Complexidade em Sistemas Dinâmicos: Formalismo Termodinâmico e Mecânico Estatísticos

Autor: *Marcus Vinicius Mesquita de Sousa*

Orientadores: Prof. Dra. Áurea Rosas Vasconcellos
Prof. Dr. Roberto Luzzi

UNIVERSIDADE ESTADUAL DE CAMPINAS

Complexidade em Sistemas Dinâmicos: Formalismo Termodinâmico e Mecânico Estatísticos

POR

Marcus Vinicius Mesquita de Sousa

Universidade Estadual de Campinas

Instituto de Física "Gleb Wagathin" — UNICAMP

Este exemplar corresponde à redação final da tese de doutoramento de M.V.M. Sousa aprovada pela Comissão Julgadora

Aurea R. Vasconcellos

TESE submetida ao Instituto de Física da Universidade Estadual de Campinas como requerimento para obtenção do título de Doutor em Física.

Campinas - SP - Brasil

16 de dezembro de 1998

UNIVERSIDADE ESTADUAL DE CAMPINAS

Complexidade em Sistemas Dinâmicos: Formalismo Termodinâmico e Mecânico Estatísticos

POR

Marcus Vinicius Mesquita de Sousa
Universidade Estadual de Campinas
Instituto de Física "Gleb Wagathin" — UNICAMP

Orientadores: **Prof. Dra. Áurea Rosas Vasconcellos,**
Prof. Dr. Roberto Luzzi,
no Grupo "Mecânica Estatística
de Sistemas Dissipativos"

TESE submetida ao Instituto de Física da Universidade Estadual de Campinas como requerimento para obtenção do título de Doutor em Física.

Campinas - SP - Brasil
16 de dezembro de 1998

FICHA CATALOGRÁFICA ELABORADA PELA
BIBLIOTECA DO IFGW - UNICAMP

So85c

Sousa, Marcus Vinicius Mesquita de
Complexidade em sistemas dinâmicos: formalismo termodinâmico e mecânico estatístico. - Campinas, SP : [s. n.], 1998.

Orientadores: Áurea Rosas Vasconcellos e Roberto Luzzi.
Tese (doutorado) - Universidade Estadual de Campinas, Instituto de Física "Gleb Wataghin".

1. Termodinâmica de sistemas em não-equilíbrio. 2. Processos irreversíveis. 3. *Fröhlich, Efeito. 4. Biopolímeros. 5. Sólitons. 6. Fonons. I. Vasconcellos, Áurea Rosas. II. Luzzi, Roberto. III. Universidade Estadual de Campinas. Instituto de Física "Gleb Wataghin". IV. Título.

INSTITUTO DE FÍSICA
GLEB WATAGHIN

Instituto de Física "Gleb Wataghin"
UNIVERSIDADE ESTADUAL DE CAMPINAS

MEMBROS DA COMISSÃO JULGADORA DA TESE DE DOUTORADO DO Sr. **MARCUS VINÍCIUS MESQUITA DE SOUSA, RA 905159** APRESENTADA E APROVADA AO INSTITUTO DE FÍSICA "GLEB WATAGHIN", DA UNIVERSIDADE ESTADUAL DE CAMPINAS, EM 16 DE DEZEMBRO DE 1998.

COMISSÃO JULGADORA:

Profa. Dra. Áurea Rosas Vasconcellos
(Orientadora do Candidato) DFESCM/IFGW/UNICAMP

Prof. Dr. Sergio Mascarenhas Oliveira
Instituto de Estudos Avançados-USP/São Carlos

Prof. Dr. Rogério Cézar de Cerqueira Leite
Professor Emérito da UNICAMP

Prof. Dr. Newton Bernardes
Centro de Lógica e Epistemologia/UNICAMP

Mario Foglio

Prof. Dr. Mário Eusébio Fóglio
DFESCM/IFGW/UNICAMP

Agradecimentos

- Aos Profs. Áurea Rosas Vasconcellos e Roberto Luzzi, pela orientação desta tese, pela compreensão, pela amizade e pelo apoio constantes;
- A meu pai e a minha mãe, pelo incentivo e pela compreensão;
- A Dulce e Marcos, pela amizade e pelo lar;
- A Iva e Mário, pela amizade e pelo apoio;
- A Maria Emília, pela amizade e pelo apoio;
- Ao David, pela amizade e pelo apoio;
- A CAPES, pelo auxílio financeiro.
- A FAEP, pelo auxílio financeiro.

Freund, du kennst doch die Goldene Zeit
(es haben die Dichter Manche Sage von ihr rührend und einfach erzählt),
jene Zeit, da das Heilige noch in der Menschheit gewandelt,
Da jungfräulich und keusch noch der Instinkt sich bewahrt,
Da noch das große Gesetz —das oben im Sonnenlauf waltet,
Und verborgen im Ei reget den hüpfenden Punkt—
Der Notwendigkeit stilles Gesetz, das stetige, gleiche,
Auch der menschlichen Brust freiere Wellen bewegt,
Da ein sichres Gefühl noch treu, wie am Uhrwerk der Zeiger,
Auf das Wahrhaftige nur, nur auf das Ewige wies?

Friedrich von Schiller, Natur und Schule.

[Amigo, conheces a época áurea
(os poetas narraram dela muitas lendas comoventes e simples),
aquela época em que o sagrado ainda caminhava na humanidade,
em que o instinto se conservava puro e casto,
em que a grande lei —que em cima rege o curso do sol
e, em segredo, agita o ponto saltitante no ovo—
a lei silenciosa da necessidade, contínua e uniformemente
também movimentava as ondas mais livres do peito humano,
em que um sentimento seguro ainda fiel, tal como o ponteiro do relógio,
ainda mostrava o verdadeiro somente, somente o eterno?]

Friedrich von Schiller, Natureza e Escola.

ABSTRACT

We present a Statistical Mechanics for nonlinear systems and a Thermodynamics of irreversible processes capable to deal with the so-called complex systems. Two powerful approaches have been used, namely

- Predictive Statistical Mechanics — based on Information Theory — in what consists of the Nonequilibrium Ensemble Formalism (NESOM), and Zubarev's approach is used,
- Informational Statistical Thermodynamics (IST).

These theories have been applied to the study of systems of bosons, like phonons and excitons in condensed matter.

Resorting to NESOM and IST we have studied with a certain depth the behavior of condensed matter when nonlinear effects are present. We have considered optical and acoustical phonons and electronic excitons in organic polymers, biological systems, and semiconductors, evidencing complex behavior consisting of three remarkable phenomena:

- Fröhlich-Bose-Einstein condensation (Fröhlich Effect);
- Propagation of near undamped Schrödinger-Davydov solitons;
- A so-named Fröhlich-Cherenkov Effect

RESUMO

O objetivo desta tese é apresentar uma Mecânica Estatística de Sistemas Não-lineares e uma Termodinâmica de processos irreversíveis apropriadas para tratar os assim chamados sistemas complexos.

Mais precisamente, foi o de utilizar dois poderosos enfoques para o tratamento de sistemas dinâmicos não-lineares, a saber:

- a Mecânica Estatística Preditiva — baseada na Teoria da Informação — na parte correspondente ao Formalismo dos Ensembles de Não-Equilíbrio (NESOM), onde usamos o enfoque de Zubarev;
- a Termodinâmica Estatística Informacional (IST).

Estas teorias foram aplicadas ao estudo de sistemas de partículas tipo boson, como são os fonons e éxcitons em matéria condensada via o uso do formalismo MaxEnt-NESOM, e a Termodinâmica Irreversível (IST) e Teoria da Função Resposta dele derivadas, temos podido fazer um estudo com certa profundidade do comportamento de matéria condensada quando efeitos não-lineares estão presentes. No caso dos bosons considerados — fonons ópticos e acústicos e éxcitons em polímeros orgânicos, sistemas biológicos e semicondutores, -- pudemos, a partir de uma base mecânica microscópica, evidenciar comportamento complexo num nível macroscópico e analisar

particularmente tal comportamento nesses sistemas dinâmicos não-lineares, evidenciando três notáveis fenômenos, que são:

- Condensação Fröhlich-Bose-Einstein (Efeito Fröhlich);
- Propagação de sólitons de Schrödinger-Davydov de vida média muito longa;
- O efeito Fröhlich-Cherenkov.

Sumário

APÊNDICES

Capítulo 1

INTRODUÇÃO

Nesta segunda metade do século XX temos assistido ao enorme desenvolvimento da *Física Não-linear* [Nicolis 1995; Haken 1978]. É difícil definir não-linearidade em uma forma precisa, a não ser, é claro, *a posteriori* pelo caráter das equações de evolução ou cinéticas que modelam um problema. Assim, em primeiro lugar, em tais sistemas o princípio da superposição de soluções — fundamental na física linear — não se aplica. Afirma-se que a não-linearidade é uma forma de descrição que trata de fenômenos que admitem mudanças qualitativas (às vezes de caráter "catastrófico") quando são impostas modificações sobre os vínculos aplicados sobre o sistema. Caos, hoje de enorme interesse e desenvolvimento, é dito ser um sintoma da não-linearidade. Outro, aquele que nos interessa aqui, é o caso de sistemas macroscópicos abertos e levados fora do equilíbrio por fontes externas, quando pode resultar possível a emergência de padrões ordenados em escala macroscópica. Processos como estes têm sido trazidos à tona pelo trabalho do prêmio Nobel Ilya Prigogine e da assim chamada Escola de Bruxelas. Estes autores têm desenvolvido uma ciência da Termodinâmica de sistemas longe do equilíbrio acompanhada de uma teoria cinética fenomenológica, em especial para o estudo de reações químicas autocatalíticas [Prigogine 1947, 1955; Glansdorff &

Prigogine 1971; Nicolis & Prigogine 1977; Nicolis 1986, 1989]. Desta forma, tem sido evidenciada a natureza criativa dos processos dissipativos em sistemas abertos, em oposição à velha idéia de decaimento por dissipação em sistemas isolados. Prigogine e colaboradores, com base nesses resultados, têm proposto a idéia de que tal tipo de auto-organização macroscópica em sistemas não-lineares abertos (a assim chamada formação de *estruturas dissipativas* [Luzzi & Vasconcellos 1991]) pode auxiliar a encurtar o fosso hoje existente entre a Física e a Biologia [Prigogine 1969; Prigogine *et al.* 1972*a,b*]. Ao mesmo tempo o assunto encaixa-se dentro da emergente *teoria da complexidade* [Anderson 1972, 1991; Gell-Mann 1995] da qual Prigogine tem sido um dos pioneiros.

Devemos ressaltar que a característica fundamental deste tipo de comportamento complexo é, como dito, que os processos sejam governados por leis não-lineares. Isto é conseqüência de que no regime linear (ou de Onsager) não há possibilidade de ordem, i. e. de comportamento complexo, devido ao teorema de Prigogine de produção mínima de entropia. De acordo com esse teorema, o sistema é levado para um estado caracterizado pela regressão de flutuações e pela validade das relações de simetria de Onsager [Prigogine 1947, 1955; Glansdorff & Prigogine 1971; Nicolis & Prigogine 1977]. A não-linearidade é ubíqua. Fenômenos não-lineares são importantes em tecnologia, particularmente na engenharia elétrica moderna, o caso típico sendo o laser. Também no caso de matéria condensada os efeitos não-lineares não são novos, e podemos mencionar a teoria de fluxo plástico de deslocações, ou o caso de que as vibrações harmônicas da rede não podem explicar a expansão térmica dos sólidos, requerendo a introdução de anarmonicidades, i. e., forças não-lineares. Contudo, como tem sido manifestado [Landauer 1987], há um interesse renovado por parte dos físicos em olhar seu caráter básico, i. e., a procura dos princípios fundamentais que estão por trás dos fenômenos não-lineares: "O que estava perdido há uma década não era a sensibilidade em relação aos fenômenos não-lineares, porém somente a apreciação da notável diversidade de comportamento disponível em sistemas não-lineares. O que é novo é o desejo de celebrar a não-linearidade."

O objetivo principal deste trabalho de tese consiste em apresentar o que se poderia denominar, seguindo G. Nicolis — de uma **Mecânica Estatística da Não-linearidade** e de uma **Termodinâmica de Sistemas Complexos** [Nicolis 1995; Nicolis & Daems 1998]: para sermos mais precisos, mostramos como um poderoso enfoque em Mecânica Estatística de sistemas fora do equilíbrio, acompanhado de uma teoria cinética quântica não-linear, uma teoria da Função Resposta para sistemas longe do equilíbrio, e uma Termodinâmica de sistemas dissipativos, mostra-se muito apropriado para tratar sistemas com comportamento dito complexo.

Nesse aspecto, tal objetivo ajusta-se aos interesses do Grupo de pesquisa/ensino "Mecânica Estatística de Sistemas Dissipativos" no DFSCM do IFGW/Unicamp, consistindo no desenvolvimento de estudos na área da Termodinâmica e Mecânica Estatística de sistemas abertos longe do equilíbrio. Esta é uma questão atual em ativo processo de desenvolvimento, e, deve dizer-se, ainda não resolvida satisfatoriamente. Assim há várias Escolas de pensamento enfocadas na questão, e, evidentemente, controvérsias surgem — resultado de que os diferentes enfoques têm suas virtudes e seus defeitos. Há um caminho a ser percorrido para chegar-se ao aprimoramento de uma teoria satisfatória, para ter-se uma Termodinâmica de processos irreversíveis confiável e aceitável.

Nesta direção é interessante mencionar o comentário de Otto Redlich [1976]:

> TERMODINÂMICA, *como Helena de Tróia — parafraseando Goethe — "bewundert viel und viel gescholten".*[1]

Mais recentemente, podemos citar G. Nicolis [1995], que escreveu:

> *Graças a sua notável flexibilidade e sua habilidade de auto-renovação, a Termodinâmica está hoje tão pronta como sempre para cumprir seu papel único na Ciência.*

Notemos que a Termodinâmica tem, como dito, várias Escolas de pensamento associadas. O renomado Laszlo Tisza [1991] listou como principais enfoques para uma construção desta disciplina:

1. O enfoque baseado nas duas leis da Termodinâmica e das regras de operação dos ciclos de Carnot, denominado enfoque da engenharia ou termodinâmica CK (de Clausius e Kelvin).
2. O enfoque matemático, que é baseado em geometria diferencial em vez dos ciclos de Carnot, denominado Termodinâmica CB (de Caratheodory e Born).
3. O ponto de vista axiomático, substituindo os ciclos de Carnot e a geometria diferencial por um conjunto de axiomas básicos, que tentam abranger os anteriores e estendê-los, denominada Termodinâmica axiomática ou TC (de Tisza e Callen).

---

[1] Muito admirada e muito censurada. W. Goethe, *Fausto*, segunda parte, terceiro ato: Diante do palácio de Menelau em Esparta.

4. O ponto de vista estatístico-mecânico, baseado obviamente no substrato provido pela mecânica microscópica (no nível molecular, ou atômico, ou de partículas, ou de quasi-partículas) mais a teoria da probabilidade, que pode ser denominada como Termodinâmica de Gibbs ou Termodinâmica Estatística.

Citamos aqui, porém sem entrar na descrição, duas tentativas recentes para uma descrição globalizada da física de sistemas de grande escala, ligando os níveis micro-, meso- e macroscópicos: a teoria GENERICS [Grmela & Öhttinger 1997] e a teoria HOLOTRÓPICA [Bernardes 1996].

Podemos mencionar exemplos já existentes nestes níveis de descrição:

1. Da Termodinâmica CK:
    - Termodinâmica de Onsager, ou Clássica Linear;
    - Termodinâmica Generalizada de Prigogine, ou Clássica Não-Linear.
2. Da Termodinâmica CB:
    - Termodinâmica Racional, baseada na mecânica dos meios contínuos.
3. Da Termodinâmica TC
    - Termodinâmica Irreversível Estendida, que introduz os fluxos como variáveis de base e hipóteses *ad hoc*.
4. Da Termodinâmica Estatística:
    - Termodinâmica Estatística Informacional, baseada, evidentemente, no substrato proporcionado pela Mecânica Estatística.

O próprio Tisza manifestou que o enfoque estatístico-mecânico — o último dos acima listados — "é o mais rico, assim como o ponto de partida para um grande arranjo de generalizações".

Como mencionado no início, é nosso intuito contribuir para o desenvolvimento deste enfoque, no que se denomina de Termodinâmica Estatística Informacional (IST, acrossemia de *Informational Statistical Thermodynamics*). Considera-se que essa IST teve início com o trabalho de Hobson [1966*a*,*b*] na década de 60. Vários Grupos desenvolveram e desenvolvem esta teoria, entre os quais se conta o Grupo no IFGW/Unicamp referido acima, às vezes mencionado como Escola de Campinas. Em particular, o enfoque do Grupo baseia-se no uso de determinada forma de tratamento, fundamentado nas idéias originais de Gibbs e Boltzmann, dentro do esquema do formalismo dos *ensembles*, porém para sistemas arbitrariamente longe do equilíbrio. Usamos o enfoque do chamado Método do Operador Estatístico de Não-Equilíbrio (NESOM, na acrossemia em Inglês), iniciado por vários autores e sistematizado e estendido pela Escola Russa de Mecânica Estatística (Bogoliubov, Krylov, Zubarev, Peletminskii, etc.). Uma descrição completa pode ser consultada nos artigos de revisão e livros listados nas referências como [Grupo GMESD, 1990-1998].

O esquema da tese consiste numa aplicação do formalismo — dentro do intento de testar resultados básicos já desenvolvidos sobre o NESOM e a IST — ao estudo de fenômenos físicos reais, experimentáveis no laboratório. Particularmente, como já dissemos anteriormente, trataremos aqui uma situação de interesse atual e muito atraente, como é o caso de sistemas não-lineares mostrando o assim denominado comportamento complexo, usualmente sendo referidos em forma resumida como sistemas complexos.

Reforçando o que dissemos sobre a tentativa de validação da teoria, via o caminho usual de aplicação da teoria e comparação com o experimento, vale a pena mencionar o renomado Ryogo Kubo [1978], que afirmou que o progresso da Mecânica Estatística dos fenômenos não-lineares fora do equilíbrio somente pode ser esperado através de uma estreita colaboração entre teoria e experimento. Mencionemos também Heisenberg [1930]:

> *Se o físico não exigisse uma teoria para explicar os resultados de um experimento, tudo seria simples e não haveria a necessidade de uma discussão epistemológica. Dificuldades surgem apenas na tentativa de classificar e sintetizar os resultados, em estabelecer a relação entre causa e efeito entre eles.*

Especificamente nosso intuito aqui é o estudo de um particular conjunto de fenômenos em certos sistemas complexos, com implicações em física da matéria condensada, assim como em biologia e em tecnologia industrial para dispositivos opto-eletrônicos e aparelhos de detecção de imagem em medicina.

Isto é feito nos próximos capítulos, que estão organizados como se segue:

No Cap. 2, deduzimos equações não-lineares de evolução para um sistema de bosons fora do equilíbrio.

No Cap. 3, tratamos sobre os sólitons do tipo Schrödinger-Davydov.

No Cap. 4, consideramos com detalhes o efeito Fröhlich.

No Cap. 5, tratamos sobre ondas solitárias em matéria condensada.

No Cap. 6, tecemos algumas considerações sobre sistemas biológicos.

No Cap. 7 é apresentada uma discussão dos resultados, com comentários e conclusões. O formalismo do NESOM está descrito de forma resumida no Apêndice A, seguido de uma Teoria da Função Resposta para sistemas longe do equilíbrio e um formalismo de funções de Green Termodinâmicas de não-equilíbrio.

Chamamos a atenção para a forma particular de apresentação desta tese, consistindo em que nos capítulos de 2 até 6, após uma Introdução ao assunto, segue a reprodução de artigos publicados ou submetidos para publicação resultantes da pesquisa realizada durante a preparação desta tese.

Nestes diversos artigos, há repetição de algumas partes, especialmente as descrições do formalismo e equações de evolução, o que é necessário para fazer auto-suficiente cada artigo submetido. Também a ênfase difere neles, dependendo da audiência a que estão destinados.

Finalmente enfatizamos que neste trabalho os assuntos de Física Não-Linear e referentes a Sistemas Dinâmicos com comportamento complexo — cuja Termodinâmica e Cinética temos desenvolvido — têm-se concentrado em:

- Propagação de *Ondas Solitárias de Schrödinger-Davydov* em condições normais.
- A chamada *Condensação tipo Fröhlich-Bose-Einstein* em sistemas de bosons, que preferimos chamar de *Efeito Fröhlich.*
- *A Termodinâmica Estatística Informacional do Efeito Fröhlich.*

- Algumas aplicações a *sistemas biológicos modelados e tecnologias médicas de imagem.*

SISTEMA DE BOSONS FORA DO EQUILÍBRIO

2.1 Introdução

Neste capítulo, estudaremos um sistema de bosons em interação anarmônica com um meio circundante — um banho térmico, o qual se considera permanentemente em equilíbrio a uma temperatura T_0, e com uma fonte externa agindo sobre o sistema, levando-o para fora do equilíbrio, ou seja, produzindo populações de estados em condições de não-equilíbrio. Na figura 2.1 é mostrado o equivalente mecânico do sistema usado.

Aplicaremos a teoria cinética descrita no Apêndice A para deduzir

- equações não-lineares de evolução para o número de ocupação dos modos de vibração desse sistema;
- equações para as amplitudes de movimento do tipo oscilatório desse sistema.

O subsistema que denominamos S_1 é composto de uma cadeia periódica de N_1 osciladores de massa m e freqüência ω_j, com $j = 1, \ldots, N_1$, e introduzimos x_j e p_j para o deslocamento ao redor da posição de equilíbrio e seu momento linear conjugado.

O subsistema denominado S_2 é composto de uma cadeia periódica de N_2 oscilado-

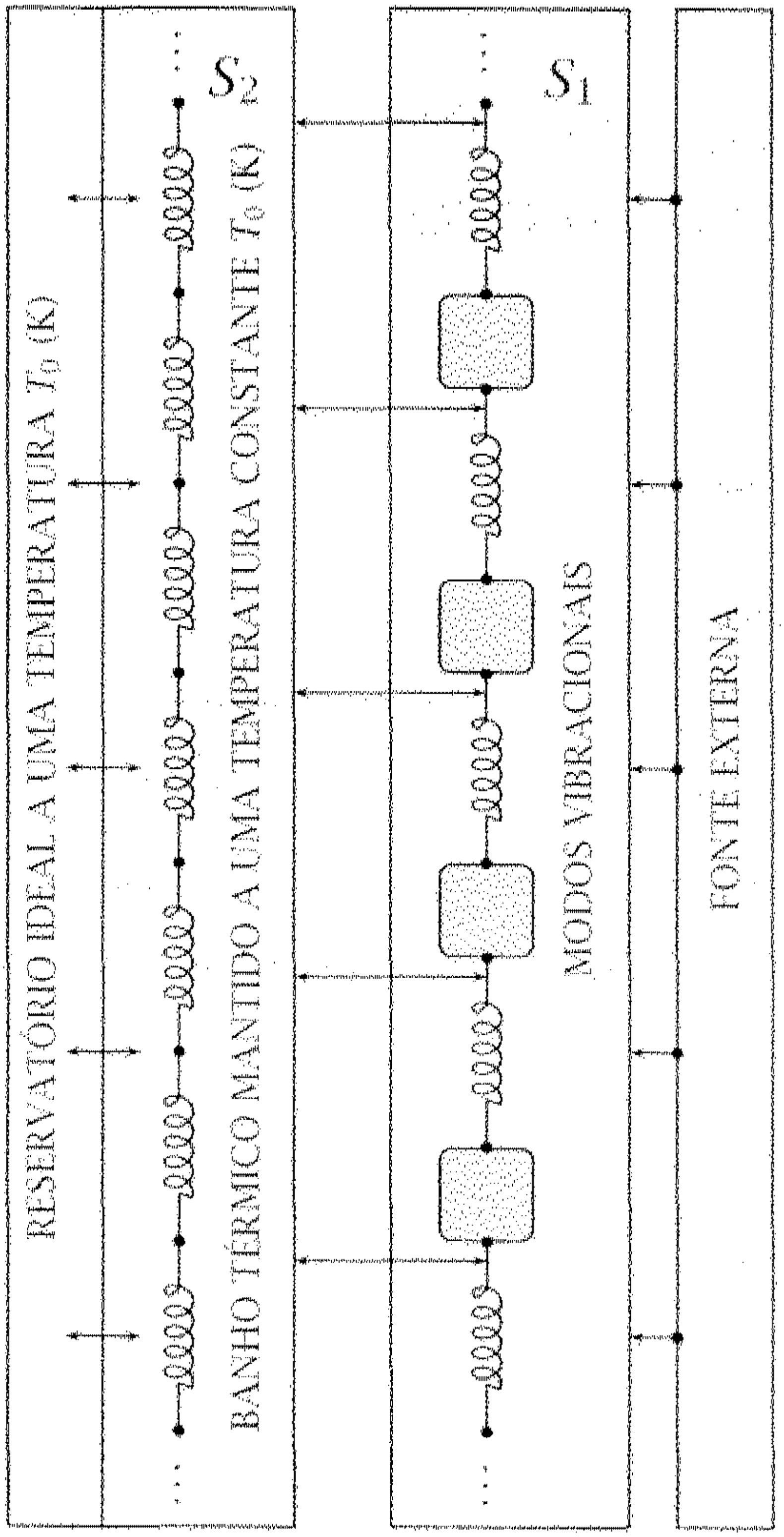

Figura 2.1: Equivalente mecânico do modelo usado, que consiste em dois subsistemas de osciladores interagindo através de um potencial anarmônico.

res de massa M e freqüências Ω_k, com $k = 1, \ldots, N_2$ e X_k e P_k são, respectivamente, o deslocamento ao redor da posição de equilíbrio e seu momento conjugado.

Assumimos um contato térmico muito bom entre S_2 e o reservatório térmico, tal que a temperatura de S_2 é sempre a do reservatório, T_0. Uma fonte externa bombeia energia em S_1. Muitos sistemas reais podem ser descritos dessa maneira, por exemplo, nos casos quase-unidimensionais como vibrações de rede em fios quânticos semicondutores quase unidimensionais, polímeros moleculares orgânicos, polímeros biológicos. Nesta tese, esse modelo será aplicado ao caso de proteínas cuja estrutura é a hélice-α e para polímeros.

O hamiltoniano do sistema pode ser escrito como:

$$\hat{H} = \hat{H}_0 + \hat{H}', \tag{2.1}$$

onde

$$\hat{H}_0 = \sum_j \left[\frac{\hat{p}_j^2}{2m} + \frac{1}{2} m \omega_j^2 \hat{x}_j^2 \right] + \sum_k \left[\frac{\hat{P}_k^2}{2M} + \frac{1}{2} M \Omega_k^2 \hat{X}_k^2 \right] \tag{2.2}$$

e

$$\hat{H}' = \sum_{jkk'} A_{jkk'} \hat{x}_j \hat{X}_k \hat{X}_{k'} + \sum_{jj'k} B_{jj'k} \hat{x}_j \hat{x}_{j'} \hat{X}_k + \sum_{jf} \hat{\varphi}_f \hat{x}_j \,. \tag{2.3}$$

A forma da Eq. (2.1) é apropriada para o uso no formalismo MaxEnt-NESOM que utilizamos aqui, descrito no Apêndice A. O termo $\hat{H}_0$ é composto pelos hamiltonianos dos osciladores livres. Por outro lado, $\hat{H}'$ é composto pelas interações anarmônicas (a contribuição de primeira ordem mais baixa), que são os dois primeiros termos do lado direito da Eq. (2.3), com A e B sendo as intensidades do acoplamento, enquanto o último é responsável pela interação entre a fonte externa e o sistema, com $\hat{\varphi}$ sendo o operador associado à intensidade da fonte com a intensidade de acoplamento já incluída e apenas estamos considerando a criação de uma única oscilação simples através de tal acoplamento.

A seguir, por conveniência, introduzimos, em primeiro lugar, as coordenadas normais

$$\hat{x}_j = \sum_{\boldsymbol{q}} \hat{x}_{\boldsymbol{q}} e^{i\boldsymbol{q}\cdot\boldsymbol{R}_j} , \qquad \hat{p}_j = \sum_{\boldsymbol{q}} \hat{p}_{\boldsymbol{q}} e^{i\boldsymbol{q}\cdot\boldsymbol{R}_j} , \tag{2.4}$$

$$\hat{X}_k = \sum_{\boldsymbol{q}'} \hat{X}_{\boldsymbol{q}'} e^{i\boldsymbol{q}'\cdot\boldsymbol{\xi}_k} , \qquad \hat{P}_k = \sum_{\boldsymbol{q}'} \hat{P}_{\boldsymbol{q}'} e^{i\boldsymbol{q}'\cdot\boldsymbol{\xi}_k} , \tag{2.5}$$

onde $\boldsymbol{q}$ e $\boldsymbol{q}'$ são números de onda no espaço recíproco, $\boldsymbol{R}_j$ e $\boldsymbol{\xi}_k$ são a posição do centro de massa dos osciladores em S_1 e S_2 respectivamente, e as somas são feitas varrendo a zona de Brillouin de cada sistema respectivamente. Em segundo lugar, introduzimos as amplitudes parciais $a_{\boldsymbol{q}}$ e $b_{\boldsymbol{q}'}$ e suas conjugadas $a^\dagger_{\boldsymbol{q}}$ e $b^\dagger_{\boldsymbol{q}'}$,

$$\hat{x}_{\boldsymbol{q}} = \left(\frac{\hbar}{2m\omega_{\boldsymbol{q}}}\right)^{1/2} (a_{\boldsymbol{q}} + a^\dagger_{-\boldsymbol{q}}) \tag{2.6}$$

$$\hat{p}_{\boldsymbol{q}} = -i\left(\frac{\hbar m\omega_{\boldsymbol{q}}}{2}\right)^{1/2} (a_{\boldsymbol{q}} - a^\dagger_{-\boldsymbol{q}}) \tag{2.7}$$

$$\hat{X}_{\boldsymbol{q}'} = \left(\frac{\hbar}{2m\Omega_{\boldsymbol{q}'}}\right)^{1/2} (b_{\boldsymbol{q}'} + b^\dagger_{-\boldsymbol{q}'}) \tag{2.8}$$

$$\hat{P}_{\boldsymbol{q}'} = -i\left(\frac{\hbar m\Omega_{\boldsymbol{q}'}}{2}\right)^{1/2} (b_{\boldsymbol{q}'} - b^\dagger_{-\boldsymbol{q}'}) \tag{2.9}$$

onde $\omega_{\boldsymbol{q}}$ e $\Omega_{\boldsymbol{q}'}$ são as freqüências dos osciladores nos modos correspondentes, e a seguir, usamos segunda quantização, com $a_{\boldsymbol{q}}(a^{\dagger}_{\boldsymbol{q}})$ e $b_{\boldsymbol{q}'}$ $(b^{\dagger}_{\boldsymbol{q}'})$ sendo os operadores de aniquilação (criação) no modo $\boldsymbol{q}$ em S_1 e $\boldsymbol{q}'$ de S_2. O hamiltoniano da Eq. (2.1) na nova representação é composto das contribuições

$$\hat{H}_0 = \hat{H}_{0S} + \hat{H}_{0B} \ , \tag{2.10}$$

com

$$\hat{H}_{0S} = \sum_{\boldsymbol{q}} \hbar\omega_{\boldsymbol{q}}(a^{\dagger}_{\boldsymbol{q}}a_{\boldsymbol{q}} + \frac{1}{2}) \ , \tag{2.11a}$$

$$\hat{H}_{0B} = \sum_{\boldsymbol{q}'} \hbar\Omega_{\boldsymbol{q}'}(b^{\dagger}_{\boldsymbol{q}'}b_{\boldsymbol{q}'} + \frac{1}{2}) \ . \tag{2.11b}$$

e

$$\hat{H}' = \hat{H}_1 + \hat{H}_2 + \hat{H}_{SF} \ , \tag{2.12}$$

com

$$\hat{H}_1 = \hat{H}_{11} + \hat{H}_{12} + \hat{H}_{13} + \hat{H}_{14} \ , \tag{2.13}$$

$$\hat{H}_2 = \hat{H}_{21} + \hat{H}_{22} + \hat{H}_{23} + \hat{H}_{24} \tag{2.14}$$

com os diversos termos do lado direito das Eq. (2.13) e (2.14) sendo dados por

$$\hat{H}_{11} = \sum_{q_1 q_2} \left\{ V^{(1)}_{q_1 q_2} a_{q_1} b_{q_2} b^{\dagger}_{q_1+q_2} + \text{h.c.} \right\} , \tag{2.15a}$$

$$\hat{H}_{12} = \sum_{q_1 q_2} \left\{ V^{(1)}_{q_1 q_2} a_{q_1} b^{\dagger}_{q_2} b_{-q_1+q_2} + \text{h.c.} \right\} , \tag{2.15b}$$

$$\hat{H}_{13} = \sum_{q_1 q_2} \left\{ V^{(1)}_{q_1 q_2} a_{q_1} b_{q_2} b_{-q_1-q_2} + \text{h.c.} \right\} , \tag{2.15c}$$

$$\hat{H}_{14} = \sum_{q_1 q_2} \left\{ V^{(1)}_{q_1 q_2} a_{q_1} b^{\dagger}_{q_2} b^{\dagger}_{q_1-q_2} + \text{h.c.} \right\} , \tag{2.15d}$$

$$\hat{H}_{21} = \sum_{q_1 q_2} \left\{ V^{(2)}_{q_1 q_2} a_{q_1} a_{q_2} b^{\dagger}_{q_1+q_2} + \text{h.c.} \right\} , \tag{2.15e}$$

$$\hat{H}_{22} = \sum_{q_1 q_2} \left\{ V^{(2)}_{q_1 q_2} a_{q_1} a_{q_2} b_{-q_1-q_2} + \text{h.c.} \right\} , \tag{2.15f}$$

$$\hat{H}_{23} = \sum_{q_1 q_2} \left\{ V^{(2)}_{q_1 q_2} a^{\dagger}_{q_1} a_{q_2} b_{q_1-q_2} + \text{h.c.} \right\} , \tag{2.15g}$$

$$\hat{H}_{24} = \sum_{q_1 q_2} \left\{ V^{(2)}_{q_1 q_2} a_{q_1} a^{\dagger}_{q_2} b^{\dagger}_{q_1-q_2} + \text{h.c.} \right\} , \tag{2.15h}$$

$$\hat{H}_{SF} = \sum_{q} \left\{ \varphi_q a^{\dagger}_q + \text{h.c.} \right\} , \tag{2.15i}$$

onde o último termo é responsável pela interação com a fonte externa, com φ_q e $\varphi^{\dagger}_q$ ligados às amplitudes Fourier da intensidade da fonte, a serem especificadas mais adiante.

Nas contribuições das Eqs. (2.15) é levada em conta a conservação de momento linear, e os coeficientes $V^{(1)}$ e $V^{(2)}$ são os elementos de matrizes do potencial de interação [derivados das amplitudes A e B da Eq. (2.3)].

2.2 Definição das variáveis de base

O primeiro passo para aplicar a Termodinâmica Estatística Informacional (IST) é escolher o conjunto básico de variáveis para a descrição do estado macroscópico de não-equilíbrio do sistema. Depois disso, podemos deduzir as equações de evolução para essas variáveis básicas, usando a teoria cinética quântica não-linear baseada no MOENE e tomando a aproximação de segunda ordem em teoria de relaxação, isto é, o limite markoviano da teoria cinética (ver Apêndice A).

Para o presente caso, as variáveis escolhidas são: (1) o número de ocupação dos modos de oscilação do sistema S_1

$$\nu_q(t) = \mathrm{Tr}\left\{a_q^\dagger a_q \varrho_\varepsilon(t)\right\} = \mathrm{Tr}\left\{\hat{\nu}_q \varrho_\varepsilon(t)\right\} , \tag{2.16}$$

(2) as amplitudes de oscilação

$$\langle a_q \mid t\rangle = \mathrm{Tr}\left\{a_q \varrho_\varepsilon(t)\right\} , \tag{2.17}$$

(3) suas conjugadas,

$$\langle a_q^\dagger \mid t\rangle = \mathrm{Tr}\left\{a_q^\dagger \varrho_\varepsilon(t)\right\} = \langle a_q | t\rangle^* , \tag{2.18}$$

e (4) a energia das vibrações acústicas do banho térmico,

$$E_B = \mathrm{Tr}\left\{\sum_{q'} \hbar\Omega_{q'}(b_{q'}^\dagger b_{q'} + \frac{1}{2})\varrho_\varepsilon(t)\right\} , \tag{2.19}$$

a qual é constante e independente do tempo, uma vez que o banho é mantido em equilíbrio térmico a uma temperatura constante T_0 (assim, a parte correspondente às variáveis do banho em $\varrho_\varepsilon(t)$ — uma distribuição canônica em equilíbrio — não depende do tempo).

Nas equações (2.16–2.18) $\varrho_\varepsilon(t)$ é o **OENE** na formulação de Zubarev [Zubarev 1974; Zubarev *et al.* 1996, 1997; Luzzi *et al.* 1998], que se escreve como

$$\varrho_\varepsilon(t) = \exp\{-\hat{S}(t,0) + \int_{-\infty}^{t} dt' e^{\varepsilon(t'-t)} \frac{d}{dt'} \hat{S}(t',t'-t)\} \;, \tag{2.20}$$

onde

$$\hat{S}(t,0) = -\ln \bar{\varrho}(t,0) \;, \tag{2.21}$$

com

$$\bar{\varrho}(t,0) = \exp\Big\{-\phi(t) - \sum_q [F_q(t)\hat{\nu}_q + f_q(t)a_q + f_q^*(t)a_q^\dagger] - \beta_0 \hat{H}_{0B}\Big\} \tag{2.22}$$

e

$$\hat{S}(t',t'-t) = \exp\Big\{-\frac{1}{i\hbar}(t'-t)\hat{H}\Big\}\, \hat{S}(t',0)\, \exp\Big\{\frac{1}{i\hbar}(t'-t)\hat{H}\Big\} \;. \tag{2.23}$$

Observemos que no operador auxiliar $\bar{\varrho}(t,0)$, às vezes denominado de "equilíbrio congelado" ou "quase-equilíbrio instantâneo", $\phi(t)$ assegura sua normalização (sendo uma espécie de logaritmo de uma função de partição de não-equilíbrio), $\phi(t) \equiv \ln \bar{Z}(t)$,

$F_q(t), f_q(t), f_q^*(t)$, são os parâmetros de Lagrange associados às variáveis dinâmicas de base de S_1, e $\beta_0 = 1/k_B T_0$ é a parte de distribuição canônica correspondente ao banho em equilíbrio à temperatura T_0.

Observemos, finalmente, que ϱ_ε pode ser sempre escrito na forma

$$\varrho_\varepsilon(t) = \bar{\varrho}(t,0) + \varrho'(t) , \tag{2.24}$$

onde $\bar{\varrho}$ define instantaneamente o estado macroscópico do sistema e $\varrho'(t)$ dá conta de sua evolução irreversível [Zubarev 1974; Zubarev *et al.* 1996, 1997; Luzzi *et al.* 1998].

Temos, portanto, que o conjunto básico de variáveis termodinâmicas está constituído por

$$\{Q_j(t)\} \equiv \left\{\nu_q \, , \langle a_q|t\rangle \, , \langle a_q^\dagger|t\rangle \, , E_B\right\} . \tag{2.25}$$

Observemos que a separação do hamiltoniano da Eq. (2.1) corresponde com a da Eq. (A.2), e as variáveis de base satisfazem à condição de simetria da Eq. (A.3), i. e.,

$$[\hat{H}_0, \hat{\nu}_q] = 0 , \tag{2.26a}$$

$$[\hat{H}_0, a_q] = \hbar\omega_q a_q , \tag{2.26b}$$

$$[\hat{H}_0, a_q^\dagger] = -\hbar\omega_q a_q^\dagger , \tag{2.26c}$$

$$[\hat{H}_0, \hat{H}_B] = 0 . \tag{2.26d}$$

2.3 Teoria cinética

Nesta seção obteremos as equações de evolução para cada uma das variáveis da Eq. (2.25), ou seja, determinaremos a evolução do estado macroscópico de não-equilíbrio do sistema. A equação de evolução para cada uma das variáveis é obtida calculando-se a média sobre o ensemble de não-equilíbrio da equação de Heisenberg para o conjunto de variáveis dinâmicas de base, i. e. $\hat{v}_q$, a_q, $a_q^\dagger$, H_B, com o operador estatístico de não-equilíbrio, $\varrho_\varepsilon(t)$, isto é

$$\frac{\partial}{\partial t}\hat{v}_q(t) = \mathrm{Tr}\left\{\frac{1}{\mathrm{i}\hbar}[\hat{v}_q,\hat{H}]\varrho_\varepsilon(t)\right\} , \tag{2.27a}$$

$$\frac{\partial}{\partial t}\langle a_q|t\rangle = \mathrm{Tr}\left\{\frac{1}{\mathrm{i}\hbar}[a_q,\hat{H}]\varrho_\varepsilon(t)\right\} , \tag{2.27b}$$

$$\frac{\partial}{\partial t}\langle a_q^\dagger|t\rangle = \mathrm{Tr}\left\{\frac{1}{\mathrm{i}\hbar}[a_q^\dagger,\hat{H}]\varrho_\varepsilon(t)\right\} , \tag{2.27c}$$

$$\frac{d}{dt}E_B = 0 , \tag{2.27d}$$

onde a última equação é o resultado de que o banho térmico está constantemente em equilíbrio com o reservatório.

Como indicado no Apêndice A, os membros da direita nas Eqs. (2.27) podem ser escritos em termos de operadores de colisão calculados em termos de médias com o operador auxiliar $\bar{\varrho}(t,0)$. Aqui usaremos o método, restringindo a série de operadores de colisão e mantendo somente o termo em segunda ordem na interação, ou seja, somente colisões binárias.

2.3.1 Equação para a evolução das populações dos modos de vibração

A equação para a evolução de $\nu_{\boldsymbol{q}}(t)$ é obtida a partir da Eq. (A.19), com $\hat{P}_j = \hat{\nu}_{\boldsymbol{q}}$, ou seja:

$$\frac{d}{dt}\nu_{\boldsymbol{q}}(t) = J^{(0)}_{\nu_{\boldsymbol{q}}}(\boldsymbol{q},t) + J^{(1)}_{\nu_{\boldsymbol{q}}}(\boldsymbol{q},t) + J^{(2)}_{\nu_{\boldsymbol{q}}}(\boldsymbol{q},t) \ , \tag{2.28}$$

onde, recordamos, estamos usando a aproximação em segunda ordem na interação. Destas três contribuições no lado direito desta equação, o primeiro termo é nulo, i.e.

$$J^{(0)}_{\nu_{\boldsymbol{q}}}(\boldsymbol{q},t) = \frac{1}{i\hbar}\langle[\hat{H}_0, \hat{\nu}_{\boldsymbol{q}}]|t\rangle_0 = 0 \ , \tag{2.29}$$

pois $\hat{\nu}_{\boldsymbol{q}}$ comuta com H_0, e onde, como indicado no Apêndice A [cf. Eq. (A.18)],

$$\langle \cdots |t\rangle_0 = \mathrm{Tr}\left\{\cdots \bar{\varrho}(t,0)\right\} . \tag{2.30}$$

A contribuição do segundo termo é nula, ou seja,

$$J^{(1)}_{\nu_{\boldsymbol{q}}}(\boldsymbol{q},t) = 0 \ , \tag{2.31}$$

como conseqüência de que:

$$\langle[\hat{H}', \hat{\nu}_{\boldsymbol{q}}]|t\rangle_0 = \langle[\hat{H}_{SF}, \hat{\nu}_{\boldsymbol{q}}] + [\hat{H}_{PA}, \hat{\nu}_{\boldsymbol{q}}]\rangle_0 = 0 \ . \tag{2.32}$$

onde $\hat{H}_{PA} = \hat{H}_1 + \hat{H}_2$.

De fato,

$$[\hat{H}_{SF}, \hat{\nu}_{\boldsymbol{q}}] = \varphi^{\dagger}_{\boldsymbol{q}} a_{\boldsymbol{q}} - \varphi_{\boldsymbol{q}} a^{\dagger}_{\boldsymbol{q}} \tag{2.33}$$

e $\langle\varphi\rangle_0 = \langle\varphi^{\dagger}\rangle_0 = 0$, admitindo uma fonte não-coerente, e, além disso,

$$\begin{aligned}
[\hat{H}_{PA}, \hat{\nu}_{\boldsymbol{q}}] = {} & V^{(1)}_{\boldsymbol{q}\boldsymbol{q}'}\{a_{\boldsymbol{q}} b_{\boldsymbol{q}'} b_{-\boldsymbol{q}-\boldsymbol{q}'} + a_{\boldsymbol{q}} b_{\boldsymbol{q}'} b^{\dagger}_{\boldsymbol{q}+\boldsymbol{q}'} + a_{\boldsymbol{q}} b^{\dagger}_{\boldsymbol{q}'} b_{-\boldsymbol{q}+\boldsymbol{q}'} + a_{\boldsymbol{q}} b^{\dagger}_{\boldsymbol{q}'} b^{\dagger}_{\boldsymbol{q}-\boldsymbol{q}'}\} \\
& -V^{(1)}_{\boldsymbol{q}\boldsymbol{q}'}\{a^{\dagger}_{\boldsymbol{q}} b_{\boldsymbol{q}-\boldsymbol{q}'} b_{\boldsymbol{q}'} + a^{\dagger}_{\boldsymbol{q}} b_{\boldsymbol{q}+\boldsymbol{q}'} b^{\dagger}_{\boldsymbol{q}'} + a^{\dagger}_{\boldsymbol{q}} b^{\dagger}_{-\boldsymbol{q}-\boldsymbol{q}'} b^{\dagger}_{\boldsymbol{q}'} + a^{\dagger}_{\boldsymbol{q}} b^{\dagger}_{-\boldsymbol{q}+\boldsymbol{q}'} b_{\boldsymbol{q}'}\} \\
& +2V^{(2)}_{\boldsymbol{q}\boldsymbol{q}'}\{a_{\boldsymbol{q}} a_{\boldsymbol{q}'} b^{\dagger}_{-\boldsymbol{q}-\boldsymbol{q}'} + a_{\boldsymbol{q}} a_{\boldsymbol{q}'} b^{\dagger}_{\boldsymbol{q}+\boldsymbol{q}'} + a^{\dagger}_{\boldsymbol{q}'} a_{\boldsymbol{q}} b_{-\boldsymbol{q}+\boldsymbol{q}'} + a^{\dagger}_{\boldsymbol{q}'} a_{\boldsymbol{q}} b^{\dagger}_{\boldsymbol{q}-\boldsymbol{q}'}\} \\
& -2V^{(2)}_{\boldsymbol{q}\boldsymbol{q}'}\{a^{\dagger}_{\boldsymbol{q}} a_{\boldsymbol{q}'} b_{\boldsymbol{q}-\boldsymbol{q}'} + a^{\dagger}_{\boldsymbol{q}} a_{\boldsymbol{q}'} b^{\dagger}_{-\boldsymbol{q}+\boldsymbol{q}'} + a^{\dagger}_{\boldsymbol{q}} a^{\dagger}_{\boldsymbol{q}'} b_{\boldsymbol{q}+\boldsymbol{q}'} + a^{\dagger}_{\boldsymbol{q}} a^{\dagger}_{\boldsymbol{q}'} b^{\dagger}_{-\boldsymbol{q}-\boldsymbol{q}'}\}
\end{aligned} \tag{2.34}$$

onde os termos que são lineares em b e $b^{\dagger}$ dão uma contribuição nula para o valor médio, isto é, $\langle b\rangle_0 = \langle b^{\dagger}\rangle_0 = 0$, já que em $\varrho_c(t)$ a distribuição associada a S_2 é a canônica em equilíbrio à temperatura T_0, e os termos restantes também dão contribuição nula quando seus valores médios são calculados, ou seja, $\langle b_{\boldsymbol{q}+\boldsymbol{q}'} b^{\dagger}_{\boldsymbol{q}'}\rangle_0 = 0$, já que $\boldsymbol{q} \neq \boldsymbol{q}'$, e $\langle bb\rangle_0 = \langle b^{\dagger} b^{\dagger}\rangle_0 = 0$ na média com a distribuição canônica.

Assim, os valores médios no ensemble caracterizado pelo operador auxiliar $\bar{\varrho}(t,0)$ na Eq. (2.32) se anulam. Conseqüentemente, na Eq. (2.28), o único termo com uma contribuição diferente de zero é o último termo, $J^{(2)}_{\nu_q}(\boldsymbol{q},t)$, cuja expressão é obtida utilizando-se a Eq. (A.20)

$$J^{(2)}_{\nu_q}(\boldsymbol{q},t) = \lim_{\varepsilon\to+0}(\mathrm{i}\hbar)^{-2}\int_{-\infty}^{0} dt'\,\mathrm{e}^{\varepsilon t'}\langle[\hat{H}'(t)_0, [\hat{H}', \hat{\nu}_{\boldsymbol{q}}]]|t\rangle_0 = J^{(2)}_{\varphi\boldsymbol{q}}(t) + J^{(2)}_{1\boldsymbol{q}} + J^{(2)}_{2\boldsymbol{q}}\,. \tag{2.35}$$

Notemos que na Eq. (2.35) a dependência de $\hat{H}'$ no tempo é dada, na representação de interação, com o operador $\hat{H}_0$, ou seja:

$$\hat{H}'(t)_0 = e^{\frac{1}{i\hbar}t\hat{H}_0}\hat{H}' e^{-\frac{1}{i\hbar}t\hat{H}_0} \ . \tag{2.36}$$

As diversas contribuições da Eq. (2.35) são:

$$\begin{aligned} J^{(2)}_{\varphi q}(t) &= \lim_{\varepsilon\to 0}\left[(i\hbar)^{-2}\int_{-\infty}^{0} dt'\, e^{\varepsilon t'}\,\mathrm{Tr}\left\{[\hat{H}_\varphi(t')_0,[\hat{H}_\varphi,\hat{\nu}_q]]\bar{\varrho}(t,0)\right\}\right] \\ &= \frac{1}{\hbar^2}\sum_{q'}\int_{-\infty}^{0} dt'\, e^{(\varepsilon+i\omega_q)t'}\,\mathrm{Tr}\left\{\varphi_{q'}(t')\varphi^\dagger_{q'}\,\bar{\varrho}(t,0)\right\} + \text{c.c.}\,, \end{aligned} \tag{2.37}$$

que é o termo correspondente à interação $\hat{H}_{SF}$, e

$$\begin{aligned} J^{(2)}_{1\boldsymbol{q}}(t) &= \lim_{\varepsilon\to 0}\left[(i\hbar)^{-2}\int_{-\infty}^{0} dt'\, e^{\varepsilon t'}\,\mathrm{Tr}\left\{[\hat{H}_1(t')_0,[\hat{H}_1,\hat{\nu}_q]]\bar{\varrho}(t,0)\right\}\right] \\ &= \frac{4\pi}{\hbar^2}\frac{1+\langle a_{\boldsymbol{q}}|t\rangle^2}{\nu^{(0)}_{\boldsymbol{q}}}\sum_{\boldsymbol{q}'}|V^{(1)}_{\boldsymbol{q}\boldsymbol{q}'}|^2\nu^B_{\boldsymbol{q}'}\nu^B_{\boldsymbol{q}-\boldsymbol{q}'}\left[\delta(\Omega_{\boldsymbol{q}'}+\Omega_{\boldsymbol{q}-\boldsymbol{q}'}-\omega_{\boldsymbol{q}}) + 2e^{\beta\hbar\Omega_{q'}}\delta(\Omega_{\boldsymbol{q}'}-\Omega_{\boldsymbol{q}-\boldsymbol{q}'}+\omega_{\boldsymbol{q}})\right]\,, \end{aligned} \tag{2.38}$$

que é o termo correspondente a $\hat{H}_1$ da Eq. (2.13), e onde $\nu^B_{\boldsymbol{q}}$ é a população de fonons do banho, que após o cálculo produz, como esperado, a distribuição de Planck, i.e.

$$\nu^B_{\boldsymbol{q}} = \mathrm{Tr}\left\{b^\dagger_{\boldsymbol{q}} b_{\boldsymbol{q}}\bar{\varrho}(t,0)\right\} = \left[\exp(\beta_0\hbar\Omega_{\boldsymbol{q}})-1\right]^{-1} . \tag{2.39}$$

Além disso, temos a contribuição correspondente a $\hat{H}_2$ da Eq. (2.14)

$$
\begin{aligned}
J_{2q}^{(2)}(t) &= \lim_{\varepsilon\to 0}\left[(i\hbar)^{-2}\int_{-\infty}^{0} dt'\, e^{\varepsilon t'}\,\mathrm{Tr}\left\{[\hat{H}_2(t')_0,[\hat{H}_2,\hat{\nu}_q]]\bar{\varrho}(t,0)\right\}\right] \\
&= \frac{8\pi}{\hbar^2}\sum_{q'}|V_{qq'}^{(2)}|^2\left[\nu_{q-q'}^{B}(\nu_{q'}-\nu_q)-\nu_q(1+\nu_{q'})\right]\delta(\Omega_{q-q'}+\omega_{q'}-\omega_q) \\
&+ \frac{8\pi}{\hbar^2}\sum_{q'}|V_{qq'}^{(2)}|^2\left[\nu_{q-q'}^{B}(\nu_{q'}-\nu_q)+\nu_{q'}(1+\nu_q)\right]\delta(\Omega_{q-q'}-\omega_{q'}+\omega_q) \\
&+ \frac{8\pi}{\hbar^2}\sum_{q'}|V_{qq'}^{(2)}|^2\left[\nu_{q+q'}^{B}(1+\nu_{q'})-(\nu_{q'}-\nu_{q+q'}^{B})\nu_q\right]\delta(\Omega_{q+q'}-\omega_{q'}-\omega_q) + \\
&+ \frac{8\pi}{\hbar^2}\sum_{q'}|V_{qq'}^{(2)}|^2\{|\langle a_q|t\rangle|^2(1+\nu_{q'}+\nu_{q-q'}^{B})-|\langle a_{q'}|t\rangle|^2(\nu_q-\nu_{q-q'}^{B})\} \\
&\times\delta(\Omega_{q-q'}+\omega_{q'}-\omega_q) \\
&- \frac{8\pi}{\hbar^2}\sum_{q'}|V_{qq'}^{(2)}|^2\{|\langle a_q|t\rangle|^2(\nu_{q'}-\nu_{q-q'}^{B})-|\langle a_{q'}|t\rangle|^2(1+\nu_q+\nu_{q-q'}^{B})\} \\
&\times\delta(\Omega_{q-q'}-\omega_{q'}+\omega_q) \\
&+ \frac{8\pi}{\hbar^2}\sum_{q'}|V_{qq'}^{(2)}|^2\{|\langle a_q|t\rangle|^2(\nu_{q'}-\nu_{q+q'}^{B})-|\langle a_{q'}|t\rangle|^2(\nu_q-\nu_{q+q'}^{B})\} \\
&\times\delta(\Omega_{q+q'}-\omega_{q'}-\omega_q)\,. \qquad (2.40)
\end{aligned}
$$

Com todos os termos que contribuem para o lado direito da Eq. (2.35) calculados, podemos escrevê-la numa forma compacta como

$$\frac{d}{dt}\nu_q(t) = I_q + \sum_{j=1}^{5} J_{q(j)}(t) + \zeta_q(t)\,, \qquad (2.41)$$

onde I_q representa a intensidade da fonte na freqüência ω_q e com transferência de momento $\boldsymbol{q}$ resultante da introdução da representação espectral para a fonte na forma

$$\hbar^{-2}\langle \varphi_q(t)\varphi^{\dagger}_{q'}\rangle = \delta_{qq'}\int_{-\infty}^{\infty}\frac{d\omega}{2\pi}\, I_q(\omega)\mathrm{e}^{-\mathrm{i}\omega t}\,, \tag{2.42}$$

e, como descrevemos a seguir, os $J_{q_{(i)}}(t)$ são operadores de colisão provenientes das interações anarmônicas, e $\zeta_q(t)$ é o termo que atua como uma fonte de acoplamento entre as populações dos modos vibracionais e as amplitudes de oscilação. Os diagramas de colisão correspondentes estão indicados nas figuras 2.2 e 2.3 nas páginas 26 e 27 respectivamente.

Os dois primeiros termos dos operadores de colisão correspondem a eventos de colisão envolvendo um fônon do sistema e dois fonons do banho, e dão origem a um termo de dissipação que toma a forma

$$J_{q_{(1)}}(t) + J_{q_{(2)}}(t) = -\frac{1}{\tau_q}\left[\nu_q(t) - \nu_q^{(0)}\right]\,, \tag{2.43}$$

onde $\nu_q^{(0)}$ é a população em equilíbrio a uma temperatura T_0, e τ_q tem o papel de um tempo de relaxação dado por:

$$\tau_q^{-1} = \frac{4\pi}{\hbar^2}\frac{1}{\nu_q^{(0)}}\sum_{q'}|V^{(1)}_{qq'}|^2\nu^B_{q'}\nu^B_{q-q'}\left[\delta(\Omega_{q'}+\Omega_{q-q'}-\omega_q)\right.$$
$$\left. + 2\mathrm{e}^{\beta\hbar\Omega_{q'}}\delta(\Omega_{q'}-\Omega_{q-q'}+\omega_q)\right]\,, \tag{2.44}$$

e as funções delta exprimem a conservação de energia nos eventos de espalhamento.

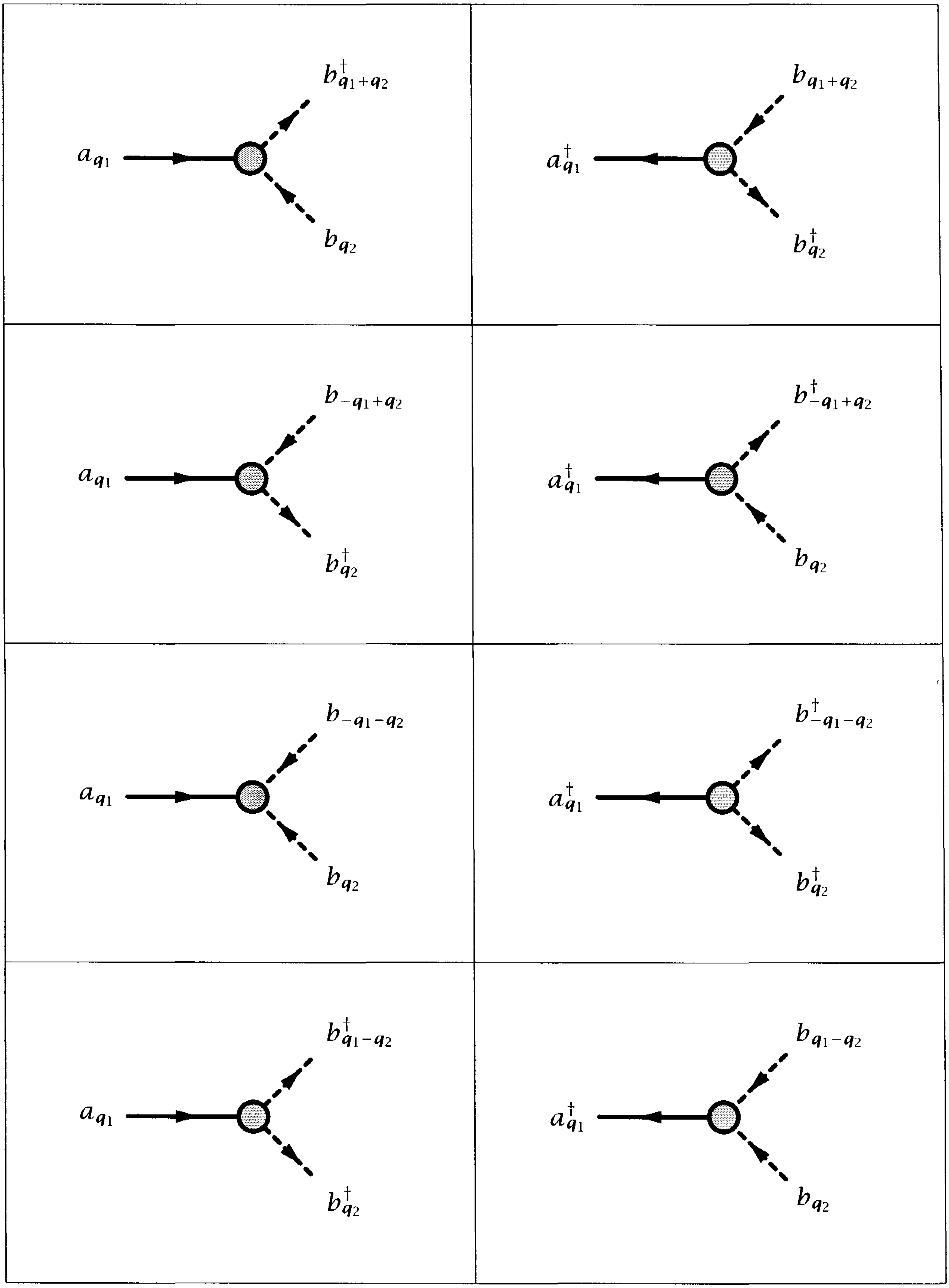

Figura 2.2: Diagramas de colisão provenientes das interações de $\hat{H}_1$.

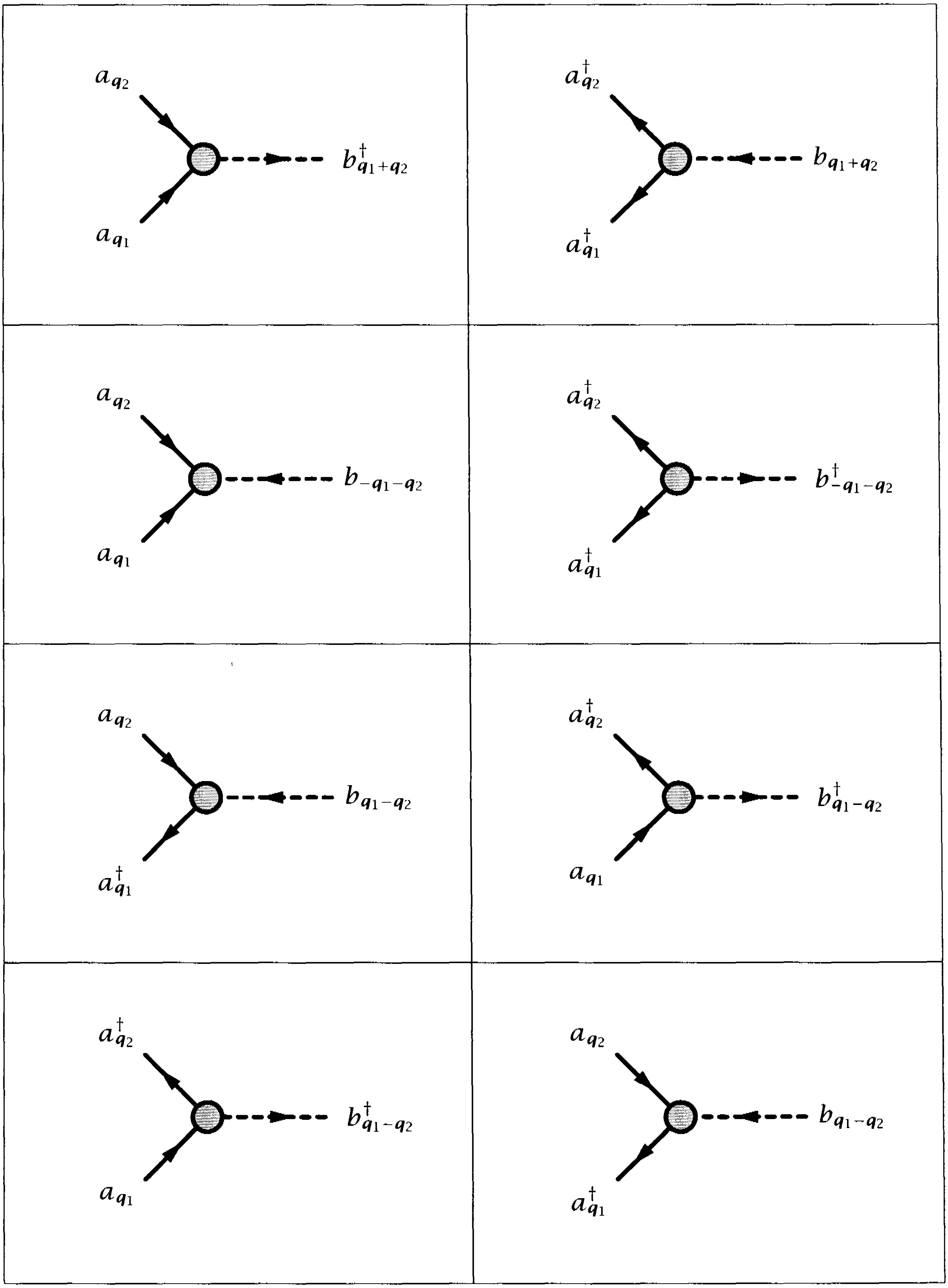

Figura 2.3: Diagramas de colisão provenientes das interações de $\hat{H}_2$.

Os outros termos, $J_{q_{(i)}}(t)$ with $i = 3, 4, 5$, são

$$J_{q_{(3)}}(t) = \frac{8\pi}{\hbar^2} \sum_{q'} |V^{(2)}_{qq'}|^2 \left[\nu^B_{q-q'}(\nu_{q'} - \nu_q) - \nu_q(1 + \nu_{q'}) \right] \delta(\Omega_{q-q'} + \omega_{q'} - \omega_q) \,, \tag{2.45a}$$

$$J_{q_{(4)}}(t) = \frac{8\pi}{\hbar^2} \sum_{q'} |V^{(2)}_{qq'}|^2 \left[\nu^B_{q-q'}(\nu_{q'} - \nu_q) + \nu_{q'}(1 + \nu_q) \right] \delta(\Omega_{q-q'} - \omega_{q'} + \omega_q) \,, \tag{2.45b}$$

$$J_{q_{(5)}}(t) = \frac{8\pi}{\hbar^2} \sum_{q'} |V^{(2)}_{qq'}|^2 \left[\nu^B_{q+q'}(1 + \nu_{q'}) - (\nu_{q'} - \nu^B_{q+q'})\nu_q \right] \delta(\Omega_{q+q'} - \omega_{q'} - \omega_q) \,. \tag{2.45c}$$

Finalmente, temos o último termo na Eq. (2.41), $\zeta_q(t)$, dado por

$$\begin{aligned}
\zeta_q(t) - \frac{|\langle a_q|t\rangle|^2}{\tau_q} &+ \frac{8\pi}{\hbar^2} \sum_{q'} |V^{(2)}_{qq'}|^2 \{ |\langle a_q|t\rangle|^2 (1 + \nu_{q'} + \nu^B_{q-q'}) - |\langle a_{q'}|t\rangle|^2 (\nu_q - \nu^B_{q-q'}) \} \\
&\times \delta(\Omega_{q-q'} + \omega_{q'} - \omega_q) \\
&- \frac{8\pi}{\hbar^2} \sum_{q'} |V^{(2)}_{qq'}|^2 \{ |\langle a_q|t\rangle|^2 (\nu_{q'} - \nu^B_{q-q'}) - |\langle a_{q'}|t\rangle|^2 (1 + \nu_q + \nu^B_{q-q'}) \} \\
&\times \delta(\Omega_{q-q'} - \omega_{q'} + \omega_q) \\
&+ \frac{8\pi}{\hbar^2} \sum_{q'} |V^{(2)}_{qq'}|^2 \{ |\langle a_q|t\rangle|^2 (\nu_{q'} - \nu^B_{q+q'}) - |\langle a_{q'}|t\rangle|^2 (\nu_q - \nu^B_{q+q'}) \} \\
&\times \delta(\Omega_{q+q'} - \omega_{q'} - \omega_q) \,.
\end{aligned} \tag{2.45d}$$

o qual envolve populações e o módulo quadrado das amplitudes.

Os operadores de colisão $J_{q_{(3)}}$ e $J_{q_{(4)}}$ são responsáveis pelo assim chamado efeito Fröhlich (ou condensação tipo Bose-Einstein em não-equilíbrio) a ser descrito no Cap. 4. Este efeito é o resultado da transferência de energia para os modos polares de freqüência mais baixa, os quais aumentam grandemente sua população. De fato, eles contêm contribuições proporcionais a

$$\sum_{\boldsymbol{q}'} |V^{(2)}_{\boldsymbol{q}\boldsymbol{q}'}|^2 \nu_{\boldsymbol{q}}(t)\nu_{\boldsymbol{q}'}(t)[\delta(\Omega_{\boldsymbol{q}\ \boldsymbol{q}'} - \omega_{\boldsymbol{q}'} + \omega_{\boldsymbol{q}}) - \delta(\Omega_{\boldsymbol{q}-\boldsymbol{q}'} + \omega_{\boldsymbol{q}'} - \omega_{\boldsymbol{q}})] \, , \tag{2.46}$$

e podemos notar que para os modos $\boldsymbol{q}'$ tal que $\omega_{\boldsymbol{q}'} > \omega_{\boldsymbol{q}}$ a conservação de energia requerida pela primeira função delta é satisfeita, enquanto isso não é possível para a segunda: assim, essa contribuição não-linear tende a aumentar a população no modo $\boldsymbol{q}$ às custas dos outros modos de freqüência mais alta. Reciprocamente, para $\omega_{\boldsymbol{q}'} < \omega_{\boldsymbol{q}}$, o modo $\boldsymbol{q}$ transfere energia para os modos de freqüência mais baixa.

O operador $J_{\boldsymbol{q}_{(5)}}$ é também um termo de relaxação que contém contribuições não-lineares nas populações dos modos, mas, como veremos, é nulo ou tem contribuição negligenciável.

2.3.2 Equação para a evolução das amplitudes de vibração

A equação para a evolução de $\langle a_{\boldsymbol{q}}|t\rangle$ é obtida a partir da Eq. (A.19), com $\hat{P}_j = a_{\boldsymbol{q}}$ e é dada por

$$\frac{d}{dt}\langle a_{\boldsymbol{q}}|t\rangle = J^{(0)}_{a_{\boldsymbol{q}}}(\boldsymbol{q},t) + J^{(1)}_{a_{\boldsymbol{q}}}(\boldsymbol{q},t) + J^{(2)}_{a_{\boldsymbol{q}}}(\boldsymbol{q},t) \, . \tag{2.47}$$

A contribuição do primeiro termo do lado direito é:

$$J^{(0)}_{a_{\boldsymbol{q}}}(\boldsymbol{q},t) = \frac{1}{i\hbar}\langle[\hat{H}_0, a_{\boldsymbol{q}}]|t\rangle_0 = -i\hbar\omega_{\boldsymbol{q}}\langle a_{\boldsymbol{q}}|t\rangle \, . \tag{2.48}$$

A contribuição do segundo termo é nula, i. e.

$$J^{(1)}_{a_q}(\boldsymbol{q},t) = 0 \, , \tag{2.49}$$

como conseqüência de que:

$$\langle [\hat{H}', a_{\boldsymbol{q}}] | t \rangle_0 = \langle [\hat{H}_{SF}, a_{\boldsymbol{q}}] + [\hat{H}_{PA}, a_{\boldsymbol{q}}] | t \rangle_0 = 0 \, , \tag{2.50}$$

ou seja, os valores médios no ensemble caracterizado por $\bar{\varrho}(t,0)$ se anulam, pela mesma razão que no caso da Eq. (2.32), como já discutido. Assim, a Eq. (2.47) pode ser escrita, utilizando-se a Eq. (A.20), como

$$J^{(2)}_{a_q}(\boldsymbol{q},t) = -\mathrm{i}\hbar\omega_{\boldsymbol{q}} \langle a_{\boldsymbol{q}} | t \rangle + \lim_{\varepsilon \to +0} (\mathrm{i}\hbar)^{-2} \int_{-\infty}^{0} dt' \, \mathrm{e}^{\varepsilon t'} \langle [H'(t), [H', a_{\boldsymbol{q}}]] | t \rangle_0 \, . \tag{2.51}$$

Igualmente, após os cálculos dos comutadores duplos terem sido feitos, os valores médios calculados e o limite quando $\varepsilon \to +0$ ter sido realizado, podemos escrever as equações de evolução para as amplitudes:

$$\frac{\partial}{\partial t} \langle a_{\boldsymbol{q}} | t \rangle = -\mathrm{i} \, \tilde{\omega}_{\boldsymbol{q}} \, \langle a_{\boldsymbol{q}} | t \rangle - \Gamma_{\boldsymbol{q}}(t) \, \langle a_{\boldsymbol{q}} | t \rangle + \Gamma_{\boldsymbol{q}}(t) \, \langle a_{\boldsymbol{q}} | t \rangle^* - \mathrm{i} W_{\boldsymbol{q}} \, \langle a_{\boldsymbol{q}} | t \rangle^* +$$

$$+ \sum_{\boldsymbol{q}_1 \boldsymbol{q}_2} R_{\boldsymbol{q}_1 \boldsymbol{q}_2} \langle a_{\boldsymbol{q}_1} | t \rangle \langle a^\dagger_{\boldsymbol{q}_2} | t \rangle \Big(\langle a_{\boldsymbol{q}-\boldsymbol{q}_1+\boldsymbol{q}_2} | t \rangle + \langle a^\dagger_{-\boldsymbol{q}+\boldsymbol{q}_1-\boldsymbol{q}_2} | t \rangle \Big) \, , \tag{2.52a}$$

$$\frac{\partial}{\partial t} \langle a^\dagger_{\boldsymbol{q}} | t \rangle = \text{o complexo conjugado do lado direito da Eq. (2.52a),} \tag{2.52b}$$

onde $\tilde{\omega}_{\boldsymbol{q}} = \omega_{\boldsymbol{q}} + W_{\boldsymbol{q}}$, com $W_{\boldsymbol{q}}$ sendo um termo de renormalização de freqüência cuja expressão é dada aproximadamente por

$$W_q = \frac{8}{\hbar^2}\wp \sum_{q'} \left(\frac{(1 + 2\nu^B_{q+q'})\omega_{q'}}{\omega^2_{q'} - \omega^2_q} \right) \tag{2.53}$$

onde $\wp$ indica valor principal, e os termos $R_{q_1 q_2}$ e $\Gamma_q(t)$ são dados por

$$R_{q_1 q_2} = \frac{2\pi}{\hbar^2} \sum_{q_1 q_2} |V^{(2)}_{q_1 q_2}|^2 \{\delta(\Omega_{q_1+q_2} + \omega_{q_1} - \omega_{q_2}) - \delta(\Omega_{q_1-q_2} - \omega_{q_1} + \omega_{q_2})\} \, , \tag{2.54}$$

$$\begin{aligned} \Gamma_q(t) = {} & \frac{1}{2}\tau^{-1}_q(t) + \frac{4\pi}{\hbar^2} \sum_{q'} |V^{(2)}_{qq'}|^2 \left[1 + \nu_{q'}(t) + \nu^B_{q-q'} \right] \delta(\Omega_{q-q'} + \omega_{q'} - \omega_q) + \\ & - \frac{4\pi}{\hbar^2} \sum_{q'} |V^{(2)}_{qq'}|^2 \left[\nu_{q'}(t) - \nu^B_{q-q'} \right] \delta(\Omega_{q-q'} - \omega_{q'} + \omega_q) + \\ & + \frac{4\pi}{\hbar^2} \sum_{q'} |V^{(2)}_{qq'}|^2 \left[\nu_{q'}(t) - \nu^B_{q+q'} \right] \delta(\Omega_{q+q'} - \omega_{q'} - \omega_q) \, , \end{aligned} \tag{2.55}$$

com τ_q dado pela Eq. (2.44). Temos, pois, que as Eqs. (2.41) e (2.52) formam um sistema de equações diferenciais não-lineares acopladas. Concentraremos nossa atenção agora na evolução da amplitude, Eq. (2.52a), uma equação não-linear muito peculiar, que será responsável pelo surgimento de um comportamento complexo de um caráter particular.

2.4 Equação tipo Schrödinger não-linear e dissipativa

Na seção precedente obtivemos as Eqs. (2.52) para os valores médios das amplitudes. Introduzamos agora uma representação no espaço direto, definindo os operadores

$$a_j = \sum_{\boldsymbol{q}} a_{\boldsymbol{q}}\, \mathrm{e}^{\mathrm{i}\,\boldsymbol{q}\cdot\boldsymbol{R}_j} \,, \tag{2.56}$$

onde $\boldsymbol{R}_j$ é a posição do j-ésimo centro oscilante; assumindo que esses centros estão espaçados periodicamente, encontramos que

$$\frac{\partial}{\partial t}\langle a_j|t\rangle = -\,\mathrm{i}\sum_{l}\left\{\left[\omega_{jl} + W_{jl} - \mathrm{i}\,\Gamma_{jl}\right]\langle a_l|t\rangle + \left[W_{jl} - \mathrm{i}\,\Gamma_{jl}\right]\langle a_l|t\rangle^*\right\}$$

$$+ \sum_{lm}\left[R_{jlm}\langle a_l|t\rangle\langle a_m|t\rangle\langle a_j|t\rangle^* + \text{c.c.}\right] \,, \tag{2.57}$$

onde

$$\omega_{jl} = \sum_{\boldsymbol{q}} \omega_{\boldsymbol{q}}\, \mathrm{e}^{\mathrm{i}\,\boldsymbol{q}\cdot(\boldsymbol{R}_j-\boldsymbol{R}_l)} \,, \qquad W_{jl} = \sum_{\boldsymbol{q}} W_{\boldsymbol{q}}\, \mathrm{e}^{\mathrm{i}\,\boldsymbol{q}\cdot(\boldsymbol{R}_j-\boldsymbol{R}_l)} \,, \tag{2.58a}$$

$$\Gamma_{jl} = \sum_{\boldsymbol{q}} \Gamma_{\boldsymbol{q}}\, \mathrm{e}^{\mathrm{i}\,\boldsymbol{q}\cdot(\boldsymbol{R}_j-\boldsymbol{R}_l)} \,, \qquad R_{jlm} = \sum_{\boldsymbol{q}_1\boldsymbol{q}_2} R_{\boldsymbol{q}_1\boldsymbol{q}_2}\, \mathrm{e}^{\mathrm{i}\,\boldsymbol{q}_1\cdot(\boldsymbol{R}_j-\boldsymbol{R}_k)}\, \mathrm{e}^{\mathrm{i}\,\boldsymbol{q}_2\cdot(\boldsymbol{R}_j-\boldsymbol{R}_m)} \,. \tag{2.58b}$$

Introduzindo a amplitude média localmente definida fazendo uma aproximação por um contínuo, i.e., as posições discretas $\boldsymbol{R}_j$ são substituídas pela variável espacial contínua $\boldsymbol{r}$, e escrevemos

$$\psi(\boldsymbol{r},t) = \sum_{\boldsymbol{q}} \langle a_{\boldsymbol{q}}|t\rangle\, \mathrm{e}^{\mathrm{i}\,\boldsymbol{q}\cdot\boldsymbol{r}} \,. \tag{2.59}$$

Consideremos o caso de uma relação de dispersão parabólica

$$\omega_{\boldsymbol{q}} = \omega_0 - \alpha|\boldsymbol{q}|^2 \, , \tag{2.60}$$

com ω_0 e α constantes (no que segue, por exemplo, o caso de éxcitons em semicondutores ou uma relação de dispersão aproximada para modos polares e no caso de modos acústicos, quando é linear na aproximação de Debye, surgirá de apropriadas expansões). Após negligenciar os termos de acoplamento lineares com a equação conjugada, o que é equivalente a introduzir um hamiltoniano truncado na assim chamada "Rotating Wave Approximation" [Haken 1970], obtemos

$$\begin{aligned} i\hbar\frac{\partial}{\partial t}\psi(\boldsymbol{r},t) &= (\hbar\omega_0 + \hbar\alpha\nabla^2)\psi(\boldsymbol{r},t) - i\hbar\int d\boldsymbol{r}'\,\Gamma(\boldsymbol{r}-\boldsymbol{r}')\psi(\boldsymbol{r}',t) + \\ &+ \int d\boldsymbol{r}'d\boldsymbol{r}''\,R(\boldsymbol{r}-\boldsymbol{r}',\boldsymbol{r}-\boldsymbol{r}'')\psi(\boldsymbol{r}'',t)\psi(\boldsymbol{r}',t)\psi^*(\boldsymbol{r},t) \, , \end{aligned} \tag{2.61}$$

onde

$$R(\boldsymbol{r}-\boldsymbol{r}',\boldsymbol{r}-\boldsymbol{r}'') = \sum_{\boldsymbol{q}_1\boldsymbol{q}_2} R_{\boldsymbol{q}_1\boldsymbol{q}_2}\; e^{i\boldsymbol{q}_1\cdot(\boldsymbol{r}-\boldsymbol{r}')+i\boldsymbol{q}_2\cdot(\boldsymbol{r}-\boldsymbol{r}'')} \, , \tag{2.62}$$

$$\Gamma(\boldsymbol{r}-\boldsymbol{r}') = \sum_{\boldsymbol{q}}\Gamma_{\boldsymbol{q}}\; e^{i\boldsymbol{q}\cdot(\boldsymbol{r}-\boldsymbol{r}')} \, . \tag{2.63}$$

A Eq. (2.61) é uma equação de Schrödinger não-linear com amortecimento [Valyasek *et al.* 1971] Introduzindo uma aproximação local, i. e., negligenciando correlações espaciais, o que é feito usando as expressões

$$R(\boldsymbol{r}-\boldsymbol{r}',\boldsymbol{r}-\boldsymbol{r}'')=K\delta(\boldsymbol{r}-\boldsymbol{r}')\delta(\boldsymbol{r}-\boldsymbol{r}'')\ , \tag{2.64}$$

$$\Gamma(\boldsymbol{r}-\boldsymbol{r}')=\gamma\delta(\boldsymbol{r}-\boldsymbol{r}')\ , \tag{2.65}$$

com K e γ sendo constantes, obtemos que a Eq. (2.61) adquire a forma

$$\mathrm{i}\hbar\frac{\partial}{\partial t}\psi(\boldsymbol{r},t)=\left(\hbar\omega_0+\hbar\alpha\nabla^2\right)\psi(\boldsymbol{r},t)-\mathrm{i}\hbar\gamma\psi(\boldsymbol{r},t)+K|\psi(\boldsymbol{r},t)|^2\psi(\boldsymbol{r},t)\ . \tag{2.66}$$

As Eqs. (2.57) e (2.66) são da forma das equações derivadas por Davydov [1982] de uma maneira alternativa, mas aqui mostrando claramente efeitos de amortecimento. Essas equações têm como soluções os assim chamados sólitons de Schrödinger-Davydov. Eles serão o assunto do próximo capítulo.

Capítulo 3

SÓLITONS DO TIPO SCHRÖDINGER-DAVYDOV

3.1 Introdução

O conceito de *sóliton* tem ganho recentemente ampla difusão em Física, Engenharia e Biologia. Sua origem, ainda não como a excitação hoje chamada sóliton, remonta ao século passado (1834), a partir de uma observação do engenheiro civil escocês John Scott-Russell [1844]: no chamado Union Canal ligando Edinburgh com Glasgow, quando estudando as relações entre as formas dos cascos dos barcos com as velocidades e as forças necessárias para movê-los, observou um fenômeno atípico que se formou quando um barco que se movimentava no canal parou subitamente. É interessante reproduzir parte de sua apresentação à *Royal Society of Edinburgh:*

> *I was observing the motion of a boat which was rapidly drawn along a narrow channel by a pair of horses, when the boat suddenly stopped — not so the mass of water in the channel which it had put in motion; it accumulated round the prow of the vessel in a state of violent agitation, then suddenly leaving it behind, rolled forward with great velocity, assuming the form of a large solitary elevation, a rounded, smooth and well defined heap of water, which continued its course along the channel apparently without change of form or diminution of speed.*

> *I followed in on horseback, and overtook it still rolling on a rate of some eight or nine miles an hour, preserving ints original figure some thirty feet long and a foot to a foot and a half in height. Its height gradually diminished, and after a chase of one or two miles I lost it in the windings of the channel. Such, in the month of August 1834, was my first chance interview with that singular and beatiful phenomenon ...*

Na Fig. 3.1 pode ser vista uma demonstração da formação de onda solitária no aqueduto Scott Russell no *Union Canal.* Essa figura foi obtida na Internet na página `http://www.ma.hw.ac.uk/solitons/press.html`.

Figura 3.1: Sóliton no aqueduto Scott Russell no *Union Canal*, perto da Universidade Heriot-Watt, em 12 de julho de 1995.

Scott Russel denominou essa onda de "Onda de Translação" e, embora estivesse convencido de tinha observado um fenômeno importante, a questão permaneceu no plano de uma simples curiosidade até aproximadamente o fim da década de 60, quando físicos e engenheiros reconheceram que as ondas solitárias eram um fenômeno intrigante e relevante muito disseminado na Natureza. Os engenheiros conseguiram criar ondas solitárias de luz em fibras ópticas [Haus 1993; Shen 1997; Snyder & Mitchell 1997]; aparecem também como importantíssimo veículo de transporte de cargas em polímeros dopados [Beardsley 1997; Heger *et al.* 1988; Anderson & Roth 1994]; astrônomos têm conjecturado que a grande mancha vermelha de Júpiter é uma formação que pode estar relacionada a uma onda solitária; em Física, aparentemente começaram a ser considerados a partir de modelos computacionais de molas e pêndulos mostrando padrões do tipo ondas solitárias. Como esses padrões eram tão bem definidos espacialmente e se mantinham compactos no tempo, de forma a parecerem um objeto único, a onda solitária foi também referida como sóliton. Isso pela similitude com fonons, elétrons e outras partículas elementares que atuam com a aparente dualidade de onda-partícula.

Nas últimas duas décadas têm sido feitos esforços para eventualmente reconhecer a presença de sólitons em biologia, e.g. em tecidos vivos. Todavia, sistemas biológicos são extremamente complicados e a observação experimental *in vivo* é muito difícil. Recentemente, os biofísicos e biomatemáticos têm começado a atacar a questão. Há indicações de que sólitons microscópicos podem atravessar as células ou eventualmente a cadeia do DNA. Em neurologia há tentativas para relacioná-los com a propagação de impulsos nervosos no cérebro, assim como o sóliton macroscópico *tsunami* atravessa o oceano. Aqui, também está presente o importantíssimo problema em bioenergética de como a energia é convertida e transmitida nos organismos vivos. Estas questões têm um tratamento parcial neste trabalho como é descrito no Cap. 6.

Os sólitons são notáveis em diversos aspectos. Um é que pacotes de onda com amplitudes maiores viajam mais rápido do que aqueles com amplitudes menores. Outro é que se observamos o movimento de sólitons antes e depois da colisão de pulsos, vemos que nem as formas nem as velocidades dos pulsos mudam, ou seja, eles são totalmente insensíveis ao processo de espalhamento.

Além disso, em certos casos, diferentemente das ondas normais que decaem mais ou menos rapidamente e tem uma vida média muito maior, como o *tsunami* no oceano, esses sólitons, é claro, não violam a segunda lei da termodinâmica, ou seja, a energia que carregam se dispersa, porém muito mais lentamente. Também é notável a coesão nos sólitons. Essa peculiaridade de aparecer como um objeto bem definido, tal como é mostrado na Fig. 3.1 é o resultado, como veremos, de que o sóliton é construído a partir de numerosos componentes (i. e. é um pacote de ondas peculiar), entre as quais a energia é transferida via efeitos não-lineares de tal forma que a energia total no pacote permanece enclausurada num envelope rígido.

Assim, enquanto ondas normais são compostas de *wavelets* que diferem em freqüência e velocidade de grupo (propagação) que se dispersam, no sóliton são mantidas num pacote de forma fixa: então os mecanismos dispersivos e de relaxação no caso de sólitons é particularmente atípico, com a questão ilustrada no restante deste capítulo e no Cap. 5.

Insistimos em que se trata de um fenômeno que somente pode existir no domínio da Física Não-linear. Esta não-linearidade, que faz com que o princípio da superposição já não seja válido, produz o mecanismo que leva à coesão do sóliton e, em circunstâncias especiais, à característica de uma relaxação ou dissipação muito fraca no tempo. Por causa da não-linearidade cada *wavelet* componente afeta constantemente todas as outras, e assim não podem ser consideradas separadamente, como é o caso de uma equação linear que pode ser atacada em termos de modos normais de vibração. Conseqüentemente as equações não-lineares não podem ser reduzidas às contribuições das partes e resolvida em membros (as componentes de Fourier).

Assim, podemos dizer que a onda solitária pode ser entendida qualitativamente como representando um equilíbrio entre os efeitos de não-linearidade e dispersão espacial e temporal. Isto será visto em continuação quando derivamos equações de evolução não-lineares — para sermos mais precisos equações do tipo chamado de Schrödinger-Davydov. Uma vez que não podemos fazer a análise de Fourier da equação não-linear, temos de recorrer ao método do espalhamento inverso, que permite resolver analiticamente a equação de evolução do sóliton. Esse método, que está estreitamente ligado à transformada de Fourier, pode ser aplicado para a resolução de equações diferenciais não-lineares. Mais detalhes podem ser vistos no Apêndice B.

No que segue neste capítulo tratamos da propagação de sólitons em polímeros e em semicondutores, no primeiro caso como um pacote de vibrações ópticas da rede e no outro por éxcitons criados por iluminação laser.

As seções a seguir são:

3.2 Tratamento Termodinâmico Estatístico de Ondas Solitárias Vibracionais na Acetanilida.

3.3 Processos Irreversíveis no Contexto do Formalismo de Ensemble Estatístico de Não-equilíbrio.

No Cap. 5 retomamos a questão para tratar da propagação de sólitons em matéria condensada sob altos níveis de excitação.

3.2 Tratamento termodinâmico estatístico de ondas solitárias vibracionais na acetanilida

Analisamos o comportamento do estado termodinâmico macroscópico de polímeros, concentrando-nos na acetanilida. São deduzidas equações não-lineares de evolução para as populações e para a média estatística das amplitudes de campo dos modos de estiramento CO. A existência de excitações do tipo onda solitária é evidenciado. O espectro infravermelho é calculado e comparado com os dados experimentaias de Careri *et al.* [1983], resultando em uma boa concordância. Consideramos também a situação de uma amostra excitada não-termicamente, predizendo a ocorrência de um grande aumento na vida média da excitação de onda solitária.

Physical Review Letter, **80** (9) 2008-11.

STATISTICAL THERMODYNAMIC APPROACH TO VIBRATIONAL SOLITARY WAVES IN ACETANILIDE

Áurea R. Vasconcellos, Marcus V. Mesquita,[1] Roberto Luzzi

Instituto de Física 'Gleb Wataghin',
Universidade Estadual de Campinas, Unicamp
13083-970 Campinas, São Paulo, Brazil

---

[1] E-mail:sousa@ifi.unicamp.br

We analyze the behavior of the macroscopic thermodynamic state of polymers, centering on acetanilide. The nonlinear equations of evolution for the populations and the statistically-averaged field amplitudes of CO-stretching modes are derived. The existence of excitations of the solitary wave type is evidenced. The infrared spectrum is calculated and compared with the experimental data of Careri *et al.* [Phys. Rev. Lett. **51**, 104 (1983)], resulting in a good agreement. We also consider the situation of a nonthermally highly excited sample, predicting the occurrence of a large increase in the lifetime of the solitary wave excitation.

PACS# 87.10.+e/05.70.Ln/82.20.Mj/87.22.-q

---

*E-mail: sousa@ifi.unicamp.br
Group Home Page: http://www.aurea.ifi.unicamp.br/index.html

The question of long range propagation of energy (signals) in polymers of technological interest [1], and in biological systems [2], has been a topic of large interest and a certain puzzlement. More than twenty years ago A. S. Davydov proposed a novel mechanism for the localization and transport of vibrational energy in such type of polymers, namely the propagation of solitary-like waves resulting from nonlinear interactions in the media (two relevant and comprehensive reviews are due to Davydov [3] and A. Scott [4]). Observation of *Davydov's soliton* in functioning biological materials is difficult. There has been alternative attempts performing experimental studies in polymers, and one has been acetanilide. The infrared spectra of crystalline acetanilide have shown an "anomalous" band that has been ascribed to the excitation of a Davydov's soliton, as reported by Careri *et al.* [5]. Fann *et al.*, on the basis of results in ultrafast time-resolved optical measurements, suggested that such band is not a result of a vibronic solitary wave but resulting from a slightly nondegenerate hydrogen-atom configuration (double-well potential) in the crystal [6]. However, recently Johnson *et al.* [7], on the basis of neutron diffraction studies, arrived to the conclusion that there is no evidence for the suggestion in [6] to explain the supplementary Amide-I mode, and the solitary vibronic excitation hypothesis is in better agreement with most of the available experimental results on the structure and dynamics of acetanilide.

In the present communication we reconsider the question on the basis of a statistical-thermodynamical description of the nonlinear vibrational dynamics in a model appropriate to describe vibrational modes in acetanilide. In that way we are able to characterize and describe—within this thermo-mechanical scheme—a Davydov-like soliton, and to derive the infrared spectra which evidences it. We discuss the dependence of the characteristics of the solitary wave (like amplitude, frequency, lifetime) on the initial conditions and on the macroscopic thermodynamic state of the system. We analyze the case of pump-probe experiments, and discuss a predicted phenomenon consisting in the propagation of nearly undamped solitary waves in a highly excited sample.

We consider a quasi-periodic polymer (e.g. acetanilide) characterized in terms of a Hamiltonian describing a system composed of polar vibrational modes (e.g. the CO-stretching) which are taken as coupled with a surrounding media (thermal bath) via anharmonic interactions (for details see [8]). The thermal bath is taken as a continuum and described in a Debye model, and is considered to constantly remain in equilibrium at a temperature T_0. Moreover, it is included an energy-pumping external source, which acts on the systems driving it out of equilibrium, that is, producing (eventually large) populations of vibrational modes in nonthermal nonequilibrium conditions. In this way we take into account, from the onset, the case of pump-probe experiments. For the thermo-mechanical description of the nonequilibrium system we resort to a statistical thermodynamics based on a particular nonequilibrium ensemble formalism, namely, the Nonequilibrium Statistical Operator Method (NESOM) [9], and Zubarev's approach to NESOM is used below [10].

In this approach the first step is the choice of the set of basic variables for the description of the nonequilibrium macroscopic state of the system, and the derivation of its irreversible evolution in time. In the present case they are the population of the polar modes, $\nu_{\boldsymbol{q}}(t)$ (where $\boldsymbol{q}$ is the mode wavevector running over the Brillouin zone), and the vibrational amplitudes $\langle a_{\boldsymbol{q}}|t\rangle$ and their conjugate $\langle a_{\boldsymbol{q}}^{\dagger}|t\rangle$ (a and $a^{\dagger}$

are, as usual, annihilation and creation operators in phonon states). Furthermore, on the basis of the condition that the thermal bath is constantly kept in equilibrium we take as basic variable its constant energy, say E_B (the bath is then characterized by a canonical distribution with temperature T_0). As already noticed, the detailed Hamiltonian is given in [8]. The equations of evolution for the time-dependent basic variables, given above, are derived in the NESOM-based nonlinear quantum transport theory [10-12]. We resort to the so-called second order approximation in relaxation theory [12], that is, the Markovian limit of the kinetic theory. Omitting the details of the quite lengthy calculation, the final expressions are

$$\begin{aligned}\frac{d}{dt}\nu_q(t) &= I_q(\omega_q) - \tau_q^{-1}(t)[\nu_q(t) - \nu_q^{(0)}] \\ &+ \frac{8\pi}{\hbar^2}\sum_{q'}|V_{qq'}^{(2)}|^2\left[\nu_{q-q'}^B(\nu_{q'} - \nu_q) - \nu_q(1+\nu_{q'})\right]\delta(\Omega_{q-q'} + \omega_{q'} - \omega_q) \\ &+ \frac{8\pi}{\hbar^2}\sum_{q'}|V_{qq'}^{(2)}|^2\left[\nu_{q-q'}^B(\nu_{q'} - \nu_q) + \nu_{q'}(1+\nu_q)\right]\delta(\Omega_{q-q'} - \omega_{q'} + \omega_q) + \\ &+ \frac{8\pi}{\hbar^2}\sum_{q'}|V_{qq'}^{(2)}|^2\left[\nu_{q+q'}^B(1+\nu_{q'}) - (\nu_{q'} - \nu_{q+q'}^B)\nu_q\right]\delta(\Omega_{q+q'} - \omega_{q'} - \omega_q)\,, \qquad (1)\end{aligned}$$

$$\begin{aligned}\frac{\partial}{\partial t}\langle a_q|t\rangle &= -\mathrm{i}\,\tilde{\omega}_q\,\langle a_q|t\rangle - \Gamma_q\,\langle a_q|t\rangle + \Gamma_q\,\langle a_q^\dagger|t\rangle + \\ &+ \sum_{q_1q_2} R_{q_1q_2}\langle a_{q_1}|t\rangle\langle a_{q_2}^\dagger|t\rangle\left(\langle a_{q-q_1+q_2}|t\rangle + \langle a^\dagger_{-q+q_1-q_2}|t\rangle\right)\,. \qquad (2)\end{aligned}$$

In Eq. (1), $I_q(\omega)$ measures the rate of production of excitations in mode q generated by the external source; $V_{qq'}^{(2)}$ are the matrix elements of the anharmonic interaction between polar modes and the bath; ω_q the polar modes frequency dispersion relation, and Ω_q that of the modes in the bath with the populations ν_q^B in thermal equilibrium at temperature T_0; τ_q is the lifetime for decay towards the equilibrium value $\nu_q^{(0)}$. In Eq. (2), $R_{q_1 q_2}$ is the coupling strength in the nonlinear contribution [8], and Γ_q is the reciprocal lifetime of the excitation, of particular relevance in what follows, given by

$$\begin{aligned}\Gamma_q(t) = \tau_q^{-1}(t) &+ \frac{4\pi}{\hbar^2}\sum_{q'}|V_{qq'}^{(2)}|^2\left[1+\nu_{q'})+\nu_{q-q'}^B\right]\delta(\Omega_{q-q'}+\omega_{q'}-\omega_q)\\ &- \frac{4\pi}{\hbar^2}\sum_{q'}|V_{qq'}^{(2)}|^2\left[\nu_{q'}-\nu_{q-q'}^B\right]\delta(\Omega_{q-q'}-\omega_{q'}+\omega_q)\\ &+ \frac{4\pi}{\hbar^2}\sum_{q'}|V_{qq'}^{(2)}|^2\left[\nu_{q'}-\nu_{q+q'}^B\right]\delta(\Omega_{q+q'}-\omega_{q'}-\omega_q)\,. \end{aligned} \tag{3}$$

We call the attention to the relevant fact consisting into the time dependence of this lifetime on the populations of the modes, with these contributions, aside from τ_q^{-1}, originating in the nonlinear anharmonic interactions. Finally, we notice that, assuming weak amplitudes $\langle a_q|t\rangle$, we have neglected their influence in the equation for the populations, Eq. (1), where they show up in quadratic contributions. Next, we introduce the average field operator for the amplitudes, namely (in the one-dimensional model we are using)

$$\psi(x,t) = \sum_q \langle a_q \mid t\rangle e^{iqx}\,, \tag{4}$$

and, moreover, we choose a parabolic dispersion relation in the form $\omega_q = \omega_0 - \alpha q^2$ (a good approximation in most cases); evidently, ω_0 is the frequency at the zone centre and α an indication of the ratio of curvature at that point. Using Eqs. (2) and (4) we find that the average amplitude field operator satisfies the equation

$$i\frac{\partial\psi(x,t)}{\partial t} - (\omega_0 - i\gamma_s)\psi(x,t) - \alpha\frac{\partial^2}{\partial x^2}\psi(x,t) + G\left|\psi(x,t)\right|^2\psi(x,t) = 0\,. \qquad (5)$$

We notice that to arrive to this Eq. (5) we have neglected its coupling with the conjugated field operator, ψ^* [Cf. Eq. (2)], what can be shown to correspond in this case to the equivalent of introducing the so-called rotating wave approximation [13]. Furthermore, we have taken a local approximation, that is, we have neglected space correlations, what is justified a posteriori because of the stringent space localization of the excitation. Equation (5) is of the form of a nonlinear Schrödinger-like equation with damping [14]. Evidently γ_s is the reciprocal lifetime and G measures the intensity of the nonlinear coupling (these two quantities γ and G are the constant values of Γ and R of Eq. (2), respectively, in direct space when the local approximation is used).

We first consider the situation of the experiment in [5], that is $I = 0$ in Eq. (1) and, then, the population ν_q is in thermal equilibrium ($\nu_q = \nu_q^{(0)}$) at temperature T_0. We solve Eq. (5) resorting to the inverse scattering method [15] for an initial condition in the form of an impulse-like excitation with an hyperbolic-secant shape, to obtain that

$$\psi(x,t) = \mathcal{A}\exp\left\{i\left[\frac{v}{2\alpha}x - (\omega_s - i\gamma_s)\,t - \frac{\theta}{2}\right]\right\}\operatorname{sech}\left[\mathcal{A}\left(\frac{|G|}{2\alpha}\right)^{1/2}(x - vt)\right]. \qquad (6)$$

In this Eq. (6), γ_s is the reciprocal lifetime of the excitation (which for $\gamma_s = 0$ is Davydov's soliton [3,4]), we used $G = |G|e^{i\theta}$, and

$$\omega_s = \omega_0 - \frac{v^2}{4\alpha} + \frac{|G|\,\mathcal{A}^2}{2}\,, \qquad (7)$$

where $\mathcal{A}$ and v are an amplitude and velocity of propagation fixed by the initial condition of excitation. Therefore it is proved the possibility of propagation of Davydov's solitons in polymers, but, we stress, of a damped character. Let us look on its experimental observation, and consider the infrared spectrum. Measurement of the IR-absorbance of ACN samples in the Amide-I region has been done by Careri *et al.* [5]. We recall that these authors report a band, red-shifted from the main Amide-I maximum by about 15 cm^{-1}, and which they ascribe to a Davydov-like solitary wave. Careri *et al.* mention the fact that Davydov [2] suggests that soliton excitation directly by light shall be small. However, they observe an absorption comparable with the one due to the normal Amide-I. Our results, as shown below, confirm such observation. We consider the second order process involving electron-laser radiation interaction and electron-vibrational mode interaction (Fröhlich potential interaction should be the relevant one as compared with deformation potential interaction). On the basis of this process, following consistently the NESOM formalism, according to the response function theory and scattering theory based on it [9, 16], we find for the expected absorbance spectrum

$$\alpha(\omega) = \sum_q \phi(q,\omega) \int_0^{\Delta t} dt \int_0^{t} dt' \mathrm{e}^{-\mathrm{i}\omega(t'-t)} \mathrm{Tr}\left\{a_q^{\dagger}(t') a_q(t) \varrho(0)\right\} , \tag{8}$$

where ϕ is an amplitude whose detailed form is not necessary for our purposes here, suffice it to say that it contains the squared modulus of the matrix elements of the electron-radiation and of the electron-phonon interaction (Fröhlich potential), and the energy denominator associated to the virtual intermediate state. Moreover $\varrho(0)$ is the statistical distribution at the initial time of preparation of the sample, and, since it is an experiment in time-integrated optical spectroscopy, Δt is the experimental resolution time. From a direct calculation it follows that

$$\mathrm{Tr}\,\{a_q{}^{\dagger}(t')a_q(t)\varrho(0)\} = \nu_q^{(0)}\,\mathrm{e}^{-\mathrm{i}\omega_q(t'-t)} + \langle a_q^{\dagger} \mid t'\rangle\langle a_q \mid t\rangle\,, \tag{9}$$

what implies that *the absorption spectrum has two bands*, the "normal" one due to the vibration around frequency ω_q, and an "anomalous" band around frequency ω_s, that is, the associated to the soliton. In fact, using Eqs. (4), (6), and (9) in Eq. (8) we find that

$$\alpha(\omega) \simeq \int_0^{\Delta t} dt \int_0^t dt'[\alpha_n(t,t') + \alpha_s(t,t')]\,, \tag{10}$$

where

$$\alpha_n(t,t') \simeq C_n[\mathrm{e}^{-2\gamma t}\mathrm{e}^{\mathrm{i}(\omega-\omega_q)(t'-t)} + \mathrm{e}^{-2\gamma t'}\mathrm{e}^{-\mathrm{i}(\omega-\omega_q)(t'-t)}], \tag{11a}$$

$$\alpha_s(t,t') \simeq C_s[\mathrm{e}^{-2\gamma_s t}\mathrm{e}^{\mathrm{i}(\omega-\omega_s)(t'-t)} + \mathrm{e}^{-2\gamma_s t'}\mathrm{e}^{-\mathrm{i}(\omega-\omega_s)(t'-t)}]\,, \tag{11b}$$

where $\gamma_s = \gamma + \mathcal{A}(|G|/2\alpha)^{\frac{1}{2}}$, and C_n and C_s are amplitudes corresponding to the "normal" and "anomalous" bands with band widths γ and γ_s respectively. Scott *et al.* [17] have detected overtones in the IR spectra, which can also be described by the present theory; here we have only considered the main band. Moreover, Careri *et al.* [18] have evidenced a fine structure present in the "anomalous" band, which may result from some kind of asymmetry arising of the nonplanarity of the amide group. Our model has ignored this fine detail. Moreover, we comment that the theory also accounts for the main (fine structure aside) Raman line in inelastic scattering of light experiments [19, 20]

We compare the NESOM-based theoretical result of Eq. (10) with the experimental data taken from [5]. It ought to be noticed that we do not have theoretical access to the initial conditions that fix $\mathcal{A}$ and v, but they can be derived from experimental data. Take the case $T = 80$ K, and then, on the basis that $\omega_0 - \omega_s = 16\ \text{cm}^{-1}$ and $\gamma_s - \gamma = 3.6\ \text{cm}^{-1}$, we obtain that $\mathcal{A}(|G|/2\alpha)^{\frac{1}{2}} = 2.3 \times 10^6 \text{cm}^{-1}$ and $v = 2.9 \times 10^4\ \text{cm}\cdot\text{s}^{-1}$. In figure 1 are indicated the experimental curves (dotted) and the theoretical ones (full line), for 20 K, 50 K, and 80 K, which show a very good agreement (The amplitudes of the bands are also fixed using the experimental results, that is, in that way it is avoided the calculation of ϕ of Eq. (8), of no relevance here, since the fundamental point to characterize is the shape and positioning of the bands). Hence, the theory described above demonstrates a very rapid decay of Davydov's soliton in situations very near to thermal equilibrium (the lifetime γ_s^{-1} is in the tens of picosecond scale). Consider now far-from-equilibrium conditions, namely, in the presence of a sufficiently intense source of strength I in Eq. (1), in, now, a pump-probe experiment. As a result of the pumping process, $I_q(\omega_q) \neq 0$ in Eq. (1), the populations $\nu_q(t)$ increase in time. Under the action of a constant-in-time pumping intensity, after a transient time (typically in the order of pico- to subpico-second range) has elapsed there follows a steady state. As indicated by Eq. (3) the lifetime of the solitary wave strongly depends on these populations.

We calculate the steady state populations by solving Eqs. (1), as done in [8], but using for the parameters involved numerical values of an order of magnitude as those characteristic of ACN. Similarly as in [8] (cf. Figs. 3 and 7 in [8]), after a threshold in the pumping intensity is achieved, the modes lowest in frequency largely increase their populations (and, then, also the energy stored) at the expenses of the others. These results are used in Eq. (3) to calculate the two characteristic reciprocal lifetimes $\bar{\Gamma}_0$ and $\bar{\Gamma}_1$ shown in Fig. 2 as a function of intensity, the one with index 1 corresponding to a mode low in frequency (one that largely increases its population), and the other corresponding to a mode higher in frequency. This reciprocal lifetimes are given in units of a characteristic time $\bar{\tau}$ (see [8]), which for ACN is roughly 0.4 picoseconds. It is evident that the modes lowest in frequency largely increase their lifetime with increasing intensity of the pumping source, while the others rapidly decay. Therefore, in the expression for the average field amplitude, Eq. (4), there survives for a long time the contribution from the modes low in frequency, which give rise to a near dissipationless Davydov-soliton-like excitation.

There remains the fundamental question of how to experimentally evidence this phenomenon. We can resort to measurements of IR-absorbance of the kind we have already considered, but now to be of the pump-probe type. With increasing intensity of the pumping source, and the consequent increase in the population of the polar modes, the bandwidth of the IR-absorbance spectrum corresponding to the solitary-wave excitation should — according to theory — be consistently reduced. This being verified the prediction would be corroborated, what may be a relevant result in bioenergetics because of the similarity of CO-stretching in ACN and in biopolymers [2–4]. A final point to consider is how to produce the nonthermal excitation of these polar modes: One possibility could be via the indirect process of free-carrier absorption of electromagnetic radiation. However, it may be noticed that this type of pumping process may be poorly efficient for providing appropriate levels of excitation, what is shown in the particular case of the photoinjected plasma in polar semiconductors [21]. Alternatively one may think of direct excitation of the polar modes via electromagnetic radiaton in the infrared region. However, for efficient results, we would need an intense source with a spectrum of frequencies covering the full extent of the width of the optical phonons dispersion relation. Apparently, nowadays the only possible way would be the use of synchroton radiaton in the IR, as, for example, in the apparatus at the Synchroton Light National Laboratory at Campinas, São Paulo, Brazil [22], where at the moment is available IR-radiation in the, say, 20 to 40 meV band, with intensities of the order of 10^{11} photons per second and milliradian.

In conclusion, we have analyzed some statistical thermodynamic aspects of polymers, with particular attention centered on acetanilide, showing that in such systems, which sustain polar vibrations of the CO-stretching type, can also be present excitations of the type of vibronic solitary waves (Davydov-like solitons). The IR-absorbance spectrum has been calculated and compared with the experimental results, following a good agreement. Also, the results confirm the very short lifetime of this excitation. However, as briefly discussed in the last part of this communication, under continuous external excitation, producing large nonthermal values of the populations of the vibrational modes, the soliton's lifetime largely increases. This implies that a coherent excitation composed by the low-lying-in-frequency excited modes, constitutes a *Davydov's solitary-like wave which travels undeformed and nearly undamped in a sufficiently highly excited steady-state background.*

REFERENCES

[1] A. J. Heger, S. Kivelson, J. R. Schrieffer, and W. P. Su, Rev. Mod. Phys. **60**, 781 (1988); T. Anderson and S. Roth, Braz. J. Phys. **24**, 746 (1994).

[2] A. S. Davydov, *Biology and Quantum Mechanics* (Pergamon, Oxford, 1982).

[3] A. S. Davydov, in *Solitons*, edited by S. E. Trullinger, V. E. Zakharov, and V. L. Prokovsky (Elsevier, New York, 1986), Chap. 1, pp. 1–51.

[4] A. C. Scott, Phys. Rep **217**, 1 (1992).

[5] G. Careri *et al.*, Phys. Rev. Lett. **51**, 304 (1983).

[6] W. Fann *et al.*, Phys. Rev. Lett. **64**, 607 (1990).

[7] S. W. Johnson *et al.*, Phys. Rev. Let. **74**, 2844 (1995).

[8] M. V. Mesquita, A. R. Vasconcellos, and R. Luzzi, Phys. Rev. E **48**, 4049 (1993).

[9] R. Luzzi and A. R. Vasconcellos, Fortschr. Phys./Prog. Phys. **38**, 887 (1990).

[10] D. N. Zubarev, *Nonequilibrium Statistical Thermodynamics* (Consultants Bureau, New York, 1974); D. N. Zubarev, V. N. Morozov, and G. Röpke, *Statistical Mechanics of Nonequilibrium Processes*, Vol. 1: *Basic principles, kinetic theory* (Akademie Verlag, Berlin, 1996).

[11] A. I. Akhiezer and S. V. Peletminskii, *Methods of Statistical Physics* (Pergamon, Oxford, 1981).

[12] L. Lauck, A. R. Vasconcellos, and R. Luzzi, Physica A **168**, 789 (1990).

[13] H. Haken, Laser Theory, in *Handbuch der Physik XXV/2C*, edited by S. Flügge (Springer, Berlin, 1970).

[14] K. Walyazek, D. N. Zubarev, and A. Z. Kuzemskii, Theor. Math. Phys. **5**, 2 (1971).

[15] V. E. Zakharov, in *Solitons*, edited by R. K. Bullough and P. J. Caudrey (Springer, Berlin, 1980), Chap. 7, pp. 243-285.

[16] V. P. Kalashnikov, Theor. Math. Phys. **9**, 1003 (1971); R. Luzzi and A. R. Vasconcellos, J. Stat. Phys, **23**, 539 (1980).

[17] A. C. Scott, E. Shyamsunder, E. Gratton, and G. Careri, Phys. Rev. B **32**, 5551 (1985).

[18] G. Careri, E. Gratton, and E. Shyamsunder, Phys. Rev. A **37**, 4048 (1988).

[19] J. L. Sauvajol *et al.*, J. Raman Spectrosc. **20**, 517 (1989).

[20] M. Sakai, N. Kuroda, and Y. Nishima, Phys. Rev. B **47**, 150 (1993).

[21] L. Lauck, A. R. Vasconcellos, and R. Luzzi, Phys. Rev. B **46**, 6150 (1992).

[22] Accelerator Physics and Instrumentation Groups of LNLS, Rev. Sci. Instrum. **63**, 1573 (1992).

FIGURE CAPTIONS

Figure 1: Infrared absorption spectra in acetanilide for three different values of temperature. Dotted curve is from the experimental data of reference [5], and the full curve the calculation in NESOM-based response function theory.

Figure 2: Reciprocal lifetime of the representative high frequency modes (index nought) and of the low frequency modes (index one) with increasing intensity of the source. Both $\bar{\Gamma}$ are in units of $\bar{\tau} \sim 0.4$ picoseconds, and the intensity S in adimensional units, but such that $1S$ corresponds to a pumping power of 1 μW per mode.

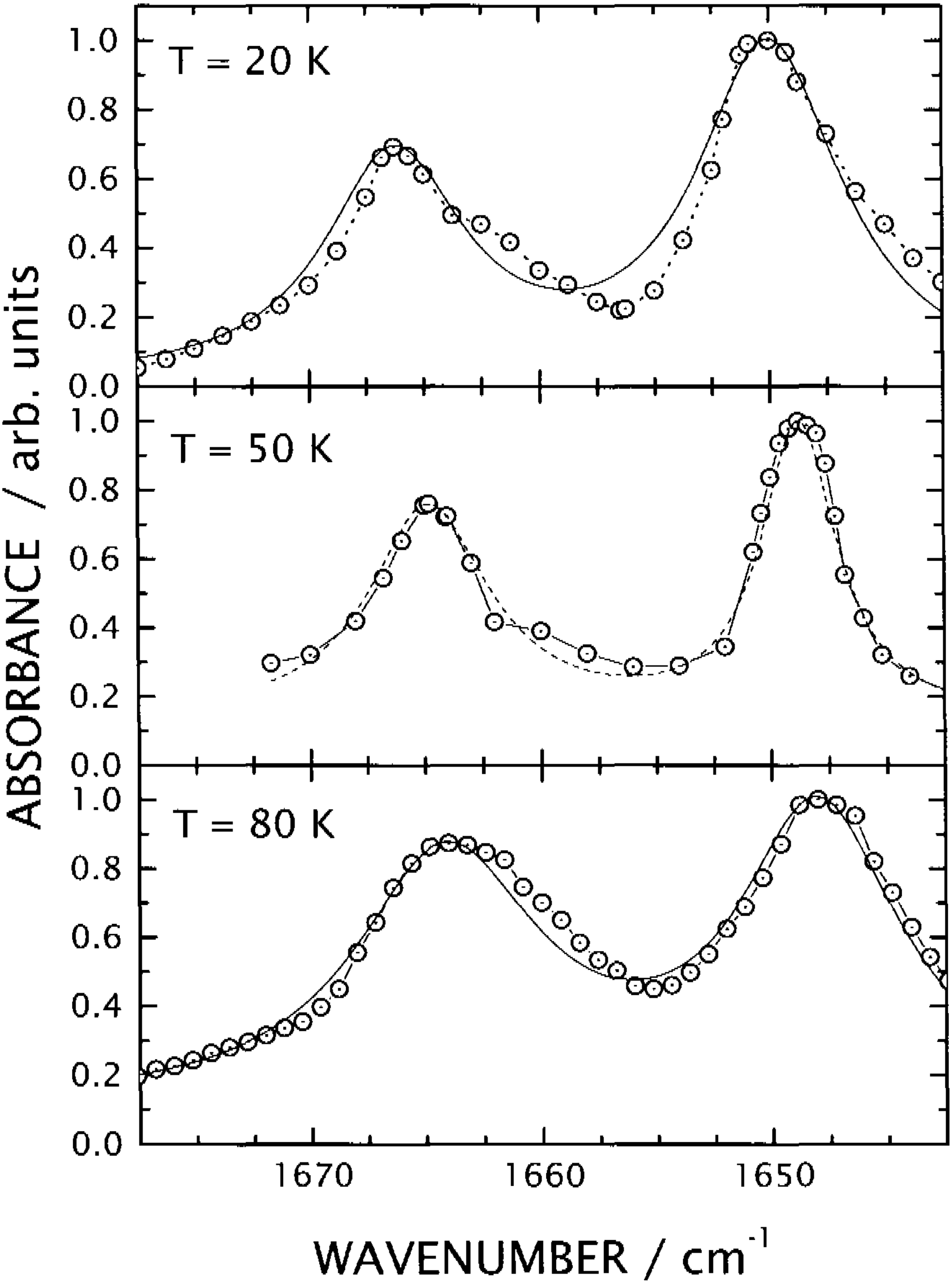

Figure 1: Infrared absorption spectra in acetanilide for three different values of temperature. Dotted curve is from the experimental data of reference 5, and the full curve the calculation in NESOM-based response function theory.

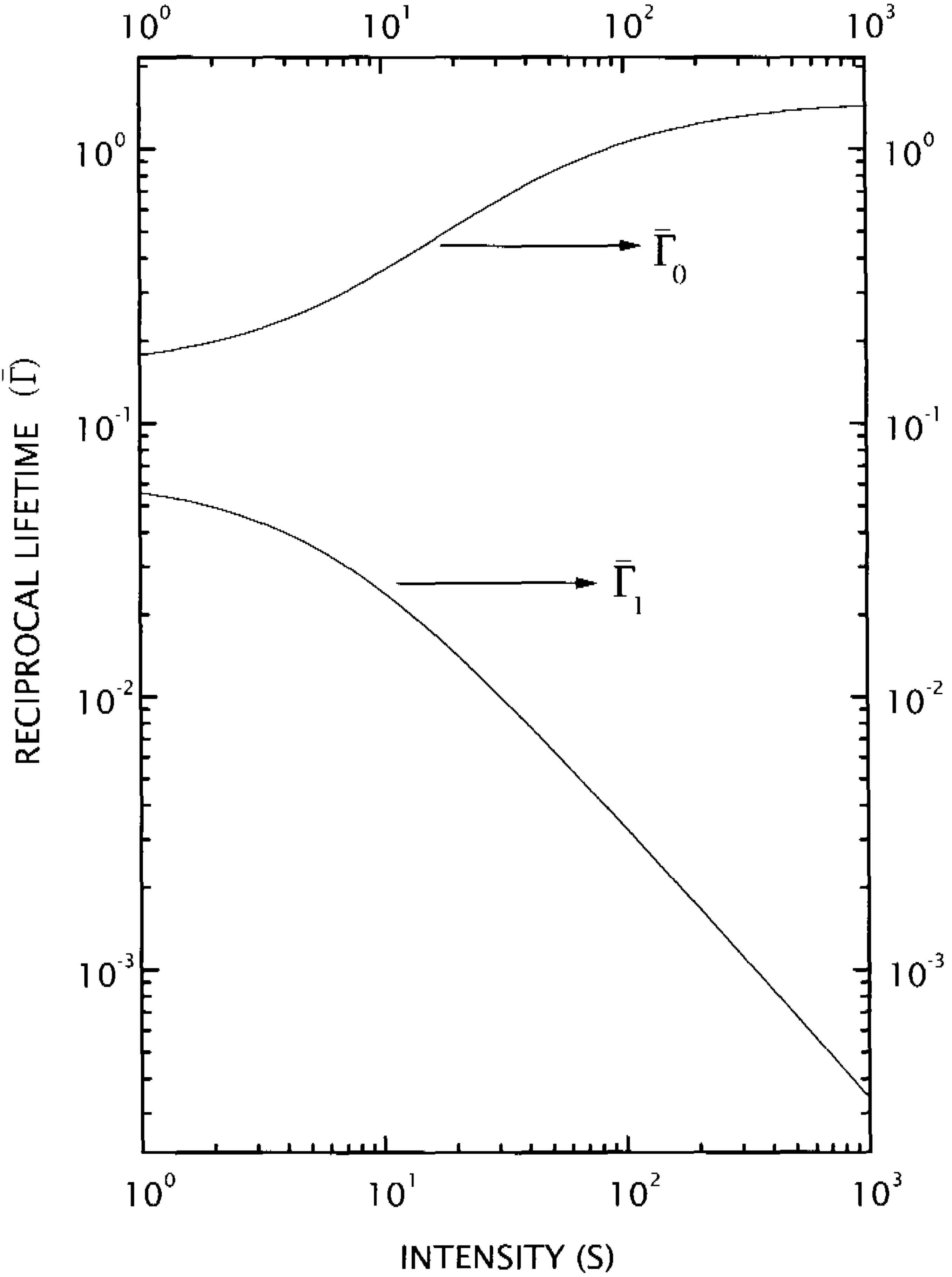

Figure 2: Reciprocal lifetime of the representative high frequency modes (index nought) and of the low frequency modes (index one) with increasing intensity of the source. Both $\bar{\Gamma}$ are in units of $\bar{\tau} \sim 0.4$ picoseconds, and the intensity S in adimensional units, but such that $1S$ corresponds to a pumping power of 1 μW per mode.

3.3 Processos irreversíveis no contexto do formalismo de ensemble estatístico de não-equilíbrio

Consideramos a questão do estudo de processos irreversíveis baseados num formalismo de ensemble de não-equilíbrio, que provê fundamentos para a assim chamada Termodinâmica Estatística Informacional. Seu funcionamento é ilustrado em uma aplicação ao estudo de processos de relaxação em um sistema de muitos bosons em interação com um banho térmico. É mostrado que a equação cinética de evolução da média da amplitude de campo bosônico é do tipo de uma equação de Schrödinger não-linear com amortecimento. A solução mostra a presença de comportamento complexo no sistema, consistindo em que o conjunto de excitações possíveis contem uma associada com uma onda solitária, o assim chamado sóliton de Davydov com amortecimento. Sistemas de matéria condensada e sistemas biofísicos são candidatos a apresentar esse tipo de comportamento. Uma comparação particular com experimento é apresentada para o caso de polímeros orgânicos.

Physica Scripta, **59** (4): 257-65 (1999).

Irreversible Processes in the Context of a Nonequilibrium Statistical Ensemble Formalism

Marcus V. Mesquita,* Áurea R. Vasconcellos, Roberto Luzzi

Instituto de Física 'Gleb Wataghin',
Universidade Estadual de Campinas, Unicamp
13083-970 Campinas, São Paulo, Brazil

We consider the question of the study of irreversible processes on the basis of a non-equilibrium ensemble formalism, which provides foundations to the so-called Informational Statistical Thermodynamics. Its functioning is illustrated in an application to the study of relaxation processes in a many-boson system in interaction with a thermal bath. It is shown that the kinetic equation for the evolution of the average boson-field amplitude is of the type of a nonlinear Schrödinger equation with damping. The solution shows the presence of complex behavior in the system, consisting in that the set of possible excitations contains one associated to a solitary-wave, the so-called Davydov's soliton with damping. Solid state and biophysical systems are candidates to present this type of behavior. A particular comparison with experiment is presented for the case of organic molecular polymers.

PACS: 05.70.Ln/82.20.Db/82.20Mj

---

*E-mail: sousa@ifi.unicamp.br
Group Home Page: http://www.ifi.unicamp.br/~aurea

1. Introduction

As well known, and universally accepted, dissipation and irreversibility are intrinsic characteristics of dynamical systems in Nature. These characteristics are quite difficult concepts to apprehend and the object of extended and lively discussions. Moreover, we recall that this question belongs to the realm of the science of Thermodynamics, in particular to the second law.

Thermodynamics has a well-deserved reputation of efficiency and elegance from its ability to make predictions, concerning macroscopic properties, on a surprisingly large variety of natural systems, with independence of the microscopic structure and the details of the processes developing in the medium. Thermodynamics of equilibrium systems is a quite well established and tremendously successful area, but the same cannot be said in the case of nonequilibrium systems, namely the area covered by the so-called *Irreversible Thermodynamics.* The latter, let us recall, is a field theory at a macroscopic and phenomenological level, dealing with states and processes in systems lying beyond equilibrium (either by a large amount or close to equilibrium, corresponding to the nonlinear and linear, respectively, divisions of it). Hence, Nonequilibrium Thermodynamics deals basically with transport phenomena involving space and time variations of macroscopic observables and their fluxes in continuum media, as well as with —in particular— the important case of steady states. In all circumstances of nonequilibrium conditions, let them be time evolving or stationary, are present dissipative processes developing in the media. Steady states in the nonlinear kinetic-thermodynamic level are of enormous relevance because of the possible emergence of complex behavior in the form of Prigogine's dissipative structures and chaos, leading to what can be dubbed as *Thermodynamics of complex systems* [1-6].

In nonequilibrium situations, in contrast with equilibrium thermodynamics which constitutes an undisputed universal discipline, the thermodynamics of irreversible processes has as yet not achieved a phenomenological formulation and a methodology which can be considered satisfactory. There exist several approaches to nonequilibrium thermodynamics: a well established one is the Classical (sometimes referred to as Linear or Onsagerian) Thermodynamics, based on the local equilibrium hypothesis, which is restricted to the limiting situations involving smooth in space and time variations (very long wavelengths and very low frequencies), and weak fluxes [7]. Outside this regime, as noted, there is not at present what may be considered as a completely satisfactory approach. On the other hand, the connection of macroscopic thermodynamics with microscopic mechanics is, as known, provided by Statistical Mechanics. Statistical Mechanics of equilibrium systems is an extremely successful theory and provides the look-after microscopic foundations to thermostatics (i. e. thermodynamics of equilibrium systems). In nonequilibrium conditions but in the strictly linear regime near equilibrium also provides the basis for Classical Irreversible Thermodynamics and response function theory [8]. Evidently it is tempting to consider that nonlinear nonequilibrium thermodynamics may have foundations on a Statistical Mechanics for arbitrarily far-from-equilibrium systems. This implies in answering the question: Is there an ensemble algorithm which is appropriate for nonequilibrium problems? An affirmative answer exists and consists in the so-called Nonequilibrium Statistical Operator Method (NESOM for short from now on). It appears to be, by far, the most appealing, practical, concise, and first principles based theory. NESOM is a far-reaching generalization of statistical methods founded on the seminal great ideas set forward by Boltzmann and Gibbs [9]. The different approaches to NESOM are based on either heuristic approaches [10–14], or projection-operator techniques [15–18]. It can be shown [19-21] that all approaches can be put under a unifying theory based on the principle of maximization of informational entropy [22, 23], (MaxEnt for short) that is, a unique variational principle. This leads to a theory which may be considered to be contained within the scope of Jayne's Predictive Statistical Mechanics [24]. This unifying approach to NESOM shall be referred to as MaxEnt-NESOM in what follows (For its application in equilibrium and near equilibrium conditions see references [25, 26], and for arbitrary nonequilibrium conditions see reference [27]).

Therefore, the above mentioned tempting consideration to put irreversible thermodynamics under the aegis of nonequilibrium statistical mechanics, appears to be possible on the basis of MaxEnt-NESOM. This is the so-called Informational Statistical Thermodynamics (IST for short; sometimes also called Information-theoretic Thermodynamics). IST may be considered to have been pioneered by Hobson [28, 29] after the publication of Jaynes seminal papers on the foundation of statistical mechanics on information theory [30, 31]. A brief review and partial historical notes are given in [32-35]. Sieniutycz and Salamon [36] also briefly review several variational approaches, and so do Nettleton and Sobolev [37].

In this paper we attempt to illustrate the use of IST resorting to the treatment of a particular dissipative problem, however of —in principle— quite large scope for being connected with a number of real situations in the physics of condensed matter.

Moreover, nonlinear interactions are present, what brings the problem within domain of *nonlinear nonequilibrium thermodynamics*, and, as known, complex behavior may arise in such systems. It is shown how nonlinear relaxation processes are present in the kinetic equations of evolution, one attaining the form of a nonlinear Schrödinger-like equation with damping, giving rise to coherent states of excitations of the solitary wave type. Solitons were first observed over a century and a half ago, namely in 1838 by the Scottish civil engineer John Scott Russell and the finding published in the Reports of the Meetings of the British Association for the Advancement of Science in 1844. This excitation, as known, presents a puzzling property of cohesiveness, namely, a propagation with a near unaltered shape, which is also recovered in the collision of two solitons after travelling through each other. They may have large relevance in bioenergetics [38], and in other areas, as, for example, the technically and economically relevant ones of transmission in optical fibers [39] and in conducting polymers (see for example reference [40]).

2. Nonlinear Schrödinger-like Equation with Damping

Let us consider a system of bosons (for example lattice vibrations, excitons, etc. in a solid state sample) in interaction with a thermal bath. We write for the system Hamiltonian

$$H = H_0 + H_I \, , \tag{1}$$

where

$$H_0 = \sum_{q} E_q (a_q^\dagger a_q + \frac{1}{2}) \, , \tag{2}$$

is the Hamiltonian of the free bosons with energy dispersion relation E_q, and where, as usual, a_q ($a_q^\dagger$) are annihilation (creation) operators in state $|\boldsymbol{q}\rangle$, and

$$H_I = \sum_{q_1,q_2} \left[\varphi_{q_1 q_2} a_{q_1}^\dagger a_{q_2} + \varphi_{q_1 q_2}^\dagger a_{q_2} a_{q_1}^\dagger \right] \, , \tag{3}$$

is the energy operator corresponding to the interaction with the thermal bath, where φ are operators acting on the thermal bath space of states (the interaction coupling strength is incorporated in φ).

According to IST, based on the MaxEnt-NESOM, the first and fundamental step for introducing the statistical method is to define the basic set of variables to be used for the description of the system. In the present case it is natural to take the populations of the modes, and the amplitudes of motion of the field of bosons, namely, the dynamical quantities

$$\{ \hat{\nu}_q = a_q^\dagger a_q \, ; \, a_q \, ; \, a_q^\dagger \} \, . \tag{4}$$

Consequently, according to the MaxEnt-NESOM [13, 20, 21, 27] the associated auxiliary coarse-grained statistical operator is given by the instantaneous-in-time Gibbsianlike distribution

$$\bar{\varrho}(t,0) = \frac{\exp\left\{-\sum_{q}\left[F_q(t)a_q^{\dagger}a_q + f_q(t)a_q + f_q^{*}(t)\,a_q^{\dagger}\right]\right\}}{\operatorname{Tr}\exp\left\{-\sum_{q}\left[F_q(t)a_q^{\dagger}a_q + f_q(t)a_q + f_q^{*}(t)\,a_q^{\dagger}\right]\right\}}\,, \tag{5}$$

where F_q, f_q, and f_q^{*} are the corresponding Lagrange multipliers that the variational method introduces. It is quite important to stress that the statistical operator of Eq. (5) *is not* the one which characterizes the macroscopic state of the system but an auxiliary coarse-grained one giving the instantaneous average values of the observables of the system, but does not account for dissipation. The fine grained statistical operator is a functional of the one of Eq. (5), taking, in Zubarev's approach to NESOM [13, 27], the form

$$\varrho_{\varepsilon}(t) = \bar{\varrho}(t,0) + \varrho_{\varepsilon}'(t) = \exp\left\{\ln\bar{\varrho}(t,0) - \int_{\infty}^{t} dt'\, e^{\varepsilon(t' \;\; t)}\frac{d}{dt'}\ln\bar{\varrho}(t',t'-t)\right\}\,, \tag{6}$$

where in $\bar{\varrho}(t',t'-t)$ the first time in the argument is related to the thermodynamic evolution of the system (the time evolution of the Lagrange parameters), while the second is related to the evolution of the mechanical quantities in Heisenberg representation (for details see, for example, Ref. [20], and in Ref. [21] the method is reviewed in a classical-mechanical approach); parameter ε is an infinitesimal that goes to zero after the trace operation in the calculation of averages has been performed, and its presence is responsible for the introduction of irreversible behavior in the macroscopic evolution of the system. As indicated by Eq. (6), the nonequilibrium statistical operator $\varrho_{\varepsilon}(t)$ is composed of two parts: one is the coarse-grained part $\bar{\varrho}(t,0)$ which, as already noticed, does not account for dissipation, while $\varrho'_\varepsilon(t)$ is responsible for describing the irreversible evolution of the system and introducing the description of the dissipative phenomena that keep developing in the media.

We introduce the IST-thermodynamic variables

$$\left\{\nu_{\boldsymbol{q}}(t);\ \langle a_{\boldsymbol{q}} \mid t\rangle;\ \langle a^{\dagger}_{\boldsymbol{q}} \mid t\rangle\right\} \tag{7}$$

which are the averages of the dynamical variables of Eq. (4) over the nonequilibrium ensemble. We recall that the associated Lagrange multipliers are [Cf. Eq. (5)]

$$\left\{F_{\boldsymbol{q}}(t);\ f_{\boldsymbol{q}}(t);\ f^{*}_{\boldsymbol{q}}(t)\right\} . \tag{8}$$

The system initially in thermal equilibrium with the thermal bath at, say, the mutual equilibrium temperature T, is assumed to receive a localized in space excitation of a very short-in-time duration. The system is then driven out of equilibrium and we look for the evolution of such state towards a final asymptotic return to equilibrium with the thermal bath. That is, we need to derive the equations of evolution for the thermodynamic variables of Eq. (7). This is done resorting to the generalized nonlinear quantum transport theory that can be built within the scope of MaxEnt-NESOM. It is worth noticing that this theory is a far-reaching generalization of Boltzmann and Mori approaches [20, 21, 27, 41]. Assuming the coupling of system and bath to be weak, we can resort to the so-called second order approximation in relaxation theory [41], sometimes referred to as the quasi-linear approximation in relaxation theory, a name we avoid because of the misleading term linear, which refers to the approximation in the order of the relaxation processes in terms of the informational-entropy production [21,41], but the equations are highly nonlinear in the basic variables; this is the Markovian approximation in the MaxEnt-NESOM-based kinetic theory.

2.1. The equation of evolution for the amplitudes

For simplicity we admit a weak perturbation (that is small amplitudes $\langle a_q \mid t \rangle$) and then we can omit the equation for the populations $\nu_q(t)$: we take in lowest approximation their values in equilibrium, since the deviations from equilibrium are shown to be proportional to the square and cubic powers in the amplitudes. The equations of evolution for the amplitudes in the Markovian approximation are

$$\frac{d}{dt}\langle a_q \mid t \rangle = J^{(0)}(q,t) + J^{(1)}(q,t) + J^{(2)}(q,t) \; . \tag{9}$$

where on the right of this Eq. (9) the first term is

$$J^{(0)}(q,t) = E_q \langle a_q \mid t \rangle, \tag{10}$$

the second term is

$$J^{(1)}(q,t) = (\mathrm{i}\hbar)^{-1} \langle [H_I, a_q] \mid t \rangle = 0 \; , \tag{11}$$

and we have written

$$\langle \ldots \mid t \rangle = \mathrm{Tr}\,\{\ldots \bar{\varrho}(t,0)\} \ , \tag{12}$$

meaning average value over the coarse-grained ensemble characterized by $\bar{\varrho}(t,0)$ of Eq. (5). The contribution of Eq. (11) is null on the basis that

$$[H_I, a_{\mathbf{q}}] = -\sum_{\mathbf{q}_1} (\varphi_{\mathbf{q}\mathbf{q}_1} + \varphi^{\dagger}_{\mathbf{q}_1\mathbf{q}}) a_{\mathbf{q}_1} \ , \tag{13}$$

and we take as null the average values of the operators φ associated to the bath system (in other words, the bath is assumed to constantly remain in equilibrium at temperature T, meaning that it is taken as an ideal reservoir). Hence, Eq. (9) can be rewritten, once Eq. (10) is taken into account and the collision operator $J^{(2)}(\mathbf{q},t)$ is explicitly written, as

$$\frac{d}{dt}\langle a_{\mathbf{q}} \mid t \rangle = (\mathrm{i}\hbar)^{-1} E_{\mathbf{q}} \langle a_{\mathbf{q}} \mid t \rangle + (\mathrm{i}\hbar)^{-2} \int_{-\infty}^{0} dt' \mathrm{e}^{\varepsilon t'} \langle [H_I(t')_0, [H_I, a_{\mathbf{q}}]] \mid t \rangle \ , \tag{14}$$

where we recall that according to the method [41] the time dependence of the dynamical operators is given in the interaction representation (i.e. dynamical evolution in terms of H_0 alone). In this Eq. (14) the last term on the right, or collision operator, involving two operations of commutation, is of second order in the interaction strengths present in H_I and, as already noticed, Markovian (memoryless) in character [41]. Once the indicated operations are performed it follows that this contribution is the equivalent of the Golden Rule of Quantum Mechanics averaged over the nonequilibrium ensemble. Moreover

$$H_I(t')_0 = \sum_{q_1 q_2} \left\{ \varphi_{q_1 q_2}(t') a^\dagger_{q_1} a_{q_2} e^{i(\omega_{q_1} - \omega_{q_2})t'} + \varphi^\dagger_{q_1 q_2}(t') a^\dagger_{q_2} a_{q_1} e^{\ i(\omega_{q_1} - \omega_{q_2})t'} \right\} , \tag{15}$$

where we used that

$$e^{\ \frac{1}{i\hbar} t H_0} a_q \, e^{\frac{1}{i\hbar} t H_0} = e^{-i\omega_q t} a_q \tag{16a}$$

$$e^{-\frac{1}{i\hbar} t H_0} a^\dagger_q \, e^{\frac{1}{i\hbar} t H_0} = e^{i\omega_q t} a^\dagger_q \tag{16b}$$

and we wrote $\hbar\omega_q = E_q$.

After some algebra and calculus together with simple algebraic manipulations briefly described in Appendix A, we obtain the equation of evolution for the boson amplitudes

$$i\hbar \frac{d}{dt} \langle a_q \mid t \rangle = E_q \langle a_q \mid t \rangle + i \sum_{q_1, q_2} T^{(1)}_{q, q_1, q_2} \langle a_{q_1} \mid t \rangle + i \sum_{q_1, q_2, q_3} T^{(2)}_{q, q_1, q_2, q_3} \langle a^\dagger_{q_1} a_{q_2} a_{q_3} \mid t \rangle , \tag{17}$$

where coefficients $T^{(1)}_{q,q_1,q_2}$ and $T^{(2)}_{q,q_1,q_2,q_3}$ are defined in Eqs. (A.5)

2.2. Calculation of averages

To evaluate the average values involved on the right of Eq. (17), which are given in terms of the auxiliary coarse-grained operator of Eq. (5), we note that the latter can be diagonalized resorting to a Glauber-like transformation appropriate to deal with coherent states, namely,

$$a_q = b_q + \lambda_q \; ; \qquad a_q^\dagger = b_q^\dagger + \lambda_q^* \; , \tag{18}$$

where λ_q is a c-number. In the new representation the coarse-grained statistical operator takes the form

$$\begin{aligned} \bar{\varrho}(t,0) = \exp\Big\{ - \phi - \sum_q \Big[& F_q(t) b_q^\dagger b_q + (F_q(t)\lambda_q^* + f_q(t)) b_q + \\ & + (F_q(t)\lambda_q + f_q^*(t)) b_q^\dagger + F_q(t)\lambda_q\lambda_q^* + f_q(t)\lambda_q + f_q^*(t)\lambda_q^* \Big] \Big\} \end{aligned} \tag{19}$$

where

$$\begin{aligned} \phi = \ln \mathrm{Tr} \exp\Big\{ - \sum_q \Big[& F_q(t) b_q^\dagger b_q + (F_q(t)\lambda_q^* + f_q(t)) b_q + \\ & + (F_q(t)\lambda_q + f_q^*(t)) b_q^\dagger + F_q(t)\; \lambda_q\lambda_q^* + f_q(t)\lambda_q + f_q^*(t)\lambda_q^* \Big] \Big\} \end{aligned} \tag{20}$$

ensures its normalization. The diagonalization of the exponential follows for the choice

$$\lambda_q = -f_q^*(t)/F_q(t) \; , \qquad \lambda_q^* = -f_q(t)/F_q(t) \; , \tag{21}$$

to finally obtain

$$\bar{\varrho}(t,0) = \exp\Big\{ - \sum_q F_q(t) b_q^\dagger b_q \Big\} / \; \mathrm{Tr} \exp\Big\{ - \sum_q F_q(t) b_q^\dagger b_q \Big\} \; . \tag{22}$$

Using Eq. (22) it follows that

$$\langle a_{\boldsymbol{q}} \mid t \rangle = \mathrm{Tr}\left\{ a_{\boldsymbol{q}} \bar{\varrho}(t,0) \right\} = \mathrm{Tr}\left\{ (b_{\boldsymbol{q}} + \lambda_{\boldsymbol{q}})\, \bar{\varrho}(t,0) \right\} = \mathrm{Tr}\left\{ b_{\boldsymbol{q}} \bar{\varrho}(t,0) \right\} + \lambda_{\boldsymbol{q}}\, \mathrm{Tr}\left\{ \bar{\varrho}(t,0) \right\} = \lambda_{\boldsymbol{q}} \tag{23a}$$

and, evidently,

$$\langle a^{\dagger}_{\boldsymbol{q}} \mid t \rangle = \lambda^{*}_{\boldsymbol{q}}\ . \tag{23b}$$

Moreover,

$$\begin{aligned} \langle a^{\dagger}_{\boldsymbol{q}_1} a_{\boldsymbol{q}_2} \mid t \rangle &= \mathrm{Tr}\left\{ a^{\dagger}_{\boldsymbol{q}_1} a_{\boldsymbol{q}_2} \bar{\varrho}(t,0) \right\} = \mathrm{Tr}\left\{ (b^{\dagger}_{\boldsymbol{q}_1} + \lambda^{*}_{\boldsymbol{q}_1})(b_{\boldsymbol{q}_2} + \lambda_{\boldsymbol{q}_2}) \bar{\varrho}(t,0) \right\} = \\ &= \mathrm{Tr}\left\{ b^{\dagger}_{\boldsymbol{q}_1} b_{\boldsymbol{q}_2} \bar{\varrho}(t,0) \right\} + \lambda_{\boldsymbol{q}_2}\, \mathrm{Tr}\left\{ b^{\dagger}_{\boldsymbol{q}_1} \bar{\varrho}(t,0) \right\} + \\ &+ \lambda^{*}_{\boldsymbol{q}_1}\, \mathrm{Tr}\left\{ b_{\boldsymbol{q}_2} \bar{\varrho}(t,0) \right\} + \lambda^{*}_{\boldsymbol{q}_1} \lambda_{\boldsymbol{q}_2}\, \mathrm{Tr}\left\{ \bar{\varrho}(t,0) \right\} \\ &= \left(e^{F_{\boldsymbol{q}_1}} - 1 \right)^{-1} \delta_{\boldsymbol{q}_1,\boldsymbol{q}_2} + \langle a^{\dagger}_{\boldsymbol{q}_1} \mid t \rangle \langle a_{\boldsymbol{q}_2} \mid t \rangle \end{aligned} \tag{24}$$

implying for $\boldsymbol{q}_1 = \boldsymbol{q}_2 = \boldsymbol{q}$ that

$$\langle a^{\dagger}_{\boldsymbol{q}} a_{\boldsymbol{q}} \mid t \rangle = \nu_{\boldsymbol{q}}(t) = \left(e^{F_{\boldsymbol{q}}(t)} - 1 \right)^{-1} + |\langle a_{\boldsymbol{q}} \mid t \rangle|^{2}, \tag{25}$$

but recalling that we are neglecting corrections out of equilibrium in the populations, then

$$F_{\boldsymbol{q}} = \left(\hbar\omega_{\boldsymbol{q}} - \mu \right) / k_B T, \tag{26}$$

and the first term in the right of Eq. (25)is the equilibrium Bose-Einstein distribution. An alternative form of Eq. (24), of practical convenience in calculations is

$$\langle a^{\dagger}_{q_1} a_{q_2} \mid t\rangle = \langle a^{\dagger}_{q_1} \mid t\rangle\langle a_{q_2} \mid t\rangle + (\nu_{q_1}(t) - |\langle a_{q_1} \mid t\rangle|^2)\delta_{q_1 q_2} \,. \tag{27}$$

Proceeding in a similar way we find that

$$\langle a^{\dagger}_{q_1} a_{q_2} a_{q_3} \mid t\rangle = (\nu_{q_1}(t) - |\langle a_{q_1} \mid t\rangle|^2)(\langle a_{q_2} \mid t\rangle\delta_{q_1,q_3} + \langle a_{q_3} \mid t\rangle\delta_{q_1,q_2}) \tag{28}$$

$$+ \langle a^{\dagger}_{q_1} \mid t\rangle\langle a_{q_2} \mid t\rangle\langle a_{q_3} \mid t\rangle \tag{29}$$

2.3. Nonlinear Damped Schrödinger-like equation

Using the results of the previous subsection Eq. (17) becomes

$$i\hbar\frac{d}{dt}\langle a_q \mid t\rangle = E_q\langle a_q \mid t\rangle + i\sum_{q_1}\Gamma_{qq_1}(t)\,\langle a_{q_1} \mid t\rangle + \tag{30}$$

$$+ i\sum_{q_1,q_2,q_3} T^{(2)}_{q,q_1,q_2,q_3}\langle a^{\dagger}_{q_1} \mid t\rangle\langle a_{q_2} \mid t\rangle\langle a_{q_3} \mid t\rangle, \tag{31}$$

where

$$\Gamma_{qq_1}(t) = \sum_{q_2}\left\{T^{(1)}_{q,q_1,q_2} + (T^{(2)}_{q,q_2,q_1,q_2} + T^{(2)}_{q,q_2,q_2,q_1})(\langle \nu_{q_2} \mid t\rangle - |\langle a_{q_2} \mid t\rangle|^2)\right\} \,. \tag{32}$$

Transforming to the direct space, introducing the boson field operator averaged over the nonequilibrium ensemble given by

$$\psi(\boldsymbol{r},t) = \sum_{q} \chi_q(\boldsymbol{r})\langle a_q \mid t\rangle \ , \tag{33}$$

where χ_q are the eigenfunctions of the free system of bosons corresponding to eigenvalues E_q, satisfying the unperturbed wave equation

$$\left\{-\frac{\hbar^2}{2m}\nabla^2 + V(\boldsymbol{r})\right\}\chi_q(\boldsymbol{r}) = E_q\chi_q(\boldsymbol{r}) \ , \tag{34}$$

where $V(\boldsymbol{r})$ is the potential energy, and the first contribution on the left is evidently the kinetic energy. Using Eqs. (31) to (34) we obtain the equation of evolution for the average field amplitude, namely

$$\mathrm{i}\hbar\frac{\partial\psi(\boldsymbol{r},t)}{\partial t} = \left\{-\frac{\hbar^2}{2m}\nabla^2 + V(\boldsymbol{r},t)\right\}\psi(\boldsymbol{r},t) + \mathrm{i}\int\Gamma(\boldsymbol{r},\boldsymbol{r}_1,t)\psi(\boldsymbol{r}_1,t)d\boldsymbol{r}_1 \tag{35}$$

$$+\int\Phi(\boldsymbol{r},\boldsymbol{r}_1,\boldsymbol{r}_2,\boldsymbol{r}_3)\psi^*(\boldsymbol{r}_1,t)\psi(\boldsymbol{r}_2,t)\psi(\boldsymbol{r}_3,t)d\boldsymbol{r}_1d\boldsymbol{r}_2d\boldsymbol{r}_3 \ , \tag{36}$$

where

$$\Gamma(\boldsymbol{r},\boldsymbol{r}_1,t) = \sum_{q,q_1}\Gamma_{qq_1}\chi_q(\boldsymbol{r})\chi^*_{q_1}(\boldsymbol{r}_1), \tag{37}$$

$$\Phi(\boldsymbol{r},\boldsymbol{r}_1,\boldsymbol{r}_2,\boldsymbol{r}_3) = \mathrm{i}\sum_{q_1,q_2,q_3} T^{(2)}_{q,q_1,q_2,q_3}\chi_q(\boldsymbol{r})\chi_{q_1}(\boldsymbol{r}_1)\chi^*_{q_2}(\boldsymbol{r}_2)\chi_{q_3}(\boldsymbol{r}_3) \ . \tag{38}$$

Equation (36) has the form of a Schrödinger equation with damping and nonlinear contributions containing space correlations (time correlations, that is memory, are not present because the approximation used — second order approximation in relaxation theory — which renders the equations of evolution Markovian in character [41].

To proceed further, and to make contact with real situations, let us introduce another approximation consisting into neglecting space correlations, what is achieved writing

$$\Gamma(\boldsymbol{r},\boldsymbol{r}_1,t) = \hbar\gamma\delta(\boldsymbol{r}-\boldsymbol{r}_1), \tag{39a}$$

$$\Phi(\boldsymbol{r},\boldsymbol{r}_1,\boldsymbol{r}_2,\boldsymbol{r}_3) = \hbar G\delta(\boldsymbol{r}-\boldsymbol{r}_1)\delta(\boldsymbol{r}-\boldsymbol{r}_2)\delta(\boldsymbol{r}-\boldsymbol{r}_3), \tag{39b}$$

As a consequence, the nonlinear Schrödinger-like equation with dissipation for the system of bosons in interaction with the reservoir takes the local-in-space and instantaneous-in-time form

$$\mathrm{i}\hbar\frac{\partial\psi(\boldsymbol{r},t)}{\partial t} = \left\{-\frac{\hbar^2}{2m}\nabla^2 + V(\boldsymbol{r}) + \mathrm{i}\hbar\gamma + \hbar G\,|\psi(\boldsymbol{r},t)|^2\right\}\psi(\boldsymbol{r},t). \tag{40}$$

2.4. An example and numerical results

We use the results just derived to analyze the case of a system of excitons in semiconductors in interaction with the thermal bath provided by the lattice vibrations (phonons). The Hamiltonian of the system is of the form [42]:

$$H = \sum_{\boldsymbol{k}} E_{\boldsymbol{k}} a^\dagger_{\boldsymbol{k}} a_{\boldsymbol{k}} + \sum_{\boldsymbol{q}} \hbar\Omega_{\boldsymbol{q}}\, b^\dagger_{\boldsymbol{q}} b_{\boldsymbol{q}} + \sum_{\boldsymbol{k}_1,\boldsymbol{k}_2} \left(M_{\boldsymbol{k}_1\boldsymbol{k}_2} a^\dagger_{\boldsymbol{k}_1} a_{\boldsymbol{k}_2} b_{\boldsymbol{k}_1-\boldsymbol{k}_2} + H.c.\right), \tag{41}$$

where $\hbar\Omega_{\boldsymbol{q}}$ is the phonon dispersion relation; $E_{\boldsymbol{k}} = E_0 - \hbar^2k^2/(2m_x)$ is the exciton energy in state $|\boldsymbol{k}\rangle, E_0$ is the value of energy at the bottom of the parabolic band, and m_x is the excitonic mass; $a(a^\dagger)$, $b(b^\dagger)$ are annihilation (creation) operators for excitons and phonons respectively (boson-like particles in both cases); M is the matrix element of the interaction potential between excitons and phonons, and therefore, comparing with Eq. (3) we have in this case that the operator φ is given by

$$\varphi_{\boldsymbol{k},\boldsymbol{k}_1} = M_{\boldsymbol{k}_1\boldsymbol{k}_2} b_{\boldsymbol{k}_1-\boldsymbol{k}_2}. \tag{42}$$

Therefore, in the conditions that led to Eq. (36), we have for the average field amplitude of the exciton system that

$$i\hbar\frac{\partial\psi(\boldsymbol{r},t)}{\partial t} - \hbar\left\{\omega_0 - i\gamma\right\}\psi(\boldsymbol{r},t) + \frac{\hbar^2}{2m_x}\nabla^2\psi(\boldsymbol{r},t) + \hbar G\left|\psi(\boldsymbol{r},t)\right|^2\psi(\boldsymbol{r},t) = 0, \tag{43}$$

where

$$\hbar\omega_0 = E_0 - \Delta E, \tag{44}$$

with ΔE being the renormalization of the exciton energy due to the interaction with the phonon field, and which follows from the terms involving the principal part in the integrations in Eqs. (A.5) in Appendix A. Moreover, we have taken plane-waves for the exciton states $\chi_{\boldsymbol{k}}(\boldsymbol{r})$, with the given parabolic dispersion relation $E_{\boldsymbol{k}}$.

Consider a sample of GaAs at room temperature which, then, contains a density of excitons of the order of 7×10^8 cm^{-3}. Let us admit, just for illustrative purposes, that a weak excitation is introduced in a small region at the sample surface, for example illumination using an ultrafast pulse of laser light, having a radial spatial distribution with a Gaussian profile, which, for practical computational reasons, is (to a good degree) approximated by a hyperbolic secant profile with a given amplitude $\mathcal{A}$ and velocity of propagation v. This localized near point-like excitation, because of isotropy, propagates radially. Then, introducing polar coordinates for the resolution of Eq. (43), separating the radial and angular parts and ignoring the latter because of isotropy, we look for the equation for the radial part. Recalling that the Laplacian in polar coordinates is of the form $\partial^2/\partial r^2 + r^{-1}\partial/\partial r$, we make the *Ansatz* that the second contribution can be neglected in comparison with the first. Hence, we need to tackle the one-dimensional equation

$$i\hbar\frac{\partial\psi(r,t)}{\partial t} - \hbar\left\{\omega_0 - i\gamma\right\}\psi(r,t) + \frac{\hbar^2}{2m_x}\frac{\partial^2}{\partial r^2}\psi(r,t) + \hbar G\left|\psi(r,t)\right|^2\psi(r,t) = 0 \quad (45)$$

For the indicated initial and boundary conditions, resorting to the inverse scattering method [43–45] we find that

$$\psi(r,t) = \mathcal{A}\exp\left\{i\left[\frac{m_x v}{\hbar}r - (\omega_s - i\gamma)\,t - \frac{\theta}{2}\right]\right\}\operatorname{sech}\left[\mathcal{A}\left(\frac{m_x\,|G|}{\hbar}\right)^{1/2}(r - vt)\right] \quad (46)$$

where we wrote $G = |G|e^{i\theta}$ (imaginary number in polar planar coordinates); $\mathcal{A}$ and v, as noticed, are fixed by the imposed initial conditions; and

$$\omega_s = \omega_0 + (2\hbar)^{-1}\left[m_x v^2 - |\hbar G|\,\mathcal{A}\right]. \quad (47)$$

The energy propagating with the excitation is proportional to the squared modulus of the field amplitude, that is, proportional to

$$|\psi(r,t)|^2 = \mathcal{A}^2 e^{-2\gamma t}\,\mathrm{sech}^2\left[\mathcal{A}\,(m_x\,|G|\,/\hbar)^{1/2}\,(r - vt)\right] , \tag{48}$$

(the proportionality constant is $\hbar\omega_s$). Introducing the scaling parameter

$$\lambda = |G|\,/\gamma , \tag{49}$$

and the adimensional coordinates

$$\bar{x} = r/a , \qquad\qquad \bar{t} = t/\tau , \tag{50}$$

where $\tau = 2m_x a^2/\hbar$, with a being the extension of the side of the cubic unit cell, we can write

$$|\,\psi(\bar{x},\bar{t}\,)\,|^2 = \mathcal{A}^2 e^{-2\bar{\gamma}\bar{t}}\,\mathrm{sech}^2\left[\mathcal{A}\,(\lambda\bar{\gamma}/2)^{1/2}\,(\bar{x} - \bar{v}\bar{t}\,)\right] \tag{51}$$

where

$$\bar{\gamma} = \left(2m_x a^2/\hbar\right)\gamma , \qquad\qquad \bar{v} = (2m_x a/\hbar)\,v\,. \tag{52}$$

Using $a = 5.6 \times 10^{-8}$ cm and $m_x = 5.7 \times 10^{-29}$ g, we draw for different values of λ, $\mathcal{A}$, γ, and v the space and time evolution of the energy of the excitation, that is,

$$\mathcal{E}(\bar{x},\bar{t}) = \hbar\omega_s|\psi(\bar{x},\bar{t}\,)|^2. \tag{53}$$

In figure 1, it is shown the quantity, $\mathcal{E}(\bar{x},\bar{t}\,)/(\hbar\omega_s\mathcal{A}^2)$, labelled energy, and where (just for illustrative purposes) $\mathcal{A} = 250$; $\lambda = 0.1$; $\gamma^{\ 1} = 5 \times 10^{-12}$ s.

The initial perturbation (hyperbolic secant mimicking a Gaussian profile) has a length of near $3a$, and propagates with velocity $v = 10^5$ cm s^{-1}. The curves correspond to the space profile at subsequent times differing from each other by intervals $\Delta\bar{t} = 5000$. It can be noticed that the profile is maintained but accompanied by a decay with lifetime of the order of $\gamma^{-1} = 5$ picoseconds; the values of $\mathcal{A}, \lambda, \bar{\gamma}$, and $\bar{v}$ are indicated in the upper right corner. In figure 2, and in the same conditions as in figure 1, the picture describes jointly the space and time evolution of the energy packed in the solitary excitation.

These figures demonstrate that the behavior of the excitation governed by the nonlinear Schrödinger equation with damping, associated to the propagation of signals in this exciton system, is of the type of the so-called *solitary wave*, which evolves conserving the profile but in the presence of a dissipation that leads to its decay with a characteristic lifetime. This type of excitation is called a Davydov's soliton[46]. In the interpretation of A. Scott [47] the excitonic energy which is originally localized, acts —through the coupling with the phonons— in such a way to distort neighboring regions. This distortion reacts —again through the coupling with the phonons— to clamp the excitation energy preventing it to disperse (this is referred to as selftrapping), in such a way to maintain the profile of this energy (signal) while it propagates.

Another relevant case when solitary waves may be present is the one of biopolymers, for example linear chains in α-helix proteins, where this so-called Davydov's solitons may have large relevance in bioenergetics [46–48]: in this case the role of these excitons is played by polar vibrations associated to the stretching of hydrogen bonds. Experimental analysis of these results is particularly difficult in both cases, namely, excitons in semiconductors (a very weak signal on the background of a number of other excitations), and in biological systems under physiological conditions. However, solitons of the type here considered seem to be present in organic compounds like polyacetylene and polythiophene [40]. Solitons in this case seem to play a quite important role in the transport properties of these compounds, which are of relevance on the technological and economical sides. Other compound, acetanilide, may have a relevant role to play: it has a structure with similarities to the biopolymers and, differently to the latter, is amenable to a possible battery of experiments. A particular one of relevance is infrared absorption, with results which point to the existence of the solitary-wave excitation [49].

In the experiment an anomalous line, red shifted in relation to an expected normal vibrational frequency and with a linewidth strongly dependent on temperature, is ascribed to an excitation of the soliton type: in Fig. 3 we reproduce the experimentally observed spectra (curve with dots). Resorting consistently to the response function theory and IST, both based on MaxEnt-NESOM [20], one may calculate the expected infrared absorption line, once the response function theory is complemented with the theoretical results reported previously in this section, to characterize the red-shifted anomalous band due to the soliton excitation; the results are shown in Fig. 3 (full curve). These results are fully described and discussed in Ref. [50]. Inspection of the experimental and theoretical curves shows that there exist a good qualitative and semiquantitative agreement. Therefore, the all important, to the scientific method, corroboration by observation and experiment of the theoretical synthesis is —at least partially— present in this case, reinforcing then the confidence in the use of MaxEnt-NESOM and IST in dealing with irreversible processes.

As noticed the question of solitons in condensed matter seems to play a relevant role for technological and biological systems [38–40, 48–51]. The field is then wide-ranging and a number of new phenomena may be expected as the research on the subject further proceeds. On this we may also mention the case of solitons in two-dimensional discrete structures, recognized as a key for understanding the excitation dynamics in many physical contexts such as theory of light pulse propagation in non-linear waveguides, charge and energy transport in condensed matther physics and biosystems [52]. In those cases the interplay of nonlinearity and discretness leads to interesting dynamical features as described, for example, by Gaididei *et al.* [53] and Christiansen *et al.* [54].

3. Concluding Remarks

Dissipative systems have been the object of a good deal of interest in recent decades. More precisely, this applies to the physics of systems in far-from-equilibrium conditions. Among other reasons for this "Renaissance" of the topic —after the relevant role it played in the "Classical" period in the nineteenth century— two particularly may be mentioned: the emergence of selforganization and chaos that dissipative systems may display when sufficiently away from equilibrium and in the domain of nonlinear physics, and the functioning of electronic semiconductor devices under high levels of excitation. The latter case has associated an enormous amount of experimental (and also, of course, theoretical) research made using quite advanced instrumentation. In that way it is obtained information of large interest on both aspects: one is the understanding of the physics of nonequilibrated many-body systems and the other, on the technological side, is understanding —as alluded earlier in this paragraph— their functioning in the fields of electronics and optoelectronics. On the other hand, the first case, namely synergetic selforganization and chaos, belongs to the emerging field of the theory of systems with complex behavior [55-59], and has a very large relevance in, among many other disciplines, hydrodynamics, meteorology and the life sciences [60].

As already noticed in the Introduction the theme belongs to the realm of Irreversible Thermodynamics and nonlinear Nonequilibrium Statistical Mechanics, which are sciences not completely established, more precisely, they are the object of several approaches and controversy among different Schools of thought. It is worth citing Ryogo Kubo [61], who stated that: "statistical mechanics of nonlinear nonequilibrium phenomena is just in its infancy and further progress can only be hoped by close cooperation with experiment". Progress has been achieved in the period intervening since this 1977 statement, but in many instances of theoretical work Kubo's admonition has been ignored, and many arguments have been shuffled without recourse to comparison with the real experimental world. We have already mentioned the fact that, because of intense technological and economical pressure, condensed matter systems, mainly semiconductors, are the object of vast experimentation of exceptionally good quality. Consequently it appears as a quite promising area for providing a testing ground for ideas and formalisms in this field of dissipative phenomena in nonequilibrated systems.

Dealing with irreversible processes has been done via different phenomenological approaches, some already cited in the Introduction, and via different kinetic-theory approaches. The point stressed in this paper is that the statistical thermodynamics founded on a particular formalism contained within the scope of Predictive Statistical Mechanics —namely, the maximization of informational-entropy-based nonequilibrium statistical operator method— provides a theoretical approach of a quite large scope, which is concise, first principles based (including Jaynes-Jeffreys scientific inference method [23, 24, 62]) and practical. Nonlinear quantum transport and hydrodynamic equations follow from the formalism, with kinetic coefficients given at the molecular (microscopic) level, and the formalism also provides a response function theory which allows to carry on the all important step of connecting theory and experiment.

The theory has been applied with a degree of success to a number of situations in semiconductor physics (one example is the case of ultrafast laser spectroscopy, briefly reviewed in reference [63, 64]), and in the present paper we have considered for illustration the excited state of a boson field coupled to a thermal bath via a nonlinear anharmonic interaction. Application of the theory shows that the averaged (over the nonequilibrium ensemble) boson field satisfies a nonlinear Schrödinger-like equation with damping evidencing that dissipative processes are developing in the system. Moreover, an additional result follows, showing that the system displays complex behavior, consisting in that the set of possible excitations include one of the soliton type. As noted in the text, this is the so-called Davydov's soliton.

We have considered several actual physical systems to which the results thus obtained may be applied, namely, excitons in interaction with lattice vibrations in semiconductors, polar vibrations (CO-stretching) in interaction with acoustic and other vibrations in biosystems (e.g. α-helix proteins), in metallic organic polymers, and, in particular, acetanilide which may approximately mimic biological polymers. Comparison of theory and experiment was presented, particularly one confronting calculated and observed spectra in infrared absorption experiments. To conclude, we restate a sentence presented in section 3: The all important, to the scientific method, corroboration of theoretical synthesis by observation and experiment is —at least partially— present in this case, reinforcing the confidence in the use of MaxEnt-NESOM and IST in dealing with irreversible processes.

4. Acknowledgments

We acknowledge financial support provided to our Group in several occasions by the State of São Paulo Research Agency(FAPESP), the National Research Council (CNPq), The Ministry of Planning (Finep), IBM-Brasil, US-National Science Foundation (US-Latin America Cooperation Project; NSF, Washington), and the John Simon Guggenheim Memorial Foundation. One of the authors (MVM) is a Ministry of Education (CAPES) pre-doctoral fellow, and the other two are CNPq Research Fellows.

Appendix A. Some steps in the derivation of Eq. (17).

Calculation of the last term on the right of Eq. (14) leads to the following explicit form for the equation of evolution of the amplitude $\langle a_q \mid t\rangle$,

$$\begin{aligned}
\frac{d}{dt}\langle a_q|t\rangle &= (\mathrm{i}\hbar)^{-1} E_q\langle a_q \mid t\rangle + \\
&+ (\mathrm{i}\hbar)^{-2} \sum_{q_1,q_2,q_3} \int_{-\infty}^{0} dt' \mathrm{e}^{\varepsilon t'} \left\{\langle \varphi^{\dagger}_{qq_3} \tilde{\varphi}_{q_1q_2}(t')\rangle \langle a_{q_3} a^{\dagger}_{q_1} a_{q_2} \mid t\rangle\right\} + \\
&- (\mathrm{i}\hbar)^{-2} \sum_{q_1,q_2,q_3} \int_{-\infty}^{0} dt' \mathrm{e}^{\varepsilon t'} \left\{\langle \tilde{\varphi}_{q_1q_2}(t') \varphi^{\dagger}_{qq_3}\rangle \langle a^{\dagger}_{q_1} a_{q_2} a_{q_3} \mid t\rangle\right\} + \\
&+ (\mathrm{i}\hbar)^{-2} \sum_{q_1,q_2,q_3} \int_{-\infty}^{0} dt' \mathrm{e}^{\varepsilon t'} \left\{\langle \varphi^{\dagger}_{qq_3} \tilde{\varphi}_{q_1q_2}(t')\rangle \langle a_{q_3} a^{\dagger}_{q_2} a_{q_1} \mid t\rangle\right\} + \\
&- (\mathrm{i}\hbar)^{-2} \sum_{q_1,q_2,q_3} \int_{-\infty}^{0} dt' \mathrm{e}^{\varepsilon t'} \left\{\langle \tilde{\varphi}_{q_1q_2}(t') \varphi^{\dagger}_{qq_3}\rangle \langle a^{\dagger}_{q_2} a_{q_1} a_{q_3} \mid t\rangle\right\} \qquad \text{(A.1)}
\end{aligned}$$

where we have introduced the notation

$$\tilde{\varphi}_{q_1q_2}(t) = \varphi_{q_1q_2} \mathrm{e}^{\mathrm{i}(\omega_{q_1}-\omega_{q_2})t}, \qquad \text{(A.2a)}$$

$$\tilde{\varphi}^{\dagger}_{q_1q_2}(t) = \varphi^{\dagger}_{q_1q_2} \mathrm{e}^{\,\mathrm{i}(\omega_{q_1}-\omega_{q_2})t} \qquad \text{(A.2b)}$$

After some simple algebraic manipulations and using the definitions

$$\langle \tilde{\varphi}^{\dagger}_{qq_1}(t')\varphi_{q_1q_2}\rangle = \frac{1}{2\pi} \int_{-\infty}^{\infty} I_{q_1q_2,qq_1}(\omega) \exp\{\mathrm{i}(\omega - \omega_{q_1} + \omega_{q_2})t'\}\, d\omega, \qquad \text{(A.3a)}$$

$$\langle \tilde{\varphi}_{qq_1}(t)\varphi^{\dagger}_{q_1q_2}\rangle = \frac{1}{2\pi} \int_{-\infty}^{\infty} K_{qq_1,q_1q_2}(\omega) \exp\{\mathrm{i}(\omega + \omega_{q_1} - \omega_{q_2})t'\}\, d\omega, \qquad \text{(A.3b)}$$

we obtain the Eq. (17) presented in the main text, namely

$$i\hbar\frac{d}{dt}\langle a_q \mid t\rangle = E_q\langle a_q \mid t\rangle + i\sum_{q_1,q_2} T^{(1)}_{q,q_1,q_2}\langle a_{q_1} \mid t\rangle + i\sum_{q_1,q_2,q_3} T^{(2)}_{q,q_1,q_2,q_3}\langle a^{\dagger}_{q_1} a_{q_2} a_{q_3} \mid t\rangle, \tag{A.4}$$

where

$$\begin{aligned} T^{(1)}_{q,q_1,q_2} &= \hbar^{-1}\int_{-\infty}^{0} dt' e^{\varepsilon t'}\left\{\langle\varphi_{qq_2}\tilde{\varphi}^{\dagger}_{q_1q_2}(t')\rangle + \langle\varphi^{\dagger}_{q_2q}\tilde{\varphi}_{q_2q_1}(t')\rangle\right\} \\ &= i/(2\pi\hbar)\int_{-\infty}^{\infty} d\omega\left[K^{*}_{qq_2,q_1q_2}(\omega) + I^{*}_{q_2q,q_2q_1}(\omega)\right][\omega + \omega_{q_1} - \omega_{q_2} + i\varepsilon]^{-1} \end{aligned} \tag{A.5a}$$

$$\begin{aligned} T^{(2)}_{q,q_1,q_2,q_3} &= \hbar^{-1}\int_{-\infty}^{0} dt' e^{\varepsilon t'}\left\{< [\varphi_{qq_3}, \tilde{\varphi}^{\dagger}_{q_2q_1}(t')] > + < [\varphi^{\dagger}_{q_3q}, \tilde{\varphi}_{q_1q_2}(t')] >\right\} \\ &= i/(2\pi\hbar)\int_{-\infty}^{\infty} d\omega\,[I_{q_2q_1,qq_3}(\omega) + K_{q_1q_2,q_3q}(\omega)]\,[\omega + \omega_{q_1} - \omega_{q_2} - i\varepsilon]^{-1} + \\ & i/(2\pi\hbar)\int_{-\infty}^{\infty} d\omega\left[I^{*}_{q_3q,q_1q_2}(\omega) + K^{*}_{qq_3,q_2q_1}(\omega)\right][\omega - \omega_{q_1} + \omega_{q_2} + i\varepsilon]^{-1}, \end{aligned} \tag{A.5b}$$

and we recall that ε is to be taken in the limit of going to zero, and then, taking into account the so-called retarded and advanced Heisenberg-Dirac generalized functions

$$\lim_{\varepsilon\to 0}(x \pm i\varepsilon)^{-1} = \mathrm{pv}\,(x)^{-1} \mp i\pi\delta(x), \tag{A.6}$$

the contributions in Eqs. (A.5) contain a contribution in principal value and another with a Dirac-delta energy conserving function.

REFERENCES

[1] Nicolis, G., Physica A **213**, 1 (1995).

[2] Nicolis, G. and Prigogine, I., *Self-organization in Nonequilibrium Systems* (Wiley-Interscience, New York, 1977).

[3] Nicolis, G., in *The New Physics.* (Edited by P. Davies) (Cambridge Univ. Press, Cambridge, 1989), p. 316.

[4] Nicolis, G. and Prigogine, I., *Exploring Complexity* (Freeman, New York, 1989).

[5] Prigogine, I., Nicolis, G. and Babloyantz, A., Phys. Today **25** (11), 23 (1972).

[6] Prigogine, I., Nicolis, G. and Babloyantz, A., Phys. Today **25** (2), 38 (1972).

[7] de Groot, S. and Mazur, P., *Nonequilibrium Thermodynamics* (North Holland, Amsterdam, 1962).

[8] Kreuzer, H. J., *Nonequilibrium Thermodynamics and its Statistical Foundations* (Clarendon, Oxford, 1981).

[9] Zwanzig, R., in *Perspectives in Statistical Physics.* (Edited by H. J. Raveché) (North Holland, Amsterdam, 1981), p. 123.

[10] Kirkwood, J. G., J. Chem. Phys. **14**, 180 (1946).

[11] Mori, H., Oppenheim, I. and Ross, J., in *Studies in Statistical Mechanics I*, (Edited by J. de Boer and G. E. Uhlenbeck) (North Holland, Amsterdam, 1962), p. 217.

[12] McLennan, J. A., *Advances in Chemical Physics*, (Academic, New York, 1963), Vol. 5, p. 261.

[13] Zubarev, D. N., *Nonequilibrium Statistical Thermodynamics* (Consultants Bureau, New York, 1974), [*Neravnovesnaia Statisticheskaia Termodinamika* (Idz. Nauka, Moscow, 1971)].

[14] Akhiezer, A. I. and Peletminskii, S. V., *Methods of Statistical Physics* (Pergamon, Oxford, 1981).

[15] Zwanzig, R., in *Lectures in Theoretical Physics.* (Edited by W. E. Brittin, B. W. Downs, and J. Downs) (Wiley-Interscience, New York, 1961).

[16] Vstovskii, V. P., Teor. Mat. Fiz., **21**, 376 (1974) [Theor. Math. Phys. (USSR) **21**: 1214 (1975)].

[17] Robertson, B., in *The Maximum Entropy Formalism.* (Edited by M. Tribus and R. D. Levine) (MIT Press, Cambridge, MA, 1978), p. 289.

[18] Grabert, H., *Projection Operators Techniques in Nonequilibrium Statistics* (Springer, Berlin, 1981).

[19] Zubarev, D. N. and Kalashnikov, V. P., Teor. Mat. Fiz. **1**, 137 (1969), [Theor. Math. Phys. (USSR)**1**, 108 (1970)].

[20] Luzzi, R. and Vasconcellos, A. R., Fortschr. Phys./Prog. Phys. **38**, 887 (1990).

[21] Ramos, J. G., Vasconcellos, A. R. and Luzzi, R., Fortschr. Phys./Prog. Phys. **43**, 265 (1995).

[22] Jaynes, E. T., in *Maximum Entropy and Bayesian Methods.* (Edited by J. Skilling) (Kluwer, Dordrecht, 1989), p. 1.

[23] Jaynes, E. T., Reprinted articles and notes, in *E. T. Jaynes Papers on Probability, Statistics, and Statistical Physics.* (Edited by R. D. Rosenkranz) (Dordrecht, Reidel, 1983).

[24] Jaynes, E. T., in *Frontiers of Nonequilibrium Statistical Physics.* (Edited by G. T. Moore and M. O. Scully) (Plenum, New York, 1986), p. 33.

[25] Grandy, W. T., *Principles of Statistical Mechanics,* Vol. 1 (Reidel, Dordrecht, 1987).

[26] Grandy, W. T., *Principles of Statistical Mechanics,* Vol. 2 (Reidel, Dordrecht, 1988).

[27] Zubarev, D. N., Morozov, V. N. and Röpke, G., *Statistical Mechanics of Nonequilibrium Processes* (Akademie Verlag, Berlin, 1996).

[28] Hobson, A., J. Chem. Phys. **45**, 1352 (1966).

[29] Hobson, A., Am. J. Phys. **34**, 411 (1966).

[30] Jaynes, E. T., Phys. Rev. **106**, 620 (1957).

[31] Jaynes, E. T., Phys. Rev. **108**, 171 (1957).

[32] Vasconcellos, A. R., Garcia-Colin, L. S. and Luzzi, R., Phys. Rev. A **43**, 6622 (1991).

[33] Vasconcellos, A. R., Garcia-Colin, L. S. and Luzzi, R., Phys. Rev. A **43**, 6633 (1991).

[34] Garcia-Colin, L. S., Vasconcellos, A. R. and Luzzi, R., J. Non-Equilib. Thermodyn. **19**, 24 (1994).

[35] Luzzi, R., Vasconcellos, A. R. and Ramos, J. G., Statistical Irreversible Thermodynamics in a Nonequilibrium Statistical Ensemble Formalism, IFGW-Unicamp Internal Report (1998), future publication.

[36] Sieniutycz, S. and Salamon, P., in *Nonequilibrium Theory and Extremum Principles.* (Edited by S. Sieniutycz and P. Salamon) (Taylor and Francis, New York, 1990), p. 1.

[37] Nettleton, R. E. and Sobolev, S. L., J. Non-Equilib. Thermodyn. **19**, 205 (1995).

[38] Scott, A. C., The Sciences **30** (2), 28 (1990), a publication of the New York Academy of Sciences.

[39] Haus, H. A., IEEE Spectrum 48 (1993).

[40] Heger, A. J., Kivelson, S., Schrieffer, J. R. and Su, W. P., Rev. Mod. Phys. **60**, 781 (1988).

[41] Lauck, L., Vasconcellos, A. R. and Luzzi, R., Physica A **168**, 789 (1990); J. R. Madureira, A. R. Vasconcellos, R. Luzzi, J. Casas-Vázquez, and D. Jou, J. Chem. Phys. **108**, 7568 (1998); *ibid.* **108**, 7580 (1998); J. R. Madureira, A. R. Vasconcellos, R. Luzzi, and L. Lauck, Phys. Rev. E **57**, 3637 (1998).

[42] Knox, R. S., *Theory of Excitons,*Solid State Physics Series. (Edited by F. Seitz and J. Turnbull) (Academic Press, New York, 1963), Suppl. 5.

[43] Zakharov, V. E. and Manakov, S. V., Teor. Mat. Fiz. **27**, 283 (1976).

[44] Zakharov, V. E., in *Solitons.* (Edited by R. K. Bullough and P. J. Caudrey) (Springer, Berlin, 1980), Chap. 7, 243.

[45] Newell, A. C., in *Solitons.* (Edited by R. K. Bullough and P. J. Caudrey) (Springer, Berlin, 1980), Chap. 6, 177.

[46] Davydov, A. S., in *Solitons.* (Edited by S. E. Trullinger, V. E. Zakharov, and V. L. Prokovsky) (Elsevier, New York, 1986), Chap. 1, 1.

[47] Scott, A. C., Phys. Rep **217**, 1 (1992).

[48] Davydov, A. S., *Biology and Quantum Mechanics* (Pergamon, Oxford, 1982).

[49] Careri, G., Buotempo, U., Carta, R., Gratton, E., Scott, A. C., Phys. Rev. Lett. **51**, 304 (1983).

[50] A. R. Vasconcellos, M. V. Mesquita, and R. Luzzi, Phys. Rev. Lett. **80**, 2008 (1998).

[51] Scott, A. C., Chu, F. Y. F., and McLaughlin, D. W., Proc. IEEE **61**, 1443 (1973).

[52] Articles and Notes in *Nonlinear Coherent Structures in Physics and Biology* (Edited by K. H. Spatscheck and F. G. Mateus) (Plenum, New York, 1994).

[53] Gaididei, Yu. B., Mingaleev, S. F., Yakimanko, I. I., Christiansen, P. L., Johannson, M., and Rasmussen, K. Ø., Phys. Scripta **T67**, 151 (1996).

[54] Christiansen, P. L., Gaididei, Yu. B., Mezentsev, V. K., Muscher, S. L., Rasmussen, K. Ø., Rasmussen, J. J., Ryzhenkova, I. V., and Turitsyn, S. K., Phys. Scripta **T67**, 160 (1996).

[55] Anderson, P. W., Science **117**, 393 (1972).

[56] Anderson, P. W., Phys. Today **44** (7), 9 (1991).

[57] Gell-Mann, M., Complexity **1**, 16 (1995).

[58] Articles and Notes in *Nonlinear Physics of Complex Systems: Current Status and Future Trends* (Edited by J. Parisi, S. C. Müller, and W. Zimmerman) (Springer, Berlin, 1996).

[59] Horgan, J., Scientific American 74 (1995).

[60] Luzzi, R. and Vasconcellos, A. R., Ciência e Cultura **43**, 423 (1992), a publication of the Brazilian Society for the Advancement of Science.

[61] Kubo, R., Oppening address to Oji Seminar on Nonlinear Nonequilibrium Statistical Mechanics, Oji, Japan, 1977. *Sup. Prog. Theor. Phys. (Japan)*, **64**:1, 1978.

[62] Jaynes, E. T., in *Maximum Entropy and Bayesian Methods.* (Edited by W. T. Grandy and L. H. Schick) (Kluwer, Dordrecht, 1991), 1.

[63] Algarte, A. C., Vasconcellos, A. R. and Luzzi, R., Phys. Stat. Sol. (b) **173**, 487 (1992).

[64] Algarte, A. C., Vasconcellos, A. R. and Luzzi, R., Braz. J. Phys. **26**, 543 (1996).

FIGURE CAPTIONS

Figure 1: Propagation of energy with the solitary excitation [cf. Eq. (53)] for the values of the parameters shown in the upper right inset. The positions are given at time intervals of 5000 (in units of τ of Eq. (47); for GaAs $a = 5.6$ Å, and $5000\tau \simeq 1.69$ ps).

Figure 2: In the same conditions as in figure 1, it is presented a "bird's view" of the space and time evolution of the packed energy.

Figure 3: Infrared spectra in acetanilide showing the band ascribed to the solitary excitation centered at 1650 cm^{-1}. Experimental data taken from reference [49], and the parameters used in the calculation shown in the upper left inset. After Ref. [50].

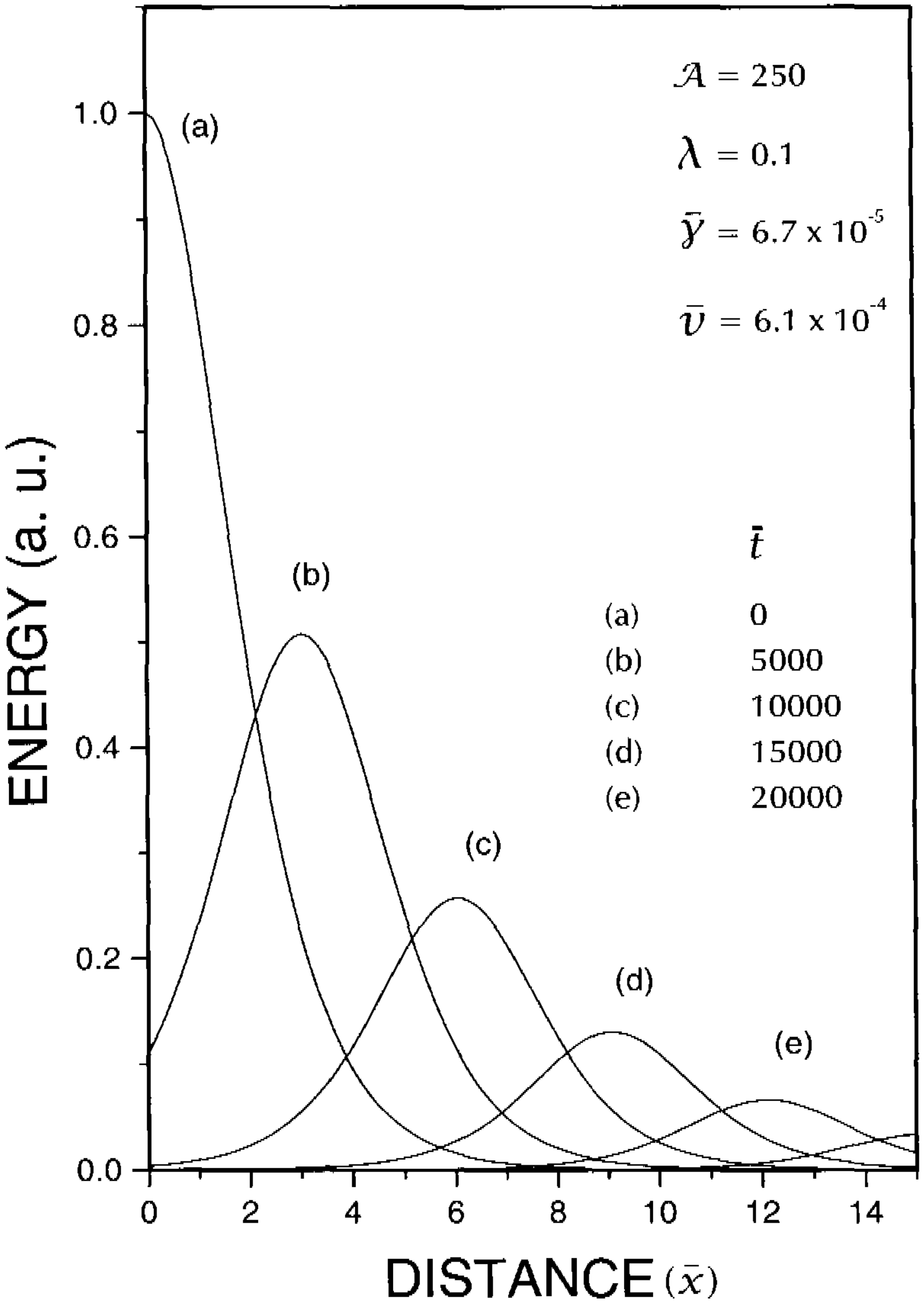

Figure 1: Propagation of energy with the solitary excitation [cf. Eq. (53)] for the values of the parameters shown in the upper right inset. The positions are given at time intervals of 5000 (in units of τ of Eq. (50); for GaAs $a = 5.6$ Å, and $\tau = 1.69$ ps).

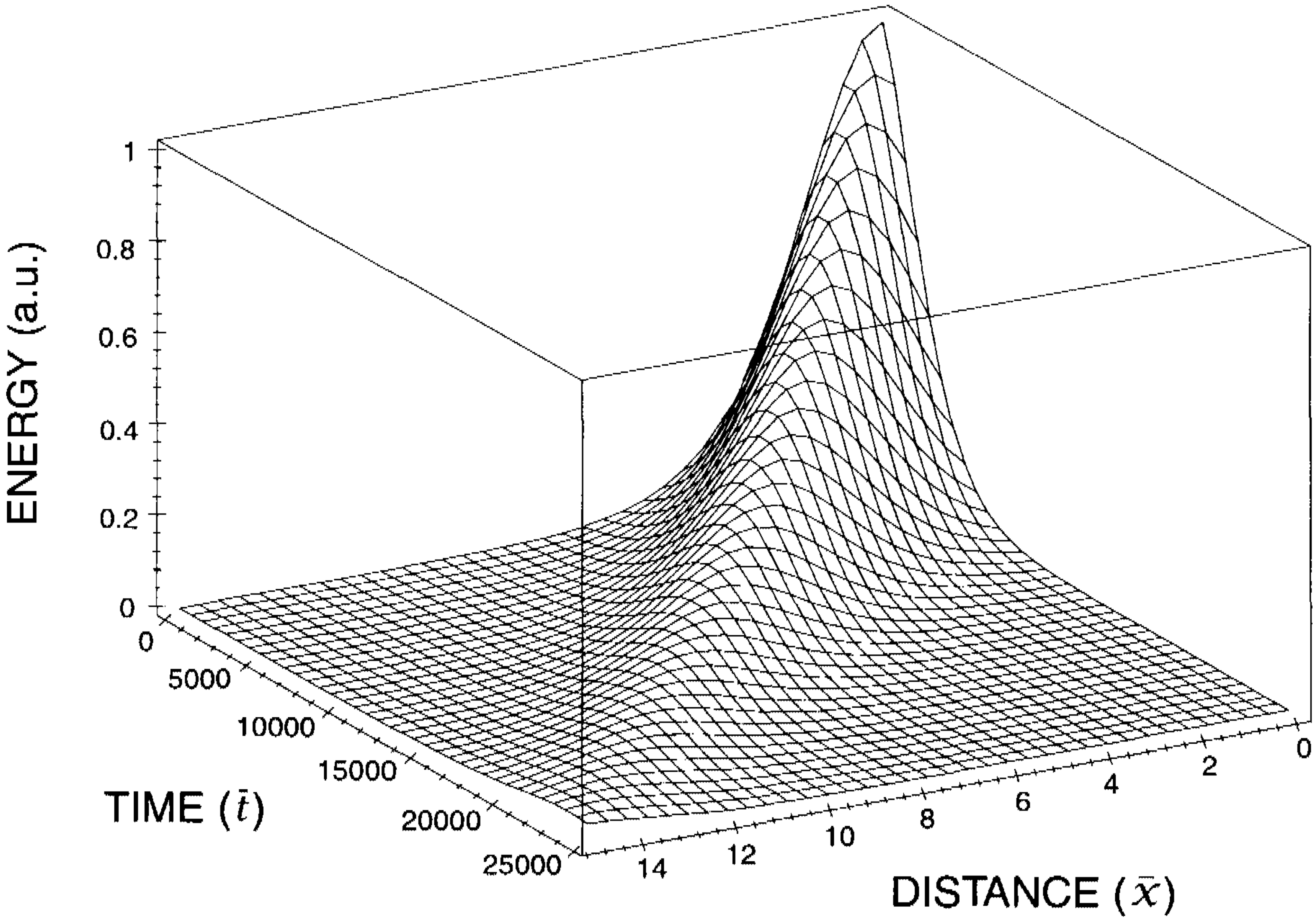

Figure 2: In the same conditions as in figure 1, it is presented a "bird's view" of the space and time evolution of the packed energy.

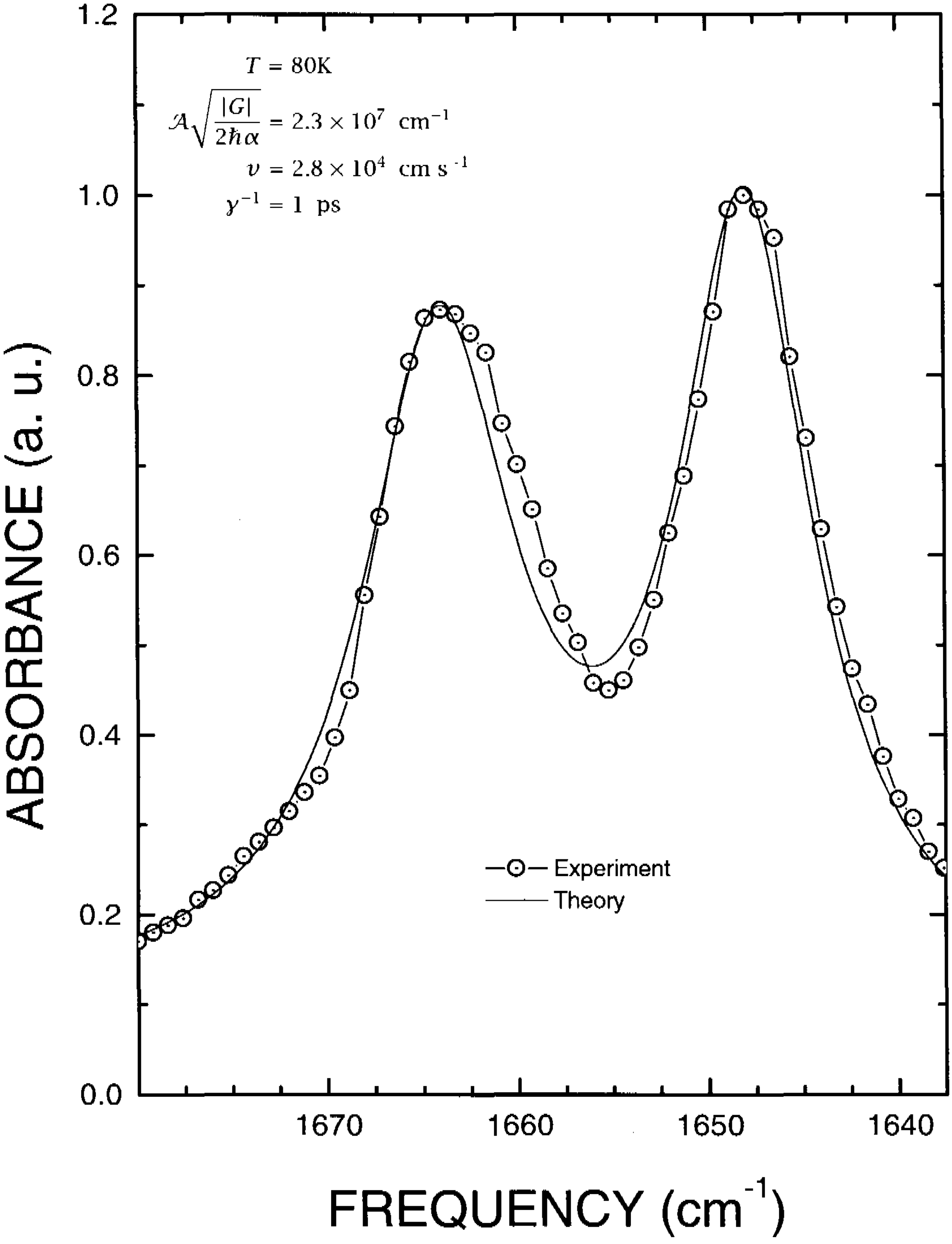

Figure 3: Infrared spectra in acetanilide showing the band ascribed to the solitary excitation centered at 1650 cm^{-1}. Experimental data taken from reference [49], and the parameters used in the calculation shown in the upper left inset. After Ref. [50].

CONDENSAÇÃO TIPO FRÖHLICH-BOSE-EINSTEIN

4.1 Introdução

Mais de trinta anos passaram-se desde que o renomado Herbert Fröhlich apresentou pela primeira vez seu conceito de coerência de longo alcance em sistemas biológicos [Fröhlich 1969], uma questão presentemente em processo de renascimento e que fornece um campo de pesquisa atrativo e relevante em Física e Biologia. De acordo com Fröhlich, sistemas biofísicos que possuem modos vibracionais elétricos longitudinais podem apresentar, sob condições apropriadas, um fenômeno coletivo semelhante a uma condensação Bose-Einstein — não em equilíbrio, mas como um comportamento complexo consistindo na emergência de uma estrutura dissipativa no sentido de Prigogine [1969]. Os resultados de Fröhlich são baseados na idéia de que sistemas biológicos ativos são sistemas abertos e muito longe do equilíbrio e têm consideráveis quantidades de energia disponível, através de processos metabólicos, que provocam mudanças não-lineares em moléculas em subsistemas biológicos maiores. Fröhlich [1973], em *Life as a Collective Phenomena*, expressou que se pensamos sem preconceitos sobre fenômenos coletivos como acontecendo em sistemas de muitos componentes onde os constituintes individuais têm seu comportamento modificado e suas partes passam a constituir um grande grupo coletivo onde o todo é maior e diferente do que a simples soma das parte, então organismos vivos seriam o exemplo ideal. Tal hipótese de explicação biológica em termos de coerência de longo alcance foi sugerida por Fröhlich no primeiro encontro do *L'Institute de la Vie* em 1967 [Fröhlich 1969].[1]

No modelo de Fröhlich, modos polares vibracionais são excitados por um suprimento constante de energia bombeada por uma fonte externa, enquanto esses modos interagem com o meio circundante, o qual age como um banho térmico. A ação recíproca desses dois efeitos — o bombeamento de energia subtraindo entropia do sistema e efeitos dissipativos internos adicionando entropia ao sistema — podem levar ao aparecimento de um comportamento complexo particular no sistema que pode ser denominado *Efeito Fröhlich:* este efeito consiste em que o sistema atinge um estado estacionário em que a energia que alimenta os modos polares é canalizada para os modos de freqüência mais baixa, cujas populações aumentam enormemente às custas dos outros modos de freqüência mais alta em uma maneira que lembra uma condensação Bose-Einstein [Fröhlich 1975, 1980]. Isso, naturalmente, desde que o fornecimento de energia seja suficientemente grande em comparação com a perda de energia.

É interessante notar que, dentro do esquema da Termodinâmica Estatística que temos usado, a descrição do estado macroscópico do sistema pode ser feita seja em termos das variáveis de base ou equivalentemente em termos dos parâmetros de Lagrange que o método variacional introduz. No caso que consideramos neste capítulo isto se refere as populações de modos polares e seu parâmetro de Lagrange associa-

---

[1] Agradecemos ao Prof. Sergio Mascarenhas (Instituto de Estudos Avançados, USP, São Carlos), convidado dessa reunião em Versailles, França, por ter chamado nossa atenção para esta importante contribuição de Herbert Fröhlich.

do. Este último pode ser adequadamente redefinido — como veremos mais adiante — em termos de uma variável termodinâmica intensiva tendo o papel de um potencial químico para fonons fora do equilíbrio (pseudo-potencial químico). Alternativamente, pode ser expresso em termos de outra variável termodinâmica intensiva tendo o papel de uma temperatura fora do equilíbrio (pseudo-temperatura, ou temperatura efetiva, ou em inglês "quasitemperature").

Na Física do Estado Sólido, mais precisamente de semicondutores, o conceito de temperatura de fonons e de portadores fora do equilíbrio foi introduzido por Cerqueira Leite e colaboradores [Shah & Leite 1969; Shah *et al.* 1970] (lembramos que no caso de elétrons em campo elétrico o conceito de uma temperatura de não-equilíbrio foi introduzido por Fröhlich [1947], para spins por Casimir & du Pré [1938], para o plasma por Landau [1936], para moléculas por Wang Chang *et al.* [1964], para supercondutores por Shklovskii [1975]; vide também [Feschbach 1987; Luzzi *et al.* 1997]).

A possibilidade de tal tipo de condensação tem levado à consideração [Mascarenhas 1987] de que na eventual nova fase condensada possa surgir um particular estado dito de eletreto, enventualmente de caráter metaestável.

Um eletreto consiste de um material dielétrico que apresenta uma carga elétrica quase permanente. Com quase permanente indica-se que as constantes de tempo características para o decaimento de carga são maiores do que o intervalo de tempo durante o qual são realizados experimentos com o eletreto.

Tem sido manifestado [Mascarenhas 1987] que armazenamento de carga e polarização via o estado de eletreto tem sido achado em muitos materias biológicos. A importância do efeito eletreto nestes materiais tem a ver com aplicações biomédicas, assim como também um possível papel em fenômenos biofísicos fundamentais. O efeito tem sido observado em biopolímeros de relevância como proteínas, polisacarídeos, e alguns polinucleotídeos. Um dos aspectos mais importantes da pesquisa de eletretos em biofísica é que a água ligada a biopolímeros, na assim chamada forma estruturada (ou água ligada, ou bioágua), pode também ser induzida num estado de eletreto. Além disso, o estado de eletreto pode apresentar-se em diversos modelos biofísicos como uma base para a compreensão de comportamento de membranas, sinais neurais, memória biológica em processos de regeneração e crescimento de tecidos, e outros fenômenos. Um dos mais interessantes modelos onde pode estar presente um tipo de ferro-elétrico, porém num estado metaestável similar ao eletreto é o resultante do modelo de Fröhlich para o comportamento das ondas longitudinais de vibrações polares nos sistemas biológicos, que poderíamos chamar de bioeletreto. O fato será evidenciado na análise a seguir nas próximas seções.

As oscilações coletivas sincrônicas em larga escala de Fröhlich implicam em emissões intercelulares de microondas que constituiriam uma interação entre as células que não é nem de natureza química nem térmica. Essas oscilações poderiam, portanto, ser reveladas por detecção de emissão de radiação em GHz ou THz. Tais sinais eletromagnéticos são de magnitude extremamente baixa e tecnologia de detecção para medi-los não estava disponível na época de Fröhlich. Somente agora é que os sinais preditos podem ser detectados mediante a adaptação da tecnologia que foi desenvolvida para a pesquisa espacial e astrofísica. Assim, uma área completamente nova em Biologia está disponível para investigação.

Experimentos mais antigos procurando pelo efeito Fröhlich não foram conclusivos, mas agora uma "segunda geração" de experimentos está-se tornando disponível. Eles necessitam aprimoramento ulterior, mas alguns resultados preliminares já são encorajadores [Grant & Hyland 1998]: evidência de uma influência não-térmica de radiação coerente de microondas no genoma do estado conformacional na bactéria *E. coli*, o que pode indicar que o DNA cromossômico poderia ser o alvo de irradiação de microondas milimétricas dentro desse sistema. Irradiação de baixa intensidade de microondas em leucócitos resulta em um aumento significante na emissão biofotônica na região óptica, cuja origem se pensa envolver o DNA. Vale a pena observar também a possível influência do conceito de biocoerência no sistema dipolar muito especial que é a água. Pode-se considerar a possibilidade que a própria água biológica possa suportar excitações dipolares coerentes extendendo-se além de regiões mesoscópicas; assim, em vez de ser um solvente passivo preenchendo o espaço, a água seria elevada a uma posição importante e singular, cuja significância plena ainda teria de ser elucidada.

Implicações não-biológicas do efeito Fröhlich também poderiam ser de amplo alcance. Podemos mencionar alguma conecção com homeopatia e física de aerossóis atmosféricos [Grant & Hyland 1998]. Com relação a estes últimos, excitações coerentes do tipo Fröhlich alimentadas via luz solar podem ter um papel na produção de anomalias no espectro de absorção da luz [Miller & Gebbie 1996]. Nesse ponto, podemos mencionar uma preocupação de saúde pública, a saber: a influência e os eventuais efeitos prejudiciais de telefones celulares devido à ação de microondas no material biológico cerebral, uma vez que eles são usados em contato direto com a cabeça do usuário.

Chamamos a atenção também para um aspecto adicional do efeito Fröhlich em conexão com a propagação de longo alcance de sinais em materiais biológicos e não-biológicos. Tais sinais são pacotes de ondas consistindo em *solitons de Scrhödinger-Davydov* [Davydov 1982], que são uma conseqüência das mesmas não-linearidades que são responsáveis pelo efeito Fröhlich. Dessa forma, fazemos contato com o capítulo anterior — onde o fato foi rapidamente mencionado —, e cuja descrição em profundidade é feita no capítulo seguinte.

Como veremos, pode ser mostrado que a onda solitária que, tanto em sistemas biológicos como não-biológicos é fortmente amortecida como resultado dos efeitos dissipativos usuais, podem propagar-se com um decaimento fraco à medida que percorrem grandes distâncias quando se locomovem no meio provido por um condensado estacionário de Fröhlich. Já existem casos onde a teoria é aparentemente validada pelo experimento, a saber: na área médica de diagnóstico via ultra-sonografia, i. e. visualização de órgãos internos do corpo via ultra-sons, está relacionada com o efeito Fröhlich em sistemas vibracionais acústicos em vez de sistemas polares. Nesse caso, o efeito Fröhlich pode aparecer também nesse caso, onde a fonte de alimentação seria então um antena emitindo sinais ultra-sônicos. Um sóliton de Davydov, ao contrário de ondas sonoras dispersivas normais, percorre distâncias longas quase que sem alteração, o que pode ser de interesse particular para a melhoria da técnica de detecção em ultrasonografia [Lu & Greenleaf 1992].

Um interessante comportamento complexo adicional ocorre quando o sóliton propaga-se com uma velocidade maior do que a velocidade de grupo dos modos normais de vibração ocorre um fenômeno semelhante ao efeito Cherenkov em teoria de radiação, a saber: um grande emissão de fonons em dois cones simétricos centrados no sóliton; isso permite interpretar as assim chamadas ondas X em ultra-sonografia como esse efeito *Fröhlich-Cherenkov* como faremos no capítulo seguinte. No que concerne a materiais biológicos, notemos primeiro o caso do polímero acenatanilida — que é uma boa imitação de certos biopolímeros — onde o sóliton de Davydov é evidenciado no espectro de absorção infravermelho, como mostrado no estudo no capítulo anterior. Nesse caso o experimentador pode procurar uma verificação indireta da formação do condensado de Fröhlich tentando encontrar a vida média (obtida via largura de linha espectral Raman) ao submeter as oscilações vibracionais polares (os modos de estiramento CO ou modos Amida I) à ação de fonte de alimentação externa (e.g. radiação infravermelha) que abranja as freqüências da relação de dispersão dos modos vibracionais.

Outro exemplo onde a condensação de Fröhlich e o sóliton de Davydov parecem estar presentes é o caso do assim chamado "excitoner", que é uma emissão coerente estimulada de éxcitons criada por excitações randômicas, em uma situação similar ao caso de fotons em um laser, com seu estudo também a ser desenvolvido no próximo capítulo. Nesse caso, éxcitons criados em um semicondutor por um pulso intenso de radiação laser percorrem a amostra como um pacote e são detectados em sua parte posterior. Um sinal fraco em condições normais de excitação térmica é grandemente ampliado quando o sistema é alimentado por uma fonte externa contínua de radiação infravermelha. A teoria sugere a formação de um condensado Fröhlich de éxcitons excitados não-termicamente onde um sóliton de Schrödinger-Davydov fracamente amortecido é criado, cuja forma está em boa concordância com a observação experimental [Vasconcellos *et al.* 1998]. Observamos aqui um comportamento complexo particularmente notável — efeito Fröhlich; sóliton de Davydov; eventualmente efeito Fröhlich-Cherenkov —, e o "excitoner", citando D. Snoke [1996], é um fenômeno que pode prover um novo tipo de fonte de luz, mas somente o tempo e a imaginação podem dizer que novas aplicações podem surgir desse novo efeito.

Em conclusão, estamos sendo confrontados com um ressurgimento estimulante do efeito Fröhlich, após certo período de hibernação parcial. Esse ressurgimento é forte no sentido de que tanto pode abrir uma área de pesquisa nova e relevante em Biologia e no âmbito de diagnóstico médico quanto em matéria inanimada como polímeros, polímeros condutores, guias de onda ópticas, envolvendo a emissão de sinais coerentes e firmes, como no caso do "excitoner" citado acima.

Apresentamos a seguir as subseções dedicadas ao efeito Fröhlich, que consistem em:

4.2 Amplificação de vibrações polares coerentes em biopolímeros: condensado de Fröhlich.

4.3 Condensação de Fröhlich tipo Bose-Einstein em Biosistemas

4.4 Considerações sobre a condensação de Fröhlich tipo Bose-Einstein.

4.5 O Regime Transiente no Fenômeno da Condensação de Fröhlich em Biosistemas.

4.6 Termodinâmica Estatística de Sistemas Complexos.

4.2 Amplificação de vibrações polares coerentes em biopolímeros: condensado de Fröhlich

Consideramos a evolução em não-equilíbrio e com dissipação e o estado estacionário da população de modos polares vibracionais em uma cadeia de biomoléculas. Esses modos polares são excitados através de um acoplamento com uma fonte energética metabólica e interagem anarmonicamente com um meio contínuo elástico. Grupos de modos polares acoplam-se dessa maneira através de termos não-lineares nas equações cinéticas. Evidencia-se que essa não-linearidade é a fonte de um fenômeno inesperado caracterizando comportamento complexo nesta espécie de sistema: após ser alcançado um limite de intensidade da fonte de alimentação, modos polares com as freqüências mais baixas têm sua população enormemente aumentada de uma maneira que lembra a condensação de Bose-Einstein (efeito Fröhlich). O transiente para que o estado estacionário ocorra é muito pequeno (da ordem de picosegundo) e o condensado aparece mesmo para valores pequenos da intensidade de acoplamento anarmonico responsável por sua ocorrência. Além disso, ele requer níveis acessíveis de energia metabólica para ser produzido e mantido.

Physical Review E, **48** (5), 4049–59 (1993).

Amplification of coherent polar vibrations in biopolymers: Fröhlich condensate

Marcus V. Mesquita, Áurea Rosas Vasconcellos, and Roberto Luzzi

Instituto de Física 'Gleb Wataghin',
Universidade Estadual de Campinas, Unicamp
13083-970 Campinas, São Paulo, Brazil

We consider the nonequilibrium and dissipative evolution, and the steady state of the population of vibrational polar modes in a chain of biomolecules. These polar modes are excited through a coupling with a metabolic pumping source and are in anharmonic interaction with an elastic continuum. Groups of polar modes are coupled in this way through nonlinear terms in the kinetic equations. This nonlinearity is shown to be the source of an unexpected phenomenon characterizing complex behavior in this kind of system: after a threshold of intensity of the pumping source is achieved, polar modes with the lowest frequencies increase enormously their population in a way reminiscent of a Bose-Einstein condensation (Froehlich effect). The transient time for the steady-state condensate to follow is very short (picosecond time scale) and the condensation appears even for weak values of the anharmonic coupling strength responsible for its occurrence. Further, it seemingly requires accessible levels of metabolic pumping power in order to be produced and sustained.

PACS number(s): 87.10.+e, 05.70.Ln

1. INTRODUCTION

Nonlinearity is known to be the source of new and unexpected phenomena that characterize complex behavior in physical systems. This is particularly the case in dissipative systems far from equilibrium [1]. The concept that many-body systems sufficiently far away from equilibrium and governed by nonlinear kinetic laws may display self-organized ordered structures at the macroscopic level, as observed in many cases, has been brought under unifying approaches such as dissipative structures [2,3], synergetics [4], and macroconcepts [5]. We may say that, in particular, biological systems are complex systems by antonomasia, which are open, driven far from equilibrium, and display a variety of nonlinear physicochemical processes. Thus, as is the case, they present an enormous number of rich and noticeable phenomena on the morphological, biochemical, biophysical, etc., levels. We emphasize that this is possible in the nonlinear thermodynamic regime far from equilibrium, since in the linear (Onsager's) regime near equilibrium, ordering is inhibited according to Prigogine's theorem of minimum entropy production (e.g., Ref. [3]) that confirms the stability of the thermally chaotic branch of solutions, i.e., the so-called thermodynamic branch that emerges continuously from the equilibrium state with increasing values of the intensity of the external perturbation.

A quite interesting and illustrative example of nonlinearity at work, producing what can be very relevant biological effects, is a model of a biophysical system proposed by Fröhlich [6,7], that may describe membranes or large chains of macromolecules possessing longitudinal electric modes. In the Fröhlich model several modes of polar vibrations are excited by a continuous supply of metabolic energy, with these polar modes interacting with a bath of acousticlike vibrations through nonlinear dynamics, which is the source for what we call the *Fröhlich effect*, namely, that under appropriate nonlinear conditions the modes with the lowest frequencies increase enormously their population in a way reminiscent of a Bose-Einstein condensation. It has been stated that these polar modes, thus largely excited, may exhibit long-range phase correlations of the electret type [8–10], that may produce observable effects in biosystems [7].

Some microscopic approaches using modeled Hamiltonians have been proposed to describe Fröhlich system [11,12]. In these treatments the nonlinear kinetic terms arise out of nonlinear anharmonic interactions resulting in the creation (decay) of a longitudinal polar excitation from (into) a single excitation of the bath system and a polar excitation.

More recently, Davydov has proposed a model for a one-dimensional α-helical protein molecular chain with oscillating peptide bonds, embedded in an elastic continuum. A theory of the transfer of metabolic energy and of electrons along the chain describe excitations accompanied by a local deformation of the chain that move uniformly and undamped in what is called a solitary exciton [13–15]. These ideas concerning the transfer of energy in biological systems have been extended mainly by Scott [16]. It should be stressed that the nonlinearity of the equations of evolution, arising out of the interaction with the elastic continuum, are responsible for the Fröhlich effect and the propagation of solitary excitons. In fact, Tuszýnski *et al.* [9] have shown the equivalence of the Hamiltonians used to describe Fröhlich and Davydov models when both are placed in a representation in terms of normal coordinates.

Along this line, we consider the case of a chain of biomolecules, taken as a quasi-unidimensional system, and study the macroscopic nonequilibrium evolution of the polar vibrational modes they possess, whose kinetic equations — derived in an appropriate mechanostatistical scheme — are numerically solved. They are assumed to be excited by the pumping of biochemical energy (usually thought of to be the energy released by hydrolysis of adenosine triphosphate) on the polar oscillations (associated to double-bonded carbon-oxygen), which sustain an anharmonic interaction with an elastic continuum, the latter being modeled in terms of a Debye acousticoscillation system. The system is far from equilibrium and. therefore its description requires nonequilibrium dissipative thermodynamics, For that purpose we resort to the powerful, and also elegant and concise, nonequilibrium statistical operator method (NESOM), reviewed and brought under a unifying variational principle based on the predictive statistical mechanics of Jaynes in Ref. [17]. NESOM allows for the construction of a nonlinear generalized transport theory — a far reaching generalization of the methods of Chapman-Enskog and also Mori— that describes the evolution of the system at the macroscopic level in arbitrary nonequilibrium situations, as shown in Ref. [18]. Among the different NESOM, we resort to the method of Zubarev [19] and the so-called [18] second order approximation in the theory of relaxation (SOART). It is also known in the literature as the quasilinear theory of relaxation [20], a name we avoid because of the misleading term "linear" that refers to a certain order of dissipation as described by the nonequilibrium statistical operator, although the equations of evolution remain highly nonlinear.

We are thus allowed to write the equations of evolution for the populations of the polar modes, with a bath of acoustic vibrations that is assumed to remain in a state of constant temperature through the action of an efficient homeostatic mechanism. The polar vibration's frequency dispersion relation is modeled by a parabolic law around the zone center in reciprocal space. We use typical values for the different parameters that enter into the equations of evolution, which results in the fact that the polar modes are coupled in groups having a small number of modes, which greatly facilitates the computational solution of the coupled system of equations.

We solve the time-dependent equations of evolution to describe the transient period before the attainment of a stationary state. In that way, it is possible to define a transient time which is expressed in units of the relaxation time of the polar modes to the thermal bath. Furthermore, the solutions for the values of the populations in the steady state are obtained in terms of the intensity of the energy pumping source.

In the next section we specify the system and write the relevant Hamiltonian and the equations of evolution for the population of the modes derived in NSOM-SOART. We deal with an exactly soluble model for a chain of biomolecules where, we anticipate, Fröhlich effect follows: with increasing values of the pumping intensity, after a threshold is achieved, there follows a large amplification of a set of modes with the lowest frequencies. It is shown that the phenomenon can be realized even under conditions of weak contribution of the nonlinear terms in the equations of evolution that are relevant for the effect to appear, and under accessible levels of excitation. Also, it follows after a very short transient time after switching on the exciting external source, and, furthermore, as shown elsewhere [10], at the critical point for the onset of the

Fröhlich effect the lifetime of the oscillatory excitations largely increases, becoming near dissipationless waves, much in the way of Davydov's solitary waves. Hence, both effects seem to have the same and simultaneous origin.

2. POLAR MODES IN BIOPOLYMERS

Let us consider a quasilinear polymeric chain of biomolecules consisting of an arrangement of periodically repeated groups of molecules. Let a be the extension of the crystallographic unit cell. An example could be the α-helix protein depicted in Fig. 1, considered by Davydov [15], more precisely three chains (channels) with peptide bonds, in a near one-dimensional array (the radius of the helix is 2.8 Å). The pitch of the spiral is 4.5 Å, and the crystallographic unit cell contains 18 peptide groups (a = 80 Å). The energy is pumped in the system by metabolic processes, typically the energy released in the hydrolysis of adenosine 5-triphosphate ATP) molecules, and it is assumed that the chain can sustain longitudinal polar vibrations. This vibrational energy is associated to the CO stretching (or amide I) oscillators. The latter have a frequency dispersion relation $\omega_{\boldsymbol{q}}$, where $\boldsymbol{q}$ is a wave vector running over the reciprocal-space (Brillouin) zone of length $2\pi/a$. The chain is assumed to be embedded in an elastic continuum represented by a Debye model, i.e., with a frequency dispersion relation $s|\boldsymbol{q}|$, where s is the sound velocity in such a medium and having a Debye cutoff frequency ω_D. On the right-hand side of Fig. 1 we proceed to analyze a rough description of the mechanical model of the chain. Such a mechanical system is completely characterized at the dynamical level by the Hamiltonian

$$H = H_{01} + H_{02} + H_{11} + H_{12} + H_{21} + H_{22} + H_f \ , \tag{1}$$

where

$$H_{01} = \sum_{\boldsymbol{q}} \hbar\omega_{\boldsymbol{q}}(a_{\boldsymbol{q}}^{\dagger}a_{\boldsymbol{q}} + \frac{1}{2}) \tag{2a}$$

is the Hamiltonian of the free polar vibrations; a ($a_{\boldsymbol{q}}^{\dagger}$), as usual, are the annihilation (creation) operators in mode q;

$$H_{02} = \sum_{q'} sq'(b^{\dagger}_{q'}b_q + \frac{1}{2}) \tag{2b}$$

is the Hamiltonian of the bath of free acousticlike vibrations; and b ($b^{\dagger}$) are the corresponding annihilation (creation) operators. The next four terms arise out of anharmonic interactions involving three-quasiparticle collisions, given by the expressions

$$H_{11} = \sum_{qq'} V^{(1)}_{qq'} a_q b_{q'} b^{\dagger}_{q+q'} + \text{H.c.}\,, \tag{2c}$$

$$H_{12} = \sum_{qq'} V_{qq'}(1) a_q b^{\dagger}_{q'} b^{\dagger}_{q-q'} + \text{H.c.}\,, \tag{2d}$$

$$H_{21} = \sum_{qq'} V^{(2)}_{qq'} a_q a_{q'} b^{\dagger}_{q+q'} + \text{H.c.}\,, \tag{2e}$$

and

$$H_{22} = \sum_{qq'} V^{(2)}_{qq'} a^{\dagger}_q a_{q'} b_{q-q'} + \text{H.c.}\,, \tag{2f}$$

where $V^{(1)}$ and $V^{(2)}$ are the corresponding matrix elements of the interaction potential. Finally,

$$H_f = \sum_{q} \varphi_q a^{\dagger}_q + \text{H.c.} \tag{2g}$$

represents the energy of interaction between the pumping source and the polar modes: φ ($\varphi^{\dagger}$) are annihilation (creation) operators of excitations in the source, also containing the coupling strength. Furthermore, we introduce — as required by NESOM — the partial Hamiltonians

$$H_0 = H_{01} + H_{02}$$

and

$$H' = H_{11} + H_{12} + H_{21} + H_{22} + H_f .$$

To deal with this system in NESOM the first step is to define the basic set of variables deemed appropriate for the description of its macroscopic state. We choose the populations of the polar vibrations

$$\nu_q = \mathrm{Tr}\{a_q^\dagger a_q \varrho(t)\} \equiv \mathrm{Tr}\{\hat{\nu}_q \varrho(t)\} , \tag{3}$$

and the energy of the free subsystem of acoustic vibrations (bath)

$$E_b(t) = \mathrm{Tr}\Big\{\sum_{q'} sq'(b_{q'}^\dagger b_q + \frac{1}{2})\Big\} , \tag{4}$$

where $\varrho(t)$ is the nonequilibrium statistical operator (NESO) in Zubarev's approach [19]. We recall that the acoustic modes act as a thermal bath for the polar mode remaining in an equilibrium state at constant temperature T, while in contact with a thermal reservoir providing a efficient homeostatic mechanism. Hence, the NESOM auxiliary operator [17,19] is, in this case,

$$\bar{\varrho}(t,0) = \exp\Big\{-\phi(t) - \sum_q F_q(t)\hat{\nu}_q - \beta H_{02}\Big\} , \tag{5}$$

where $\beta = 1/k_B T$ and $F_q(t)$ are nonequilibrium thermodynamic parameters conjugated to the dynamical variable ocupation number of polar vibrations, $\phi(t)$ is Massieu-Planck functional that ensures its normalization and β is time independent because of the assumption that T is kept constant. Therefore, we are simply left witt equations of evolution for the population of the polar modes, then characterizing the nonequilibrium dissipa tive thermodynamic state of the system.

As noted in the Introduction, these equations are derived by resorting to the nonlinear quantum generalized transport theory that NESOM provides [18]. But the collision operator they define, which contains highly nonlinear, nonlocal, and memory effects, is extremely difficult to handle in practical calculations; however, through an appropriate mathematical manipulation it can be rewritten in terms of an infinite series of partial collision operators which are instantaneous in time [given as averages over the auxiliary NESO — that of Eq. (5) in our case — at the time of measurement] and organized in increasing powers n of the interaction strengths [18]. The form of the collision operator thus obtained permits us to introduce approximations by means of a truncation of the series of partial collision operators in a given order of interaction. The lowest order that introduces relaxation effects is a truncation in second order in the interaction strengths, the SOART referred to in the Introduction: it renders the equations Markovian in character [17,18,20]. We resort here to this approximation; it produces the nonlinear contributions relevant to the question in hand, with the higher-order terms given small modifications. The NSOM-SOART equation of evolution for the mode populations are

$$\frac{d}{dt}\nu_q = J_q^{(0)} + J_q^{(1)} + J_q^{(2)} , \tag{6}$$

where

$$J_q^{(0)} = \mathrm{Tr}\{\frac{1}{\mathrm{i}\hbar}[a_q^\dagger a_q, H_0]\bar{\varrho}(t,0)\} , \tag{7a}$$

$$J_q^{(1)} = \mathrm{Tr}\{\frac{1}{\mathrm{i}\hbar}[a_q^\dagger a_q, H']\bar{\varrho}(t,0)\} , \tag{7b}$$

$$\begin{aligned} J_q^{(2)} &= (\mathrm{i}\hbar)^{-2}\int_{-\infty}^{0} dt' \mathrm{e}^{\varepsilon t'}\,\mathrm{Tr}\Big\{[H'(t'),[H',a_q^\dagger a_q]]\bar{\varrho}(t,0)\Big\} \\ &\quad + (\mathrm{i}\hbar)^{-1}\int_{-\infty}^{0} dt' \mathrm{e}^{\varepsilon t'}\frac{\delta J_q^{(1)}(t)}{\delta \nu_q(t)}\,\mathrm{Tr}\Big\{[a_q^\dagger a_q, H']\bar{\varrho}(t,0)\Big\} , \end{aligned} \tag{7c}$$

where δ stands for functional derivative, $\bar{\varrho}$ is given by Eq. (5), and Zubarev's approach was used.

In the NSOM-SOART calculation for the equations of evolution for the polar mode populations, it results that because of the symmetry properties of the system and the selected choice of the basic variables — and thus the form of the auxiliary NESO of Eq. (5) — several contributions are null, namely, $J^{(0)}$ and $J^{(1)}$. There remains only the first contribution to $J^{(2)}$, which produces a result that correspond to the golden rule of quantum mechanics averaged with the auxiliary nonequilibrium statistical operator of Eq. (5); performing the required calculations we finally obtain

$$\begin{aligned}
\frac{d}{dt}\nu_q(t) = I_q(\omega) &- \frac{2\pi}{\hbar^2}\sum_{q'}|V^{(1)}_{qq'}|^2\{\nu^b_{q'}(1+\nu^b_{q+q'})\nu_q(t)-(1+\nu^b_{q'})\nu^b_{q+q'}[1+\nu_q(t)]\}\delta(s|\mathbf{q}+\mathbf{q}'|-s|\mathbf{q}'|-\omega_q) \\
&- \frac{2\pi}{\hbar^2}\sum_{q'}|V^{(1)}_{qq'}|^2\{(1+\nu^b_{q'})(1+\nu^b_{q-q'})\nu_q(t)-\nu^b_{q'}\nu^b_{q-q'}[1+\nu_q(t)]\}\delta(s|\mathbf{q}-\mathbf{q}'|-s|\mathbf{q}'|-\omega_q) \\
&- \frac{2\pi}{\hbar^2}\sum_{q'}|V^{(2)}_{qq'}|^2\{(1+\nu^b_{q+q'})\nu_{q'}(t)\nu_q(t)-\nu^b_{q+q'}[1+\nu_{q'}(t)][1+\nu_q(t)]\}\delta(s|\mathbf{q}+\mathbf{q}'|-\omega_{q'}-\omega_q) \\
&- \frac{2\pi}{\hbar^2}\sum_{q'}|V^{(2)}_{qq'}|^2\{(1+\nu^b_{q-q'})[1+\nu_{q'}(t)]\nu_q(t)-\nu^b_{q\ q'}\nu_{q'}(t)[1+\nu_q(t)]\}\delta(s|\mathbf{q}-\mathbf{q}'|+\omega_{q'}-\omega_q) \\
&- \frac{2\pi}{\hbar^2}\sum_{q'}|V^{(2)}_{qq'}|^2\{\nu^b_{q-q'}[1+\nu_{q'}(t)]\nu_q(t)-(1+\nu^b_{q\ q'})\nu_{q'}(t)[1+\nu_q(t)]\}\delta(s|\mathbf{q}-\mathbf{q}'|-\omega_{q'}+\omega_q) \qquad (8)
\end{aligned}$$

We recall that q when referred to the polar modes runs over the Brillouin zone ($-\pi/a \le q \le \pi/a$), and that the Hamiltonian of Eq. (1) already contains information on the conservation of the linear momentum; in the equation above the δ functions take care of the conservation of energy in the collision events. Furthermore, we expressed the time-dependent correlations involving the operators associated to the external source in terms of a spectral density, namely,

$$\frac{2\pi}{\hbar^2}\langle\varphi_q(t)\varphi_q^\dagger\rangle = \int_{-\infty}^{\infty}\frac{d\omega}{\pi}I_q(\omega)\mathrm{e}^{i\omega t} \qquad (9)$$

where $I_q(\omega)$ represents the intensity of the source over the spectrum of frequencies. Finally, ν^b_q is the population of the acoustic vibrational modes, namely,

$$\nu^b_q = [\exp(\beta s q) - 1]^{-1}\,. \qquad (10)$$

Taking into account Eq. (10) and using the energy-conserving δ functions, Eqs. (8) can be rewritten as

$$\begin{aligned}
\frac{d}{dt}\nu_q(t) = I_q(\omega) &- \frac{2\pi}{\hbar^2}\sum_{q'}|V^{(1)}_{qq'}|^2\nu^b_q\nu^b_{q+q'}\mathrm{e}^{\beta\hbar\omega^b_{q'}}\left[\frac{\nu_q(t)}{\nu^0_q}-1\right]\delta(s|\mathbf{q}+\mathbf{q}'|-s|\mathbf{q}|-\omega_q) \\
&- \frac{4\pi}{\hbar^2}\sum_{q'}|V^{(1)}_{qq'}|^2\nu^b_q\nu^b_{q-q'}\left[\frac{\nu_q(t)}{\nu^0_q}-1\right]\delta(s|\mathbf{q}-\mathbf{q}'|+s|\mathbf{q}|-\omega_q) \\
&- \frac{2\pi}{\hbar^2}\sum_{q'}|V^{(2)}_{qq'}|^2\nu^b_{q+q'}\left\{[1+\nu_{q'}(t)][1+\nu_q(t)]-\nu_{q'}(t)\nu_q(t)\mathrm{e}^{\beta\hbar\Omega_{qq'}}\right\}\delta(s|\mathbf{q}+\mathbf{q}'|-\omega_{q'}-\omega_q)
\end{aligned}$$

$$-\frac{2\pi}{\hbar^2}\sum_{q'}|V^{(2)}_{\boldsymbol{q}\boldsymbol{q}'}|^2\nu^b_{\boldsymbol{q}-\boldsymbol{q}'}\left\{\nu_{\boldsymbol{q}'}(t)\,[1+\nu_{\boldsymbol{q}}(t)]-[1+\nu_{\boldsymbol{q}'}(t)]\,\nu_{\boldsymbol{q}}(t)\mathrm{e}^{\beta\hbar\Omega_{qq'}}\right\}\delta(s|\boldsymbol{q}-\boldsymbol{q}'|+\omega_{\boldsymbol{q}'}-\omega_{\boldsymbol{q}})$$
$$-\frac{2\pi}{\hbar^2}\sum_{q'}|V^{(2)}_{\boldsymbol{q}\boldsymbol{q}'}|^2\nu^b_{\boldsymbol{q}-\boldsymbol{q}'}\left\{\nu_{\boldsymbol{q}'}(t)\,[1+\nu_{\boldsymbol{q}}(t)]\,\mathrm{e}^{-\beta\hbar\Omega_{qq'}}-[1+\nu_{\boldsymbol{q}'}(t)]\,\nu_{\boldsymbol{q}}(t)\right\}\delta(s|\boldsymbol{q}+\boldsymbol{q}'|-\omega_{\boldsymbol{q}'}-\omega_{\boldsymbol{q}}) \tag{11}$$

where

$$\Omega_{\boldsymbol{q}\boldsymbol{q}'}=\omega_{\boldsymbol{q}}+\omega_{\boldsymbol{q}'} \tag{12a}$$

$$\Delta_{\boldsymbol{q}\boldsymbol{q}'}=\omega_{\boldsymbol{q}}-\omega_{\boldsymbol{q}'} \tag{12b}$$

and $\nu^0_{\boldsymbol{q}}$ is the population in equilibrium (at temperature T) of the polar vibrational mode.

Equation (11) is the type of equation proposed by Fröhlich. On the right-hand side of Eq. (11), besides the pump term, which is the first one, the next two terms are associated to relaxation (decay) of the polar excitations to the thermal bath (related to H_{11} and H_{12}); the fourth, arising out of H_{21} is also a relaxation term of the vibrational mode; the last two terms are contributions arising from H_{22}, that we call Fröhlich terms, because those are response for the transfer of excitations to the low frequency polar modes. In fact, given mode $\boldsymbol{q}$, if $\omega_{\boldsymbol{q}} \leq \omega_{\boldsymbol{q}'}$, the bilinear terms containing $\nu_{\boldsymbol{q}}(t)\nu_{\boldsymbol{q}'}(t)$ lead to an increase in population for it, at the expense of the other $\boldsymbol{q}'$ modes. It has been argued [21] that contributions coming from the fourth term wash away the effect of contributions arising out of H_{22}, but Fröhlich has countered [22] that it has a small contribution as a result of the different form of energy conservation in both processes as, in fact, characterized by the δ functions in Eq. (8); we anticipate that for the parameters we use in our numerical calculations contributions arising from H_{21} are identically null.

To proceed further, we model the dispersion relation of the polar modes by a parabolic law, namely

$$\omega_{\boldsymbol{q}}=\omega_0-\alpha q^2\,, \tag{13}$$

where ω_0 and α are constant parameters. It should be noticed that this form for the dispersion law implies a maximum value ω_0 at the zone center and a minimum value at the zone boundaries. Also, the second and third terms on the right-hand side of Eq. (11) are written as

$$-\frac{1}{\tau_{\boldsymbol{q}}}(\nu_{\boldsymbol{q}} - \nu_{\boldsymbol{q}}^0) \tag{14}$$

which introduces the relaxation time

$$\tau_{\boldsymbol{q}}^{-1} = \frac{2\pi}{\hbar^2}\frac{1}{\nu_{\boldsymbol{q}'}^0}\sum_{\boldsymbol{q}'}|V_{\boldsymbol{q}\boldsymbol{q}'}^{(1)}|\nu_{\boldsymbol{q}'}^b\nu_{\boldsymbol{q}+\boldsymbol{q}'}^b e^{\beta\hbar s|\boldsymbol{q}'|}\delta(s|\boldsymbol{q}+\boldsymbol{q}'| - s|\boldsymbol{q}'| - \omega_{\boldsymbol{q}}) + \delta(s|\boldsymbol{q}-\boldsymbol{q}'| + s|\boldsymbol{q}'| - \omega_{\boldsymbol{q}}) . \tag{15}$$

Because of the choice given by Eq. (13) we are now in condition to evaluate the energy-conserving δ functions, i.e., to determine the values of q' that they fix. This requires one to look for the roots of the equations,

$$f_{11} \equiv \omega_0 - \alpha q^2 + s|\boldsymbol{q}'| - s|\boldsymbol{q}+\boldsymbol{q}'| , \tag{16a}$$

$$f_{12} \equiv \omega_0 - \alpha q^2 - s|\boldsymbol{q}'| - s|\boldsymbol{q}-\boldsymbol{q}'| , \tag{16b}$$

$$f_2 \equiv 2\omega_0 - \alpha(q^2 + q'^2) - s|\boldsymbol{q}+\boldsymbol{q}'| , \tag{16c}$$

$$f_3 \equiv \alpha(q'^2 - q^2) - s|\boldsymbol{q}-\boldsymbol{q}'| , \tag{16d}$$

$$f_4 \equiv \alpha(q'^2 - q^2) + s|\boldsymbol{q}-\boldsymbol{q}'| . \tag{16e}$$

In one dimension the vectors $\boldsymbol{q}$ and $\boldsymbol{q}'$ take the values q and q', positive or negative. Taking this into account we have the following:

(1) The roots of f_{11} are

$$q'_{11} = \begin{cases} -(\omega_0 - \alpha q^2 + sq)/2s, & \text{if } q' > 0 \text{ and } q + q' < 0 , \\ (\omega_0 - \alpha q^2 - sq)/2s , & \text{if } q' < 0 \text{ and } q + q' > 0 ; \end{cases} \tag{17a}$$

what implies that $\omega_0 - \alpha q^2 \pm sq < 0$.

(2) The roots of f_{12} are

$$q'_{12} = \begin{cases} (\omega_0 - \alpha q^2 + sq)/2s, & \text{if } q' > 0 \text{ and } q - q' < 0\,, \\ -(\omega_0 - \alpha q^2 - sq)/2s\,, & \text{if } q' < 0 \text{ and } q - q' > 0\,; \end{cases} \tag{17b}$$

what implies that $\omega_0 - \alpha q^2 \pm sq > 0$.

(3) The roots of f_2 are

$$q'^{(1)}_{2\pm} = \frac{s}{2\alpha} \pm \sqrt{\left(\frac{s}{2\alpha}\right)^2 - q^2 + \left(\frac{s}{\alpha}\right) q + \frac{2\omega_0}{\alpha}}\,, \qquad \text{if } q + q' > 0 \tag{17c}$$

$$q'^{(2)}_{2\pm} = -\frac{s}{2\alpha} \pm \sqrt{\left(\frac{s}{2\alpha}\right)^2 - q^2 - \left(\frac{s}{\alpha}\right) q + \frac{2\omega_0}{\alpha}}\,, \qquad \text{if } q + q' < 0\,. \tag{17d}$$

(4) The roots of f_3 are $q'_2 = q$ and

$$q'_2 = \begin{cases} -q - s/\alpha\,, & \text{if } q - q' > 0 \text{ and } q > -s/2\alpha\,, \\ -q + s/\alpha\,, & \text{if } q - q' < 0 \text{ and } q < s/2\alpha\,; \end{cases} \tag{17e}$$

(5) The roots of f_4 are $q'_3 = q$ and

$$q'_3 = \begin{cases} -q - s/\alpha\,, & \text{if } q - q' < 0 \text{ and } q < -s/2\alpha\,, \\ -q + s/\alpha\,, & \text{if } q - q' > 0 \text{ and } q > s/2\alpha\,. \end{cases} \tag{17f}$$

It should be noted that the δ functions in Eqs. (11) produce δ functions in the variable of the integration q' through the known relation

$$\delta(f_j(q')) = \sum_n \left| \frac{df_j}{dq'} \right|^{-1} \delta(q' - q'_{jn}) \tag{18}$$

where n runs over all the roots of f_j.

To further simplify matters, but without losing the fundamental characteristics of the model, we take the matrix elements $V^{(1)}_{qq'}$ and $V^{(2)}_{qq'}$ as constants, V_1 and V_2, respectively. We go over the quasicontinuum (large system) in the reciprocal space, i.e., in one dimension,

$$\sum_q \to \frac{L}{2\pi} \int dq \,, \tag{19}$$

where L is the length of the chain, the limits of integration are for the values q of the polar vibrations $Q_0 = \pi/a$ and $-Q_0 = -\pi/a$, i.e., the end values of the Brillouin zone, and those for the values of q' of the mode of vibrations in the continuum are in the interval Q_D and $-Q_D$, i.e., the Debye wave number fixed by the Debye cutoff frequency; we assume that $Q_D \gg Q_0$. Introducing the time scale $\bar{\tau} = \hbar^2 s/L|V_1|^2$ and the reduced time $\tau = t/\bar{\tau}$, the coefficient $\lambda = |V_2|^2/|V_1|^2$, and taking into account the expressions for the energy conserving δ functions as given by Eqs. (17) and (18), we find that

$$\frac{d}{dt}\nu_q = S_q - \frac{\gamma(q)}{\nu_q}[\nu_q - \nu_q^0] + R_1(q) + R_2(q) \,, \tag{20}$$

where

$$S_q = I_q \bar{\tau} \,, \tag{21a}$$

$$\begin{aligned}
\gamma(q) = {} & s \int_{-Q_D}^{Q_D} dq' \, \nu_{q'}^b \nu_{q+q'}^b e^{\beta\hbar s|q'|} \left\{ \frac{1}{2s}[1 - \Theta(q + q')]\Theta(q')\delta(q' + (\omega_0 - \alpha q^2 + sq)/2s) \right. \\
& \left. + \frac{1}{2s}\Theta(q + q')[1 - \Theta(q')]\delta(q' - (\omega_0 - \alpha q^2 - sq)/2s) \right\} \\
& + s \int_{-Q_D}^{Q_D} dq' \, \nu_{q'}^b \nu_{q-q'}^b \left\{ \frac{1}{2s}[1 - \Theta(q - q')]\Theta(q')\delta(q' - (\omega_0 - \alpha q^2 + sq)/2s) \right. \\
& \left. + \frac{1}{2s}\Theta(q - q')[1 - \Theta(q')]\delta(q' + (\omega_0 - \alpha q^2 - sq)/2s) \right\} \,,
\end{aligned} \tag{21b}$$

$$\begin{aligned}
R_1(q) = {} & \lambda s \int_{-Q_D}^{Q_D} dq' \nu_{q+q'}^b [(1 + \nu_{q'})(1 + \nu_q) - \nu_{q'}\nu_q e^{\beta\hbar\Omega_{qq'}}] \\
& \times \left(\frac{\Theta(q + q')\{\delta(q' - q_{2+}'^{(1)}) + \delta(q' - q_{2-}'^{(1)})\}}{\sqrt{s^2 - 4\alpha^2 q^2 - 16\alpha s q + 8\alpha\omega_0}} \right. \\
& \left. + \frac{[1 - \Theta(q + q')]\{\delta(q' - q_{2+}'^{(2)}) + \delta(q' - q_{2-}'^{(2)})\}}{\sqrt{s^2 - 4\alpha^2 q^2 + 16\alpha s q + 8\alpha\omega_0}} \right) \,,
\end{aligned} \tag{21c}$$

$$
\begin{aligned}
R_2(q) = \lambda s \int_{-Q_0}^{Q_0} & dq' \nu^b_{q-q'} [\nu_{q'}(1+\nu_q) - (1+\nu_{q'})\nu_q e^{\beta\hbar\Delta_{qq'}}] \\
& \times \left\{ \frac{1}{|2\alpha q + s|} \Theta(q-q')\Theta(q+s/2\alpha)\delta(q'+q+s/\alpha) \right. \\
& \left. + \frac{1}{|2\alpha q - s|} [1-\Theta(q-q')][1-\Theta(q-s/2\alpha)]\delta(q'+q-s/\alpha) \right\} \\
& + \lambda s \int_{Q_0}^{Q_0} dq' \nu^b_{q-q'} [\nu_{q'}(1+\nu_q) e^{-\beta\hbar\Delta_{qq'}} - (1+\nu_{q'})\nu_q] \\
& \times \left\{ \frac{1}{|2\alpha q + s|} [1-\Theta(q-q')][1-\Theta(q+s/2\alpha)]\delta(q'+q+s/\alpha) \right. \\
& \left. + \frac{1}{|2\alpha q - s|} \Theta(q-q')\Theta(q-s/2\alpha)\delta(q'+q-s/\alpha) \right\} ,
\end{aligned}
\tag{21d}
$$

where $\Theta(x)$ is Heaviside's step function accounting for the step limitations imposed on q' by Eqs. (17). It should be noted that in R_2 the contributions from the roots $q' = q$ in f_3 and f_4 are null. Furthermore, we recall that $-Q_0 \leq q \leq Q_0$, and it should be noted that Eq. (20) is invariant under the inversion operation in which q and q' change in $-q$ and $-q'$.

For the sake of simplicity, we already take into account that for the values to be used later on for numerical calculations the first term in γ is null as well as the term R_1. Hence, leaving aside these contributions, performing the integrations in Eqs. (21) we find that (q, next, is the vector in one dimension)

$$
\begin{aligned}
\frac{d}{d\tau}\nu_q = & S_q - \frac{\gamma(q)}{\nu^0_q}[\nu_q - \nu^0_q] \\
& + \Theta(q + \frac{s}{2\alpha})\lambda\varphi(q)[\nu_{q+\frac{s}{\alpha}}(1+\nu_q) - e^{\beta\hbar s(2q+\frac{s}{\alpha})}(1+\nu_{q+\frac{s}{\alpha}})\nu_q] \\
& + [1 - \Theta(q - \frac{s}{\alpha})]\lambda\psi(q)[\nu_{q-\frac{s}{\alpha}}(1+\nu_q) - e^{-\beta\hbar s(2q-\frac{s}{\alpha})}(1+\nu_{q-\frac{s}{\alpha}})\nu_q] \\
& + [1 - \Theta(q + \frac{s}{\alpha})]\lambda\phi(q)[\nu_{q+\frac{s}{\alpha}}(1+\nu_q)e^{-\beta\hbar s(2q+\frac{s}{\alpha})} - (1+\nu_{q+\frac{s}{\alpha}})\nu_q] \\
& + \Theta(q - \frac{s}{2\alpha})\lambda\psi(q)[\nu_{q-\frac{s}{\alpha}}(1+\nu_q)e^{\beta\hbar s(2q-\frac{s}{\alpha})} - (1+\nu_{q-\frac{s}{\alpha}})\nu_q] ,
\end{aligned}
\tag{22}
$$

where now

$$y(q) = \frac{1}{2}[e^{\beta\hbar|\omega_0 - \alpha q^2 - sq|/2} - 1]^{-1}[e^{\beta\hbar|\omega_0 - \alpha q^2 + sq|/2} - 1]^{-1} \tag{23a}$$

$$\varphi(q) = \frac{s}{|2\alpha q + s|}(e^{\beta\hbar s}|q + \frac{s}{\alpha}| - 1) , \tag{23b}$$

$$\psi(q) = \frac{s}{|2\alpha q - s|}(e^{\beta\hbar s}|q - \frac{s}{\alpha}| - 1) . \tag{23c}$$

We can see that in the all important term $R_2(q)$ (the one containing the nonlinear contributions) not all the polar modes are coupled, but those that differ between them in a spacing given by $\pm s/\alpha$, and are contained in the Brillouin zone. Hence, the modes contained in each segment of the extension s/α are, each mode independently, coupled to a finite number $2\bar{n}$ of modes outside it, such that $\bar{n}$ equals the integer part of $[\pi\alpha/sa]$. For example, if the set contains the mode at the zone center, $q = 0$, then the coupled modes are $\{+0, \pm s/\alpha; \pm 2s/\alpha; \ldots; \pm js/\alpha\}$ and the set that contains the end zone vector $Q_0 = \pi/\alpha$ is $\{Q_0; Q_0 - s/\alpha; Q_0 - 2s/\alpha; \ldots; Q_0 - (\bar{n} - 1)s/\alpha\}$. The bilinear terms connect the mode q to the modes $q - s/\alpha$ and $q + s/\alpha$, in a process of transmission of energy from each mode q for the next lower in energy. Furthermore, we recall that because of symmetry considerations modes with negative wave vectors are equivalent to those with a positive value, Having set the equations of evolution for the populations of the coupled modes let us first consider the stationary states that should follow after a certain transient, to be determined later on in this section, have elapsed. The steady state is the solution of Eqs. (22) when setting $d\nu/d\tau = O$. It is worth noting that in NESOM, because of the form of the auxiliary operator of Eq. (5), one finds that

$$\nu_q = 1/[e^{F_q} - 1] , \tag{24}$$

i.e., the populations can be expressed in terms of the unknown nonequilibrium thermodynamic parameter F_q. In particular, we may choose the alternative form

$$F_q = \beta[\hbar\omega_q - \mu_q] , \tag{25}$$

and then Eq. (24) resembles a Bose-Einstein distribution but with a quasichemical potential for each mode μ_q, thus being of the form proposed by Fröhlich [7]. Clearly, replacing Eq. (25) in Eq. (24), and the latter for ν_q in the steady-state equation of evolution, one gets an equation for the quasichemical potential in terms of the populations of different modes. This quasichemical potential increases with growing external pumping energy and then may signal a kind of Bose-Einstein condensation if at some critical intensity μ_q coincides with $\hbar\omega_q$. This implies the possibility of emergence of the Fröhlich effect as described in the Introduction. The formal character of the quasichemical potential per mode, μ_q, should be stressed, while F_q is the nonequilibrium intensive thermodynamic parameter that NESOM introduces, that is, Eq. (25) is an arbitrary choice deemed appropriate for the physical discussion of the problem. A quasichemical potential for the characterization of the population of nonequilibrium photons in the case of a nonequilibrium state of radiation and carriers in semiconductors was also used by Landsberg [23].

Returning to Eqs. (22) in the steady state, we proceed to obtain their numerical solution using an adaptation of a known computational algorithm [24]. For that purpose we need to introduce numerical values for the parameters involved; we take for them values that are typical of the biopolymers involved [7,15,16], namely,

$$\omega_0 = 10^{13}\ \text{Hz}\,; \qquad a = 100\ \text{Å}\,;$$

$$s = 10^{5}\text{cm/s}\,; \qquad \alpha = 0.19\ \text{cm}^2/\text{s}\,;$$

that is we simply take values within the order of magnitude to be expected in such types of systems, e.g., the α-helix protein of Fig. 1. We stress that the characteristic behavior to be derived, as shown in Figs. 2–7, is independent of the numerical parameters, that is, the qualitative aspects remain but, of course, with changing numeric results. With these values it results that the end Brillouin-zone wave number is $Q_O = 3.14\times10^{6}\ \text{cm}^{-1}$; the width of the frequency spectrum of the polar modes $\Gamma = 1.87\times10^{12}$ Hz; the ratio $s/\alpha = 5.27\times10^{5}\ \text{cm}^{-1}$ and then the number $\bar{n}$ of coupled modes is 12. The bath temperature is taken as 300 K. There is an open parameter, viz. λ, that measures —

as its definition indicates the ratio of the coupling strengths involved in the nonlinear and linear (in the polar mode populations) anharmonic interactions; we will obtain solutions for sever values of this parameter.

We consider the set that contains the mode at the zone center ($q = 0$), which is assumed to be the only one pumped by the external source, and we solve the equations of evolution for the populations ν_q for the values $\lambda = 1$ and 0.01; the results are shown in Figs. 2(a) and (2b).

Next, we consider the more realistic case of all modes being pumped, and such that $S_q = S$, and $\lambda = 1$ with the corresponding curves shown in Fig. 3.

Inspection of these curves clearly shows a complex behavior of the system: at a given threshold of the intensity S of the pumping source (we recall that S is a scaled quantity for the amplitude of the intensity in the spectral representation of Eq. (9); cf. Eq. (21a)] the mode with the lowest frequency begins to grow enormously, in a very steep fashion with increasing intensity S. The quasichemical potential associated with this mode tends asymptotically from below to the value of the frequency of the mode, but does not coincide with it; see Fig. 4. At and beyond the threshold intensity (indicated in an estimative way by the arrows) this very close approach of the quasichemical potential to the frequency of this lowestfrequency mode leads to a near Bose-Einstein condensation, in the sense that the distribution in the modes corresponds to a very large accumulation in the lowest-energy state. The comparison in Fig. 3 of the populations in the presence of the nonlinear coupling with those in the absence of coupling, allows us to better visualize the Fröhlich effect: the mode with the lowest energy has increased its population by almost an order of magnitude above the value expected for $\lambda = 0$, at the expenses of the other modes whose populations rest below the dashed line; some of them tend to a constant saturated value. After the critical intensity threshold has been achieved ν_1 grows quite steeply.

The first threshold intensity (at which there follows the steep increase in population of the lowest-frequency mode) is not strongly dependent on λ, which, we recall, measures the strength of the anharmonic interaction responsible for the nonlinear terms in the equations of evolution. This is shown in Fig. 5. Hence, the effect follows an intense form even at weak nonlinear contributions in the relevant (nonlinear) term that needs to be present for the phenomenon to arise.

Also, as previously mentioned, it has been argued that the anharmonic contribution contained in the fourth term in the Hamiltonian of Eq. (1) opposes and may eventually cancel the Fröhlich effect [21]. Fröhlich has replied that this is not so because the term should involve less important contributions to the kinetic equations [22]. Our calculations show this clearly; furthermore, for the particular numerical values of the parameters we use, the contribution from that term vanishes, because in the scattering events it produces it cannot be simultaneously satisfied by the conservation of energy and momentum.

Our results then show that protein polymers of the type considered by Davydov [13-15] display complex behavior manifested in the emergence of the Fröhlich effect.

As already noted, the Fröhlich effect seems to be accompanied by the formation of an electret state [8,9] and the propagation of undamped waves [10,13-15]. Therefore, it is of relevance to determine the transient time. For that purpose, we solve the equations of evolution (22), using as an initial condition the values for the populations in equilibrium, resorting to an adaptation of a known computer program [25]. Figure 6 shows the evolution of the population of the six modes for case $\lambda = 1$ and $S = 5000$ (slightly above the critical value for the condensation to follow). We are then in a condition to evaluate the transient time before the steady state is reached. Comparing Eqs. (12) and (19b) we find that

$$\tau_q^{-1} = L|V_1|^2\gamma(q)/\hbar^2 s\nu_q^{(0)} = \gamma(q)/\nu_q^0\bar{\tau} \ . \tag{26}$$

Assuming these relaxation times to the bath being of the order of tens of picoseconds [7,16], we estimate the scale factor $\bar{\tau}$ to be roughly 20 ps, and so the transient times are of this order or smaller (see Fig. 4).

Finally, after solving the set of 12 coupled equations for several different sets of 12 coupled modes, we are able to show in Fig. 7 the dependence of the mode populations along the interval of frequencies in the polar branch of vibrations. The region of low frequencies privileged by the onset of the Fröhlich effect is evident. We have already noted that the results described in the series of figures retain their qualitative characteristics when the numerical values of the parameters of the system are changed. Consider, for example, the case when the cell parameter is reduced by a factor of 4 (i.e., $a \simeq 25$ Å) to maintain the width of the frequency dispersion spectrum of the vibrations, parameter α needs to be reduced by a factor of 16. But now the number of coupled modes is 48. Numerical results are similar, but the main change is that the length of the region in frequency space (cf. Fig. 7) that includes the modes in the condensate is stretched by a factor of 4.

Furthermore, using the given value of $\bar{\tau}$, we find that for the critical intensity (for the onset of Fröhlich effect) $S^* = I^*\bar{\tau}$ being roughly 5000 (cf. Figs. 3 and 4), the value of the critical intensity I^* is roughly 5×10^{13} Hz, which implies for $\omega_0 = 10^{13}$ Hz a pumping power of 5×10^{-8} W per mode. Since the number of modes is LQ_0/π (where L is the length of the chain), for the numbers used this is $10^6 L$, and then the total pumped power is 5×10^{-2} W. Assuming that this power is provided through the hydrolysis of adenosine 5'-triphosphate (ATP), which produces 7.3 kcal/mol, in the event of absorption of a fraction f of this metabolic energy, to maintain the power intensity required would imply a rate of $-(L/f)(1.6 \times 10^{6})$ mol/s, or (Lf) mg/s of ATP. To obtain the stationary Fröhlich condensate, as seen, a time interval of the order of 10 ps is required, and then an expense of $-(L/f)(10^{-14})$ g of ATP, which seems to be very accessible values for the phenomenon to occur. Moreover, we have considered here that the source creates single excitations in the vibrational modes (cf. Eq. (2g)] but multiple excitations are also energetically possible, which, furthermore, are enhanced by the same effect of condensation when the modes lowest in frequency are externally pumped. In the next section we summarize and comment on the relevance of the phenomenon evidenced in this section.

3. CONCLUDING REMARKS

We have studied a model of a biological polymer, namely a chain of biomolecules such as the a-helix considered by Davydov [15], which is expected to possess polar modes of vibration. The latter are assumed to receive energy from an external pumping source, say, a metabolic feeding of these modes. At the same time, the polar modes interact with an elastic continuum via a nonlinear anharmonic-type potential. Equation (1) presents the Hamiltonian of this system. We studied the dissipative nonequilibrium state of the polar modes which is characterized by the populations of these modes of vibration. We derived for them the corresponding equations of evo lution resorting to the nonequilibrium statistical operator method [17], but in the approximation SOART for the nonlinear transport equations that can be built within the framework of NESOM [18]. Even though the equations couple, in principle, all the modes characterized by the wave vector $\boldsymbol{q}$ running over the whole Brillouin zone, conservation of energy and momentum in the scattering events allows for the separation of the whole set of coupled equations in reduced independent sets of equations composed of a certain number of modes. The equations of evolution for the populations of the polar modes of vi bration are solved under the assumption of a constant pumping of energy by the external source, and that the thermal bath of acousticlike vibrations is constantly kept in equilibrium with a reservoir at a constant temperature T (i.e., it is regulated by an efficient homeostatic mechanism),

We have been able to demonstrate that such a system displays a complex behavior, namely, that at a certain distance from equilibrium, i.e., for a threshold value of the pump intensity, there occurs a steep increase in the population of the modes with the lowest frequencies, in a way reminiscent of a Bose-Einstein condensation that we term *Fröhlich effect*. There is a kind of self-organization in the system, governed by the nonlinear effects in the equations of evolution and, thus, this phenomenon may be considered as the emergence of a dissipative structure in Prigogine's sense [26].

Clearly, a very large population in certain modes implies large amplitudes of vibrations, which may lead to a coherent effect among the vibrating units and to formation of some kind of space ordering; it has been suggested that this is an electretlike state, however, of a metastable character [8,9].

Furthermore, as is also shown elsewhere [10], a restudy of the propagation of the excitations in this media, not at the quantum-mechanical level but at the nonequilibrium statistical mechanical level that may describe, within NESOM, the far-from-equilibrium thermodynamic state of the open system, seems to indicate that beyond the point of emergence of Fröhlich's effect, polar waves propagate with a very weak damping. This appears to be of large interest for an eventual explanation of the effective energy transfer at the biomolecular level. At normal lifetimes, estimated in the picosecond range, vibrations cannot propagate further than a few micrometers, but beyond the critical point, as noted, the vibration lifetime is markedly increased and can propagate energy at long distances. Therefore, it is of relevance to determine the time interval (transient time) between the onset of excitation of the modes and the establishment of the steady state after the threshold for the Fröhlich effect: as shown in the last section it is estimated to be of the order of the relaxation time to the bath; if the latter is, as expected, in the tens of picosecond time scale, then the time of the transient is of the order of a few tens of picoseconds. Also, the threshold for Fröhlich effect, as our estimative presented in last section shows, may be attained with the use of the expending of low levels of power, i.e., a exceedingly small fraction of a mol of ATP molecules participating in energy-providing hydrolysis reactions.

The Fröhlich effect is then demonstrated to be present in biopolymers, like a large chain of protein molecules, that can sustain polar vibrations-like those originating in peptide groups. Its occurrence implies that the leading term for the phenomenon to arise-namely the nonlinear terms in Eq. (22) — whose origin was the anharmonic contribution contained in the term H_{22} of Eq. (2f) overcomes the opposing effects of relaxation to the thermal bath, arising out of H_{11} and H_{12} of Eqs. (2c) and (2d), and the contribution from the anharmonic interaction in H_{21} of Eq. (2e), which, we recall, has a null contribution in the particular case we used for numerical calculations. We stress that the Fröhlich effect is of purely quantum-mechanical origin, i.e., the Planckian form of the mean populations of the vibrations of the bath and the zero-point energy of their states: Taking the classical limit in Eq. (6) results in the cancellation of the nonlinear Fröhlich term. Finally, as shown, the phenomenon is dependent on the value of the coupling intensity, i.e., parameter λ, but it may follow even for very small values of it, and then it is possible under very broad circumstances.

It has been suggested as experimental evidence of the phenomenon [7] the investigation of the buildup of the reaction rate of enzyme molecules as a function of the enzyme density. In principle, it can be evidenced by direct observation of the excited vibrations, for example, with the use of scattering efflects, since the intensity of the Raman line is proportional to the population of the mode. It should be noticed that Raman scattering allows us to probe only long-wavelength modes, because of the small value of photon wave number in the visible, IR, and UV regions of the spectrum. The nonthermal amplification of polar modes has been determined in several experiments in materials displaying biological activity [27]. Additional possible experimental evidences have been discussed in Refs. [6], [7], [12], [16], and [28].

In conclusion, we can summarize the result by saying that, the Fröhlich effect, which can be related to important biophysical aspects in biopolymers (i) may be of easy realization (it suffices to have even a very weak nonlinear anharmonic coupling strength of the type described, and a weak threshold of pumping power), (ii) is produced very rapidly after the initial release of the pumping (metabolic) energy, and (iii) also, as preliminary calculations seem to indicate [10], once in its domain, signals can be propagated in the medium with almost no decay, and, then, at very long distances (the lifetime of the excitation is very large). Furthermore, it can be shown [10] that the vibrations propagate in a coherent way, and then all the characteristics for the propagation of biochemical energy in this kind of biosystem formally resemble the situation one finds for the case of electromagnetic waves in laser devices.

ACKNOWLEDGMENTS

One of us (M.V.M.) acknowledges support from the Brazilian National Research Council (CNPq); the other two authors (A.R.V., R.L.) acknowledge financial support from the Sao Paulo State Research Agency (FAPESP) and the Brazilian National Research Council (CNPq).

REFERENCES

[1] G. Nicolis, in *The New Physics,* edited by P. Davies (Cambridge University, Cambridge, 1989).

[2] I. Prigogine, in *Theoretical Physics and Biology,* edited by M. Marois (North-Holland, Amsterdam, 1969); Nature **246**, 67 (1973); Acta Phys. Austriaca Suppl. X, 401 (1973); I. Prigogine and G. Nicolis, Q. Rev. Biophys. **4**, 107 (1971); P. Glansdorff and I. Prigogine, *Thermodynamics of Structures, Stability, and Fluctuations* (Wiley interscience, New York, 1971).

[3] G. Nicolis and I. Prigogine, *Self-Organization in Nonequilibrium Systems* (Wiley Interscience, New York, 1977).

[4] H. Haken, *Synergetics* (Springer, Berlin, 1978).

[5] H. Fröhlich, Riv. Nuovo Cimento **3**, 490 (1973).

[6] H. Fröhlich, Phys. Lett. **26A**, 402 (1968); Int. J. Quantum Chem. **2**, 641 (1968); Nature **228**, 1093 (1970); Phys. Lett. **44A**, 385 (1973); **51A**, 21 (1975); Collect. Phenom. **3**, 139 (1981).

[7] H. Fröhlich, in *Advances in Electronics and Electron Physics,* edited by L. Marton (Academic, New York, 19801, Vol. 53, pp. 85-162.

[8] S. Mascarenhas, in *Electrets,* edited by G. M. Sessler, 2nd ed. (Springer, Berlin, 1987); H. Biltz, H. Büttner, and H. Fröhlich, Z. Naturforsch. B **36**, 208 (1981).

[9] J. A. Tuszýnski, R. Paul, R. Chatterjee, and S. R. Sreenivasan, Phys. Rev. A **30**, 2666 (1984).

[10] A. R. Vasconcellos and R. Luzzi, Phys. Rev. E **48**, 2246 (1993).

[11] T. M. Wu and S. Austin, Phys. Lett. **69A**, 151 (1977); J. Theor. Biol. **71**, 209 (1978).

[12] R. E. Mills, Phys. Rev. A **28**, 379 (1983).

[13] A. S. Davydov and N. I. Kislukha, Phys. Stat. Sol. B **59**, 465 (1973); A. S. Davydov, *ibid.* **75**, 735 (1976); J. Theor. Biol. **66**, 379 (1977); Int. J. Quantum Chem. **26**, 5 (1979); Phys. Scripta **20**, 387 (1979); Physica D **3**, 1 (1981).

[14] A. S. Davydov, in *Nonlinear and Turbulent Processes in Physics,* edited by R. Z. Sagdeev (Harwood, London, 1984).

[15] A. S. Davydov, *Biology and Quantum Mechanics* (Pergamon, Oxford, 1982).

[16] A. C. Scott, Phys. Rev. A **26**, 578 (1982); Phys. Scripta **25**, 651 (1982); The Sciences, March/April (1990), pp. 28–35; in *Dynamical Problems in Soliton Systems,* edited by S. Takeno (Springer, Berlin, 1985); Phys. Rep. **217**, 1 (1992).

[17] R. Luzzi and A. R. Vasconcellos, Fortschr. Phys. **38**, 887.

[18] L. Lauck, A. R. Vasconcellos, and R. Luzzi, Physica A **168**, 789 (1990).

[19] D. N. Zubarev, *Nonequilibrium Statistical Thermodynamics* (Plenum, New York, 1974).

[20] D. N. Zubarev, Nonequilibrium Statistical Thermodynamics (Ref. [19]), Chap. IV, Sec. 25.1; also V. P. Kalashnikov, Teor. Mat. Fiz. **9**, 94 (1971) [Theor. Math. Phys. (USSR) **9**, 1003 (1972)].

[21] M. A. Lifshitz, Biofiz. **17**, 694 (1972); also M. Y. Yushina, Phys. Lett. **91A**, 372 (1982).

[22] H. Fröhlich, Phys. Lett. **93A**, 105 (1982).

[23] P. T. Landsberg, J. Phys. C **14**, L1025 (1981).

[24] L. O. Chua and P. M. Lin, *Computer-Aided Analysis of Electronic Circuits* (Prentice-Hall, Englewood Cliffs, NJ, 1975).

[25] J. R. Cash, *Stable Recursions* (Academic, London, 1979).

[26] I. Prigogine and I. Stengers, *Order out of Chaos* (Bantam, New York, 1984); I. Prigogine, G. Nicolis, and A. Babloyantz, Phys. Today **25**, 28 (1972); **25**, 39 (1972).

[27] S. J. Webb, Phys. Rep. **60**, 201 (1980).

[28] R. Paul, O. G. Fritz, and R. Chatterjee, Int. J. Quantum Chem. Symp. **15**, 191 (1988).

FIGURE CAPTIONS

Figure 1: An atomic model of the α-helix structure in a protein (Refs. [15] and [16]), and on the right a rough description of the mechanical model considered in the text.

Figure 2: The population of the different coupled modes, in a set that contains $q = 0$, as a function of the scaled intensity S for (a) $\lambda = 1$ and (b) $\lambda = 0.01$. Mode $q = 0$ is the only one pumped. Index 6 stands for $q = 0$; 5 for $q - s/\alpha, \ldots, 1$ for $q - 5s/\alpha$ (mode 1 is the one with the lowest frequency).

Figure 3: As in the case of Fig. 1 but now with all modes equally pumped and $\lambda = 1$. The dashed curve is the result $\lambda = 0$ (uncoupled modes), when the population of the different twelve modes is roughly the same.

Figure 4: The dependence on the scaled intensity of the quasichemical potential of the lowest-frequency mode (arrows indicate the approximate onset of condensation).

Figure 5: Behavior of population of the lowest-frequency mode ν_1, for different values of the coupling strength.

Figure 6: Evolution in time of the populations of the modes for $\lambda = 1$ and $S = 5000$.

Figure 7: The population of the modes in the band containing their frequencies of vibration, namely, $\omega_0 - \alpha(\pi/a)^2 \leq \omega \leq \omega_0$.

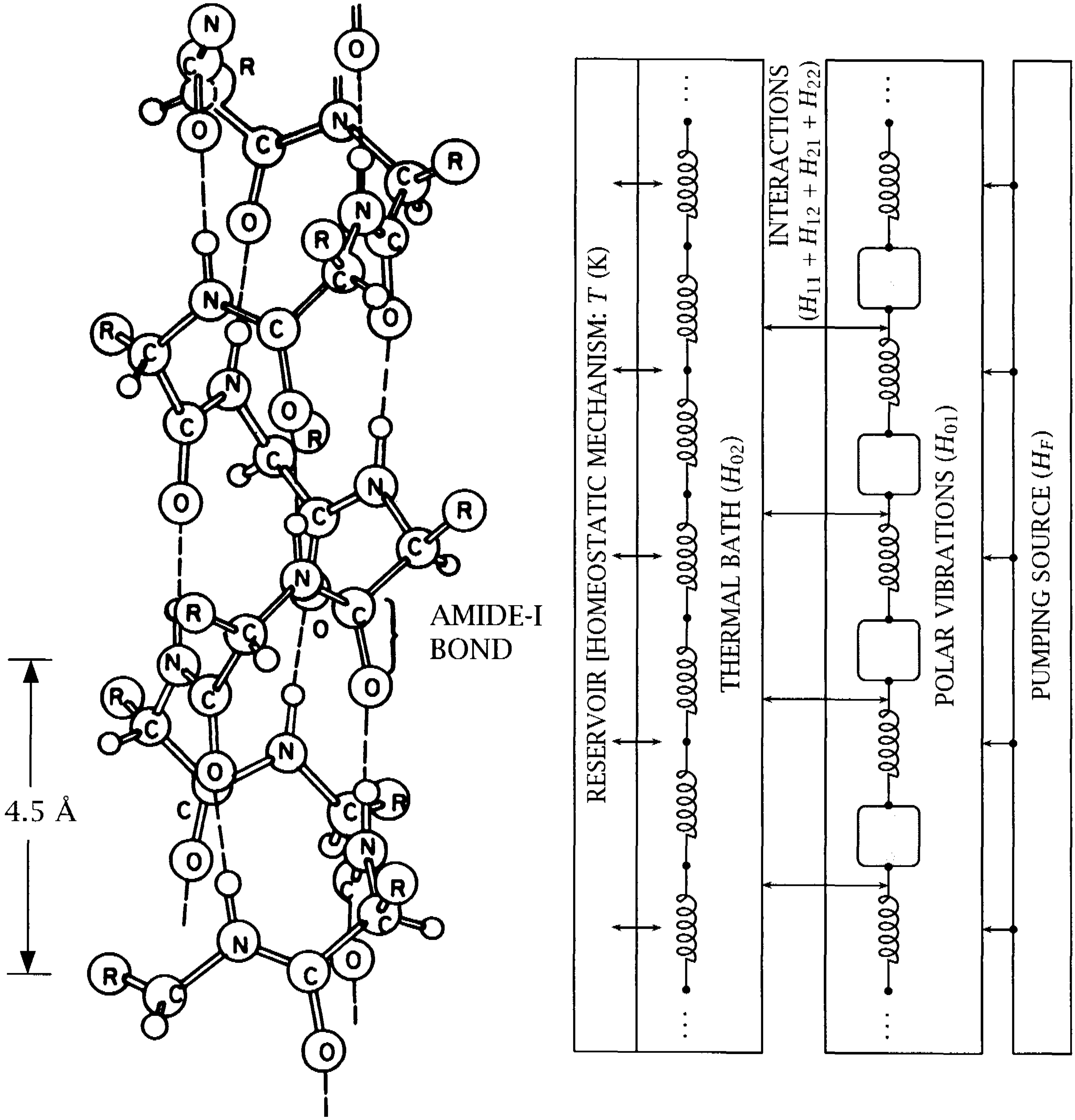

Figure 1: An atomic model of the α-helix structure in a protein (Refs. [15] and [16]), and on the right a rough description of the mechanical model considered in the text.

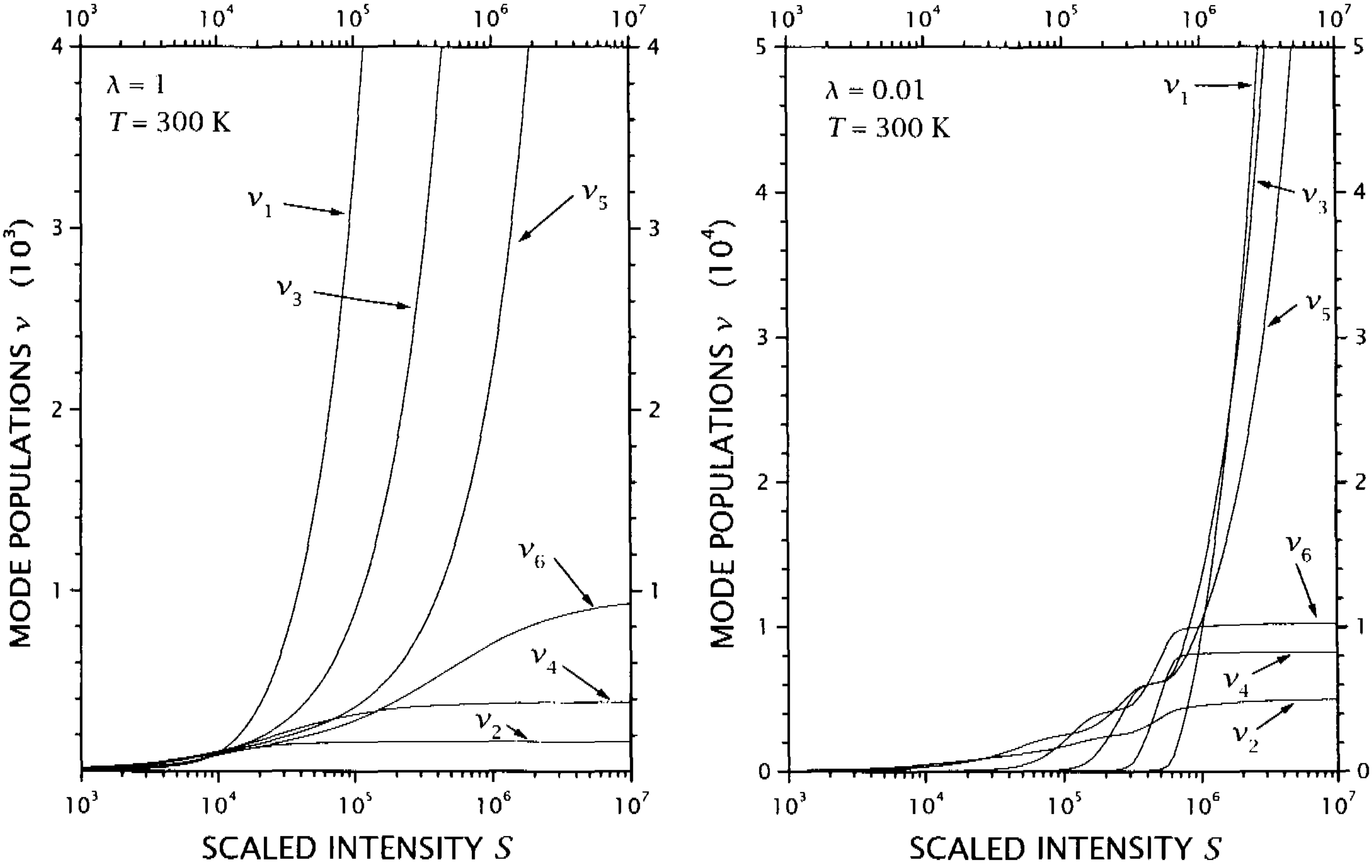

Figure 2: The population of the different coupled modes, in a set that contains $q = 0$, as a function of the scaled intensity S for (a) $\lambda = 1$ and (b) $\lambda = 0.01$. Mode $q = 0$ is the only one pumped. Index 6 stands for $q = 0$; 5 for $q - s/\alpha, \ldots, 1$ for $q - 5s/\alpha$ (mode 1 is the one with the lowest frequency).

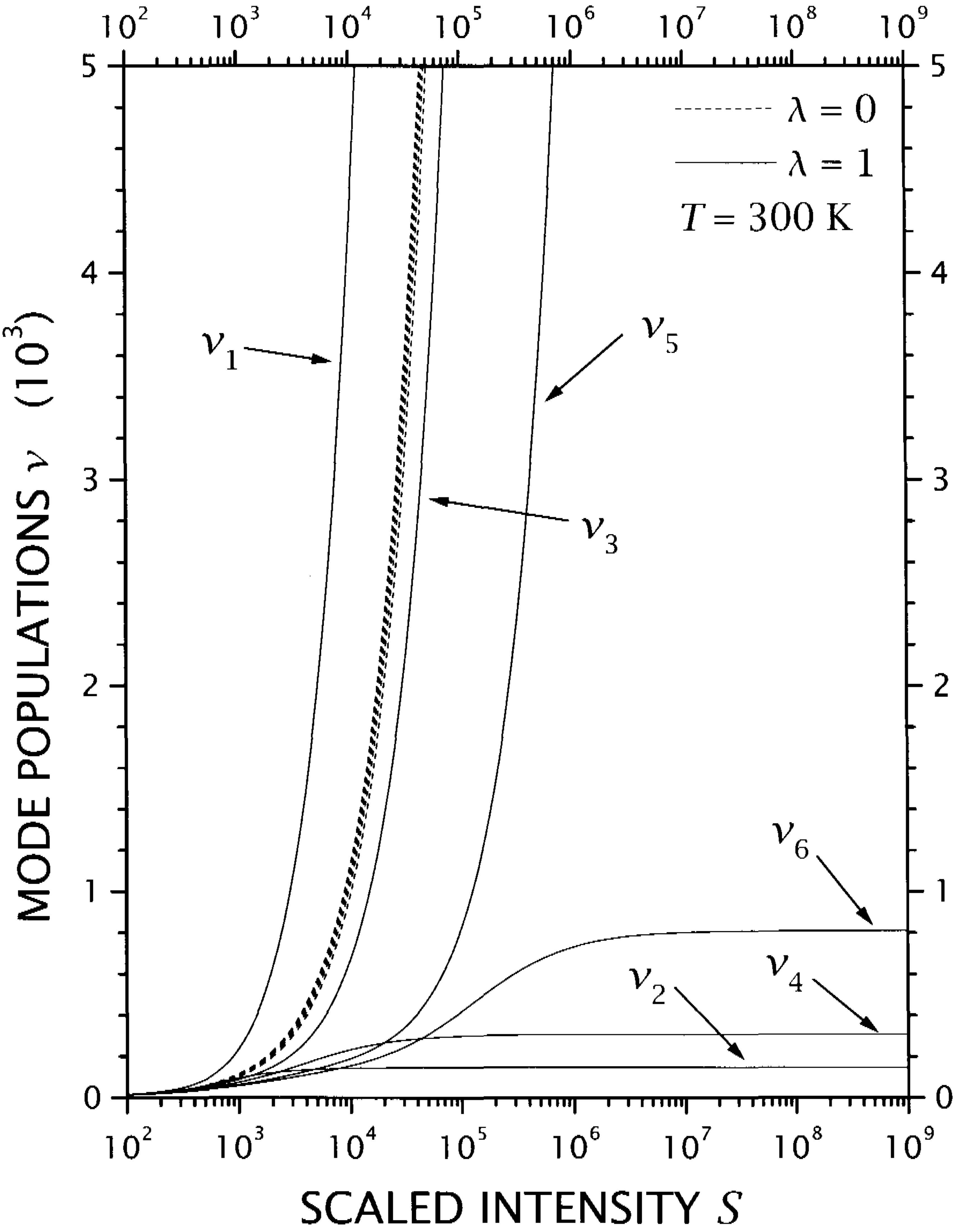

Figure 3: As in the case of Fig. 1 but now with all modes equally pumped and $\lambda = 1$. The dashed curve is the result $\lambda = 0$ (uncoupled modes), when the population of the different twelve modes is roughly the same.

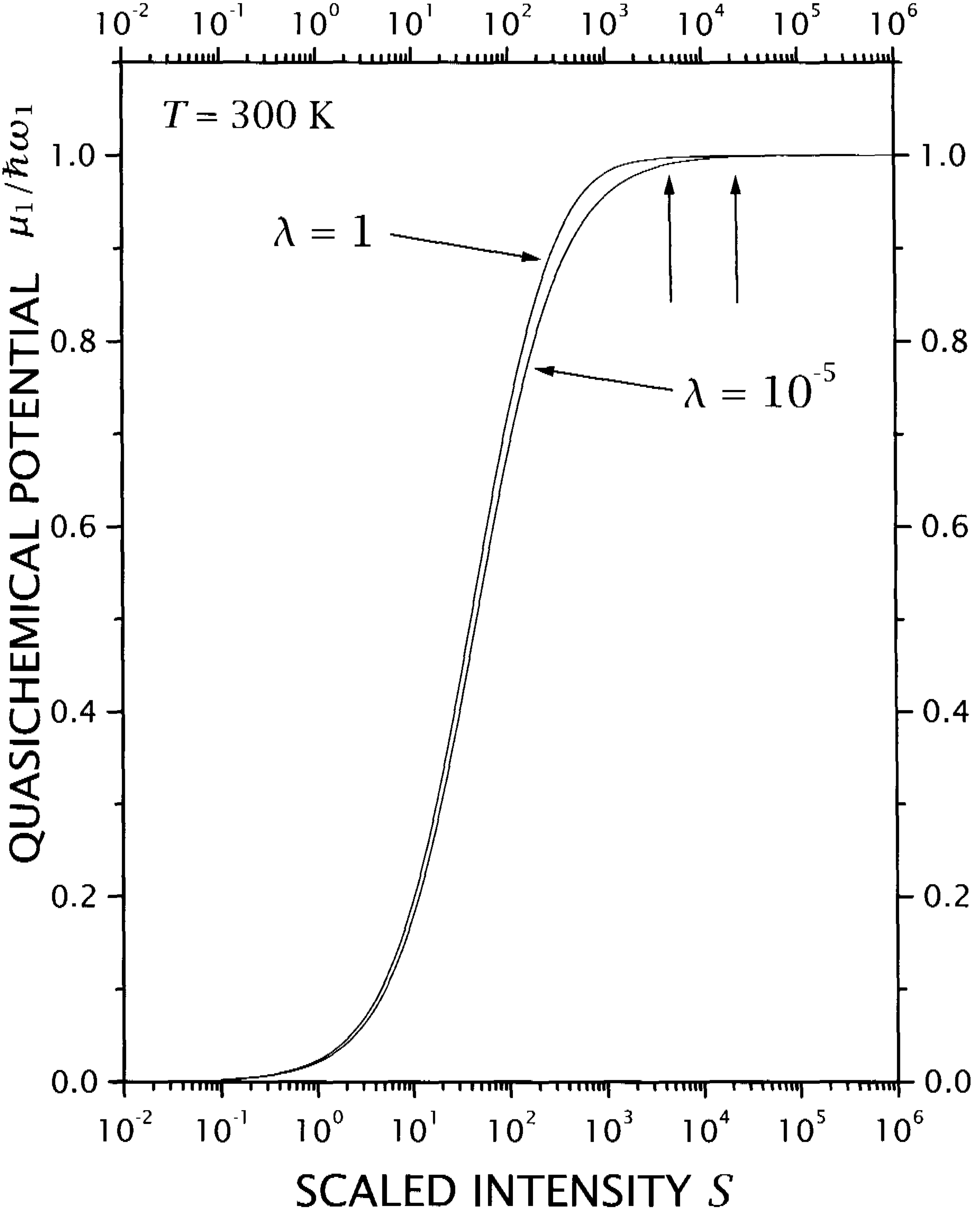

Figure 4: The dependence on the scaled intensity of the quasichemical potential of the lowest-frequency mode (arrows indicate the approximate onset of condensation).

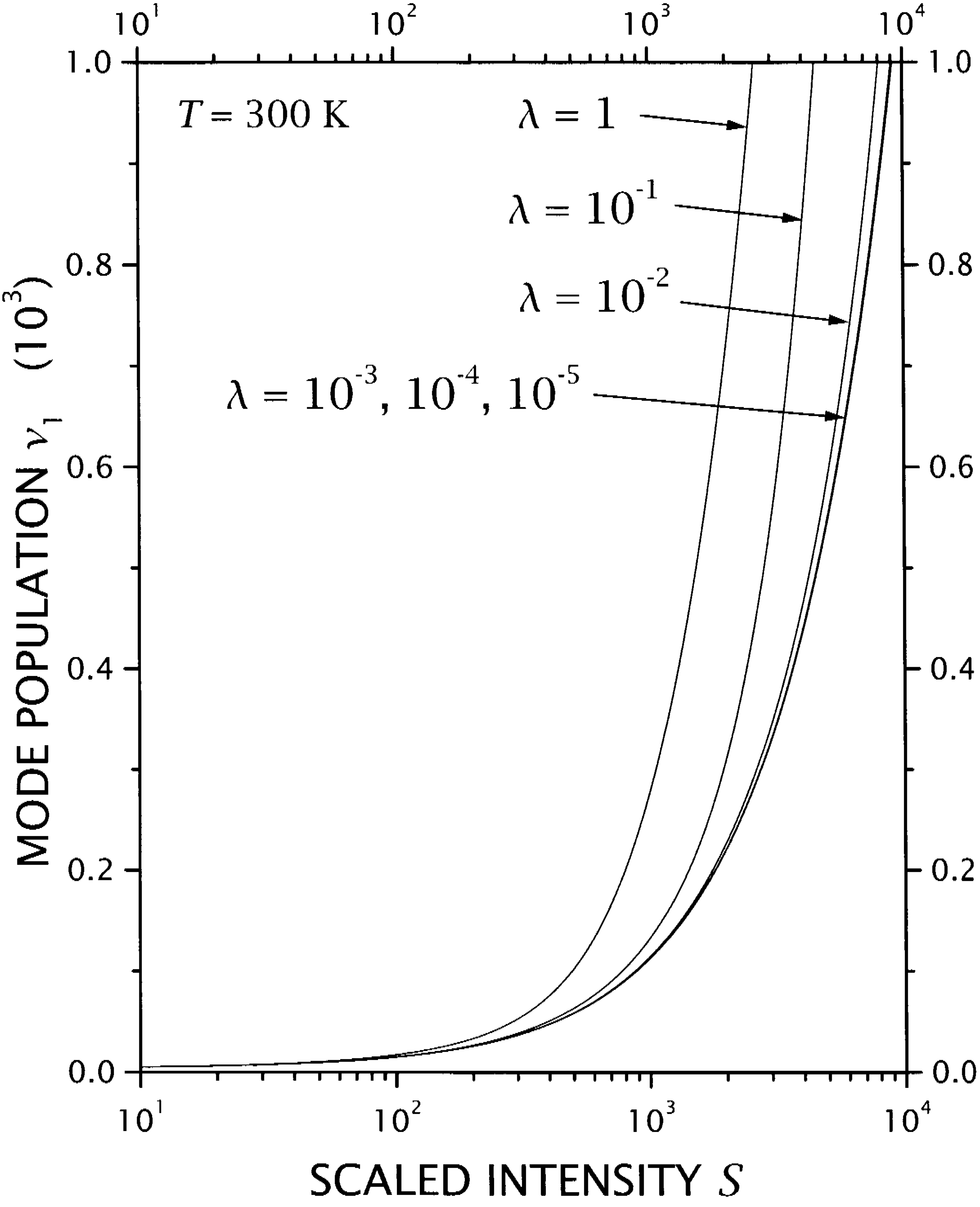

Figure 5: Behavior of population of the lowest-frequency mode ν_1, for different values of the coupling strength.

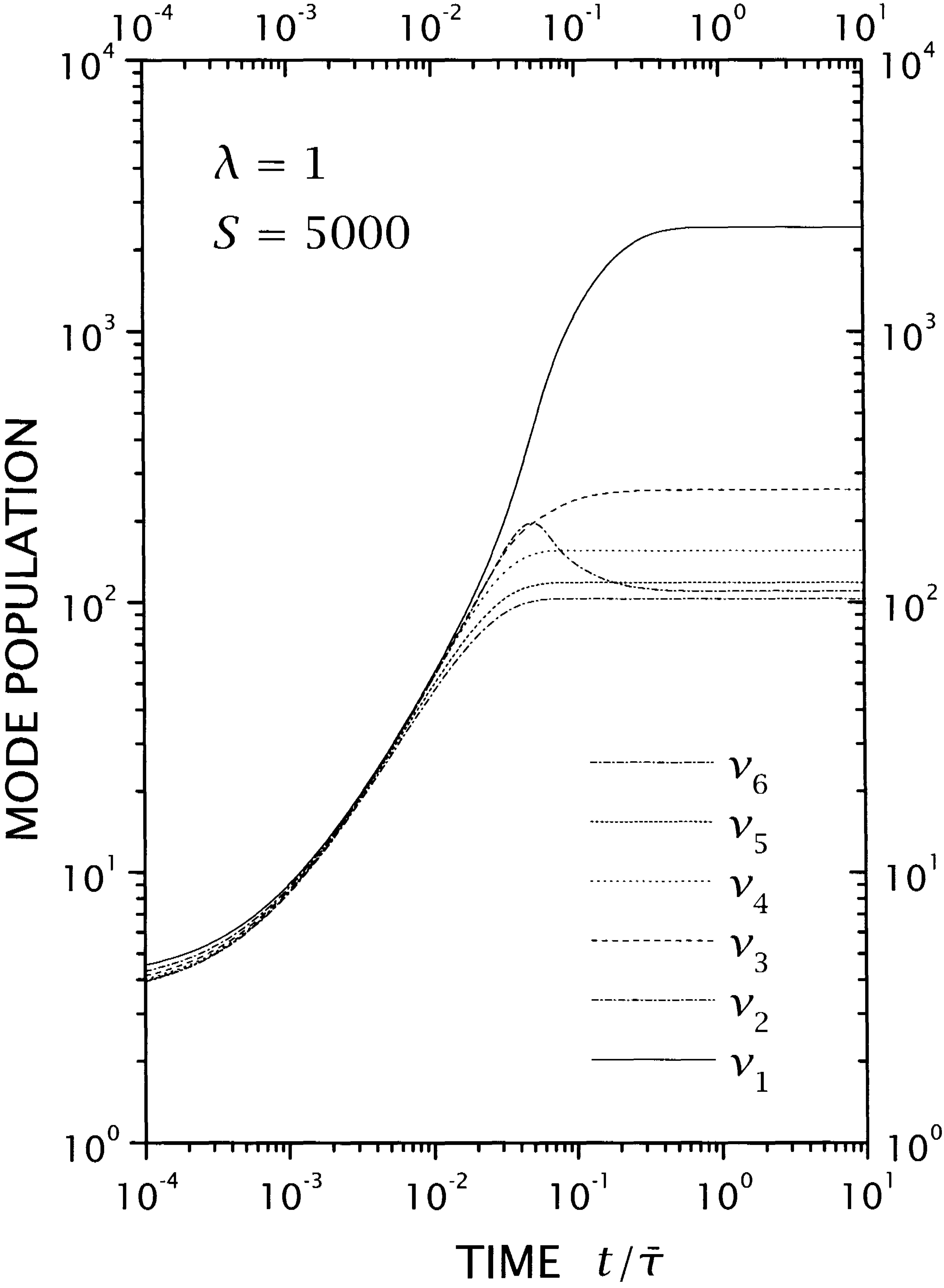

Figure 6: Evolution in time of the populations of the modes for $\lambda = 1$ and $S = 5000$.

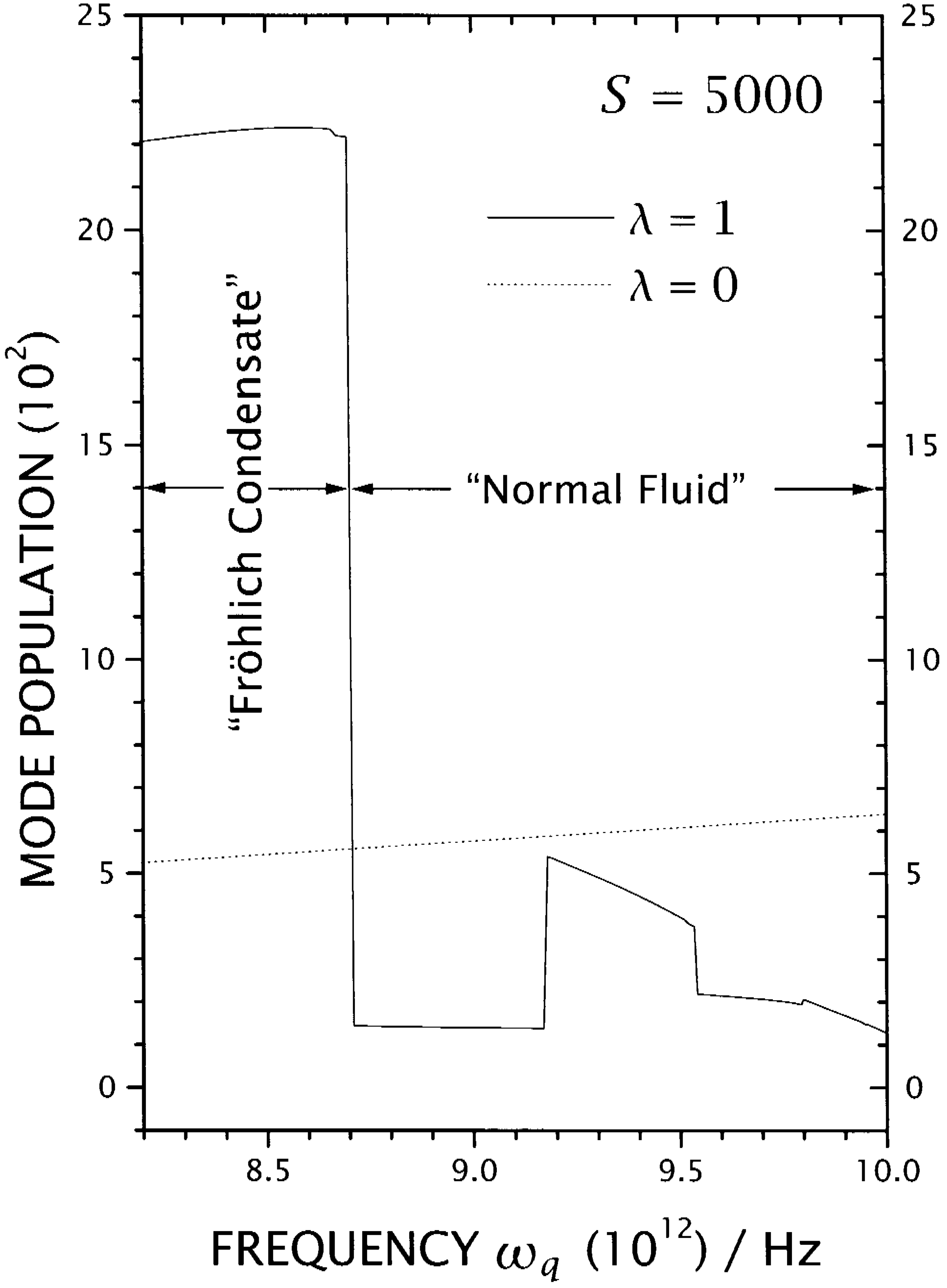

Figure 7: The population of the modes in the band containing their frequencies of vibration, namely, $\omega_0 - \alpha(\pi/a)^2 \leq \omega \leq \omega_0$.

4.3 Condensação de Fröhlich tipo Bose-Einstein ampliada por retro-alimentação positiva em biosistemas

Apresentamos um estudo mecânico-estatístico do assim chamado efeito Fröhlich, a saber: a amplificação não-térmica de vibrações polares que levam a comportamento complexo em biosistemas, como biopolímeros e agrandes agregrados de macromoléculas. O condensado de Fröhlich é considerado de relevância para determinada classe de processos biológicos, em particular em conexão com o problema de propagação a longa distância de sinais em temperatura fisiológica. Recorrendo a uma teoria termomecânica apropriada para lidar com processos irreversíveis em sistemas longe do equilíbrio, resultados anteriores são estendidos. Realizamos uma análise do caso em que a produção de uma dupla excitação de vibrações polares, gerada pela ação de uma fonte externa de alimentação de energia metabólica é possível. É mostrado que, quando esse é o caso, o processo envolve um mecanismo de retroalimentação positiva que facilita grandemente e aumenta o fenômeno do condensado de Fröhlich e, conseqüentemente, os possíveis processos biológicos que o acompanha. Os resultados são discutidos e uma eventual conexão com observações experimentais é indicada.

International Journal of Quantum Chemistry, **66** (2), 177–87 (1998).

POSITIVE-FEEDBACK-ENHANCED FRÖHLICH'S BOSE-EINSTEIN-LIKE CONDENSATION IN BIOSYSTEMS

Marcus V. Mesquita, Áurea R. Vasconcellos, Roberto Luzzi

Instituto de Física 'Gleb Wataghin',
Universidade Estadual de Campinas, Unicamp
13083-970 Campinas, São Paulo, Brazil

We present a mechano-statistical study of the so-called Fröhlich effect, namely nonthermal amplification of polar vibrations leading to complex behavior in biosystems, like biopolymers and large aggregates of macromolecules. Fröhlich condensation is considered to be of relevance for a certain class of biological processes, in particular in connection with the problem of long range propagation of signals at physiological temperature. Resorting to a thermo-mechanical theory appropriate to deal with irreversible processes in systems far from equilibrium, earlier results are extended. We perform an analysis of the case when production of a double excitation of polar vibrations, generated by the action of an external pumping source of metabolic energy, is possible. It is shown that, when this is the case, the process involves a positive feedback mechanism that greatly facilitates and enhances the phenomenon of Fröhlich's condensation, and consequently the possible accompanying biological processes. The results are discussed and eventual connection with experimental observations pointed out.

Group Home Page: http://www.ifi.unicamp.br/~aurea

1. INTRODUCTION

It is certainly a truism to say that the complicate heterogeneous spatial structure and functioning(temporal evolution) of living organisms, starting with the individual cell, set down quite difficult problems at the biophysical and biochemical levels. In recent decades a good amount of effort has in particular been devoted to some physico-chemical aspect of biosystems like, how to increase our knowledge of the chemical composition of the life forms; to determine the structure of large macromolecules; to determine the reactions that lead to processes of sintetization of multiple components; to understand the mechanisms and codes required to determine the structure of proteins; and so on. For considering living systems at the biophysical level we must be well aware of the fact that we are dealing with macroscopic open systems in non-equilibrium conditions. In other words, one observes macroscopic organization — at the spatial and temporal levels — of the microscopic components of the systems, namely, molecules, atoms, radicals, ions, electrons. The macroscopic behavior is of course correlated to the details of the microscopic structure. However, it must be emphasized that this does not mean that knowing the microscopic details shall reveal the interesting macroscopic properties.

Quite recently, this question concerning the theoretical description of the macroscopic behavior of dissipative open many-body systems in arbitrarily far-from-equilibrium conditions has been encompassed in a seemingly powerful, concise, and elegant formalism, established on sound basic principles. This is the Nonequilibrium Statistical Operator Method (NESOM) [1–3] which may be considered as pertaining to Jaynes'

Predictive Statistical Mechanics [4,5]. The NESOM allows for the construction of a nonlinear quantum transport theory of a large scope [1,3,6,7] and a thermodynamics of irreversible processes, termed Informational Statistical Thermodynamics (IST; sometimes referred to as Information-theoretic Thermodynamics, which is briefly reviewed with accompanying historical notes in [8]), which provides the foundations for the treatment of dissipative open macrosystems away (either near or far) from equilibrium. This is, as already noticed, the situation in biosystems, a result which is a general feature of biological systems where energy is always available, through metabolic processes, that is, the open biosystem "feeds" on this energy and is driven away from equilibrium. A quite fundamental point is that the evolution of the system has associated a nonlinear kinetics, and from this point of view the physics we are thus involved here with consists in the description of nontrivial nonlinear effects that change in time and space and are maintained through a constant energy supply.

As pointed out by Fröhlich [9,10], biological systems are relatively stable from a microscopic point of view, e. g. the thermal vibrations of single atoms are practically the same as in a corresponding nonbiological system. In some conditions, however, when they are very far from thermal equilibrium, a restricted set of phase space points dominate the overall behavior of the rest. This implies in collective properties of organization that are carried out by a great number of molecules requiring, as noted, a description in terms of macro-concepts which are outside the domain of the purely mechanicist-reductionist scheme. These collective properties evolve as a consequence of the supply of energy (metabolism), and virtually represent extreme nonlinear displacements. This nonlinearity of the equations of evolution of the macroscopic properties of the system is of fundamental relevance. Nonlinearity is nowadays known to be the source of new and quite unexpected phenomena that give rise to the so called *complex behavior in dynamical systems* [11, 12].

Biological systems are evidently complex systems by antonomasia, displaying a large variety of nonlinear physico-chemical processes. Hence, as it is the case, they present an enormously large number of rich and noticeable phenomena at the morphological, biochemical, biophysical, etc., levels. We consider in this paper a conjectured complex behavior in a biophysical system consisting of a long quasi one-dimensional array of proteins, or biopolymers, in terms of a quite simplified model that contains the main physical characteristics of a real system that are relevant to the present study. The system has already been described in a previous paper [13], heretofore referred as (I), whose study is here broadened with the inclusion of an analysis of the case when — as it seems to be possible in real systems — *the pumping of metabolic energy is accompanied by a feedback (auto-catalytic) mechanism that reinforces the predicted complex behavior eventually leading to bioenergetic phenomena that may have large relevance in the functioning of living systems.*

We consider the dissipative evolution and the steady state of the population of vibrational polar modes in a chain of biomolecules. In our model these polar modes are excited through the coupling with a pumping source of metabolic energy and are in anharmonic interaction with an elastic continuum. Groups of polar modes are coupled in this way through nonlinear terms in the kinetic equations that describe the evolution of the macroscopic state of the system. This nonlinearity is thought to be the source of a new and unexpected phenomenon characterizing complex behavior in this kind of systems: After a threshold in the intensity of the pumping source is achieved, polar modes with the lowest frequencies increase enormously their populations at the expense of the other modes. The possibility of this phenomenon was advanced by H. Fröhlich [9, 10], and, therefore, is termed *Fröhlich effect*, which resembles a kind of nonequilibrium Bose-Einstein condensation.

For the model chosen in (I), our calculations show that the transient times for the steady state of Fröhlich's condensate to appear is very short, namely in the ten-fold picosecond time scale. Moreover, the condensation in the low lying in frequency modes should follow even for weak values of the anharmonic coupling strength responsible for its occurrence. Furthermore, the condensation seemingly requires reasonable levels of metabolic pumping power to be produced and sustained. The phenomenon of condensation may lead to a coherent effect among the vibrating units and to the formation of some kind of spatial ordering, which is suggested to be an electret-like state of a metastable character [14, 15]. Current trends indicate that Fröhlich effect may have important biological consequences as a result of the long range action of the electric forces, like the enhancement of the reaction rate of enzyme molecules, roleaux formation in erithocytes, and others as considered in [15–18]. Also, the connection between Fröhlich's and Davydov's effects has been recently shown. Davydov's theory contains a proposition for a novel mechanism for the localization and transport of vibrational energy consisting in the formation of solitary-like waves in biopolymers as those considered in (I) [19–22]. There is an indication that excitations of the Davydov's soliton type propagating through the system, while they are strongly damped in near equilibrium conditions, become almost dissipationless once the threshold of

Fröhlich condensate is attained [23]. This suggests a relevant phenomenon of propagation of excitations at long distances in such biosystems, a question of interest in bioenergetics.

Hence, the possible relevance of Fröhlich's effect at the biological level clearly calls for a deeper analysis of the phenomenon. Our calculations in (I) were based on a pumping mechanism involving the production of a single excitation. Nevertheless, the metabolic pumping source being, for example, the one resulting from hydrolysis of ATP providing near 420 meV per molecule, allows for production of double or higher order excitations, depending on the system, as already suggested by Alwyn Scott [22]. Hence we reconsider the case of paper (I) introducing as before the production of single excitations, and adding to it double excitations: as shown below this leads to a positive feedback effect that greatly enhances and favors the emergence of Fröhlich's effect. In last section we further discuss this phenomenon and related experimental observations.

2. THEORY: THE FEEDBACK EFFECT

We reconsider the system of (I), which we analyze in terms of the nonlinear quantum transport theory that the NESOM provides, as done in (I). However, since the anharmonic interaction responsible for the dissipative processes is weak, we can greatly simplify matters by resorting to the lowest order approximation in the NESOM-based kinetic theory. It is the Markovian limit, in which one only retains the memoryless two-particle collisions, that is, the collision operator contains the strength of the interaction between system and thermal bath only up to second order (we recall that in the present case it consists into the anharmonic interaction) [7]. Moreover, because of the particular characteristcs of the system Hamiltonian, together with the fact that the thermal bath is taken as an ideal reservoir characterized by a canonical distribution with temperature T_0, the collision operator in the kinetic equation for the populations is simply reduced to the Golden Rule of Quantum Mechanics averaged over the nonequilibrium statistical ensemble.

The cited possibility of double excitation is incorporated in our theory by simply introducing instead of the interaction Hamiltonian of Eq. (2g) in (I) the new expression

$$H_f = \sum_{\boldsymbol{q}} W^{(1)}_{\boldsymbol{q}} \varphi_{\boldsymbol{q}} a^\dagger_{\boldsymbol{q}} + \sum_{\boldsymbol{q},\boldsymbol{q}'} W^{(2)}_{\boldsymbol{q},\boldsymbol{q}'} \varphi_{\boldsymbol{q}+\boldsymbol{q}'} a^\dagger_{\boldsymbol{q}} a^\dagger_{\boldsymbol{q}'} + H.c. \tag{1}$$

containing the contributions corresponding to single(as in I) and double excitations, respectively, and where $W^{(1)}_{\boldsymbol{q}}$ and $W^{(2)}_{\boldsymbol{q},\boldsymbol{q}'}$ are their coupling strengths, φ is the annihilation operator of excitations in the source, and $a^\dagger_{\boldsymbol{q}}$ is the creation operator of a polar excitation in mode $\boldsymbol{q}$. The other contributions to the Hamiltonian are the same as in (I) (Cf. Eqs. (1) and (2) in (I)), which, we recall, contain three quasiparticle collisions involving the polar vibrations and the acoustic-like excitations of the thermal bath. Hence the equations of evolution for the populations of the polar modes, that is, Eqs. (6) to (11) in (I), remain the same except for an additional source term associated to the new contribution in Eq. (1).

Taking the coupling amplitudes $W^{(1)}$ and $W^{(2)}$ as weakly wavevector dependent, the term associated to the pumping process takes the form

$$\frac{\partial}{\partial t}\nu_q(t)\bigg|_{\text{pump}} = |W^{(1)}|^2 I(\omega_q) + \sum_{q'} |W^{(2)}|^2 I(\omega_q + \omega_{q'})\,[1 + \nu_q(t) + \nu_{q'}(t)]\,, \qquad (2)$$

where the first term on the right corresponds to the one of (I), and the second is the one arising from double excitations, ω_q is the polar mode frequency dispersion relation, and ν_q is the population in polar mode $\boldsymbol{q}$. Moreover, the presence of the quantity $I_q(\omega)$ is the result of introducing a spectral representation for the description of the pumping source, namely,

$$\frac{2\pi}{\hbar^2}\left\langle \varphi_q^\dagger(t)\varphi_q \right\rangle = \int_{-\infty}^{\infty} \frac{d\omega}{\pi} I_q(\omega) e^{i\omega t}. \qquad (3)$$

Therefore, taking into account Eq. (2), the equation of evolution for the population of the vibrational polar modes is now

$$\begin{aligned}
\frac{d}{dt}\nu_q(t) = {} & |W^{(1)}|^2 I(\omega_q) + \sum_{q'} |W^{(2)}|^2 I(\omega_q + \omega_{q'})\,[1 + \nu_q(t) + \nu_{q'}(t)] + \\
& - \tau_q^{-1}(t)[\nu_q(t) - \nu_q^0] + \\
& - \frac{2\pi}{\hbar^2}\sum_{q'} |V_{qq'}|^2 [1 + \nu^b_{q+q'}]\nu_{q'}(t)\nu_q(t)\delta(\Omega_{q+q'} - \omega_{q'} - \omega_q) + \\
& + \frac{2\pi}{\hbar^2}\sum_{q'} |V_{qq'}|^2 \nu^b_{q+q'}[1 + \nu_{q'}(t)][1 + \nu_q(t)]\delta(\Omega_{q+q'} - \omega_{q'} - \omega_q) + \\
& - \frac{2\pi}{\hbar^2}\sum_{q'} |V_{qq'}|^2 [1 + \nu^b_{q-q'}][1 + \nu_{q'}(t)]\nu_q(t)\delta(\Omega_{q-q'} + \omega_{q'} - \omega_q) + \\
& + \frac{2\pi}{\hbar^2}\sum_{q'} |V_{qq'}|^2 \nu^b_{q-q'}\nu_{q'}(t)[1 + \nu_q(t)]\delta(\Omega_{q-q'} + \omega_{q'} - \omega_q) + \\
& - \frac{2\pi}{\hbar^2}\sum_{q'} |V_{qq'}|^2 \nu^b_{q-q'}[1 + \nu_{q'}(t)]\nu_q(t)\delta(\Omega_{q-q'} - \omega_{q'} + \omega_q) + \\
& + \frac{2\pi}{\hbar^2}\sum_{q'} |V_{qq'}|^2 (1 + \nu^b_{q-q'})\nu_{q'}(t)[1 + \nu_q(t)]\delta(\Omega_{q-q'} - \omega_{q'} + \omega_q)\,, \qquad (4)
\end{aligned}$$

that is, Eq. (8) in (I), which now presents the new pumping term as given by Eq. (2) above. In this Eq. (4), we recall, ν_q^b are the population of the acoustic-like vibrations in the thermal bath, having the frequency dispersion relation Ω_q and being kept at the equilibrium temperature T_0. Quantities $V_{qq'}$ are the matrix elements associated to the anharmonic interaction, τ_q is a relaxation time [Cf. Eq. (15) in (I)], crystalline momentum conservation is included and the delta functions account for energy conservation in the scattering events.

We notice in Eq. (2) that the term associated with the production of double excitations is proportional to the populations ν_q which are growing under the action of the pump, and, therefore, a *positive feedback mechanism* is present. Let us see its consequences.

We now proceed with numerical calculations using the same parameters than in (I), which, we stress, are simply chosen as an order of magnitude approximation in comparison with those to be expected in real systems (e. g. the α-helix protein in [19, 22]). We recall that in the model of (I), and for the proposed characteristic parameters, the equations of evolution which, in principle, couple all the modes in the Brillouin zone (of the order of 10^{22}), separate out — because of the concurrent energy and momentum conservation in the collision processes —, in independent (and equivalent) sets of twelve coupled modes. Moreover, these twelve modes are equivalent in pairs (those symmetrically distributed on both sides of the one-dimensional Brillouin zone), and then we need only to account for the six populations we labell ν_1 to ν_6. In Fig. 1 we reproduce the results reported in (I) showing the dependence of the polar mode populations on the pump intensity (for a set of coupled modes as described in (I)). The pump intensity is a scaled one, namely $S = |W^{(1)}|^2 I_0 \bar{\tau}$ where I_0 is the intensity of the source which has been assumed to have a white spectrum. In other words, all spectral intensities in Eq. (3) are approximated by a constant I_0. Furthermore, $\bar{\tau}$ is a reference time defined in (I), where the parameter λ is also defined: it measures the relative intensity of the nonlinear to the linear interactions of the polar vibrations with the thermal bath. In Figs. 2 and 3 are shown the results that follow when the pumping term with double excitation production is introduced. There is an open parameter to be chosen, namely the ratio of the squared coupling constants $|W^{(2)}|^2/|W^{(1)}|^2$ which we write as $(a/L)w$, where L is the length of the chain, a is the length of the crystallographic unit cell, and w is an open weight parameter (L cancels in the calculation as it should). The set of curves in Fig. 2 corresponds to the choice $w = 1$ and those in Fig. 3 to $w = 0.01$. Comparison with Fig. 1 clearly demonstrates how the additional pumping process favors Fröhlich's effect: First the threshold of intensity for the phenomenon to follow is largely decreased. And, second, the phenomenon is particularly more pronounced. In the case in which $w = 1$, the intensity threshold for Fröhlich's effect to appear(which we define as the point corresponding to the intensity for which ν_1 is roughly an order of magnitude larger than the other modes) is nearly five hundred times smaller than in the case when only production of a single excitation is considered (when $w = 0$ as it is the case of Fig. 1). For $w = 0.01$ the intensity threshold is five times smaller. A most noticeable effect is the very steep increase in the population of the mode with the lowest frequency in Figs. 2 and 3 as compared with Fig. 1.

We also consider the transient regime. The numerical solution of the equations of evolution is shown in Fig. 4. Comparison with the results of (I) shows that the steady-state Fröhlich's condensate appears after a much shorter transient time has elapsed, namely one of the order of magnitude of picosecond to subpicosecond instead of the ten or more picoseconds obtained in the calculations in (I). However, it ought to be noticed a kind of instability at high levels of pumping intensity, consisting in the fact that strictly under the given modelled conditions the system attains stationary condition at not too high pumping intensity but no stationary condition follows at sufficiently high values of S. This effect is a consequence of the presence of the feedback mechanism, which occurs for $w = 0.01$ at a value of intensity roughly given by $S \sim 2480$. Finally, in Fig. 5 the steady-state population of the modes in the frequency spectrum for a value of pumping intensity $S = 2400$ (with $w = 0.01$) are shown. This phenomenon therefore exhibits a kind of separation in a "two fluid system", like in the theories for superfluid He and superconductivity, which display Bose-Einstein-like phase transitions in equilibrium. These two fluids consist of the one composed by the modes in the condensate at low frequencies (as indicated in Fig. 5) and the remaining modes (at intermediate to high frequencies) which are those which transfer energy to the former (through the nonlinear anharmonic coupling).

3. RESULTS AND DISCUSSION

The results so far derived show that pumping of energy that can produce double excitations in biosystems which can sustain polar vibrations (governed by nonlinear kinetic laws), involves a positive feedback mechanism that largely facilitates and enhances Fröhlich's effect, a phenomenon that may play an important role in biological processes. We emphasize that the steady state condensate follows very rapidly after the switching on of the pumping source (namely, in the pico- to subpico-second time scale) and for low levels of pumping power. Hence, it is greatly enhanced the complex behavior of the modelled biosystem, which, when at a certain distance from equilibrium, that is, for a threshold value of the intensity of the pumping source, displays a steeply increase in the population of the vibrational modes lowest in frequency. This is reminiscent of a Bose-Einstein condensation, but it must be clearly kept in mind that while the latter is a phase transition in equilibrium and defined by a critical temperature, Fröhlich's effect is a nonequilibrium phenomenon. The transition point is defined in terms of the intensity of the pumping source, and this phenomenon may be considered as the emergence of a dissipative structure in Prigogine's sense [24].

As already noticed, this effect, apparently possible in biosystems, may be of relevance for biological mechanisms. Some of them, as already stressed, may be associated to the formation of a metastable electret state [10, 14, 15], and another, of eventually particular relevance, is related to the propagation at long distances of signals without decay in these biosystems. These are Davydov's solitary waves [19] already referred to in the Introduction. This phenomenon is extensively covered in two relevant and comprehensive review articles due to Davydov [21] and Scott [22]. In the case of an α-helix region of protein this mechanism is described as follows [22]: Vibrational energy of the CO-stretching (or Amide-I) oscillators that is localized on the quasi-periodic helix (see Fig. 1 in (I)) acts — through a phonon coupling effect — to distort the structure of the helix. The helical distortion reacts — again through phonon coupling — to trap the Amide-I oscillation energy and prevent it to dispersion, in a so called self-trapping.

Davydov's theory has received plenty of attention. It has been pointed out that [22], although its novelty and large relevance in bioenergetics, it has associated some questions that have been of particular concern. One is that if the soliton is stable at normal physiological temperature (310K). We have derived the equivalent of Davydov's equation in general nonequilibrim thermodynamic conditions, for the same model as the one presented here, then showing that Fröhlich effect and Davydov soliton are a result of the same nonlinearities in the equations of evolution [23]: Our calculations show that, in principle, the damping effect of Davydov's solitary wave in equilibrium at normal physiological conditions is present, and should give rise to a very rapid decay (the signal can travel only a few micrometers). But these calculations allowed us to demonstrate that this damping is dependent on the macroscopic nonequilibrim dissipative thermodynamic state of the system, and therefore influenced by the same nonlinearities responsible for both Fröhlich's effect and Davydov's soliton. As a consequence, after Fröhlich's condensation sets in, the lifetime of the vibrational modes lowest in frequency (namely, those in the Fröhlich's condensate in Fig. 5) increases enormously, while those for the other vibrational modes decrease. This implies that a *coherent excitation composed by the surviving low-lying-in-frequency excited states follows in the form of a Davydov's solitary excitation which travels nearly undamped, and then propagates at long distances, while Fröhlich condensation is maintained by the pumping of metabolic energy.* Hence, these two phenomena described on the basis of a unified statistical thermo-mechanics appear to be linked together in a quite interesting and relevant way.

As stated in (I) and in the Introduction, some experimental evidence of Fröhlich effect is available, however of an indirect nature and not at all conclusive. A clear cut and direct experimental signature of the phenomenon would follow from the determination of the population of the vibrational modes via scattering experiments. However since the vibrational modes in the condensate are those that lie at the Brillouin zone boundary, their wavelengths are of the order of the extension of the crystallographic cell. Hence it requires the use of neutron scattering, an experimental tool of difficult use and, more importantly, inappropriate for the case of probing functioning biological material. Light scattering experiments are possible, but they probe the modes with long wavelengths near the Brillouin zone center. However, this Raman scattering can provide indirect proof of the phenomenon since, according to the theory (see figures), beyond the critical point the population of some set of modes outside the condensate attain a kind of saturation, that is, their population remains nearly constant with increasing intensity of the pumping source.

The above referred to amplification of the vibrational modes through metabolic processes was evidenced in Raman scattering experiments using *escherichia coli* [25]. The Raman bands correspond to Raman shifts of the order of 120 cm^{-1} (3.6×10^{12} s^{-1}). As known, the population ν of this mode is related to the ratio of the intensities of the anti-Stokes (I_{AS}) to Stokes (I_S) lines by

$$R = \frac{I_{AS}}{I_S} = \frac{\nu}{\nu + 1}. \tag{5}$$

In equilibrium ν is the Planck distribution function, which, at the room temperature in the experiment is near one, and then it results that $R \simeq 0.5$. But the observed value was $R \simeq 1$, what implies $\nu \gg 1$, and so much larger than the value in equilibrium. This demonstrates that, in the active (metabolizing) phase the vibrational mode is largely nonthermally excited. A similar experiment was performed with live and metabolizing cells of the algae *chlorella pyrenoidosa*, which showed also a large increase of the intensity of the Raman lines involved in this case [26].

Moreover, it has been conjectured that Fröhlich's effect may have a relevant presence in cellular division: it has been observed an increase in the rate of cellular division of certain cultures of yeast after irradiation by short wavelengths, with the source of electromagnetic radiation being the external pumping source in this case [27]. It is also suggested that enzymes are activated by the phenomenon of Fröhlich condensation: in that state there follows a reduction in the activation energy, and may explain its high catalytic power [28]. Another situation when Fröhlich effect may be in action is the case of aggregation of red blood cells [29, 30]. This would provide an indirect evidence: if Fröhlich effect is accompanied by the formation of a metastable electret state [14, 15], it arises an electric interaction of long range which may lead to the formation of linear aggregates, known as "rouleaux". They dissociate in principle together with the disappearance of the effect, when the cellular membrane is disorganized and the supply of metabolic energy is withdrawn. But, it must be stressed that the formation of "rouleaux" of human erythrocytes on the basis of Fröhlich's condensation is not conclusive [31].

Experiments on functioning biological materials is of difficult realization. An alternative to test Fröhlich's effect and Davydov's soliton may be the use of polyacetilene and other organic polymers. Using infrared absorption techniques it was obtained experimental evidence of Davydov's soliton in acetanilide [32]. But in those cases the question is how to excite the systems to levels allowing for Fröhlich's condensation to follow. In these organic materials the polar modes can be indirectly excited by means of laser illumination producing phonon amplification in single-photon absorption by free carriers. But this process of excitation of the polar modes is poorly effective, as a result that energy and momentum conservation in the interaction events makes that the process only weakly excites a reduced number of modes in an off-center region of the Brillouin zone. As a consequence the critical point where Fröhlich's condensation arises would occur at a level of power excitation so high as to produce extensive material damage in the sample [33]. One may alternatively think of using current excitation at intermediate to high electric fields in doped samples, but we do not have a definitive report so far. We expect that the results and comments presented in (I), here, and in [23], would encourage experimental work, however difficult, in these interesting, engaging, and seemingly relevant topics of Fröhlich's effect and Davydov's soliton.

Before closing this section we would like to comment that, as already stressed, Fröhlich's effect and Davydov's solitary waves have one and the same origin, meaning that they arise from the macroscopic kinetic equations, which are the statistical average over the nonequilibrium ensemble of Heisenberg equations of motion governed by the corresponding quantum energy operator. Earlier attempts looking for a general theory of Fröhlich effect and Davydov's solitons, were based on truncated Hamiltonians, (the so-called Rotating Wave Approximation) and, as a result, certain collision processes were missing what gave rise to some unnecessary controversy and unphysical results [34–36].

In conclusion, we have approached the question of eventual complex behavior of a system modelling the polar modes of long quasi-linear and quasi-periodic arrays of macromolecules, as described in Fig. 1 in (I). The theoretical treatment of the problem, as here presented, was based on an irreversible thermodynamics of large scope, namely IST, involving the description of the system at the microscopic level provided by Quantum Mechanics, with the accompanying macroscopic level provided by a statistical approach in terms of the NESOM. As final words we ought to emphasize that the reported results are based on a simplified model, which, however, introduces the elements considered to be fundamental. Of course in biological systems myriads of other processes may be accompanying the considered one. Nevertheless, resorting to a well established methodology, starting with this concept of a general nature refinements and modifications may be added for a more detailed discussion of properties of the system under observation.

As final words we may say, following Fröhlich, that it is particularly auspicious to see that biological systems — dealt with at the biophysical level — may display a complex behavior describable in terms of appropriate physical concepts. The question of the phenomenon of the enhanced Fröhlich effect via the positive feedback mechanism has been briefly reported in [37], and the present paper was originally intendend for the SANIBEL-97 Conference Proceedings.

Acknowledgments

We acknowledge financial support provided by the State of São Paulo Research Agency (FAPESP). Two of the authors (ARV, RL) are National Research Council (CNPq) research fellows. The other author (MVM) is a Ministry of Education (CAPES) pre-doctoral fellow. We also acknowledge the support to our Group received from the Ministry of Planning (Finep) and the John Simon Guggenheim Memorial Foundation.

REFERENCES

[1] D. N. Zubarev, *Nonequilibrium Statistical Thermodynamics* (Consultants Bureau, New York, 1974), [*Neravnovesnaia Statisticheskaia Termodinamika* (Idz. Nauka, Moscow, 1971)].

[2] D. N. Zubarev, in *Reviews of Science and Technology: Modern Problems of Mathematics*, edited by R. B. Gamkreludze (Izd. Nauka, Moscow, 1980), Vol. 16, [English Transl.: Soviet Math. **16**, 1509 (1981)].

[3] D. N. Zubarev, V. N. Morozov, and G. Röpke, *Statistical Mechanics of Nonequilibrium Processes* (Akademie Verlag, Berlin, 1996).

[4] E. T. Jaynes, in *Frontiers of Nonequilibrium Statistical Physics*, edited by G. T. Moore and M. O. Scully (Plenum, New York, 1986), pp. 33-55.

[5] E. T. Jaynes, in *Complex Systems: Operational Approaches*, edited by H. Haken (Springer, Berlin, 1985).

[6] A. I. Akhiezer and S. V. Peletminskii, *Methods of Statistical Physics* (Pergamon, Oxford, 1981).

[7] L. Lauck, A. R. Vasconcellos, and R. Luzzi, Physica A **168**, 789 (1990).

[8] L. S. Garcia-Colin, A. R. Vasconcellos, and R. Luzzi, J. Non-Equilib. Thermodyn. **19**, 24 (1994).

[9] H. Fröhlich, in *From Theoretical Physics to Biology*, edited by M. Marois (North Holland, Amsterdam, 1969), pp. 13–22.

[10] H. Fröhlich, *Advances in Electronics and Electron Physics* (Academic Press, New York, 1980), Vol. 17, pp. 85–152.

[11] P. W. Anderson, Science **117**, 393 (1972).

[12] G. Nicolis and I. Prigogine, *Exploring Complexity* (Freeman, New York, 1989).

[13] M. V. Mesquita, A. R. Vasconcellos, and R. Luzzi, Phys. Rev. E **48**, 4049 (1993).

[14] S. Mascarenhas, in *Electrets*, edited by G. M. Sessler (Springer, Berlin, 1987), pp. 321-346.

[15] H. Biltz, H. Bütner, and H. Fröhlich, Z. Naturforsch. B **36**, 206 (1981).

[16] H. Fröhlich, Nature **228**, 1093 (1970).

[17] R. E. Mills, Phys. Rev. A **28**, 379 (1983).

[18] R. Paul, O. G. Fritz, and R. Chatterjee, Int. J. Quantum Chem. Symp. **15**, 191 (1988).

[19] A. S. Davydov, *Biology and Quantum Mechanics* (Pergamon, Oxford, 1982).

[20] A. C. Scott, Phys. Rev. A **26**, 578 (1982).

[21] A. S. Davydov, in *Solitons*, edited by S. E. Trullinger, V. E. Zakharov, and V. L. Prokovsky (Elsevier, New York, 1986), Chap. 1, pp. 1–51.

[22] A. C. Scott, Phys. Rep **217**, 1 (1992).

[23] R. Luzzi and A. R. Vasconcellos, Phys. Rev. E **48**, 2246 (1993).

[24] I. Prigogine, in *From Theoretical Physics to Biology*, edited by M. Marois (North Holland, Amsterdam, 1969).

[25] S. J. Webb, M. E. Stoneham, and H. Fröhlich, Phys. Lett. A **63**, 407 (1977).

[26] F. Drissler and R. M. MacFarlane, Phys. Lett. A **69**, 65 (1978).

[27] T. M. Wu and S. Austin, J. Theor. Biol. **71**, 209 (1978).

[28] H. Fröhlich, Collective Phenomena **3**, 139 (1981).

[29] S. Rowlands, L. S. Sewchand, R. E. Lovlin, J. S. Beck, and E. G. Enns, Phys. Lett. A **82A**, 436 (1981).

[30] S. Rowlands, L. S. Sewchand, and E. G. Enns, Phys. Lett. A **87**, 256 (1982).

[31] J. A. Tuszyński, J. Theor. Biol. **132**, 31 (1988).

[32] G. Careri, U. Buotempo, R. Carta, E. Gratton, and A. C. Scott, Phys. Rev. Lett. **51**, 304 (1983).

[33] L. Lauck, A. R. Vasconcellos, and R. Luzzi, Phys. Rev. B **46**, 6150 (1992).

[34] R. E. Mills, Phys. Rev. A **43**, 3176 (1991).

[35] J. A. Tuszyński and R. Paul, Phys. Rev. A **43**, 3179 (1991).

[36] H. Bolterauer and L. A. Ludwig, Phys. Rev. E **47**, 2122 (1993).

[37] M. V. Mesquita, A. R. Vasconcellos, and R. Luzzi, Phys. Lett. A, textbf238, 206 (1998).

FIGURE CAPTIONS

Figure 1: The population of a set of coupled modes in terms of the pumping source intensity involving only production of single excitations. All modes are equally pumped. The mode labelled 1 is the one with the lowest frequency in the set. The composition of the set of modes is described in reference [13].

Figure 2: The population of a set of coupled modes (the same of Figure 1) in terms of the pumping source intensity, when production of double excitations is taken into account. Parameters λ and w are shown in the upper left inset.

Figure 3: Same as caption to Figure 2.

Figure 4: Time evolution of the mode populations using the parameters shown in the upper left inset.

Figure 5: Distribution in frequency of the population of the modes, using the parameters shown in the upper right inset, with indication of the positioning of the Fröhlich condensate at low frequencies.

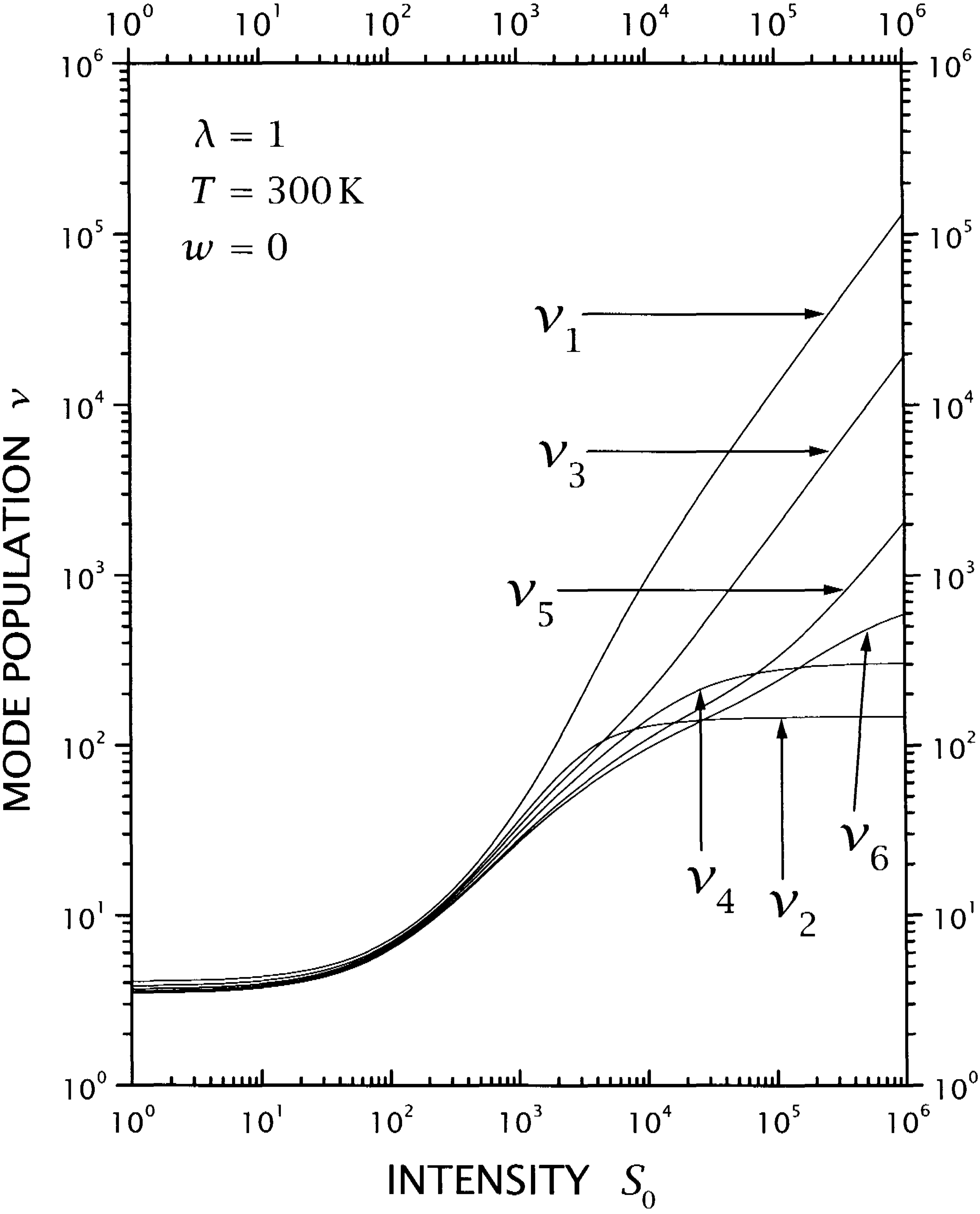

Figure 1: The population of a set of coupled modes in terms of the pumping source intensity involving only production of single excitations. All modes are equally pumped. The mode labelled 1 is the one with the lowest frequency in the set. The composition of the set of modes is described in reference [13].

MESQUITA *et al.* — *J. Biol. Phys.* FIGURE 1

172.

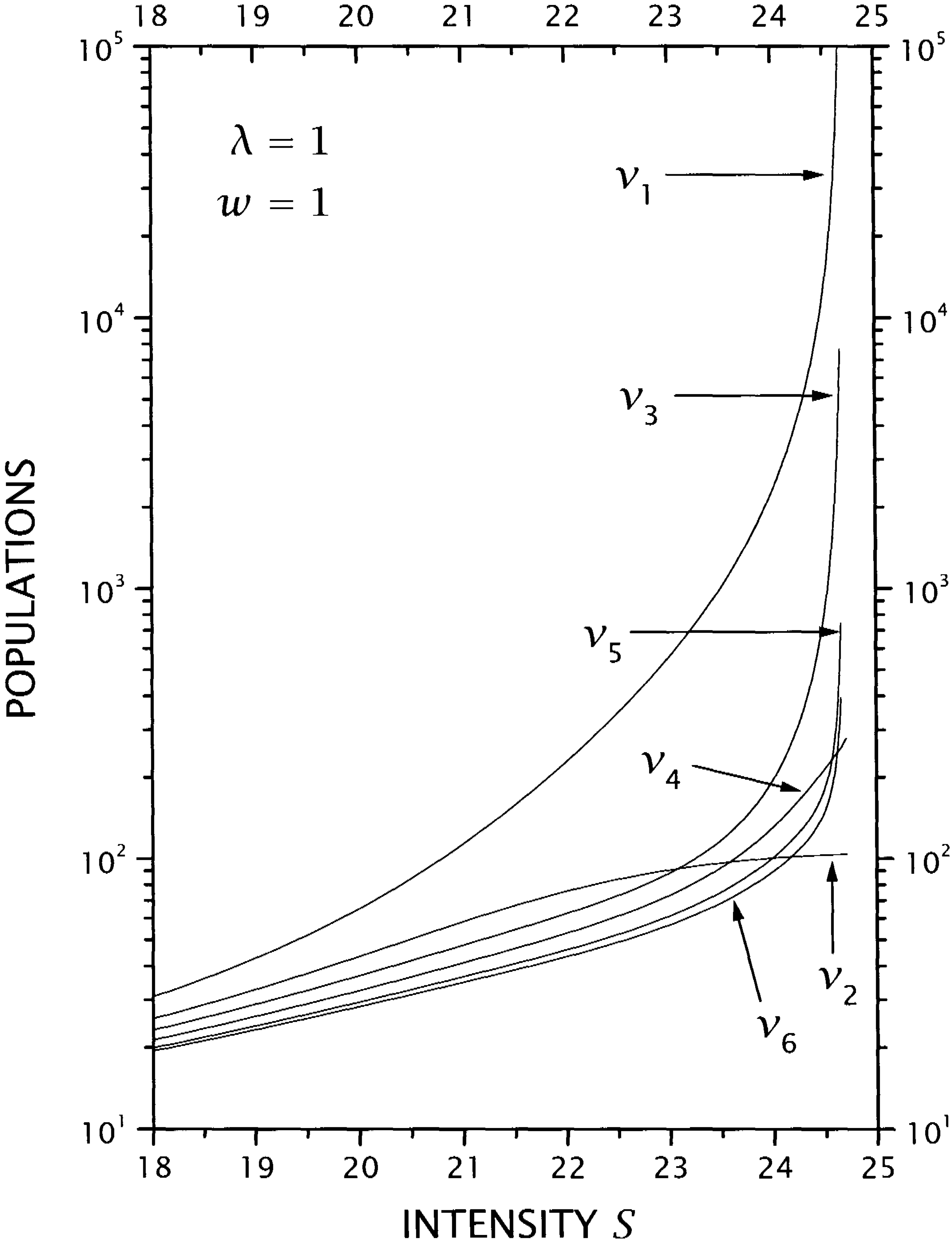

Figure 2: The population of a set of coupled modes (the same of Figure 1) in terms of the pumping source intensity, when production of double excitations is taken into account. Parameters λ and w are shown in the upper left inset.

MESQUITA *et al.* — *J. Biol. Phys.* FIGURE 2

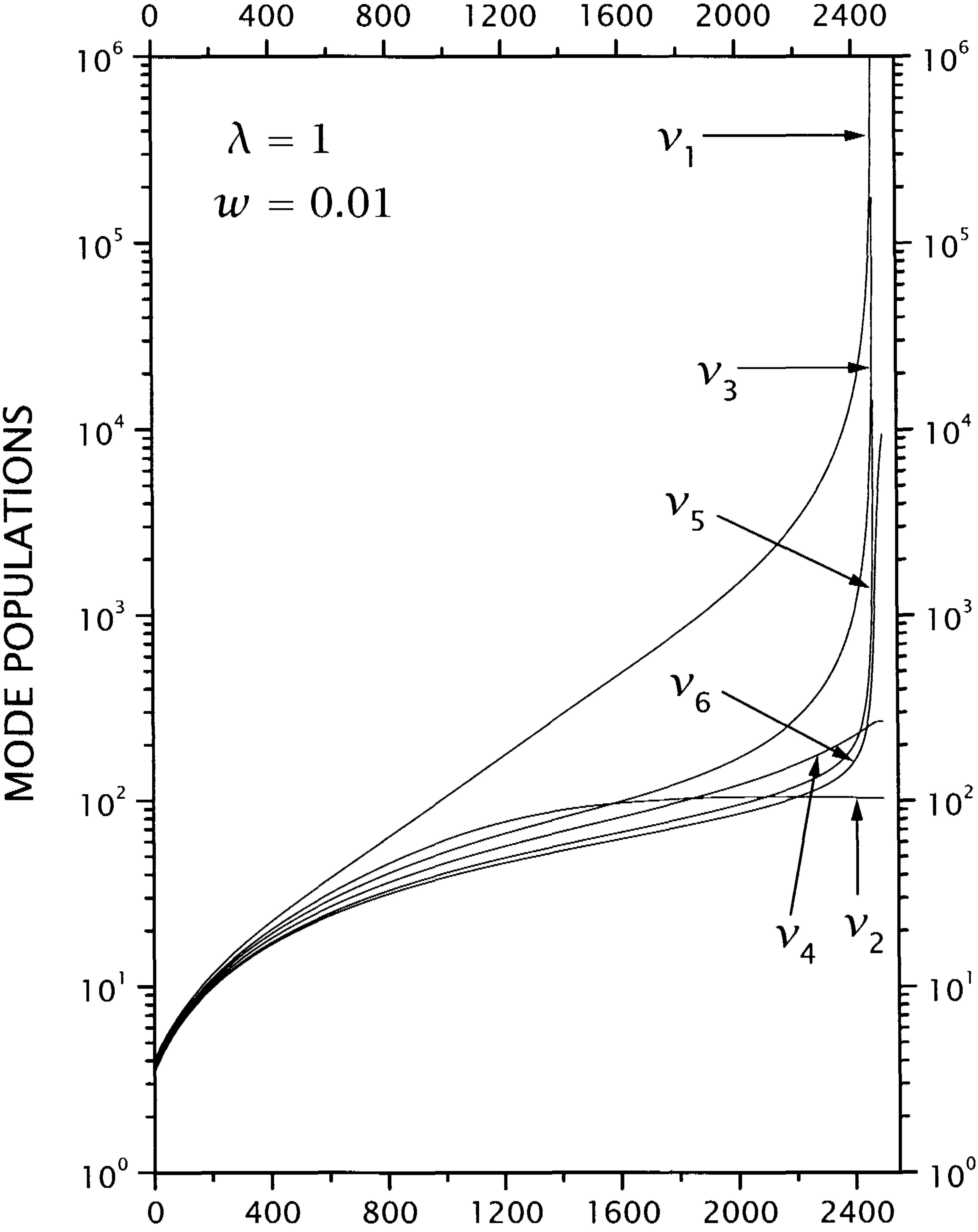

Figure 3: Same as caption to Figure 2.

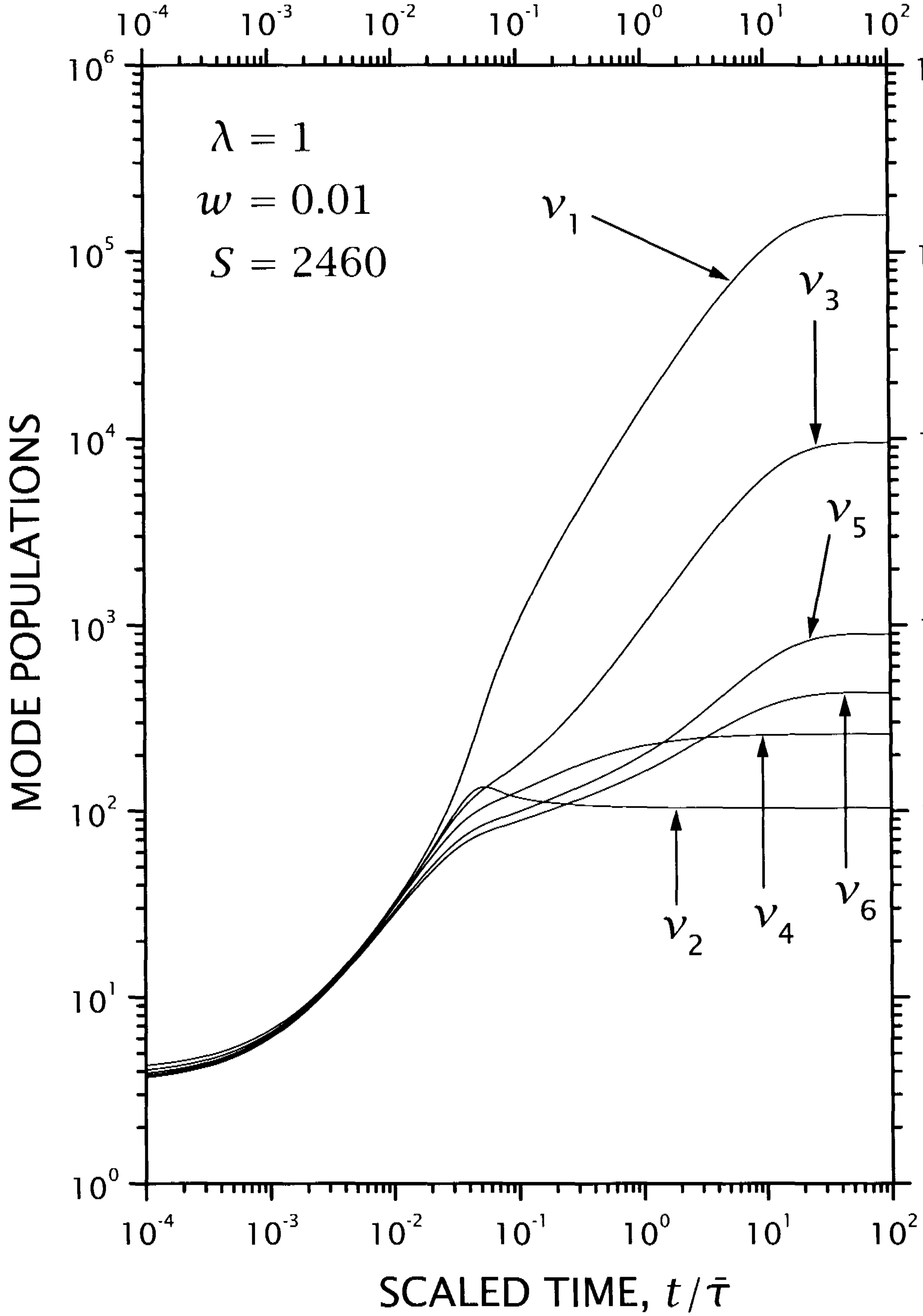

Figure 4: Time evolution of the mode populations using the parameters shown in the upper left inset.

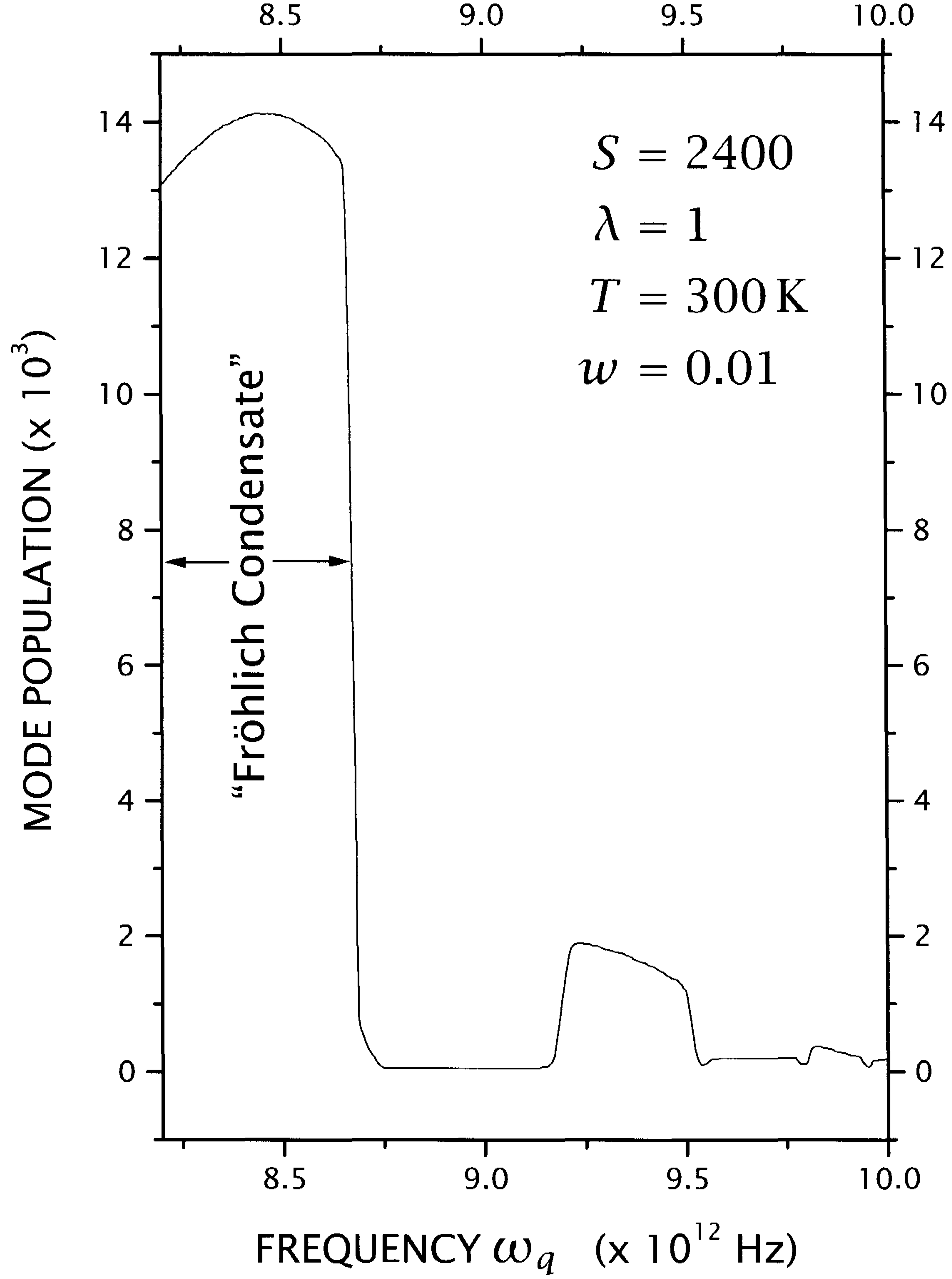

Figure 5: Distribution in frequency of the population of the modes, using the parameters shown in the upper right inset, with indication of the positioning of the Fröhlich condensate at low frequencies.

4.4 Considerações sobre a condensação de Fröhlich tipo Bose-Einstein

O assim chamado *efeito Fröhlich* — que consiste em um conjecturado comportamento coerente de excitações tipo bóson em polímeros biológicos e orgânicos — é deduzido e analisado completamente em termos de uma teoria termo-mecânica. Esta é a assim chamada Termodinâmica Estatística Informacional, baseada em uma generalização da teoria estatística de Gibbs para sistemas longe do equilíbrio. Além disso, é mostrado que quando processos duplos (ou múltiplos) de excitação do sistema de bosons são possíveis, ocorre um *fenômeno de retroalimentação positiva* que favorece e aumenta grandemente o efeito.

Physics Letters A, **238**, 206-11 (1998).

CONSIDERATIONS ON FRÖHLICH'S BOSE-EINSTEIN-LIKE CONDENSATION

Marcus V. Mesquita, Áurea R. Vasconcellos, Roberto Luzzi

Instituto de Física 'Gleb Wataghin',
Universidade Estadual de Campinas, Unicamp
13083-970 Campinas, São Paulo, Brazil

The so-called *Fröhlich effect* — consisting in a conjectured coherent behavior of boson-like excitations in biological and molecular polymers — is fully derived and analized in terms of a thermo-mechanical theory. This is the so-dubbed Informational Statistical Thermodynamics, based on a generalization of Gibbs statistical theory to systems far from equilibrium. Moreover, it is shown that when double (or multiple) processes of excitation of the boson system are possible there follows a *positive-feedback phenomenon* that greatly favors and enhances the effect.

In a communication in this Journal [1] it was recalled that more than 25 years have elapsed since the renowned late Herbert Fröhlich first presented his concept of long-range coherence in biological systems [2-5]. Eichwald [1] discussed a microscopic approach to the question which he presents in the form of a scheme considered simple and transparent and within a nonlinear dynamical modelling appropriate in biophysics. We reconsider the question from a macroscopic point of view, that is, within the field of the Thermodynamics of irreversible processes and the accompanying Statistical Mechanics of nonequilibrium systems. We focus on a treatment leading to Fröhlich condensation on the basis of a thermo-mechanical theory which shows particular success in dealing with irreversible processes in systems far from equilibrium. In particular we are extending a previous paper [6] with the inclusion of a possible additional excitation process which may lead to a particular effect of positive feedback, which greatly enhances the feasibility of the phenomenon.

Quite recently, this question concerning the theoretical description of the macroscopic behavior of dissipative open many-body systems in arbitrarily far-from-equilibrium conditions has been encompassed in a seemingly powerful, concise, and elegant formalism, established on sound basic principles. This is the Nonequilibrium Statistical Operator Method (NESOM) [7–10], which is based on Jaynes' Predictive Statistical Mechanics [11, 12]. The NESOM allows for the construction of a nonlinear quantum transport theory of a large scope [7, 13, 14] and a thermodynamics of irreversible processes, termed Informational Statistical Thermodynamics (IST; sometimes referred to as Information-theoretic Thermodynamics, pioneered by Hobson [15] after the publication of Jaynes' seminal papers on the foundations of statistical mechanics on information theory; see for example [16, 17]) which provides the foundations for the treatment of dissipative open macrosystems away (either near or far) from equilibrium.

We consider an open biopolymer away from equilibrium described by the so-called Fröhlich-Davydov model [18, 19]. This model consists of a quasi-linear chain of macromolecules in a periodically repeated array, of which an example could be found in the α-helix protein. Energy is pumped in the system by a metabolic external process, and the chain can sustain longitudinal polar vibration, namely, those associated to the CO-stretching — or Amide I — oscillations; a mechanical model is described in Fig. 1 in [6], where the details of the Hamiltonian operator which completely characterizes the system at the microscopic level is given. This Hamiltonian [cf. Eq. 1 in [6]] is the complete one that can be written describing the longitudinal polar vibrations, which are in contact with the surrounding media. The latter is described as an elastic continuum media interacting with the polar vibrations via anharmonic interactions: they lead to a nonlinear effect, in the kinetic equations, with the contribution consisting in a scattering of a polar vibration by an elastic vibration, which is the source of Fröhlich effect. To deal with the question the first, and fundamental, step required in IST is the choice of the basic set of macrovariables which provides for the characterization of the non-equilibrium thermodynamic state of the system. As described in [6], a proper choice consists of the time-dependent populations (number of excited quantum phonons) of the polar vibrational modes (the CO-stretching modes), and the energy of the surrounding media which is assumed to remain at a constant temperature, ensured by an efficient homeostatic mechanism. The corresponding mechanical Hermitian operators are designated by $\hat{\nu}_q$ (the number occupation operator) and $\hat{H}_B$ (the Hamiltonian of the surrounding thermal bath). According to the method [7–10, 20] the statistical operator depends on these quantities and on a set of accompanying Lagrange multipliers (intensive thermodynamic variables in IST), which we call $F_q(t)$ and $\beta_R = (k_B T_R)^{-1}$ (where T_R is the bath temperature) respectively. An important role is played by an auxiliary coarse-grained statistical operator, $\bar{\varrho}(t,0)$ (which is not the complete statistical operator, $\varrho(t)$, this being a superoperator expressed in terms of the former [7–10, 20] and carrying the information on the irreversible processes that develop in the system, which are absent in $\bar{\varrho}$), given by the instantaneous Gibbs-like distribution (sometimes referred to as a "frozen quasi-equilibrium distribution")

$$\bar{\varrho}(t,0) = \exp\{-\phi(t) - \beta_R \hat{H}_R - \sum_q F_q(t)\hat{\nu}_q\}, \tag{1}$$

where $\phi(t)$, playing in NESOM the role of the logarithm of a nonequilibrium partition function, ensures the normalization of $\bar{\varrho}(t,0)$ at any time.

Next step is the derivation of the equations of movement for the basic variables, thus obtaining the description of the evolution of the macrostate of the system. As noticed E_B is constant in time, and then we only need the kinetic equations for the polar mode populations, $\nu_q(t)$, given by $\nu_q(t) = \mathrm{Tr}\left\{\hat{\nu}_q \varrho_\varepsilon(t)\right\}$. These are (for each $\boldsymbol{q}$ mode)

$$\frac{d}{dt}\nu_q(t) = \mathrm{Tr}\{\frac{1}{i\hbar}[\hat{\nu}_q, \hat{H}]\varrho_\varepsilon(t)\}, \tag{2}$$

that is, the average over the nonequilibrium ensemble (here $\varrho_\varepsilon(t)$ is the statistical operator in Zubarev's approach [7]) of the corresponding quantum mechanical Heisenberg equation of evolution for the number occupation operator and where $\hat{H}$ is the system Hamiltonian as given in [6]. We stress that this is the complete Hamiltonian of the system; earlier attempts looking for a microscopic-based theory of Fröhlich effect relied on truncated Hamiltonians, and, as a result, certain collisional processes were missing, what gave rise to some unnecessary controversy around unphysical results [21–23].

Equation (2) is of unmanageable proportions, but it can be rewritten, in the context of a quantum nonlinear kinetic theory [14, 24], in terms of a conserving term plus an infinite series of collision integrals involving scattering by two, three, etc. particles, which are nonlocal in space, memory dependent (that is correlations in space and time are present) and are highly nonlinear in the basic variables. We resort to the use of the lowest approximation in the theory consisting in retaining only the second order contribution in the interaction strength (the anharmonic processes involving the polar modes and the continuum representing the thermal bath), which is the Markovian limit in the theory [14, 24]. Within this approximation we obtain a generalized form of Fröhlich original equations, as shown in [6]. We extend here those results taking into account the fact that, while in [6] the calculations were based on a pumping mechanism involving the production of a single excitation in the system of polar modes — this source being for example the one resulting from hydrolysis of ATP providing near 420 meV per molecule — production of double or higher order excitations may be possible, as already suggested in [19]. This fact is incorporated in our theory when replacing the interaction Hamiltonian of Eq. (2g) in [6] by the new expression

$$\hat{H}_f = \sum_{q} W_q^{(1)} \varphi_q a_q^\dagger + \sum_{qq'} W_{qq'}^{(2)} \varphi_{q+q'} a_q^\dagger a_{q'}^\dagger + \text{h. c.}. \tag{3}$$

containing the contributions corresponding to single and double excitations, respectively, and where $W_q^{(1)}$ and $W_{qq'}^{(2)}$ are their coupling strengths, φ is the annihilation operator of excitations in the source, and $a_q^\dagger$ is the creation operator of a polar excitation in mode $\boldsymbol{q}$. The other contributions to the Hamiltonian are the same as in [6] (Cf. Eqs. (1) and (2) in [6]).

The equation of evolution for the populations of the $\boldsymbol{q}$-mode polar mode is now given by

$$\begin{aligned}
\frac{d}{dt}\nu_q(t) = {} & |W_q^{(1)}|^2 I_q(\omega_q) + \sum_{q'} |W_{qq'}^{(2)}|^2 I_{q+q'}(\omega_q + \omega_{q'})[1 + \nu_q(t) + \nu_{q'}(t)] \\
& - \frac{2\pi}{\hbar^2} \sum_{q'} |V_{qq'}^{(1)}|^2 \left\{ \nu_{q'}^b (1 + \nu_{q+q'}^b)\nu_q(t) - (1 + \nu_{q'}^b)\nu_{q+q'}^b [1 + \nu_q(t)] \right\} \delta(\Omega_{q+q'} - \Omega_{q'} - \omega_q) \\
& - \frac{2\pi}{\hbar^2} \sum_{q'} |V_{qq'}^{(1)}|^2 \left\{ (1 + \nu_{q'}^b)(1 + \nu_{q-q'}^b)\nu_q(t) - \nu_{q'}^b \nu_{q-q'}^b [1 + \nu_q(t)] \right\} \delta(\Omega_{q-q'} - \Omega_{q'} - \omega_q) \\
& - \frac{2\pi}{\hbar^2} \sum_{q'} |V_{qq'}^{(2)}|^2 \left\{ (1 + \nu_{q+q'}^b)\nu_{q'}(t)\nu_q(t) - \nu_{q+q'}^b [1 + \nu_{q'}(t)][1 + \nu_q(t)] \right\} \delta(\Omega_{q+q'} - \omega_{q'} - \omega_q) \\
& - \frac{2\pi}{\hbar^2} \sum_{q'} |V_{qq'}^{(2)}|^2 \left\{ (1 + \nu_{q-q'}^b)[1 + \nu_{q'}(t)]\nu_q(t) - \nu_{q-q'}^b \nu_{q'}(t)[1 + \nu_q(t)] \right\} \delta(\Omega_{q-q'} + \omega_{q'} - \omega_q) \\
& - \frac{2\pi}{\hbar^2} \sum_{q'} |V_{qq'}^{(2)}|^2 \left\{ \nu_{q-q'}^b [1 + \nu_{q'}(t)]\nu_q(t) - (1 + \nu_{q-q'}^b)\nu_{q'}(t)[1 + \nu_q(t)] \right\} \delta(\Omega_{q-q'} - \omega_{q'} + \omega_q)
\end{aligned} \tag{4}$$

We recall that ω_q and Ω_q are the frequency dispersion relations of the polar modes and of those in the continuum (the thermal bath); ν_q^b are the populations of the excitations in the bath; $V^{(1)}$ and $V^{(2)}$ the matrix elements of the anharmonic interactions between polar vibrations and those in the surrounding continuum; and the presence of $I_q(\omega)$ in the contribution corresponding to the coupling with the external pumping source, is the result of introducing a spectral representation

$$\frac{2\pi}{\hbar^2}\langle\varphi_q^\dagger(t)\varphi_q\rangle = \int_{-\infty}^{\infty}\frac{d\omega}{\pi}I_q(\omega)e^{i\omega t}. \tag{5}$$

where $I(\omega)$ is the intensity of the source at frequency ω.

We notice that in Eq. (4) the term associated with the production of double excitations is proportional to the populations ν_q which are growing under the action of the pump, and, therefore, a *positive feedback mechanism* is present. This is a revelant new feature in the picture; let us see its consequences. First, for simplicity, we take the coupling amplitudes $W^{(1)}$ and $W^{(2)}$ as weakly wavevector dependent, and then the term associated to the pumping process takes the form

$$\frac{\partial}{\partial t}\nu_q(t)\bigg|_{\text{pump}} = |W^{(1)}|^2 I(\omega_q) + \sum_{q'}|W^{(2)}|^2 I(\omega_q+\omega_{q'})\left[1+\nu_q+\nu_{q'}\right], \tag{6}$$

where the first term on the right corresponds to the one of Eq. (11) in [6], and the second is the one arising from double excitations, and responsible for the positive-feedback process.

We now proceed with numerical calculations using the same parameters than in [6], which, we stress, are simply chosen as an order of magnitude approximation in comparison with those to be expected in real systems (e. g. the α-helix protein in [18, 25]). We introduce a scaled pump intensity, namely $S = |W^{(1)}|^2 I_0\bar{\tau}$ where I_0 is the intensity of the source which is assumed to have a white spectrum. In other words, all spectral intensities in Eq. (6) are approximated by a constant I_0. Furthermore, $\bar{\tau}$ is a scaling time defined in [6], where the parameter λ is also defined. This λ measures the relative intensity of the nonlinear to the linear interactions between the polar vibrations and the thermal bath. Equations (4), where $\boldsymbol{q}$ and $\boldsymbol{q}'$ run over the whole Brillouin zone, couple all the polar modes in the zone (of the order of 10^{22}); however, as shown in [6], the concurrent conservation of energy and momentum in the collision processes restricts such coupling to independent (but equivalent) sets of twelve modes (also equivalent in pairs on each side of the linear Brillouin zone in the considered one dimensional chain). Therefore, it suffices to consider only one of these sets and, in what follows, we label the population of the corresponding modes from ν_1 to ν_6. Under continuous pumping, after a very rapid (picosecond scale) transient a steady state is achieved. The dependence on the source intensity S of the stationary population of the polar modes in the typical set is shown in Fig. 1. We notice that there are two open parameters in the theory, namely, the λ already mentioned, and the ratio of the squared coupling constants $|W^{(2)}|^2/|W^{(1)}|^2$ which we write as $(a/L)w$, where where L is the length of the chain, a is the length of the crystallographic unit cell, and w is an open weight parameter (L cancels in the calculation as it should). The set of curves in Fig. 1 corresponds to the choice $\lambda = 1$ and $w = 1$, arbitrarily done in order to proceed with the numerical calculation, but we call the attention to the fact that the phenomenon is always present for any value of these parameters; what changes is only the numerical final values in the calculation.

Let us compare this result with the one shown in Fig. 3 in [6], that is, the one coresponding only to production of single excitations ($w = 0$ in such case). Such comparison clearly demonstrates how the additional pumping process favors Fröhlich's effect: First the threshold of intensity for the phenomenon to follow is largely decreased, and, second, the phenomenon is particularly more pronounced. In this case in which $w = 1$, the intensity threshold for Fröhlich's effect to appear(which we define as the point corresponding to an intensity such that the population ν_1 is roughly an order of magnitude larger than that of the other modes) is nearly five hundred times smaller than in the case when only production of a single excitation is considered (that is, for $w = 0$ as it is the case of Fig. 3 in [6]). Our calculations show that for $w = 0.01$ the intensity threshold is five times smaller. A most noticeable effect is the very steep increase in the population of the mode with the lowest frequency in Fig. 1 as compared with Fig. 3 in [6].

We also consider the transient regime. The numerical solution of the equations of evolution is shown in Fig. 2. Comparison with the results in [6] shows that the steady-state Fröhlich's condensate appears after a much shorter transient time has elapsed, namely one of the order of magnitude of picosecond to subpicosecond instead of the ten or more picoseconds obtained in the calculations in [6]. Finally, in Fig. 3 the steady-state population of the modes for each frequency and for a value of pumping intensity $S = 2400$ (with $w = 0.01$) are shown. It may be noticed that the phenomenon exhibits a kind of separation in a "two-fluid system", like in the theories for superfluid He and superconductivity, which display Bose-Einstein-like phase transitions in equilibrium. These two fluids consist of the one composed by the modes in the condensate at low frequencies (as indicated in Fig. 3) and the remaining modes (at intermediate to high frequencies) which are those which transfer energy to the former (through the nonlinear anharmonic coupling).

The results we have derived show that pumping of energy producing double excitations in polymers which can sustain polar vibrations, say, the CO-stretching in α-helix protein or acetanilide, and whose evolution is governed by nonlinear kinetic laws, may involve a *positive feedback mechanism* which largely facilitates and enhances a possible Fröhlich's effect, a phenomenon that may play an important role in biological processes. We emphasize that the steady-state condensate follows very rapidly after the switching on of the pumping source (namely, in the pico- to subpico-second time scale) and for low levels of pumping power. Hence, the complex behavior of the system is greatly enhanced, once a certain distance from equilibrium is attained, that is, for a threshold value of the intensity of the pumping source, the system displays a steeply increase in the population of the vibrational modes lowest in frequency. This is reminiscent of a Bose-Einstein condensation, but it must be clearly kept in mind that while the latter is a phase transition in equilibrium and at a critical temperature, Fröhlich's effect is a nonequilibrium phenomenon, following at a transition point defined in terms of the intensity of the pumping source.

Clearly an important question to consider is the experimental corroboration of the theoretical results. Some evidence of Fröhlich's condensation is available, however of an indirect nature and not at all conclusive. A clear cut and direct experimental signature of the phenomenon would follow from the determination of the population of the vibrational modes via scattering experiments. But, the vibrational modes in the condensate are those that lie at the Brillouin zone boundary (where reside the modes lowest in frequency), which have wavelengths of the order of the extension of the crystallographic unit cell. Hence it is required the use of neutron scattering, an experimental tool of difficult use and, more importantly, inappropriate for probing functioning biological material. Light scattering experiments are possible, but they probe the modes with long wavelengths near the Brillouin zone center. However, this Raman scattering can provide indirect proof of the phenomenon if it allows to verify that, according to the theory (see figures 1 and 3), beyond the critical point the population of some the modes outside the condensate (in particular the long-wavelength ones) attain a kind of saturation, that is, their population remains nearly constant with increasing intensity of the pumping source.

In conclusion, we have approached the question of eventual complex behavior of a system modelling the polar modes of long quasi-linear and quasi-periodic arrays of macromolecules, as described in Fig. 1 in [6]. The theoretical treatment of the problem was based on an irreversible thermodynamics of large scope, namely IST, involving the description of the system at the microscopic level provided by Quantum Mechanics, with the accompanying macroscopic level provided by a statistical approach in terms of the NESOM. We emphasize that the reported results are based on a simplified model, which, however, introduces the elements considered to be fundamental. Of course in biological systems myriads of other processes may be accompanying the considered one. Nevertheless, resorting to a well established methodology, starting with this concept of a general nature, refinements and modifications may be added for a more detailed discussion of properties of the system under observation.

We acknowledge financial support provided by the State of São Paulo Research

Agency (FAPESP). Two of the authors (ARV, RL) are National Research Council (CNPq) research fellows. The other author (MVM) is a Ministry of Education (CAPES) pre-doctoral fellow.

REFERENCES

[1] C. F. Eichwald, Phys. Lett., 207 (1995) 194.

[2] H. Fröhlich, Quantum Mechanical Concepts in Biology, in M. Marois, editor, *From Theoretical Physics to Biology*, pages 13–22, North Holland, Amsterdam, 1969.

[3] H. Fröhlich, Int. J. Quantum Chem., 2 (1968) 641.

[4] H. Fröhlich, Nature, 228 (1970) 1093.

[5] H. Fröhlich, The Biological Effects of Microwaves and Related Questions, in *Advances in Electronics and Electron Physics*, volume 17, pages 85–152, Academic Press, New York, 1980.

[6] M. V. Mesquita, A. R. Vasconcellos, and R. Luzzi, Phys. Rev. E, 48 (1993) 4049.

[7] D. N. Zubarev, *Nonequilibrium Statistical Thermodynamics*, Consultants Bureau, New York, 1974, [*Neravnovesnaia Statisticheskaia Termodinamika* (Idz. Nauka, Moscow, 1971)].

[8] D. N. Zubarev, V. N. Morozov, and G. Röpke, *Statistical Mechanics of Nonequilibrium Processes*, volume 1: Basic Concepts, Kinetic Theory, Akademie Verlag, Berlin, 1996.

[9] R. Luzzi and A. R. Vasconcellos, Fortschr. Phys./Prog. Phys., 38 (1990) 887.

[10] J. G. Ramos, A. R. Vasconcellos, and R. Luzzi, Fortschr. Phys./Prog. Phys., 43 (1995) 265.

[11] E. T. Jaynes, Macroscopic Prediction, in H. Haken, editor, *Complex Systems: Operational Approaches*, Springer, Berlin, 1985.

[12] E. T. Jaynes, Predictive Statistical Mechanics, in G. T. Moore and M. O. Scully, editors, *Frontiers of Nonequilibrium Statistical Physics*, pages 33-55, Plenum, New York, 1986.

[13] A. I. Akhiezer and S. V. Peletminskii, *Methods of Statistical Physics*, Pergamon, Oxford, 1981.

[14] L. Lauck, A. R. Vasconcellos, and R. Luzzi, Physica A, 168 (1990) 789.

[15] A. Hobson, J. Chem. Phys., 45 (1966) 1352.

[16] L. S. Garcia-Colin, A. R. Vasconcellos, and R. Luzzi, J. Non-Equilib. Thermodyn., 19 (1994) 24.

[17] M. A. Tenan, A. R. Vasconcellos, and R. Luzzi, Fortschr. Phys./Prog. Phys., 47 (1996) 1.

[18] A. S. Davydov, *Biology and Quantum Mechanics*, Pergamon, Oxford, 1982.

[19] A. C. Scott, Phys. Rev. A, 26 (1982) 578.

194.

[20] D. N. Zubarev, Modern Methods of the Statistical Theory of Nonequilibrium Processes, in R. B. Gamkreludze, editor, *Reviews of Science and Technology: Modern Problems of Mathematics*, volume 16, Izd. Nauka, Moscow, 1980, [English Transl.: Soviet Math. **16**, 1509 (1981)].

[21] R. E. Mills, Phys. Rev. A, 43 (1991) 3176.

[22] J. A. Tuszyński and R. Paul, Phys. Rev. A, 43 (1991) 3179.

[23] H. Bolterauer and L. A. Ludwig, Phys. Rev. E, 47 (1993) 2122.

[24] A. J. Madureira, A. R. Vasconcellos, R. Luzzi, and L. Lauck, IFGW-Unicamp Internal Report, (1996), future publication.

[25] A. C. Scott, Phys. Rep, 217 (1992) 1.

FIGURE CAPTIONS

Figure 1: The population of the set of coupled modes described in [6] in terms of the pumping souce intensity, when production of double excitations is taken into account. Parameters λ and w are shown in the upper left inset.

Figure 2: Time evolution of the mode populations using the parameters shown in the upper left inset.

Figure 3: Distribution in frequency of the population of the modes, using the parameters shown in the upper right inset, with indication of the positioning of the Fröhlich condensate at low frequencies.

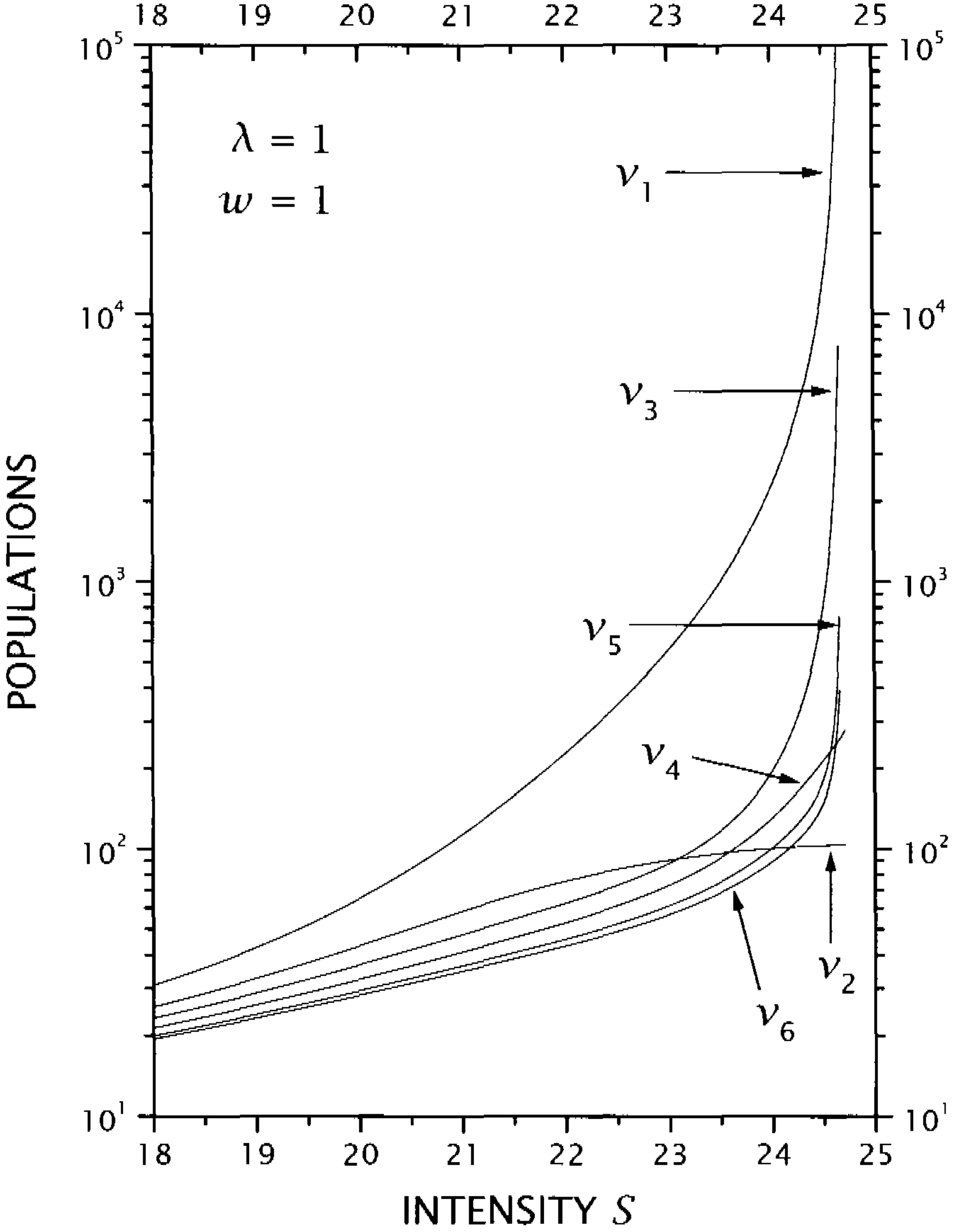

Figure 1: The population of the set of coupled modes described in [6] in terms of the pumping souce intensity, when production of double excitations is taken into account. Parameters λ and w are shown in the upper left inset.

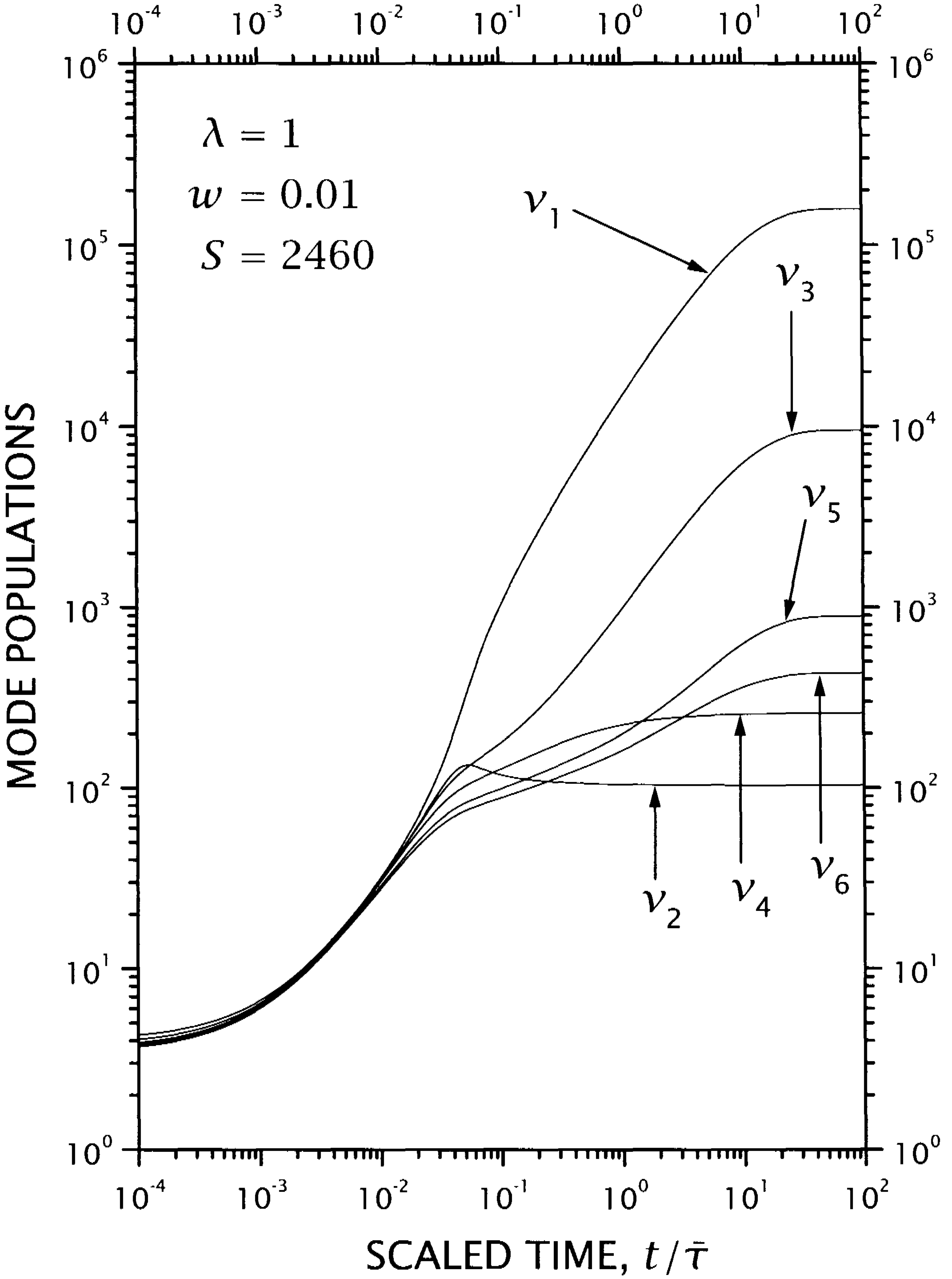

Figure 2: Time evolution of the mode populations using the parameters shown in the upper left inset.

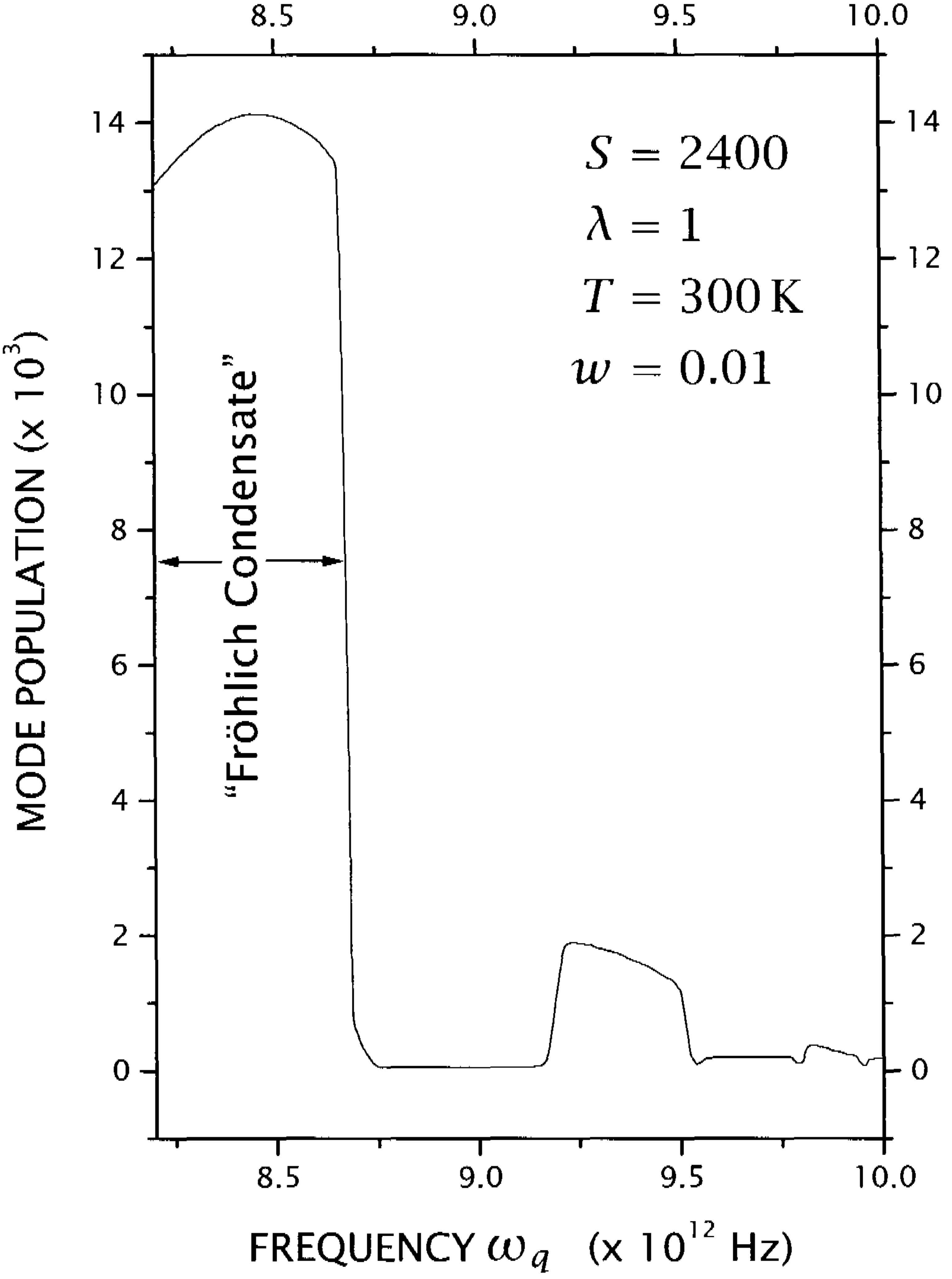

Figure 3: Distribution in frequency of the population of the modes, using the parameters shown in the upper right inset, with indication of the positioning of the Fröhlich condensate at low frequencies.

4.5 O regime transiente no fenômeno da condensação de Fröhlich em biosistemas

Consideramos a emergência do assim chamado efeito Fröhlich em um biosistema, um fenômeno que consiste na condensação de excitações dos modos vibracionais polares que estão na parte inferior do espectro de freqüências desses modos. Esse comportamento complexo do sistema, que parece ter relevância em bioenergética, pode surgir em biomaterial não-isolado, que é governado por equações cinéticas não-lineares, e quando sob a ação de uma fonte de alimentação de energia metabólica. Analisamos aqui em detalhe a dinâmica (i) do estágio transiente antes do estabelecimento de uma estado estacionário e (ii) da relaxação para o estado de equilíbrio termodinâmico original após a fonte de alimentação ser desligada.

International Journal of Quantum Chemistry, **62** (4), 363-72 (1997).

The Transient Regime in Fröhlich's Condensation Phenomenon in Biosystems

Mario A. Tenan, Marcus V. Mesquita, Ricardo A. Mosna

Instituto de Física 'Gleb Wataghin',
Universidade Estadual de Campinas, Unicamp
13083-970 Campinas, São Paulo, Brazil

We consider the emergence of the so-called Fröhlich's effect in a biosystem, a phenomenon consisting of the condensation of excitations in the polar vibrational modes lying at the bottom of these modes' frequency spectrum. This complex behavior of the system, which seems to have relevance in bioenergetics, may arise in open biomaterials, which is governed by nonlinear kinetic equations, and when under the action of a pumping source of metabolic energy. We analyze here in detail the dynamics of (i) the transient stage before the establishment of a steady state and (ii) the relaxation to the original thermodynamic equilibrium state after the pumping source is turned off.

Key words: bioenergetics; organized collective behavior; nonlinear kinetic equations; nonequilibrium thermodynamics; informational statistical thermodynamics.

PACs Number(s): 87.10.+e, 05.701n, 82.20.Mj

1. Introduction

In 1969, Herbert Fröhlich [1] advanced the idea that in systems not near equilibrium they may follow organized collective behavior at a macroscopic level. At that time, he speculated on the possible occurrence of such a type of behavior in biosystems where longitudinal electric oscillations are present. The question was further developed by him [2,3] and other authors [4–6].

Fröhlich's effect consists of that, under appropriate conditions, a phenomenon quite similar to a Bose condensation may occur in substances that possess polar vibrational modes. This phenomenon shall also be referred to as *Fröhlich's condensation.* If energy is constantly pumped into these modes and thence transferred to other degrees of freedom of the substance (a thermal bath), a stationary state may be attained in which the energy content of the vibrational modes is larger than in thermal equilibrium. This excess energy is found to be channeled into the modes lowest in frequency-similarly to the case of a Bose condensation-provided that the rate of pumped energy exceeds a critical value. Under these circumstances, a random supply of energy is thus not completely thermalized but partly used in maintaining a coherent state of these vibrational modes.

Several approaches to Fröhlich's effect were developed during recent decades [1–6]. One is based on the treatment of the question in terms of the emerging Informational Statistical Thermodynamics [5,6]. All cases involved detailed study of the stationary state of Fröhlich's condensation. In the present article, we report a complement to such work including an analysis in depth, based on Informational Statistical Thermodynamics, of the transient regime that develops prior to the attainment of the steady state and the return of the system to its initial conditions following the suppression of the pumping source of metabolic energy. This is described in the next section, while in the third section, we summarize and discuss the results, adding some concluding remarks.

2. The Model and the Transient in Fröhlich's Condensate

Let us consider a model biosystem consisting of a linear chain that can sustain longitudinal polar vibrations (e.g., the co-stretching of amide I groups in a-helix protein chains) in interaction with a thermal bath of acousticlike excitations. The polar modes are assumed to interact with an external pumping source as well. For the sake of conciseness, we restrict the description of the model only to some physical aspects at a qualitative and semiquantitative level. Explicit expressions for the system Hamiltonian and application of Informational Statistical Thermodynamics, both to be used in what follows, are given in [5] and [6].

The interactions between the polar modes and the elastic continuum are described by an anharmonic potential which contains linear and nonlinear terms, the latter leading to processes involving three-quasiparticle collisions, namely, two polar phonons in the chain and one acoustic phonon in the bath. These processes (at a microscopic level) play a fundamental role in the model, for they are responsible for the introduction of non-linearities (at a macroscopic level) in the dynamical equations governing the thermodynamic evolution of the system. The pumping action of the external source is determined by coupling terms between the source and the chain, which lead to the generation of single and double excitations [6].

We also assume in the model that the acousticlike modes act as an ideal thermal bath kept in a state of equilibrium at a constant temperature, say T_0. Accordingly, the population of a vibrational mode of the bath is given by the Planck distribution

$$\eta_q = [\exp(\beta\hbar\Omega_q)]^{-1} , \tag{1}$$

where Ω_q is the mode frequency, $\beta = 1/(k_B T_0)$, and k_B is the Boltzmann constant. The equations of evolution for the populations of the polar vibrations are obtained in the framework of the nonequilibrium statistical method described in [5], where these equations are given (cf. Eq. (8) in [5]).

The equation for the rate of change of the population of a phonon mode of wave vector q has the typical form

$$\frac{d\nu_q}{dt} = I_q - \mathcal{J}_q \, . \tag{2}$$

In Eq. (1), I_q stands for the pumping term (coupling to the external sources of metabolic energy), which is composed of two terms, corresponding to generation of single and double excitations-the latter one (not present in [5] but considered in [6] implies a very effective mechanism of positive feedback that largely enhances the efficiency of the pumping action of the source. The last term $\mathcal{J}_q$ on the rhs of Eq. (1) is a collision integral, which is composed of the five terms described in [5]; it consists (in the approximation to the kinetic theory that we used) in contributions which are the equivalent of the Golden Rule of Quantum Mechanics averaged over the nonequilibrium ensemble that the method introduces. Of the five contributions, which are a result of the anharmonic interactions between the chain and the elastic continuum, two are linear in the populations of the polar modes, which account for the usual relaxation of the excess energy of those modes toward the thermal bath. The other three terms are *nonlinear* in the population of the polar phonons, and although they also involve relaxation to the surrounding bath, they contain, among others, the nonlinear contributions that are responsible for the complex behavior of the system, i.e., the emergence of *Fröhlich's effect*. This was shown in [5] and [6].

The rate Eq. (1) consists of a complicated set of integrodifferential equations for the populations of the modes, since the collision integral involves a sum over all modes contained in the Brillouin zone. We circumvent this difficulty by resorting to a simplified model. Taking into account the established fact that high-frequency modes transfer energy to the low-frequency ones, we introduce a crude model in which we consider a representative set of energy-transferring modes, with a unique frequency ω_0 and contained in a region $\mathcal{R}_0$ of the Brillouin zone, and a representative set (with frequency ω_1) in another region $\mathcal{R}_1$ of the Brillouin zone. We are then left with only two coupled equations for the two sets of representative modes in the model, namely:

$$\frac{d}{dt}\nu_0(t) = I_0 - \frac{1}{\tau_0}[\nu_0 - \nu_0^{\mathrm{eq}}] - g_1\eta e^{\beta\hbar\Delta}\nu_0(t) + g_1\eta\nu_1(t) - g_1\nu_0(t)\nu_1(t) \tag{3a}$$

and

$$\frac{d}{dt}\nu_1(t) = I_1 - \frac{1}{\tau_1}[\nu_1 - \nu_1^{\mathrm{eq}}] - g_0\eta e^{\beta\hbar\Delta}\nu_1(t) + g_0\eta\nu_1(t) + g_0\nu_0(t)\nu_1(t) \,, \tag{3b}$$

where

$$\Delta = \omega_0 - \omega_1 \qquad\qquad \eta = [\exp(\beta\hbar\Delta) - 1]^{-1} \,,$$

$$\begin{aligned}
\tau_i^{-1} &= \frac{2\pi}{\hbar^2}\frac{1}{\nu_i^{\mathrm{eq}}}\sum_{\boldsymbol{q}} |V^{(1)}_{\boldsymbol{q}_i\boldsymbol{q}}|^2 \Big\{\eta_{\boldsymbol{q}}\eta_{\boldsymbol{q}_i+\boldsymbol{q}} e^{\beta\hbar\Omega_{\boldsymbol{q}}}\delta(\Omega_{\boldsymbol{q}_i+\boldsymbol{q}} - \Omega_{\boldsymbol{q}} - \omega_i) \\
&\quad + \eta_{\boldsymbol{q}}\eta_{\boldsymbol{q}-\boldsymbol{q}_i}\delta(\Omega_{\boldsymbol{q}_i-\boldsymbol{q}} + \Omega_{\boldsymbol{q}} - \omega_i)\Big\} \qquad (i = 0, 1) \\
I_i &= |W^{(1)}_{\boldsymbol{q}_i}|^2 \mathcal{K}_{\boldsymbol{q}_i}(\omega_0) + \sum_{\boldsymbol{q}} |W^{(1)}_{\boldsymbol{q}_i\boldsymbol{q}}|^2 \mathcal{K}_{\boldsymbol{q}_i+\boldsymbol{q}}(\omega_i + \omega_{\boldsymbol{q}})[1 + \nu_i(t) + \nu_{\boldsymbol{q}}(t)] \,, \qquad (i = 0, 1) \\
g_0 &= \frac{2\pi}{\hbar^2}\sum_{\boldsymbol{q}\in\mathcal{R}_0} |V^{(2)}_{\boldsymbol{q}_i\boldsymbol{q}}|^2 \delta(\Omega_{\boldsymbol{q}_i-\boldsymbol{q}} - \Delta) \,, \\
g_1 &= \frac{2\pi}{\hbar^2}\sum_{\boldsymbol{q}\in\mathcal{R}_1} |V^{(2)}_{\boldsymbol{q}_1\boldsymbol{q}}|^2 \delta(\Omega_{\boldsymbol{q}_0-\boldsymbol{q}} - \Delta) \,.
\end{aligned}$$

ν_0^{eq} and ν_1^{eq} are the distributions in equilibrium, and $\boldsymbol{q}_0$ and $\boldsymbol{q}_1$ label each type of representative modes. The symbols $V^{(1)}_{\boldsymbol{q}_i\boldsymbol{q}}$ and $V^{(1)}_{\boldsymbol{q}_i\boldsymbol{q}}$ are the matrix elements of the anharmonic potential for the interactions between the chain and the elastic continuum, $W^{(1)}_{\boldsymbol{q}_i}$ and $W^{(2)}_{\boldsymbol{q}_i}$ represent the coupling strengths for the interactions of the source with the chain, and $\mathcal{K}(\omega)$ stands for the intensity of the source over the spectrum of frequencies.

It is worth mentioning that quantities g_0 and g_1, are a measure of the intensity of the coupling between the two sets of modes. These quantities (i) depend on the strength of the interaction contained in the matrix element $V^{(2)}_{\boldsymbol{q}_i\boldsymbol{q}}$ involve (ii) the region in energy-momentum space available for the three-quasiparticle scattering events determined by the energy conserving delta function (momentum conservation is automatically accounted for in the expression for the Hamiltonian of the system [5, 6]).

More specifically, we consider the model of a one-dimensional chain embedded in an elastic continuum, with the following dispersion relations:

$$\omega_q = \omega_0 - \alpha q^2 , \tag{4}$$

for the polar modes in the chain, and

$$\Omega_q = sq , \tag{5}$$

for the acousticlike vibrations of the surrounding elastic medium.

For the sake of definiteness, we consider in our calculations the following set of values for the system parameters: $\omega = 3.1 \times 10^{14}$ rad/s, $\alpha = 2.4 \times 10^{-2}$ cm^{2}s^{-1}, $q_0 = 0$, $q_1 = s/\alpha = 6.6 \times 10^6$ cm^{-1}, $a = 27$ Å, and $L = 1500$ Å. The parameters a and L are the crystallographic unit cell extension and the chain length, respectively. The values that we have taken for a and L as well as that for ω_0, are typical of a biomolecule such as the myosin molecule [7]. As a typical value for s, we have taken that of the speed of sound in liquids [8]. Finally, the value that we chose for α is such that if we take $q_0 = 0$ as the representative mode in region $\mathcal{R}_0(|\boldsymbol{q}_0| < s/\alpha)$ [5] then the delta functions in the quantitie g_0 and g_1 of Eqs. (2a) and (2b) couple that mode to just one mode $q_1 = s/\alpha$ in region $\mathcal{R}_1(|\boldsymbol{q}_1| < s/\alpha)$. In fact, mode $-q_1$, is also coupled to mode q_0, However, the equivalence between the symmetric modes $\pm q_1$ allows us to consider only two kinetic equations Coupling modes q_0 and q_1 which will be and denoted from now on as mode 0 and mode 1 respectively.

To further simplify matters, but without losing the fundamental features of the model, we take the matrix elements $V^{(i)}$ and $W^{(i)}$ $(i = 1,2)$ as constands and write $|V^{(1)}_{q_jq}|^2 = |V_1|^2$, $|V^{(2)}_{q_jq}|^2 = \lambda |V_1|^2$, $|W^{(1)}_{q_j}|^2 = |W_1|^2$, and $|W^{(}_{q_jq}2)|^2 = d\varpi |W_1|^2/L$, with $j = 1,2$. We introduce a further simplification: $\mathcal{K}_{q+q_i} \approx \mathcal{K}_q(\omega_q)$, with $i = 0, 1$, i.e., we assume that the intensity $\mathcal{K}$ does not change appreciably over the range of frequencies of the polar modes' spectrum.

Using the assumptions above and introducing the time scale $\bar{\tau} = \hbar^2 s/(L|V_1|^2)$ and the dimensionless quantities $t^* = t/\bar{\tau}$, $\tau_i^* = \tau_i/\bar{\tau}$ and $S_i = |W^{(1)}|^2 \mathcal{K}_i \tau$, $i = 0, 1$, the kinetic equations, Eqs. (2a) and (2b), can be rewritten as

$$\frac{d}{dt^*}\nu_0 = [1 + \varpi[1 + (1 + r/2)]\nu_0 + r\nu_1]S_0 - (\tau_0^*)^{1}[\nu_0 - \nu_0^{\mathrm{eq}}]$$

$$- 2\lambda\eta e^{\beta\hbar\Delta}\nu_0 + 2\lambda\eta\nu_1 - 2\lambda\nu_0\nu_1 \quad (6)$$

and

$$\frac{d}{dt^*}\nu_1 = [1 + \varpi[1 + r\nu_0/2 + (1 + r)\nu_1]S_1 - (\tau_1^*)^{1}[\nu_1 - \nu_1^{\mathrm{eq}}]$$

$$+ \lambda\eta e^{\beta\hbar\Delta}\nu_0 - \lambda\eta\nu_1 + \lambda\nu_0\nu_1 \ , \quad (7)$$

where $r = as/(\pi\alpha)$.

Next, we proceed to analyze the steady-state solutions of Eqs. (3a) and (3b). To provide better evidence of the emergence of Fröhlich's effect, we further simplify our analysis by considering from now on that only the set of polar modes higher in frequency (identified by the index nought) are pumped by the external source, i.e., we set $S_1 = 0$ in Eqs. (3a) and (3b).

The steady-state solutions of the nonlinear dynamical system, represented by the coupled set of Eqs. (3a) and (3b), follow by setting the rates $d\nu_i/dt^*$ equal to zero. The resulting system of algebraic equations admits two distinct solutions that we denote by $\boldsymbol{\nu}_-^0 \equiv (\nu_{0-}^0, \nu_{1-}^0)$ and $\boldsymbol{\nu}_+^0 \equiv (\nu_{0+}^0, \nu_{1+}^0)$. Figure 1 shows these solutions as functions of S_0 for the choice $\lambda = \varpi = 10^{-2}$ (a variety of choices of parameter values, each parameter ranging independently from 10^{-3} to 1, leads to similar results).

An investigation of the local stability of the steady-state solutions was performed on the basis of the usual linear stability analysis. This analysis shows that $\boldsymbol{\nu}_-^0$ as well as the branch of $\boldsymbol{\nu}_+^0$ corresponding to (unphysical) negative values of ν_{1+}^0 are always unstable. On the other hand, the branch of $\boldsymbol{\nu}_+^0$ corresponding to positive values of both ν_{0+}^0 and ν_{1+}^0 is always stable, being either a stable node or a stable focus (after using the nomenclature of [9]. Thus, only the physically meaningful steady-state solution is mathematically stable.

Prior to a discussion of the emergence of the Fröhlich effect, we consider first the asymptotic behavior of the solution of Eqs. (3a) and (3b) for large values of S_0, i.e., for values of S_0 greater than $\approx$ 184, and, we recall, $\lambda = \varpi = 10^{-2}$ [this range of S_0 corresponds to the unstable branch of the steady-state solution ν_+^0 in Fig. 11. In those cases, there is no possibility for the system to attain a steady state: At long times, the population ν_0 tends to saturate while the population ν_1 keeps growing exponentially. In fact, making $d\nu_0/dt^* \approx 0$ and considering that $\nu_1 \gg \nu_0$, we get from Eqs. (3a) and (3b)

$$\nu_0 \approx \eta + \frac{\varpi r S_0}{2\lambda} \tag{8}$$

and

$$\frac{d}{dt^*}\nu_1 \approx \left(\frac{\varpi r S_0}{2} - \frac{1}{\tau_1}\right)\nu_1 \tag{9}$$

a result that can be verified once numerical solutions of Eqs. (3a) and (3b) for any value S_0 greater than $\approx$ 184 are obtained.

Let us consider next the question of the onset of Fröhlich's effect. Figure 2 shows the stable steady state populations as functions of the pumping parameter S_0, for $\lambda = \varpi = 10^{\ 2}$. Inspection of that figure tells us that the steady-state population ν_1^0 of the lower-frequency modes overcomes the corresponding population of the pumped modes, ν_0^0, for S_0 above $\approx$ 41. This value of the pumping parameter can be taken as a threshold value for the onset of Frölich's effect in the present case when $\lambda = \varpi = 10^{-2}$. Beyond such a threshold, there follows a large increase of ν_1^0, and, e.g., for $S \approx 183$, the modes in the condensate attain a steady-state population near three orders of magnitude larger than that of the pumped modes.

We are now in a position to examine the transient behavior of the system as it is driven by the external source of energy from the initial state of equilibrium to the final steady state. As an illustration, we consider the following set of parameter values: $S_0 = 180$ and, as before, $\lambda = \varpi = 10^{-2}$. Figure 3(a) and (b) shows the evolution of the populations during the first stages of the pumping process. That figure shows that the population of the modes labeled 0 (Pumped modes) increases very rapidly and then relaxes, also rapidly (peak "width" $\Delta t^* \approx 2$), to levels comparable to its final steady-state value ($\nu_0^0 \approx 100$). On the other hand, the population of the modes labeled 1 starts to increase significantly only during the fist relaxation process undergone by type-0 modes. However, contrasting with the behavior of the pumped modes, type-1 modes evolve very slowly toward a final population ($\nu_1^0 \approx 1.7 \times 10^4$). This is confirmed by the numerical calculation: For example, the Population of type-0 modes at $t^* = 15$ differs by ≈ 4% from its steady-state value, whereas the corresponding difference for type-1 modes is ≈ 84%.

For a more detailed analysis of the transient process, let us rewrite Eqs. (3a) and (3b) in the following form:

$$\frac{d}{dt^*}\nu_0 = r_0^{\text{abs}} + r_0^{\text{fdb}} + r_0^{\text{bath}} + r_0^{\text{net transf}} \tag{10}$$

and

$$\frac{d}{dt^*}\nu_0 = r_1^{\text{abs}} + r_1^{\text{fdb}} + r_1^{\text{bath}} + r_1^{\text{net transf}} , \tag{11}$$

where the term

$$r_0^{\text{abs}} \equiv S_0$$

in Eq. (4a) represents the rate of population growth of type-0 modes due to the production of single excitations by the external source; the next term,

$$r_0^{\text{fdb}} \equiv \varpi S_0[1 + (1 + r/2)\nu_0 + r\nu_1] ,$$

is the contribution to the rate of population growth due to double excitations (containing the feedback effect); the third term,

$$r_0^{\text{bath}} \equiv -\frac{1}{\tau_0^*}[\nu_0 - \nu_0^{\text{eq}}] ,$$

is the rate at which the population of the type-0 modes relaxes to the thermal bath; and, finally, the fourth term,

$$r_0^{\text{net transf}} \equiv -2\lambda[\eta e^{\beta\hbar\Delta}\nu_0 - \eta\nu_1 + \nu_0\nu_1] ,$$

is related to energy transfer from type-0 modes to type-I modes in processes mediated by the anharmonic interactions between the chain and the elastic continuum. In this sense, r net tran,f is a measure of the net rate of population exchange between the two sets of polar modes. Correspondingly, we can identify on the rhs of Eq. (4b) the following terms:

$$r_1^{\text{abs}} \equiv S_1$$

$$r_1^{\text{fdb}} \equiv \varpi S_1[1 + r\nu_0/2 + (1 + r)\nu_1] ,$$

$$r_1^{\text{bath}} \equiv -\frac{1}{\tau_1^*}[\nu_1 - \nu_1^{\text{eq}}] ,$$

and

$$r_1^{\text{net transf}} \equiv \lambda[\eta e^{\beta\hbar\Delta}\nu_0 - \eta\nu_1 + \nu_0\nu_1] .$$

The evolution in time of the rates defined above is displayed in Figure 4. Taking into account the linearity between the rates r_i^{bath} and the respective populations ν_i, we can also follow in Figure 4 the time evolution of the populations. As can be noticed by inspection of the figure, the energy exchange between the two sets of modes begins to be effective only when type-0 modes (pumped modes) become significantly populated. The exchange proceeds at high rates even after the decrease of vo has occurred, due to the high levels of population then reached by type-1 modes (the modes in the condensate).

Finally, we analyze the relaxation process that takes place in the system when the power source is turned off after the condensation has taken place. Figures 3(c) and (d) and 5 show the time evolution of the populations ν_i and of the rates r_i^{bath} and $r^{\text{net transf}}$

We can distinguish two time scales for the relaxation process for type-0 modes. The first, very short ($\Delta t^* \approx 0.02$) corresponds essentially to a fast energy transfer from the pumped type-0 modes to type-1 modes. During this process, the population of type-0 modes is reduced to ≈ 50% of its initial nonequilibrium value [Fig. 3(c)]. The second time scale, much longer ($\Delta t^* \approx 20$), is characterized by energy transfer to (and also from) type-1 modes and to the bath, at very small rates [compared to those in the first stage, see Fig. 5(a) and inset].

On the other hand, there are no appreciable changes in behavior for the type-1 mode population during the relaxation toward equilibrium. Although type-1 modes are favored by an energy flow from type-0 modes during the very first moments of the process and, later on, disfavored by a reverse flow [Fig. 5(a) and (b)], the relaxation can be considered as taking place in an exponential-like fashion starting at the initial time [Fig. 3(d)].

The transient regimes can be appreciated globally (pumping and relaxation stages) in Figure 6. The figure shows the phase trajectory described by the system as it evolves from the equilibrium state to the nonequilibrium Fröhlich's state and its return again to the equilibrium state after suppressing the pumping action of the external source of energy. The main features of the evolution of the populations, as determined by the nonlinear coupling between the two sets of modes, can be distinguished clearly in the "hysteresis loop" that can be observed in Figure 6. In particular, we can identify the initial growth of the type-0 mode population and the subsequent energy transfer to type-I modes, during the pumping process. It can also be noticed that the population of the type-1 modes remains at levels close to that of the condensate during the very first moments of the relaxation process following the turning off of the external energy source, at the expense of the flow of energy it is receiving from the type-0 modes.

In closing this section, we present numerical estimates for the transient times as well as for the energy consumption during the pumping process. On the assumption that the relaxation time to the bath, τ_q, is of the order of tens of picoseconds [10], we can estimate the time scale $\bar{\tau}$ to be about 20 ps. Using this value, in the case of $\lambda = \varpi = 0.5$, we find a time $t_p \approx 0.17$ ps for the system to reach a population ratio

ν_1/ν_0, when all modes are pumped at equal rates $S_0 = S_1 = 950$. On the other hand, for the process of irreversible relaxation that follows after turning off the power source, we can estimate that it takes the system a much longer time, $t_R \approx 0.68$ ns, to get its population reduced to a level of about 10% above the equilibrium value.

Now let us make an estimate of the energy to be expended by the source during the pumping process. Using the given time scale $\bar{\tau} = 20$ ps, we find that a power $\hbar\omega_0 S_0/\bar{\tau} \approx 9.7\times 10^{12}$ eV/s per mode should be delivered by the external source (we are considering, as above, $S_0 = S_1 = 950$). For a system such as the myosin molecule, with two α-helices, each containing three chains [7], there would be $6(L/a) \approx 330$ modes per molecule to be pumped by the external source. This implies an energy consumption of about $6(L/a) \times (\hbar\omega_0 S/\bar{\tau})t_P \approx 5.4 \times 10^2$ eV/molecule, as the system is driven from the initial state of thermodynamic equilibrium to a state in which the population ratio attains a value $\nu_1/\nu_0 \approx 10$, after an elapsed pumping time $t_P \approx 0.17$ ps. Assuming that this energy is provided by means of the hydrolysis of adenosine triphosphate (ATP), which under metabolic conditions in a cell can deliver 0.54 eV/molecule [11], we conclude that ≈ 103 molecules of ATP per pumped molecule would be expended in the process. It Should be stressed that, due to the simplifications introduced in the present illustrative model, this result is an overestimation of the order of magnitude [12]. More realistic approaches predict values which seem to be very accessible for the phenomenon to occur [5].

As a final comment, it is worth mentioning a possible connection between the Fröhlich's condensation phenomenon and the propagation of coherent excitations in a biomolecule, the so-called Davydov's solitons [13]. Both phenomena result from the same nonlinearities in the evolution equations as those we consider in this article. As shown in [14], the presence of a condensate in the system allows for the propagation of nearly undamped Davydov's solitons composed of the low-lying-in-frequency polar modes excitations in the molecule. This result may be of relevance in the understanding of energy propagation in biosystems.

3. Conclusions

The simple but representative model of two coupled sets of modes that we have introduced has allowed us to analyze some relevant features of Fröhlich's condensation phenomenon. As shown, the anharmonic interactions between the polar modes in the chain with the acousticlike excitations in the elastic continuum provide the necessary conditions for the system to attain a nonequilibrium steady state as it absorbs energy from an external source. Above a threshold value of the pumping intensity, the system can exhibit the phenomenon of condensation of excitations in the polar modes lowest in frequency. It was considered the role played by the action of a source producing double excitations, which enhances considerably the population growth rates of the pumped polar modes, and being capable of suppressing the *steadiness* of the condensate state. However, it should be stressed that the phenomenon of condensation into the lowest-in-frequency modes persists even in these circumstances.

We also analyzed the role played by the interactions of the chain with its surroundings in determining the nonequilibrium thermodynamic evolution of the system during the pumping stage when going from equilibrium to the steady state, as well as the return of the system to equilibrium, after turning off the external energy source. We verified that in both stages the anharmonic interactions between the chain and the elastic medium induce a rapid exchange of energy between the two types (if modes once the populations attain large values. It follows that during the pumping process initially only the population of the pumped modes increases rapidly. Noticeable energy transfer to the modes of low frequency occurs only after the pumped-mode population attains a certain threshold value. For the transient stage following the turning off of the energy source, we found the existence of two time scales characterizing the evolution of the population of the modes high in frequency: The first, a very short one, characterizes the rapid energy transfer to the condensed low-infrequency modes (since both modes are highly populated high-energy exchange rates are expected in this case); the second, a much longer one, corresponds to energy transfer (at low rates) to the bath as well as to and from the low-infrequency modes. The population of the modes in the condensate, on the other hand, relaxes exponentially, without any remarkable change in behavior.

4. Acknowledgments

We would like to thank Professors R. Luzzi and A. R. Vasconcellos for valuable discussions. This work was supported in part by the São Paulo State Research Foundation (FAPESP), the National Research Council (CNPq), and the Ministry of Education (MEC/CAPES).

REFERENCES

[1] H. Fröhlich, in Theoretical Physics and Biology, M. Marois, Ed. (North-Holland, Amsterdam, 1969).

[2] H. Fröhlich, Adv. Electron. Electron. Phvs. **53**, 85 (1980).

[3] H. Fröhlich, Int. J. Quantum Chem. **2**, 641 (1968); Ibid., 14 Nature **228**, 1093 (1970).

[4] T. M. Wu and S. Austin, J. Theor. Biol. **71**, 209 (1978); R. K. Mishra, K. Bhaumik, S. C. Mathur, and S. Mitra, Int. J. Quantum Chem. **26**, 691 (1979); S. A. Moskalenko, E. P. Pokatilov, M. F. Miglei, and I. S. Kiselyova, Int. J. Quantum Chem. **26**, 745 (1979); R. E. Mills, Phys. Rev. A **28**, 379 (1983); R. Paul, J. A. Tuszyński, and R. Chatterjee, Phys. Rev. A **30**, 2676 (1984); J. Hirsch, Phys. Lett. A **121**, 447 (1987); R. E. Mills, Phys. Rev. A **43**, 3176 (1991); J. A. Tuszynski and R. Paul, Phys. Rev. A **43**, 3179 (1991); C. F. Eichwald, Phys. Lett. A **207**, 194 (1995).

[5] M. V. Mesquita, A. R. Vasconcellos, and R. Luzzi, Phys. Rev. E **48**, 4049 (1993).

[6] M. V. Mesquita, A. R. Vasconcellos, and R. Luzzi, Nuovo Cim., **17**, 569 (1995).

[7] A. S. Davydov, Biology and Quantum Mechanics (Pergamon, Oxford, 1982), pp. 44, 45, 165.

[8] D. R. Lide, Ed., *CRC Handbook of Chemistry and Physics*, 72nd ed. (CRC Press, Boca Raton, FL, 1991), p. 14–35.

[9] R. Serra, M. Andretta, M. Compiani, and G. Zanarini, *Introduction to the Physics of Complex Systems* (Pergamon, Oxford, 1986), Chap. 5.

[10] S. J. Webb, Phys. Rep. **60**, 201 (1980).

[11] A. S. Davydov, *Biology and Quantum Mechanics* (Pergamon, Oxford, 1982), p. 111.

[12] S. E. Bresler, *Introduction to Molecular Biology* (Academic Press, New York, 1971), p. 188.

[13] See, e.g., A. Scott, Phys Rep. **217**, 1 (1992); A. S. Davydov, in *Solitons*, S. E. Trullinger, V. E. Zakharov, and V. L. Prokrovsky, Eds. (Elsevier, Amsterdam, 1986); see also A. S. Davydov, *Biology and Quantum Mechanics* (Pergamon, Oxford, 1982), p. 190. M. V. Mesquita, A. R. Vasconcellos, and R. Luzzi, Int. Quantum Chem. **60**, 689 (1996).

FIGURE CAPTIONS

Figure 1: Steady-state solutions of Eqs. (3a) and (3b) as functions of the pumping parameter S_0 for $\lambda = \varpi = 10^{-2}$ and $S_1 = 0$. Attention should be paid to the marked differences in scales on the vertical axes.

Figure 2: Steady-state populations as functions of the pumping parameter S_0, for $\lambda = \varpi = 10\ ^{2}$ and $S_1 = 0$.

Figure 3: (a, b): Evolution of the populations ν_0 and ν_1, during the first stages of the pumping process, for $\lambda = \varpi = 10\ ^{2}$, $S_0 = 180$, and $S_1 = 0$. (c, d): Evolution during the relaxation process toward the thermodynamic equilibrium state, after turning off the external source.

Figure 4: Early stages of the pumping process: evolution of the various components of the population growth rates for (a) type-0 modes and (b) type-1 modes. Parameters: $\lambda = \varpi = 10\ ^{2}$, $S_0 = 180$, and $S_1 = 0$.

Figure 5: Evolution of the components of the population relaxation rates for (a) type-0 modes and (b) type-1 modes. Parameters: $\lambda = \varpi = 10^{-2}$.

Figure 6: Phase trajectory described by the system as it evolves from the equilibrium state to Fröhlich's state and its return to the initial state of equilibrium after turning off the external energy source. Parameters: $\lambda = \varpi = 10^{-2}$, $S_0 = 180$ and $S_1 = 0$ (pumping stage).

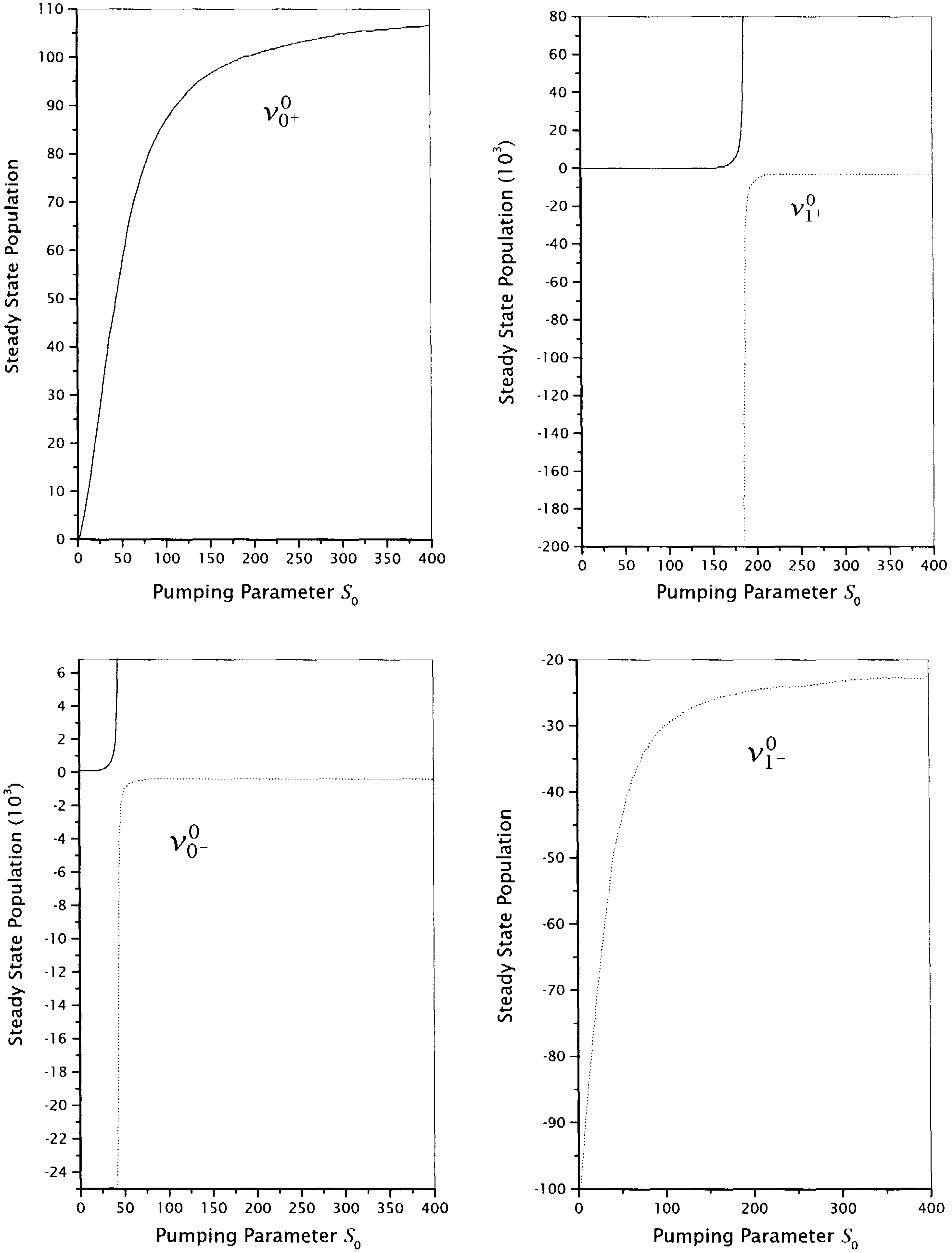

Figure 1: Steady-state solutions of Eqs. (3a) and (3b) as functions of the pumping parameter S_0 for $\lambda = \varpi = 10^{-2}$ and $S_1 = 0$. Attention should be paid to the marked differences in scales on the vertical axes.

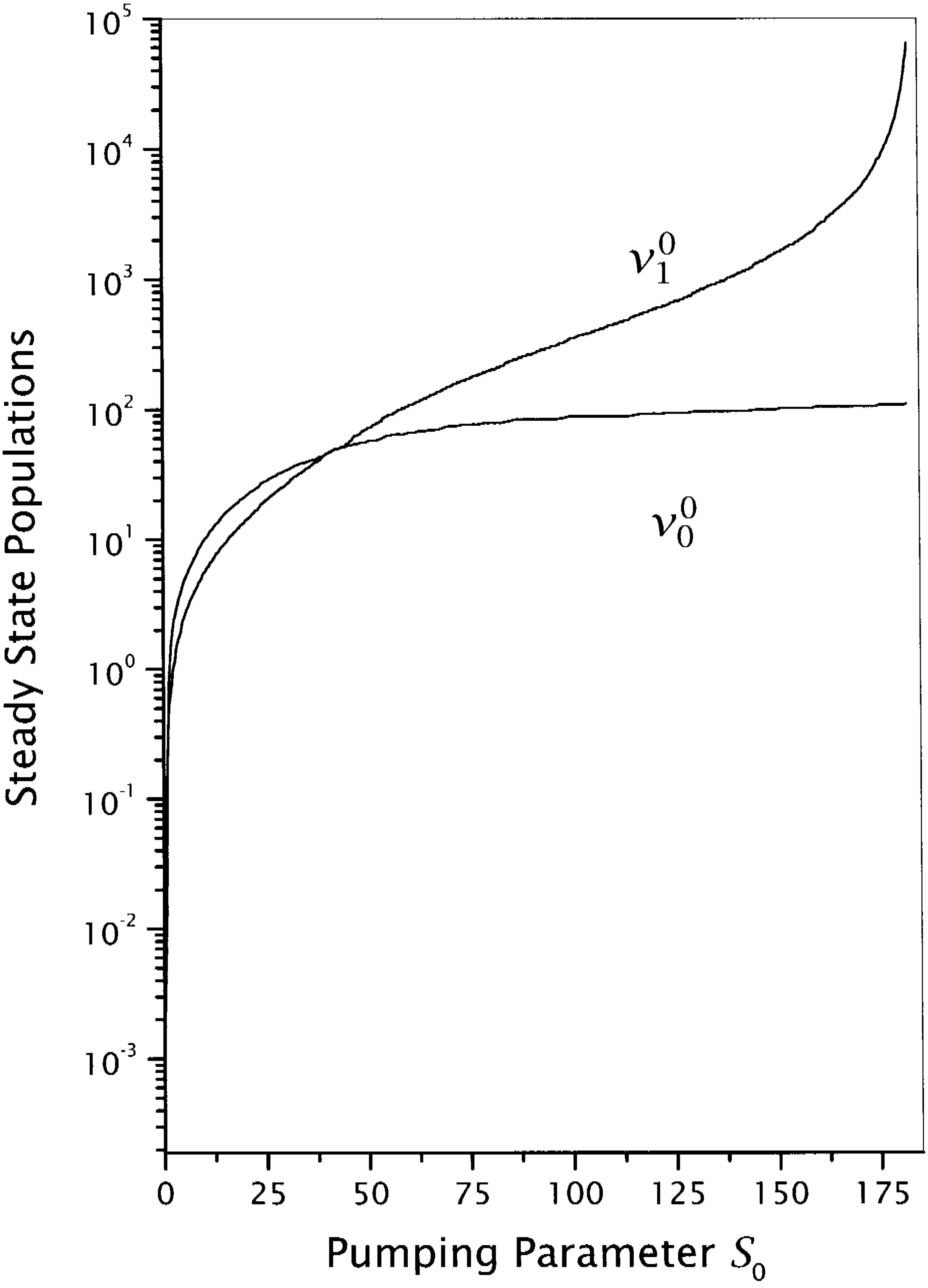

Figure 2: Steady-state populations as functions of the pumping parameter S_0, for $\lambda = \varpi = 10^{-2}$ and $S_1 = 0$.

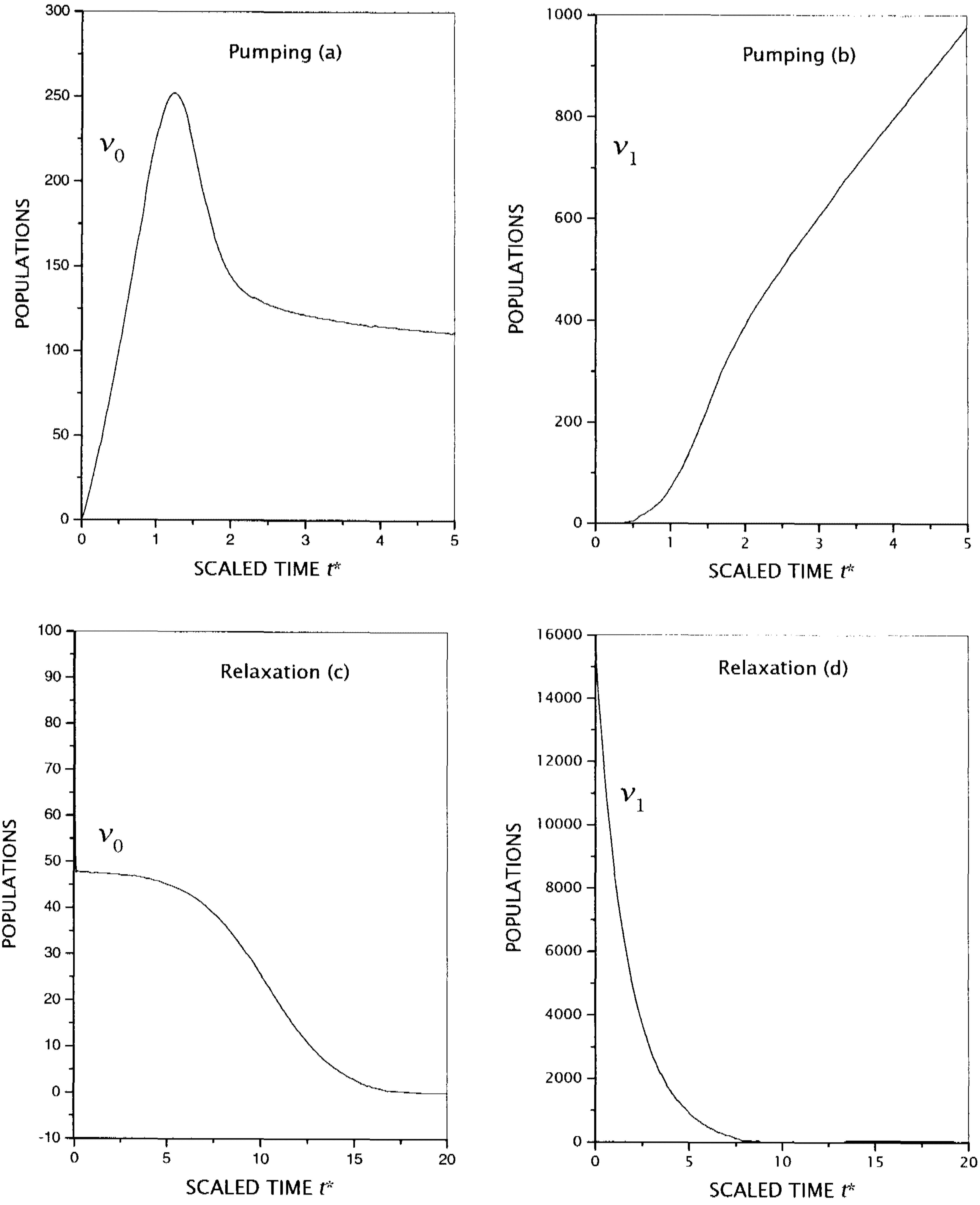

Figure 3: (a, b): Evolution of the populations ν_0 and ν_1, during the first stages of the pumping process, for $\lambda = \varpi = 10^{-2}$, $S_0 = 180$, and $S_1 = 0$. (c, d): Evolution during the relaxation process toward the thermodynamic equilibrium state, after turning off the external source.

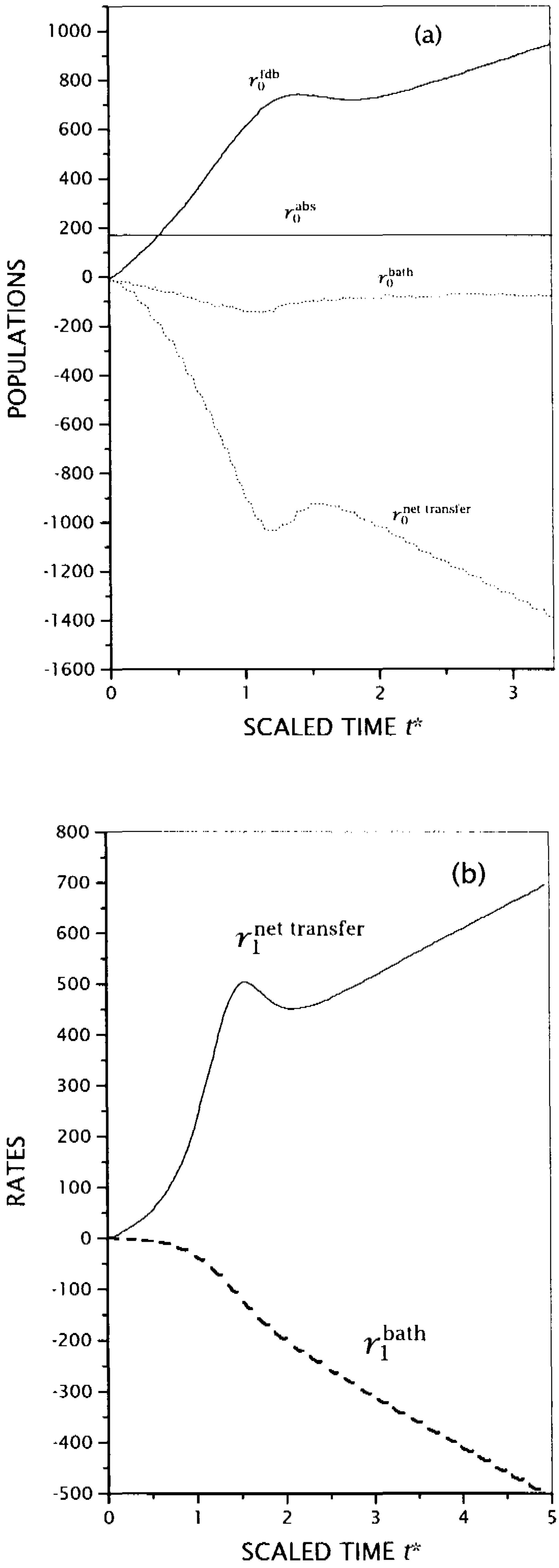

Figure 4: Early stages of the pumping process: evolution of the various components of the population growth rates for (a) type-0 modes and (b) type-1 modes. Parameters: $\lambda = \varpi = 10^{-2}$, $S_0 = 180$, and $S_1 = 0$.

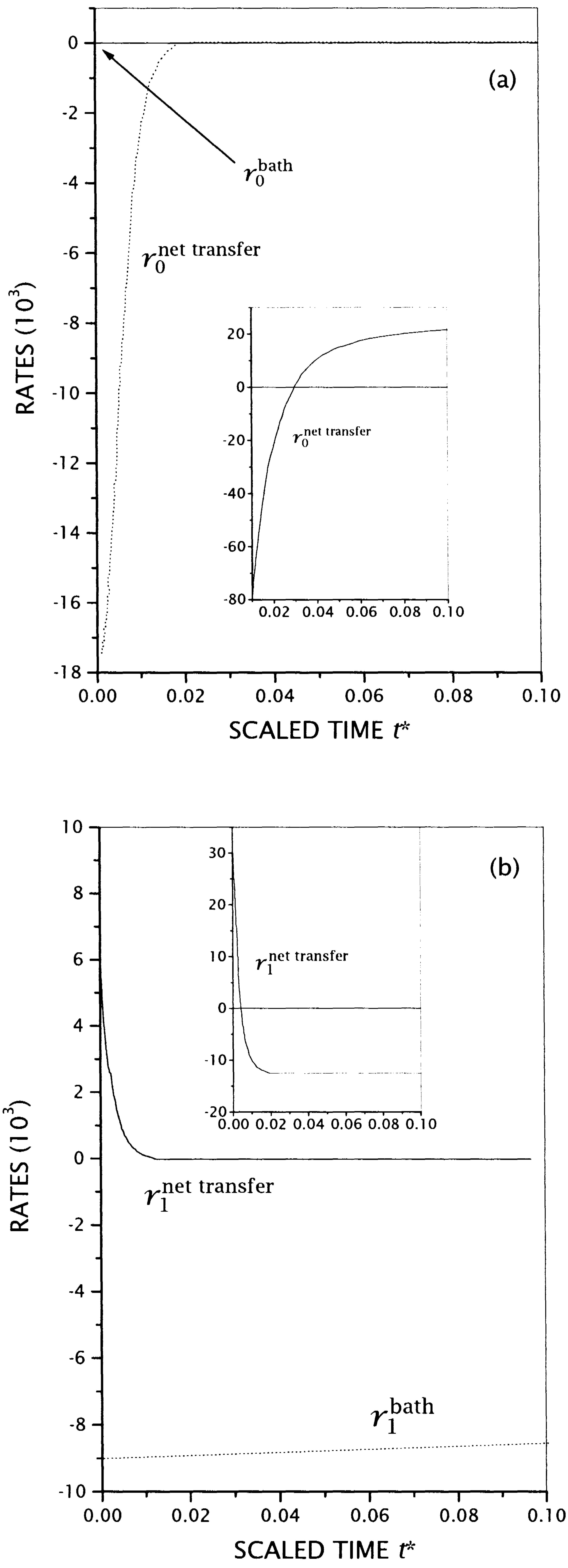

Figure 5: Evolution of the components of the population relaxation rates for (a) type-0 modes and (b) type-1 modes. Parameters: $\lambda = \varpi = 10^{-2}$.

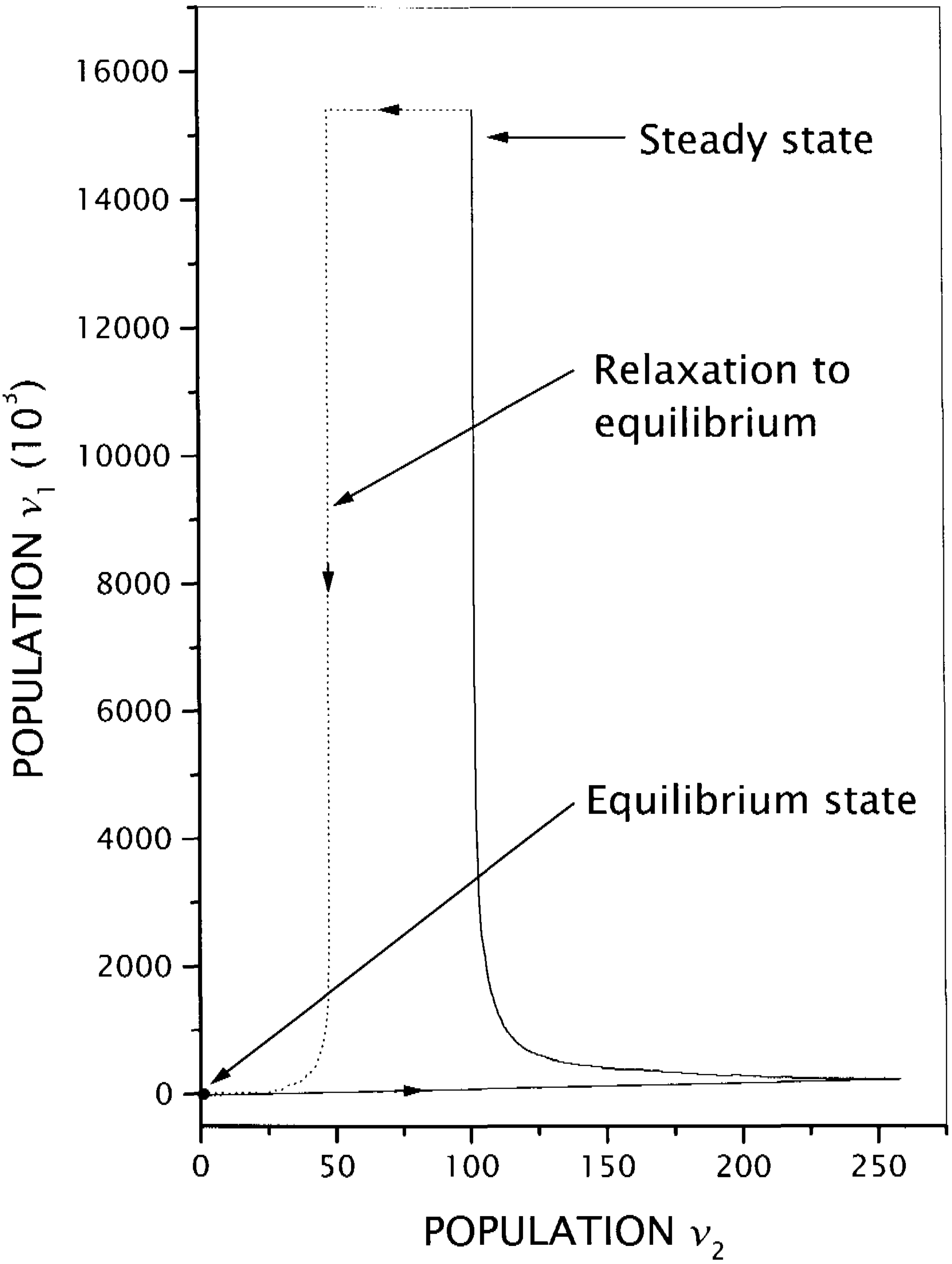

Figure 6: Phase trajectory described by the system as it evolves from the equilibrium state to Fröhlich's state and its return to the initial state of equilibrium after turning off the external energy source. Parameters: $\lambda = \varpi = 10^{-2}$, $S_0 = 180$ and $S_1 = 0$ (pumping stage).

4.6 Termodinâmica estatística de sistemas complexos

Aplicamos um tratamento termodinâmico estatístico ao estudo de um sistema físico particular (dois conjutos de osciladores acoplados não-lineares) levado para longe do equilíbrio. Tal sistema apresenta um tipo de comportamento complexo consistindo no assim chamado efeito Fröhlich, que leva, em condições de estado estacionário, a um condensação de fase de não-equilíbrio que se assemelha a uma condensação de Bose-Einstein de sistemas em equilíbrio. Uma espécie de "modelo de dois fluidos" surge: a "fase normal de não-equilíbrio" e o condensado de Fröhlich ou "superfase de não-equilíbrio". Trabalhamos com detalhes a termodinâmica desse sistema complexo dissipativo.

Submetido para publicação em *Chaos* (Am. Inst. Phys.)

Statistical Thermodynamics of Complex Systems

Alexandre F. Fonseca, Marcus V. Mesquita,[1]
Áurea R. Vasconcellos, Roberto Luzzi

Instituto de Física 'Gleb Wataghin',
Universidade Estadual de Campinas, Unicamp
13083-970 Campinas, São Paulo, Brazil

---

[1] E-mail:sousa@ifi.unicamp.br

We apply a statistical-thermodynamic approach to the study of a particular physical system (two sets of nonlinearly coupled oscillators), driven far away from equilibrium. Such system displays a kind of complex behavior consisting in the so-called Fröhlich effect leading in steady-state conditions to a nonequilibrium phase condensation resembling the Bose-Einstein condensation of systems in equilibrium. A kind of "two-fluid model" arises: the "normal nonequilibrium phase" and Fröhlich condensate or "nonequilibrium superphase", which is shown to be an attractor of the system. We work out some aspects of the irreversible thermodynamics of this dissipative complex system. Particular nonlinear properties are discussed and Lyapunov exponents determined.

Group Home Page: http://www.ifi.unicamp.br/~aurea

Nowadays *Complex Systems* constitutes a fashionable area of research, and we recall that complex systems is a short expression for the correct one of Dynamical Systems with Complex Behavior [1-3]. Particularly, complex physico-chemical and biological dynamical systems are of special relevance, the first ones mainly for technological interest and the second ones for their relevance related to the origin, evolution and functioning of life and also for technical-comercial interest in, for example, bioengineering and medical-imaging techniques.

We first notice that complexity must not be confused with a system being of a complicated struture: the dynamical system may be quite simply modelled but showing complex behavior, that is, displaying, in principle, unexpectedly rich and diversified characteristics at a macroscopic level of description. A particular example could be Lorentz meteorological model — a protype of chaotic (complex) behavior [4]. Other aspect of complexity is the one associated to selforganization or synergetic ordering (spatial, temporal, or different kinds of homogeneous stationary states) in matter [5-8]. We address here this latter type of complexity.

1. Introduction

Complexity, it must be noticed, can emerge only in the case of systems governed by *nonlinear kinetic laws of evolution.* In the linear domain it is ruled out by Prigogine's theorem of minimum entropy production [9, 10], basically because in such conditions applies the principle of superposition of solutions (of the equations of evolution) and no synergetically-coherent order can follow.

The scientific disciplines appropriate to deal with complex behavior in matter are the Thermodynamics of Irreversible Processes, nonlinear kinetic theories and, mainly, Statistical Mechanics of systems far from equilibrium which provides an umbrella for covering the two others. In this case the first one is sometimes dubbed *Thermodynamics of Complex Systems* [11].

It is presented in continuation what we consider an illustrative didactical example of a system with complex behavior, for which it is possible to derive a complete theory which covers in full all its nonequilibrium thermodynamical and kinetic characteristics.

2. A Model of Coupled Linear Oscillators

For the purpose stated in the Introduction of describing as completely as possible the thermodynamics and kinetics of the macroscopic state of a complex system, we choose: (1) The model of coupled linear oscillators described below, and (2) the description of the nonequilibrium thermodynamics of its time-envolving dissipative macroscopic state in terms of the so-called *Informational Statistical Thermodynamics.*

2.1. Thermodynamics of Irreversible Processes

First we notice that the thermodynamics of irreversible processes has had a development beginning — if we leave aside the attempts done in the nineteenth century — with Classical (sometimes referred to as Linear or Onsagerian) Irreversible Thermodynamics (see for example the classical textbook of Ref. [12] and also [9]). It was extended to the nonlinear regime mainly by Ilya Prigogine and so-called Brussels' School (see for example Ref. [10]). To account for processes involving not too long wavelength and not too small frequencies, when classical irreversible thermodinamics begins to fail, were developed several approaches of which we highlight Rational Thermodynamics [13] and Extended Irreversible Thermodynamics [14].

Moreover, as Thermodynamics of equilibrium, or Thermostatics, is connected to the microscopic level of Mechanics by Gibbs ensemble formalism for Statistical Mechanics, one may expect something similar for nonlinear irreversible thermodynamics of systems arbitrarily away from equilibrium. A promising start with a successful development is provided by Informational Statistical Thermodynamics (IST for short). IST was initiated by Hobson [15] sometime after the publication of Jaynes' seminal papers [16] on the foundations of Statistical Mechanics on Information Theory (of Shannon-Brillouin style [17, 18]). It is worth noticing that the above mentioned thermodynamic formulations belong, one way or another, to the main four levels listed by Laszlo Tisza in Ref. [19].

The present day statistical foundations of IST are provided by a nonequilibrium ensemble formalism referred to as the *Nonequilibrium Statistical Operator Method* (NESOM for short) [20–24]. NESOM is based on a variational principle, namely the maximization of the informational statistical entropy (MaxEnt for short) [25–28], and can be considered as belonging to the domain of Jaynes' Predictive Statistical Mechanics [29–31]. For explicit calculations we resort to Zubarev's approach to this MaxEnt-NESOM [25–28, 32, 33], by far the most concise, practical and soundly based method. Moreover, MaxEnt-NESOM-based IST is going to be described as long as we proceed with the presentation of the physical system we are introducing.

2.2. The Model and The Evolution of its Macrostate

The model system we are considering — schematically described in Fig. 1 – consists of two subsystems of linear oscillators interacting through an anharmonic potencial. The subsystem we label as S_1 is composed of a periodic array of N_1 oscillators of equal mass m and frequencies ω_j with $j = 1, 2, \ldots, N_1$, and we introduce x_j and p_j for the displacement from the position of equilibrium and the conjugated linear momentum respectively. The subsystem labelled S_2 is composed of a periodic array of N_2 oscillators of equal mass M and frequencies Ω_k with $k = 1, 2, \ldots, N_2$, and X_k and P_k stand for the displacement and its conjugated momentum respectively.

It is assumed a very good thermal contact between S_2 and a thermal reservoir, such that the temperature of S_2 is always the one of the reservoir, T_0. An external source pumps energy on S_1. Several realistic systems can be described in this way, for example, lattice vibrations in near one-dimensional semiconductor quantum wires, organic molecular polymers, biological polymers, etc.; our model here covers the case of polymeric α-proteins [35] and acetanilide [36].

The Hamiltonian of the proposed model is taken as:

$$\hat{H} = \hat{H}_0 + \hat{H}' , \tag{1}$$

where

$$\hat{H}_0 = \sum_j \left[\frac{\hat{p}_j^2}{2m} + \frac{1}{2} m \omega_j^2 \hat{x}_j^2 \right] + \sum_k \left[\frac{\hat{P}_k^2}{2M} + \frac{1}{2} M \Omega_k^2 \hat{X}_k^2 \right] \tag{2}$$

and

$$\hat{H}' = \sum_{jkk'} A_{jkk'}\hat{x}_j\hat{X}_k\hat{X}_{k'} + \sum_{jj'k} B_{jj'k}\hat{x}_j\hat{x}_{j'}\hat{X}_k + \sum_{jf}\hat{\varphi}_f\hat{x}_j \, . \tag{3}$$

The form of Eq. (1) is the appropriate for use in MaxEnt-NESOM in this case, where $\hat{H}_0$ is evidently composed of the Hamiltonians of the free oscillators. On the other hand $\hat{H}'$ is composed of the anharmonic interactions (the first lower order contribution), which are the first two terms on the right of Eq. (3), while the last accounts for the interaction between the external source (to be better specified later on) and the system, with $\hat{\varphi}$ standing for an operator associated to the source with the coupling strength included in it, and we are considering a linear coupling.

Next, for convenience we introduce, first, normal coordinates

$$\hat{x}_j = \sum_q \hat{x}_q e^{iqR_j} \, , \qquad \hat{p}_j = \sum_q \hat{p}_q e^{iqR_j} \, , \tag{4}$$

$$\hat{X}_k = \sum_{q'} \hat{X}_{q'} e^{iq'\xi_k} \, , \qquad \hat{P}_k = \sum_{q'} \hat{P}_{q'} e^{iq'\xi_k} \, , \tag{5}$$

where q and q' are wavenumbers in reciprocal (one-dimensional) space, R_j and ξ_k the positioning in the lattice of the center of mass of the oscillators in S_1 and S_2 respectively, and the sumation runs in the intervals $(-\pi/a_1, \pi/a_1)$ and $(-\pi/a_2, \pi/a_2)$ with a_1 and a_2 being the lattice parameters in S_1 and S_2. Second, we introduce the amplitudes a_q and $b_{q'}$ and their conjugates $a_q^\dagger$ and $b_{q'}^\dagger$,

$$\hat{x}_q = \left(\frac{\hbar}{2m\omega_q}\right)^{1/2} (a_q + {a^\dagger}_{-q}) \, , \qquad \hat{p}_q = -\mathrm{i}\left(\frac{\hbar m\omega_q}{2}\right)^{1/2} (a_q - {a^\dagger}_{q}) \, , \tag{6}$$

$$\hat{X}_{q'} = \left(\frac{\hbar}{2m\Omega_{q'}}\right)^{1/2} (b_{q'} + b^{\dagger}{}_{q'}) \,, \qquad \hat{P}_{q'} = -\mathrm{i}\left(\frac{\hbar m\Omega_{q'}}{2}\right)^{1/2} (b_{q'} - b^{\dagger}_{-q'}) \,, \tag{7}$$

where ω_q and $\Omega_{q'}$ are the frequencies of vibration in the corresponding modes, and next second quantization is used, with $a_q(a_q^{\dagger})$ and $b_{q'}$ $(b_{q'}^{\dagger})$ then being the annihilation (creation) operators in mode q in S_1 and q' in S_2.

The Hamiltonian of Eq. (1) is composed in the new representation of the contributions

$$\hat{H}_0 = \hat{H}_{OS} + \hat{H}_{OB} \,, \tag{8}$$

$$\hat{H}_{OS} = \sum_q \hbar\omega_q \left(a_q^{\dagger}a_q + \frac{1}{2}\right) \,, \tag{9}$$

$$\hat{H}_{OB} = \sum_{q'} \hbar\Omega_{q'} \left(b_{q'}^{\dagger}b_{q'} + \frac{1}{2}\right) \,, \tag{10}$$

$$\hat{H}' = \hat{H}_1' + \hat{H}_2' + \hat{H}_3' + \hat{H}_{\varphi} \,, \tag{11}$$

where

$$\hat{H}_1' = \sum_{qq'} \left(V_{qq'}^{(1)} a_q b_{q'} b_{q+q'}^{\dagger} + V_{qq'}^{(1)} a_{q+q'}^{\dagger} b_q b_{q'} + H.C.\right) \,, \tag{12}$$

$$\hat{H}_2' = \sum_{qq'} \left(V_{qq'}^{(2)} a_q^{\dagger} a_{q'} b_{q-q'} + H.C.\right) \,, \tag{13}$$

$$\hat{H}_3' = \sum_{qq'} \left(V_{qq'}^{(2)} a_q a_{q'} b_{q+q'}^{\dagger} + H.C.\right) \,. \tag{14}$$

We notice that in $\hat{H}'$ of Eq. (11) we have kept only the terms consisting of scattering-like processes (Eqs. (12), (13) and (14), and we have neglected terms involving only creation (e.g. $a^\dagger b^\dagger b^\dagger$, etc.) and only destruction of particles (e.g. abb, etc.) which have no contribution for the phenomena we are going to study. Finally the last term in Eq. (11) account for the interaction with the external pumping source, namely

$$\hat{H}_{\varphi} = \sum_q \left(\hat{\varphi}_q a_q^\dagger + H.C.\right) \ , \tag{15}$$

momentum conservation has been considered, and $\hat{\varphi}_q$ ($\hat{\varphi}_q^\dagger$) is the second quatization operator for annihilation (creation) of an excitation of wavevector q in the source, and the coupling strength with the system is incorporated into it.

Next we need to characterized in MaxEnt-NESOM the macroscopic state of the system, and for that purpose we take as the basic set of dynamical variables

$$\left\{\{\hat{\nu}_q = a_q^\dagger a_q\} \ ; \ \hat{H}_{OB}\right\} \ , \tag{16}$$

that is, the occupation numbers in the modes of S_1, which are driven out of equilibrium by the action of the external source, and the Hamiltonian of the system S_2 since it remains in thermal equilibrium at temperature T_0; q, as noticed, takes all possible values in the Brillouin zone.

Therefore, the auxiliary statistical operator in MaxEnt-NESOM (sometimes referred to as "coarse-grained" distribution or "freezed instantaneous quasiequilibrium" distribution) is according to MaxEnt-NESOM [25-28] given in the present case by

$$\bar{\varrho}(t,0) = \exp\left\{-\phi(t) - \sum_q F_q(t)\hat{\nu}_q - \beta_0 \hat{H}_{OB}\right\} . \tag{17}$$

We recall the important point that *this is not the statistical operator of the system,* the latter being a superoperator defined in terms of the $\bar{\varrho}$ of the Eq. (17) which is given by (see Refs. [25–28, 32, 33]),

$$\varrho_{\varepsilon} = \exp\left\{ \ln \bar{\varrho}(t,0) - \int_{\infty}^{t} dt' \, e^{\varepsilon(t'-t)} \frac{d}{dt'} \ln \bar{\varrho}(t', t' \quad t) \right\} , \tag{18}$$

where

$$\bar{\varrho}(t', t'-t) = \exp\left\{ -\frac{1}{i\hbar}(t'-t)\hat{H} \right\} \bar{\varrho}(t,0) \, \exp\left\{ \frac{1}{i\hbar}(t'-t)\hat{H} \right\} . \tag{19}$$

In Eq. (17) we have introduced the Lagrange multipliers that the variational MaxEnt-NESOM produces, namely

$$\left\{ \{F_q(t)\} \; ; \; \beta_0 = \frac{1}{k_B T_0} \right\} , \tag{20}$$

and we recall that $\phi(t)$ ensures the condition of normalization of $\bar{\varrho}(t,0)$, playing the role of a kind of logarithm of a nonequilibrium partition function, say, $\phi(t) = \ln \bar{Z}(t)$. Finally we designate by

$$\left\{ \{\nu_q(t)\} \; ; \; E_B \right\} \tag{21}$$

the macrovariables in the nonequilibrium thermodynamic state space (or Gibbs' thermodynamic space), that is

$$\nu_q(t) = \mathrm{Tr}\left\{\hat\nu_q \varrho_\varepsilon(t)\right\} = \mathrm{Tr}\left\{\hat\nu_q \bar\varrho(t,0)\right\} \ , \tag{22}$$

$$E_B = \mathrm{Tr}\left\{\hat H_{OB} \varrho_\varepsilon(t)\right\} = \mathrm{Tr}\left\{\hat H_{OB} \bar\varrho(t,0)\right\} \ , \tag{23}$$

where $\varrho_\varepsilon(t)$ is the nonequilibrium statistical operator in Zubarev's approach, and we recall that $\varrho_\varepsilon(t)$ and $\bar\rho(t,0)$ give the same average values for the basic dynamical variables and only for these (see Refs. [25–28, 32, 33]). We are now in conditions to derive the equations of motion for the basic macrovariables of Eq. (21). Consider first the populations $\nu_q(t)$; we find that

$$\frac{d}{dt}\nu_q(t) = J_q^{(0)}(t) + J_q^{(1)}(t) + J_q^{(2)}(t) \ , \tag{24}$$

once we use the Markovian approximation in the MaxEnt-NESOM-based kinetic theory [37], where

$$J_q^{(0)}(t) = \mathrm{Tr}\left\{\frac{1}{i\hbar}[\hat\nu_q, \hat H_0]\bar\varrho(t,0)\right\} = 0 \ , \tag{25}$$

$$J_q^{(1)}(t) = \mathrm{Tr}\left\{\frac{1}{i\hbar}[\hat\nu_q, \hat H']\bar\varrho(t,0)\right\} = 0 \ , \tag{26}$$

$$J_q^{(2)}(t) = J_{\varphi q}^{(2)}(t) + J_{1q}^{(2)}(t) + J_{2q}^{(2)}(t) + J_{3q}^{(2)}(t) \ , \tag{27}$$

and the partial contributions on the right of Eq. (27), arising out of the four contributions to the interaction Hamiltonian of Eq. (11), are

$$J_{\varphi q}^{(2)}(t) = \lim_{\varepsilon \to +0}\left[(i\hbar)^{-2}\int_{-\infty}^{0} dt' \, e^{\varepsilon t'} \, \mathrm{Tr}\left\{[\hat H_\varphi(t')_0, [\hat H_\varphi, \hat\nu_q]]\bar\varrho(t,0)\right\}\right]$$

$$= \lim_{\varepsilon\to+0} \frac{1}{\hbar^2} \sum_{q'} \int_{-\infty}^{0} dt' \left\{ e^{(\varepsilon+i\omega_q)t'} \operatorname{Tr}\left\{ \hat{\varphi}_{q'}(t')\hat{\varphi}^{\dagger}_{q'}\, \bar{\varrho}(t,0) \right\} + \text{c.c.} \right\}, \tag{28}$$

$$\begin{aligned} J^{(2)}_{1q}(t) &= \lim_{\varepsilon\to+0} \left[(i\hbar)^{-2} \int_{-\infty}^{0} dt' e^{\varepsilon t'} \operatorname{Tr}\left\{ [\hat{H}'_1(t')_0, [\hat{H}'_1, \hat{\nu}_q]]\bar{\varrho}(t,0) \right\} \right] \\ &= \frac{2\pi}{(i\hbar)^2} \sum_{q'} \Big\{ |V^{(1)}_{qq'}|^2 \left[\nu_q \left(1+\nu^B_{q+q'}\right) \nu^B_{q'} - \left(1+\nu_q\right)\left(1+\nu^B_{q'}\right)\nu^B_{q+q'} \right] \delta\left(\omega_q + \Omega_{q'} - \Omega_{q+q'}\right) \\ &\quad - 2|V^{(1)}_{q-q',q'}|^2 \left[\left(1+\nu_q\right) \nu^B_{q'} \nu^B_{q-q'} - \nu_q \left(1+\nu^B_{q'}\right)\left(1+\nu^B_{q-q'}\right) \right] \delta\left(\omega_q - \Omega_{q'} - \Omega_{q-q'}\right) \Big\}, \end{aligned} \tag{29}$$

$$\begin{aligned} J^{(2)}_{2q}(t) &= \lim_{\varepsilon\to+0} \left[(i\hbar)^{-2} \int_{-\infty}^{0} dt' e^{\varepsilon t'} \operatorname{Tr}\left\{ [\hat{H}'_2(t')_0, [\hat{H}'_2, \hat{\nu}_q]]\bar{\varrho}(t,0) \right\} \right] \\ &= \frac{2\pi}{(i\hbar)^2} \sum_{q'} |V^{(2)}_{qq'}|^2 \Big\{ \left[\nu_{q'} \left(1+\nu_q\right) \nu^B_{q-q'} - \nu_q \left(1+\nu_{q'}\right)\left(1+\nu^B_{q-q'}\right) \right] \delta\left(\omega_q - \omega_{q'} - \Omega_{q-q'}\right) \\ &\quad + \left[\nu_{q'} \left(1+\nu_q\right)\left(1+\nu^B_{q'-q}\right) - \nu_q \left(1+\nu_{q'}\right) \nu^B_{q'-q} \right] \delta\left(\omega_q - \omega_{q'} + \Omega_{q'-q}\right) \Big\}, \end{aligned} \tag{30}$$

$$\begin{aligned} J^{(2)}_{3q}(t) &= \lim_{\varepsilon\to+0} \left[(i\hbar)^{-2} \int_{-\infty}^{0} dt' e^{\varepsilon t'} \operatorname{Tr}\left\{ [\hat{H}'_3(t')_0, [\hat{H}'_3, \hat{\nu}_q]]\bar{\varrho}(t,0) \right\} \right] \\ &= \frac{8\pi}{(i\hbar)^2} \sum_{q'} |V^{(2)}_{qq'}|^2 \left[\left(1+\nu_q\right)\left(1+\nu_{q'}\right) \nu^B_{q+q'} - \nu_q \nu_{q'} \left(1+\nu^B_{q+q'}\right) \right] \delta\left(\omega_q + \omega_{q'} - \Omega_{q+q'}\right). \end{aligned} \tag{31}$$

In these equations the notation $\hat{O}(t)_0$ means that the operator $\hat{O}$ is given in the interaction representation, that is, its evolution is with Hamiltonian H_0, namely

$$\hat{O}(t)_0 = e^{-\frac{1}{i\hbar}t\hat{H}_0} \hat{O} e^{\frac{1}{i\hbar}t\hat{H}_0}. \tag{32}$$

In Eqs. (29), (30) and (31) ν^B_q is the distribution of the vibrational modes in the thermal bath represented by S_2, which is being kept in equilibrium with an ideal thermal reservoir at temperature T_0, and then it is given by the Planck distribution function

$$\nu_q^B = \left[\exp\{\beta_0\hbar\Omega_q\} - 1\right]^{-1} , \tag{33}$$

with $\beta_0 = 1/k_B T_0$, and the relation

$$1 + \nu_q^B = \nu_q^B \exp\{\beta_0\hbar\Omega_q\} \tag{34}$$

will be used below.

It can be noticed that the scattering operators in Eq. (27) take in the present case (use of the Markovian approximation and the property that $J_q^{(1)}(t)$ is null) the form of the Golden Rule of Quantum Mechanics however averaged over the nonequilibrium ensemble.

Using Eq. (34) and taking the energy conserving delta-function present in the collision operators into account, we can rewrite Eq. (27) in the form

$$\begin{aligned}
\frac{d}{dt}\nu_q(t) = I_q(\omega_q) - \frac{1}{\tau_q}\left(\nu_q - \nu_q^{(0)}\right) \\
- \frac{2\pi}{\hbar^2}\sum_{q'} |V_{qq'}^{(2)}|^2 \nu_{q-q'}^B \left[\nu_{q'}\nu_q\left(e^{\beta_0\hbar(\omega_q-\omega_{q'})} - 1\right) - \nu_{q'} + e^{\beta_0\hbar(\omega_q-\omega_{q'})}\nu_q\right] \\
\times\,\delta\left(\omega_q - \omega_{q'} - \Omega_{q-q'}\right) \\
- \frac{2\pi}{\hbar^2}\sum_{q'} |V_{qq'}^{(2)}|^2 \nu_{q'-q}^B \left[\nu_{q'}\nu_q\left(1 - e^{\beta_0\hbar(\omega_{q'}-\omega_q)}\right) + \nu_q - e^{\beta_0\hbar(\omega_{q'}-\omega_q)}\nu_{q'}\right] \\
\times\,\delta\left(\omega_q - \omega_{q'} + \Omega_{q'-q}\right) \\
- \frac{8\pi}{\hbar^2}\sum_{q'} |V_{qq'}^{(2)}|^2 \nu_{q+q'}^B \left[\nu_{q'}\nu_q\left(e^{\beta_0\hbar(\omega_q+\omega_{q'})} - 1\right) - \nu_q - \nu_{q'} - 1\right]
\end{aligned}$$

$$\times\, \delta\left(\omega_q + \omega_{q'} - \Omega_{q+q'}\right) \ , \tag{35}$$

where it has been introduced the relaxation time τ_q given by

$$\frac{1}{\tau_q} = \frac{2\pi}{\hbar^2 \nu_q^{(0)}} \sum_{q'} \Big\{ |V^{(1)}_{qq'}|^2 \nu^B_{q'} \nu^B_{q+q'} e^{\beta_0 \hbar \Omega_{q'}} \delta\left(\omega_q + \Omega_{q'} - \Omega_{q+q'}\right) + 2|V^{(1)}_{q-q,q'}|^2 \nu^B_{q'} \nu^B_{q-q'} \delta\left(\omega_q - \Omega_{q'} - \Omega_{q-q'}\right) \Big\} \ , \tag{36}$$

and $\nu_q^{(0)}$ is the distribution in equilibrium at temperature T_0, namely

$$\nu_q^{(0)} = \left[\exp\{\beta_0 \hbar \omega_q\} - 1\right]^{-1} \ . \tag{37}$$

Moreover, the first term on the right of Eq. (35) is the rate of production of q-mode excitations in the systems arising out of the contribution of Eq. (28) after introduction of the spectral representation for the pumping source, as given by

$$\frac{1}{\hbar^2} \mathrm{Tr}\left\{\hat{\varphi}^\dagger_q(t)\hat{\varphi}_{q'}\bar{\varrho}(t,0)\right\} = \delta_{qq'} \int \frac{d\omega}{2\pi} I_q(\omega) e^{i\omega t} \ . \tag{38}$$

On the other hand, the equation of evolution for the other basic macrovariable, i. e. the energy E_B of the thermal bath (or subsystem S_2) is

$$\frac{d}{dt} E_B(t) = J^{(2)}_B(t) + J^{(2)}_{TD}(t) = 0 \ , \tag{39}$$

which is null because of the fact that the thermal bath is constantly kept in equilibrium with the ideal thermal reservoir. In the equation above

$$J_B^{(2)}(t) = -\sum_q \hbar\omega_q \left[J_{q1}^{(2)}(t) + J_{q2}^{(2)}(t) + J_{q3}^{(2)}(t)\right] \tag{40}$$

because it is minus the energy exchanged with S_1, and

$$J_{TD}^{(2)}(t) = -\frac{E_B(t) - E_{B,\text{equil.}}}{\tau_{TD}} \tag{41}$$

is the term which accounts for thermal diffusion to the reservoir with a thermal diffusion time τ_{TD} ; the assumption made implies that this thermal diffusion effects is sufficiently rapid for keeping S_2 constantly in equilibrium with the reservoir.

To proceed further in order to obtain numerical solutions we introduce: (1) the dispersion relation

$$\omega_q = \omega_0 - \alpha|q|^2 , \tag{42}$$

a reasonable approach to the realistic ones; (2) a Debye model is taken for S_2, i.e. $\Omega_{q'} = s|q'|$, with a cut-off frequency Ω_D; (3) the matrix $V_{qq'}^{(1)}$ and $V_{qq'}^{(2)}$ are taken outside the summation (integration) sign in the spirit of the mean value theorem of calculus and indicated by $\bar{V}^{(1)}$ and $\bar{V}^{(2)}$, and we introduce the parameter $\lambda = |\bar{V}^{(2)}/\bar{V}^{(1)}|^2$; (4) we define a scaling time $\bar{\tau}$ given by

$$\bar{\tau}^{-1} = \frac{L|\bar{V}^{(1)}|^2}{\hbar^2 s} , \tag{43}$$

where L is the length of the onedimensional sample; and (5) is defined the adimensional intensity $\bar{I_q}(\omega_q) = \bar{\tau} I_q(\omega_q)$. Using the five items above and after performing the integrations in Eq. (35), we obtain that the equations of evolution for the populations of the vibrational modes of S_1 are

$$\begin{aligned}
\frac{d}{d\bar{t}}\nu_{|q|}(\bar{t}) &= \bar{I}_{|q|} - \gamma(|q|)\left(\nu_{|q|}(\bar{t}) - \nu_{|q|}^{(0)}\right) \\
&+ \frac{\lambda s}{2\alpha|q| - s}\left[\frac{\nu_{|q|-\frac{s}{\alpha}}(\bar{t})}{1 - e^{-\beta_0\hbar s(2|q|-\frac{s}{\alpha})}} + \frac{\nu_{|q|}(\bar{t})}{1 - e^{\beta_0\hbar s(2|q|-\frac{s}{\alpha})}} + \nu_{|q|}(\bar{t})\nu_{||q|-\frac{s}{\alpha}|}(\bar{t})\right] \\
-\frac{\lambda s\left[1 - \theta\left(|q| - q_B + \frac{s}{\alpha}\right)\right]}{2\alpha|q| + s}&\left[\frac{\nu_{|q|+\frac{s}{\alpha}}(\bar{t})}{1 - e^{\beta_0\hbar s(2|q|+\frac{s}{\alpha})}} + \frac{\nu_{|q|}(\bar{t})}{1 - e^{-\beta_0\hbar s(2|q|+\frac{s}{\alpha})}} + \nu_{|q|}(\bar{t})\nu_{|q|+\frac{s}{\alpha}}(\bar{t})\right],
\end{aligned} \tag{44}$$

where $\bar{t} = t/\bar{\tau}$, and

$$\gamma(q) = \frac{2\left(e^{\beta_0\hbar\omega_q} - 1\right)}{\left(e^{\frac{\beta_0\hbar}{2}|\alpha q^2 - sq - \omega_0|} - 1\right)\left(e^{\frac{\beta_0\hbar}{2}|\alpha q^2 + sq - \omega_0|} - 1\right)} . \tag{45}$$

In this Eq. (44) the last contribution on the right side of Eq. (35) is not present, because it is null as a result that energy conservation in the scattering event, represented by the delta function, is not satisfied. Moreover, θ is Heaveside step function, which takes care of the fact that for modes with wavenumber $|q| + s/\alpha$ larger than the Brillouin wavenumber q_B are not present.

A relevant fact can be noticed in Eq. (44), namely, that the equation of evolution for the population of a given mode $|q|$ is coupled only to the equations for two other modes, namely those with wavenumbers $|q| - s/\alpha$ and $|q| + s/\alpha$. This is a result of energy and crystalline momentum conservation, and implies then that the modes are coupled in independent blocks involving a finite number $\bar{n}$ of modes: $\pm|q|, \pm|q| \pm (s/\alpha), \ldots, \pm|q| \pm \bar{n}(s/\alpha)$, with

$$\bar{n} = \lfloor 2q_B\alpha/s \rfloor , \tag{46}$$

where, we recall, $q_B = \pi/a_1$, and $\lfloor x \rfloor$ stands for the greatest integer not larger than x, this because of the limiting wavenumber upper value set by q_B.

Furthermore, we notice that a direct calculation tells us that the population $\nu_q(t)$ and its associated Lagrange multiplier $F_q(t)$ are related by the expression

$$\nu_q(t) = \mathrm{Tr}\left\{\hat{\nu}_q \bar{\varrho}(t,0)\right\} = \left[\exp\left\{F_q(t) - 1\right\}\right]^{-1} . \tag{47}$$

It is worth noticing that this Lagrange multiplier can be alternatively written in either of two forms, namely

$$F_q(t) = \beta_0 \left[\hbar\omega_q - \mu_q(t)\right] , \tag{48}$$

introducing a so-called quasi-chemical potential per mode, $\mu_q(t)$, as done by Landsberg [38] and Fröhlich [39], or

$$F_q(t) = \beta_q(t)\hbar\omega_q = \frac{\hbar\omega_q}{k_B T_q(t)} , \tag{49}$$

introducing a quasi-temperature per mode as it is done in the physics of semiconductors [40], and in radiation theory by Landau and Lifshitz [41].

2.3. A Specific Case

We proceed next to obtain numerical results which illustrate the previous theory, which will show how complex behavior in this system may arise. For that purpose we use a set of parameters typical of biopolymers [35], namely

$$\omega_0 = 10^{13}\ s^{-1}\ ; \qquad s = 10^5\ \mathrm{cm\,s^{-1}}\ ; \tag{50}$$

$$a_1 = 100\ \text{Å}\ ; \qquad \alpha = 0.19\ \mathrm{cm^2\,s^{-1}}\ ; \tag{51}$$

and then $q_B = 3.14 \times 10^6\ \mathrm{cm}^{-1}$. With these parameters the number $\bar{n}$ [cf. Eq. (46)] of coupled modes in each independent set is $\bar{n} = 12$. The numerical results are shown in Figs. 2 to 5.

Using the scaled time $\bar{t} = t/\bar{\tau}$ with $\bar{\tau}$ defined by Eq. (43), and $\lambda = |\bar{V}^{(2)}/\bar{V}^{(1)}|^2$, both already defined, we look first for the steady state which sets in, after a certain transient has elapsed, under the application of a constant pumping intensity $\bar{I}_q = \bar{\tau} I_q$ which we take as being the same for all mode q. The result is shown in Fig. 2; for simplicity we have chosen the set which includes the center zone mode $q = 0$ and then each curve corresponds to the symetrical modes $\pm|q_\kappa|$, which we have labelled from $\kappa = 1$ (the lowest frequency mode in the set, $q_1 = 5s/\alpha$) to $\kappa = 6$ (the highest frequency mode $q_6 = 0$). We have taken $T_0 = 300$ K and, for illustration, we have fixed λ as equal to 1.

This Fig. 2 evidences the complex behavior of the system when sufficiently far from equilibrium: after a certain distance from equilibrium is achieved, roughly for $\bar{I} \sim 10^4$, the expected similar increase in population of all the modes is drastically altered, with the mode lowest in frequency (population ν_1) largely increasing its population at the expenses of the other modes higher in frequency. A calculation for all the modes is shown in Fig. 3, for $\bar{I} = 2.6 \times 10^5$, where is shown the comparison with the result which follows for $\lambda = 0$, i.e. in the absence of the anharmonic interactions in $\hat{H}_2'$ and $\hat{H}_3'$ of Eqs. (13) and (14).

This complex behavior is what we call *Fröhlich effect* [39], sometimes referred to as Bose-Einstein-like Condensation in nonequilibrium conditions. We can see by inspection of Fig. 3 that we can talk of a kind of a "two fluid model", as in the theories of superfluidity and superconductivity; we have indicated the "normal fluid" region of modes and the "super fluid" region we called the *Fröhlich condensate*. In this case the complex behavior is a result of the nonlinear contributions to the kinetic equations of evolution, i. e. those contained in the collision operators $J_{2q}^{(2)}(t)$ and $J_{3q}^{(2)}(t)$, and proportional to λ in Eq. (35), which contain the term

$$-\nu_q(t)\nu_{q'}(t)\left[1 - \exp\left\{-\beta_0\hbar(\omega_q - \omega_{q'})\right\}\right] , \tag{52}$$

which is positive for $\omega_q < \omega_{q'}$, and then mode q is "fed" by mode q', while for $\omega_q > \omega_{q'}$ the contribution is negative, and mode q "feeds" mode q'. In Figs. 4 and 5 it is shown the evolution of the quasi-temperature of Eq. (49) and of the quasi-chemical potential of Eq. (48) for the modes described in Fig. 2.

3. Statistical Thermodynamics of Fröhlich-Bose-Einstein-like Condensation

We consider now the thermodynamics of the Fröhlich effect. The informational entropy in IST is given by [23, 24, 42]

$$\bar{S}(t) = -\operatorname{Tr}\left\{\varrho_\varepsilon(t)\wp_\varepsilon(t)\ln\varrho_\varepsilon(t)\right\} , \tag{53}$$

where $\wp_\varepsilon(t)$ is a time-dependent projection operator (it is characterized by the non-equilibrium state of the system at any time t), defined in Ref. [26], which has the property that

$$\wp_\varepsilon(t)\ln\varrho_\varepsilon(t) = \ln\bar{\varrho}(t,0) , \tag{54}$$

and we recall that $\varrho_\varepsilon(t)$ is the systems' nonequilibrium statistical operator in Zubarev's approach, and $\bar{\varrho}$ is given in Eq. (17). Hence,

$$\bar{S}(t) = -\operatorname{Tr}\left\{\varrho_\varepsilon(t)\ln\bar{\varrho}(t,0)\right\} = \phi(t) + \sum_q F_q(t)\nu_q(t) + \beta_0 E_B , \tag{55}$$

where, we recall,

$$\phi(t) = \ln\operatorname{Tr}\exp\left\{-\sum_q F_q(t)\hat{\nu}_q - \beta_0\hat{H}_{OB}\right\} \equiv \ln\bar{Z}(t) \tag{56}$$

is the logarithm of a nonequilibrium partition function which we have called $\bar{Z}(t)$.

It can be shown that this informational entropy has a particularly differentiated dependence on λ only after the onset of Fröhlich effect, i.e. for, roughly, $\bar{I} \sim 10^4$, resulting in that the informational entropy decreases for increasing values of λ (which, we recall, measures the strength of the nonlinear contribution responsible for the complex behavior of the system): this can be interpreted as some kind of increase in order, or of increase of information as a result of the formation of Fröhlich condensate. To characterize this point, we introduce the order parameter

$$\Delta(\lambda) = \frac{\bar{S}_0^{\text{ss}} - \bar{S}_\lambda^{\text{ss}}}{\bar{S}_0^{\text{ss}}} , \tag{57}$$

where $\bar{S}_0^{\text{ss}}$ and $\bar{S}_\lambda^{\text{ss}}$ are the entropies in the steady-state for $\lambda = 0$ and $\lambda \neq 0$, which is shown in Fig. 6, where it is evidenced the above mentioned characteristics.

Next we go over the function informational-entropy production given by

$$\bar{\sigma}(t) = \frac{d}{dt}\bar{S}(t) = \sum_q F_q(t)\frac{d\nu_q(t)}{dt} = \sum_q \frac{d\nu_q(t)}{dt} \ln \frac{\nu_q(t) + 1}{\nu_q(t)} , \tag{58}$$

where we have used Eq. (47), and the fact that E_B does not change in time. In Fig. 7 it is displayed the evolution of the informational entropy-production (the full line), $\bar{I} = 2.6 \times 10^5$, i.e. beyond the onset of Fröhlich effect), which becomes null when the steady-state is attained as it should.

IST-entropy production has two contributions:

$$\bar{\sigma}(t) = \bar{\sigma}_i(t) + \bar{\sigma}_e(t) , \tag{59}$$

consisting of the so-called internal one, $\bar{\sigma}_i(t)$, which results from the internal interactions in the system, and the external one, $\bar{\sigma}_e(t)$, due to interactions with the surroundings, in this case with the source and the thermal reservoir. They are given by

$$\bar{\sigma}_i(t) = \sum_q \left[F_q(t) - \beta_0 \hbar \omega_q\right] \left[J_{1q}^{(2)}(t) + J_{2q}^{(2)}(t) + J_{3q}^{(2)}(t)\right] , \tag{60}$$

$$\bar{\sigma}_e(t) = \sum_q F_q(t) J_{\varphi q}^{(2)}(t) + \beta_0 J_{TD}^{(2)}(t) = \sum_q F_q(t) J_{\varphi q}^{(2)}(t) - \beta_0 J_B^{(2)}(t) , \tag{61}$$

whose evolutions are indicated in Fig. 7, and where it is clear that $\bar{\sigma}_i(t)$ is definite positive and at the steady-state $\bar{\sigma}_e(t) = -\bar{\sigma}_i(t)$. The positiveness of $\bar{\sigma}_i(t)$ can be considered as a manifestation of a kind of *H*-theorem in MaxEnt-NESOM-based IST. We can in this figure see the relevant point that in the presence ($\lambda = 1$) and in the absence ($\lambda = 0$) of the nonlinear contributions responsible for Fröhlich effect, the total production of informational entropy is the same (and this is valid for any λ). This is a consequence (Cf. Fig. 9 below) that the nonlinear terms do not produce dissipative effects but redistribute the energy, without loss, between the polar modes.

We consider in continuation two additional important results in IST [23], which are generalization of those of Generalized Irreversible Thermodynamics [5, 10]. One is the criterion for evolution: the change in time of IST-entropy production can be separated out into two parts, namely

$$\frac{d}{dt}\bar{\sigma}(t) = \frac{d_F}{dt}\bar{\sigma}(t) + \frac{d_Q}{dt}\bar{\sigma}(t) , \tag{62}$$

where

$$\frac{d_F}{dt}\bar{\sigma}(t) = \sum_q \frac{d}{dt}F_q(t)\frac{d}{dt}\nu_q(t) \ , \tag{63}$$

$$\frac{d_Q}{dt}\bar{\sigma}(t) = \sum_q F_q(t)\frac{d^2}{dt^2}\nu_q(t) \ , \tag{64}$$

that is, the change in time of the informational-entropy production due to the change in time of the Lagrange multipliers, and the other due to the change in time of the basic variables (the populations), and we recall that $dE_B/dt = 0$. After a simple calculation of Eq. (63) using Eq. (47) we find that

$$\frac{d_F}{dt}\bar{\sigma}(t) = -\sum_q \frac{1}{\nu_q(t)\left(\nu_q(t)+1\right)}\left(\frac{d}{dt}\nu_q(t)\right)^2 \leq 0 \ , \tag{65}$$

verifying for this system the generalization [23] of Glansdorff-Prigogine's thermodynamic (originally called universal) criterion of evolution. That is, along the trajectory of the macrostate of the system in the thermodynamic (or Gibbs) space of states, the quantity of the Eq. (63) is always non-negative, a quantity which in classical Onsagerian thermodynamics is the product of the change in time of the thermodynamic forces times the fluxes of matter and energy [5, 10, 23].

Finally, we look for the criterion for (in)stability, which requires the analysis of the quantity called the excess of entropy production. First we introduce the quantity

$$\frac{1}{2}\delta^2\bar{S}(t) = \frac{1}{2}\sum_{qq'}\left[\frac{\delta^2\bar{S}(t)}{\delta\nu_q(t)\delta\nu_{q'}(t)}\right]^{ss}\Delta\nu_q(t)\Delta\nu_{q'}(t) \ , \tag{66}$$

where $\Delta\nu_q(t)$ represents at a later time t the value of an imposed arbitrary deviation from the steady-state of the system ($\delta^2\bar{S}$ is the second functional differential of the IST entropy). A direct calculation tell us that

$$\frac{\delta^2\bar{S}(t)}{\delta\nu_q(t)\delta\nu_{q'}(t)} = -\frac{\delta_{qq'}}{\nu_q(t)\,(\nu_q(t)+1)}\,, \tag{67}$$

and consequently

$$\frac{1}{2}\delta^2\bar{S}(t) = -\frac{1}{2}\sum_q\left[\frac{1}{\nu_q^{ss}\,(\nu_q^{ss}+1)}\right]|\Delta\nu_q(t)|^2 \le 0\,, \tag{68}$$

what is a manifestation of the convexity of the maximized informational entropy. Differentiation in time of Eq. (68) introduces the quantity called excess of entropy production function, namely

$$\delta^2\bar{\sigma}(t) = \frac{1}{2}\frac{d}{dt}\delta^2\bar{S}(t) = -\sum_q\frac{\Delta\nu_q(t)}{\nu_q^{ss}\,(\nu_q^{ss}+1)}\frac{d}{dt}\Delta\nu_q(t) = \sum_q\Delta F_q(t)\Delta\nu_q(t)\,, \tag{69}$$

a quantity shown in Fig. 8. We can see that this quantity is non-negative, and therefore

$$\frac{1}{2}\delta^2\bar{S}(t)\,\delta^2\bar{\sigma}(t) \le 0 \tag{70}$$

is always non-negative and then, according to Lyapunov theorem in linear stability analysis (see for example [5]) the macroscopic state of this system displaying Fröhlich effect, is always stable. This is a manifestation of the generalization in IST [23] of Glansdorff-Progogine's (in)stability criterion [5, 10].

The stability of the macroscopic state of the system can be characterized in an alternative way, consisting in that — for the particular present case — it can be proved a generalization of Prigogine's theorem of minimum entropy production, which ensures the stability of any thermodynamic system in the immediate neighborhood of the state of equilibrium, i. e. within a strictly linear (or Onsagerian) regime of classical irreversible thermodynamics where Onsager's reciprocity relations are satisfied [5, 10]. The theorem proves that in Onsager's regime and in the generalization to IST [23], $\bar{\sigma}_i^{ss} \geq 0$ and $d\bar{\sigma}_i^{ss}/dt \leq 0$ are always satisfied and ensure the stability of the macrostate. In the model we are presenting it can be verified that in any condition, that is even far away from equilibrium, and then in the nonlinear regime outside Onsager's domain, the condition above is satisfied everywhere, as shown in Fig. 7, and then $\bar{\sigma}_i$ plays the role of a thermodynamic potential whose minimum defines an attractor for the steady states of the system.

4. Further Aspects of Fröhlich-Bose-Einstein-like Condensation

First we notice that of the three contributions implying relaxation processes, $J_{q1}^{(2)}$, $J_{q2}^{(2)}$, and $J_{q3}^{(2)}$ [Eqs. (28), (29) and (30)] the first one gives rise to the one expressed in terms of the relaxation time τ_q [$\gamma(|q|)$ in Eq. (44)], while in the other two correspond in Eq. (44) to the terms with coefficient λ. They arise out of the interactions with matrix elements A and B respectively in the Hamiltonian of Eq. (3). It can be shown — see Fig. 9 — that $J_{q1}^{(2)}$ is exclusively responsible for dissipation, while the other two contributions (with λ) produce only redistribution of energy among the modes: the lines with open circles, the sum of all three contributions for $\lambda = 0$, and with triangles, for $\lambda = 1$, coincide. Moreover, for $q \gtrsim 2.6 \times 10^8$ cm^{-1} or $\omega \gtrsim 8.7 \times 10^{12}$ Hz (cf. Fig. 4), the contributions of J_{q2} plus J_{q3} are, for $\lambda = 1$, positive, that is, they act as a source term, the one in fact responsible for the "feeding" of the modes in the Fröhlich condensate, resulting in the large increase of their populations.

Furthermore, we are dealing with a nonlinear dissipative system and to it applies other relevant results in Nonlinear Science [43]. As Nicolis and Daems noticed [44] the equations of evolution [Eqs. (35) or (44)] are nonlinear owing to the cooperativity inherent in the interactions. Moreover, the dissipative character of the set of equations is reflected in that when embedding the equations of evolution into the space of nonequilibrium thermodynamic state spawned by the set of variables of Eq. (21) one has, on average, a contraction of a volume element each point of which follows the evolution laws. This very important property is shown to be equivalent in the case of Fröhlich condensation to

$$\frac{1}{t - t_0} \int_{t_0}^{t} dt' \left\{ \sum_{q} \frac{\partial}{\partial \nu_q} J_q^{(2)}(t') + \frac{\partial}{\partial E_B} [J_B^{(2)}(t') + J_{TD}^{(2)}(t')] \right\} < 0 , \qquad (71)$$

where the latter contribution is null because of Eq. (39), and the expression between curly brackets is the so-called divergence of the evolution operator of Eqs. (24) and (39) [43].

We have that

$$\frac{\partial}{\partial \nu_q} [J_q^{(1)}(t) + J_q^{(2)}(t')] = -\frac{1}{2} \tau_q^{-1}(t) - \frac{4\pi}{\hbar^2} \sum_{q'} |V_{qq'}^{(2)}|^2 \left[1 + \nu_{q'}(t) + \nu_{q-q'}^{B} \right] \delta(\Omega_{q-q'} + \omega_{q'} - \omega$$

$$+ \frac{4\pi}{\hbar^2} \sum_{q'} |V_{qq'}^{(2)}|^2 \left[\nu_{q'}(t) - \nu_{q-q'}^{B} \right] \delta(\Omega_{q-q'} - \omega_{q'} + \omega_q)$$

$$-\frac{4\pi}{\hbar^2}\sum_{q'}|V^{(2)}_{qq'}|^2\left[\nu_{q'}(t)-\nu^B_{q+q'}\right]\delta(\Omega_{q+q'}-\omega_{q'}-\omega_q)\equiv D_q(t)\ . \tag{72}$$

These quantities $D_q(t)$ are predominantly negative for any t (they are shown in Fig. 10 for a particular value of the intensity) and then Eq. (71) is verified.

Let us consider the Lyapunov exponents, λ_j, of the dynamical system when it has achieved the steady state, that is the eigenvalues of the linearized evolution operator, which are given by Eq. (72) once ν_q is taken in the steady state. They are given in Fig. 11 for a range of values of the intensity of the pumping source. Inspection of this Fig. 11 tells us that the Lyapunov exponents are negative, what then ensures the stability of the solution for any value of the intensity, a point we have previously demonstrated through an alternative treatment. Other interesting point is that the modulus of the one corresponding to the mode labelled 1 (the one in Fröhlich condensate) is very small. This has the consequence that, since the population ν_1 in the steady state can be shown to be proportional to the inverse of the modulus of λ_1, then it is the very large one corresponding to the mode in Fröhlich condensate. Moreover, Fig. 12 shows the sum of the Lyapunov exponents, namely the divergence of the supervector corresponding to the different contributions of the evolution operator [Cf. Eq. (69)], which is negative and increasing in modulus with the pumping intensity. This points to the fact that the trajectories are winding towards an attractor consisting in the Fröhlich-Bose-Einstein-like condensation. Hence, this indicates an increasing contraction of the elementary volumes in the space of thermodynamic states with increasing intensity of the pumping source. This is related to the interesting fact that the condensation becomes more and more effective, in the sense that the ratio — for each intensity — between the number of excitations in the condensate and the total number is increasing with $\bar{I}$, what is shown in Fig. 13. Again there is a similarity with Bose-Einstein condensation of bosons in equilibrium where the number of particles in the condensate increases with decreasing temperature.

We notice that in this case, with all Lyapunov exponents being negative, Kolmogorov entropy [43] is null, and then, as noted before, this implies that the trajectories are stable, the system does not produce information by itself (no selforganization follows) as would be for positiveness of some Lyapunov coefficient, but the system shows loss of information as evidenced by the increase in time of the informational entropy. However, as described by the order parameter of Fig. 9, with increasing nonlinearity (increasing values of λ) the informational entropy, for a giving pumping intensity, diminishes implying in smaller loss of information as ordering increases in the form of a more "dense" Fröhlich condensate, as noticed above.

5. Summary and Conclusions

Summarizing, to illustrate the thermodynamic aspects of systems with complex behavior, we have resorted to a particular model of linear oscillators coupled through anharmonic interactions. It can be a good representation of vibrational modes in quasi-linear semiconductors (the so-called quantum wires), molecular polymers, and biopolymers. The system is driven out of equilibrium by an external pumping source of energy, for example, illumination by a constantly applied electromagnetic field, v.g.

a continuous-wave laser, or in biosystems by a metabolic mechanism, the so-called dark excitations. One of the two subsystems of oscillators is taken as a thermal bath at constant temperature, being kept in this condition by a good thermal contact (an efficient "homeostatic" process) with an ideal thermal reservoir. The other system can attain high levels of excitation with increasing intensity of the pumping source to which it is coupled (see Fig. 1).

The study has been performed resorting to Informational Statistical Thermodynamics and a nonlinear quantum kinetic theory, both based on the Nonequilibrium Statistical Operator Method founded on the principle of maximization of the informational entropy — and considered to belong to the realm of Jaynes' Predictive Statistical Mechanics.

The equations of evolution for the populations $\nu_q(t)$ of the vibrational modes, and then the energy per mode $\hbar\omega_q\nu_q(t)$, are derived, and it has been clearly evidenced a kind of complex behavior in such system, consisting in the so-called Fröhlich-effect or Fröhlich-Bose-Einstein condensation in a nonequilibrium thermodynamic phase. After a certain threshold in the value of the intensity of the pumping source has been attained, in a cascading-down-type process, the energy pumped on the system is transferred from the modes higher in frequency to those lower in frequency. The modes of lowest energy are then largely populated at the expenses of the other modes with higher frequencies.

The thermodynamic of Fröhlich effect has been analized in depth. On the one hand it has been characterized the Lagrange parameters that the variational method introduces, those we called $F_q(t)$. These Lagrange parameters are the intensive nonequilibrium thermodynamic variables, which completely characterize the macrostate of the system as the basic variables, in this case $\nu_q(t)$, do. As shown they can be interpreted in terms of either a quasi-temperature $T_q(t)$ per mode, or a quasi-chemical potential $\mu_q(t)$ per mode.

In section 3 we have worked out in certain detail the nonequilibrium thermodynamic characteristics of the Fröhlich condensate, hence an example of the thermodynamics of complexity. The so-called informational entropy in IST is derived and its temporal evolution described, from the initial time of preparation of the sample up to the steady-state displaying Fröhlich's condensation. When the external pumping source is switched off there follows a return to the value in equilibrium with the reservoir recovering the usual Clausius-Gibbs thermodynamic entropy. As shown, the informational entropy in the condensed state is smaller than the entropy when the nonlinear interaction responsible for the onset of Fröhlich effect is disregarded. As the order parameter shown in Fig. 6 demonstrates, the system increases in order with increasing coupling strength λ, and the informational entropy decreases since information is gained as organization of the system is developing.

Another important quantity in irreversible thermodynamics has been analized, namely the informational-entropy production function. In terms of it we have verified that the, generalized to IST, Glansdorff-Prigogine's evolution principle is satisfied, as it should, and from the generalization of Glansdorff-Prigogine's (in)stability principle we have shown that the thermodynamic state of the system we have derived, is stable under any condition. However, it needs be stressed, such stability has been only derived against other possible homogeneous steady-states, but an instability against the onset of a spatially ordered state cannot be ruled out a priori [45]. This latter point will be considered in a future article.

We end this conclusions citing Nicolis and Daems [44] who stated that this new field of statistical mechanics of dynamical systems is nowadays a unique laboratory in which ideas, conjectures, and methods can be used.

We gratefully acknowledge finantial support to our research Group that in differents opportunities was provided by the State of São Paulo Research Foundation (FAPESP); the National Research Council (CNPq); the Ministry of Planning (Finep); IBM-Brasil; USA-National Science Foundation (USA-Latin America Cooperation Project Washington, USA); and the John Simon Guggenheim Memorial Foundation (New York, USA). One of the authors (AFF) thanks CNPq for finantial help, other two (ARV, RL) are CNPq Research Fellows.

REFERENCES

[1] P. W. Anderson, Science **177**, 393 (1972); Physics Today, July 1991, pp. 9–11.

[2] M. Gell-Mann, Complexity **1**, 16 (1995).

[3] G. Nicolis and I. Prigogine, *Exploring Complexity* (Freeman, New York, 1989).

[4] E. Lorentz, J. Atm. Sc. **20**, 130 (1963).

[5] G. Nicolis and I. Prigogine, *Self-Organization in Nonequilibrium Systems* (Wiley-Interscience, New York, 1977).

[6] G. Nicolis, in *The New Physics*, P.Davies, Ed. pp. 316–47 (Cambridge Univ. Press, Cambridge, 1989).

[7] H. Haken, *Synergetics, An Introduction* (Springer, Berlin, 1978).

[8] S. Kauffman, *The Origins of Order* (Oxford Univ. Press, New York, 1993); *At Home in the Universe* (Oxford Univ. Press, New York, 1995).

[9] I. Prigogine, *Etude Thermodinamique des Phènomènes Irreversibles* (Desrer, Liège, 1947), and *Introduction to the Thermodynamics of Irreversible Processes* (Thomas, New York, 1955).

[10] P. Glansdorff and I. Prigogine, *Thermodynamics of Structure, Stability and Fluctuations* (Wiley-Interscience, New York, 1971).

[11] G. Nicolis, Physica A **213**, 1 (1995).

[12] S. R. de Groot, and P. Mazur, *Nonequilibrium Thermodynamics* (North Holland, Amsterdam, 1962).

[13] C. Truesdell, *Rational Thermodynamics.* (McGraw-Hill, New York, 1969); 2nd edition (Springer, Berlin, 1988).

[14] D. Jou, J. Casas-Vazquez, and G. Lebon, *Extended Irreversible Thermodynamics.* (Springer, Berlin, 1993); 2nd enlarged edition (Springer, Berlin, 1996).

[15] A. Hobson, J. Chem. Phys. **45**, 1352 (1966).

[16] E. T. Jaynes, Phys. Rev. **106**, 620 (1957); *ibid.* **108**, 171 (1957).

[17] C. E. Shannon and W. Weaver, *The Mathematical Theory of Communication.* (Univ. Illinois Press, Urbana, 1964).

[18] L. Brillouin, *Science and Information Theory,* (Academic, New York, 1962).

[19] L. Tisza, in *Thermodynamics: History and Philosophy,* edited by K. Martinas, L. Ropolyyi, and P. Szegedi (World Scientific, Singapore, 1991), pp. 515-22.

[20] L. S. Garcia-Colin, A. R. Vasconcellos and R. Luzzi, J. Non-Equil. Thermodyn. **19**, 24 (1994).

[21] R. Luzzi and A. R. Vasconcellos, Physica A, **241**, 677 (1997).

[22] R. Luzzi, A. R. Vasconcellos, D. Jou and J. Casas-Vazquez, J. Chem. Phys., **107**, 7383 (1997); Phys. A **248**, 111 (1998).

[23] M. A. Tenan, A. R. Vasconcellos and R. Luzzi, Fortschr. Phys./Prog. Phys., **45**, 1 (1997).

[24] R. Luzzi, A. R. Vasconcellos and J. G. Ramos, *Statistical Foundations of Irreversible Thermodynamics,* in *Texte zur Physik Series,* W. Ebeling, Ed. (Teubner, Berlin, in press).

[25] D. N. Zubarev, V. N. Morozov, and G. Röpke, *Statistical Mechanics of Nonequilibrium Processes. Vol. 1: Basic Concepts, Kinetic Theory; Vol. 2: Relaxation and Hydrodynamic Processes* (Akademie Verlag, Berlin, 1996 and 1997 respectively).

[26] R. Luzzi and A. R. Vasconcellos, Fortschr. Phys./Prog. Phys. **38**, 887 (1990).

[27] J. G. Ramos, A. R. Vasconcellos and R. Luzzi, Fortschr. Phys./Prog. Phys. **43**, 265 (1995).

[28] R. Luzzi, A. R. Vasconcellos and J. G. Ramos, *Foundations of a Nonequilibrium Statistical Ensemble Formalism*, in Fundamental Theories of Physics Series, van der Merwe, Ed. (Kluwer Academics, Dordrecht, in preparation).

[29] E. T. Jaynes, Predictive Statistical Mechanics, in G. T. Moore and M. O. Scully, editors, *Frontiers of Nonequilibrium Statistical Physics*, pp. 33–55, Plenum, New York, 1986.

[30] E. T. Jaynes, Reprinted Articles and Notes in *E. T. Jaynes' Papers on Probability, Statistics and Statistical Physics*, D. Rosenkrantz, Ed. (Reidel-Kluwer Academics, Dordrecht, 1983); see also J. N. Kapur and H. K. Kesavan, *Entropy Optimization Principles with Applications* (Academic, San Diego, CA, 1992).

[31] E. T. Jaynes, in *Maximum Entropy and Bayesian Methods*, edited by J. Skilling (Kluwer, Dordrecht, 1989), pp. 1–27.

[32] D. N. Zubarev, Fortschr. Phys./Prog. Phys. **18**, 125 (1970).

[33] D. N. Zubarev, *Neravnovesnaia Statisticheskaia Termodinamica* (Idz. Nauka, Moscou, 1971) [England Transl.: *Nonequilibrium Statistical Thermodynamics* (Consultants Bureau-Plenum, New York, 1974).

[34] M. V. Mesquita, A. R. Vasconcellos, and R. Luzzi, Phys. Rev. E **48**, 4049 (1993)

[35] A. S. Davydov, *Biology and Quantum Mechanics* (Pergamon, Oxford, 1982).

[36] A. R. Vasconcellos, M. V.Mesquita and R. Luzzi, Phys. Rev. Lett. **80**, 2008 (1998).

[37] L. Lauck, A. R. Vasconcellos, and R. Luzzi, Physica A **168**, 789 (1990); J. R. Madureira, A. R. Vasconcellos, R. Luzzi, and L. Lauck, Phys. Rev. E **57**, 3637 (1998); J. R. Madureira, A. R. Vasconcellos, R. Luzzi, J. Casas-Vázquez, and D. Jou, J. Chem. Phys. **108**, 7568 (1998)

[38] P. T. Landsberg, J. Phys. C **14**, L1025 (1981).

[39] H. Fröhlich, Int. J. Quantum Chem. 2, 641 (1968); in *From Theoretical Physics to Biology*, edited by M. Marois (North Holland, Amsterdam, 1969); Nature **228**, 1093 (1970); H. Fröhlich, in *Advances in Electronics and Electrons Physics*, Vol. 53, pp. 85–192 (Academic, New York, 1980).

[40] D. Kim and P. Y. Yu, Phys. Rev. Lett. **64**, 946 (1990); A. C. Algarte, A. R. Vasconcellos, and R. Luzzi, Phys. Rev. B **54**, 11311 (1996).

[41] L. D. Landau and E. M. Lifshitz, *Statistical Physics,* Vol. 5 of *Course of Theoretical Physics* (Pergamon, Oxford and New York, 1980), p. 189.

[42] S. A. Hassan, A. R. Vasconcellos, and R. Luzzi, Physica A, in press.

[43] G. Nicolis, *Introduction to Nonlinear Science* (Cambridge Univ. Press, Cambridge, 1995).

[44] G. Nicolis and D. Daems, Chaos **8**, 311 (1998).

[45] S. A. Hassan, A. R. Vasconcellos, and R. Luzzi, Eur. J. Phys., submitted.

FIGURE CAPTIONS

Figure 1: A schematical description of the two interacting subsystems, S_1 and S_2.

Figure 2: Populations of a set of modes in the steady state under a constant pumping intensity $\bar{I}$.

Figure 3: Populations of the modes in the steady state for $\bar{I} = 2.6 \times 10^5$, compared with the case of absence of nonlinear interactions.

Figure 4: The quasitemperatures associated to the set of modes in Fig. 2.

Figure 5: The quasi-chemical potential associated to the set of modes in Fig. 2.

Figure 6: The order parameter of Eq. (55) as a function of the strength of the nonlinear coupling.

Figure 7: Evolution of the informational-entropy production.

Figure 8: The excess entropy production around the steady state.

Figure 9: The different contributions to the relaxation processes for $\lambda = 1$ and in the absence of a nonlinear coupling ($\lambda = 0$).

Figure 10: Quantities $D_q(t)$ of Eq. 72 for the set of modes of Fig. 2.

Figure 11: Lyapunov coefficient in the steady state for the set of modes of Fig. 2.

Figure 12: Sum of Lyapunov coefficients or divergence of the evolution operator in the steady state for the set of modes of Fig. 2.

Figure 13: Fraction of excitations in the steady state.

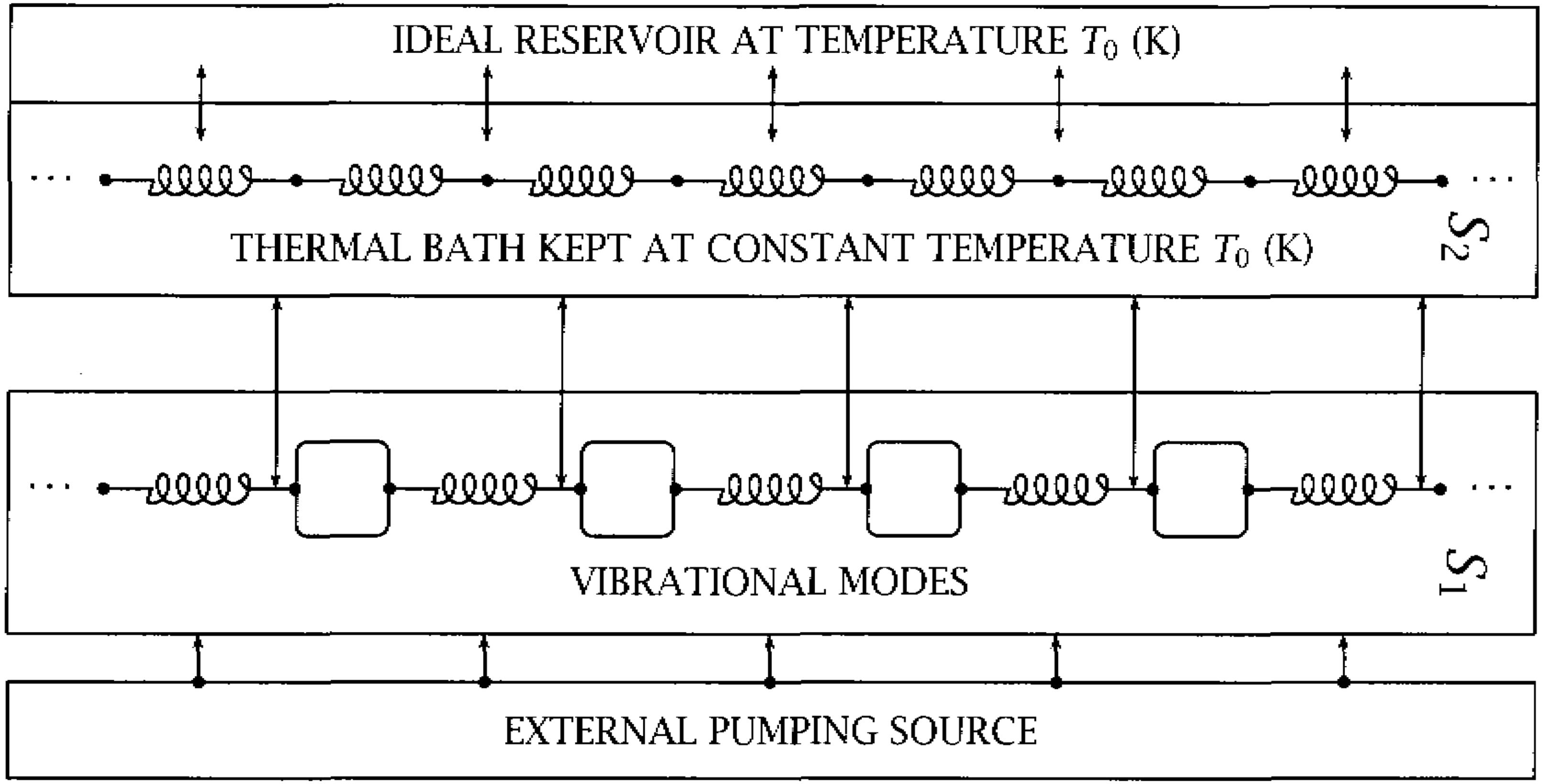

Figure 1: A schematical description of the two interacting subsystems, S_1 and S_2.

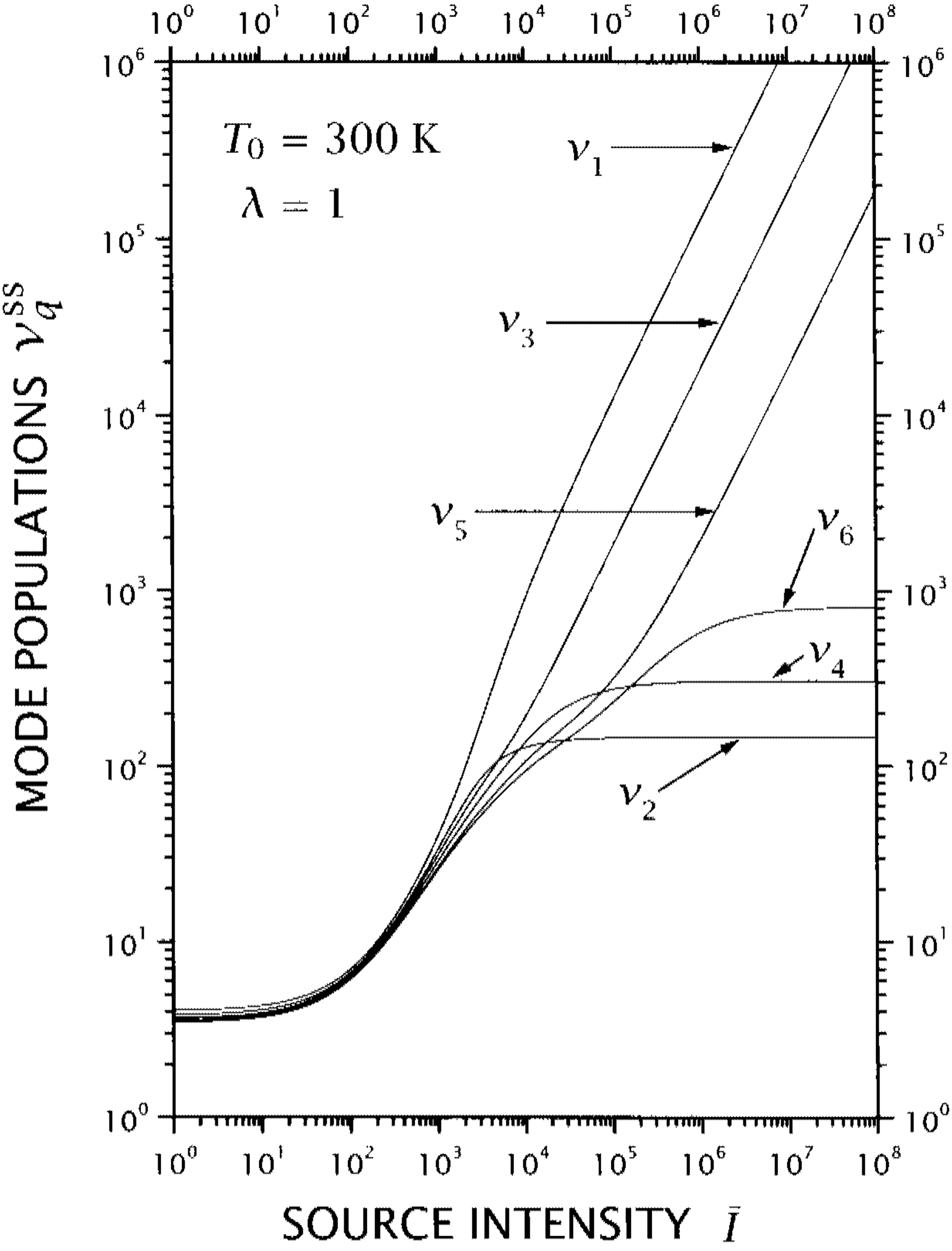

Figure 2: Populations of a set of modes in the steady state under a constant pumping intensity $\bar{I}$.

FONSECA *et al.* FIGURE 2

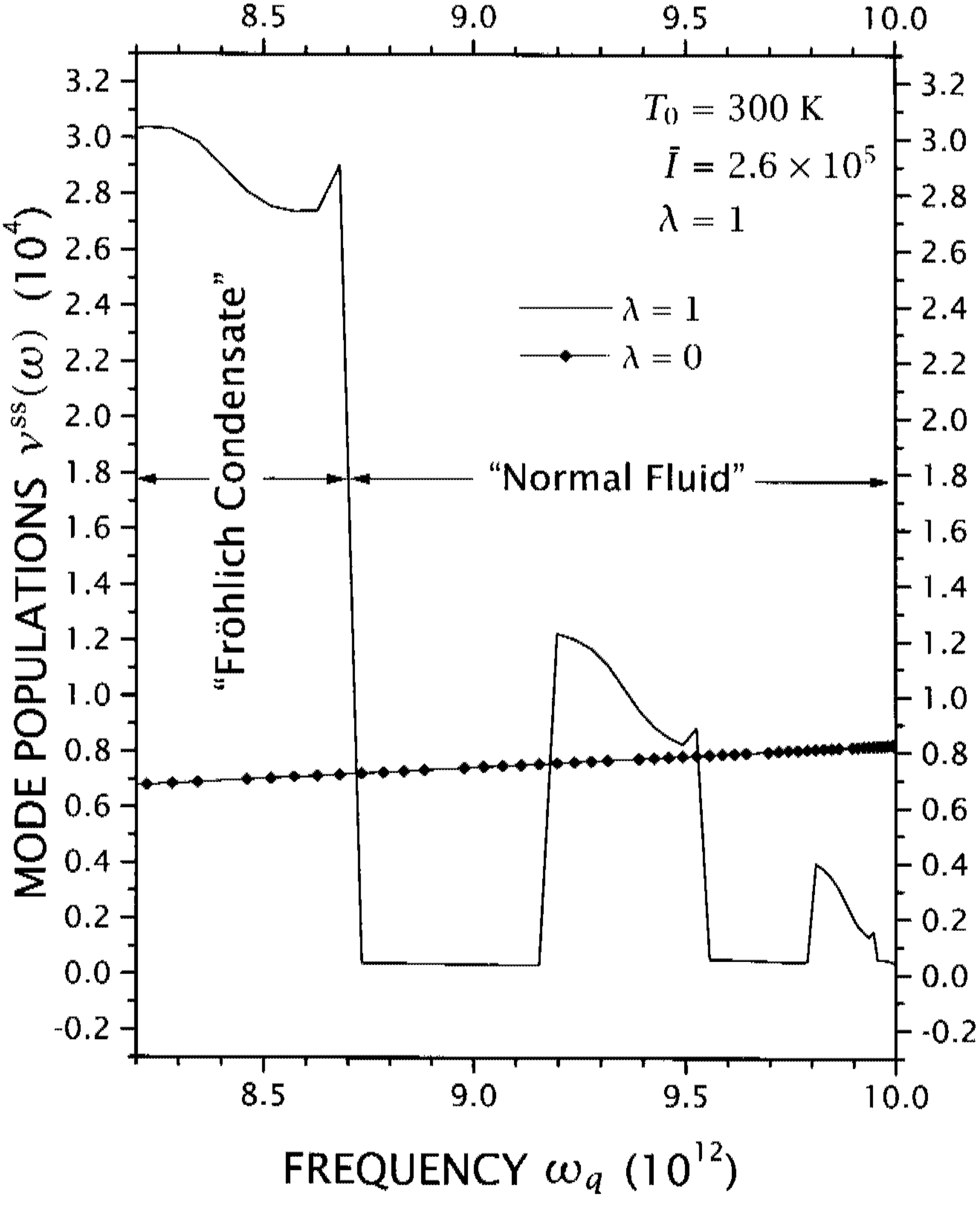

Figure 3: Populations of the modes in the steady state for $\bar{I} = 2.6 \times 10^5$, compared with the case of absence of nonlinear interactions.

FONSECA *et al.* FIGURE 3

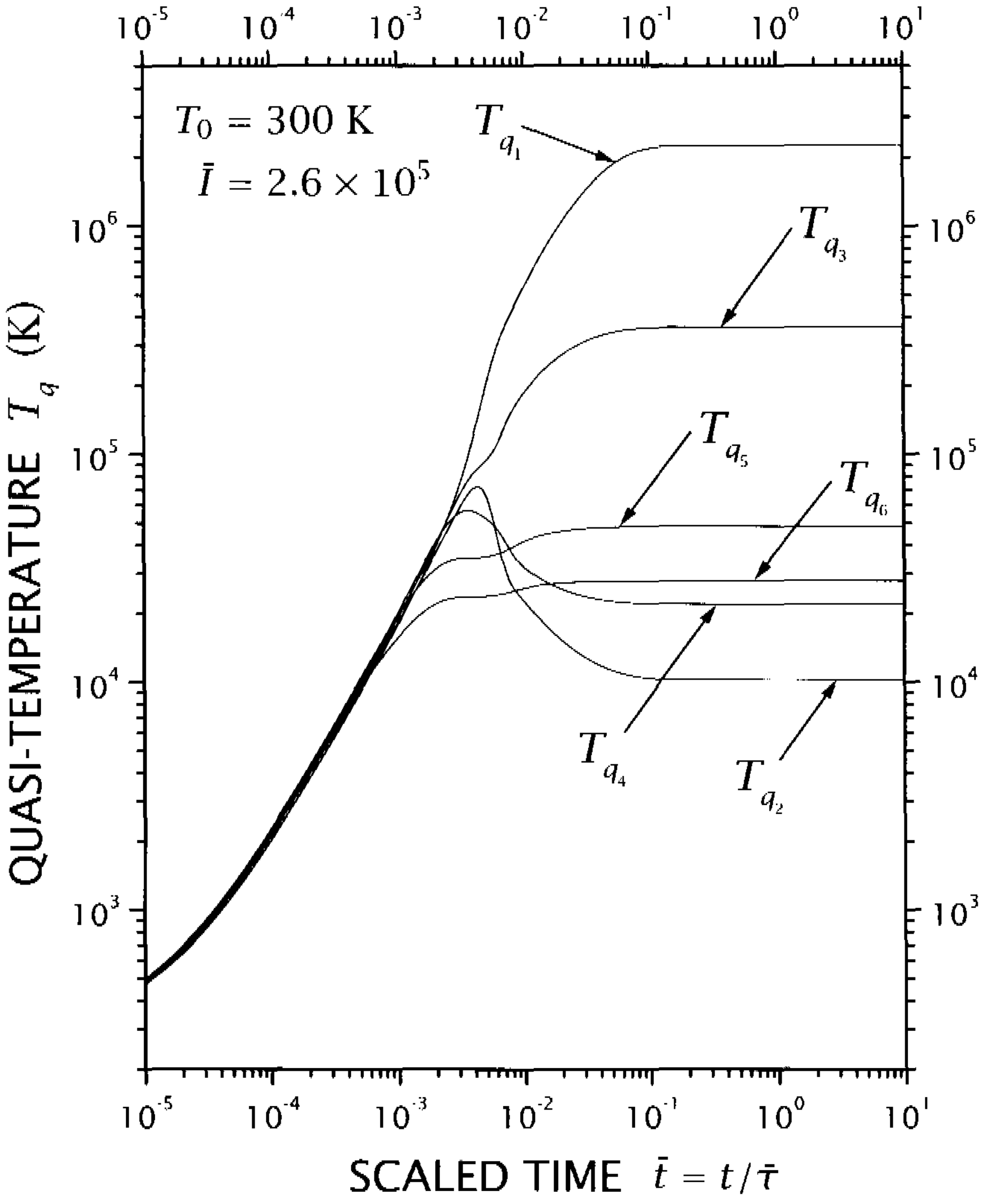

Figure 4: The quasitemperatures associated to the set of modes in Fig. 2.

FONSECA *et al.* FIGURE 4

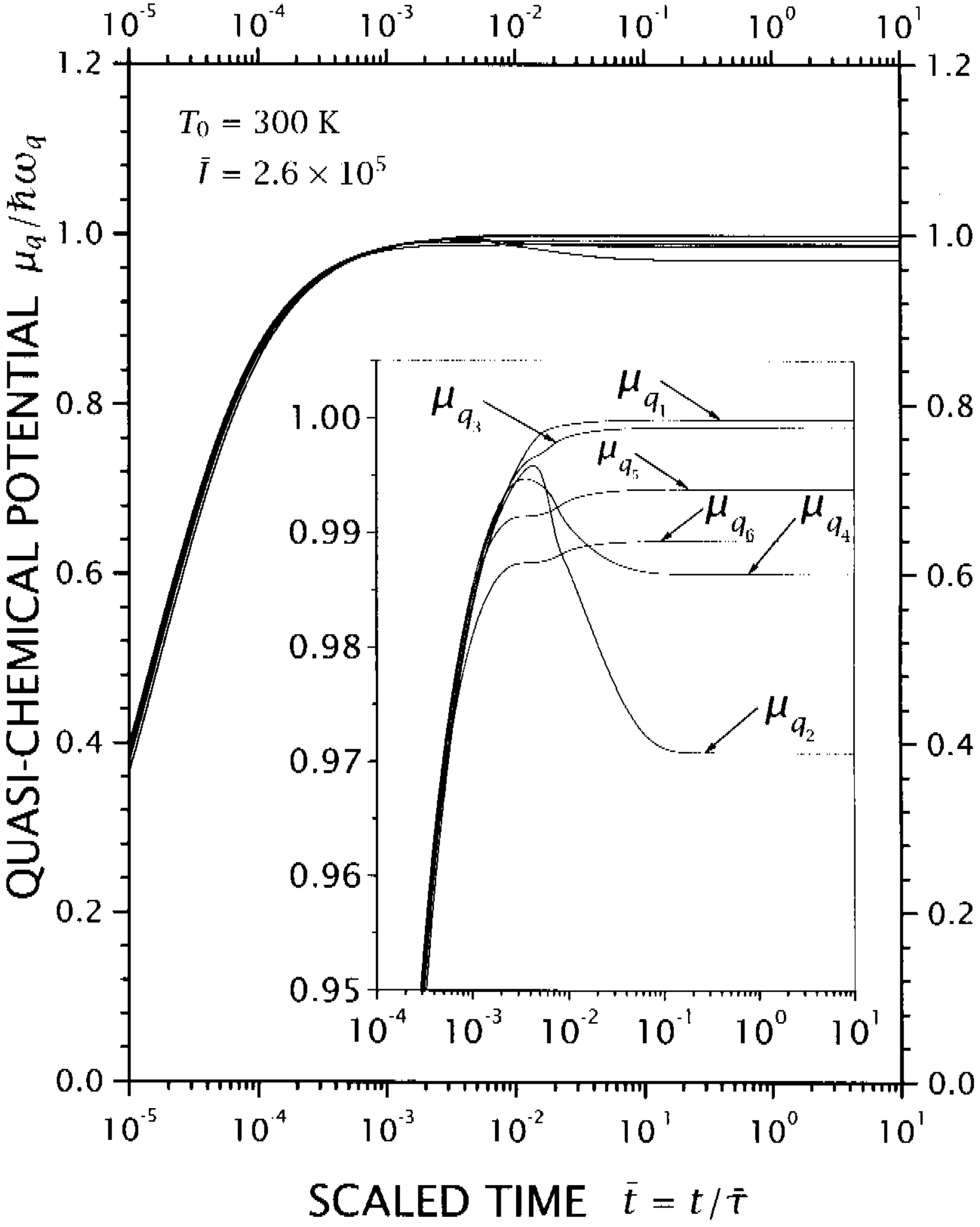

Figure 5: The quasi-chemical potential associated to the set of modes in Fig. 2.

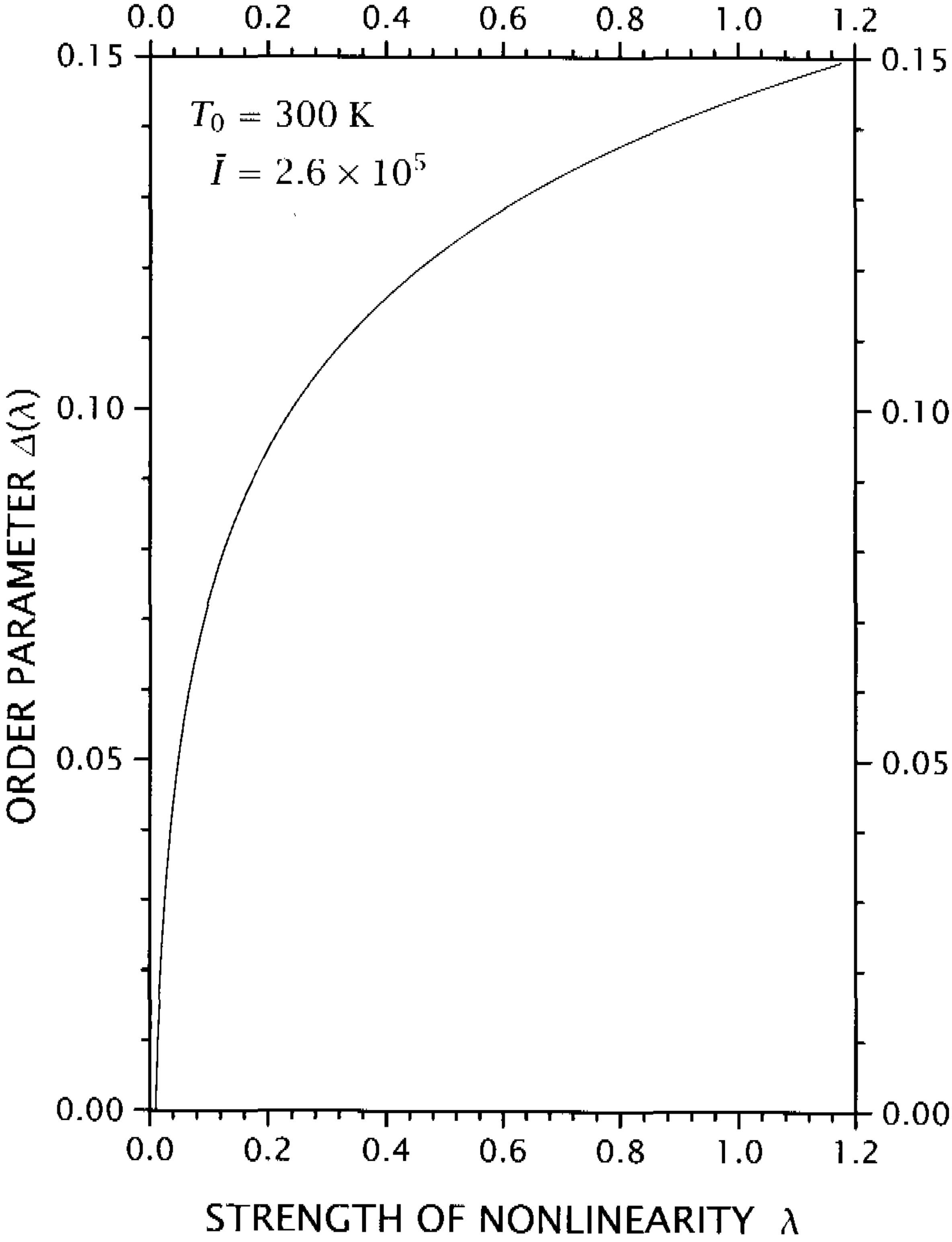

Figure 6: The order parameter of Eq. (55) as a function of the strength of the nonlinear coupling.

FONSECA *et al.* FIGURE 6

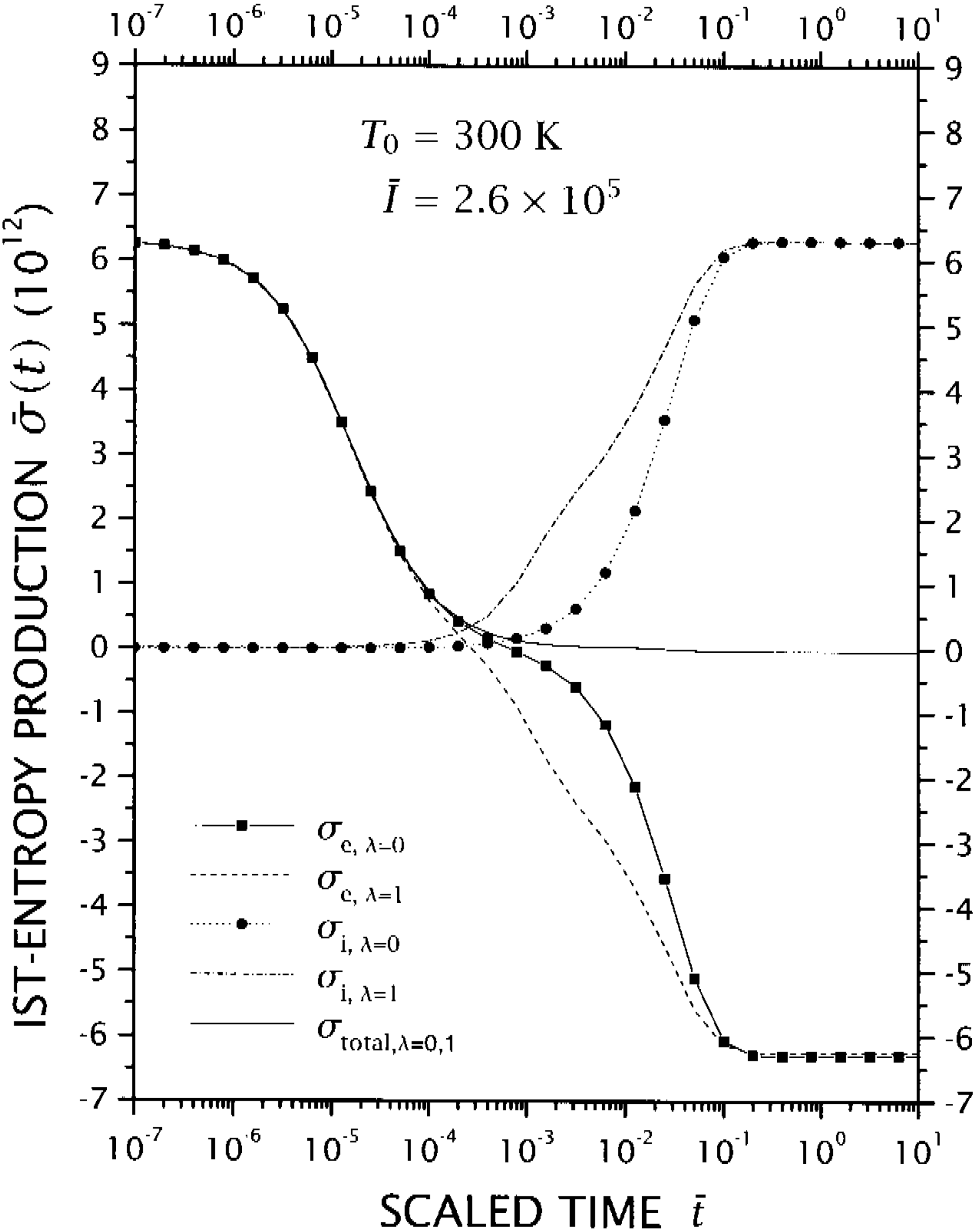

Figure 7: Evolution of the informational-entropy production.

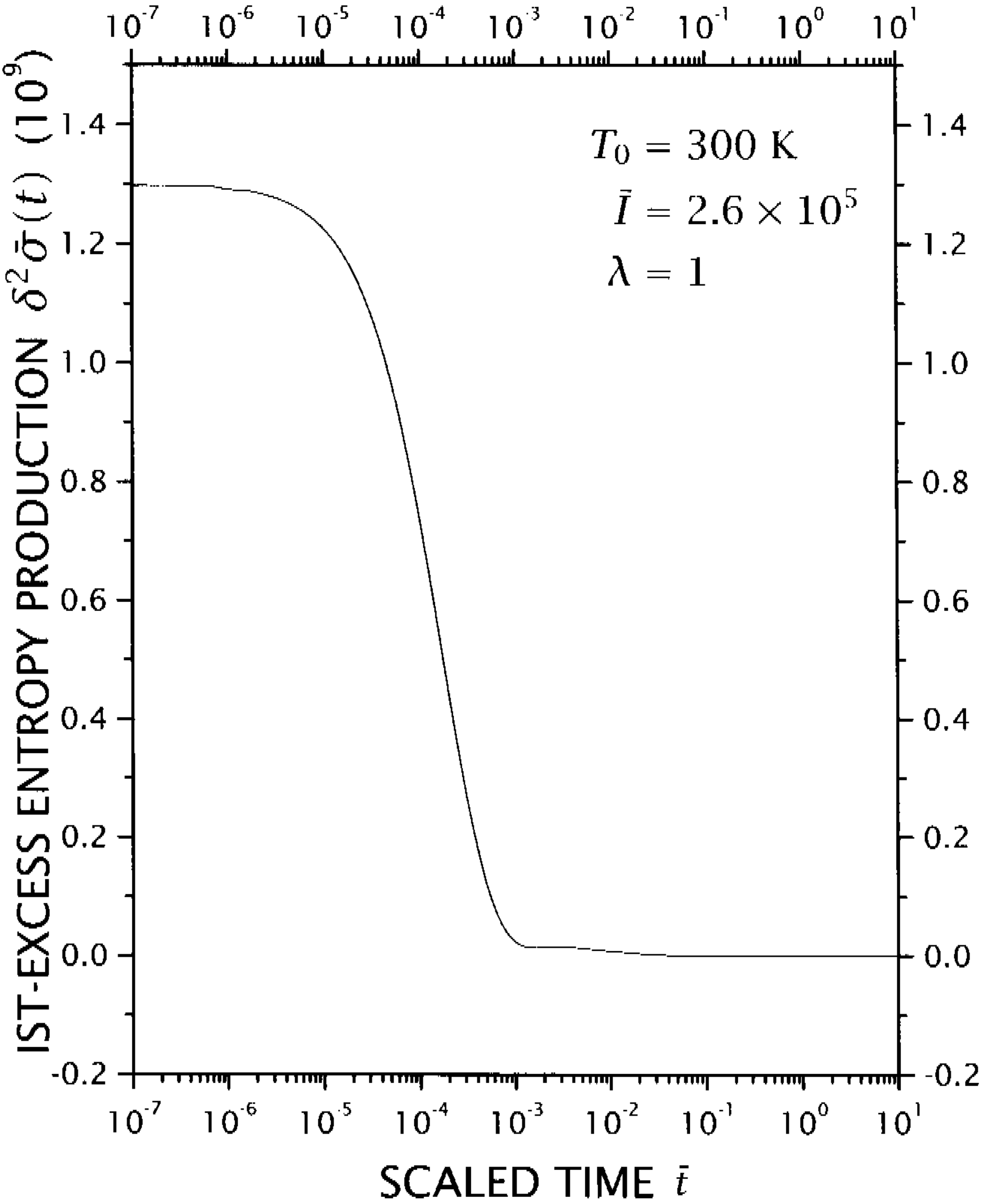

Figure 8: The excess entropy production around the steady state.

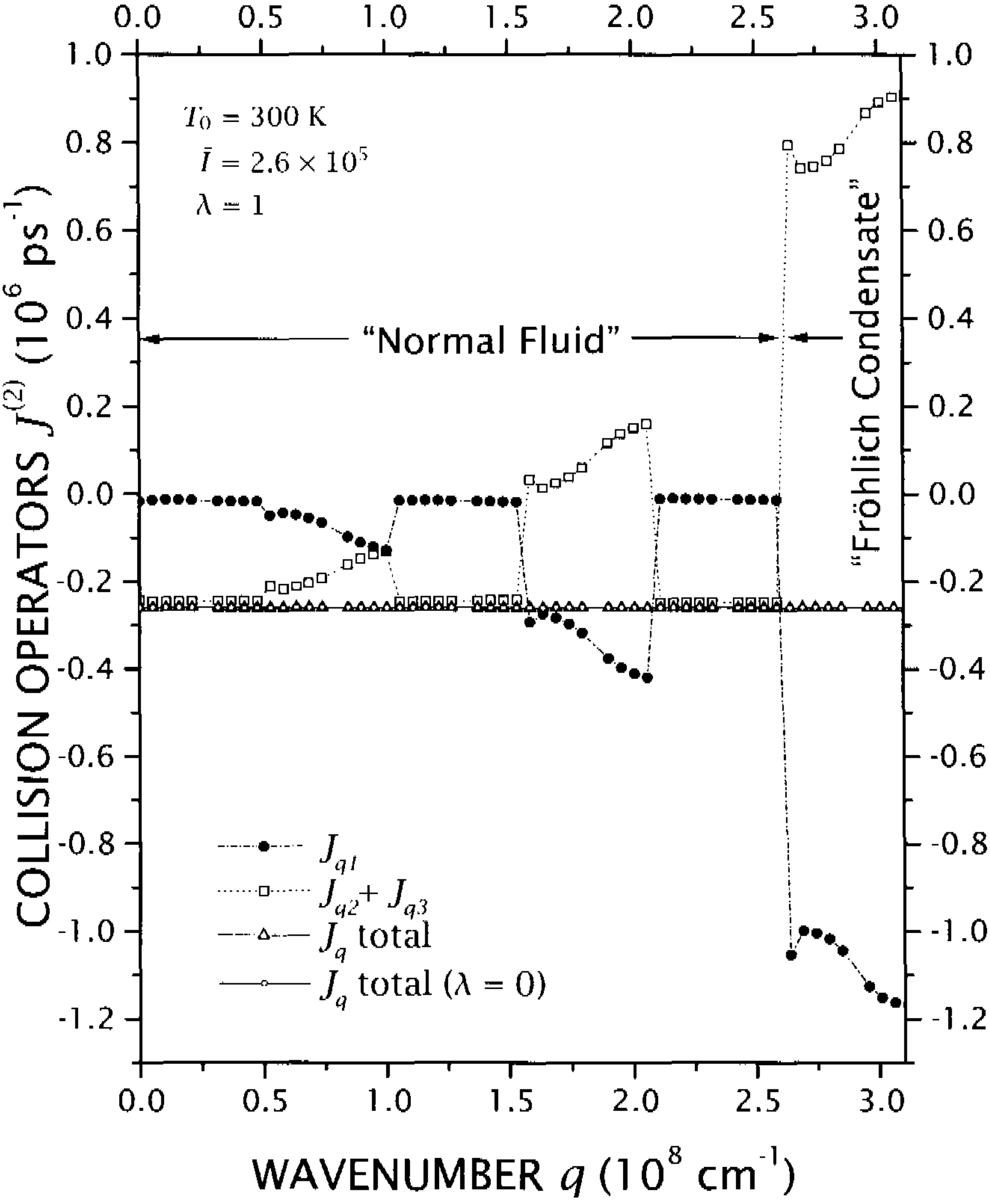

Figure 9: The different contributions to the relaxation processes for $\lambda = 1$ and in the absence of a nonlinear coupling ($\lambda = 0$).

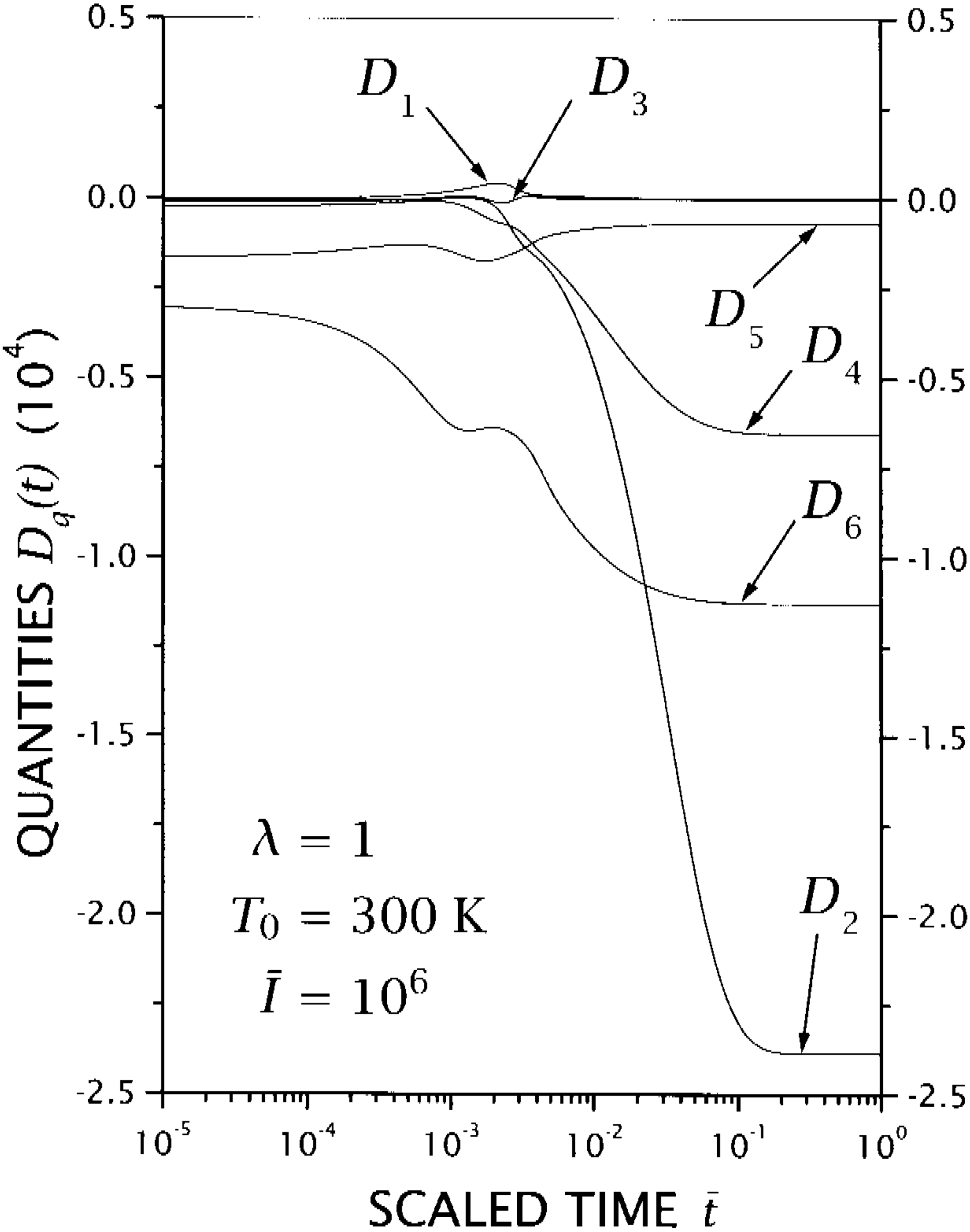

Figure 10: Quantities $D_q(t)$ of Eq. 72 for the set of modes of Fig. 2.

FONSECA *et al.* FIGURE 10

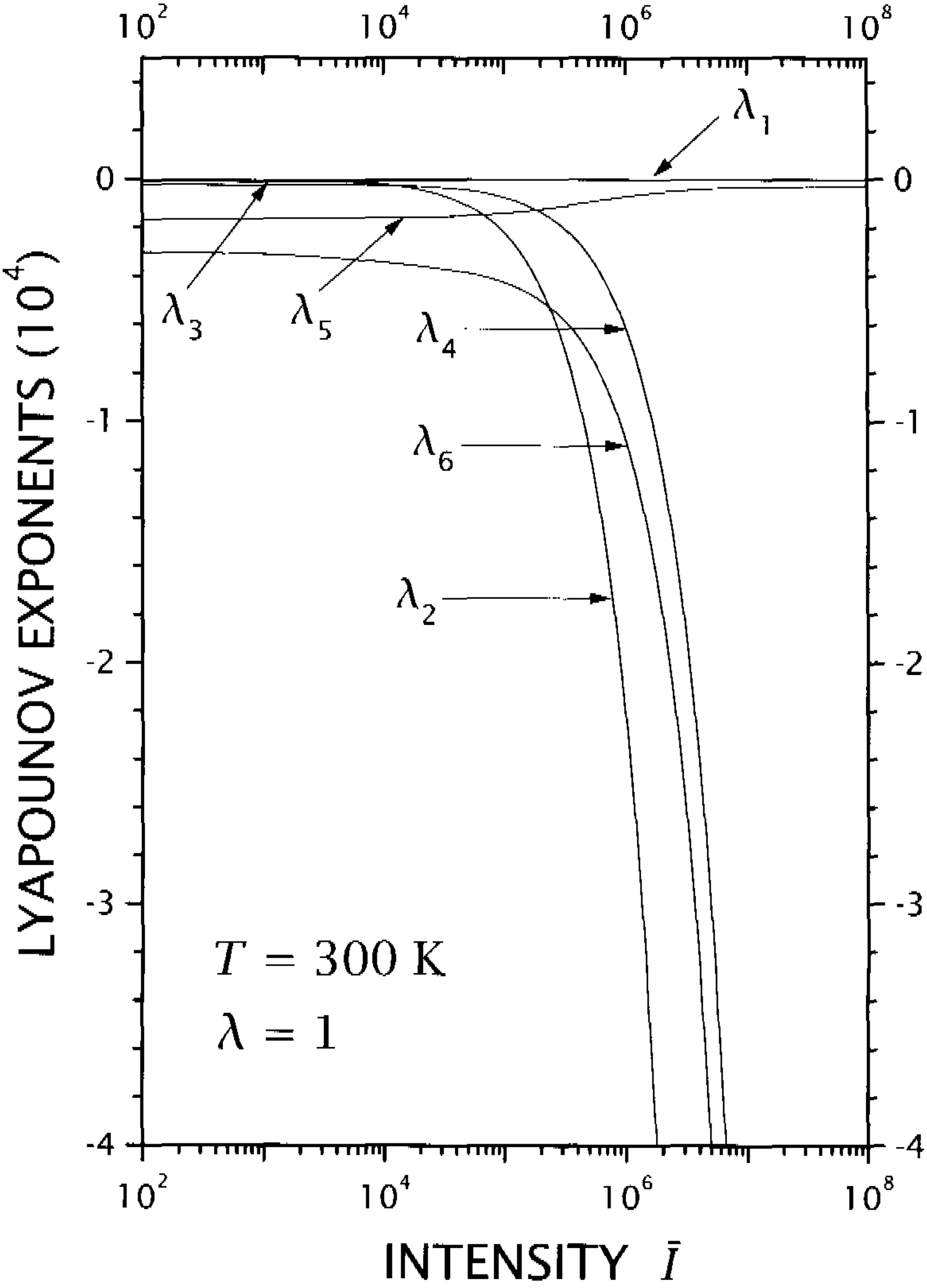

Figure 11: Lyapunov coefficient in the steady state for the set of modes of Fig. 3.

FONSECA *et al.* FIGURE 11

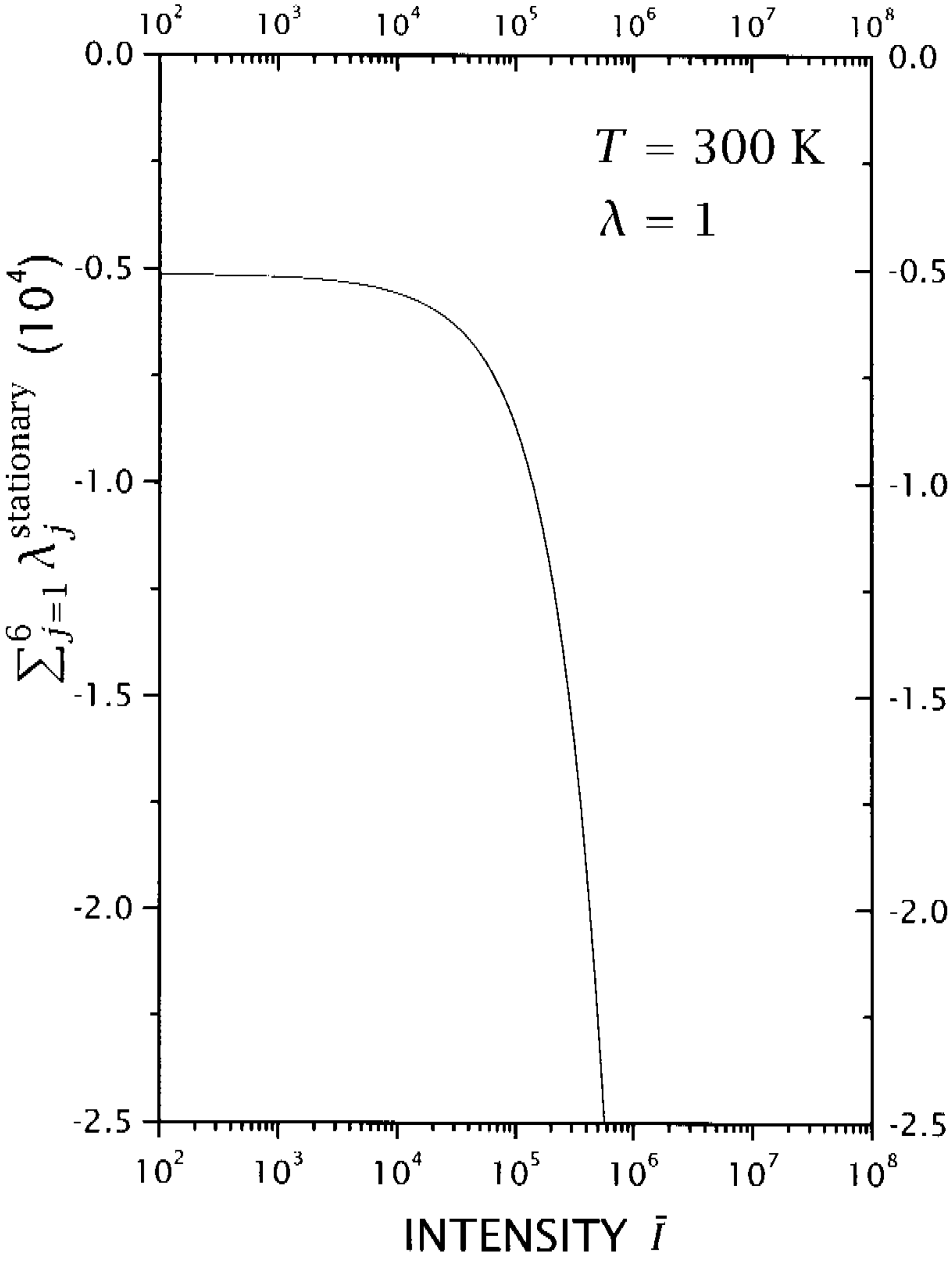

Figure 12: Sum of Lyapunov coefficients or divergence of the evolution operator in the steady state for the set of modes of Fig. 2.

FONSECA *et al.* FIGURE 12

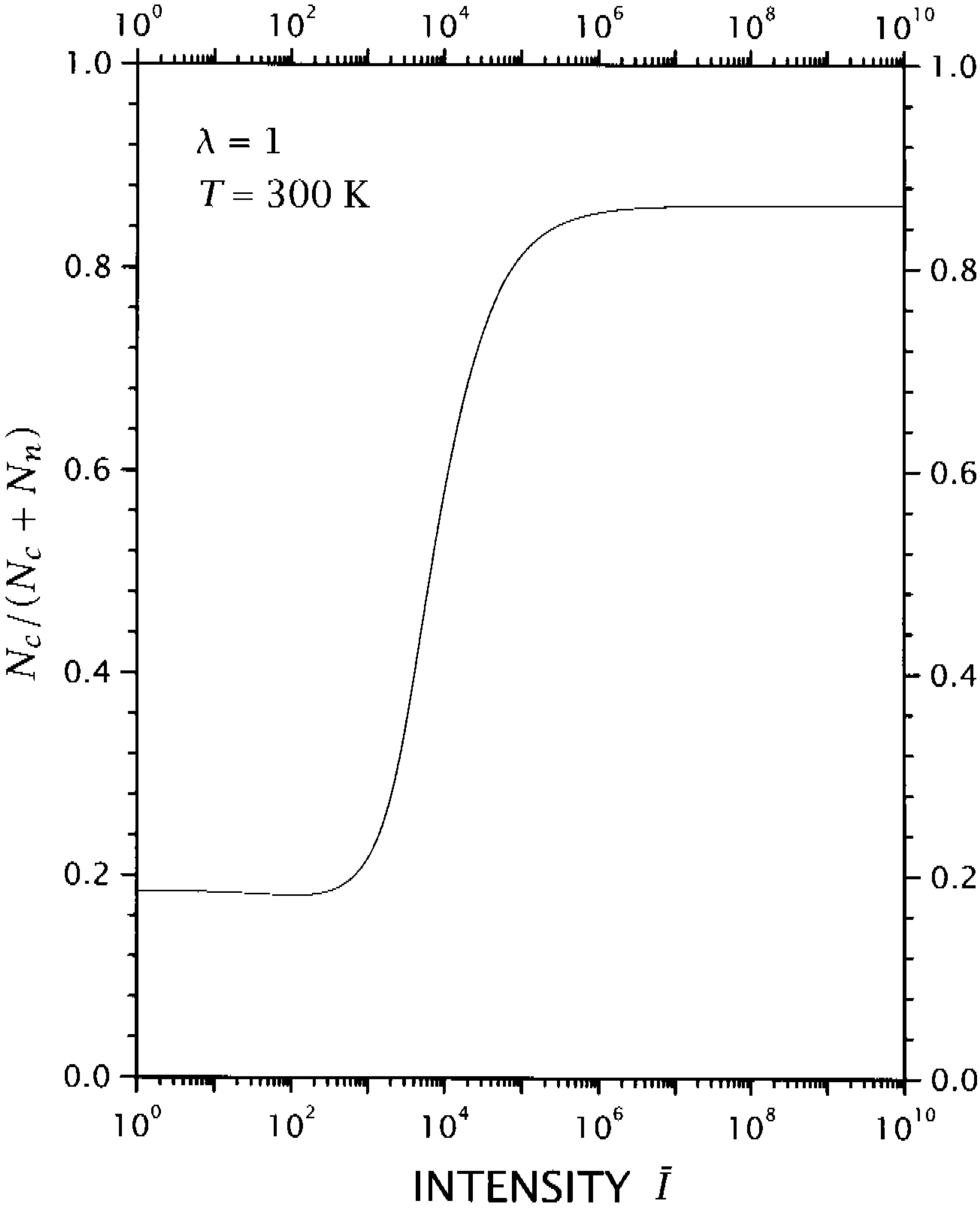

Figure 13: Fraction of excitations in the steady state.

Capítulo 5

ONDAS SOLITÁRIAS EM MATÉRIA CONDENSADA SOB CONDIÇÕES DE FORTE EXCITAÇÃO

5.1 Introdução

Neste capítulo estabelecemos a conexão com os dois capítulos anteriores.

Já tínhamos notado que o efeito Fröhlich e a propagação de sólitons do tipo Schrödinger-Davydov são uma conseqüência das *mesmas* contribuições não-lineares: os termos de interação anarmônica na descrição mecânica do sistema.

Assim vêm imediatamente a idéia de explorar o comportamento do sóliton no condensado de Fröhlich. Como este último surge em forma efetiva após certo limiar de excitação por uma fonte externa constante no tempo, e então em condições de afastamento do equilíbrio, vamos tratar o sóliton — diferentemente do que foi feito no Cap. 3 — quando em condições de forte excitação produzida pela alimentação da fonte externa.

Mostramos que em tais circustâncias acontece um fenômeno notável, que consiste num aumento enorme da vida média do sóliton. Nessas condições, o sóliton propaga-se então a longas distâncias, por causa do fraco decaimento e, como vimos, conservando sua forma de pacote e sem dispersão.

No que segue analisamos em detalhe o caso, i. e. deduzimos a demonstração do fenômeno e acrescentamos a aplicação dos resultados ao estudo de uma observação experimental particular e notável. Esta última consiste na existência do assim chamado "excitoner", que é a amplificação espontânea de pacotes de éxcitons incoerentes. A situação assemelha-se — ainda que apenas formalmente — ao caso do laser. Mostramos que o sinal detectado é um sóliton (de éxcitons) de Schrödinger-Davydov acompanhado de uma nuvem de éxcitons incoerentes.

Em continuação seguem as seções:

5.2 Sólitons em Matéria Fortemente Excitada: Efeitos Dissipativos Termodinâmicos e Supersônicos.

5.3 Amplificação Estimulada e Propagação de Feixe de Éxcitons.

5.2 Sólitons em matéria fortemente excitada: efeitos dissipativos termodinâmicos e supersônicos

Ondas solitárias — que surgem da coerência induzida de modos vibracionais ópticos e acústicos em sistemas abertos dissipativos (polímeros e matéria condensada) — são descritas em termos de uma termodinâmica estatística baseada em um formalismo de ensemble de não-equilíbrio. A onda progressiva não-deformada está acoplada às vibrações normais, e três fenômenos relevantes surgem em condições suficientemente distante das condições de equilíbrio: (1) um grande aumento das populações dos modos normais de freqüência mais baixa, (2) acompanhado por um grande aumento do tempo de vida da onda solitária, e (3) emergência de um efeito tipo Cherenkov, consistindo em uma grande emissão de fonons em direções privilegiadas, quando a velocidade de propagação do sóliton é maior do que a velocidade de grupo das vibrações normais. Comparação com experimentos é apresentada, o que aponta para a validade da teoria.

Physical Review E, **58** (6), 7913 (1998).

SOLITONS IN HIGHLY EXCITED MATTER: Dissipative-Thermodynamic and Supersonic Effects

Marcus V. Mesquita,* Áurea R. Vasconcellos, Roberto Luzzi

Instituto de Física 'Gleb Wataghin',
Universidade Estadual de Campinas, Unicamp
13083-970 Campinas, São Paulo, Brazil

---

*E-mail: sousa@ifi.unicamp.br
Group Home Page: http://www.ifi.unicamp.br/~aurea

Solitary waves — arising out of nonlinearity-induced coherence of optical and acoustical vibrational modes in dissipative open systems (polymers and bulk matter) — are described in terms of a statistical thermodynamics based on a nonequilibrium ensemble formalism. The undistorted progressive wave is coupled to the normal vibrations, and three relevant phenomena follow in sufficiently away-from-equilibrium conditions: (1) A large increase in the populations of the normal modes lowest in frequency, (2) accompanied by a large increase of the solitary wave lifetime, and (3) emergence of a Cherenkov-like effect, consisting in a large emission of phonons in privileged directions, when the velocity of propagation of the soliton is larger than the group velocity of the normal vibrations. Comparison with experiments is presented, which points out to the corroboration of the theory.

PACS # 63.70+h; 05.70Ln; 11.10.Lm; 87.22.-q

1. Introduction

Solitary waves are a particular kind of excitation in condensed matter, which nowadays are evidenced as ubiquitous and of large relevance in science and technology. Its role as a new concept in applied science was already emphasized by A. C. Scott *et al.* in 1973 [1], who discussed the case of several wave systems where the phenomenon may arise. Recently, solitons have been shown to play a very important role in three significant areas: conducting polymers [2, 3], fiber optics in communication engineering [4, 5], and as conveyors of energy in biological and organic polymers [6–8].

We consider here solitary waves arising out of vibronic modes, both optical and acoustical, when in the presence of external pumping sources driving the open system arbitrarily away from equilibrium. We evidence the possibility of emergence of a particular complex behavior brought about by the nonlinearities present in the kinetic equations which govern the evolution of the nonequilibrium (dissipative) macroscopic state of the system. For that purpose we resort to the so-called Informational Statistical Thermodynamics (IST for short [9], and see for example references [10–14]). IST is based on a particular nonequilibrium ensemble formalism, namely, the Nonequilibrium Statistical Operator Method (NESOM; see for example references [15–17]), and D. N. Zubarev's approach is by far the most concise, soundly based, and a quite practical one [16, 17]. Besides providing microscopic foundations to IST, Zubarev's NESOM yields a nonlinear quantum kinetic theory of a large scope [16–22], the one we used to derive the results we report in what follows.

2. Frölich Condensation and Schrödinger-Davydov Soliton

Let us consider a system which can sustain longitudinal vibrations, optical and acoustical (e.g. polar semiconductors, polymers and biopolymers, etc.), with, say, a frequency dispersion relation $\omega_{\boldsymbol{q}}$; $\boldsymbol{q}$ is a wave-vector in reciprocal space running over the Brillouin zone. The vibronic system is taken to be in contact with a thermal bath, modeled as a continuum of acoustic-like vibrations, with frequency dispersion relation $\Omega_{\boldsymbol{p}} = s_B|\boldsymbol{p}|$, and a cut-off Debye frequency Ω_D. System and bath interact via an anharmonic potential, and the whole Hamiltonian is taken as

$$H = H_0 + H_I = H_{0S} + H_{0B} + H_I \ , \tag{1}$$

where

$$H_{0S} = \sum_q \hbar\omega_q (a_q^\dagger a_q + \frac{1}{2}) \tag{2a}$$

$$H_{0B} = \sum_p \hbar\Omega_p (b_p^\dagger b_p + \frac{1}{2}), \tag{2b}$$

$$\begin{aligned} H_I = & \sum_q Z_q \varphi_q a_q^\dagger + \sum_{q_1 p} V^{(1)}_{q_1 p} a_{q_1} b_p b^\dagger_{q_1+p} + \sum_{q_1 p} V^{(1)}_{q_1 p} a_{q_1} b^\dagger_p b_{-q_1+p} \\ & + \sum_{q_1 p} V^{(1)}_{q_1 p} a_{q_1} b_p b_{-q_1-p} + \sum_{q_1 p} V^{(1)}_{q_1 p} a_{q_1} b^\dagger_p b^\dagger_{q_1-p} + \sum_{q_1 q_2} V^{(2)}_{q_1 q_2} a_{q_1} a_{q_2} b^\dagger_{q_1+q_2} \\ & + \sum_{q_1 q_2} V^{(2)}_{q_1 q_2} a_{q_1} a_{q_2} b_{-q_1-q_2} + \sum_{q_1 q_2} V^{(2)}_{q_1 q_2} a^\dagger_{q_1} a_{q_2} b_{q_1-q_2} + \sum_{q_1 q_2} V^{(2)}_{q_1 q_2} a_{q_1} a^\dagger_{q_2} b^\dagger_{q_1-q_2} + \text{H.c.} \end{aligned} \tag{2c}$$

It consists of the energy of the free system and bath, H_{0S} and H_{0B} respectively, and in H_I are present the interaction of the system with an external source (a mechanism for excitation which pumps energy on the system), which is the first term on the right, and the anharmonic interaction composed of several contributions, namely, those associated with three-particle (phonons) collisions involving one of the system and two of the bath (we call $V^{(1)}_{qq'}$ the corresponding matrix element), and two of the system and one of the bath (we call $V^{(2)}_{qq'}$ the associated matrix element). Moreover, a_q ($a_q^\dagger$), b_p ($b_p^\dagger$), are, as usual, annihilation (creation) operators of, respectively, normal-mode vibrations in the system and bath, and φ_q ($\varphi_q^\dagger$) of excitations in the source with Z_q being the coupling strength. (see also reference [23]). We recall that the wavevector runs over the system Brillouin zone in the case of the vibronic modes, and between zero and Debye cut-off wavevector in the bath.

Next, following NESOM-based IST, we need to define the thermodynamic space for the description of the nonequilibrium macroscopic state of the system. In other words, the set of basic variables relevant for the problem in hands: They are in the present case, first, the number of excitations in each mode, i.e. the operator $\hat{\nu}_q = a_q^\dagger a_q$. Second, once the formation of a coherent state of vibronic modes (the solitary wave) is expected, we must introduce the amplitudes a_q and $a_q^\dagger$ averaged over the nonequilibrium ensemble. Finally, we take the thermal bath as constantly remaining in equilibrium at a temperature T_0, and then we introduce its Hamiltonian H_{0B} as a basic dynamical variable. Therefore the basic set of chosen microdynamical variables consists of

$$\{\hat{\nu}_q\, , a_q\, , a_q^\dagger\, , H_{0B}\}\ . \tag{3a}$$

The nonequilibrium statistical operator in NESOM — we recall that we use Zubarev's approach and call it $\varrho_\varepsilon(t)$ —, is a superoperator depending on the above said basic dynamical microvariables, and an associated set of Lagrange multipliers (which constitute the corresponding set of intensive variables in IST, which also completely describes the nonequilibrium macroscopic-thermodynamic state of the system) [10, 13–17], which we designate as

$$\left\{F_q(t),\ f_q(t),\ f_q^*(t),\ \beta_0\right\}\ , \tag{3b}$$

and in the first part of Appendix A we describe ϱ_ε.

The set of basic macrovariables is indicated by

$$\left\{\nu_q(t),\ \langle a_q|t\rangle, \langle a_q^\dagger|t\rangle,\ \ E_B\right\}\ , \tag{4}$$

that is,

$$\nu_q(t) = \operatorname{Tr}\{\hat{\nu}_q \varrho_\varepsilon(t)\}, \tag{5}$$

$$\langle a_q|t\rangle = \operatorname{Tr}\{a_q \varrho_\varepsilon(t)\}, \tag{6}$$

$$E_B = \operatorname{Tr}\{H_{0B} \varrho_\varepsilon(t)\}\ . \tag{7}$$

Moreover, E_B (the energy of the thermal bath) is time independent and so is $\beta_0 = (k_B T_0)^{-1}$, because of the assumption that the bath is constantly kept in equilibrium at temperature T_0. Hence, the whole statistical operator is $\varrho_\varepsilon(t) = \tilde{\varrho}_\varepsilon(t) \times \varrho_B$, where now $\tilde{\varrho}_\varepsilon(t)$ is Zubarev's statistical operator of the vibronic system, and ϱ_B the canonical statistical distribution of the free thermal bath at temperature T_0 (which then plays the role of an ideal reservoir).

The equations of evolution for the three basic variables describing the evolution of the vibronic system are derived in the NESOM-based kinetic theory [15-22]. Taking into account that the anharmonic interaction is weak, we restrict the calculation to the Markovian limit, that is, we consider only collision integrals only up to second order in the interaction strength [16, 19-21]. We briefly describe in the second part of the Appendix A the fundamentals of these kinetic equations, particularly the origin of the collision operators that are present on the right of Eq. (8).

After some lengthy calculation we find that

$$\frac{d}{dt}\nu_{\boldsymbol{q}}(t) = I_{\boldsymbol{q}} + \sum_{j=1}^{5} J_{\boldsymbol{q}(j)}(t) + \zeta_{\boldsymbol{q}}(t) \, , \tag{8}$$

where $I_{\boldsymbol{q}}$ represents the rate of production of $\boldsymbol{q}$-mode phonons generated by the external pumping source,

$$J_{\boldsymbol{q}(1)}(t) + J_{\boldsymbol{q}(2)}(t) = -\tau_{\boldsymbol{q}}^{-1}[\nu_{\boldsymbol{q}}(t) - \nu_{\boldsymbol{q}}^{(0)}] \, , \tag{9}$$

with $\nu_{\boldsymbol{q}}^{(0)}$ being the $\boldsymbol{q}$-mode-population in equilibrium, i.e. Planck distribution at temperature T_0, and $\tau_{\boldsymbol{q}}$ is a relaxation time given by

$$\tau_{\boldsymbol{q}}^{-1} = \frac{4\pi}{\hbar^2}\frac{1}{\nu_{\boldsymbol{q}}^{(0)}}\sum_{\boldsymbol{p}}|V_{\boldsymbol{q}\boldsymbol{p}}^{(1)}|^2\nu_{\boldsymbol{p}}^B\nu_{\boldsymbol{q}-\boldsymbol{p}}^B[\delta(\Omega_{\boldsymbol{p}} + \Omega_{\boldsymbol{q}-\boldsymbol{p}} - \omega_{\boldsymbol{q}}) + 2e^{\beta\hbar\Omega_{\boldsymbol{p}}}\delta(\Omega_{\boldsymbol{p}} - \Omega_{\boldsymbol{q}-\boldsymbol{p}} + \omega_{\boldsymbol{q}})] \, , \tag{10}$$

where $\nu_{\boldsymbol{p}}^B$ is the population (Planck distribution) of the phonons in the bath at temperature T_0, and the other terms are

$$J_{\boldsymbol{q}(3)}(t) = \frac{8\pi}{\hbar^2}\sum_{\boldsymbol{q}'}|V_{\boldsymbol{q}\boldsymbol{q}'}^{(2)}|^2\left[\nu_{\boldsymbol{q}-\boldsymbol{q}'}^B(\nu_{\boldsymbol{q}'} - \nu_{\boldsymbol{q}}) - \nu_{\boldsymbol{q}}(1 + \nu_{\boldsymbol{q}'})\right]\delta(\Omega_{\boldsymbol{q}-\boldsymbol{q}'} + \omega_{\boldsymbol{q}'} - \omega_{\boldsymbol{q}}) \, , \tag{11}$$

$$J_{q(4)}(t) = \frac{8\pi}{\hbar^2}\sum_{q'} |V^{(2)}_{qq'}|^2 \left[\nu^B_{q-q'}(\nu_{q'} - \nu_q) + \nu_{q'}(1+\nu_q)\right]\delta(\Omega_{q-q'} - \omega_{q'} + \omega_q)\ , \tag{12}$$

$$J_{q(5)}(t) = \frac{8\pi}{\hbar^2}\sum_{q'} |V^{(2)}_{qq'}|^2 \left[\nu^B_{q+q'}(1+\nu_{q'}) - (\nu_{q'} - \nu^B_{q+q'})\nu_q\right]\delta(\Omega_{q+q'} - \omega_{q'} - \omega_q)\ , \tag{13}$$

and, finally, the term ζ_q is the one which couples the populations with the amplitudes, namely

$$\begin{aligned}
\zeta_q(t) = {} & \frac{|\langle a_q|t\rangle|^2}{\tau_q} + \frac{8\pi}{\hbar^2}\sum_{q'} |V^{(2)}_{qq'}|^2\{|\langle a_q|t\rangle|^2(1+\nu_{q'}+\nu^B_{q-q'}) - |\langle a_{q'}|t\rangle|^2(\nu_q - \nu^B_{q-q'})\} \\
& \times \delta(\Omega_{q-q'} + \omega_{q'} - \omega_q) \\
& - \frac{8\pi}{\hbar^2}\sum_{q'} |V^{(2)}_{qq'}|^2\{|\langle a_q|t\rangle|^2(\nu_{q'} - \nu^B_{q-q'}) - |\langle a_{q'}|t\rangle|^2(1+\nu_q+\nu^B_{q-q'})\} \\
& \times \delta(\Omega_{q-q'} - \omega_{q'} + \omega_q) \\
& + \frac{8\pi}{\hbar^2}\sum_{q'} |V^{(2)}_{qq'}|^2\{|\langle a_q|t\rangle|^2(\nu_{q'} - \nu^B_{q+q'}) - |\langle a_{q'}|t\rangle|^2(\nu_q - \nu^B_{q+q'})\} \\
& \times \delta(\Omega_{q+q'} - \omega_{q'} - \omega_q)\ .
\end{aligned} \tag{14}$$

In Eqs. (11) to (14) is evident the presence of Dirac's delta function accounting for energy conservation in the anharmonic-interaction-generated collisional processes; momentum conservation is taken care of in the energy operators of Eqs. (2). In the case of acoustical vibrational excitations the matrix elements of the anharmonic interaction are proportional to the square roots of the three wavenumbers involved, typically $K^{(1),(2)}[|\mathbf{q}||\mathbf{q}'||\mathbf{q}-\mathbf{q}'|]^{\frac{1}{2}}$, with indexes 1 or 2 in K corresponding to the matrix elements $V^{(1)}$ and $V^{(2)}$ respectively; $K^{(1)}$ can be determined via measurements of bandwidths in scattering experiments and $K^{(2)}$ is left an open parameter.

The equations of evolution for the amplitudes are

$$\begin{aligned}
\frac{\partial}{\partial t}\langle a_q|t\rangle = {} & -\mathrm{i}\,\tilde{\omega}_q\,\langle a_q|t\rangle - \Gamma_q\,\langle a_q|t\rangle + \Gamma_q\,\langle a^\dagger_q|t\rangle^* - \mathrm{i}W_q\,\langle a^\dagger_q|t\rangle^* + \\
& + \sum_{q_1q_2} R_{q_1q_2}\langle a_{q_1}|t\rangle\langle a^\dagger_{q_2}|t\rangle\left(\langle a_{q-q_1+q_2}|t\rangle + \langle a^\dagger_{q+q_1-q_2}|t\rangle\right)\ ,
\end{aligned} \tag{15}$$

$$\frac{\partial}{\partial t}\langle a^\dagger_q|t\rangle = \text{the complex conjugate of the right hand side of Eq. (15)}\ , \tag{16}$$

where $\tilde{\omega}_q$ is the frequency renormalized by the anharmonic interaction, with W_q being a term of renormalization of frequency, and the lengthy expression for $R_{q_1q_2}$ is given elsewhere [24] (their detailed expressions are not necessary for our purposes here). Finally, $\Gamma_q(t)$, which has a relevant role in what follows, is the reciprocal of a relaxation time, given by

$$\begin{aligned}\Gamma_q(t) = \tau_q^{-1}(t) &+ \frac{4\pi}{\hbar^2}\sum_{q'}|V^{(2)}_{qq'}|^2\left[1+\nu_{q'}+\nu^B_{q-q'}\right]\delta(\Omega_{q-q'}+\omega_{q'}-\omega_q)\\ &+ \frac{4\pi}{\hbar^2}\sum_{q'}|V^{(2)}_{qq'}|^2\left[\nu_{q'}-\nu^B_{q-q'}\right]\delta(\Omega_{q-q'}-\omega_{q'}+\omega_q)\\ &+ \frac{4\pi}{\hbar^2}\sum_{q'}|V^{(2)}_{qq'}|^2\left[\nu_{q'}-\nu^B_{q+q'}\right]\delta(\Omega_{q+q'}-\omega_{q'}-\omega_q)\,.\end{aligned} \tag{17}$$

Equations (15) and (16) are coupled together, and contain linear and trilinear terms. They give rise to two types solutions: one is a superposition of normal vibrations and the other is of the Davydov's soliton type [6, 25, 26], as we proceed to show. First, we neglect the coupling of the amplitude $\langle a_q|t\rangle$ and its conjugate, what can be shown that straightly follows when the original Hamiltonian is truncated in the so-called Rotating Wave Approximation [27], which can be used in this case. Next, we introduce the averaged (over the nonequilibrium ensemble) field operator

$$\psi(x,t) = \sum_q \langle a_q|t\rangle \mathrm{e}^{\mathrm{i}qx}. \tag{18}$$

for one-dimensional propagation along x-direction (the only one in the case of quasi-one-dimensional polymers or semiconductor quantum wires). At this point we need to define the dispersion relation ω_q: we may consider two cases, namely, optical and acoustical vibrations. The first case has already been considered [28] in the particular case of acetanilide (in which the CO-stretching polar modes are of the same type as those in biopolymers, e.g., the α-helix protein). It is shown that a *Davydov's soliton-type excitation*, in the form of an undeformed wavepacket consisting in a coherent state of CO-stretching (or Amide-I) vibration is present. But it is damped when propagating in the dissipative medium, a damping dependent on the thermodynamic state of the system, as evidenced in the NESOM-IST calculation. Moreover, a calculation in NESOM-based response function theory has allowed us to derive the infrared absorption spectra [28], characterizing the soliton and obtaining an excellent agreement with the experimental data of Careri *et al.* [29]. For illustration we present in Fig. 1 the IR-spectra in three different conditions, namely at temperatures of 20 K; 50 K; and 80 K.

Let us consider next the case of acoustic vibrations, with a frequency dispersion relation $\omega_{\boldsymbol{q}} = s|\boldsymbol{q}|$ (s being the velocity of sound in the system). Using this dispersion relation, and proceeding on the *Ansatz* that a well localized and spatially undeformed solitary-wave-type solution is expected, using Eqs. (15) and (18), we find (see Appendix B) that the field amplitude satisfies the local (space correlations neglected, as noticed) equation

$$i\hbar\frac{\partial}{\partial t}\psi(x,t)+\frac{\hbar^2}{2M_S}\frac{\partial^2}{\partial x^2}\psi(x,t)+i\hbar\gamma_s\psi(x,t)=\hbar G|\psi(x,t)|^2\psi(x,t)\,, \tag{19}$$

which is formaly identical to the one for the optical vibrations [28], where $\hbar^2/2M_S = \hbar s w$, with w being the width of the wavepacket (see below) and M_S a pseudo-mass. This is a nonlinear Schrödinger-type equation with damping [1, 30], and where γ_s and G are the values in the local approximation of the transforms of $\Gamma_{\boldsymbol{q}}$ of Eq. (17) and $R_{q_1 q_2}$ in Eq. (15) to direct space (see reference [28]). Equation (19) for the average field amplitude admits two types of solutions. One is a simple plane wave composed by the superposition of the normal-mode vibrations (corresponding to *first-sound-like waves* associated to the motion of density). Other is a *Schrödinger-Davydov soliton-type excitation*: Let us consider as an initial and boundary condition, an impinged signal with a hyperbolic secant shape, which satisfactorily approaches a Gaussian profile. It has an amplitude, say, $\mathcal{A}$, which defines its energy content, and a momentum characterized by a velocity of propagation v. Resorting to the inverse scattering method [31] we obtain that the solution of Eq. (19) is

$$\psi(x,t)=\mathcal{A}\exp\Big\{i\Big[\frac{M_S v}{\hbar}x-(\omega_s-i\gamma_s)t-\frac{\theta}{2}\Big]\Big\}\,\mathrm{sech}\Big[\mathcal{A}\Big[\frac{|G|M_S}{\hbar}\Big]^{1/2}(x-vt)\Big]\,, \tag{20}$$

where γ_s is the reciprocal lifetime of the excitation, we used $G = |G|e^{i\theta}$, and

$$\omega_s = \frac{|G|\mathcal{A}^2}{2} - \frac{M_S v^2}{4\hbar}, \tag{21}$$

which is an amplitude- and velocity-dependent frequency.

We recall that the amplitude $\mathcal{A}$ and the velocity v are determined by the initial and boundary conditions of excitation determined by the perturbing source (the "exciting antenna array"). Davydov's soliton of Eq. (20) can be interpreted as that the vibrational acoustic modes are localized by means of the nonlinear coupling with the external bath; the distortion then reacts — also through anharmonic coupling — to trap the oscillations and keeping the packet undistorted, in a process also referred-to as selftrapping [1, 7]. Moreover, as noticed, in conditions of excitation in near equilibrium with the bath, the solitary wave is damped, relaxing with a lifetime γ_s^{-1}. However, the situation is substantially modified in sufficiently far-from-equilibrium conditions, i.e. for high values of the pumping intensity I_q in Eq. (8). In this equation it can be noticed that $J_{q(4)}$ and $J_{q(5)}$ contain nonlinear contributions in the populations of the modes. These nonlinear contributions have the remarkable characteristic that when $\omega_q < \omega_{q'}$, there follows a net transmission of the energy, received from the external source, from the modes higher in frequency to those lower in frequency, in a cascade-down process: This a consequence of the presence of the nonlinear terms (containing the product $\nu_q \nu_{q'}$) in the collision integrals of Eqs. (11–13), which are present in the equation of evolution for the population in mode $\boldsymbol{q}$, viz. Eq. (8). For $\omega_q < \omega_{q'}$, the collision integrals of Eqs. (11) and (13) do not contribute, as a consequence that energy conservation in the collisional events (accounted for the delta functions) cannot be satisfied. Hence, there survives the collision integral of Eq. (12) giving rise to the already mentioned increase of population in mode $\boldsymbol{q}$, at the expenses of all the other modes $\boldsymbol{q}'$ having higher frequencies than ω_q. For $\omega_q > \omega_{q'}$ there survives only the collisional integral of Eq. (15) implying in a transmission of energy from the mode to those with lower frequencies, that is, these nonlinear terms redistribute energy among the modes.

As a consequence the populations of the modes lowest in frequency (i.e. those around the zone center) are largely increased. Such phenomenon was predicted by H. Fröhlich near thirty years ago [32]. This so-called *Fröhlich effect*, in sufficiently far-from-equilibrium conditions, has a dramatic effect on the propagation of the Davydov soliton described above. With increasing population ν_q in the modes lowest in frequency, the lifetime of these modes of vibration, as given by the reciprocal of the Γ_q of Eq. (17), is largely increased. Therefore, in the field amplitude $\psi(x,t)$, as given by Eq. (18), after typically a fraction of picosecond has elapsed after switch-on of the excitation, the amplitudes $\langle a_q|t\rangle$ for modes at intermediate to high frequencies in the dispersion relation band die down, but those for the modes lowest in frequency (in the neighborhood of the zone center) survive for long times (their lifetime being larger and larger for increasing values of the pump intensity). We illustrate the point in figures 2 and 3: Consider a sample with the soliton traveling in a given direction along the extension L of the sample. Then the permitted vibrational modes are those in the interval of wavenumbers $\pi/L \leq q \leq q_B$, where q_B is the Brillouin zone-end wavenumber. We take $L = 10$cm, and values for the parameters involved in an order of magnitude for typical polymers and thermal bath, namely $q_B = 3.14 \times 10^7$ cm^{-1} (hence the lattice parameter has been taken as $a = 10$ Å), $s \simeq 1.8 \times 10^5$ cm/s, $s_B \simeq 1.4 \times 10^5$ cm/s, $\tau_q \simeq 10$ ps for all $\mathbf{q}$, and from the latter we can estimate in the matrix elements $K^{(1)}$, while we keep as an open parameter the ratio $\lambda = |K^{(2)}|^2/|K^{(1)}|^2$. For these characteristic values it follows that, because of energy and momentum conservation in the scattering events, the set of equations of evolution, Eqs. (8), which in principle couple all modes among themselves, can be grouped into independent sets each one having nine modes. For example, taking the mode with the lowest wavenumber π/L, the set to which it belongs contains the modes $\kappa^{n-1}\pi/L$, where $\kappa = (s + s_B)/(s - s_B) = 8$ in this case, and $n = 2, 3, \ldots, 9$. Let us call $\nu_1, \ldots, \nu_9$ the corresponding populations, and their frequencies are $\omega_1 = 5.6 \times 10^4$ Hz, $\omega_2 = 4.5 \times 10^5$ Hz, $\omega_3 = 3.6 \times 10^6$ Hz, $\omega_4 = 2.9 \times 10^7$ Hz, $\omega_5 = 2.3 \times 10^8$ Hz, $\omega_6 = 1.8 \times 10^9$ Hz, $\omega_7 = 1.5 \times 10^{10}$ Hz, $\omega_8 = 1.2 \times 10^{11}$ Hz, $\omega_9 = 9.5 \times 10^{11}$ Hz. Moreover, for illustration, the open parameter λ is taken equal to 1, and we consider that only the modes 2 and 3 (in the ultrasonic region) are pumped with the same constant intensity $S = I\bar{\tau}$, where $I_2 = I_3 = I$, and I_1 and I_n with $n = 4, \ldots, 9$ are null, and $\bar{\tau}$ is a characteristic time used for scaling purposes (as in [22]) here equal to 0.17 s. It is evident the large enhancement of the population in the mode lowest in frequency (ν_1), for $S_0 \simeq 10^{19}$, at the expenses of the two pumped modes ν_2 and ν_3, while the modes ν_4 to ν_9 have minor modifications acquiring populations which are very near that in equilibrium with the thermal bath at temperature T_0; that is to say that they are practically unaltered. The emergence of Fröhlich effect is clearly evidenced for this case of acoustical vibrations: In fact, pumping of the modes in a restricted ultrasonic band (in the present case in the interval 4.5×10^5 Hz $\leq \omega \leq 2.8 \times 10^7$ Hz), leads at sufficiently high intensity of excitation to the transmission of the pumped energy in these modes to those with lower frequencies ($\omega < \omega_2$), while those with larger frequencies ($\omega > 2.8 \times 10^7$ Hz) remain in near equilibrium. It may be noticed that for the given value of $\bar{\tau}$, $S = 10^{19}$ corresponds to a flux power, provided by the external source in the given interval of ultrasound frequencies being excited, of the order of milliwatts.

The dependence of the lifetime with the level of excitation is illustrated in Fig. 3: It is evidenced the mentioned fact of a large increase of the lifetime for the mode lowest in frequency, that is, the reciprocal of the lifetime, Γ_1, largely decreases.

Fröhlich effect can be evidenced in an alternative way. A straightforward calculation in NESOM, leads to the result that, in terms of the intensive nonequilibrium thermodynamic variables of Eq. (3b), the population and the amplitude are given by

$$\nu_q(t) = \left[e^{F_q(t)} - 1\right]^{-1} + |\langle a_q|t\rangle|^2 \, , \tag{22}$$

$$\langle a_q|t\rangle = -f_q(t)^* / F_q(t) \, . \tag{23}$$

Moreover, the intensive thermodynamic variable F_q can alternatively be written in either of two forms: One is

$$F_q(t) = \beta_0(\hbar\omega_q - \mu_q(t)) \, , \tag{24}$$

introducing a pseudo-chemical potential per mode μ_q, usually referred-to as a quasi-chemical potential, as done by Fröhlich [32] and P. T. Landsberg [33] (we recall that $\beta_0 = (k_B T_0)^{-1}$). The steady state values of the quasi-chemical potential of mode populations $\bar{\nu}_j$, with $j = 1, 2$ and 3 in Fig. 2 vs. the intensity of the external source are shown in Fig. 4., being evident that μ_1 approaches ω_1 for S of the order of 10^{19}, what results in a near singularity in $\bar{\nu}_1$ (This phenomenon is sometimes referred-to as a kind of non-equilibrium "Bose-Einstein-like condensation" because of the characteristic of "piling up"of excitations in the lowest levels of vibronic energy. Also a "two-fluid-like" model may be considered in a descriptive way, as, in a sense, shown in Fig. 5).

Otherwise, it can be written

$$F_q(t) = \hbar\omega_q / k_B T_q^*(t) \ , \tag{25}$$

introducing a nonequilibrium pseudo-temperature (or quasitemperature) per mode, as used in the physics of the photoinjected plasma in semiconductors (e.g. [34–36]); its dependence on the intensity of the external source is displayed in Fig. 6.

3. Fröhlich-Cherenkov Effect or X-Waves

Moreover, another novel phenomenon may be expected in the out-of-equilibrium non-linear system we are considering. In both cases of "optical" or "acoustical" Schrödinger-Davydov solitons we have described, the amplitude and the velocity of propagation are determined by the initial condition of excitation. Hence, the velocity v can be either smaller or larger than the group velocity of the normal waves. For the polymer acetanilide in the conditions of the experiment of Careri *et al.* [29], v is larger than the group velocity of the phonons of the CO-stretching vibrations [28]. In the case of acoustic vibrations in bulk we may have $v > s$, leading to the emergence of a kind of Cherenkov-like effect (a so-called superluminal effect in the case of charges moving in a dielectric with a velocity larger than the velocity of light in the medium [37, 38]) as we proceed to show. This could be the case in the experiments of Lu and Greenleaf [39]; in Fig. 7 we reproduce a related figure [40] showing on the one side the excitation of a normal sound wave, and the other an apparent, in our interpretation, "superluminal" solitary wave, or better to say a *supersonic solitary wave.* accompanied with a Cherenkov-like large emission of phonons, as next described. Such excitation has been dubbed an X-wave, and interpreted in terms of an undeformed progressive wave [40, 41], created by the particular excitation provided by the pumping transducer.

Consider propagation of a soliton with velocity $v(> s)$ in, say, x-direction in bulk, what introduces a privileged direction in the system. It can be noticed that according to Eq. (8) [cf. also Eq. (22)] the populations of the vibronic modes increase as a result of the direct excitation provided by the source with intensity I_q in Eq. (8), with, as previously shown, such pumped energy being concentrated in the modes lowest in frequency (see Figs. 2 and 3), and as a consequence of such so-called Fröhlich effect, the lifetime of the soliton is largely increased. Moreover, we notice that for the modes in the Fröhlich condensate it can be estimated that $|\langle a_q \mid t\rangle|^2 \simeq w^2\mathcal{A}^2/L^2$, where, we recall, $\mathcal{A}$ is the amplitude and we have written w for the width of the solitary wave packet. On the other hand, for the preferentially populated modes with small q, using Eqs. (22) and (24) it follows that

$$\begin{aligned}\mu_q &= \hbar sq[1 - \frac{k_B T_0}{\hbar sq}\ln(1 + \frac{1}{\nu_q - |\langle a_q\rangle|^2})] = \\ &= \hbar sq[1 - \frac{k_B T_0}{\hbar sq}F_q] = \hbar v q\cos\theta_q\,, \end{aligned} \tag{26}$$

where we have introduced the angle θ_q whose cosinus is

$$\begin{aligned}\cos\theta_q &= \frac{s}{v}[1 - \frac{k_B T_0}{\hbar sq}\ln(1 + \frac{1}{\nu_q - |\langle a_q\rangle|^2})] \\ &= \frac{s}{v}[1 - \frac{T_0}{T_q^*}] \equiv \frac{s}{v n_q}\,, \end{aligned} \tag{27}$$

after Eq. (25) is used, and n_q defines a "pseudo-refraction index" introduced simply for giving an expression resembling the case of Cherenkov effect in radiation theory (when then ν_q is the Planck distribution of photons) [37, 38]. Hence, since

$$\nu_q = [\exp[\beta_0\hbar sq[1 - (v/s)\cos\theta_q]] - 1]^{-1} + |\langle a_q\rangle|^2\,, \tag{28}$$

(where $|\langle a_{\boldsymbol{q}}\rangle|^2 \simeq w^2\mathcal{A}/L^2$) then, it follows that a large emission of phonons follows when $\cos\theta_{\boldsymbol{q}}$ approaches the value s/v, that is, for T_q^* much larger than T_0 [cf. Fig. 6], and which are emitted in the direction $\boldsymbol{q}$ forming an angle $\theta_{\boldsymbol{q}}$ with the direction of propagation of the supersonic soliton ($v > s$). Forward and backwards symmetrical propagations are present because modes $\pm\boldsymbol{q}$ are equivalent ($\mu_{\boldsymbol{q}}$ depends on the modulus of $\boldsymbol{q}$). This is here a particular characteristic of what in radiation theory are the normal and anomalous Cherenkov effect in a spatially dispersive medium [38]. As already noticed, the phenomenon, which we call *Fröhlich-Cherenkov effect*, may provide a microscopic interpretation of the X-waves in experiments of ultrasonography [39], shown in the lower part of Fig. 7 [40]. From this figure we roughly estimate that $\theta \simeq 13°$, and then $v/s \simeq 1.02$, that is, the velocity of propagation of the ultrasonic soliton is 2% larger than the velocity of sound in the medium, once we admit an excitation strong enough to imply that $T_q^* \gg T_0$.

These X-waves have been described in terms of a mathematical approach pertaining to the theory of undeformed progressive waves [40, 41]. This appears to be a particularly interesting applied mathematical treatment for a practical handling of the phenomenon, for example in engineering for medical imaging [39, 41], as other applied mathematical method does for engineering in communications [42, 43]. The interesting case of medical imaging is treated in detail elsewhere [44], where we use the results presented in this communication.

Summarizing, we have described, resorting to a statistical thermodynamics based on a nonequilibrium ensemble formalism, the solitary waves which arise out of nonlinearity-induced coherence of optical and acoustical vibrations in open systems driven away from equilibrium. The resulting Schrödinger-Davydov soliton is coupled to the normal vibrations, and complex behavior is evidenced in the form of three relevant phenomena, namely: (1) a large increase in the populations of the normal modes lowest in frequency (the so-called Fröhlich condensation); (2) an accompanying large extension of the solitary wave lifetime (producing a near undamped soliton); (3) large emission of phonons in privileged directions when the velocity of propagation of the soliton is larger than the group velocity of the normal vibrations (or Fröhlich-Cherenkov effect).

Finally, we call the attention to the fact that, in any material system, mass and thermal motions are coupled together through thermo-striction effects (in the case of charged particles is the thermo-electric effect). Thermal motion consists into the so-called second sound propagation, for which apply all the considerations we have presented here. Also, it may be added the case of the zero-sound-like excitation in the double photoinjected plasma in semiconductors (the so-called acoustic plasmons, with the corresponding first-sound-like excitation being the optical plasmons) [45, 46]. Similarly, one may consider as candidates for these kind of phenomena a large variety of normal-mode vibrations in matter, like, e.g., polaritons, plasmaritons, phonoritons, and all kind of excitonic waves propagating in nonlinear media. A particular case of eventual large relevance may be the case of the so-called "excitoner", that is, the stimulated amplification of excitons low in energy (dubbed a kind of Bose condensation), and their propagation in the form of a weakly undamped packet [47, 48]. It is analyzed on the basis of the statistical thermodynamics as described in [49].

We acknowledge financial support provided to our Group, in different opportunities, by the São Paulo State Research Foundation (FAPESP), the National Research Council (CNPq), the Ministry of Planning (Finep), Unicamp Foundation (FAEP), IBM Brasil, the US-National Science Foundation (USA-Latin American Cooperation, Washington, USA), and the John Simon Guggenheim Memorial Foundation (New York, USA).

Appendix A. The Statistical Operator and the Equations of Evolution

The nonequilibrium statistical operator in Zubarev's approach (e.g. [15-17]) is

$$\varrho_\varepsilon(t) = \exp\{\ln\bar{\varrho}(t,0) - \int_{-\infty}^{t} dt'\, e^{\varepsilon(t'-t)}\frac{d}{dt'}\ln\bar{\varrho}(t',t'-t)\} \tag{A.1}$$

where $\bar{\varrho}$ is the auxiliary (sometimes called "coarse-grained" or "instantaneous" quasi-equilibrium) statistical operator, in the present case given by

$$\bar{\varrho}(t,0) = \exp\left\{ \phi(t) - \sum_q \left[F_q(t)\hat{\nu}_q + f_q(t)a_q + f_q^*(t)a_q^\dagger - \beta_0 H_{0B}\right]\right\} \tag{A.2}$$

where $\phi(t)$ ensures its normalization, and

$$\bar{\varrho}(t',t'-t) = \exp\{-\frac{1}{i\hbar}(t'-t)H_S\}\bar{\varrho}(t',0)\exp\{\frac{1}{i\hbar}(t'-t)H_S\} \tag{A.3}$$

with H_S being the Hamiltonian of Eq. (1) excluding the interaction with the external source (i.e. the free system Hamiltonian in an interaction representation).

We recall that ε is a positive infinitesimal which goes to zero after the trace operation in the calculation of averages has been performed. Its presence in the exponential introduces a so-called fading memory in the formalism, from which follows irreversible behavior from an initial condition of preparation of the nonequilibrated system [15-17].

The equations of evolution for the basic macrovariables, Eqs. (8), (15) and (16) consists in the averaging over the nonequilibrium ensemble of Heisenberg equations of motion, that is,

$$\frac{\partial}{\partial t}\nu_q(t) = \mathrm{Tr}\,\{\frac{1}{i\hbar}[\hat{\nu}_q,H]\varrho_\varepsilon(t)\}\,, \tag{A.4a}$$

$$\frac{\partial}{\partial t}\langle a_q|t\rangle = \mathrm{Tr}\,\{\frac{1}{i\hbar}[a_q,H]\varrho_\varepsilon(t)\}\,, \tag{A.4b}$$

$$\frac{\partial}{\partial t}\langle a_q^\dagger|t\rangle = \mathrm{Tr}\,\{\frac{1}{i\hbar}[a_q^\dagger,H]\varrho_\varepsilon(t)\}\,. \tag{A.4c}$$

and $dE_B/dt = 0$ because of the assumption that the system of acoustical vibrations remains constantly in equilibrium with an ideal thermal reservoir at fixed temperature T_0.

The right sides of Eqs. (A.4) have a formidable structure of almost unmanageable proportions. But an appropriate way to handling them is provided by the NESOM-based kinetic theory [16–22]. Details are given in these references, where is shown that in general we can write, for example for Eqs. (A.4a) and (A.4b),

$$\frac{d}{dt}\nu_q(t) = \sum_{n=0}^{\infty} \Omega^{(n)}\{\nu_q(t)|t\} , \tag{A.5}$$

$$\frac{d}{dt}\langle a_q|t\rangle = \sum_{n-0}^{\infty} \Omega^{(n)}\{\langle a_q|t\rangle|t\} , \tag{A.6}$$

where the Ω's for $n \geq 2$ are interpreted as collision operators corresponding to scattering by 2, 3, etc. particles, n is the order of the interaction strength in H' present in $\Omega^{(n)}$, and memory effects are included.

On the other hand, each one of these collision operators can be rewritten in the form of a series of partial collision operators instantaneous in time, and expressed in the form of correlations functions over the auxiliary ensemble characterized by the coarse-grained operator $\bar{\varrho}(t)$, that is

$$\Omega^{(n)}\{\nu_q|t\} = \sum_{m=n}^{\infty} {}_{(n)}J^{(m)}\{\nu_q|t\} , \tag{A.7}$$

and similarly for the case of Eq. (A.6) (Details in [19]). Introducing Eq. (A.7) in Eq. (A.5) their right hand sides consists into a double series of partial collision operators. This still involves extremely complicated calculations, which, however, are greatly simplified when the Markovian limit is taken [19, 50]. We recall that the Markovian approach consists into retaining only memoryless-binary-like collisions, an approximation valid in the weak coupling limit [50–52], which stands in the present case of anharmonic interactions. The correspondig Markov equations retain only the three lowest order contributions $\Omega^{(0)}$, $\Omega^{(1)}$, and ${}_{(2)}J^{(2)}$ in $\Omega^{(2)}$, which are the right-hand sides of Eqs. (8) and (15). We notice that in the present case, ${}_{(2)}J^{(2)}$ simply reduces to the Golden Rule of Quantum Mechanics averaged over the nonequilibrium ensemble.

Appendix B. Schrödinger-Davydov Equation, Eq. (19).

In direct space, after the terms that couple the amplitude $\langle a_q \rangle$ with its conjugate are neglected, what, as noticed in the main text is accomplished using the rotating wave approximation, Eq. (15 takes the form:

$$i\hbar \frac{\partial}{\partial t}\psi(x,t) = -i\sum_q \hbar\omega_q \int \frac{dx'}{L} e^{iq(x-x')}\psi(x',t) - i\hbar\sum_q \Gamma_q \int \frac{dx'}{L} e^{iq(x-x')}\psi(x',t)$$
$$+\sum_{q_1 q_2} R_{q_1 q_2} \int \frac{dx'}{L} \int \frac{dx''}{L} e^{iq_1(x-x')} e^{iq_2(x-x'')} \psi(x',t)\psi(x'',t)\psi^*(x,t), \quad \text{(B.1)}$$

where, we recall, $\omega_q = sq$. Considering that it is expected the formation of a highly localized packet (the soliton), centered in point x and with a Gaussian-like profile with a width, say, w (fixed by the initial condition of excitation) extending along a certain large number of lattice parameter a (i.e. $w \gg a$), in Eq. (A.1) we make the expansion

$$\psi(x',t) \approx \psi(x,t) - \xi \frac{\partial}{\partial x}\psi(x,t), \quad \text{(B.2)}$$

where $\xi = x - x'$ is roughly restricted to be smaller or at most of the order of w. The first term on the right of Eq. (A.1) is

$$-i\sum_q s|q| \int \frac{dx'}{L} e^{iq(x-x')}\psi(x',t) =$$
$$= -\frac{Ls}{2\pi}\frac{\partial}{\partial x}\int_0^{\frac{\pi}{a}} dq \int_0^L \frac{dx'}{L}\left[e^{iq(x-x')} - e^{-iq(x-x')}\right]\psi(x',t)$$
$$\approx -\frac{is}{\pi}\frac{\partial}{\partial x}\int_0^{\frac{\pi}{a}} dq \int_{x-w/2}^{x+w/2} d\xi\, \sin(q\xi)\left[\psi(x,t) - \xi\frac{\partial}{\partial x}\psi(x,t)\right]$$
$$= \frac{is}{\pi}\frac{\partial}{\partial x}\left[\int_{x-\frac{1}{2}w}^{x+\frac{1}{2}w}(1-\cos\frac{\pi}{a}\xi)\,\frac{d\xi}{\xi}\right]\psi(x,t)$$
$$+\frac{is}{\pi}\left[\int_{x-\frac{1}{2}w}^{x+\frac{1}{2}w}(1-\cos\frac{\pi}{a}\xi)\,\frac{d\xi}{\xi}\right]\frac{\partial}{\partial x}\psi(x,t)$$
$$-\frac{is}{\pi}\left[\int_{x-\frac{1}{2}w}^{x+\frac{1}{2}w}(1-\cos\frac{\pi}{a}\xi)\,d\xi\right]\frac{\partial}{\partial x}\psi(x,t)$$

$$-\frac{is}{\pi}\left[\int_{x-\frac{1}{2}w}^{x+\frac{1}{2}w}(1-\cos\frac{\pi}{a}\xi)\,d\xi\right]\frac{\partial^2}{\partial x^2}\psi(x,t)\ . \tag{B.3}$$

But, of the four terms after the last equal sign in this Eq. (A.3), the second and third are null, because of the *Ansatz* that a soliton would follow, since the derivative at the center of the packet is null. Consider now the last term, which after the integrations are performed becomes

$$-\frac{isw}{\pi}[1-\frac{2a}{\pi w}\sin\frac{\pi}{a}\frac{w}{2}\cos\frac{\pi}{a}x]\frac{\partial^2}{\partial x^2}\psi(x,t)\ . \tag{B.4}$$

But, we notice that the width of the packet is $w \gg a$, and the cosine in Eq. (A.4) has a period $2a$, and then it oscillates very many times in w, and with amplitude $(2a/\pi w) \ll 1$, and can be neglected. Similarly, the first term becomes proportional to

$$\frac{is}{\pi}\frac{\psi(x)}{x^2-(w/2)^2}\left\{w\left[1-\cos\left(\frac{\pi x}{a}\right)\cos\left(\frac{\pi w}{2a}\right)\right]-2x\sin\left(\frac{\pi x}{a}\right)\sin\left(\frac{\pi w}{2a}\right)\right\}\ , \tag{B.5}$$

where, on the one hand, the oscillatory terms cancel on average, and, on the other hand, the term decays as x^{-2}. Consequently, using these results in Eq. (B.1), after introducing the notation $(\hbar s w/\pi) = \hbar^2/(2M_s)$, and the local approximation in the second and third term on the right of Eq. (B.1), we find Eq. 19.

BIBLIOGRAPHY

[1] A. C. Scott, F. Y. F. Chu, and D. W. McLaughlin, Proc. IEEE **61**, 1443 (1973).

[2] A. J. Heger, S. Kivelson, J. R. Schrieffer, and W. P. Su, Rev. Mod. Phys. **60**, 781 (1988).

[3] K. Leutwyler, Scientific American **275**(6), 26 (1996).

[4] H. A. Haus, IEEE Spectrum **33**(3), pp. 48 (1996).

[5] D. Marcuse, *Theory of Dielectric Optical Waveguides* (Academic, Boston, 1991), Chap. 9, pp. 335–365.

[6] A. C. Scott, The Sciences (NYAS) **30**(2), 28 (1990).

[7] A. C. Scott, Phys. Rep **217**, 1 (1992).

[8] A. C. Scott, I. J. Bigio, and C. T. Johnston, Phys. Rev. B **39**, 12883 (1989).

[9] A. Hobson, J. Chem. Phys. **45**, 1352 (1966).

[10] L. S. Garcia-Colin, A. R. Vasconcellos, and R. Luzzi, J. Non-Equilib. Thermodyn. **19**, 24 (1994); R. Luzzi, A. R. Vasconcellos, and J. G. Ramos, Fortschr. Phys./Prog. Phys., in press; *Statistical Foundations of Irreversible Thermodynamics,* intended for Texte zur Physik series, W. Ebeling, Ed. (Teubner, Berlin).

[11] R. Luzzi and A. R. Vasconcellos, Physica A **241**, 677 (1997).

[12] R. Luzzi, A. R. Vasconcellos, D. Jou, and J. Casas-Vazquez, J. Chem. Phys. **107**, 7383 (1997).

[13] R. Luzzi, A. R. Vasconcellos, and J. G. Ramos, Fort. Phys./Prog. Phys. , in press.

[14] M. A. Tenan, A. R. Vasconcellos, and R. Luzzi, Fortschr. Phys./Prog. Phys. **45**, 1 (1997).

[15] R. Luzzi and A. R. Vasconcellos, Fortschr. Phys./Prog. Phys. **38**, 887 (1990); R. Luzzi, A. R. Vasconcellos, and J. G. Ramos, *Foundations of a Nonequilibrium Statistical Ensemble Formalism,* intended for Fundamental Theories of Physics Series, A. van der Merwe, Ed. (Kluwer Academics, Dordrecht).

[16] D. N. Zubarev, *Nonequilibrium Statistical Thermodynamics* (Consultants Bureau, New York, 1974), [*Neravnovesnaia Statisticheskaia Termodinamika* (Izd. Nauka, Moscow, 1971)].

[17] D. N. Zubarev, V. N. Morozov, and G. Röpke, *Statistical Mechanics of Nonequilibrium Processes. Vol. 1: Basic Concepts, Kinetic Theory; Vol. 2: Relaxation and Hydrodynamic Processes* (Akademie Verlag, Berlin, 1996 and 1997 respectively).

[18] A. I. Akhiezer and S. V. Peletminskii, *Methods of Statistical Physics* (Pergamon, Oxford, 1981).

[19] L. Lauck, A. R. Vasconcellos, and R. Luzzi, Physica A **168**, 789 (1990).

[20] J. R. Madureira, A. R. Vasconcellos, R. Luzzi, J. Casas-Vazquez, and D. Jou, J. Chem. Phys. **108**, 7568 (1998); ibid. **108**, 7580 (1998).

[21] J. R. Madureira, A. R. Vasconcellos, and R. Luzzi J. Chem. Phys., **109**, 2099 (1998).

[22] J. G. Ramos, A. R. Vasconcellos, and R. Luzzi, Fortschr. Phys./Prog. Phys. **43**, 265 (1995).

[23] M. V. Mesquita, A. R. Vasconcellos, and R. Luzzi, Phys. Rev. E **48**, 4049 (1993).

[24] M. V. Mesquita, A. R. Vasconcellos, and R. Luzzi, Int. J. Quantum Chem. **60**, 689 (1996).

[25] A. S. Davydov, in *Solitons,* edited by S. E. Trullinger, V. E. Zakharov, and V. L. Prokovsky (Elsevier, New York, 1986), Chap. 1, pp. 1–51.

[26] A. S. Davydov, *Biology and Quantum Mechanics* (Pergamon, Oxford, 1982); also P. L. Christiansen and A. C. Scott (Eds.), *Davydov's Soliton Revisited* (Plenum, New York, 1990).

[27] H. Haken, *Handbuch der Physik XXV/2C* (Springer, Berlin, 1970).

[28] A. R. Vasconcellos, M. V. Mesquita, and R. Luzzi, Phys. Rev. Lett. **80**, 2008 (1998).

[29] G. Careri, U. Buotempo, R. Carta, E. Gratton, and A. C. Scott, Phys. Rev. Lett. **51**, 304 (1983).

[30] K. Valyasek, D. N. Zubarev, and A. L. Kuzemskii, Theor. Math. Phys. (USSR) **5**, 2 (1971).

[31] V. E. Zakharov, in *Solitons*, edited by R. K. Bullough and P. J. Caudrey (Springer, Berlin, 1980), Chap. 7, pp. 243-285.

[32] H. Fröhlich, Nature **228**, 1093 (1970); in *Advances in Electronics and Electron Physics* (Academic Press, New York, 1980), Vol. 17, pp. 85-152.

[33] P. T. Landsberg, J. Phys. C: Solid State Phys. **14**, L1025 (1981).

[34] A. C. Algarte, A. R. Vasconcellos, and R. Luzzi, Phys. Status Solidi (B) **173**, 487 (1992).

[35] A. C. Algarte, A. R. Vasconcellos, and R. Luzzi, Braz. J. Phys. **26**, 543 (1996).

[36] D. Kim and P. Y. Yu, Phys. Rev. Lett. **64**, 946 (1990).

[37] V. L. Ginsburg, Soviet Phys.-Uspekhi **2**, 874 (1960).

[38] V. M. Agranovich and V. L. Ginsburg, *Spatial Dispersion in Crystal Optics and the Theory of Excitons* (Wiley-Interscience, London, 1966).

[39] J. Lu and J. F. Greenleaf, IEEE Trans. Ultrason. Ferroelect. Freq. Contr. **39**, 19 (1992).

[40] W. A. Rodrigues and J. Lu, Found. Phys. **27**, 435 (1997), we thank W. A. Rodrigues and J. A. Majorino for providing us with a postscript file of Fig. 7.

304.

[41] J. Lu and J. F. Greenleaf, IEEE Trans. Ultrason. Ferroelect. Freq. Contr. **39**, 441 (1992).

[42] Y. R. Shen, Science **276**, 1520 (1997).

[43] A. W. Snyder and D. J. Mitchell, Science **276**, 1538 (1997).

[44] M. V. Mesquita, A. R. Vasconcellos, and R. Luzzi, J. Biol. Phys., submitted.

[45] A. R. Vasconcellos, R. Luzzi, and A. S. Esperidião, Phys. Rev. B **52**, 5021 (1995).

[46] S. A. Hassan, A. R. Vasconcellos, and R. Luzzi, Solid State Commun. **66**, 177 (1998).

[47] D. Snoke, Science **273**, 1351 (1996).

[48] A. Mysyrowicz, E. Benson, and E. Fortin, Phys. Rev. Lett. **77**, 896 (1996).

[49] A. R. Vasconcellos, M. V. Mesquita, and R. Luzzi, Phys. Rev. Letters, submitted.

[50] J. R. Madureira, L. Lauck, A. R. Vasconcellos, and R. Luzzi, Phys. Rev. E **57**, 3637 (1998).

[51] J. R. Madureira, Phys. Rev. E , submitted.

[52] E. B. Davies, Commun. Math. Phys. **34**, 91 (1974).

FIGURE CAPTIONS

Figure 1: The infrared absorption spectrum of acetanilide in the frequency range of the CO-stretching mode, showing the normal band and a red-shifted one adjudicated to the soliton. After reference [28]: full line is the calculation in NESOM and the dots are experimental points taken from reference [29].

Figure 2: Populations of the three relevant modes in the set—as described in the main text–, with increasing values of the intensity of the external source pumping modes labeled 2 and 3 in the ultrasonic region.

Figure 3: The reciprocal of the lifetime of the modes whose population is shown in Fig. 2.

Figure 4: The quasi-chemical potential of the modes labeled 1 to 3 in Fig. 2, with mode 1 corresponding to the one with the lowest frequency in the given set: It is evident the emergence of a "Bose-Einstein-like condensation" for S approaching a critical value of the order of 10^{19}.

Figure 5: The population in the steady state for a pumping intensity $S = 10^{23}$, of the modes along the spectrum of frequencies of the acoustic modes. Dots indicate the modes in the first set (the remaining part of the spectrum up to the highest Brillouin frequency $\omega_B = 9.5 \times 10^{11}$ Hz has been omitted).

Figure 6: The quasi-temperature, defined in Eq. (25), for the modes in Fig. 2.

Figure 7: Excited normal sound wave (upper figure), and the undistorted progressive X-wave (lower figure) [40].

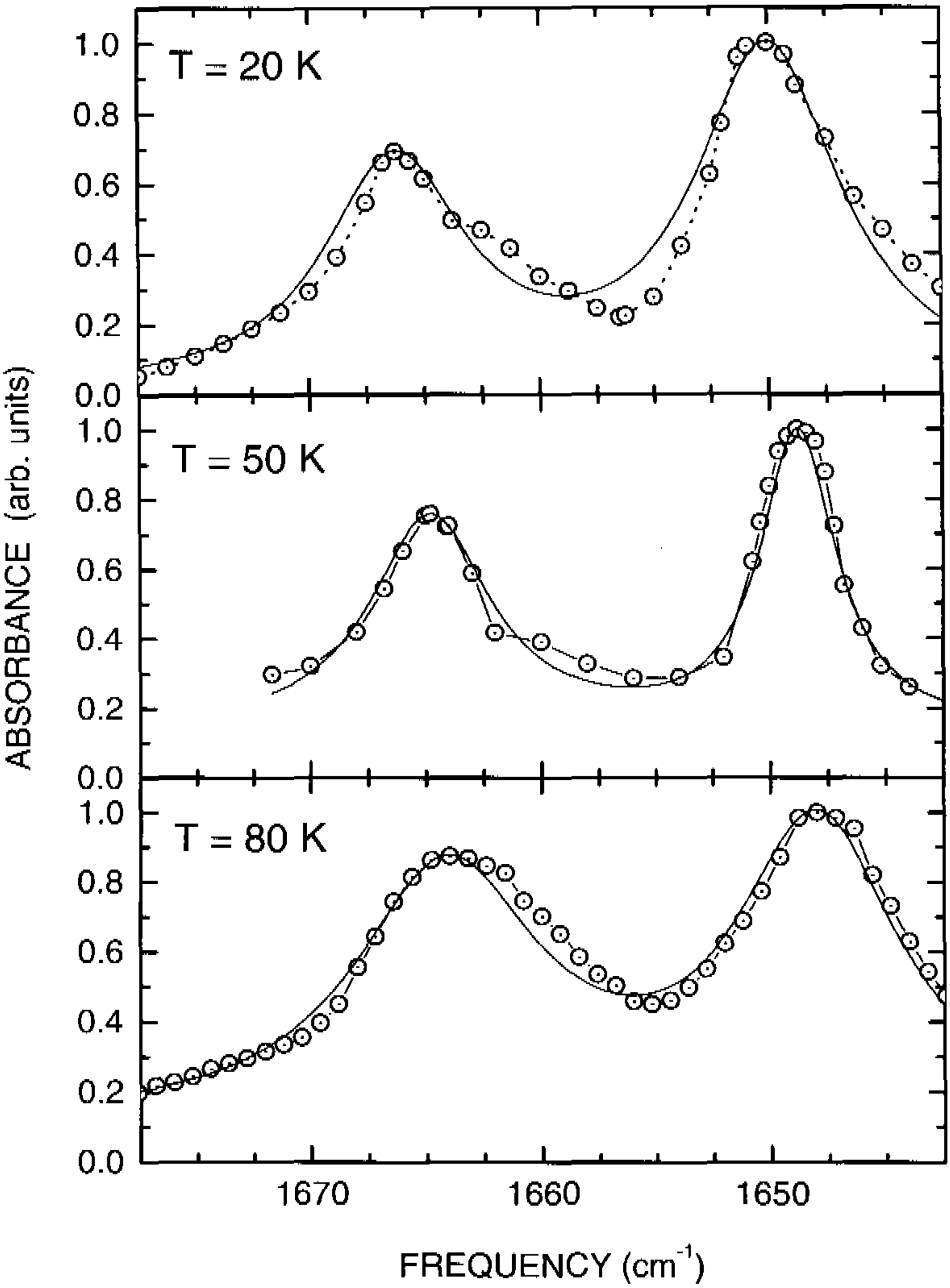

Figure 1: The infrared absorption spectrum of acetanilide in the frequency range of the CO-stretching mode, showing the normal band and a red-shifted one adjudicated to the soliton. After reference [28]: full line is the calculation in NESOM and the dots are experimental points from reference [29].

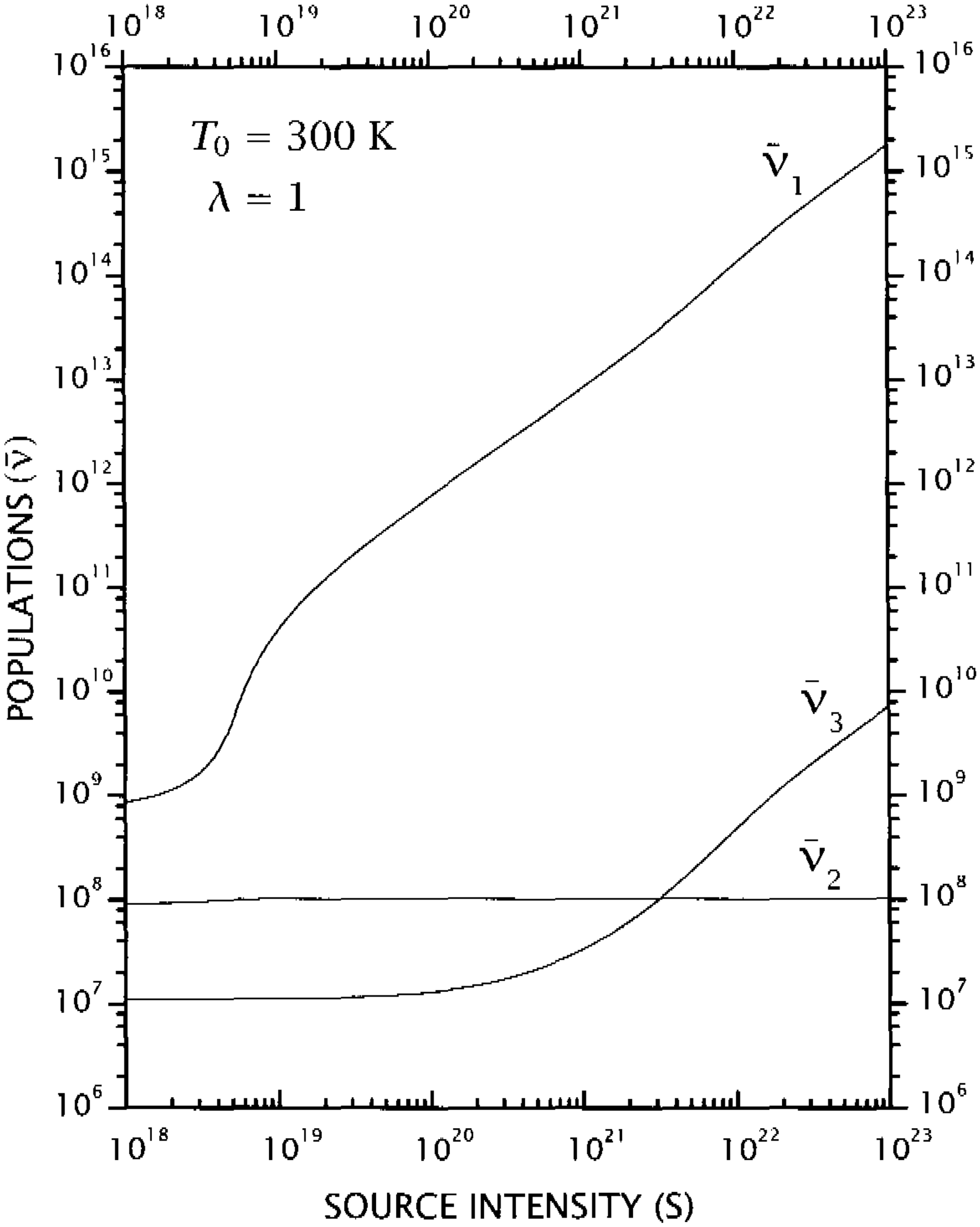

Figure 2: The steady state populations of the three relevant modes in the set — as described in the main text —, with increasing values of the intensity of the external source pumping modes labeled 2 and 3 in the ultrasonic region.

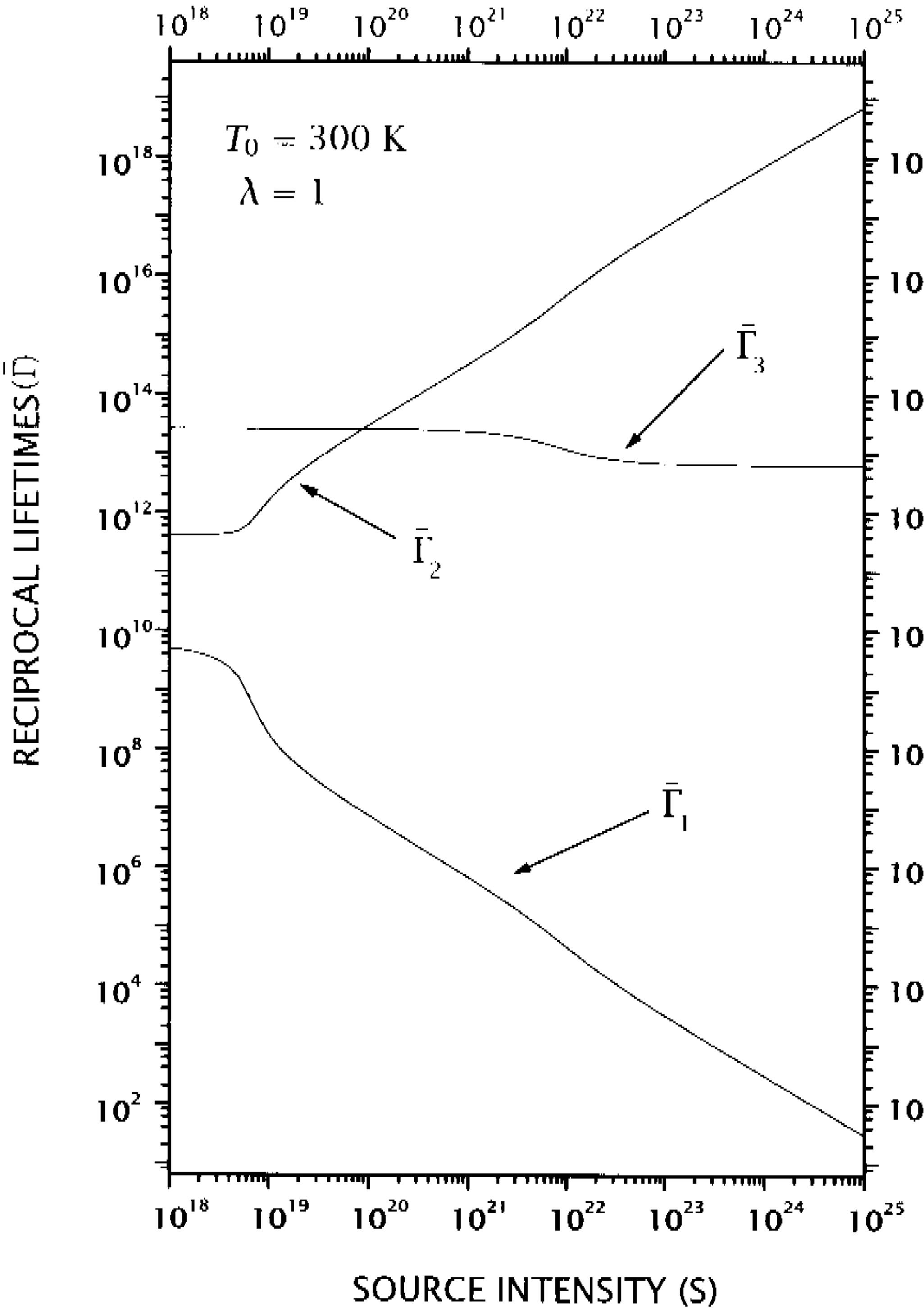

Figure 3: The reciprocal of the lifetime of the modes whose populations are shown in Fig. 2 (multiplied by the scaling time $\bar{\tau} \simeq 0.17$ s, $\bar{\Gamma} = \Gamma\bar{\tau}$).

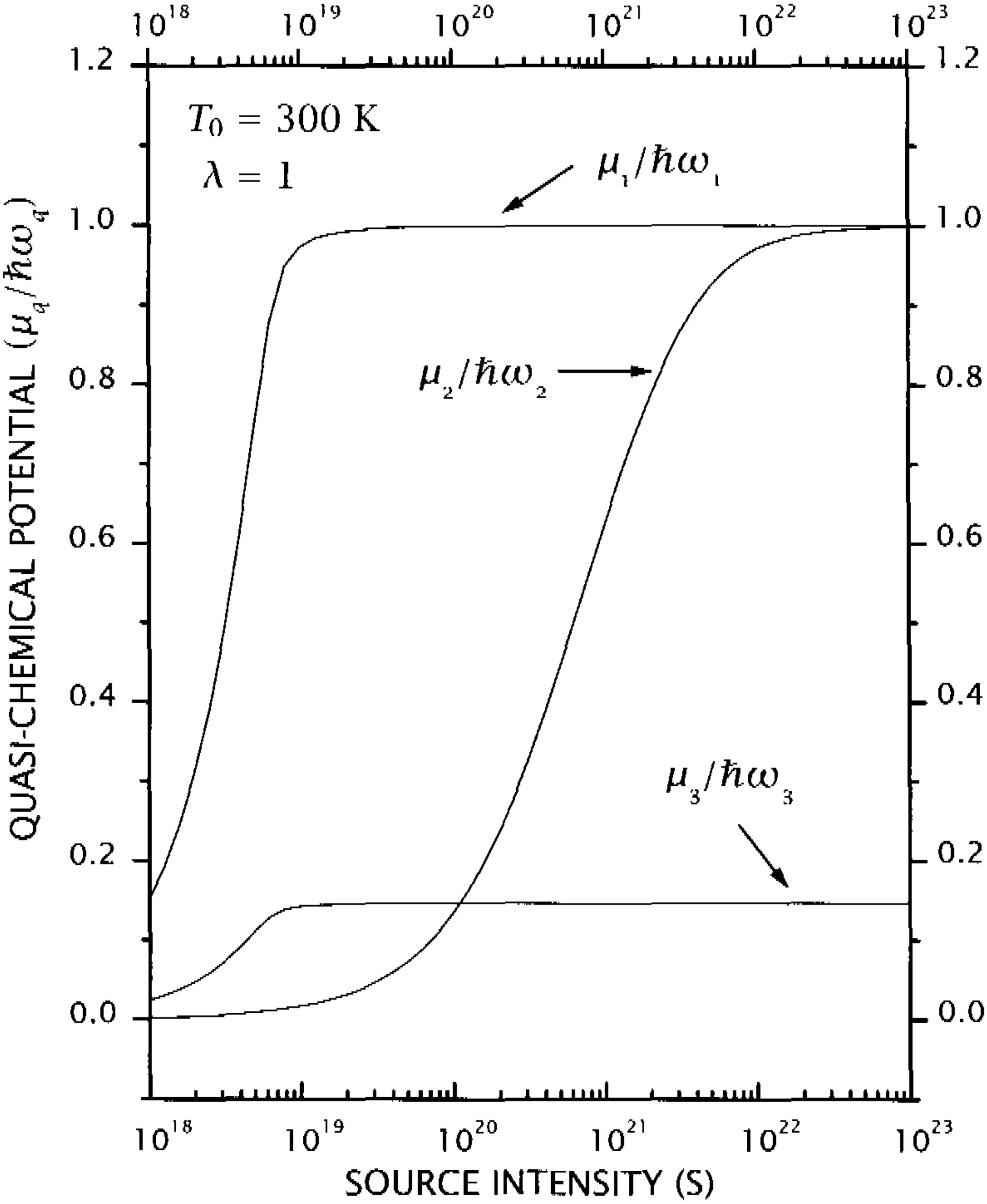

Figure 4: The quasi-chemical potential of the modes labeled 1 to 3 in Fig. 2, with mode 1 corresponding to the one with the lowest frequency in the given set: It is evident the emergence of a "Bose-Einstein-like condensation" for S approaching a critical value of the order of 10^{19}.

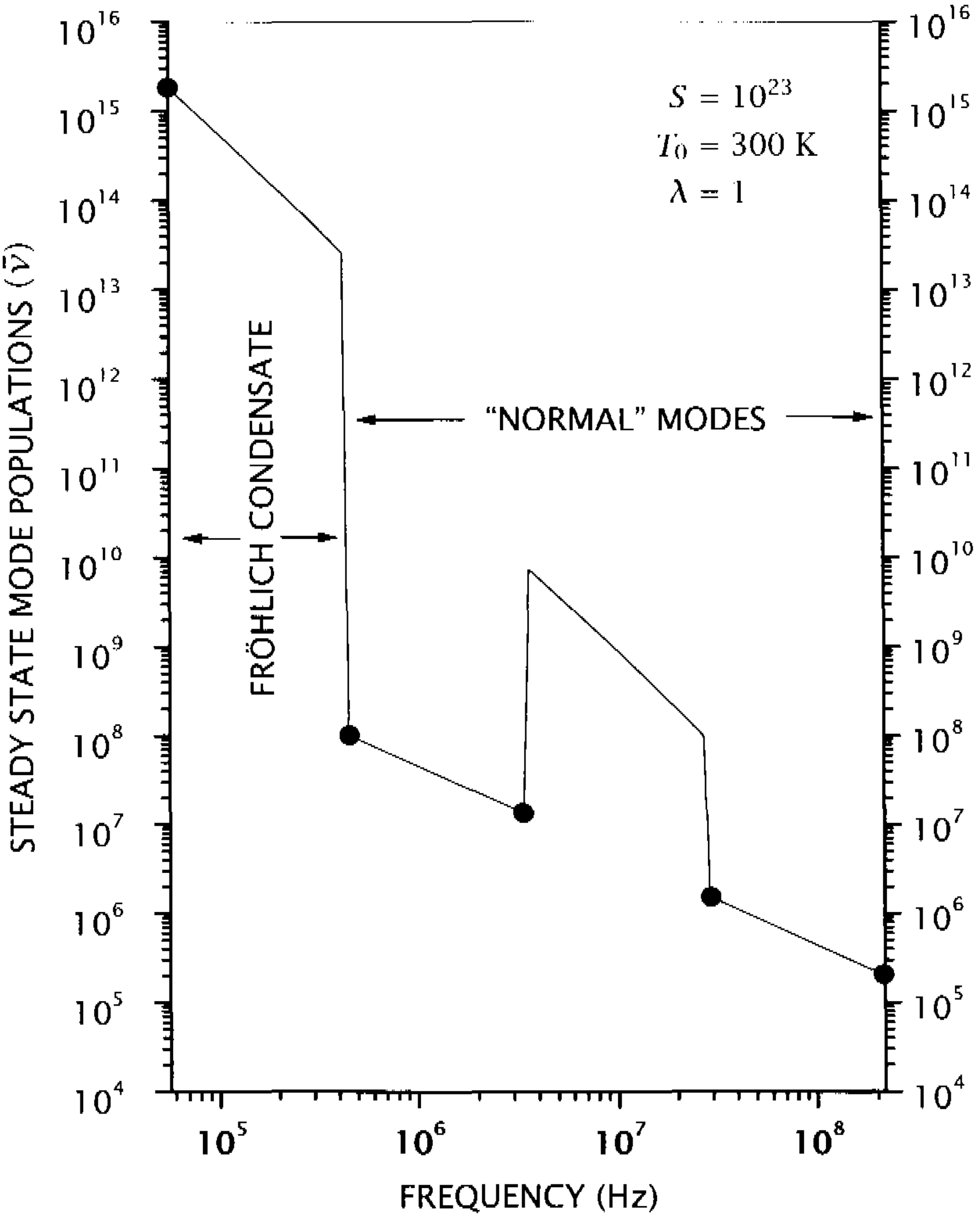

Figure 5: The population in the steady state for a pumping intensity $S = 10^{23}$ of the modes along the spectrum of frequencies of the acoustic modes. Dots indicate modes in the first set (the remaining part of the spectrum up to the highest Brillouin frequency $\omega_B = 9.5 \times 10^{11}$ Hz has been omitted).

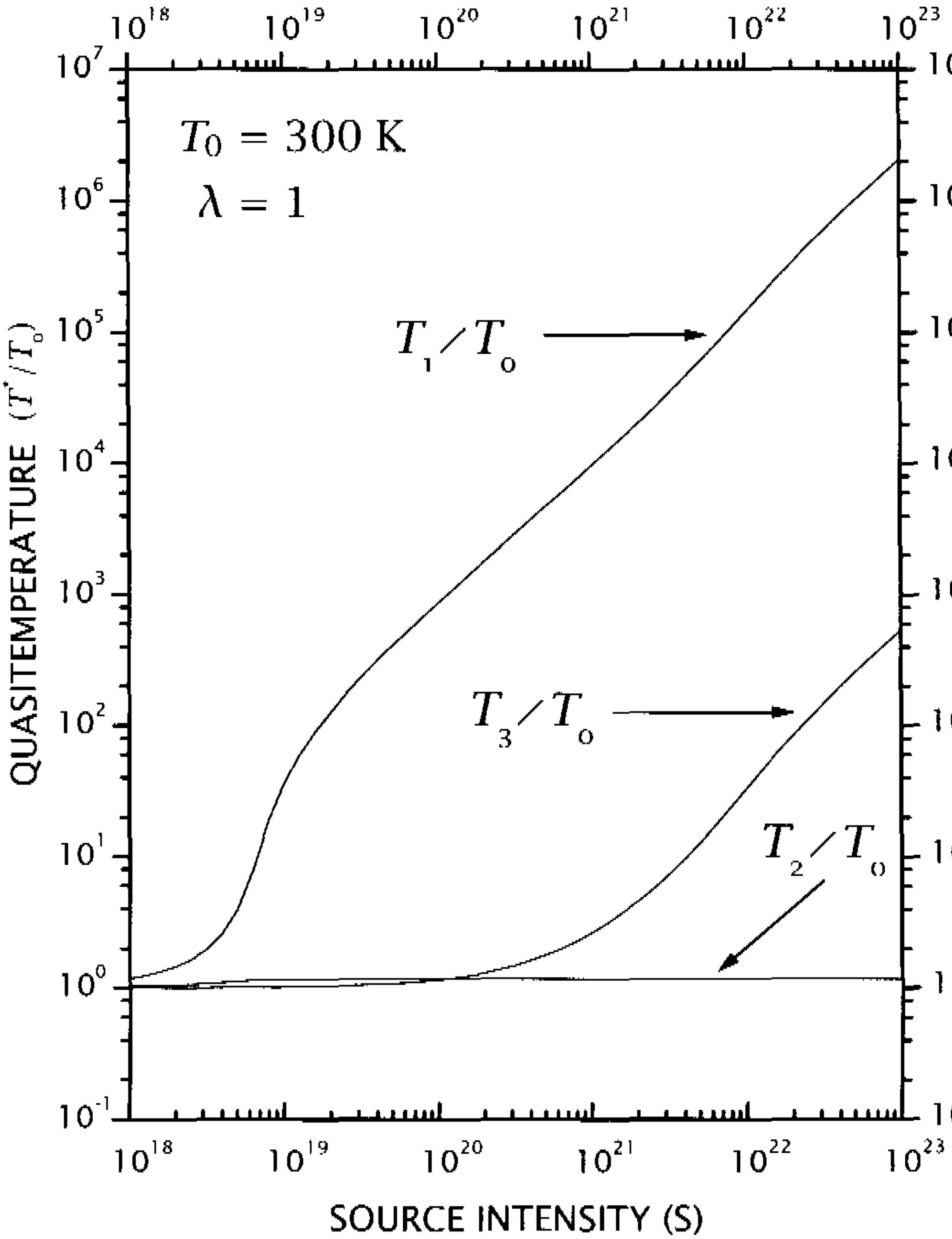

Figure 6: The quasi-temperature, defined in Eq. (25), for the modes in Fig. 2.

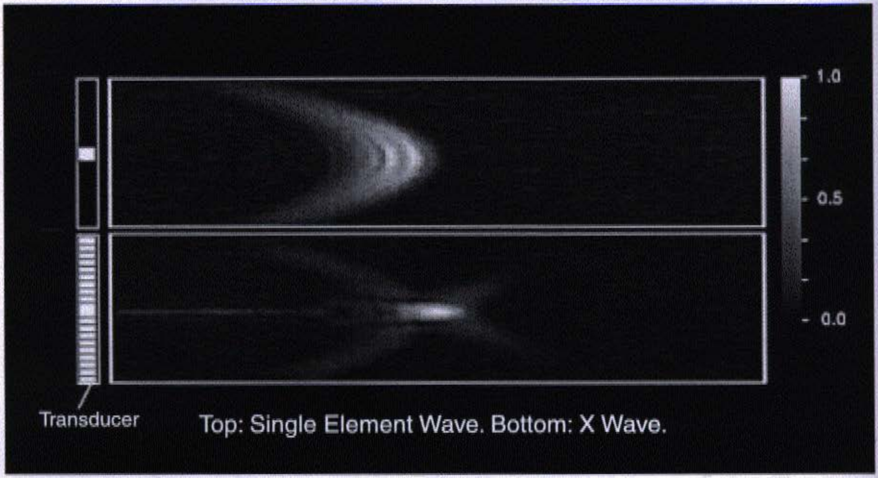

Figure 7: Excited normal sound wave (upper figure), and the undistorted progressive X-wave (lower figure) [40].

5.3 Amplificação estimulada e propagação de feixe de éxcitons

É apresentada uma teoria termodinâmica estatística do fenômeno de amplificação estimulada das populações de éxciton que estão no fundo de sua banda de energia mais baixa. Ele constitui um caso particular do *efeito Fröhlich*. Além disso, a não-linearidade nas equações também é responsável pelos efeitos dinâmicos de propagação de sólitons de Schrödinger-Davydov e de um conjecturável *efeito Cherenkov*. Mostra-se que o "pacote" de éxcitons detectado experimentalmente, fluindo balisticamente, consiste em tal onda solitária, revestida com um nuvem de éxcitons incoerentes.

Submetido para publicação em *Physical Review Letters*.

Stimulated Amplification and Propagation of Excitons' Beams

Áurea R. Vasconcellos, Marcus V. Mesquita, Roberto Luzzi

Instituto de Física 'Gleb Wataghin',
Universidade Estadual de Campinas, Unicamp
13083-970 Campinas, São Paulo, Brazil

It is presented a statistical-thermodynamic theory of the phenomenon of stimulated amplification of the population of excitons which lie at the bottom of their lowest energy band. The experimentally detected “packet” of excitons flowing ballistically is shown to consist of a Schrödinger-Davydov solitary wave, dressed with a cloud of incoherent excitons. Moreover, a secondary excitation by a c.w. laser beam promotes a Fröhlich-Bose-Einstein-like condensation, which is responsible for the relevant phenomenon that the lifetime of the soliton is largely increased with increasing pumping power.

Group Home Page: http://www.ifi.unicamp.br/~aurea

Recently it has been evidenced the phenomenon of stimulated amplification of low-energy exciton populations (SALEEP for short in what follows; the term ‘excitoner’ or ‘beamer’ has also been coined for this phenomenon on the basis of the resulting amplification of a cloud of coherent excitons using random excitons, much as a laser beam can be amplified with incoherent photons) [1, 2]. The experiment consists in that a laser beam pulse incident on the sample front produces a gas of excitons, a c.w. laser pumps energy on this photoinjected excitons, and a packet of them is detected on the other side of the platelet. We proceed with a theoretical analysis of the phenomenon on the basis of a nonequilibrium ensemble formalism for statistical thermodynamics (dubbed MaxEnt-NESOM), and we resort to Zubarev’s approach [3–5]. It is shown that the signal is consistent with the propagation of a weakly damped Schrödinger-Davydov soliton dressed with a cloud of incoherent excitons. Moreover, the nonlinearities that are responsible for the formation of the soliton are also responsible for the manifestation of what we call *Fröhlich effect* [6], sometimes referred to as a Bose-Einstein condensation in nonequilibrium phases a misleading name which we avoid introducing the former thus recognizing the contribution of the renowned late Herbert Fröhlich [7]. For the case of excitons Fröhlich model seems to have been firstly adapted by Duffield [8], and later on by Tikhodeev [9] and Imamoglu *et al.* [10].

An explanation of the phenomena on the basis of solitary wave propagation has been considered by Mysyrowicz *et al.* [2]. But they are disregarding dissipative effects which rapidly would damp out the excitation. This is not what is observed in the experiment, which also shows an increase of amplitude and narrowing band width with increasing intensity of the c.w. pumping source.

Our point, as we demonstrate below, is that a Schrödinger-Davydov soliton propagating in Fröhlich condensate has its lifetime greatly increased as a result of the nonlinear kinetics which is the same responsible for Fröhlich effect and soliton formation, a phenomenon of large relevance for eventual technological application of the ‘excitoner’.

The Hamiltonian which describes this system is composed of the energy operator for the exciton gas, the lowest exciton state ($n = 1$) is considered and the exciton energy dispersion relation is $E_{1k} = -R_y^x + \hbar^2 k^2/2M$, with R_y^x being the excitonic Rydberg (=150 meV in Cu_2O), $\boldsymbol{k}$ runs over the Brillouin zone, M is the mass of the exciton ($\simeq 2.7m_0$ in Cu_2O) and zero of energy is at the bottom of the conduction band. The exciton gas produced by the exciting ultrashort beam interacts with the lattice (exciton-phonon interaction), and differently to the case of free carriers, the interaction with optical phonons can be disconsidered in comparison with the one associated with the acoustical phonons [11], the one we introduce: formally this contribution is the same as given in [12] once excitons enter in place of the polar vibrations. It is also included the interaction with the electromagnetic field of the c.w. laser and the one associated to spontaneous recombination effects (luminescense) [11]. Other interactions leading to relaxation effects are incorporated in the kinetic equations on a phenomenological basis. Once the Hamiltonian has been defined we need to introduce the statistical thermodynamic level of description, what we do — as noticed — resorting to MaxEnt-NESOM. The first fundamental step is the choice of the relevant macrovariables (or mesovariables in this case) for the description of the nonequilibrium thermodynamic state of the system. In analogy with the case in [12] we introduce the time-dependent exciton populations which we call $\nu_k(t)$, and the energy of the acoustic phonons $\mathcal{E}_B(t)$ (B for bath) with these phonons assumed to constantly remain in equilibrium with an external reservoir at temperature T_0 (2 K in the experiment of Ref. [2]), and then $\mathcal{E}_B$ is time independent. The accompanying intensive nonequilibrium thermodynamic variables (Lagrange multipliers in the variational approach to MaxEnt-NESOM [4, 5]) are designated by $F_k(t)$ and $\beta_0 = (k_B T_0)^{-1}$ respectively, the latter being the reciprocal of the reservoir temperature since the thermal bath is described by a canonical distribution in equilibrium. Variables ν_k and F_k are connected, once the corresponding calculations in MaxEnt-NESOM are performed, by the expression

$$\nu_k(t) = [\exp\{F_k(t)\} - 1]^{-1} . \tag{1}$$

Alternatively, the intensive thermodynamic variable $F_k(t)$ can be rewritten in either of two forms, one is $F_k(t) = E_{1k}/k_B T_k^*(t)$, introducing the so-called quasi-temperature

$T_{\mathbf{k}}^{*}$ for each state $|\mathbf{k}\rangle$, as it is done for phonons in semiconductors physics [13], and the other is $F_{\mathbf{k}}(t) = [E_{1\mathbf{k}} - \mu_{\mathbf{k}}(t)]/k_B T_0$, introducing a quasi-chemical potential $\mu_{\mathbf{k}}(t)$ for each state $|\mathbf{k}\rangle$, as proposed, for example, by H. Fröhlich [6] and P. T. Landsberg [14].

The equations of evolution for the mesoscopic variables $\nu_{\mathbf{k}}(t)$ are calculated in the MaxEnt-NESOM-based kinetic theory [3–5, 15], and since the interactions are weak the Markovian approximation is used [16]. They are quite similar to those in [12]. Without going into details we notice the quite relevant result that, once the steady state (ss) has been achieved (under the action of a constant pumping source), the populations are given by

$$\nu_{\mathbf{k}}^{(ss)} = \mathcal{N}_{\mathbf{k}}/\Gamma_{\mathbf{k}} \,, \tag{2}$$

where

$$\begin{aligned}\Gamma_{\mathbf{k}} = {} & \frac{1}{2}\tau_{\mathbf{k}}^{-1} + \frac{4\pi}{\hbar^2}\sum_{\mathbf{k}'} |V_{\mathbf{k}\mathbf{k}'}^{(2)}|^2 [1 + \nu_{\mathbf{k}-\mathbf{k}'}^{B} + \nu_{\mathbf{k}'}]\delta(\Omega_{\mathbf{k}-\mathbf{k}'} + \omega_{\mathbf{k}'} - \omega_{\mathbf{k}}) \\ & + \frac{4\pi}{\hbar^2}\sum_{\mathbf{k}'} |V_{\mathbf{k}\mathbf{k}'}^{(2)}|^2 [\nu_{\mathbf{k}-\mathbf{k}'}^{B} - \nu_{\mathbf{k}'}]\delta(\Omega_{\mathbf{k}-\mathbf{k}'} - \omega_{\mathbf{k}'} + \omega_{\mathbf{k}}) \\ & - \frac{4\pi}{\hbar^2}\sum_{\mathbf{k}'} |V_{\mathbf{k}\mathbf{k}'}^{(2)}|^2 [\nu_{\mathbf{k}-\mathbf{k}'}^{B} - \nu_{\mathbf{k}'}]\delta(\Omega_{\mathbf{k}+\mathbf{k}'} - \omega_{\mathbf{k}'} - \omega_{\mathbf{k}})\end{aligned} \tag{3}$$

In Eq. (3) $\tau_{\mathbf{k}}$ is the relaxation time due to exciton-phonon collisions (see [12]), and $V^{(2)}$ the matrix element of the interaction of one phonon with two excitons (we noticed that $\tau_{\mathbf{k}}$ is associated to the interaction of one exciton with two phonons). The cumbersome expression for $\mathcal{N}_{\mathbf{K}}$ is omitted, since it is not relevant for the analysis in continuation.

It follows that the population of the states lowest in energy are largely enhanced, that is, for them $\Gamma_{\mathbf{k}}$ largely decreases, and for this characteristic the phenomenon sometimes has been called a Bose-Einstein-like condensation. Next we illustrate numerically these results using parameters characteristic of Cu_2O, and the conditions of the experiment in Ref. [2].

Front sample is illuminated with a laser pulse with $\lambda = 532$ nm, 10 ns duration, and intensity ≈ 6.3 MW cm^{-2}; it is imposed illumination by a c.w. laser with $\lambda =$

605.4 nm, and 4 W cm^{-2} of intensity (at this wavelength the absorption coefficient is roughly 30 cm^{-1}). We also use for the mass of the exciton $M = 2.7m_0$, a static dielectric constant $\epsilon_0 = 10$ and the optical one $\epsilon_\infty = 4$. Moreover, we consider a nearly wavevector independent relaxation time resulting from exciton-phonon interaction, i.e. $\bar{\tau}_{\boldsymbol{k}} \equiv \bar{\tau}$, which is used as a scaling parameter defining a scaled time $\tilde{t} = t/\bar{\tau}$.

Figure 1 shows two characteristic populations in the steady state depending on the intensity $S = I\bar{\tau}$ of the source, which we take as equal for each exciton state, We recall that I times the excitonic Rydberg is a fraction — determined by the absorption coefficient — of the intensity 4 W cm^{-2} of the pumping c.w. laser. The mode labelled with index nought corresponds to a low-lying-in-energy exciton, and index one for an exciton higher in energy. In the inset is described the evolution of the quasi-chemical potential associated to ν_0, which we have written as $\mu_0^x = \mu_0 - R_y^x$.

We can notice that the quasi-chemical potential never coincides with the energy of the exciton state, i.e. μ_0^x is always negative and different from zero, but tends asymptotically to this value as the pumping intensity tends to infinity; hence a, say, Bose-Einstein-like condensation does not occur. We stress that what emerges is a large amplification of the populations over a certain region of the exciton states low in energy, contituting the so-called *Fröhlich condensate.* It is worth noticing that we can see the presence of a kind of "two-fluid system": excitons in the Fröhlich condensate (a "superphase") and incoherents excitons in a "normal phase", similarly to the situation shown by Fig. 7 in [12].

Let us next go over the formation of the Schrödinger-Davydov soliton. Again, in MaxEnt-NESOM and the Markovian approach, the creation, $a_{\boldsymbol{k}}$, and annihilation, $a_{\boldsymbol{k}}^\dagger$, operators in exciton states $|\boldsymbol{k}\rangle$, averaged over the nonequilibrium ensemble, and denoted by $\langle a_{\boldsymbol{k}}|t\rangle$ and $\langle a_{\boldsymbol{k}}^\dagger|t\rangle = \langle a_{\boldsymbol{k}}|t\rangle^*$, satisfy the equations

$$\frac{d}{dt}\langle a_{\boldsymbol{k}}|t\rangle = -\mathrm{i}\tilde{\omega}_{\boldsymbol{k}}\langle a_{\boldsymbol{k}}|t\rangle - \Gamma_{\boldsymbol{k}}\langle a_{\boldsymbol{k}}|t\rangle - \mathrm{i}W_{\boldsymbol{k}}\langle a_{\boldsymbol{k}}|t\rangle^* + \\ + \Gamma_{\boldsymbol{k}}\langle a_{\boldsymbol{k}}|t\rangle^* + \sum_{\boldsymbol{k}_1\boldsymbol{k}_2}\left[R_{\boldsymbol{k}_1\boldsymbol{k}_2}\langle a_{\boldsymbol{k}_1}|t\rangle\langle a_{\boldsymbol{k}_2}|t\rangle\langle a_{\boldsymbol{k}_1+\boldsymbol{k}_2-\boldsymbol{k}}|t\rangle^* + \text{c.c.}\right], \quad (4)$$

and the equation for $\langle a_{\boldsymbol{k}}^\dagger|t\rangle$ is the complex conjugated of this. In Eq. (4) $\Gamma_{\boldsymbol{k}}(t)$ is the quantity which in the steady state is given by Eq. (3), which, clearly, is the reciprocal of a relaxation time; W_k is a frequency renormalization factor which is disconsidered; and $R_{kk'}$ is the strength of the trilinear term (we do not give its cumbersome expression which is not explicitly used in what follows).

Once the populations have achieved a steady state, the reciprocal lifetimes for the two states of Fig. 1 are shown in Fig. 2 for increasing values of the intensity of the pumping source. This clearly tells us that the states lowest in energy tend to have a long-lived amplitude $\langle a_q|t\rangle$. To proceed further in the equation for this amplitude we neglect the linear terms in its conjugate; this can also be obtained from the start if one introduces the so-called rotating wave approximation (RWA), as it is done in laser theory [17]. For linear propagation, as in Ref. [2], we introduce the amplitude field in an onedimensional continuum model, namely

$$\psi(x,t) = \sum_k \langle a_k|t\rangle e^{ikx} \,. \tag{5}$$

where x is the direction of propagation of the excitons' beam.

Using Eq. (4) in RWA, we obtain that $\psi(x,t)$ satisfies the equation:

$$\begin{aligned} i\hbar\frac{\partial}{\partial t}\psi(x,t) &= \frac{\hbar^2}{2M_s}\frac{\partial^2}{\partial x^2}\psi(x,t) - i\hbar\int_0^L \frac{dx'}{L}\,\Gamma(x-x')\psi(x',t) + \\ &\quad + \int_0^L \frac{dx'}{L}\int_0^L \frac{dx''}{L}\,\mathcal{R}(x-x',x-x'')\psi(x',t)\psi(x'',t)\psi^*(x,t), \end{aligned} \tag{6}$$

where Γ and $\mathcal{R}$ are the expressions in direct space of the corresponding quantities in Eq. (4). Proceeding on the Ansatz that a narrow solitary wave is to follow, we introduce a local-in-space approximation, by writing $\Gamma(x-x') = \gamma_s\delta(x-x')$, $R(x-x',x-x'') = G_s\delta(x-x')\delta(x-x'')$

$$i\frac{\partial}{\partial t}\psi(x,t) + \frac{\hbar}{2M_s}\frac{\partial^2}{\partial x^2}\psi(x,t) + i\gamma_s\psi(x,t) - G_s|\psi(x,t)|^2\psi(x,t) = 0 \tag{7}$$

Using the inverse scattering method we obtain the solution of this equation, which is:

$$\psi(x,t) = \mathcal{A}\exp\{\mathrm{i}[\kappa x - (\omega_s - \mathrm{i}\gamma_s)t] - \theta/2\}\mathrm{sech}\,[W(\kappa x - vt)]\ , \tag{8}$$

where $\mathcal{A}$ is the amplitude; $\omega_s = \mathcal{A}^2|G_s|/2 - \kappa v_s/4$ is the frequency; v is the velocity of propagation; γ_s is the damping coefficient; $\kappa = Mv_s/\hbar$ is the wavenumber; $W = [\mathcal{A}^2 M|G|/\hbar]^{1/2}$, and $G = |G|e^{i\theta}$ is the nonlinear coupling strength, in complete analogy with the acoustic-phonon-composed solution reported in [18]; $\mathcal{A}$ and v are determined by the energy and momentum transferred by the impinging exciting photons.

But in Eq. (5), as shown, the amplitudes corresponding to the states higher in frequency decay very rapidly – typically in the subpicosecond scale —, while the amplitudes associated to the states lowest in energy have long lifetimes. Thus, after a very rapid transient, the quantity $\psi(x,t)$ is formed by the latter type of coherent excitons, and γ_s is very small. Inspection of Fig. (2) indicates that it goes to zero as the amplitude of the excitation goes to infinity.

Using Eq. (8) for the case in Ref. [2], and that Wv_s is of the order of the width of the signal which is roughly 20.8 μs^{-1}, and taking $\mathcal{A} \simeq 0.87$, the strength in the nonlinear terms responsible for Fröhlich and Davydov phenomena can be estimated to be $|G| \approx 2000\ s^{-1}$. We stress that the just described behavior of the system follows for a weak nonlinear kinetic term coupling excitons and thermal bath; this coupling strength and the amplitude of the signal are the only open parameters fixed by best fitting.

These results then indicate that *the packet of excitons flowing ballistically from the condensate* (in Ref. [2] with a velocity of roughly 4.5×10^5 cm/s) *is an exciton-composed Schrödinger-Davydov soliton.* This is something similar to what is the case in conducting polymers [19] when it is composed of carriers and in optical fibers [20] when is composed of photons. This is reinforced by the fact that the larger amplitude of the signal when the c.w. laser is present, as compared with the one in its absence as reported in Ref. [2], is consistent with the result that the lifetime of the soliton is increased with increasing levels of excitation [21,22]. Moreover, it can be shown that the profile of the signal in Ref. [2] is well fitted by the squared hyperbolic secant of Eq. (8) characteristic of Schrödinger-Davydov soliton [23], as shown in Fig. 3. To draw the full line — the theoretical calculation — we have taken into account that the registered signal is composed of the solitary wave formed by the coherent excitons plus the contribution of an accompanying cloud of incoherent excitons. The former, as noticed, consists of the squared modulus of the Schrödinger-Davydov soliton-field amplitude of Eq. (8); the other is composed by the travelling normal excitons produced in the active region defined by the extinction length of the laser field, of the order of 0.033 cm, and are decaying with a halftime of the order of 0.5 μs. These are the parameters used in the calculation, while the amplitude and width of the solitary wave have been fitted.

Furthermore, we notice, that in [18] it has been shown and verified that in the case when the soliton is composed by vibrational modes propagating with a speed v_s larger than the average one, $\bar{v}$, velocity of the normal vibrational background there follows a kind of Cherenkov effect (two Cherenkov cones, a normal and an anomalous however symmetric in this case) composed, evidently, in that case, of phonons instead of the photons in radiation theory. This effect is apparently evidenced in the case of propagation of solitons involving vibrational modes in experiments with ultrasound waves, the so-called 'X-waves' [24]. Although the excitons are not truly bosons it is conjectured, using the same arguments than in [18], that when the exciton-composed soliton is travelling with a speed larger than that of the incoherent excitons, the latter may be driven preferentially in two Fröhlich-Cherenkov-like symmetrically oposed cones. This is a result that, using Eqs. (2) and (4) it can be obtained that $F_k = (E_{1k} - \mu_{1k})/k_B T \approx (E_{1k}/k_B T)[1 - (\bar{v}/v_s)\cos\theta_{1k}]$, and $\cos\theta_{1k} = (v_s/\bar{v})[1 - \ln(1 + \nu_k^{1})]$.

In conclusion, the phenomenon of stimulated amplification of low-energy exciton populations arises as a result of the propagation of coherent excitons in the form of a long-lived Schrödinger-Davydov soliton. The relevant point, and an important one for eventual technological use, is that the lifetime is largely increased by illuminating the system with an energy pumping-source: this improves the amplitude of the signal, and reduces the width at half-height, as the experimental results show.

As final words, citing D. Snoke [1], the phenomenon may provide a new kind of light source (the 'excitoner'), but only time and imagination can tell what new applications may arise from this novel effect.

REFERENCES

[1] D. Snoke, Science **273**, 1351 (1996).

[2] A. Mysyrowicz, E. Benson, and E. Fortin, Phys. Rev. Lett. **77**, 2844 (1996).

[3] D. N. Zubarev, Fortschr. Phys./Prog. Phys. **18**, 125 (1970).

[4] D. N. Zubarev, V. N. Morozov, and G. Röpke, *Statistical Mechanics of Nonequilibrium Processes. Vol. 1: Basic Concepts, Kinetic Theory; Vol. 2: Relaxation and Hydrodynamic Processes* (Akademie Verlag, Berlin, 1996, 1997).

[5] R. Luzzi and A. R. Vasconcellos, Fortschr. Phys./Prog. Phys. **38**, 887 (1990).

[6] H. Fröhlich, Nature **228**, 1093 (1970).

[7] H. Fröhlich, in *Cooperative Phenomena*, edited by H. HAKEN and M. Wagner (Springer, Berlin, 1973).

[8] N. G. Duffield, Helv. Phys. Acta **3**, 363 (1988).

[9] S. G. Tikhodeev, Solid State Commun. **11**, 1075 (1989).

[10] A. Imamoglu, R. J. Ram, S. Pau, and Y. Yamamoto, Phys. Rev. A **53**, 4250 (1996).

[11] R. S. Knox, in *Theory of Excitons*, edited by F. Seitz and J. Turnbull (Academic Press, New York, 1963), No. Solid State Physics Series, Suppl. 5.

[12] M. V. Mesquita, A. R. Vasconcellos, and R. Luzzi, Phys. Rev. E **48**, 4049 (1993).

[13] D. Kim and P. Y. Yu, Phys. Rev. Lett. **64**, 946 (1990).

[14] P. T. Landsberg, J. Phys. C: Solid State Phys. **14**, L1025 (1981).

[15] A. I. Akhiezer and S. V. Peletminskii, *Methods of Statistical Physics* (Pergamon, Oxford, 1981).

[16] J. R. Madureira, A. R. Vasconcellos, R. Luzzi, and L. Lauck, Phys. Rev. E **57**, 3637 (1998).

[17] H. Haken, *Handbuch der Physik XXV/2C* (Springer, Berlin, 1970).

[18] M. V. Mesquita, A. R. Vasconcellos, and R. Luzzi, Phys. Rev. E , **58**, 7913 (1998).

[19] A. J. Heger, S. Kivelson, J. R. Schrieffer, and W. P. Su, Rev. Mod. Phys. **60**, 781 (1988).

[20] D. Marcuse, *Theory of Dielectric Optical Waveguides* (Academic, Boston, 1991), Chap. 9, pp. 335–65.

[21] M. V. Mesquita, A. R. Vasconcellos, and R. Luzzi, Int. J. Quantum Chem. **60**, 689 (1996).

[22] A. R. Vasconcellos, M. V. Mesquita, and R. Luzzi, Phys. Rev. Lett. **80**, 2008 (1998).

[23] A. S. Davydov, *Biology and Quantum Mechanics* (Pergamon, Oxford, 1982).

[24] J. Lu and J. F. Greenleaf, IEEE Trans. Ultrason. Ferroelect. Freq. Contr. **39**, 19 (1992).

FIGURE CAPTIONS

Figure 1: The populations in the steady state of a characteristic mode in Fröhlich condensate, ν_0, and a "normal" mode, ν_1, for intensities $S = I\bar{\tau}$. In the inset is shown the quasi-chemical potential $\mu_0^x = \mu_0 - R_y^x$ of the mode in Fröhlich condensate, in units of R_y^x.

Figure 2: The reciprocal of the lifetimes of the modes of Fig. 1, where $\bar{\Gamma}_{1(0)} = \bar{\tau}/\tau_{1(0)}$, the scaling time $\bar{\tau}$ given in the main text.

Figure 3: Comparison of the shape of the voltaic signal in [2] with the shape of the energy density of Schrödinger-Davydov's soliton [proportional to the squared modulus of the amplitude field of Eq. (8)] plus the contribution of the incoherent excitons.

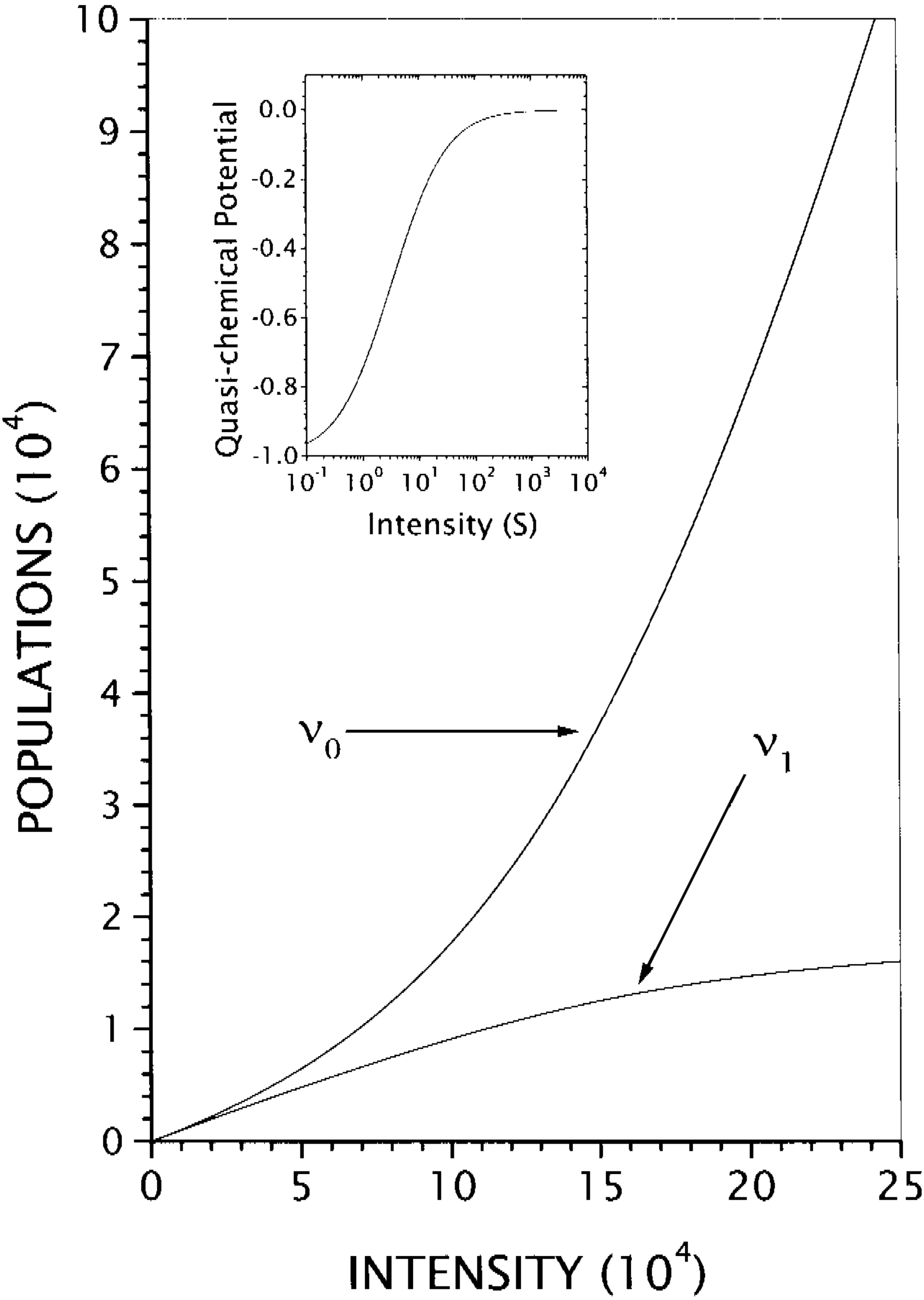

Figure 1: The populations in the steady state of a characteristic mode in Fröhlich condensate, ν_0, and a "normal" mode, ν_1, for intensities $S = I\bar{\tau}$. In the inset is shown the quasi-chemical potential $\mu_0^x = \mu_0 - R_y^x$ of the mode in Fröhlich condensate, in units of R_y^x.

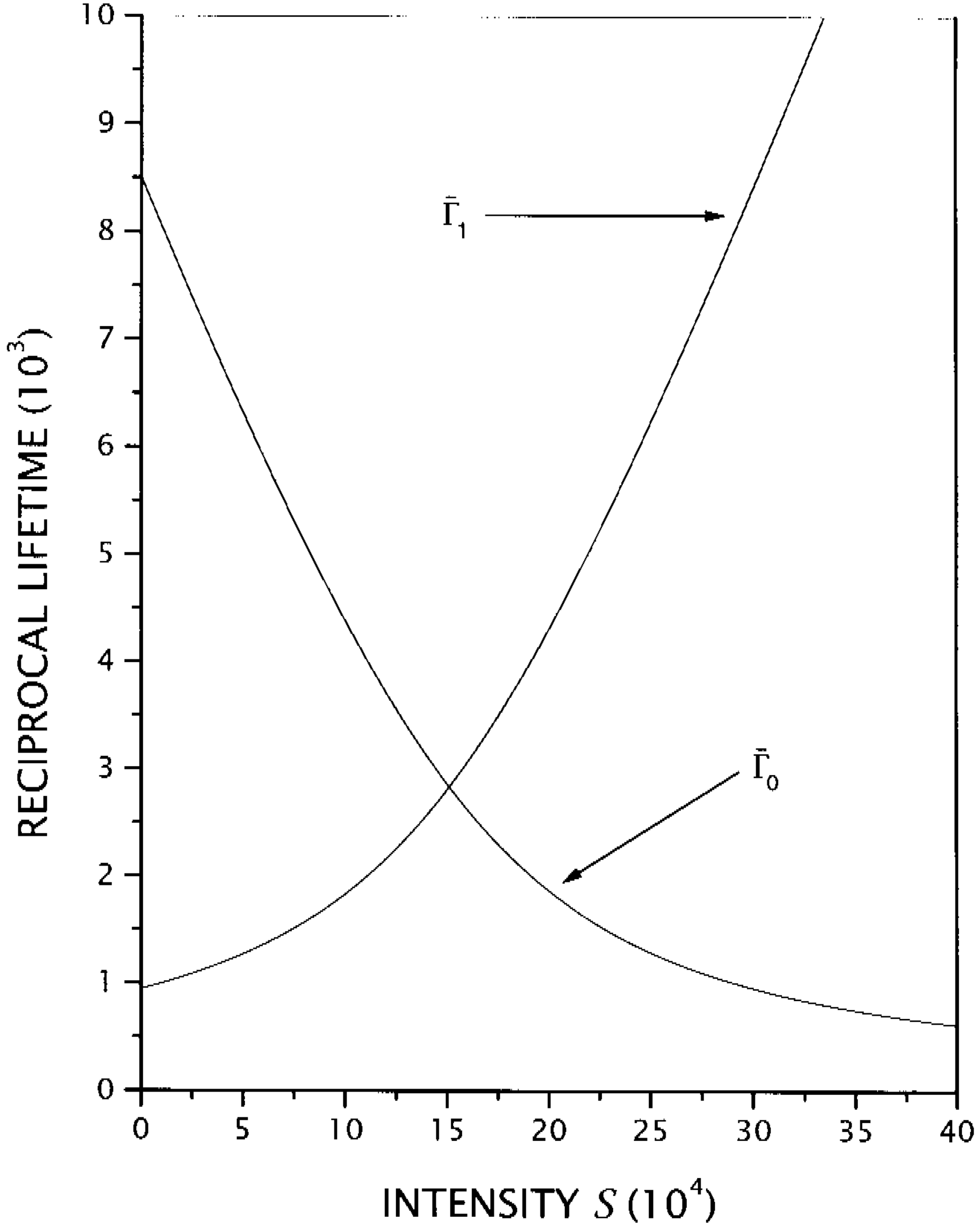

Figure 2: The reciprocal of the lifetimes of the modes of Fig. 1, where $\bar{\Gamma}_{1(0)} = \bar{\tau} / \tau_{1(0)}$.

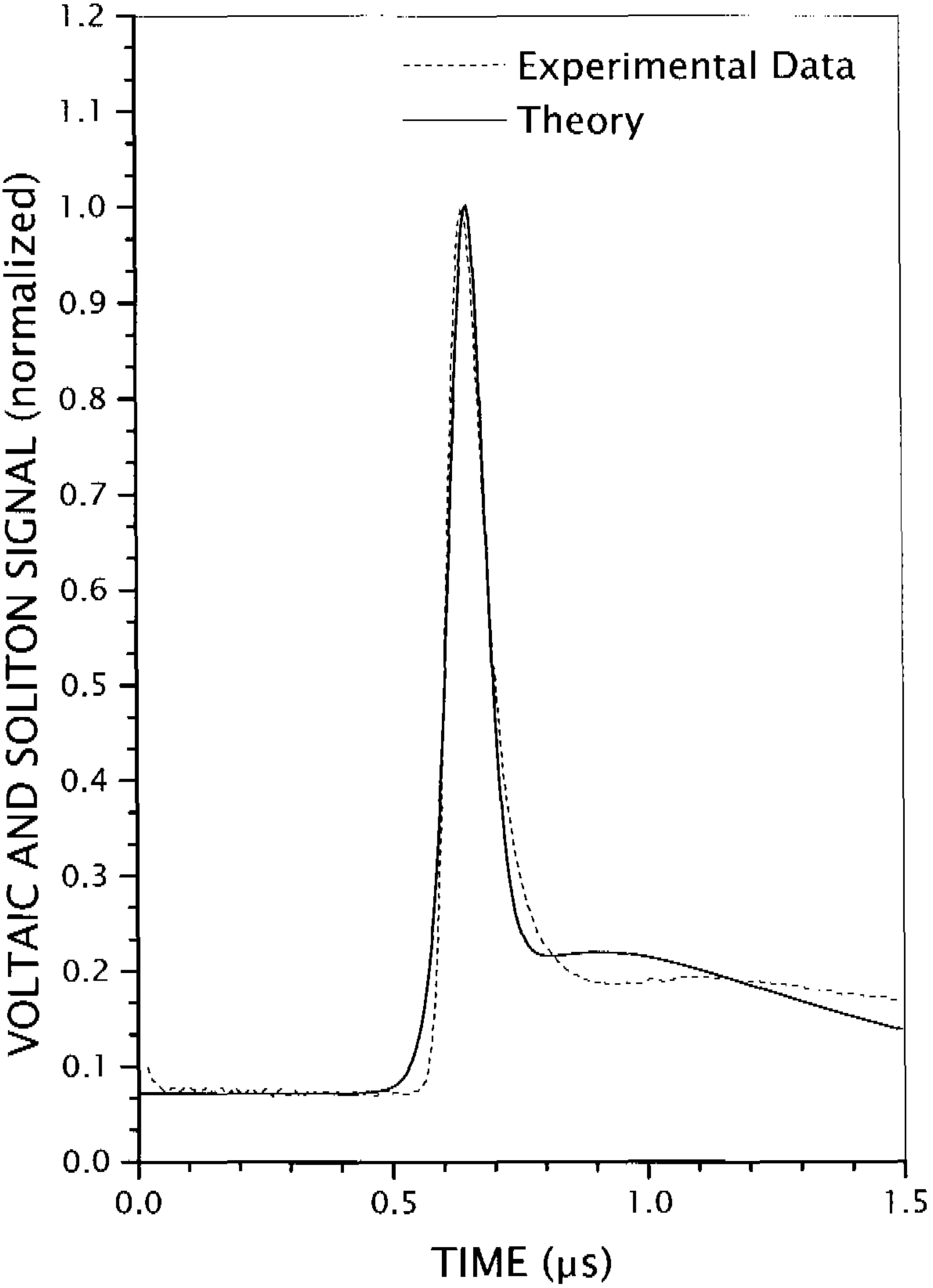

Figure 3: Comparison of the shape of the voltaic signal in [2] with the shape of the energy density of Schrödinger-Davydov's soliton [proportional to the squared modulus of the amplitude field of Eq. (8)] plus the contribution of the incoherent excitons.

Capítulo 6

ALGUMAS CONSIDERAÇÕES SOBRE SISTEMAS BIOLÓGICOS

6.1 Introdução

Iniciamos este capítulo citando S. Mascarenhas,[1] que manifestou que para nós o mais importante fenômeno da Natureza é a vida. Ela é muito complexa e para conseguir compreendê-la é necessário recorrer a vários ramos da ciência. O uso de conceitos biológicos e físicos levou ao conceito de Biofísica. Mas outras disciplinas que não a Física são necessárias neste difícil empreendimento. Assim, a *Biofísica* hoje deve melhor ser interpretada como uma ampla ciência interdisciplinar que envolve, além da Biologia, a Física, a Química, a Matemática, a Teoria de Informação, Computação, etc. Assim, ela é uma porção muito rica da ciência moderna e que apresenta tremendas oportunidades para a pesquisa básica e aplicada. O amplo campo da Biofísica faz contato com muitas outras áreas como a Genética, a Engenharia Genética, aplicações em Medicina, Biologia molecular, Bioenergética, etc.

Também seguindo Mascarenhas, que sendo os sistemas vivos constituídos por um número enorme de átomos, moléculas, organelas e células, comportamento dito complexo está amplamente presente neles. Contudo, complexidade leva, paradoxalmente,

---

[1] *Biophysics*, na *MacMillan Encyclopædia of Physics*.

à simplicidade, se reconhecermos que, não obstante o vasto número de componentes, os processos da vida evoluem harmoniosamente no tempo e no espaço. Isto certamente é o resultado de efeitos cooperativos. Assim, uma questão fundamental é: Podemos obter a partir das leis da Física Estatística, da Termodinâmica e da Química os conceitos básicos que levam aos particulares fenômenos de organização nos seres vivos? Este capítulo constitui-se numa tentativa de mostrar uma possível trilha no sentido de responder a essa pergunta. Tal tentativa de nossa parte consiste simplesmente, já que não somos biofísicos, em mostrar o uso da Mecânica Estatística e da Termodinâmica Estatística propostas na metodologia em que se baseia esta tese, ao estudo de sistemas biológicos modelados. Isto é descrito nas seções seguintes, que são:

6.2 Complexidade em sistemas biológicos

6.3 Considerações sobre ondas X e sólitons de Davydov em ultrasonografia.

6.4 Comportamento complexo em biosistemas: uma abordagem teórico-informacional.

6.2 Complexidade em sistemas biológicos

Descrevemos alguns aspectos do comportamento complexo que pode estar presente em biopolímeros. O estudo é baseado em uma termodinâmica não-linear de de sistemas em não-equilíbrio e dissipativos. Semelhante complexidade consiste numa condensação tipo Fröhlich-Bose-Einstein e na propagação de excitações tipo onda solitária de Schrödinger-Davydov, que são de relevância e bioenergética. A questão do tempo de vida do sóliton em condições fisiológicas é discutida, e comparação com resultados de experimentos é mostrada. Além disso, é discutido brevemente um comportamento complexo aparentemente presente em imagens para diagnóstico médico via ultrasom, fenômeno que denominamos de efeito Fröhlich-Cherenkov, o qual é brevemente discutido.

Aceito para publicação em *Contemporary Physics.*

Complexity in Biological Systems

Marcus V. Mesquita, Áurea R. Vasconcellos, Roberto Luzzi

Instituto de Física 'Gleb Wataghin',
Universidade Estadual de Campinas, Unicamp
13083-970 Campinas, São Paulo, Brazil

We describe some aspects of complex behavior that can be present in biopolymers. The study is based on a nonlinear thermodynamics of non-equilibrium, and then dissipative, systems. Such complexity consists of a Fröhlich-Bose-Einstein-like condensation and propagation of Schrödinger-Davydov solitary-wave-like excitations, which are of relevance in Bioenergetics. The question of the soliton lifetime under physiological conditions is discussed, and comparison with experiments performed in the case of an organic molecular polymer is shown. Further complex behavior apparently present in ultrasonic medical imaging, dubbed Fröhlich-Cherenkov effect, is briefly discussed.

Group Home Page: http://www.ifi.unicamp.br/~aurea

1. INTRODUCTION

Biological systems are complex systems by antonomasia, that is, notable representatives of the class of systems which show complex behavior. They present an enormous number of rich and noticeable phenomena on the morphological, biochemical, biophysical, biomechanical, etc., levels. We recall that living organisms are open systems driven (generally far) away from equilibrium and, then, one relevant area of Biophysics for their study is that of the nonlinear irreversible thermodynamics of open systems and its microscopic foundations (at the classical or quantal, nonlinear, memory-dependent, nonlocal, etc., levels) provided by nonequilibrium nonlinear statistical mechanics. These disciplines, irreversible thermodynamics of open systems and statistical mechanics of arbitrarily far-from-equilibrium systems, even though initiated in last century with the great contributions of Maxwell, Boltzmann, and Gibbs, have been marred by conceptual and practical difficulties, but have recently shown vigorous development. We discuss in this Note the use of an informational-statistical approach to irreversible thermodynamics for dealing with biophysical systems with complex behavior.

It is certainly a truism to say that the complicated heterogeneous spatial structure and functioning (temporal evolution) of living organisms, starting with the individual cell, pose quite difficult problems at the biophysical and biochemical levels of Biology. In recent decades a good deal of effort has been devoted in particular to specific physico-chemical aspects of biosystems, such as, how to increase our knowledge of the chemical composition of life forms; to determine the structure of macromolecules, proteins, etc. (as noted in Ref. [1], understanding of structure is the first vital step, without which any further analyses run aground); to determine the reactions that lead to processes of synthesis of multiple components; to understand the mechanisms and codes required to determine the structure of proteins; and so on. Moreover, as already noticed, to consider living systems at the biophysical level we must be well aware of the fact that we are dealing with macroscopic open systems in nonequilibrium conditions. In other words, we observe macroscopic organization — at the spatial and temporal levels — of the microscopic components of the system, namely, molecules, atoms, radicals, ions, electrons. The macroscopic behaviour is of course correlated to the details of the microscopic structure.

An immediate question to ask is: Which could be the theoretical approaches in Physics to carry on a programme to deal with the microscopic (molecular) level and, at the same time, be capable of describing the all important macroscopic level of biosystems and their synergetic aspects? During the last decades this question concerning the theoretical description of the macroscopic behaviour of dissipative open many-body systems in arbitrarily far-from-equilibrium conditions has been encompassed in a seemingly powerful, concise, and elegant formalism, established on sound basic principles. This is the so-called Nonequilibrium Statistical Operator Method (NESOM for short; [2–6]), which we consider [7] to be encompassed within the scope of Edwin T. Jaynes' Predictive Statistical Physics, based on Information theory, and the accompanying principle of maximization of informational-statistical entropy (MaxEnt for short; [8–13]).

The MaxEnt-NESOM formalism is based on a particular kind of scientific inference and the Bayesian approach to probability theory. According to the Nobel awarded Philip Anderson [14] the latter appears to be the most appropriate to use in science since it provides the degree of confidence consistent with retaining the idea that a proposition is correct when based on the fact to accept that other conditioning propositions are true: "These statistics are the correct way to do inductive reasoning from necessarily imperfect experimental data."

The MaxEnt-NESOM allows for the construction of a nonlinear quantum transport theory — covering a large class of situations [3–7, 15] — and a response function theory for far-from-equilibrium systems [6]. It also provides a thermodynamics of irreversible processes, dubbed as Informational Statistical Thermodynamics (IST, sometimes referred-to as Information-theoretic Thermodynamics). IST was apparently pioneered by Hobson [16] after the publication of Jaynes' seminal articles on the information-theoretic foundations of Statistical Mechanics [17, 18] (the MaxEnt-NESOM-based IST is described in references [19] and [20]). This irreversible statistical thermodynamics provides the foundations for the treatment of dissipative open macrosystems away (either near or far) from equilibrium. This is, as already noticed, the situation in biosystems, a result of the evident general feature that to function they require to have energy available which is provided by metabolic processes: That is, the open biosystem "feeds" on this energy and is driven away from equilibrium.

A quite fundamental point is that the evolution of the system has associated a nonlinear kinetics. This nonlinearity of the equations that describe the evolution in time of the macroscopic properties of the system is of enormous relevance for being the source for complex behaviour in matter. Complexity manifests itself in different situations involving this nonlinear domain of dynamical systems theory, and two relevant aspects are the nowadays fashionable deterministic chaos [21,22] and self-organization in dissipative systems [23–26]. This latter type of complex behaviour in macroscopic systems is one that could apparently have enormous importance in biosystems, in that it is related to the origin of life, its functioning, and evolution [25,27–29]. Two questions naturally arise concerning self-organization in matter: What is the microscopic origin of dissipative structures?, and How can we deal theoretically with and be able to perform a rigorous analysis of them? As noted in an earlier paragraph a promising approach may be the irreversible statistical thermodynamics IST founded on the framework of the MaxEnt-NESOM. We attempt to illustrate the point by reviewing an application to a modelled biosystem [30,31], which reveals two relevant complex phenomena, namely Fröhlich synchronous modes leading to a kind of Bose-Einstein condensation in a nonequilibrium steady state, and the dynamical effect consisting of Schrödinger-Davydov solitary waves propagating signals at long distances in a coherent way, and also a peculiar phenomenon we are calling Fröhlich-Cherenkov effect.

2. FRÖHLICH-DAVYDOV'S SYSTEM AND BIOENERGETICS

As pointed out by Fröhlich [32], biological systems are relatively stable from a microscopic point of view, for example, the thermal vibrations of single atoms are practically the same as in a corresponding nonbiological system. In some conditions, however, when they are very far from thermal equilibrium, a restricted set of phase space points dominate the overall behaviour of the rest. This implies in the emergence of collective properties of organization that are carried out by a great number of vibrational modes. These collective properties evolve as a consequence of the supply of energy (metabolism) and have associated extreme nonlinear displacements, a complex behaviour that may be of large relevance in bioenergetics, as we shall see as we proceed. We consider this in the framework of IST applied to the so-called Fröhlich-Davydov model which consists in a quasi-linear chain of macromolecules in a periodically repeated array, of which an example could be found in the α-helix protein, what is illustrated in Fig. 1. Energy is pumped in the system by a metabolic external process, and the chain can sustain longitudinal polar vibrations (those associated to the CO-stretching, or Amide-I, oscillations), with the corresponding mechanical model described in Fig. 1. Details of the Hamiltonian operator (or energy operator) that completely characterizes the system at the microscopic mechanical level are given in Refs. [30]. Moreover, the polar modes are in anharmonic interaction with an elastic continuum (describing the surrounding media). In the MaxEnt-NESOM-based IST, the basic macrovariables used for the description of the nonequilibrium thermodynamics state of the system are the time-dependent populations (number of excited quantum phonons) and amplitudes of the polar vibrational modes, and the energy of the surrounding media. The equations of evolution for these variables are derived in the MaxEnt-NESOM generalized nonlinear quantum transport theory [15], and solved for given initial conditions [30, 31]. The solutions provide evidence of complex behaviour — already expected — in the system, consisting of two particular phenomena, namely, the *Fröhlich effect* [32–34], and propagation of solitary-like waves, or *Schrödinger-Davydov solitons* [35–37].

Consider the first: More than thirty years have elapsed since the renowned late Herbert Fröhlich first presented his concept of long-range coherence in biological systems [32], a question presently in a process of strong revival providing an attractive and relevant field of research in Physics and Biology. According to Fröhlich biophysical systems possessing longitudinal electric vibrational modes may display, under appropriate conditions, a collective phenomenon akin to a Bose-Einstein condensation — not in equilibrium but as a complex behavior consisting in the emergence of a dissipative structure in Prigogine's sense [25]. Fröhlich's results are based on the idea that active biological systems are open and very far from equilibrium and have considerable amounts of energy available, through metabolic processes, that cause non-linear changes in molecules and larger biological subsystems. Fröhlich in 'Life as a Collective Phenomenon' [38], expressed that if one thinks without preconceptions of collective phenomena in which the discrete constitutive individuals are modified in their behavior, and indeed in their constituting a large collective group where the whole is more than and different from a simple addition of its parts, living organisms would seem to be the ideal example. Such a hypothesis of biological explanation in terms of long-range coherence was originally suggested by Fröhlich at the first meeting of *L'Institute de la Vie* in 1967 [32].

In Fröhlich model vibrational-polar modes are excited by a continuous supply of energy pumped by an external source, while these modes interact with the surrounding medium acting as a thermal bath. The interplay of these two effects — pumping of energy subtracting entropy from the system and dissipative internal effects adding entropy to the system —, may lead to the emergence of complex behavior in the system consisting in what can be called *Fröhlich effect:* Provided the energy supply is sufficiently large compared with the energy loss, the system attains a stationary state in which the energy that feeds the polar modes is channelled into the modes with the lowest frequencies. The latter largely increase their populations at the expenses of the other higher-in-frequency modes, in a way reminiscent of a Bose-Einstein condensation [30]. This highly excited subset of modes may exhibit long-range phase correlations of an electret type as discussed in Ref. [39]. Details of the theory, the description of the system, the accompanying kinetic theory, possible experimental situations, and discussion of the phenomenon is available in the extensive literature on the subject (partially listed in, for example, Refs. [30]). The nonlinearities responsible for Fröhlich effect are also of relevance to the other phenomenon consisting of propagation of Davydov soliton, which we consider next.

The solution of the equations of evolution for the statistically averaged field amplitude of vibration $\psi(x,t)$ (see Eq. (5) below) of the polar (CO-stretching) modes in the quasi-linear biopolymer, takes the form of a nonlinear Schrödinger-like equation with damping, namely [31]

$$i\frac{\partial\psi(x,t)}{\partial t}-\{\omega_0-i\gamma\}\,\psi(x,t)-\alpha\frac{\partial^2}{\partial x^2}\psi(x,t)+G\,|\psi(x,t)|^2\,\psi(x,t)=0, \qquad (1)$$

where ω_0, α, γ, and G are parameters characteristic of the material (frequency and curvature of the dispersion relation at the zone-centre, reciprocal lifetime, and the nonlinear coupling strength of the modes, respectively). For a given impulse-like initial excitation of amplitude $\mathcal{A}$ and velocity υ, a solution of Eq. (1) is

$$\psi(x,t)=\mathcal{A}\exp\left\{i\left[\frac{\upsilon}{2\alpha}x-(\omega_s-i\gamma)\,t-\frac{\theta}{2}\right]\right\}\operatorname{sech}\left[\mathcal{A}\left(\frac{|G|}{2\alpha}\right)^{1/2}(x-\upsilon t)\right] \qquad (2)$$

where we wrote $G=|G|e^{i\theta}$ (complex number in polar planar coordinates); $\mathcal{A}$ and υ, as noticed, are fixed by the imposed initial conditions; and

$$\omega_s=\omega_0-\frac{\upsilon^2}{4\alpha}+\frac{|G|\mathcal{A}^2}{2}\,. \qquad (3)$$

is the frequency of oscillation of the soliton.

Except for the exponential decay, Eq. (2) describes Davydov soliton, that is, an excitation (the soliton) which propagates undamped (for $\gamma=0$) and undeformed. This is the novel mechanism for the localization and transport of vibrational energy in protein proposed by A. S. Davydov [35–37]. In the case of the α-helix region of protein this mechanism is described as follows: Vibrational energy of the CO-stretching oscillators that is localized on the quasi-periodic helix, acts — through the phonon coupling effect — to distort the structure of the helix. The helical distortion reacts — again through phonon coupling — to trap the Amide-I oscillation energy preventing its dispersion, in a so-called selftrapping [40]

As noted, Eq. (1) is the equation of evolution for a Davydov soliton, which propagates (for the given initial conditions) in the form given by Eq. (2). But a quite important fact should be noticed, namely that Davydov soliton corresponds to $\gamma=0$, that is, its original quantum mechanical derivation did not include relaxation effects, which are of course accounted for in the nonequilibrium thermodynamic approach which leads to Eq. (1). Therefore, the result is a solitary-like wave (a nondeformed wave packet) but subject to dissipation. Typically, the lifetime is of the order of 10 picoseconds, and then, for a typical velocity of propagation in the range of 10^6 cm/s, the excitation would propagate energy only along a few micrometers. Therefore it would be a quite inefficient mechanism for the propagation of energy (signals), which in living systems travels distances in the centimeter range. Some effort has been devoted to this question trying to circumvent such drawback. A quite attractive result, which has been derived consistently within the above described approach, shows that the lifetime of the solitary exciton increases enormously, and so does the distance which is travelled by the signal, when the propagation occurs in a nonequilibrium background where Fröhlich condensation is present [31]. That is, *a coherent excitation in the form of a Davydov solitary excitation can travel nearly undamped, and undeformed, while a nonequilibrium-dissipative state consisting of Fröhlich-Bose-Einstein-like condensation is maintained by the action of an external energy pumping process.*

But, evidently, these theoretical results are in need of corroboration through application of the well established scientific method, namely, observation and measurement. Experiments of the physical and chemical type are quite difficult to realize in biological systems under normal physiological conditions. Raman scattering experiments have demonstrated the enhancement of polar vibrations in biological active systems [41], a fundamental condition for leading eventually to the emergence of Fröhlich effect. Also, it has been tentatively attempted to evidence Fröhlich effect in experiments measuring reaction rates of enzyme molecules, rouleaux formation in erythrocytes (see second of Refs. [34]), etc., with no conclusive results. However, a circumventing alternative can be used in a first approach to the question, consisting of the use of inanimate organic polymers that roughly reproduce the structure of some biopolymers. Solitons of the type here considered seem to be present in organic compounds such as polyacetylene and polythiophene. These solitons appear to have an important influence on the conducting properties of these substances, properties which have technological and industrial/economic relevance [42,43]. Another particular compound, acetanilide, may have an important role to play: it has a structure resembling biopolymers with the presence of the relevant CO-stretching modes. Several careful experiments testing optical properties, such as infrared absorption and Raman scattering, have been performed in acetanilide. The infrared spectrum shows an anomalous line, later ascribed precisely to the presence of a Davydov soliton [44].

Following consistently the MaxEnt-NESOM formalism, according to the response function theory based on it [6], we find for the optical absorption coefficient

$$\alpha(\omega) = \sum_{q} A(q,\omega) \int_{0}^{\Delta t} dt \int_{0}^{t'} dt' \, e^{-i\omega(t'-t)} \, \mathrm{Tr}\,\{a_q^{\dagger}(t-t')a_q\varrho(t)\} \,, \tag{4}$$

where A is an amplitude whose detailed form is not necessary for our purposes here, $\varrho(t)$ is the statistical distribution at time t, in this experiment in time-integrated optical spectroscopy Δt is the experimental resolution time, and $a_q(a_q^{\dagger})$ are as usual annihilation (creation) operators in mode $\boldsymbol{q}$. From a direct calculation, and using

$$\psi(x,t) = \sum_{q} a_q(t) e^{ix} \,, \tag{5}$$

with $\psi(x,t)$ given in Eq. (2) it follows that

$$\mathrm{Tr}\,\{a_q^{\dagger}(t-t')a_q\varrho(t)\} = \nu_{\boldsymbol{q}}^{0} e^{-i\omega(t'-t)} + \langle a_q^{\dagger}|t\rangle\langle a_q|t'\rangle \,, \tag{6}$$

what implies that the absorption spectrum has two bands, the "normal" one due to the vibrations with frequency $\omega_{\boldsymbol{q}}$, (the population of this mode being ν_q^0) and an "anomalous" band around frequency ω_0, that is, the associated to the soliton. In fact, using Eqs. (4) to (6) and (2) it follows that

$$\alpha(\omega) \simeq \int_{0}^{\Delta t} dt \int_{0}^{t'} dt' [\alpha_n(t,t') + \alpha_s(t,t')], \tag{7}$$

where

$$\alpha_n(t,t') \simeq C_n[\mathrm{e}^{-2\gamma t}\mathrm{e}^{\mathrm{i}(\omega-\omega_q)(t'-t)} + \mathrm{e}^{-2\gamma t'}\mathrm{e}^{-\mathrm{i}(\omega-\omega_q)(t'-t)}, \tag{8}$$

$$\alpha_s(t,t') \simeq C_s[\mathrm{e}^{-2\gamma_s t}\mathrm{e}^{\mathrm{i}(\omega-\omega_s)(t'-t)} + \mathrm{e}^{-2\gamma_s t'}\mathrm{e}^{-\mathrm{i}(\omega-\omega_s)(t'-t)}, \tag{9}$$

where $\gamma_s = \gamma + \mathcal{A}(|G|/2\alpha)^{\frac{1}{2}}$, γ is the decay time of the vibrational modes, and C_n and C_s are amplitudes corresponding to the "normal" and "anomalous" bands with band widths γ and γ_s respectively. We have compared the NESOM-based theoretical result of Eq. (7) with the experimental data taken from Ref. [44]. Since there is not a theoretical access to the initial conditions that fix $\mathcal{A}$ and v, they have been derived from the experimental data, using Eq. (3), and, for instance, for the case of $T = 80$ K, and then, on the basis that $\omega_0 - \omega_s = 16\ \mathrm{cm}^{-1}$ and $\gamma_s - \gamma = 3.6\ \mathrm{cm}^{-1}$, we obtain that $\mathcal{A}(|G|/2\alpha)^{\frac{1}{2}} = 2.3 \times 10^6\mathrm{cm}^{-1}$ and $v = 2.9 \times 10^4\ \mathrm{cm\ s}^{-1}$. In Fig. 2 are indicated the experimental curves (dotted) and the theoretical ones (full line), for 20 K, 50 K, and 80 K, which are in a very good agreement. The amplitudes of the bands have been normalized that is, in that way it is avoided the calculation of A of Eq. (9), of no relevance here, since the fundamental point to characterize is the shape and positioning of the bands. Details are given in Refs. [45–47].

Figure 3 depicts the calculated shape of the squared modulus of the soliton propagating along a given direction x, which is proportional to its energy density, provided at several delay times after initial excitation. In Fig. 4 is shown a picture of the soliton amplitude over the plane of the spatial and temporal coordinates. The decay of the solitary exciton is evident in this near equilibrium conditions.

Successful experiments — for example those reported in [44] — are quite promising results which open up the possibility of carrying on additional experiments in acetanilide, now in the presence of intense excitation by a continuous pumping of energy in order to attempt to corroborate the phenomena previously discussed. Probing it in infrared or Raman scattering experiments, we should look for the theoretically predicted large enhancements of the lifetime of the soliton, that is, a noticeable narrowing of the Raman bandwidth, as the system eventually approaches the threshold for Fröhlich condensation.

In acetanilide the relevant vibrations, which are related to the Amide-I vibrations in biopolymers, are of the optical dipolar type. But the phenomena just described can also be present in the case of acoustical vibrations, which may have relevance to the medical technique of ultrasound imaging. This is described in Refs. [46] and [47]: longitudinal acoustic phonons (sound-like waves) excited by the action of a pumping source acting in the region of ultrasound frequencies, as in the previous case of optical phonons, also display a very large enhancement of the populations of the modes lowest in frequency, and solitary-like waves can be produced.

In both cases of "optical" or "acoustical" Schrödinger-Davydov solitons we have described, the amplitude and the velocity of propagation are determined by the initial condition of excitation. Hence, the velocity v can be either smaller or larger than the group velocity of the normal waves. For the polymer acetanilide in the conditions of the experiment of Careri *et al.* [44], v is larger than the group velocity of the phonons of the CO-stretching vibrations. In the case of acoustic vibrations in bulk we may have v larger than the velocity of sound s in the medium, leading to the emergence of a kind of Cherenkov-like effect (a so-called superluminal effect in the case of charges moving in a dielectric with a velocity larger than the velocity of light in the medium [48]) as we proceed to show. This could be the case in supersonic medical imaging as reported by Lu and Greenleaf [49]; in Fig. 4 we reproduce a pair of results, one the excitation of a normal sound wave, and the other an apparent, in our interpretation, "superluminal" solitary wave, or better to say a supersonic solitary wave accompanied with a Cherenkov-like large emission of phonons, as next described. Such excitation has been dubbed an X-wave, and interpreted in terms of an undeformed progressive wave [50], created by the particular excitation provided by the pumping transducer.

Consider propagation of a soliton with velocity $v(> s)$ in, say, x-direction in bulk, what introduces a privileged direction in the system. The population of the vibronic modes increase as a result of direct excitation, and as noticed, such pumped energy is concentrated in the modes lowest in frequency, that is, there follows the emergence of Fröhlich effect. It can be shown that the population of the acoustic phonon states takes the form [46, 47]

$$\nu_q = \left[\exp[\beta_0 \hbar s q[1 - (v/s)\cos\theta]] - 1\right]^{-1}, \tag{10}$$

after the small corrections due to the amplitude of the oscillation are neglected, where $\beta_0 = 1/k_B T_0$, T_0 being the temperature of the system, a Debye dispersion relation $\omega_q = sq$ is used, and we have introduced the angle θ_q such that

$$\cos\theta_q = \frac{s}{v}\left[1 - \frac{k_B T_0}{\hbar s q}\ln\left(1 + \frac{1}{\nu_q}\right)\right] = \frac{s}{v n_q}, \tag{11}$$

and n_q defines a "pseudo-refraction index" introduced simply for giving an expression resembling the case of Cherenkov effect in radiation theory (when then ν_q is the Planck distribution of photons [48]). Hence it follows that a large emission of phonons follows when $\cos\theta_q$ approaches the value s/v, that is, for large values of ν_q in the Fröhlich condensate, and which are emitted in the direction $\boldsymbol{q}$ forming an angle θ_q with the direction of propagation of the "supersonic soliton" ($v > s$). Forward and backward symmetrical propagations are present because modes $\pm\boldsymbol{q}$ are equivalent (θ_q depends on the modulus of $\boldsymbol{q}$). This is here a particular characteristic of what in radiation theory are the normal and anomalous Cherenkov effect in a spatially dispersive medium [48]. As already noticed, the phenomenon, which we call *Fröhlich-Cherenkov effect*, may provide a microscopic interpretation of the X-waves in ultrasonic medical imaging [49, 50], shown in the lower part of Fig. 5. From this figure we roughly estimate that $\theta \simeq 13°$, and then $v/s \simeq 1.02$ (i.e. the velocity of propagation of the ultrasonic soliton is 2% larger than the velocity of sound in the medium, once we admit strong excitation implying in that ν_q greatly increases for modes q in Fröhlich condensate, and then $\cos\theta_q \to (s/v)[1 - (k_B T_0/\hbar s q \nu_q)] \approx s/v$. This seems to be the case noticed in ultrasonic medical imaging [49], where the propagating excitation was dubbed an X-wave. Rodrigues and Lu have described this kind of motion in terms of a mathematical treatment in the context of the so-called undistorted propagating wave [50]: the statistical thermodynamic approach here described provides a microscopic foundation for the phenomenon. Figure 4 shows a normal sound wave (upper part) and the X-wave (lower part), the latter being the soliton accompanied of the Cherenkov-like effect referred to above.

3. DISCUSSIONS AND CONCLUSIONS

We have considered the question of complex behavior in biosystems and its possible description — involving the microscopic level of many-particle physics —, in terms of a particularly promising approach, namely, Informational-Statistical Thermodynamics.

Complexity is regarded presently to be one of the frontier fields in Physics [51]. The 1972 article in *Science* [52] by Philip W. Anderson, titled 'More is Different' is considered to constitute one of the main "Manifestos" on the subject (see also Refs. [23-29, 38, 53-55]). Complex behaviour in matter is nowadays a topic attracting increasing interest. Complex systems are not necessarily complicated (even though they can be), but characterized by the fact of displaying highly coherent behaviour involving a collective organization in a vast number of constituent elements. It is said that it is one of the universal miracles of Nature that huge assemblages of particles, subject only to the blind forces of nature, are nevertheless capable of organizing themselves into patterns of cooperative activity [51]. Complex behaviour in matter can only arise in the nonlinear domain of the theory of dynamical systems (one of its founders being Ludwig von Bertalanffy in the thirties [53]), since in the linear domain the principle of superposition of states cannot give rise to any unexpected behaviour of a synergetic character. For thermodynamic systems, as the biological ones, coherent behaviour is only possible in the nonlinear regime far from equilibrium, once in the linear (also referred to as Onsagerian) regime around equilibrium synergetic organization is inhibited according to Prigogine's theorem of minimum entropy production [24, 26].

On the other hand, the mechanical-statistical approach above mentioned is based on Predictive Statistical Mechanics, which is not a physical theory, but a method of reasoning that accomplishes the description of the macroscopic state of the system by finding, not the particular things that the equations of motion say in any particular case, but the general things that they say, in 'almost-all' cases consistent with our information, for those are the reproducible things. Evidently, there remain quite difficult points to be cleared up, mainly how to determine in which extension this information reside in us, or up to what degree it is a "property" of Nature, or, better to say, of dynamical systems in general. Again according to Jaynes, the question as to how the theoretically valid and pragmatically useful ways to apply Probability theory in science was faced by Sir Harold Jeffrey [56, 57], in the sense that he stated the general philosophy of what scientific inference is, and proceeded to develop a mathematical theory and its implementations. At the beginning of his book on Probability theory [57], Jeffreys maintains that the fundamental problem of scientific progress and a fundamental one of everyday life, is that of learning from experience. Knowledge obtained in this way is partly merely description of what we have already observed, but part consists of making inferences from past experience to predict future experiences. It is worth noticing that MaxEnt-NESOM appears to have points in common with an alternate engaging approach, namely the one of Prigogine and the Brussels' school, referred-to as subdynamics (see for example reference [58]). A comparison, with an attempt to relate both approaches, has been presented by J. P. Dougherty, and we refer the reader to his work in references [59–61].

The formalism has been applied to the study of a particular physicochemical subsystem present in biological material. We have reviewed in this paper the case of polar modes of vibration (of the CO-stretching type) in anharmonic interaction with a bath of acoustic-like vibrations (also present in some polymers like, for example, vinyls and acetanilide). Complex behavior may follow consisting of two particular phenomena we have described here. One is *Fröhlich effect* where synchronous large-scale collective oscillations imply in intercellular microwave emissions which would constitute a non-chemical and non-thermal interaction between cells. These oscillations could therefore be revealed by detection of emissions of GHz or THz radiation. Such electromagnetic signals are of extremely low magnitude and the receiver technology to measure them was not available during Fröhlich's time. It is only now that the predicted signals can be detected by adapting successful technology that has been developed for space and astrophysical research [62].

Earlier experiments looking after Fröhlich effect were not conclusive, but now - as notice above - a 'second generation' of experiments are becoming available. They require further improvement, but already some preliminary results are encouraging [62]: Some evidence of a non-thermal influence of coherent microwave radiation on the genome conformational state in *E. coli* has been reported, which may indicate that chromosomal DNA could be the target of mm microwave irradiation within this system. Also low intensity microwave irradiation of leukocytes results in a significant increase in biophoton emission in the optical range, the origin of which is thought to involve DNA. Also it is worth noticing the possible influence of the concept of biocoherence on the very particular dipolar system which is water. It can be considered the possibility that biological water might itself support coherent dipolar excitations extending over mesoscopic regions; thus water instead of being a passive space-filling solvent would be risen to an important singular position whose full significance has yet to be elucidated. Hence, a whole new area of biology is now ready for investigation.

Nonbiological implications of Fröhlich effect could also be far-reaching. It can be mentioned some connection with homeopathy and atmospheric aerosol physics [62]. Regarding the latter, sunlight-pumped Fröhlich-like coherent excitations may play a role in producing anomalies in the spectrum of light absorption [63]. At this point we may mention a question related to a public safety concern, namely, the influence and eventual deleterious effects of mobile phones in close proximity to the head of the user as a result of the action of microwaves on the biological material, which could eventually be better analyzed in connection with studies related to the Fröhlich effect here described.

The other complex phenomena we have considered consists in the propagation of *Schrödinger-Davydov solitary waves*. As it was shown the solitary wave in biological as well as nonbiological systems, although strongly damped in a sample not excited by external pumping sources as a result of the usual dissipative effects, may propagate with weak decay and travelling long distances when moving in the background provided by a steady-state Fröhlich's condensate [46]. There already exist cases where theory is seemingly validated by experiment, and we have noticed in the previous Section the case in ultrasound medical imaging, where another kind of complex behavior may follow, namely the so-called Fröhlich-Cherenkov emission.

Other example where Fröhlich's condensation and Davydov's soliton appear to be present is the case of the so-called *'Excitoner'*, meaning stimulated coherent emission of excitons created by random excitations, in a situation similar to the case of photons in a laser [64, 65]. In this case excitons, created in a semiconductor by an intense pulse of laser radiation, travel through the sample as a packet and are detected on the back of the sample. A weak signal in normal conditions of thermal excitation is largely enhanced when the system is pumped by a continuous external source of infrared radiation. The theory suggests the formation of a nonthermally excited Fröhlich condensate of excitons where a weakly damped Schrödinger-Davydov soliton is created, whose shape is in very good agreement with the experimental observation [66]: We reproduce in Fig. 6 a comparison of the experimental result and the one provided by the theory. We notice here a particularly noticeable complex behavior — Fröhlich effect; Davydov soliton; eventually Fröhlich-Cherenkov effect —, and the 'Excitoner', citing D. Snoke [64], is a phenomenon which may provide a new kind of light source, but only time and imagination can tell what new applications may arise from this novel effect.

In conclusion, the results we have described, resulting from a promising and particularly successful marriage of nonlinear nonequilibrium Statistical Thermodynamics and Biology, lead us to paraphrase Herbert Fröhlich saying that it is particularly auspicious to see that biological systems may display complex behaviour describable in terms of appropriate physical concepts.

We acknowledge finantial support to our research Group that in different opportunities was provided by the State of São Paulo Research Foundation (FAPESP); the National Research Council (CNPq); The Ministry of Planning (Finep); IBM-Brasil; USA-National Science Foundation (USA-Latin America Cooperation Project, Washington, USA); and the John Simon Guggenheim Memorial Foundation (New York, USA). One of the authors (MVM) is a Ministry of Education (CAPES) Pre-Doctoral Fellow, and the other two (ARV, RL) are CNPq Research Fellows. We are grateful to Prof. Sergio Mascarenhas (Institute for Advanced Studies, USP, São Carlos (São Paulo), Brazil) for calling our attention to the Proceedings of the first Meeting of *L'Institute de la Vie,* mainly the works of H. Fröhlich and I. Prigogine.

REFERENCES

[1] J. Glanz, Science **272**, 646 (1996).

[2] D. N. Zubarev, Fortschr. Phys./Prog. Phys. **18**, 125 (1970); D. N. Zubarev and M. Yu. Novikov, Fortschr. Phys./Prog. Phys. **21**, 703 (1973).

[3] D. N. Zubarev, *Nonequilibrium Statistical Thermodynamics* (Consultants Bureau, New York, 1974), [*Neravnovesnaia Statisticheskaia Termodinamika* (Idz. Nauka, Moscow, 1971)].

[4] D. N. Zubarev, V. N. Morozov, and G. Röpke, *Statistical Mechanics of Nonequilibrium Processes*, Vol. 1: Basic concepts, Kinetic Theory; Vol. 2: Relaxation and Hydrodynamic Processes (Akademie Verlag, Berlin, 1996 and 1997 respectively).

[5] A. I. Akhiezer and S. V. Peletminskii, Methods of Statistical Physics (Pergamon, Oxford, 1981).

[6] R. Luzzi and A. R. Vasconcellos, Fortschr. Phys./Prog. Phys. **38**, 887 (1990); R. Luzzi, A. R. Vasconcellos, and J. G. Ramos, *Foundations of a Nonequilibrium Statistical Ensemble Formalism*, intended for Fundamental Theories of Physics, A. van der Merwe, Ed. (Kluwer Academics, Dordrecht).

[7] J. G. Ramos, A. R. Vasconcellos, and R. Luzzi, Fortschr. Phys./Prog. Phys. **43**, 265 (1995).

[8] E. T. Jaynes, in *Frontiers of Nonequilibrium Statistical Physics*, edited by G. T. Moore and M. O. Scully (Plenum, New York, 1986).

[9] E. T. Jaynes, in *E. T. Jaynes Papers on Probability, Statistics, and Statistical Physics*, edited by R. D. Rosenkrantz (Dordrecht, Reidel, 1983).

[10] E. T. Jaynes, in *Maximum Entropy and Bayesian Methods,* edited by J. Skilling (Kluwer, Dordrecht, 1989).

[11] E. T. Jaynes, in *Maximum Entropy and Bayesian Methods,* edited by W. T. Grandy and L. H. Schick (Kluwer, Dordrecht, 1991).

[12] J. N. Kapur and H. K. Kesavan, *Entropy Optimization Principles with Applications* (Academic, San Diego, CA, 1992).

[13] W. T. Grandy, *Foundations of Statistical Mechanics* (Reidel, Dordrecht, 1987).

[14] P. W. Anderson, Phys. Today **45**(1), 9 (1992).

[15] L. Lauck, A. R. Vasconcellos, and R. Luzzi, Physica A **168**, 789 (1990); J. R. Madureira, A. R. Vasconcellos, R. Luzzi, and L. Lauck, Phys. Rev. E **57**, 3637 (1998); J. R. Madureira, A. R. Vasconcellos, R. Luzzi, J. Casas-Vázquez, and D. Jou, J. Chem. Phys. **108**, 7568–79 (1998); *ibid.* **108**, 7580–87 (1998).

[16] A. Hobson, J. Chem. Phys. **45**, 1352 (1966).

[17] E. T. Jaynes, Phys. Rev. **106**, 620 (1957).

[18] E. T. Jaynes, Phys. Rev. **108**, 171 (1957).

[19] L. S. Garcia-Colin, A. R. Vasconcellos, and R. Luzzi, J. Non-Equilib. Thermodyn. **19**, 24 (1994); A. R. Vasconcellos, R. Luzzi, and L. S. Garcia-Colin, Phys. Rev. A **43**, 6622 (1991); *ibid.* **43**, 6633 (1991); R. Luzzi, A. R. Vasconcellos, and J. G. Ramos, Fortschr. Phys./Prog. Phys., in press; *Statistical Foundations of Irreversible Thermodynamics,* intended for Texte zur Physik series, W. Ebeling, Ed. (Teubner, Berlin).

[20] M. A. Tenan, A. R. Vasconcellos, and R. Luzzi, Fortschr. Phys./Prog. Phys. **45**, 1 (1997); R. Luzzi and A. R. Vasconcellos, Physica A **241**, 677 (1997); R. Luzzi, A. R. Vasconcellos, J. Casas Vázquez, and D. Jou, J. Chem. Phys. **107**, 7383 (1997); Physica A **248**, 111 (1998).

[21] S. H. Kellert, *In the Wake of Chaos* (Univ. of Chicago Press, Chicago, 1993).

[22] G. Nicolis, Physica A **213**, 1 (1995).

[23] I. Prigogine and I. Stengers, *Order out of the Chaos: Man's New Dialogue with Nature* (Bantam, New York, 1984).

[24] G. Nicolis and I. Prigogine, *Self-organization in Nonequilibrium Systems* (Wiley-Interscience, New York, 1977).

[25] I. Prigogine, in *From Theoretical Physics to Biology*, edited by M. Marois (North Holland, Amsterdam, 1969).

[26] P. Glansdorff and I. Prigogine, *Thermodynamic Theory of Structure, Stability, and Fluctuations* (Wiley-Interscience, New York, 1971).

[27] I. Prigogine, G. Nicolis, and A. Babloyantz, Phys. Today **25** (11), 23 (1972); *ibid.* **25** (12), 38 (1972).

[28] S. Kauffman, *The Origins of Order: Self-organization and selection in evolution* (Oxford Univ. Press, New York, 1995).

[29] A. Babloyantz, *Molecules, Dynamics and Life* (Wiley-Interscience, New York, 1986).

[30] M. V. Mesquita, A. R. Vasconcellos, and R. Luzzi, Phys. Rev. E **48**, 4049 (1993); Phys. Lett. A **238**, 206 (1998); Int. J. Quantum Chem. **66**, 177 (1998); M. A. Tenan, M. V. Mesquita, and R. A. Mosna, Int. J. Quantum Chem. **62**, 363 (1997); L. Lauck, A. R. Vasconcellos, and R. Luzzi, J. Theor. Biol. **158**, 1 (1992).

[31] A. R. Vasconcellos and R. Luzzi, Phys. Rev. E **48**, 2246 (1993); M. V. Mesquita, A. R. Vasconcellos, and R. Luzzi, Int. J. Quantum Chem **60**, 689 (1996).

[32] H. Fröhlich, in *From Theoretical Physics to Biology*, edited by M. Marois (North Holland, Amsterdam, 1969).

[33] H. Fröhlich, Int. J. Quantum Chem. **2**, 641 (1968).

[34] H. Fröhlich, Nature **228**, 1093 (1970); H. Fröhlich, in *Advances in Electronics and Electrons Physics*, Vol. 53, pp. 85-192 (Academic, New York, 1980).

[35] A. S. Davydov, in *Solitons*, Chap. 1, edited by S. E. Trullinger, V. E. Zakharov, and V. L. Prokovsky (Elsevier, New York, 1986).

[36] A. S. Davydov, *Biology and Quantum Mechanics* (Pergamon, Oxford, 1982).

[37] A. C. Scott, F. Y. F. Chu, and D. W. McLaughling, Proc. IEEE **61**, 1443 (1973).

[38] H. Fröhlich, 'Life as a Collective Phenomenon', in *Cooperative Phenomena*, Dedicated to Herbert Fröhlich, edited by H. Haken and M. Wagner (Springer, Berlin, 1973).

[39] S. Mascarenhas, Bioelectrets, in *Electrets*, edited by G. M. Sessler (Springer, Berlin, 1987).

[40] A. C. Scott, Phys. Rep **217**, 1 (1992).

[41] S. J. Webb, Phys. Rep. **60**, 201 (1980).

[42] A. J. Heger, S. Kivelson, J. R. Schrieffer, and W. P. Su, Rev. Mod. Phys. **60**, 781 (1988).

[43] A. S. Kivelson, in *Solitons*, edited by S. E. Trullinger, V. E. Zahkarov, and V. L. Prokovsky (Elsevier, New York, 1986), pp. 301-387.

[44] G. Careri, U. Buotempo, R. Carta, E. Gratton, and A. C. Scott, Phys. Rev. Lett. **51**, 304 (1983); G. Careri, U. Buotempo, F. Galluzzi, A. C. Scott, E. Gratton, and E. Shyamsunder, Phys. Rev. B **30**, 4869 (1984).

[45] A. R. Vasconcellos, M. V. Mesquita, and R. Luzzi, Phys. Rev. Lett. **80**, 2008 (1998).

[46] M. V. Mesquita, A. R. Vasconcellos, and R. Luzzi, Phys. Rev. E **58** (6), xxx (1998).

[47] A. R. Vasconcellos, M. V. Mesquita, and R. Luzzi, J. Biol. Phys., submitted.

[48] V. L. Ginsburg, Phys.-Uspekhi 2, 874 (1960); V. M. Agranovich and V. L. Ginsburg, *Spatial Dispersion in Crystal Optics and the Theory of Excitons* (Wiley-Interscience, London, 1966).

[49] J. Lu and J. F. Greenleaf, IEEE Trans. Ultrason. Ferroelect. Freq. Contr. **39**, 19 (1992); **39**, 441 (1992).

[50] W. A. Rodrigues and J. Lu, Found. Phys. **27**, 435 (1997).

[51] P. Davies, in *The New Physics*, edited by P. Davies (Cambridge Univ. Press, Cambridge, 1989).

[52] P. W. Anderson, Science **117**, 393 (1972).

[53] L. von Bertalanffy, *General Systems Theory*, 3rd ed. (Braziller, New York, 1968).

[54] H. Haken, *Synergetics* (Springer, Berlin, 1978).

[55] G. Nicolis and I. Prigogine, *Exploring Complexity* (Freeman, New York, 1989).

[56] H. Jeffrey, *Scientific Inference* (Cambridge Univ. Press, Cambridge, 1973).

[57] H. Jeffrey, *Probability Theory* (Clarendon, Oxford, 1961).

[58] R. Balescu, *Equilibrium and Nonequilibrium Statistical Mechanics* (Wiley-Interscience, New York, 1975).

[59] J. P. Dougherty, in *Maximum entropy and Bayesian Methods*, edited by J. Skilling (Kluwer, Dordrecht, 1989).

[60] J. P. Dougherty, Stud. Hist. Phil. Sci. **24**, 843 (1993).

[61] J. P. Dougherty, Phil. Trans. R. Soc. Lond. A **346**, 259 (1994).

[62] G. J. Hyland, Coherent GHz and THz Excitations in Active Biosystems, and their Implications, invited talk in the *Advances in Microwave Detection and Applications Workshop*, to be held in the University of São Paulo (São Paulo, Brazil, in the Autumn (Southern Hemisphere) of 1998). We thank Dr. Norman Grant (Matra-Marconi Space-United Kingdom) and Prof. Oswaldo Massambani (Univ. of São Paulo) for providing us in advance the invited talks' preprints to this workshop.

[63] P. F. Miller and H. A. Gebbie, Int. J. Infrared Milli. **17**, 1573 (1996).

358.

[64] D. Snoke, Science **273**, 1351 (1996).

[65] Mysyrowicz, E. Benson, and E. Fortin, Phys. Rev. Lett. **77**, 896 (1996).

[66] A. R. Vasconcellos, M. V. Mesquita, and R. Luzzi, Phys. Rev. Lett., submitted.

Authors' brief biographical information

Roberto Luzzi: Argentina born and educated. Ph. D. in Physics in 1966. Formely at Purdue University and the University of Southern California, is presently Professor of Physics at the State University of Campinas (UNICAMP). Visiting scientist in Universities of USA and Spain. 1976-John Simon Guggenheim Memorial Foundation Fellow. Member of the São Paulo Academy of Sciences, the NYAS, and the International Centre for Theoretical Physics.

Áurea Rosas Vasconcellos: Brazil born and educated. Ph. D. in Physics in 1976. Visiting Scientist in Universities of USA, Spain, and Belgium. Presently Associate Professor of Physics at UNICAMP.

Marcus Vinicius Mesquita: Brazil born and educated. Presently pre-Doctoral Fellow at the Institue of Physics, UNICAMP.

Our interest on the subject began after the invited talks by H. Fröhlich and I. Prigogine at the first meeting of *L'Institute de la Vie* in 1967, to which Prof. Sergio Mascarenhas (Institut for Advanced Studies, University of São Paulo at São Carlos) called our attention.

FIGURE CAPTIONS

Figure 1: An atomic model of the α-helix structure in a protein, and a rough description of the mechanical model we used (After first of Refs. [30]).

Figure 2: Infrared absorption spectra of acetanilide: curves with points are experimental data from reference [44], and full curves the result of theoretical calculations. Thermal bath temperature are 20 K, 50 K and 80 K, as indicated on the upper left (after Ref. [45]).

Figure 3: The solitary exciton spatial shape at several delay times after initial excitation. Bath temperature is 80 K and in the conditions of the experiment of [44], with $\gamma = 9.2 \times 10^{11}\ \mathrm{s}^{-1}$.

Figure 4: Shape of the solitary excitation: its space and time dependence in the conditions indicated in the caption to Fig. 2.

Figure 5: Normal sound propagation (upper figure), and the excitation interpreted as a supersonic soliton (lower figure); from reference [50] (We thank W. A. Rodrigues and J. E. Maiorino for providing us with a postscript file of this picture).

Figure 6: Comparison of the shape of the voltaic signal in [65] with the shape of the energy density of Schrödinger-Davydov's soliton [proportional to the squared modulus of the amplitude field of Eq. (2)] plus the contribution of the incoherent excitons [66].

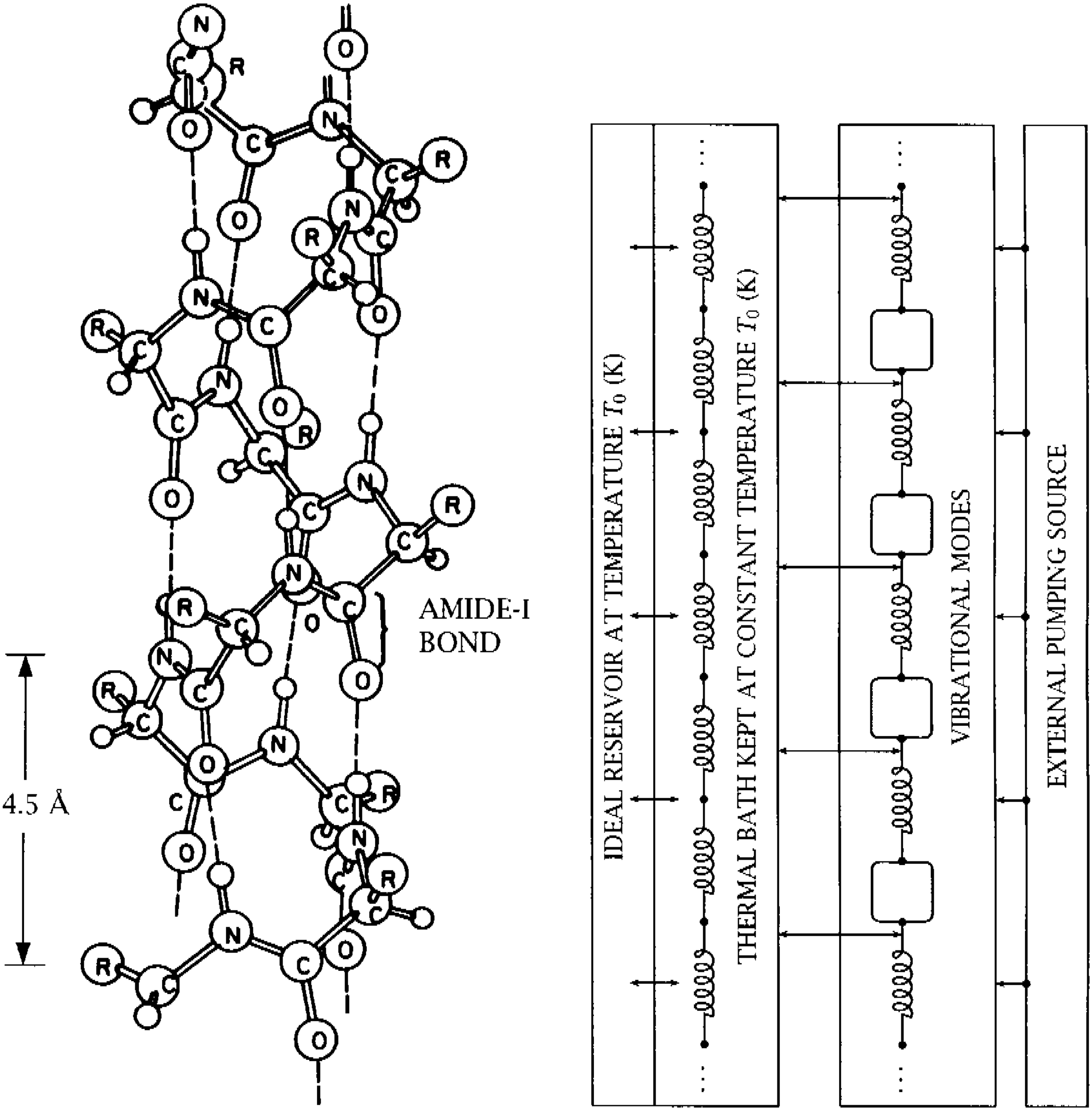

Figure 1: An atomic model of the α-helix structure in a protein, and a rough description of the mechanical model we used (After first of Refs. [30]).

MESQUITA *et al.* — *Contemp. Phys.* FIGURE 1

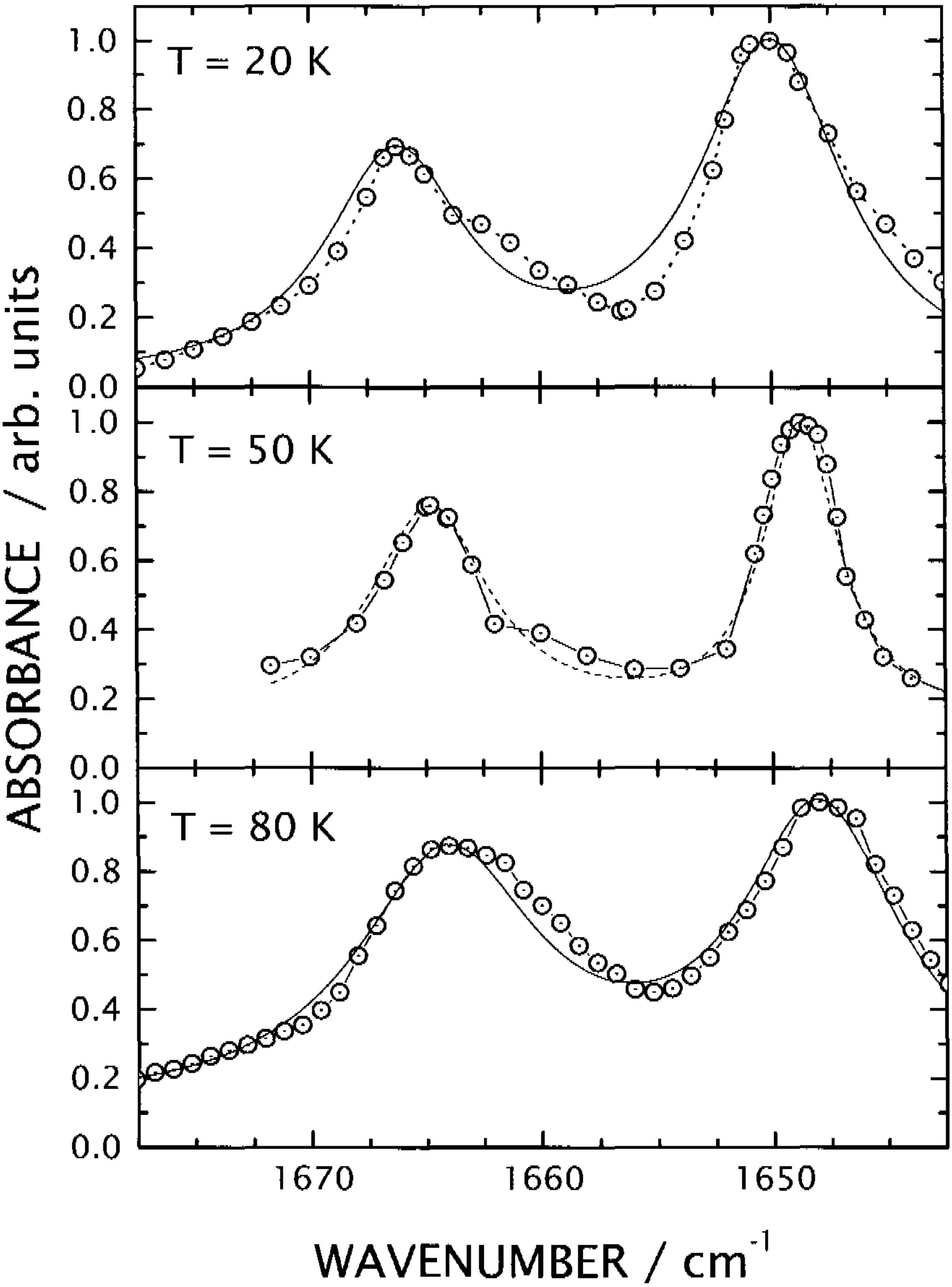

Figure 2: An Infrared absorption spectra of acetanilide: curves with points are experimental data from reference [44], and full curves the result of theoretical calculations. Thermal bath temperature are 20 K, 50 K and 80 K, as indicated on the upper left (after Ref. [45]).

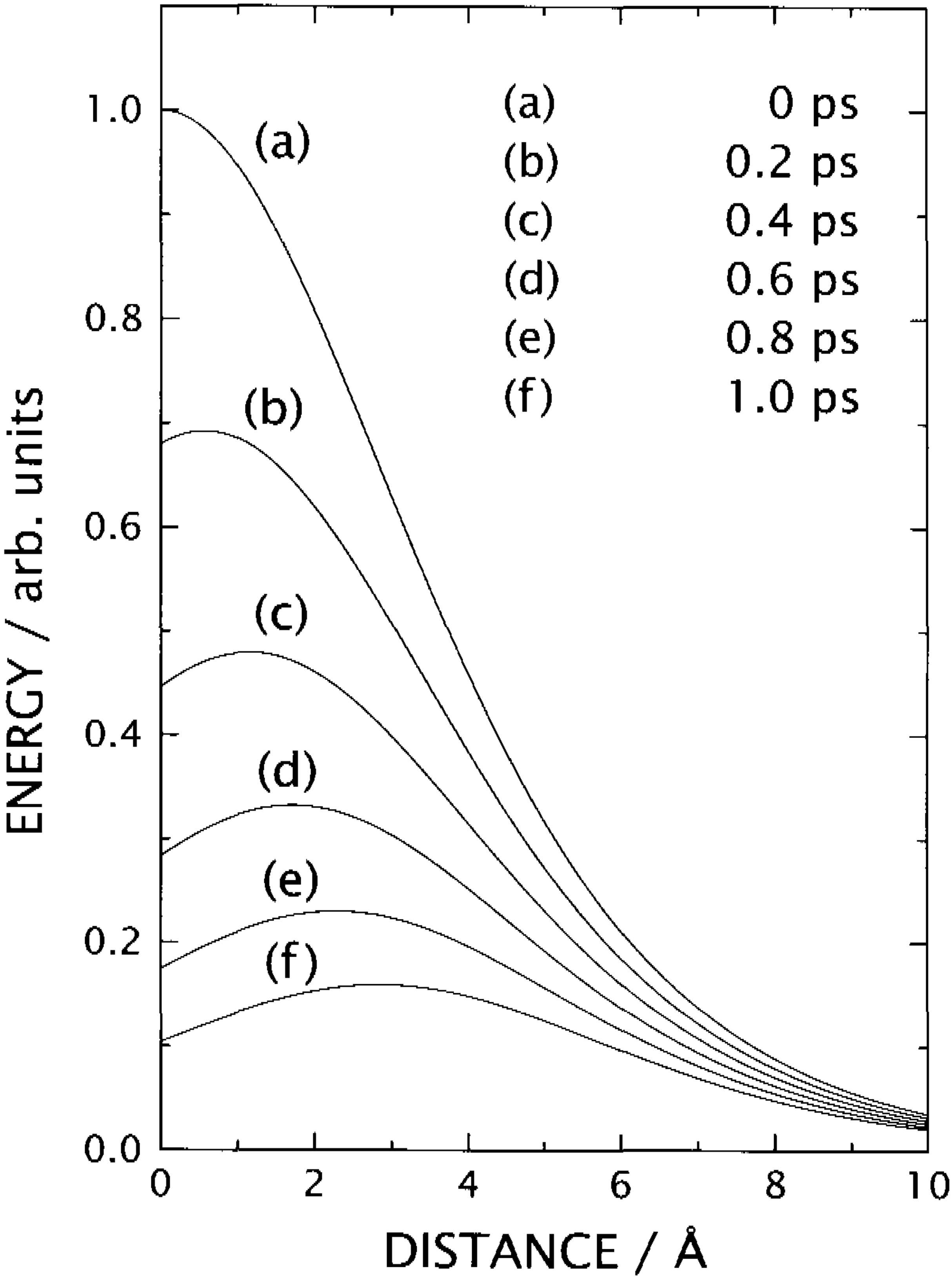

Figure 3: The solitary exciton spatial shape at several delay times after initial excitation. Bath temperature is 80 K and in the conditions of the experiment of [44], when $\gamma = 9.2 \times 10^{11}$ s ^{1}.

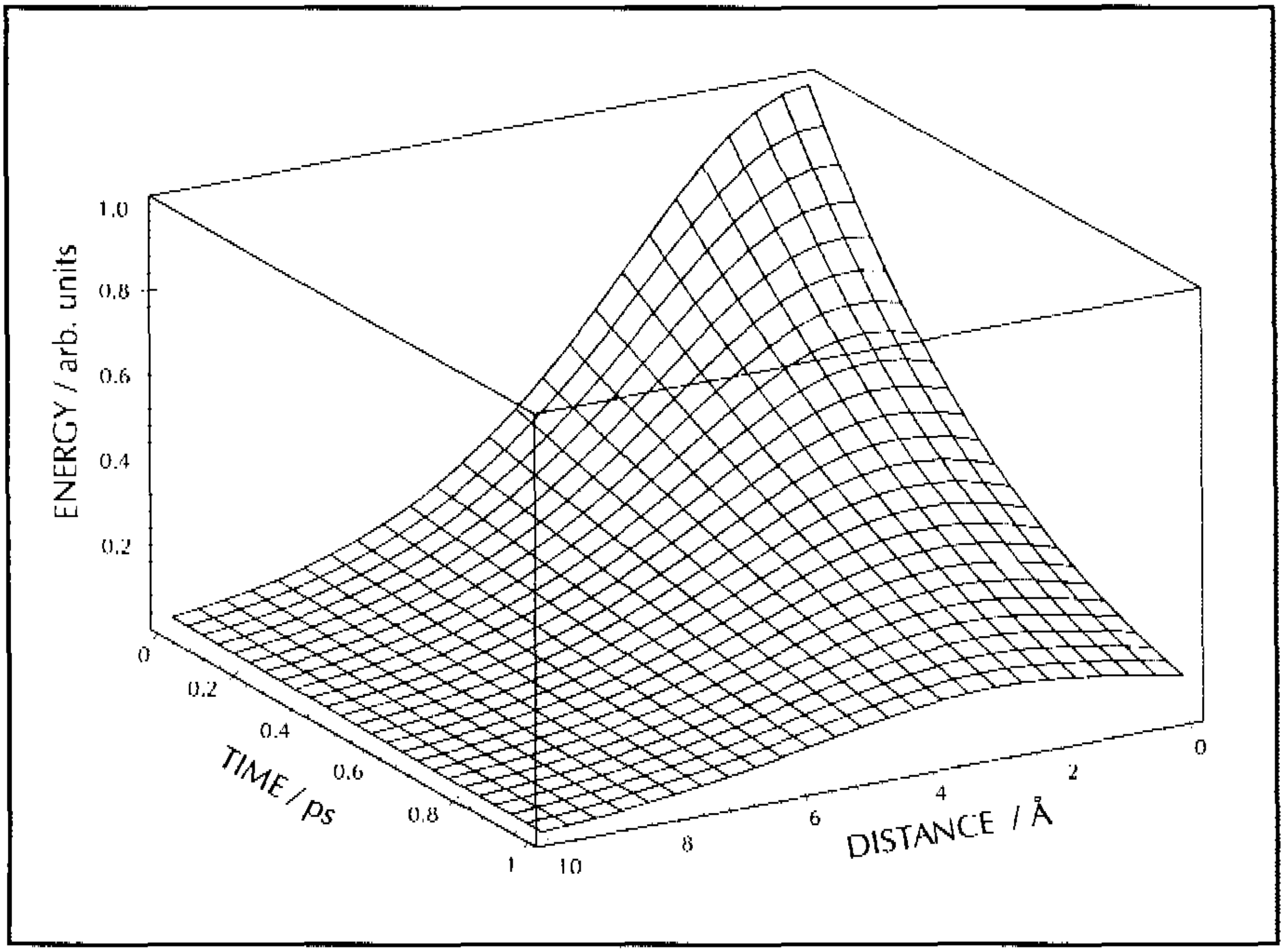

Figure 4: Shape of the solitary excitation: its space and time dependence in the conditions indicated in the caption to figure 2.

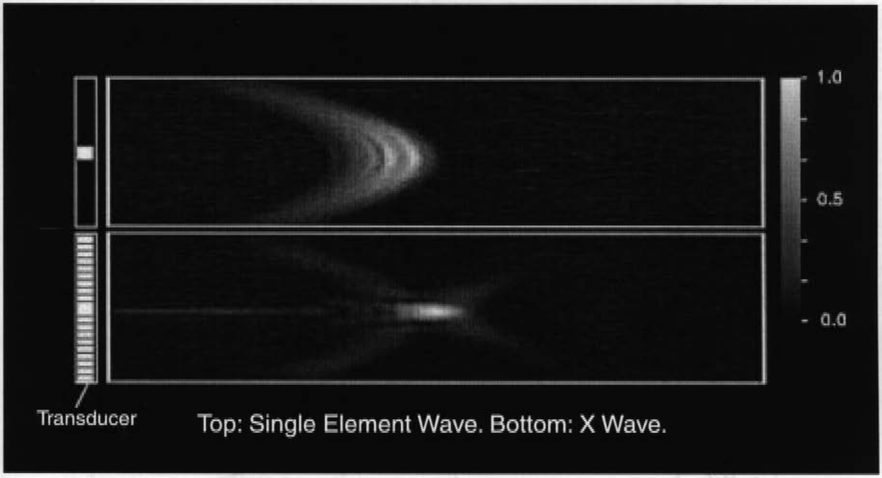

Figure 5: Normal sound propagation (upper figure), and the excitation interpreted as a supersonic soliton (lower figure); from reference [50] (We thank W. A. Rodrigues and J. E. Maiorino for providing us with a postscript file of this picture).

MESQUITA *et al.* — *Contemp. Phys.* FIGURE 5

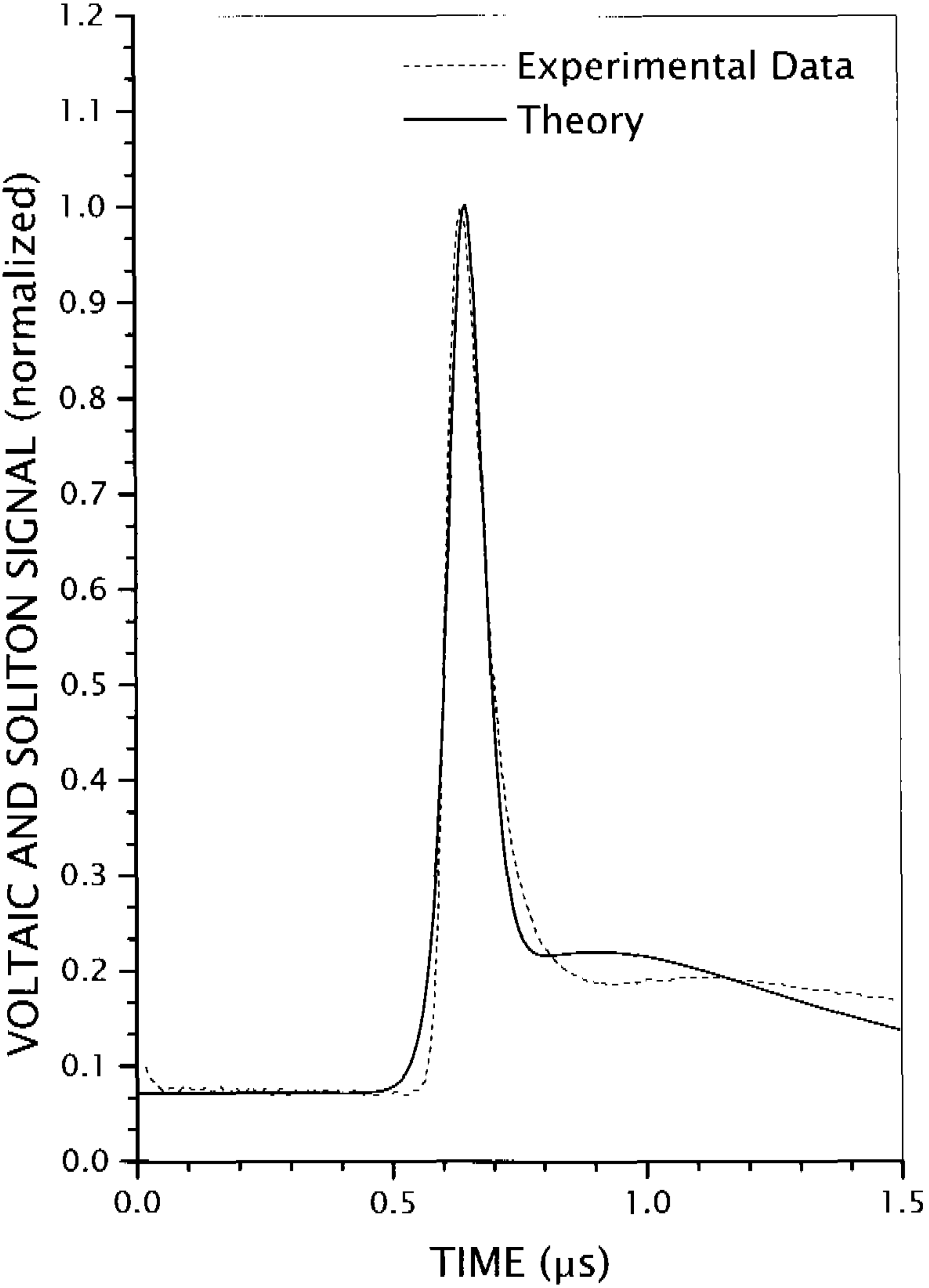

Figure 6: Comparison of the shape of the voltaic signal in [65] with the shape of the energy density of Schrödinger-Davydov's soliton [proportional to the squared modulus of the amplitude field of Eq. (2)] plus the contribution of the incoherent excitons [66].

6.3 Considerações sobre ondas X e sólitons de Davydov em ultrasonografia

Pesquisa recente em ultrasonografia evidenciou a propagação de um tipo peculiar de excitação em fluidos. Tal excitação, denominada onda X, tem características que se assemelham às de uma onda solitária. Considerando sua possível relevância para o melhoramento de imagens para diagnóstico médico via ultrasom, reconsideramos o problema em um meio que consiste em um material biológico do tipo proteínas que apresentam a estrutura da hélice α. Pode ser mostrado que neste caso é esperada uma excitação do tipo onda solitária de Davydov, contudo fortemente amortecida em condições normais. O caso da acetanilida, um polímero orgânico que se assemelha a biopolímeros, é considerado, e o espectro infravermelho analisado. O sóliton de Davydov é evidenciado como um estado coerente de vibrações polares. O caso de vibrações acústicas também é considerado aqui, onde, também, uma onda solitária amortecida de Davydov pode ser excitada. Contudo, é mostrado que quando propagando-se em condições suficientemente longe do equilíbrio, o tempo de vida da onda solitária é bastante ampliado. Além disso, um sóliton movendo-se com uma velocidade maior do que a velocidade de grupo das ondas vibracionais normais produzem uma emissão de fonons que dão origem ao padrão tipo onda X que é observado experimentalmente.

Submetido para publicação em *Journal of Biological Physics*.

Considerations on X-Waves and Davydov Solitons in Ultrasonography

Marcus V. Mesquita, Áurea R. Vasconcellos, Roberto Luzzi

Instituto de Física 'Gleb Wataghin',
Universidade Estadual de Campinas, Unicamp
13083-970 Campinas, São Paulo, Brazil

370.

Recent research in ultrasonography has evidenced the propagation of a peculiar kind of excitation in fluids. [Lu and Greenleaf, IEEE Trans. on Ultrasonics Ferroeletrics and Frequency Control, 39, 441–446 (1992)]. Such excitation, dubbed a X-wave, has characteristics resembling that of a solitary-wave type. Considering its possible relevance for improving ultrasound medical imaging, we reconsider the problem in a medium consisting of a biological material of the like of α-helix proteins. It can be shown that in this case is expected an excitation of the Davydov's solitary wave type, however strongly damped in normal conditions. The case of acetanilide, an organic polymer which resembles biopolymers, is considered, and the infrared spectrum analyzed. Davydov's soliton is evidenced as a coherent state of polar vibrations. The case of acoustic (sound) vibrations is also considered, where, also, a damped Davydov-like solitary wave may be excited. However, it is shown that when traveling in conditions sufficiently away from equilibrium,the lifetime of the solitary wave is largely enhanced. Moreover, a soliton moving in bulk with a velocity larger than that of the group velocity of the normal vibrational waves would produce a Cherenkov-like emission of phonons giving rise to the observed X-wave-like pattern.

Group Home Page: http://www.ifi.unicamp.br/~aurea

1. Introduction

Recently, experiments in ultrasonography have evidenced a particular kind of wave propagation, dubbed as X-waves [1,2]. They have the characteristic of propagating without dispersion, and may result of relevance for ultrasound medical imaging. Later on, they were ascribed to some kind of the so-called undistorted propagating waves [3]. They are waves traveling in a material media, and the reported characteristics point to the possibility of they belonging to the category of *solitary waves. Soliton* is the name coined to describe a pulse-like nonlinear wave (the solitary wave referred to above) which emerges from a collision with a similar pulse having unchanged shape or speed. Its relevance in applied sciences has been described in a 1973 review paper by A. C. Scott *et al.* [4] Because of the above mentioned technological/medical relevance we reanalyze the question in the case of propagation in biological materials.

The original category of solitary waves consists in the one observed by the Scottish engineer Scott-Russell in August 1834 in an English water channel, and reported in a 1844 meeting of the British Society for the Advancement of Science [5,6]. During the second half of this century many other types of solitary waves have been associated to a number of physical situations in condensed matter physics. Several, seemingly, have a fundamental role in important technological areas of large relevance for contemporary society. Among them we may highlight the case of doped organic polymers with very large conductivity for, e. g., use in very light, almost two-dimensional (sheets) batteries [7-9], and the case of propagation of light in optical fibers [10]. Another example is that of the so-called Davydov's solitons [11,12], which may have a quite relevant role in bioenergetics.

Davydov's theory has received plenty of attention, and a long list of results published up to the first half of 1992 are discussed in a comprehensive review due to A. C. Scott [13]. As pointed out in that review, one question concerning Davydov's soliton is that of its stability at normal physiological conditions, that is, the ability of the excitation to transport energy (and so information) at long distances in the living organism, in spite of the relaxation mechanisms that are expected to damp it out at very short (micrometers) distances. On the assumption that the X-waves in ultrasonography may belong to the category of solitary waves in the material media, we consider this question on the basis of a model in nonequilibrium thermodynamic conditions, since any biological system is an open system out of thermal equilibrium. For that purpose we resort to an informational statistical thermodynamics (see for example [14–16]), based on the Nonequilibrium Statistical Operator Method (NESOM) [17–20]. The NESOM, which provides microscopic foundations to phenomenological irreversible thermodynamics [21], also allows for the construction of a nonlinear generalized quantum transport theory — a far-reaching generalization of the Chapman-Enskog's and Mori's methods — which describes the evolution of the system at the macroscopic level in arbitrary nonequilibrium situations [17, 18, 22, 23], a formalism to be used in what follows. We notice that the method has been applied with particular success to the study of optical and transport properties in solids [24] and also to modelled biopolymers [25, 26], of the kind we consider here, and to techno-industrial processes [27]. Consequently, we do not go over the details of the formalism, just adapting those earlier results for the present discussion, giving in each case the reference where they are reported. We separate the presentation into two parts: After a general derivation of the equations of evolution, a first analysis is concentrated on the case of polar vibrations (with frequencies in the infrared region of the spectrum), for which are available experimental results, particularly the case of acetanilide, which we analyze, comparing theory and experiment. This is done in subsection 2.1, while in subsection 2.2 we deal with the case of longitudinal acoustic vibrations.

As stated, we first consider a system where modes of polar vibrations are excited by a continuous supply of energy. These polar modes are coupled through a nonlinear kinetics with a bath consisting of a continuous medium modelled by a system of acoustic-like vibrations. The equations of evolution for the population of the vibrational modes are derived resorting to the nonlinear quantum kinetic theory that the NESOM provides. This corresponds to the description of polar vibrations of the CO-stretching type (Amide-I) in, for example, α-helix proteins [11–13]. Experiments, of the class of Raman or neutron scattering or radiation absorption, in active biological systems are particularly difficult. For that reason, the comparison of the theory of next section with experiment is done in the case of the organic polymer acetanilide, which constitutes a good mimic of biopolymers [28]. The infrared spectrum in the frequency region corresponding to the CO-stretching oscillation is derived, and compare very well with the experimental measurements, confirming the presence of *Davydov's soliton.* Finally, we comment on the possibly very large increase of the lifetime of Davydov's soliton when propagating in an open medium sufficiently far from equilibrium.

In subsection 2.2, we consider a system of longitudinal acoustic vibrations in interaction with the above said thermal bath. We find a behavior of the acoustic modes quite similar to the one evidenced for the optical modes, namely, existence of the solitary-wave excitation, damped near equilibrium conditions but whose lifetime is greatly enhanced when propagating in a highly excited background.

Finally, it is demonstrated the possible emergence of a particular phenomenon, which we call *Fröhlich-Cherenkov effect*, consisting in that when the soliton is propagating with a velocity larger than the group velocity of the normal modes of vibration in the medium, a large number of phonons are emitted at a certain angle with the direction of propagation of the soliton.

2. The Solitary Wave

Let us consider a model biosystem which can sustain longitudinal vibrations and in interactions with a thermal bath of acoustic-like vibrations, which is described by the so-called Fröhlich-Davydov Hamiltonian given in [11] and [25]: This Hamiltonian is given in the so-called Random Wave Approximation, while the full Hamiltonian — to be used in what follows — is given by

$$H = H_0 + H_I = H_{0S} + H_{0B} + H_I \ , \tag{1}$$

where

$$H_{0S} = \sum_q \hbar\omega_q (a_q^\dagger a_q + \frac{1}{2}) \ , \tag{2a}$$

$$H_{0B} = \sum_{q} \hbar\Omega_{q}(b_{q}^{\dagger}b_{q} + \frac{1}{2}) , \tag{2b}$$

$$\begin{aligned} H_{I} = {} & \sum_{q} Z_{q}\varphi_{q}a_{q}^{\dagger} + \sum_{q_1q_2} V_{q_1q_2}^{(1)} a_{q_1} b_{q_2} b_{q_1+q_2}^{\dagger} + \sum_{q_1q_2} V_{q_1q_2}^{(1)} a_{q_1} b_{q_2}^{\dagger} b_{-q_1+q_2} \\ & + \sum_{q_1q_2} V_{q_1q_2}^{(1)} a_{q_1} b_{q_2} b_{-q_1-q_2} + \sum_{q_1q_2} V_{q_1q_2}^{(1)} a_{q_1} b_{q_2}^{\dagger} b_{q_1-q_2}^{\dagger} + \sum_{q_1q_2} V_{q_1q_2}^{(2)} a_{q_1} a_{q_2} b_{q_1+q_2}^{\dagger} \\ & + \sum_{q_1q_2} V_{q_1q_2}^{(2)} a_{q_1} a_{q_2} b_{-q_1-q_2} + \sum_{q_1q_2} V_{q_1q_2}^{(2)} a_{q_1}^{\dagger} a_{q_2} b_{q_1-q_2} + \sum_{q_1q_2} V_{q_1q_2}^{(2)} a_{q_1} a_{q_2}^{\dagger} b_{q_1-q_2}^{\dagger} + \text{H.c.} \end{aligned} \tag{2c}$$

Figure 1 in [25] describes a particular biological system and the mechanical analog we are using. The Hamiltonian consists of the energy of the free subsystems, namely, that of the free vibrations, with $\omega_{\boldsymbol{q}}$ being their frequency dispersion relation ($\boldsymbol{q}$ is a wave-vector running over the reciprocal-space Brillouin zone), and that of the thermal bath composed by oscillations with frequency dispersion relation $\Omega_{\boldsymbol{q}}$, with a Debye cut-off frequency Ω_D. The interaction Hamiltonian H_I contains the interaction of the system of polar vibrations with an external source [which pumps energy on the system and is the first term on the right side of Eq. (2c)], and, finally, the anharmonic interactions between both subsystems. The latter are composed of several contribution, namely, those associated with three quasi-particle (phonons) collisions involving one of the system and two of the thermal bath (we call $V_{qq'}^{(1)}$ the corresponding matrix element), and two of the system and one of the bath (we call $V_{qq'}^{(2)}$ the corresponding matrix element). Finally, $a_{\boldsymbol{q}}$ ($a_{\boldsymbol{q}}^{\dagger}$), $b_{\boldsymbol{q}}$ ($b_{\boldsymbol{q}}^{\dagger}$), are, as usual, annihilation (creation) operators of, respectively, normal-mode vibrations in the system and bath in mode $\boldsymbol{q}$, and the one corresponding to the quantum excitations in the pumping source, with Z being the coupling strength.

Next step consists in the choice, within the tenets of NESOM, of the basic set of dynamical variables relevant for the present problem. Since we are dealing with excitation of vibrations in modes $\boldsymbol{q}$ (with energy $\hbar\omega_{\boldsymbol{q}}$), we need to introduce the number of excitations in each mode, $\hat{\nu}_{\boldsymbol{q}} = a_{\boldsymbol{q}}^{\dagger}a_{\boldsymbol{q}}$. Moreover, once the formation of a coherent state is expected (Davydov's soliton), we must introduce the field amplitudes $a_{\boldsymbol{q}}$ and $a_{\boldsymbol{q}}^{\dagger}$. Finally, since the thermal bath is taken as remaining constantly in a stationary state at a temperature T_0, via an efficient homeostatic mechanism, we introduce its Hamiltonian, H_B. The average of these quantities over the NESOM nonequilibrium ensemble constitute the basic set of macrovariables, which we designate as

$$\left\{\nu_q(t),\, \langle a_q^\dagger|t\rangle,\, \langle a_q|t\rangle,\, E_B\right\}, \tag{3}$$

that is, they define Gibbs's space of nonequilibrium thermodynamic states. This is the thermodynamic state space in Informational Statistical Thermodynamics (IST for short). IST is the thermodynamic theory for irreversible processes based on the nonequilibrium ensemble formalism NESOM [14–16]. The basic thermodynamic macrovariables of Eq. (3) are then given by

$$\nu_q(t) = \mathrm{Tr}\left\{\hat{\nu}_q \varrho(t)\right\} ; \tag{4a}$$

$$\langle a_q|t\rangle = \mathrm{Tr}\left\{a_q \varrho(t)\right\} ; \tag{4b}$$

$$\langle a_q^\dagger|t\rangle = \langle a_q|t\rangle^* = \mathrm{Tr}\left\{a_q^\dagger \varrho(t)\right\} ; \tag{4c}$$

$$E_B = \mathrm{Tr}\left\{\hat{H}_B \varrho_B\right\} \tag{4d}$$

where $\varrho(t)$ is the nonequilibrium statistical operator of the system, and ϱ_B the canonical distribution of the thermal bath at temperature T_0. The statistical operator $\varrho(t)$ is taken in Zubarev's approach [17, 18], in this case given by

$$\varrho(t) = \mathrm{e}^{-\hat{S}_\varepsilon(t)} \tag{5}$$

where

$$\hat{S}_\varepsilon(t) = \hat{S}(t,0) - \int_{\infty}^{t} dt'\, \mathrm{e}^{\varepsilon(t'-t)} \frac{d}{dt'} \hat{S}(t', t'-t), \tag{6a}$$

with

$$\hat{S}(t,0) = \phi(t) + \sum_q \left[F_q(t)\hat{\nu}_q + f_q(t) a_q + f_q^*(t) a_q^\dagger\right] \tag{6b}$$

being the so-called informational-statistical-entropy operator [29],

$$\hat{S}(t',t'-t) = \exp\left\{-\frac{1}{i\hbar}(t'-t)H\right\}\hat{S}(t,0)\exp\left\{\frac{1}{i\hbar}(t'-t)H\right\}, \tag{6c}$$

and ε is a positive infinitesimal that goes to zero after the calculation of averages has been performed [17–22]. Moreover, $\phi(t)$ — playing the role of a nonequilibrium partition function — ensures the normalization of the statistical operator.

In Eq. (6b) are present the Lagrange multipliers that the method introduces, namely those we have called

$$\left\{F_{q}(t),\, f_{q}(t),\, f_{q}^{*}(t),\, \beta_{0}\right\}, \tag{7}$$

where $\beta_0 = (k_B T_0)^{-1}$, since the thermal bath remains in a stationary state at fixed temperature T_0, and the total statistical operator is the direct product of $\varrho(t)$ and ϱ_B; k_B is Boltzmann universal constant.

In continuation we proceed to derive, in the corresponding NESOM nonlinear quantum kinetic theory [17–23] the equations of motion for the basic variables of Eq. (3). Since β_0 is assumed to be constant in time, and so is E_B, we are simply left to calculate the equations of evolution for the population of the vibrational modes, $\nu_q(t)$, and of the amplitude $\langle a_q|t\rangle$ and its complex conjugate. As noticed, these equations are derived resorting to the nonlinear quantum generalized transport theory that the NESOM provides. We introduce an approximated treatment, however appropriate for the present case since the anharmonic interactions are weak, consisting of the so-called second order approximation in relaxation theory, SOART for short [22]. It is usually referred to as the quasi-linear theory of relaxation [30], which is a Markovian approximation involving only the second order in the interaction strengths [22], in the present case involving contributions proportional to $|V_{qq'}^{(1)}|^2$ and $|V_{qq'}^{(2)}|^2$.

The calculation shows that, because of the symmetry properties of the system and the selected choice of basic variables, several contributions in NESOM-SOART vanish in this case: The surviving one corresponds to the Golden Rule of quantum mechanics averaged over the nonequilibrium ensemble [25]. In compact form, the one for the population is

$$\frac{d}{dt}\nu_q(t) = I_q + \sum_{j=1}^{5} J_{q_{(j)}}(t) + \zeta_q(t), \tag{8}$$

where the first term on the right hand side is the one associated to the pumping source, where I_q is then the rate of population increase that it generates, and the remaining five collisions operators $J_{q_{(i)}}(t)$ are those arising out of the anharmonic interactions. The first two correspond to collisional events involving a single vibration and two of the bath, and gives rise to a pure dissipative term which takes the form

$$J_{q_{(1)}}(t) + J_{q_{(2)}}(t) = -\frac{1}{\tau_q}\left[\nu_q(t) - \nu_q^{(0)}\right], \tag{9}$$

where $\nu_q^{(0)}$ is the population in equilibrium at temperature T_0, and τ plays the role of a relaxation time given by

$$\tau_q^{-1} = \frac{4\pi}{\hbar^2}\frac{1}{\nu_q^{(0)}}\sum_{q'} |V_{qq'}^{(1)}|^2 \nu_{q'}^B \nu_{q-q'}^B \left[\delta(\Omega_{q'} + \Omega_{q-q'} - \omega_q) + 2e^{\beta\hbar\Omega_{q'}}\delta(\Omega_{q'} - \Omega_{q-q'} + \omega_q)\right], \tag{10}$$

where ν_q^B is the population of the phonons in the bath, namely, the Planck distribution

$$\nu_q^B = [\exp(\beta_0\hbar\Omega_q) - 1]^{-1}, \tag{11}$$

and the delta functions account for conservation of energy in the scattering events. The other terms, $J_{q_{(i)}}(t)$ with $i = 3, 4, 5$, are

$$J_{q_{(3)}}(t) = \frac{8\pi}{\hbar^2}\sum_{q'} |V_{qq'}^{(2)}|^2 \left[\nu_{q-q'}^B(\nu_{q'} - \nu_q) - \nu_q(1 + \nu_{q'})\right]\delta(\Omega_{q-q'} + \omega_{q'} - \omega_q), \tag{12a}$$

$$J_{q_{(4)}}(t) = \frac{8\pi}{\hbar^2}\sum_{q'} |V_{qq'}^{(2)}|^2 \left[\nu_{q-q'}^B(\nu_{q'} - \nu_q) + \nu_{q'}(1 + \nu_q)\right]\delta(\Omega_{q-q'} - \omega_{q'} + \omega_q), \tag{12b}$$

$$J_{q_{(5)}}(t) = \frac{8\pi}{\hbar^2}\sum_{q'} |V_{qq'}^{(2)}|^2 \left[\nu_{q+q'}^B(1 + \nu_{q'}) - (\nu_{q'} - \nu_{q+q'}^B)\nu_q\right]\delta(\Omega_{q+q'} - \omega_{q'} - \omega_q), \tag{12c}$$

and, finally, the term $\zeta_q(t)$ is the one which couples the populations with the amplitudes, namely

$$\begin{aligned}
\zeta_q(t) &= \frac{4\pi}{\hbar^2}\sum_{q'}|V^{(1)}_{qq'}|^2|\langle a_q|t\rangle|^2\Big\{(1+\nu^B_{q'}+\nu^B_{q-q'})\delta(\Omega_{q-q'}+\Omega_{q'}-\omega_{q'}) \\
&\qquad\qquad + 2(\nu^B_{q'}-\nu^B_{q-q'})\delta(\Omega_{q-q'}-\Omega_{q'}-\omega_{q'})\Big\} \\
&+\frac{8\pi}{\hbar^2}\sum_{q'}|V^{(2)}_{qq'}|^2\Big\{|\langle a_q|t\rangle|^2(1+\nu_{q'}+\nu^B_{q-q'})-|\langle a_{q'}|t\rangle|^2(\nu_q-\nu^B_{q-q'})\Big\}\delta(\Omega_{q-q'}+\omega_{q'}-\omega_q) \\
&-\frac{8\pi}{\hbar^2}\sum_{q'}|V^{(2)}_{qq'}|^2\Big\{|\langle a_q|t\rangle|^2(\nu_{q'}-\nu^B_{q-q'})-|\langle a_{q'}|t\rangle|^2(1+\nu_q+\nu^B_{q-q'})\Big\}\delta(\Omega_{q-q'}-\omega_{q'}+\omega_q) \\
&+\frac{8\pi}{\hbar^2}\sum_{q'}|V^{(2)}_{qq'}|^2\Big\{|\langle a_q|t\rangle|^2(\nu_{q'}-\nu^B_{q+q'})-|\langle a_{q'}|t\rangle|^2(\nu_q-\nu^B_{q+q'})\Big\}\delta(\Omega_{q+q'}-\omega_{q'}-\omega_q)\,.
\end{aligned} \tag{12d}$$

The collision operator $J_{q(5)}$ is also a relaxation term (containing contributions nonlinear in the mode populations); and the first two terms are those responsible for the so-called *Fröhlich effect*, as a result that they account for, through the nonlinear terms, of the transfer of energy to the polar modes lowest in frequency. In fact, they contain nonlinear contributions proportional to

$$\sum_{q'}|V^{(2)}_{qq'}|^2\nu_q(t)\nu_{q'}(t)\Big[\delta(\Omega_{q-q'}-\omega_{q'}+\omega_q)-\delta(\Omega_{q-q'}+\omega_{q'}-\omega_q)\Big]\,, \tag{13}$$

and we may notice that for modes $\boldsymbol{q}'$ such that $\omega_{q'} > \omega_q$ the energy conservation as required by the first delta function is satisfied, while this is not possible for the second: hence this nonlinear contribution tends to increase the population in mode $\boldsymbol{q}$ at the expenses of the other modes higher in frequency. Reciprocally, for $\omega_{q'} < \omega_q$, the mode $\boldsymbol{q}$ transfers energy to the modes lower in frequency. Moreover, in Eq. (12d) the term $\zeta_q(t)$ acts as a source coupling the populations of the vibrational modes with the amplitudes of the expected coherent excitation (Davydov's soliton as shown a posteriori).

On the other hand, the equations of evolution for the field amplitudes are

$$\frac{\partial}{\partial t}\langle a_q|t\rangle = -\mathrm{i}\,\tilde{\omega}_q\,\langle a_q|t\rangle - \Gamma_q\,\langle a_q|t\rangle + \Gamma_q\,\langle a_q\,|t\rangle^* - \mathrm{i}W_q\,\langle a_q\,|t\rangle^* +$$

$$+\sum_{q_1q_2} R_{q_1q_2}\langle a_{q_1}|t\rangle\langle a^\dagger_{q_2}|t\rangle\left(\langle a_{q-q_1+q_2}|t\rangle + \langle a^\dagger_{-q+q_1-q_2}|t\rangle\right), \tag{14a}$$

$$\frac{\partial}{\partial t}\langle a^\dagger_q|t\rangle = \text{the c.c. of the r.h.s. of Eq. (14a)}, \tag{14b}$$

where $\tilde{\omega}_q = \omega_q + W_q$, with W_q being a term of renormalization of frequency which will not be of interest in the following analysis, and the lengthy expression for $R_{q_1q_2}$ is given elsewhere [26]; its detailed expression is unnecessary for the analysis here. Finally, $\Gamma_q(t)$, which has a quite relevant role in what follows, is given by

$$\Gamma_q(t) = \frac{1}{2}\tau_q^{-1}(t) + \frac{4\pi}{\hbar^2}\sum_{q'}|V^{(2)}_{qq'}|^2\left[1 + \nu_{q'} + \nu^B_{q\ \ q'}\right]\delta(\Omega_{q-q'} + \omega_{q'} - \omega_q) +$$

$$-\frac{4\pi}{\hbar^2}\sum_{q'}|V^{(2)}_{qq'}|^2\left[\nu_{q'} - \nu^B_{q-q'}\right]\delta(\Omega_{q-q'} - \omega_{q'} + \omega_q) +$$

$$\frac{4\pi}{\hbar^2}\sum_{q'}|V^{(2)}_{qq'}|^2\left[\nu_{q'} - \nu^B_{q+q'}\right]\delta(\Omega_{q+q'} - \omega_{q'} - \omega_q)\,. \tag{15}$$

The coupled equations (14) contain linear and tri-linear terms. Ignoring the latter, the resulting linearized equation has as solutions the normal damped wave motion, proceeding with a renormalized frequency and lifetime Γ_q^{-1}. The complete equations, i.e. including the nonlinear terms, are of the Davydov's soliton type, but with damping, or more precisely, are nonlinear damped Schrödinger-like equations [4, 31]. We introduce a representation in direct space, defining the averaged (over the nonequilibrium ensemble) field operator

$$\psi(x,t) = \sum_q\langle a_q|t\rangle \mathrm{e}^{\mathrm{i}qx}. \tag{16}$$

for linear propagation along the, say, x direction on bulk or along the one-dimensional polymer.

2.1. Polar (Optical) Vibrational Modes

At this point we introduce a first type of analysis, specifying the vibrational modes as being of the class of longitudinal polar-modes (optical modes with frequencies in the infrared), as in Davydov's and Fröhlich's works [11, 12, 32, 33]. Their frequency dispersion relation is approximated (to a good degree of accuracy) by the parabolic-law $\omega_q = \omega_0 - \alpha q^2$, where ω_0 and α are constants, standing for the frequency at the zone centre (the maximum one) and the curvature at this centre, respectively. Next, using Eqs. (14), after neglecting the coupling terms with the conjugated amplitude (what can be shown to be the case when we introduce from the outset a truncated Hamiltonian in the so-called Rotating Wave Approximation [34]), it follows that the average field amplitude satisfies the equation

$$i\hbar\frac{\partial}{\partial t}\psi(x,t) = (\hbar\omega_0 + \hbar\alpha\frac{\partial^2}{\partial x^2})\psi(x,t) - i\hbar\int_0^L \frac{dx'}{L}\,\Gamma(x-x')\psi(x',t) + \\ + \int_0^L \frac{dx'}{L}\int_0^L \frac{dx''}{L}\,\mathcal{R}(x-x', x-x'')\psi(x',t)\psi(x'',t)\psi^*(x,t), \quad (17)$$

where Γ and $\mathcal{R}$ are the back-transforms to direct space of Γ_q in Eq. (15) and $R_{q_1 q_2}$ in Eq. (14a), and L is the length of the sample. Moreover, we have taken a time-independent population ν_q, that is, according to Eq. (8) it is either the equilibrium distribution at temperature T_0 when no external pumping source is present (i. e. $I_q(\omega_q) = 0$), or when in the presence of a constant pumping source leading, after a short transient has elapsed, to a steady state and, moreover, the term ζ_q is weakly dependent on time (a condition to be characterized *a posteriori*).

Equation (17) is a nonlinear Schrödinger-type equation with damping [31]. Introducing a local approximation, that is, neglecting space correlations, after using the expressions

$$\mathcal{R}(x-x', x-x'') = \hbar G\delta(x-x')\delta(x-x''), \quad (18a)$$

$$\Gamma(x-x') = \gamma_s\delta(x-x'), \quad (18b)$$

we obtain that Eq. (17) becomes

$$\mathrm{i}\frac{\partial\psi(x,t)}{\partial t} - (\omega_0 - \mathrm{i}\gamma_s)\psi(x,t) - \alpha\frac{\partial^2}{\partial x^2}\psi(x,t) - G\,|\psi(x,t)|^2\,\psi(x,t) = 0, \qquad (19)$$

Equations (14) and (19) are of the form of the equations derived by Davydov in an alternative way, but, with the present thermodynamic treatment clearly showing the damping effects. In equilibrium conditions at temperature 300 K, the damping constants have values corresponding to lifetimes in the order of a few picoseconds. For the case of a Gaussian signal impinged at the beginning of the polymer chain, which can be approximated to a good degree of accuracy by a hyperbolic secant shape, and next using the Inverse Scattering Method [35] we obtain the solution

$$\psi(x,t) = \mathcal{A}\exp\left\{\mathrm{i}\left[\frac{\upsilon}{2\alpha}x - (\omega_s - \mathrm{i}\gamma_s)\,t - \frac{\theta}{2}\right]\right\}\operatorname{sech}\left[\mathcal{A}\left(\frac{|G|}{2\alpha}\right)^{1/2}(x - \upsilon t)\right], \qquad (20)$$

where γ_s is, evidently, the reciprocal lifetime of the excitation (taking $\gamma_s = 0$ and $\omega_0 = 0$, Eq. (20) is the expression for Davydov's soliton in its original version [11, 12]), and we used $G = |G|\mathrm{e}^{\mathrm{i}\theta}$. Moreover,

$$\omega_s = \omega_0 - \frac{\upsilon^2}{4\alpha} + \frac{|G|\,\mathcal{A}^2}{2}, \qquad (21)$$

is the reciprocal period of the solitary wave and $\mathcal{A}$ and υ are an amplitude and a velocity of propagation fixed by the initial condition of excitation imposed by the external source.

Hence, it is proved the possible presence of Davydov's solitons in polymers, like the α-helix protein in biological matter, but, we stress, of a damped character. The mechanism for the formation of the soliton is in this case interpreted as follows [13]: Vibrational energy of the CO-stretching (Amide-I) oscillators that is localized on the quasi-periodic helix acts — through a phonon coupling effect — to distort the structure of the helix. The helical distortion reacts — again through phonon coupling — to trap the Amide-I oscillation and prevents its dispersion in a self-trapping.

Let us consider the experimental observation of this excitation. As already noticed, experimental observation is difficult in active biological materials. A way around this difficulty consists into the experimental study of polymers whose vibronic characteristics resemble those of biopolymers, and a quite favorable one is acetanilide. Experiments of infrared absorption in acetanilide showed an "anomalous" band in the IR spectrum, which was ascribed to a Davydov's soliton [36], and later on reproduced in other experiments, and also observed in Raman scattering experiments [37–41].

We analyze the experiment of Careri *et. al* [36], resorting to a response function theory consistently derived in the framework of NESOM [19, 42, 43]. Without going into details (see [51]), the absorbance in the region of the CO-stretching mode has the expression

$$\alpha(\omega) = \alpha_n(\omega) + \alpha_s(\omega), \tag{22}$$

which describes two bands: one centered around ω_q, the frequency of the normal mode, ($\boldsymbol{q}$ being equal to the IR-photon wave-vector) and with intensity proportional to the population in equilibrium ν_q at temperature T_0, since no external pump is present, $I_q = 0$ in Eq. (8); and the other is centered around ω_s, the frequency of the soliton. The band widths are $\gamma_n = \tau_0^{-1}$ and $\gamma_s = \tau_0^{\ 1} + \mathcal{A}(|G|/2\alpha)^{1/2}$, where τ_0^{-1} is the one of Eq. (10), for $\boldsymbol{q}$ near the zone center. Let us consider the experiments of reference [36], and take, for example, the case of $T_0 = 80$ K; on the basis of the red shift of the band due to the soliton in relation to the normal CO-stretching band, that is, $\omega_0 - \omega_s \approx 16$ cm^{-1}, and that $\gamma_s - \gamma_n \approx 3.6$ cm^{-1}, we find that $\mathcal{A}(|G|/2\alpha)^{1/2} \approx 2.3 \times 10^6$ cm^{-1} and $\upsilon \approx 3 \times 10^4$ cm s^{-1}. The calculated spectra is shown as a full line in Fig. 1, while the dots are experimental points, evidencing a satisfactory agreement.

In Fig. 2 it is shown the propagation of the energy accompanying the soliton (proportional to $|\psi(x,t)|^2$) along a few picoseconds after the application of the initial Gaussian-like excitation. It is clearly evidenced the conservation of the shape characteristic of the soliton, but accompanied, as already described, with a decay in amplitude in the picosecond range. Hence, a pulse signal impinged on the system would be carried a few micrometers, since the velocity of propagation is $\approx 3 \times 10^4$ cm s^{-1}.

However, the situation may be substantially modified if the excitation propagates in a nonequilibrium background, namely the one provided by the presence of a constant pumping source [$I_q \neq 0$ in Eq. (8)] leading the system to a steady state, with populations, say, $\bar{\nu}_q$, constant in time but much larger than the population in equilibrium. At a sufficient distance from equilibrium, as proposed by Fröhlich near thirty years ago [32,33], and later on verified by several authors (in the framework of IST in [25]), is expected to arise a particular complex behavior in the system, namely a phenomenon akin to a Bose-Einstein condensation, consisting in that [because of the presence of the terms of Eq. (9)], and as already noticed, the energy stored in the polar vibrational modes is preferentially channeled to the modes lowest in frequency. The latter greatly increase in population, while the modes at intermediate and high frequencies remain nearly constant on further increase of the intensity of the pump. As expressed above, this is similar to a Bose-Einstein condensation, but, it must be stressed, not in equilibrium but in nonequilibrium conditions, and then the phenomenon — *Fröhlich effect* — may be considered a kind of emergence of a dissipative structure in Prigogine's sense [44–46]. This is illustrated in Fig. 3, where the steady state populations in terms of the intensity of the pumping source are shown. We have used numerical parameters characteristic of a polymer of the α-helix protein type [25]. The figure evidences the large increase (after an intensity threshold has been attained) of a mode lowest in frequency (the one labelled 1), at the expenses of other modes higher in frequency. In Fig. 4 it is evidenced the Fröhlich-Bose-Einstein-like condensate at the lowest frequencies in the vibrational spectrum.

The relevant point to be stressed is that *Fröhlich effect* and *Davydov soliton are phenomena arising out of the same nonlinear kinetic effects* that are present in Eq. (9) for the populations $\nu_q(t)$, and in Eq. (15) for the reciprocal lifetimes Γ_q. As a consequence of the fact that, because of Fröhlich effect, the population of the modes lowest in frequency largely increase, concomitantly their lifetime also largely increases (i.e. the reciprocal lifetime Γ_q in Eq. (15) largely decreases), while for the modes at intermediate to high frequencies their lifetime largely decreases (the reciprocal of Γ_q largely increases). This is illustrated in Fig. 5 [26]. Hence, in the expression for the average field amplitude of Eq. (16), after a fraction of picosecond following the application of the exciting pulse has elapsed, there survive for a long time the contributions from the modes lowest in frequency, a survival time that keeps increasing as the intensity I increases [26]. This implies that it may be expected that an excitation composed by a coherent interplay of the low-lying-in frequency excited polar (optical) modes in biopolymers, may propagate in the form of a *Davydov solitary wave traveling undeformed and nearly undamped while Fröhlich condensate state is maintained.*

2.2. Acoustical Vibrational Modes

So far we have considered propagation of vibronic waves in biological media, via Eq. (16), but restricted to the case of polar modes. We briefly consider next the case of longitudinal acoustic modes. For that purpose we return to Eqs. (14), where now we take into account that the dispersion relation ω_q is, for acoustic-like vibrations, sq, where s is the velocity of sound in the media, this meaning that we are using a Debye model. Using this dispersion relation, and the *Ansatz* that the excitation is expected to be a closed-packet solitary wave, we arrive at the equivalent of Eq. (19), in this case acquiring the expression

$$\mathrm{i}\frac{\partial}{\partial t}\psi(x,t) + \frac{\hbar}{2M_s}\frac{\partial^2}{\partial x^2}\psi(x,t) + \mathrm{i}\,\gamma_s\psi(x,t) - G_s|\psi(x,t)|^2\psi(x,t) = 0 \tag{23}$$

as shown in Appendix A.

Evidently, this Eq. (23) is formally identical with Eq. (19) if in the latter we take $\omega_0 = 0$ and, of course with the coefficients being those corresponding to this case of LA (longitudinal acoustic) vibrations. However, a remarkable difference may be noticed, namely, while in Eq. (19) the coefficient in front of the second derivative in space is determined, through α, by the bandwidth of the LO (longitudinal optical) vibrations dispersion relation, in this case, as shown in Appendix A, it depends through the pseudo-mass M_s on the characteristics of the experiment, that is, depends on the width of the solitary wave packet which is determined by the initial condition. The solution for a given hyperbolic secant-profile signal impinged on the system, say, the same as in the previous subsection, is given by

$$\psi(x,t) = \mathcal{A} \exp\left\{ \mathrm{i}\left[\frac{M_s v}{\hbar} x - (\omega_s - \mathrm{i}\,\gamma_s)t - \frac{\theta}{2} \right] \right\} \operatorname{sech}\left\{ \mathcal{A}\left[\frac{|G_s| M_s}{\hbar} \right]^{1/2} (x - vt) \right\}, \tag{24}$$

where

$$\omega_s = -\frac{|G_s|\mathcal{A}^2}{2} - \frac{M_s v^2}{4\hbar}, \tag{25}$$

As in the case of LO vibrations, the "acoustic" solitary wave is damped, and one may wonder if, as in the case of the "optical" solitary wave, this lifetime may be largely extended by the action of nonlinear kinetic terms enhanced by the pumping of energy on the system. We reconsider Eqs. (11), now specialized for the LA vibrations, and look for the stationary states when a constant exciting source is continuously applied.

To perform numerical calculations we choose a set of parameters in a typical order of magnitude approximation. We take for the Brillouin zone-end wavenumber $q_B = 3.14 \times 10^7$ cm^{-1}, $\omega_q = sq$ with $s = 1.8 \times 10^5$ cm s^{-1}, $\Omega_q = s_B q$ with $s_B = 1.4 \times 10^5$ cm s^{-1}. Moreover, the matrix elements $V^{(1)}$ and $V^{(2)}$ are proportional to the square roots of the wavenumbers [48], say $V^{(1,2)}_{qq'} = K^{(1,2)}[|\boldsymbol{q}_1||\boldsymbol{q}_2||\boldsymbol{q}_1 - \boldsymbol{q}_2|]^{\frac{1}{2}}$, and $K^{(1)}$ is determined from a typical value of 10 ps for the lifetime of Eq. (10) (for any system it can be determined from the linewidth in Raman scattering experiments). An open parameter $\lambda = |K^{(2)}/K^{(1)}|^2$ is introduced, and we take $\lambda = 1$ to draw Fig. 6. Finally, L, the length of the sample in the direction of propagation is taken as 10 cm. Therefore, the permitted wavenumbers for propagation of vibrations are contained in the interval $\pi/L \leq q \leq q_B$. For these characteristic values it follows that, because of energy and momentum conservation in the scattering events, the set of equations of evolution, Eqs. (8), which in principle couple all modes among themselves, can be separated into independent sets each one having nine modes. For example, taking the mode with the lowest wavenumber π/L, the set to which it belongs contains the modes $\kappa^{n-1}\pi/L$, where $\kappa = (s + s_B)/(s - s_B) = 8$ in this case, and $n = 2, 3, \ldots, 9$. Let us call $\nu_1, \ldots, \nu_9$ the corresponding populations, having frequencies $\omega_1 = 5.6 \times 10^4$ Hz,

$\omega_2 = 4.5 \times 10^5$ Hz. $\omega_3 = 3.6 \times 10^6$ Hz, $\omega_4 = 2.9 \times 10^7$ Hz, $\omega_5 = 2.3 \times 10^8$ Hz, $\omega_6 = 1.8 \times 10^9$ Hz, $\omega_7 = 1.5 \times 10^{10}$ Hz, $\omega_8 = 1.2 \times 10^{11}$ Hz, $\omega_9 = 9.5 \times 10^{11}$ Hz. Moreover, for illustration, the open parameter λ is taken equal to 1, and we consider that only the modes 2 and 3 (in the ultrasonic region) are pumped with the same constant intensity $S = I\bar{\tau}$, where $I_2 = I_3 = I$, and I_1 and I_n with $n = 4,\ldots,9$ are null, and $\bar{\tau}$ is a characteristic time used for scaling purposes (as in [25]) here equal to 0.17 s. The results are shown in Fig. 6, where it is evident the large enhancement of the population in the mode lowest in frequency (ν_1), for $S_0 \simeq 10^{19}$, at the expenses of the two pumped modes ν_2 and ν_3, while the modes ν_4 to ν_9 (higher in frequency) are practically unaltered. The emergence of Fröhlich effect is clearly evidenced for this case of acoustical vibrations: In fact, pumping of the modes in a restricted ultrasonic band (in the present case in the interval 4.5×10^5 Hz $\leq \omega \leq 2.8 \times 10^7$ Hz), leads at sufficiently high intensity of excitation to the transmission of the pumped energy in these modes to those with lower frequencies ($\omega < \omega_2$), while those with larger frequencies ($\omega > 2.8 \times 10^7$ Hz) remain in near equilibrium, as shown in Fig. 7. It may be noticed that for the given value of $\bar{\tau}$, for $S = 10^{23}$, the flux power provided by the external source, in the given interval of ultrasound frequencies being excited, is of the order of milliwatts. Modes in the interval $5.6 \times 10^4 \leq \omega_q \leq 4.5 \times 10^5$, those lowest in frequency, have large populations in comparison with those higher in frequency. As already noticed, because of these characteristics of Fröhlich's effect, it is sometimes referred-to as a Bose-Einstein-like condensation. However, it must be stressed that not in equilibrium, but in nonequilibrium conditions, then being a kind of nonequilibrium phase transition or better to say, a kind of emergence of a dissipative structure in Prigogine's sense [44–46]. Moreover, we may say, in a descriptive way, that it is present a kind of a "two fluid system", the normal one and the Fröhlich condensate.

Another relevant result is that, also as in the case of the optical vibrations, the modes in the condensate largely increase their lifetimes; this is shown in Fig. 8. Therefore, the soliton, composed by the coherent interplay of low-frequency acoustical modes, travels nearly undamped in the Fröhlich condensate.

We proceed now to consider another possible novel phenomenon in this kind of systems.

2.3. The accompanying Cherenkov-like emission

Considering either an "optical" or an "acoustical" soliton of the Davydov type respectively described in the previous subsections, we recall that the amplitude and the velocity of propagation are determined by the initial condition of excitation (that is, the energy and the momentum transferred in the process of interaction with the external source). For example, in the case of the acetanilide we have considered in subsection 2.1, and in the conditions of the experiment of Careri *et al.* [36], the velocity of propagation is larger than the group velocity of the phonons in the optical branch corresponding to the CO-stretching vibrations, which is small because the dispersion relation is flat.

When the soliton velocity of propagation, say v, is larger than the group velocity of the normal vibrations, (the velocity of sound s when the acoustic modes are involved), it may follow a *Cherenkov-like effect.* We recall that originally it was observed in electromagnetic radiation (e.g. [47]) by Cherenkov in 1934. It is a result that in a material media with an index of refraction n, the velocity of propagation of light is c/n, smaller than the velocity c in vacuum (since $n > 1$), and if an electron with velocity $u > c/n$ (but with the relativistic limitation of $u < c$) travels in this medium then, along a cone defined by the angle $\cos\theta = c/n\,u$ is emitted the so-called Cherenkov radiation: that is, along such direction photons are strongly emitted. This is the so-called superluminal radiation [48, 49].

Something similar is present in the case of phonons in the photoinjected plasma in semiconductors in the presence of an electric field: when the drift velocity of the carriers exceeds the group velocity of the $\boldsymbol{q}$-mode optical phonon, then along a cone whose axis is along the electric field, and with an aperture with angle $\theta_{\boldsymbol{q}}$ defined by

$$\cos\theta = \omega_{q}/vq, \tag{26}$$

there follows a large emission of q-mode optical phonons [50].

This is also the case when the soliton, either optical or acoustical, travels in bulk with a velocity v larger than the group velocity of the normal vibronic waves. This is described elsewhere [51], and next we briefly outline the results. Inspection of Eq. (8) tells us that the presence of the direct coupling to the external source via I_q, and indirectly through ζ depending on the squared amplitude of the soliton, tends to increase the population of phonons. But, as already noticed, because of Fröhlich effect, such pumped energy tends to concentrate in the modes lowest in frequency, those at the Brillouin zone boundary in the case of optical vibrations and around the zone center in the case of acoustic vibrations.

Take the case of acoustic phonons, when there should be a large increase in the population of the modes with very small wavenumber. A straightforward calculation of Eq. (4a) leads to the result that

$$\nu_q(t) = [e^{F_q}(t) - 1]^{-1} + \left| \frac{f_q(t)}{F_q} \right|^2 . \tag{27}$$

Evidently, in the absence of the perturbation, that is, $I_q = 0$ and $\langle a_q \rangle = 0$ and then $f_q = 0$, it follows that $F_q(t) = \hbar s q / k_B T_0$, and we recover the usual Planck distribution in equilibrium. In the presence of the perturbation we need to obtain both $F_q(t)$ and $f_q(t)$. On the one hand, a direct calculation tell us that

$$|f_q(t)/F_q(t)|^2 = |\langle a_q | t \rangle|^2 \approx \int_0^L \frac{dx}{L} |\psi(x,t)|^2 \approx (\mathcal{A}^2 w^2 / L^2) e^{-\gamma_s t} , \tag{28}$$

where we have used Eqs. (16) and (20), and, we recall, under a sufficiently intense excitation γ_s is small and then $|\langle a_q | t \rangle|^2$ becomes near time independent; we have called w the width of the solitary wave packet.

On the other hand, F_q in steady state conditions after application of the constant external excitation, depends on the intensity of the pumping source. This Lagrange multiplier may be rewritten in either of two alternative forms, which resemble well known results in equilibrium theory. One is

$$F_q(t) = [\hbar s q - \mu_q]/k_B T_0, \tag{29}$$

where μ_q plays the role of a quasi-chemical potential (this kind of choice was done by Fröhlich [33] and Landsberg [52]). In Fig. 9 is shown the dependence of the quasi-chemical potential, corresponding to the modes in Fig. 6, with the pumping intensity. Another is

$$F_q = \hbar s q / k_B T_q^* \tag{30}$$

introducing a quasitemperature T^*, as it is done in semiconductor physics [24]. In Fig. 10 is shown the dependence of the dependence of the quasitemperature, corresponding to the modes in Fig. 6, with the pumping intensity.

Let us take the choice of Eq. (30), then the quasitemperature T^* is given by

$$k_B T_q^* = \hbar s q \ln[1 + \frac{1}{\nu_q - |\langle a_q \rangle|^2}] \tag{31}$$

and we recall that

$$|\langle a_q \rangle|^2 \approx \mathcal{A}^2 w^2 / L^2, \tag{32}$$

(for $\gamma_s \to 0$, with ν_q determined in each case solving Eq. (8)). Using Eqs. (29) to (32) we have that [51]

$$\mu_q = \hbar v q \cos \eta_q \tag{33}$$

where

$$\cos \eta_q = \frac{s}{v}\left[1 - \frac{k_B T_0}{\hbar s q} \ln[1 + (\nu_q - |\langle a_q \rangle|^2)^{-1}]\right] = \frac{s}{v}[1 - \frac{T_0}{T_q^*}]. \tag{34}$$

These results imply in this case in a phenomenon of a peculiar character which we call

Fröhlich-Cherenkov-effect. In fact, we note, first, that there follows a large enhancement of phonons in mode $\boldsymbol{q}$ for μ_q approaching $\hbar sq$, and second, the linear motion of the soliton defines a particular direction, the one given by its velocity of propagation $\boldsymbol{v}$. Therefore, there is a preferential direction of production of vibrational waves given by

$$\hbar sq \approx \hbar vq \cos\eta_q = \mu_q \tag{35}$$

or

$$\cos\eta_q \approx s/v. \tag{36}$$

Equation (35) defines the direction of propagation $\boldsymbol{q}$ of the longitudinal vibration and its modulus. Since η_q depends only on the modulus of $\boldsymbol{q}$, there follows two Cherenkov-like privileged directions of emission of $\boldsymbol{q}$-mode phonons, one forward and one backwards, like the normal and anomalous Cherenkov cones in radiation theory as illustrated in Fig. 9 adapted from [49]. In the present case both directions are symmetrical on both sides of the centre defined at each time by the position occupied by the soliton. This may account for the observed so-called X-waves [1,3,53]. In Fig. 12 is illustrated the cases of propagation of the normal sound wave (upper figure) and of the, presumably, solitary wave-packet selectively excited by the transducer (lower figure) with velocity larger than the sound velocity in the medium. The figure has appeared in [3]. Given the angle η_q (called the axicon angle in [1]), then v is larger than s in the percentage $[(v/\cos\eta_q) - s]/v$. Same arguments are valid for the case of the optical soliton, when $\nabla_q \omega_q$ (the group velocity of the normal mode) enters in place of s. In the case of Fig. 12, a rough estimate gives $\eta \sim 13^\circ$ and $v_s/s \sim 1.02$, that is, the velocity of propagation of the soliton, v, is roughly 2% larger than the velocity of sound in the medium.

3. CONCLUDING REMARKS

We have considered the propagation of vibronic excitations in nonlinear condensed matter media, like biological material. Because of the nonlinearities in the kinetic equations that describe the evolution of the macroscopic collective modes (nonlinearities having their origin in the microscopic anharmonic interactions between the system and the surroundings) it is expected that complex behavior shall arise.

Resorting to an appropriate thermo-mechanical statistical approach, we have shown that such complex behavior consists of four particular phenomena. One is that the normal vibrational modes are accompanied by another type of excitation, consisting in the propagation of *solitary waves of the Schrödinger-Davydov type.* They are undeformed waves composed by a coherent state of normal modes. Although the wavepacket is spatially undeformed, it presents, as it should, decay in time with a given lifetime resulting from the dissipative effects that develop in the excited sample. The amplitude, velocity, and frequency of the solitary wave are determined by the initial and boundary conditions. Another phenomenon, arising out of the same nonlinearities that allows for the creation of the soliton, consists in that, under conditions of excitation which lead the system sufficiently away from equilibrium, there follows a large increase of the population of the modes lowest in frequency. This effect has a reminiscence of a Bose-Einstein condensation but here in nonequilibrium conditions, and we have termed it *Fröhlich effect.*

A third phenomenon consists in that, and again because of the nonlinearities which are responsible for both, Fröhlich effect and formation of a Schrödinger-Davydov soliton, the latter acquires a very long lifetime, that is, *the soliton becomes nearly undamped*, when travelling in the Fröhlich-Bose-Einstein-like condensate.

Finally, the fourth phenomenon refers to a situation when, because of appropriate initial and boundary conditions, the soliton travels with a speed larger than that of the normal vibronic modes. In this case, as shown, there follows what can be termed as *Fröhlich-Cherenkov effect*: along two symmetrical privileged directions centered on the position of the soliton, is produced a large number of long wavelengths phonons. This could be the origin of the so-called X-waves observed in experiments of ultrasonography, as noticed in previous sections.

We conclude with the remark that solitary waves appear to be ubiquitous, and having large relevance in a number of important situations. Some at the technological level, like propagation in optical fibers (e.g., in a projected trans-Atlantic cable), in conducting polymers (for electric-car batteries; microcircuits; etc.), and the case of biological systems (long range propagation of nervous signals; the here mentioned case of medical imaging; etc.).

4. Acknowledgments

We gratefully acknowledge financial support to our Group, provided in different opportunities by the São Paulo State Research Foundation (FAPESP), the National Research Council (CNPq), the Ministry of Planning (Finep), Unicamp Foundation (FAEP), IBM Brasil, the John Simon Guggenheim Memorial Foundation (New York, USA).

Appendix A. The Acoustic Solitary Wave

In direct space, after the terms that couple the amplitude $\langle a_q \rangle$ with its conjugate are neglected, what, as noticed in the main text is accomplished using the rotating wave approximation, Eq. (14) takes the form:

$$\begin{aligned} \mathrm{i}\hbar\frac{\partial}{\partial t}\psi(x,t) = & -\mathrm{i}\sum_q \hbar\omega_q \int \frac{dx'}{L}\,\mathrm{e}^{\mathrm{i}q(x-x')}\,\psi(x',t) - \mathrm{i}\hbar\sum_q \Gamma_q \int \frac{dx'}{L}\,\mathrm{e}^{\mathrm{i}q(x-x')}\,\psi(x',t) \\ & + \sum_{q_1 q_2} R_{q_1 q_2} \int \frac{dx'}{L} \int \frac{dx''}{L}\,\mathrm{e}^{iq_1(x-x')}\,\mathrm{e}^{iq_2(x-x'')}\,\psi(x',t)\psi(x'',t)\psi^*(x,t), \quad \text{(A.1)} \end{aligned}$$

where, we recall, $\omega_q = sq$. Considering that it is expected the formation of a highly localized packet (the soliton), centered in point x and with a Gaussian-like profile with a width, say, w (fixed by the initial condition of excitation) extending along a certain large number of lattice parameter a (i.e. $w \gg a$), in Eq. (A.1) we make the expansion

$$\psi(x',t) \approx \psi(x,t) - \xi \frac{\partial}{\partial x} \psi(x,t), \tag{A.2}$$

where $\xi = x - x'$ is roughly restricted to be smaller or at most of the order of w. The first term on the right of Eq. (A.1) is

$$\begin{aligned}
& -\mathrm{i} \sum_q s|q| \int \frac{dx'}{L} \mathrm{e}^{\mathrm{i}q(x-x')} \psi(x',t) = \\
& = -\frac{Ls}{2\pi} \frac{\partial}{\partial x} \int_0^{\frac{\pi}{a}} dq \int_0^L \frac{dx'}{L} \left[\mathrm{e}^{\mathrm{i}q(x-x')} - \mathrm{e}^{-\mathrm{i}q(x-x')}\right] \psi(x',t) \\
& \approx -\frac{\mathrm{i}s}{\pi} \frac{\partial}{\partial x} \int_0^{\frac{\pi}{a}} dq \int_{x-w/2}^{x+w/2} d\xi \, \sin(q\xi) \left[\psi(x,t) - \xi \frac{\partial}{\partial x} \psi(x,t)\right] \\
& = \frac{\mathrm{i}s}{\pi} \frac{\partial}{\partial x} \left[\int_{x-\frac{1}{2}w}^{x+\frac{1}{2}w} (1 - \cos \frac{\pi}{a} \xi) \, \frac{d\xi}{\xi}\right] \psi(x,t) \\
& \quad + \frac{\mathrm{i}s}{\pi} \left[\int_{x-\frac{1}{2}w}^{x+\frac{1}{2}w} (1 - \cos \frac{\pi}{a} \xi) \, \frac{d\xi}{\xi}\right] \frac{\partial}{\partial x} \psi(x,t) \\
& \quad - \frac{\mathrm{i}s}{\pi} \left[\int_{x-\frac{1}{2}w}^{x+\frac{1}{2}w} (1 - \cos \frac{\pi}{a} \xi) \, d\xi\right] \frac{\partial}{\partial x} \psi(x,t) \\
& \quad - \frac{\mathrm{i}s}{\pi} \left[\int_{x-\frac{1}{2}w}^{x+\frac{1}{2}w} (1 - \cos \frac{\pi}{a} \xi) \, d\xi\right] \frac{\partial^2}{\partial x^2} \psi(x,t) \, .
\end{aligned} \tag{A.3}$$

But, of the four terms after the last equal sign in this Eq. (A.3), the second and third are null, because of the *Ansatz* that a soliton would follow, since the derivative at the center of the packet is null. Consider now the last term, which after the integrations are performed becomes

$$-\frac{\mathrm{i}sw}{\pi} \left[1 - \frac{2a}{\pi w} \sin \frac{\pi}{a} \frac{w}{2} \cos \frac{\pi}{a} x\right] \frac{\partial^2}{\partial x^2} \psi(x,t) \, . \tag{A.4}$$

But, we notice that the width of the packet is $w \gg a$, and the cosine in Eq. (A.4) has a period $2a$, and then it oscillates very many times in w, and with amplitude $(2a/\pi w) \ll 1$, and can be neglected. Similarly, the first term becomes proportional to

$$\frac{is}{\pi}\frac{\psi(x)}{x^2-(w/2)^2}\left\{w\left[1-\cos\left(\frac{\pi x}{a}\right)\cos\left(\frac{\pi w}{2a}\right)\right]-2x\sin\left(\frac{\pi x}{a}\right)\sin\left(\frac{\pi w}{2a}\right)\right\}, \quad (A.5)$$

where, on the one hand, the oscillatory terms cancel on average, and, on the other hand, the term decays as x^{-2}. Consequently, using these results in Eq. (A.1), after introducing the notation $(\hbar sw/\pi) = \hbar^2/(2M_s)$, and the local approximation in the second and third term on the right of Eq. (A.1), we find Eq. 23.

REFERENCES

[1] J. Lu and J. F. Greenleaf, Nondiffracting X-waves, IEEE Trans. Ultrason. Ferroelect. Freq. Contr. **39**, 19–31 (1992).

[2] J. Lu and J. F. Greenleaf, Experimental Verification of Nondiffracting X-waves, IEEE Trans. Ultrason. Ferroelect. Freq. Contr. **39**, 441–6 (1992).

[3] W. A. Rodrigues and J. Lu, On the Existence of Undistorted Progressive Waves, Found. Phys. **27**, 435–508 (1997).

[4] A. C. Scott, F. Y. F. Chu, and D. W. McLaughlin, The Soliton: A new concept in applied Science, Proc. IEEE **61**, 1443 (1973).

[5] J. Scott-Russell, Report on Waves, Proc. Roy. Soc. Edinburgh , 319–20 (1844).

[6] A. C. Scott, The Solitary Wave, The Sciences (NYAS) **30**(2), 28–35 (1990).

[7] T. Beardsley, Plastic Power, Scientific American, pp. 31–2 (April, 1997).

[8] A. J. Heger, S. Kivelson, J. R. Schrieffer, and W. P. Su, Solitons in Conducting Polymers, Rev. Mod. Phys. **60**, 781–850 (1988).

[9] T. Anderson and S. Roth, Conducting Polymers: Electrical Transport and Current Applications, Braz. J. Phys. **24**, 746—54 (1994).

[10] H. A. Haus, Molding light into solitons, IEEE Spectrum , 48-53 (March 1993).

[11] A. S. Davydov, *Biology and Quantum Mechanics*, Pergamon, Oxford, 1982.

[12] A. S. Davydov, Solitons in Biology, in *Solitons*, edited by S. E. Trullinger, V. E. Zakharov, and V. L. Prokovsky, Chapter 1, pages 1–51, Elsevier, New York, 1986.

[13] A. C. Scott, Davydov's Soliton, Phys. Rep **217**, 1–67 (1992).

[14] L. S. Garcia-Colin, A. R. Vasconcellos, and R. Luzzi, On Informational Statistical Thermodynamics, J. Non-Equilib. Thermodyn. **19**, 24–46 (1994); R. Luzzi, A. R. Vasconcellos, and J. G. Ramos, On the Statistical Foundations of Irreversible Thermodynamics, IFGW-Unicamp Internal Report (1997) and Fortschr. Phys./Prog. Phys., submitted; R. Luzzi and A. R. Vasconcellos, The Basic Principles of Irreversible Thermodynamics in the Context of an Informational-Statistical Approach, Physica A **241**, 677–703 (1997).

[15] A. R. Vasconcellos, L. S. Garcia-Colin, and R. Luzzi, A Microscopic Approach to Irreversible Thermodynamics: (I), Phys. Rev. A **43**, 6622–32 (1991); (II) *ibid.* **43**, 6633–41 (1991); A. R. Vasconcellos, R. Luzzi, J. Casas-Vázquez, and D. Jou, Thermodynamic variables in the context of a nonequilibrium statistical ensemble approach, J. Chem. Phys. **107**, 7383–96 (1997).

[16] M. A. Tenan, A. R. Vasconcellos, and R. Luzzi, Mechano-Statistical Foundations for Generalized Nonequilibrium Thermodynamics, Fortschr. Phys./Prog. Phys. **47**, 1–30 (1996).

[17] D. N. Zubarev, *Nonequilibrium Statistical Thermodynamics*, Consultants Bureau, New York, 1974, [*Neravnovesnaia Statisticheskaia Termodinamika* (Idz. Nauka, Moscow, 1971)].

[18] D. N. Zubarev, V. N. Morozov, and G. Röpke, *Statistical Mechanics of Nonequilibrium Processes*, volume 1: Basic Concepts, Kinetic Theory, Akademie-Verlag, Berlin, 1996.

[19] R. Luzzi and A. R. Vasconcellos, On the Nonequilibrium Statistical Operator Method, Fortschr. Phys./Prog. Phys. **38**, 887–922 (1990).

[20] J. G. Ramos, A. R. Vasconcellos, and R. Luzzi, A Classical Approach in Predictive Statistical Mechanics: A Generalized Boltzmann Formalism, Fortschr. Phys./Prog. Phys. **43**, 265–300 (1995).

[21] R. Luzzi, A. R. Vasconcellos, and J. G. Ramos, Statistical Irreversible Thermodynamics in a Nonequilibrium Statistical Ensemble Formalism, IFGW-Unicamp Internal Report (1997), and future publication.

[22] L. Lauck, A. R. Vasconcellos, and R. Luzzi, A Nonlinear Quantum Transport Theory, Physica A **168**, 789–819 (1990); J. R. Madureira, A. R. Vasconcellos, and R. Luzzi, A nonequilibrium grand-canonical ensemble, J. Chem. Phys. **00**, 0000-0000 (1998); J. R. Madureira, A. R. Vasconcellos, and R. Luzzi, J. Casas-Vázquez, and D. Jou, Evolution of dissipative processes via a statistical thermodynamic approach: I. Generalized Mori-Heisenberg-Langevin equations, J. Chem. Phys. **108**, 7568–79 (1998); II. Thermodynamic properties of a fluid of bosons, ibid. **108**, 7580–87 (1998).

[23] A. I. Akhiezer and S. V. Peletminskii, *Methods of Statistical Physics*, Pergamon, Oxford, 1981; S. V. Peletminskii and A. Yatsenko, Contribution to the Quantum Theory of Kinetic and Relaxation Processes, JETP **26**, 773–8 (1968).

[24] A. C. Algarte, A. R. Vasconcellos, and R. Luzzi, Kinetic of Hot Elementary Excitations in Photoexcited Polar Semiconductors, Phys. Stat. Sol. (b) **173**, 487–514 (1992); A. R. Vasconcellos and R. Luzzi, Coherent phonon modulation in time-resolved transmission in plasma in semiconductors, Phys. Rev. Lett. (1997), submitted; L. Lauck, A. R. Vasconcellos, and R. Luzzi, Nonlinear Effects in the Production of Highly Photoexcited Polar Vibrations, Phys. Rev. B **46**, 6150–59 (1992); A. R. Vasconcellos, A. C. Algarte, and R. Luzzi, Diffusion of Photoinjected Carriers in Plasma in Nonequilibrium Semiconductors, Phys. Rev. B **48**, 10873-84 (1993).

[25] M. V. Mesquita, A. R. Vasconcellos, and R. Luzzi, Selective Amplification of Coherent Polar Vibrations in Biopolymers, Phys. Rev. E **48**, 4049–59 (1993).

[26] M. V. Mesquita, A. R. Vasconcellos, and R. Luzzi, Near-dissipationless Coherent Excitations in Biosystems, Int. J. Quantum Chem **60**, 689–97 (1996).

[27] R. Luzzi, M. F. Scarparo, J. G. Ramos, A. R. Vasconcellos, M. Barros, and A. Kiel, Informational Statistical Thermodynamics and Thermal Laser Stereolithography, J. Non-Equilib. Thermodyn. **22**, 197–216 (1997).

[28] A. R. Vasconcellos, M. V. Mesquita, and R. Luzzi, Statistical Thermodynamic Approach to Solitary Waves in Acetanilide, Phys. Rev. Lett. **80**, 2008–11 (1998).

[29] S. A. Hassan, A. R. Vasconcellos, and R. Luzzi, The informational entropy operator in a nonequilibrium statistical ensemble formalism, IFGW-Unicamp Internal Report(1997), and Physica A, submitted.

[30] V. P. Kalashnikov, Linear relaxation equations in the nonequilibrium statistical operator method, Teor. Mat. Fiz. **34**, 263–72 (1978).

[31] K. Walyazek, D. N. Zubarev, and A. Z. Kuzemskii, Schrödinger-type equation with damping for a dynamical system in a thermal bath, Theor. Math. Phys. **5**, 1150–58 (1971).

[32] H. Fröhlich, Long-Range Coherence and the Action of Enzymes, Nature **228**, 1093 only (1970).

[33] H. Fröhlich, The Biological Effects of Microwaves and Related Questions, in *Advances in Electronics and Electron Physics*, volume 17, pages 85–152, Academic Press, New York, 1980.

[34] H. Haken, Laser Theory, in *Handbuch der Physik XXV/2C*, edited by S. Flügge, Springer, Berlin, 1970.

[35] V. E. Zakharov, The Inverse Scattering Method, in *Solitons*, edited by R. K. Bullough and P. J. Caudrey, Chapter 7, pages 243–85, Springer, Berlin, 1980.

[36] G. Careri, U. Buotempo, R. Carta, E. Gratton, and A. C. Scott, Infrared Absorption in Acetanilide by Solitons, Phys. Rev. Lett. **51**, 304–7 (1983).

[37] J. L. Sauvajol, R. Almaraic, J. Moret, M. Barthes, and J. L. Ribet, Temperature Dependence of the Raman spectrum of fully deuterated acetanilide, J. Raman Spectrosc. **20**, 517–21 (1989).

[38] G. Careri and E. Gratton, Fine Structure of the Amide-I Band in Acetanilide, Phys. Rev. A **37**, 4048–51 (1988).

[39] M. Sakai, N. Kuroda, and Y. Nishima, High-pressure Raman Study of Vibrational Spectra in Crystalline Acetanilide, Phys. Rev. B **47**, 150–7 (1993).

[40] M. Barthes, R. Almaraic, J. L. Sauvajol, , R. Currat, J. Moret, , and J. L. Ribet, Neutron scattering investigation of deuterated crystalline acetanilide, Europhys. Lett. **7**, 55–60 (1988).

[41] M. Barthes, J. Eckert, S. W. Johnson, J. Moret, B. I. Swanson, and C. J. Unjeker, Anomalous Vibrational Modes in acetanilide as studied by inelastic neutron scattering, J. Phys. I France **2**, 1929–39 (1992).

[42] R. Luzzi and A. R. Vasconcellos, Response function theory for systems far from equilibrium, J. Stat. Phys. **23**, 539–59 (1980).

[43] V. P. Kalashnikov, Response to a mechanical perturbation and the Green's functions for nonequilibrium systems, Theor. Math. Phys. **9**, 1003–12 (1971).

[44] I. Prigogine, Structure, Dissipation, and Life, in *From Theoretical Physics to Biology*, edited by M. Marois, North Holland, Amsterdam, 1969.

[45] G. Nicolis and I. Prigogine, *Self-organization in Nonequilibrium Systems*, Wiley-Interscience, New York, 1977.

[46] R. Luzzi and A. R. Vasconcellos, Dissipation and Order in Complex Systems: An overview, Ciência e Cultura **43**, 423–31 (1992), a publication of the Brazilian Society for the Advancement of Science.

[47] L. D. Landau and E. M. Lifshitz, *Electrodynamics of Continuous Media*, Pergamon, Oxford, 1960.

[48] V. L. Ginsburg, Certain Theoretical Aspects of Radiation due to Superluminal Motion in a Medium, Phys.-Uspekhi **2**, 874–93 (1960).

[49] V. M. Agranovich and V. L. Ginsburg, *Spatial Dispersion in Crystal Optics and the Theory of Excitons*, Wiley-Interscience, London, 1966.

[50] P. Kocevar, Hot phonon dynamics, Physica B **34**, 155–63 (1985).

[51] M. V. Mesquita, A. R. Vasconcellos, and R. Luzzi, Solitons in Highly Excited Matter: Dissipative thermodynamic and supersonic effects, Phys. Rev. Lett., submitted (1998).

[52] P. T. Landsberg, Photons at non-zero chemical potential, J. Phys. C: Solid State Phys. **14**, L1025–27 (1981).

[53] J. Lu, Z. Hehong, and J. F. Greenleaf, Biomedical ultrasound beam forming, Ultrasound Med. Biol. **20**, 403–28 (1994).

FIGURE CAPTIONS

Figure 1: Optical vibrations: The IR absorption spectrum in acetanilide at 80 K. Points are from the experimental data reported in [36], and the full line the calculation after Eq. (23).

Figure 2: Optical vibrations: Profile of the soliton energy (proportional to $|\psi(x,t)|^2$) along a few picoseconds after application of the initial Gaussian-like perturbation (in the experimental conditions of Fig. 1 for $T = 80$ K).

Figure 3: Optical vibrations: The steady-state populations vs. the intensity of the pumping source, for a selected set of modes: After an intensity $S = 10^3$ is reached, there follows a large increase in the population ν_6 of the mode lowest in frequency in the said set (After Ref. [25]).

Figure 4: Optical vibrations: The steady-state populations for $S = 10^4$, showing a "two fluid" separation consisting in the "condensate" at low frequencies and the "normal" contributions at higher frequencies (After reference [25])

Figure 5: Optical vibrations: The lifetime of the same modes as in Fig. 3, in terms of the intensity of the pumping source.

Figure 6: Acoustic vibrations: The steady state populations of the three relevant modes in the set — as described in the main text —, with increasing values of the intensity of the external source pumping modes labeled 2 and 3 in the ultrasonic region. (After Ref. [51]).

Figure 7: Acoustic vibrations: The population in the steady state for a pumping intensity $S = 10^{23}$, of the modes along the spectrum of frequencies of the acoustic modes. Dots indicate the modes in the first set (the remaining part of the spectrum up to the highest Brillouin frequency $\omega_B = 9.5 \times 10^{11}$ Hz has been omitted). (After Ref. [51]).

Figure 8: Acoustic vibrations: The lifetime of the same modes as in Fig. 7, in terms of the intensity of the pumping source (After Ref. [51]).

Figure 9: The quasi-chemical potential of the modes labeled 1 to 3 in Fig 6, with mode 1 corresponding to the one with the lowest frequency in the given set: it is evident the emergence of a "Bose-Einstein-like condensation" for S approaching a critical value of the order of 10^{19}.

Figure 10: The quasi-temperature, defined in Eq. (30) for the modes in Fig. 6.

Figure 11: The direction of propagation of the waves of Cherenkov radiation, when spatial dispersion is taken into account, for the ordinary wave (subscript 1) and the anomalous wave (subscript 2) (Adapted from Ref. [49]).

Figure 12: Normal sound propagation (upper figure), and the excitation interpreted as a supersonic soliton (lower figure); from reference [3] (We thank W. A. Rodrigues and J. E. Maiorino for providing us with a postscript file of this picture).

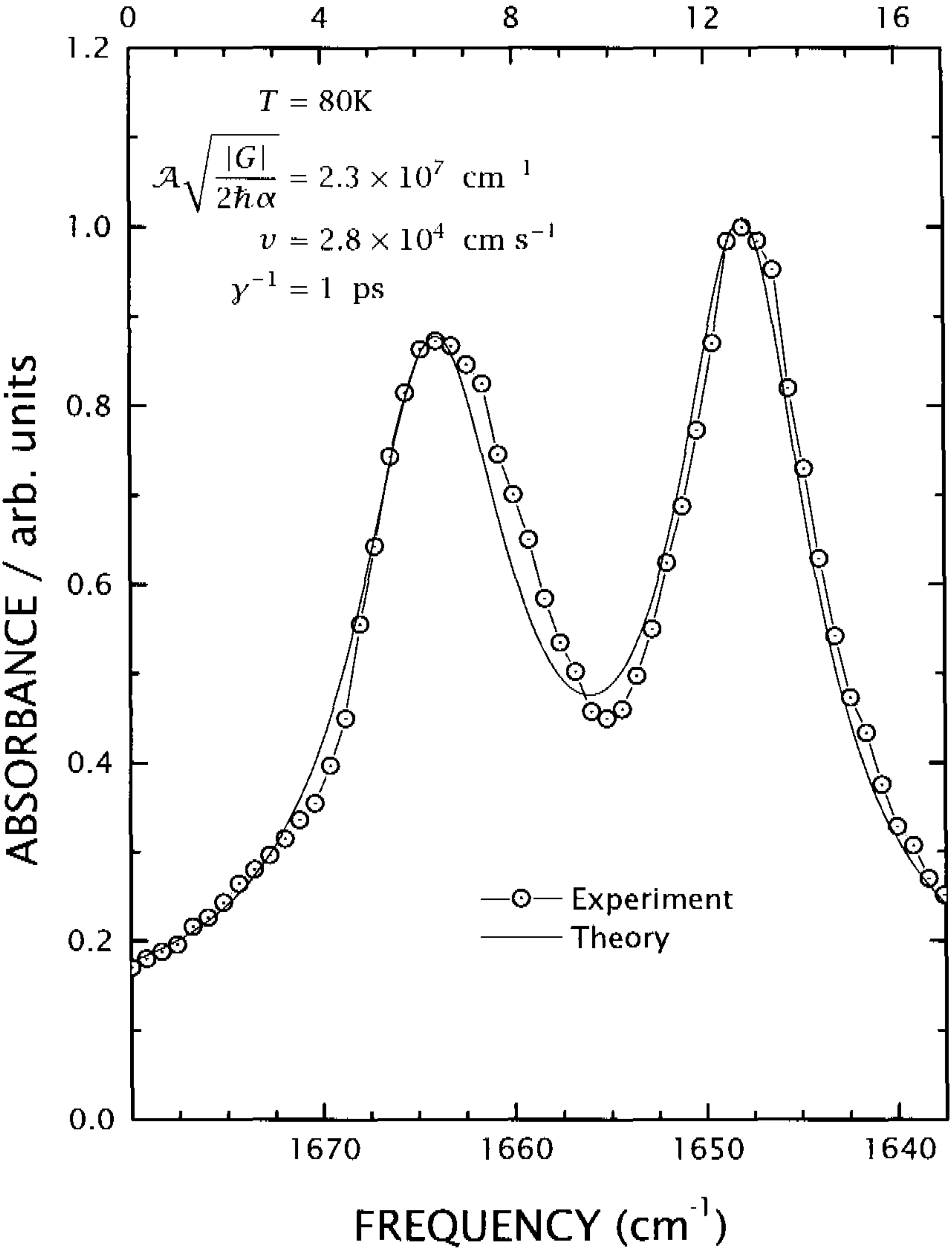

Figure 1: Optical vibrations: The IR absorption spectrum in acetanilide at 80 K. Points are from the experimental data reported in [36], and the full line the calculation after Eq. (23).

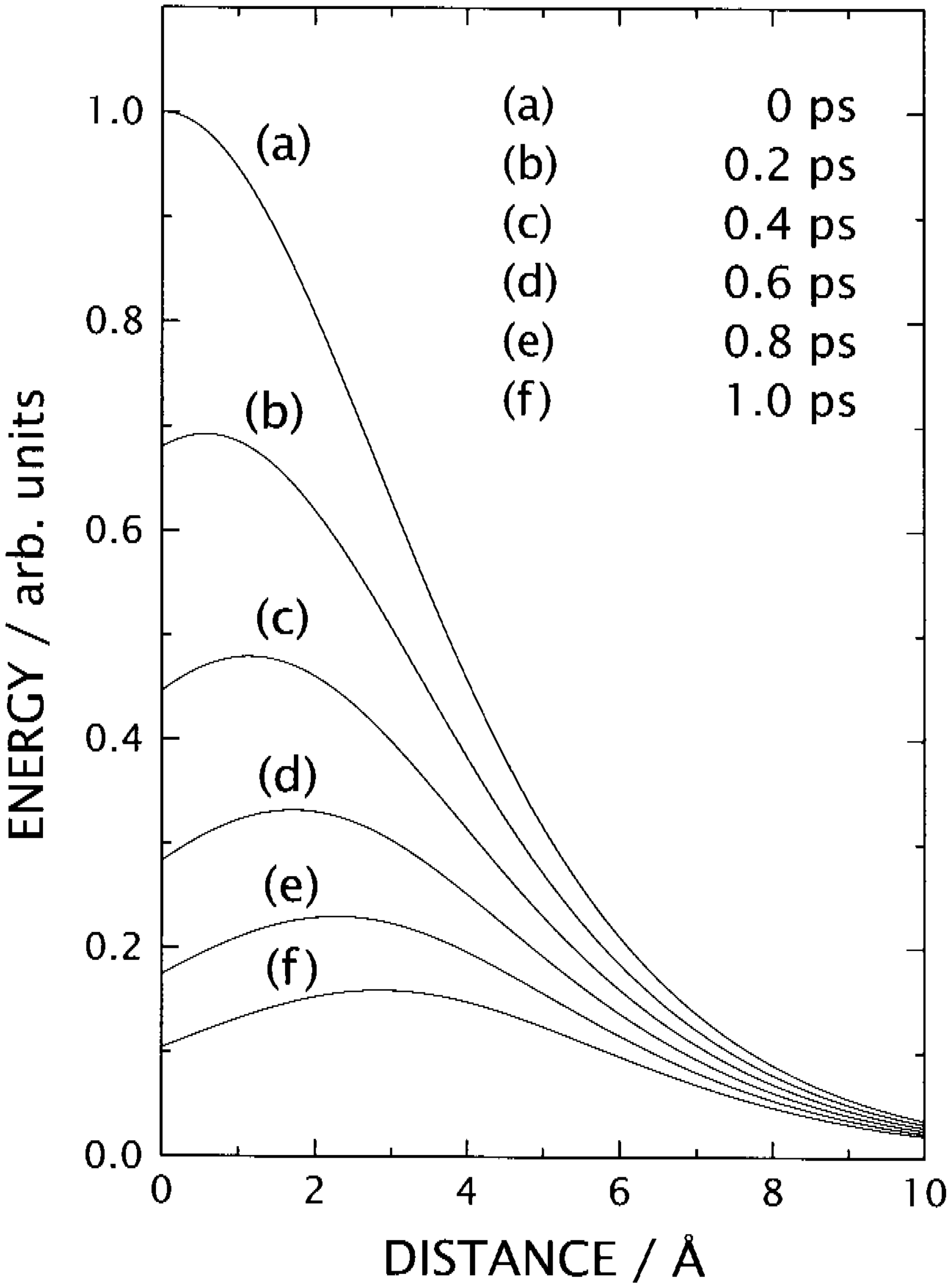

Figure 2: Optical vibrations: Profile of the soliton energy (proportional to $|\psi(x,t)|^2$) along a few picoseconds after application of the initial Gaussian-like perturbation (in the experimental conditions of Fig. 1 for $T = 80$ K).

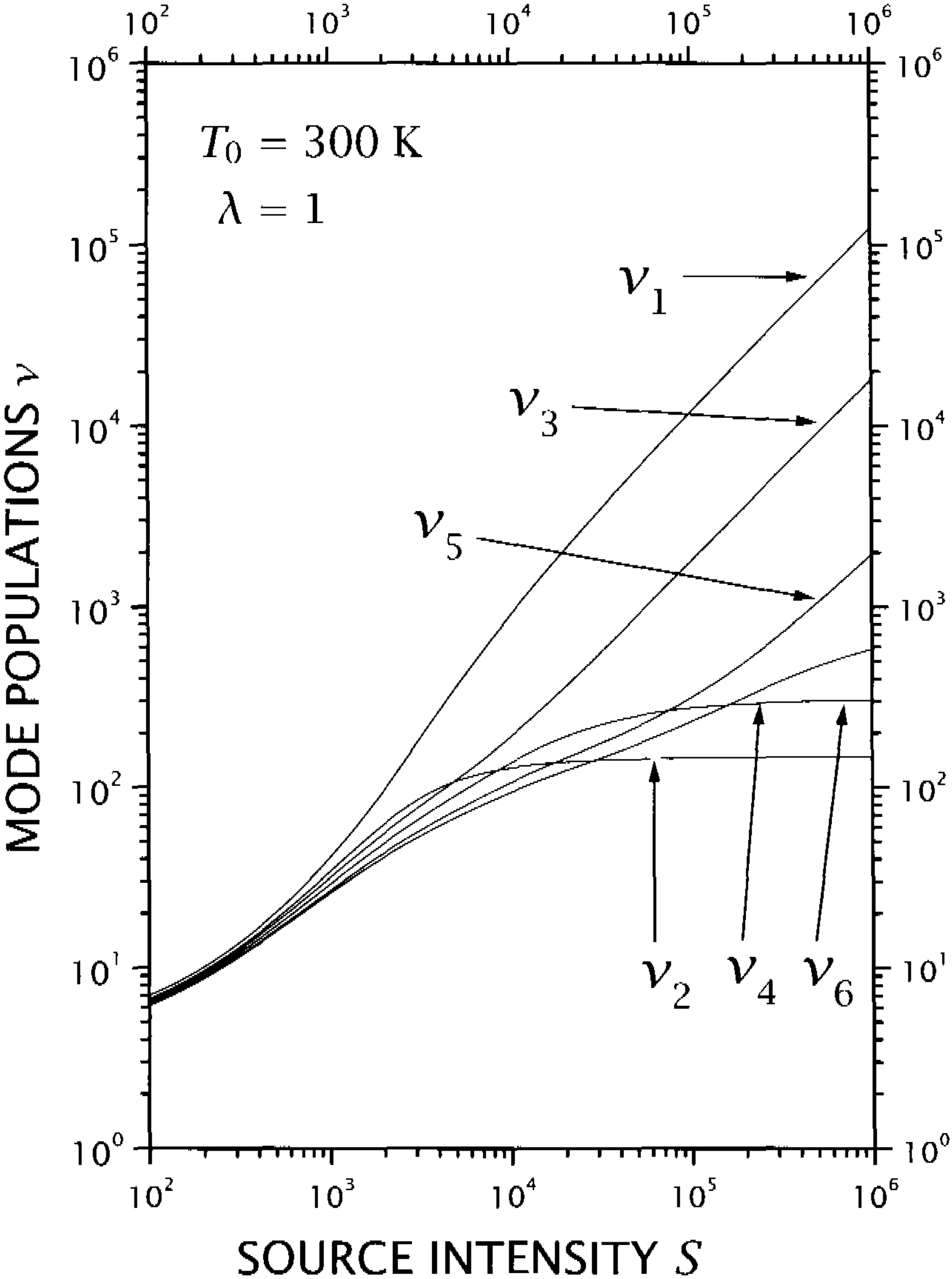

Figure 3: Optical vibrations: The steady-state populations vs. the intensity of the pumping source, for a selected set of modes: After an intensity $S = 10^3$ is reached, there follows a large increase in the population ν_6 of the mode lowest in frequency in the said set (After Ref. [25]).

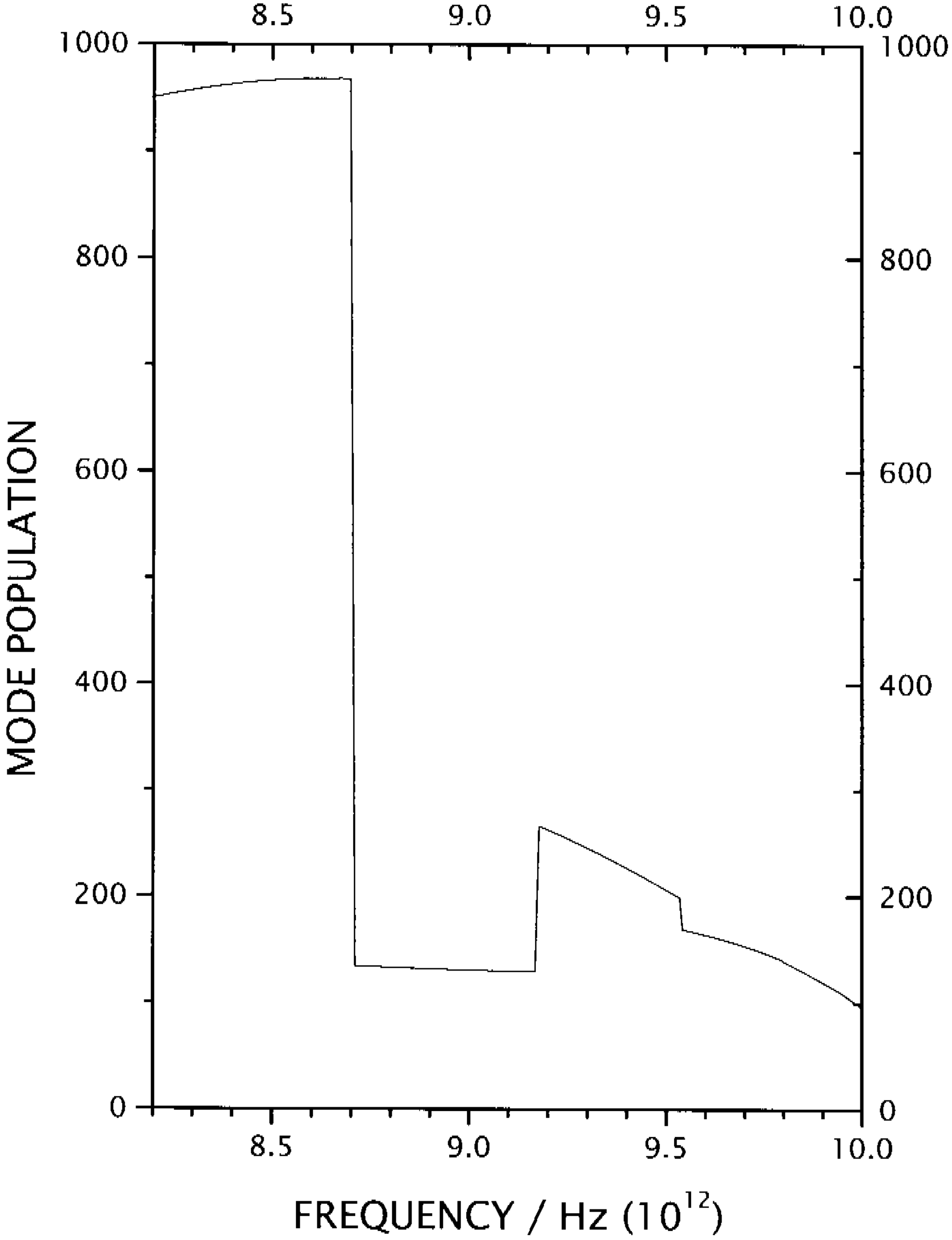

Figure 4: Optical vibrations: The steady-state populations for $S = 10^4$, showing a "two fluid" separation consisting in the "condensate" at low frequencies and the "normal" contributions at higher frequencies (After reference [25])

MESQUITA *et al.* — *J. Biol. Phys.* FIGURE 4

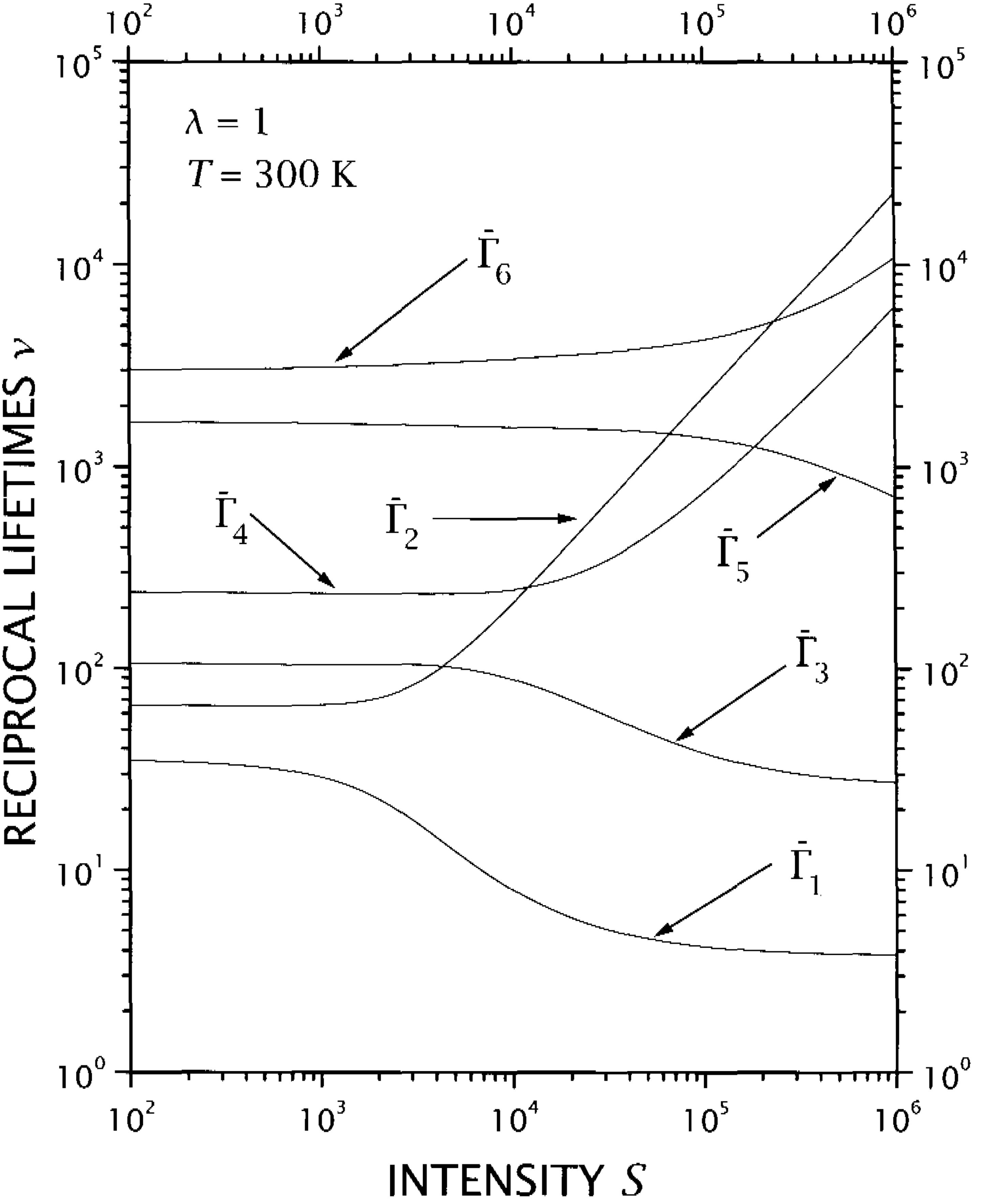

Figure 5: Optical vibrations: The lifetime of the same modes as in Fig. 3, in terms of the intensity of the pumping source.

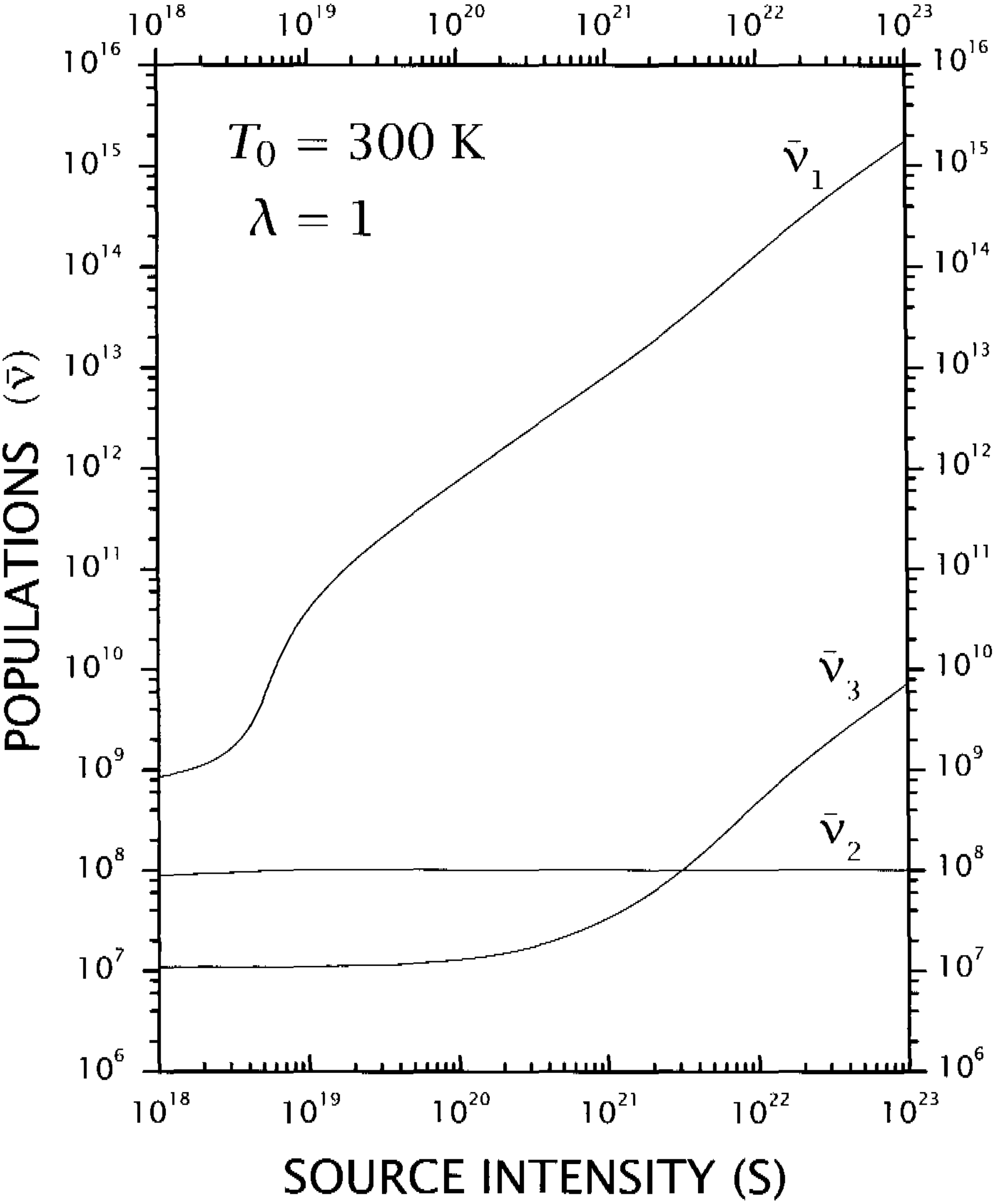

Figure 6: Acoustic vibrations: The steady state populations of the three relevant modes in the set — as described in the main text —, with increasing values of the intensity of the external source pumping modes labeled 2 and 3 in the ultrasonic region. (After Ref. [51]).

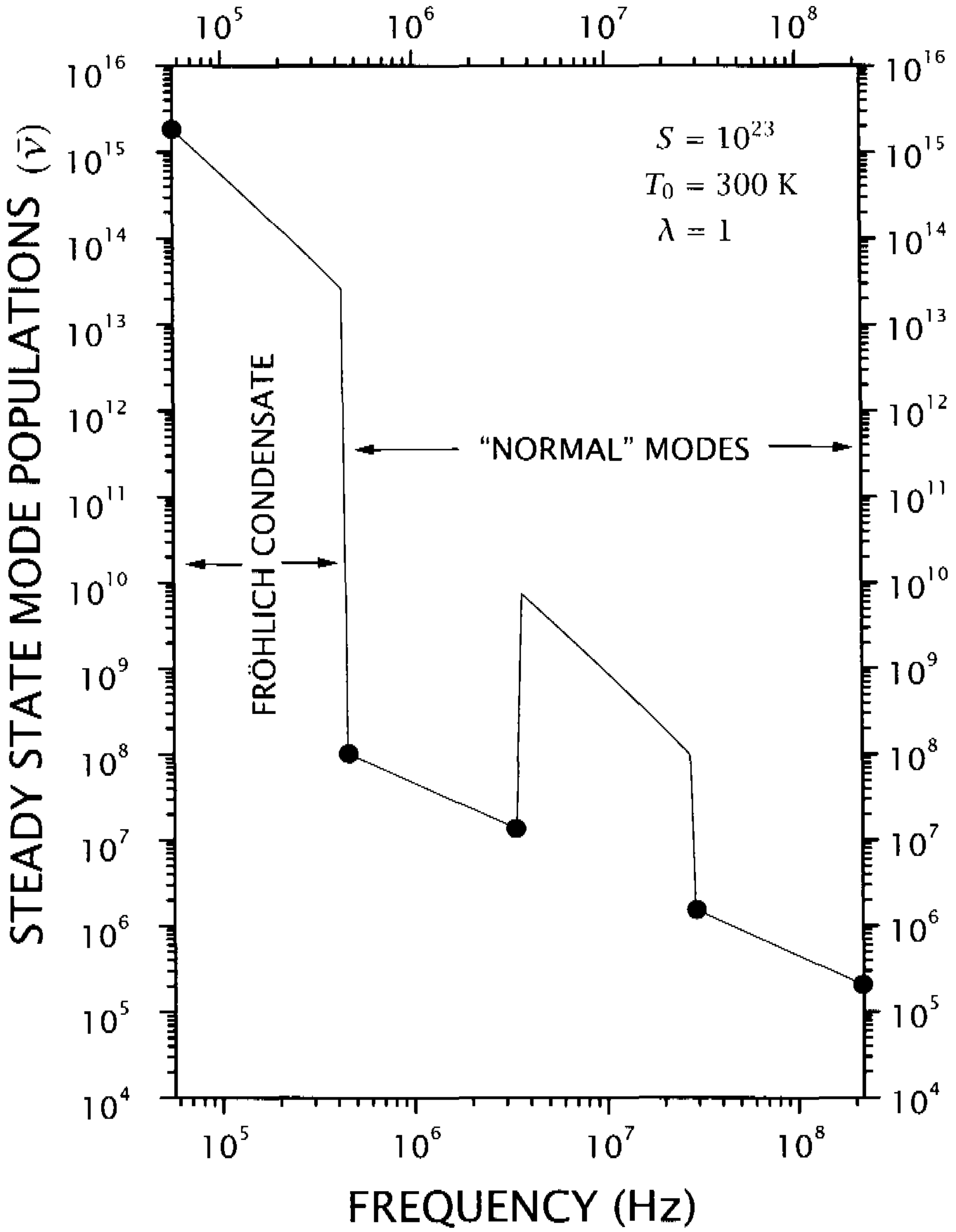

Figure 7: Acoustic vibrations: The population in the steady state for a pumping intensity $S = 10^{23}$, of the modes along the spectrum of frequencies of the acoustic modes. Dots indicate the modes in the first set (the remaining part of the spectrum up to the highest Brillouin frequency $\omega_B = 9.5 \times 10^{11}$ Hz has been omitted). (After Ref. [51]).

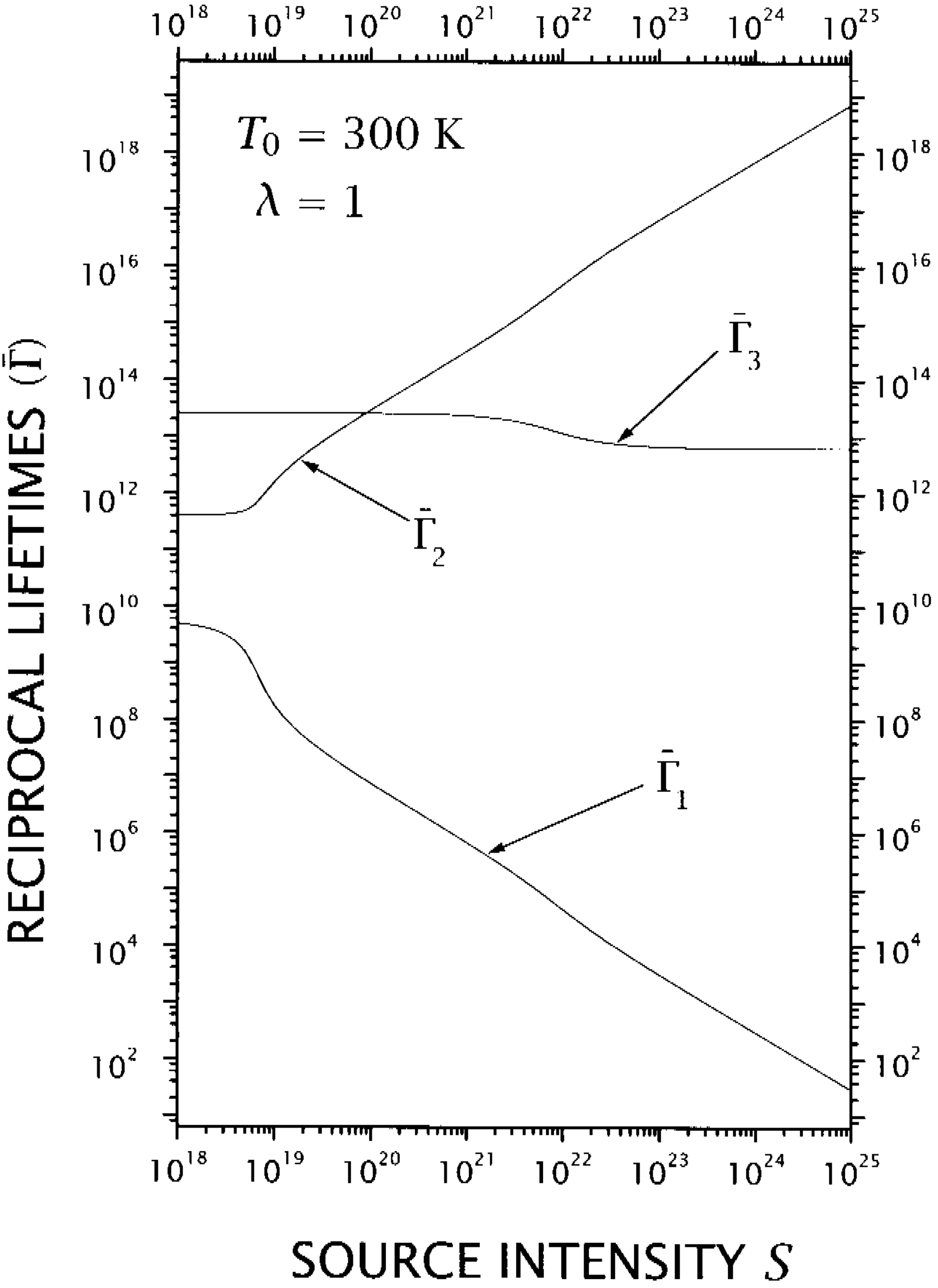

Figure 8: Acoustic vibrations: The lifetime of the same modes as in Fig. 7, in terms of the intensity of the pumping source (After Ref. [51]).

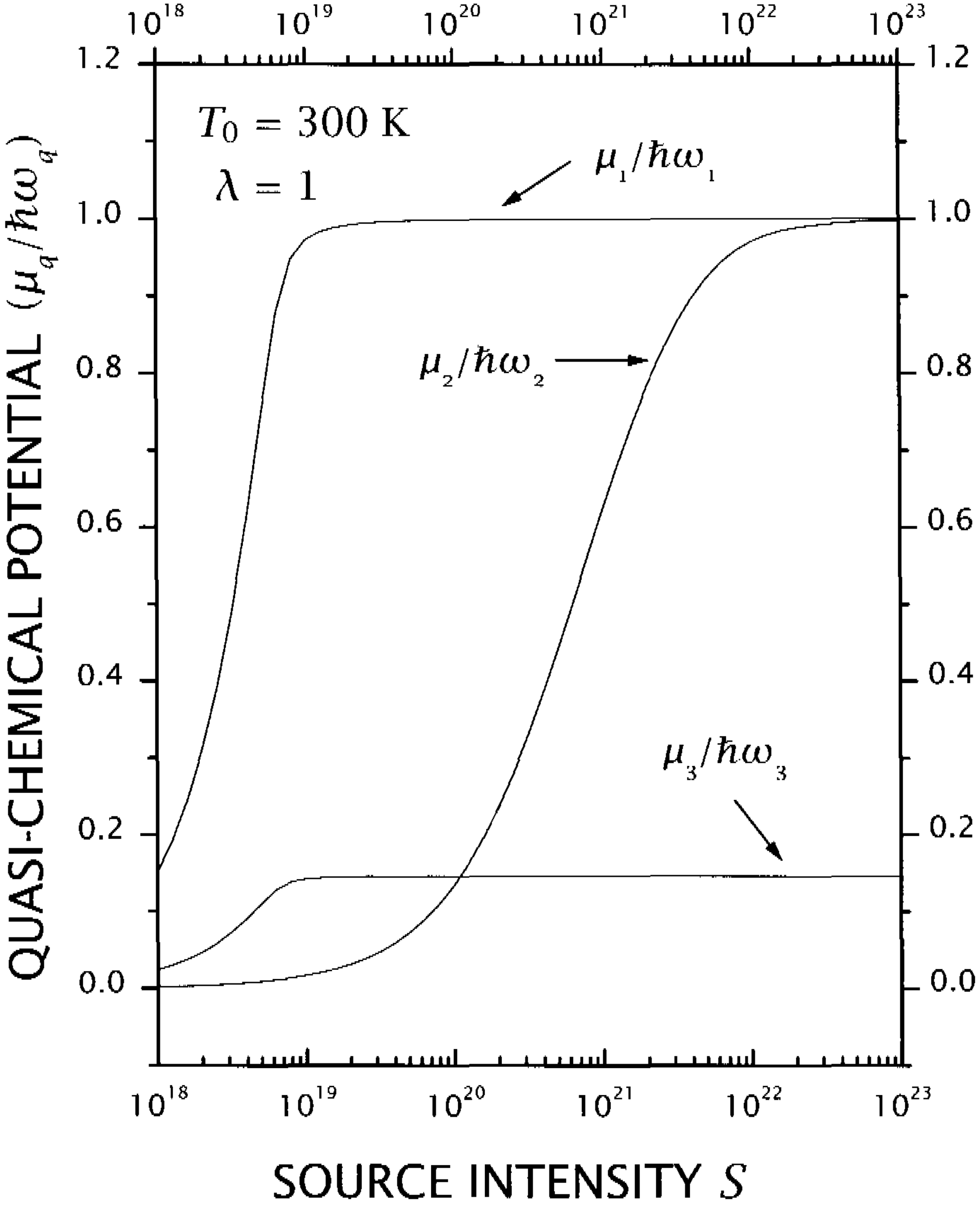

Figure 9: The quasi-chemical potential of the modes labeled 1 to 3 in Fig 6, with mode 1 corresponding to the one with the lowest frequency in the given set: it is evident the emergence of a "Bose-Einstein-like condensation" for S approaching a critical value of the order of 10^{19}.

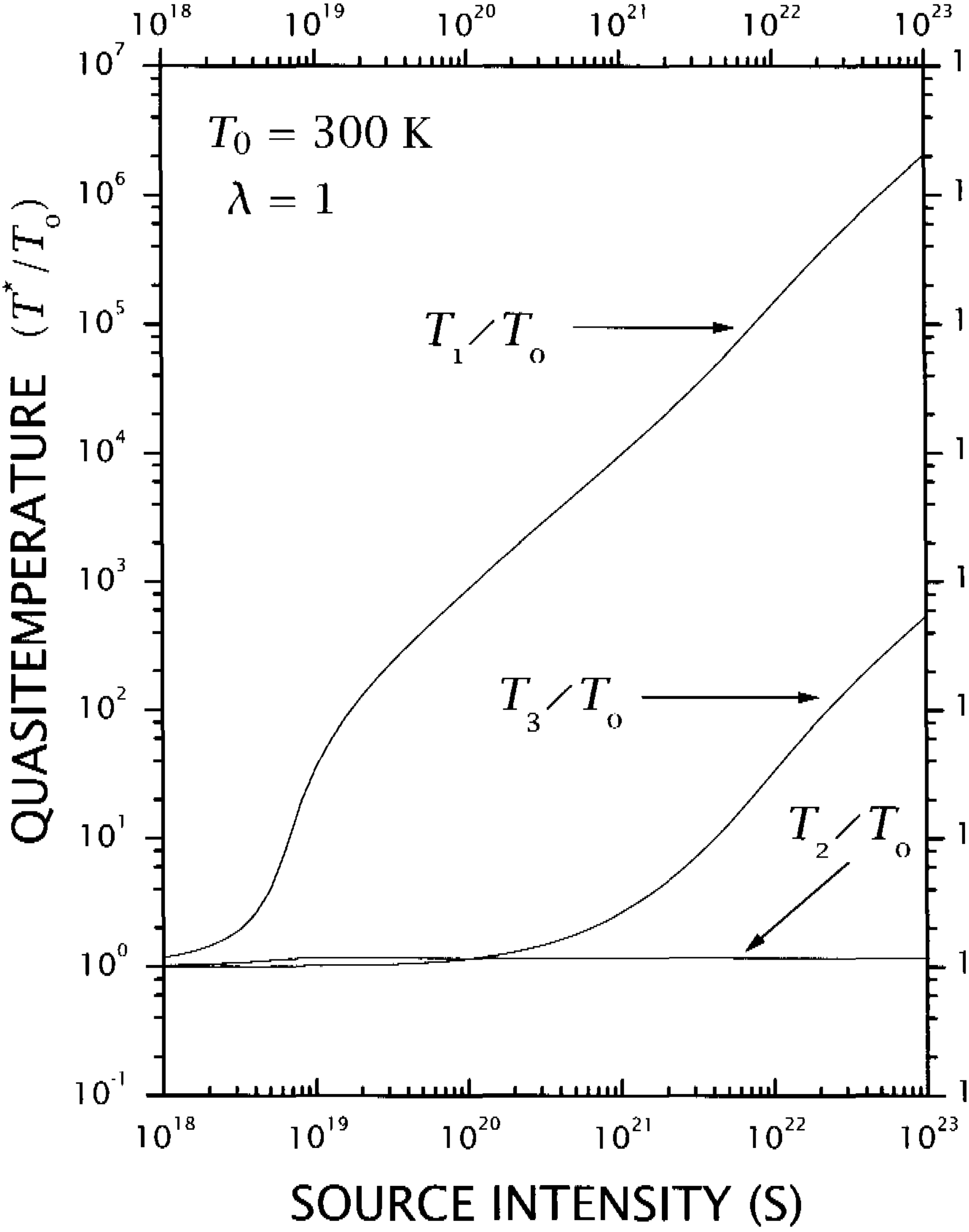

Figure 10: The quasi-temperature, defined in Eq. (30) for the modes in Fig. 6.

MESQUITA *et al.* — *J. Biol. Phys.* FIGURE 10

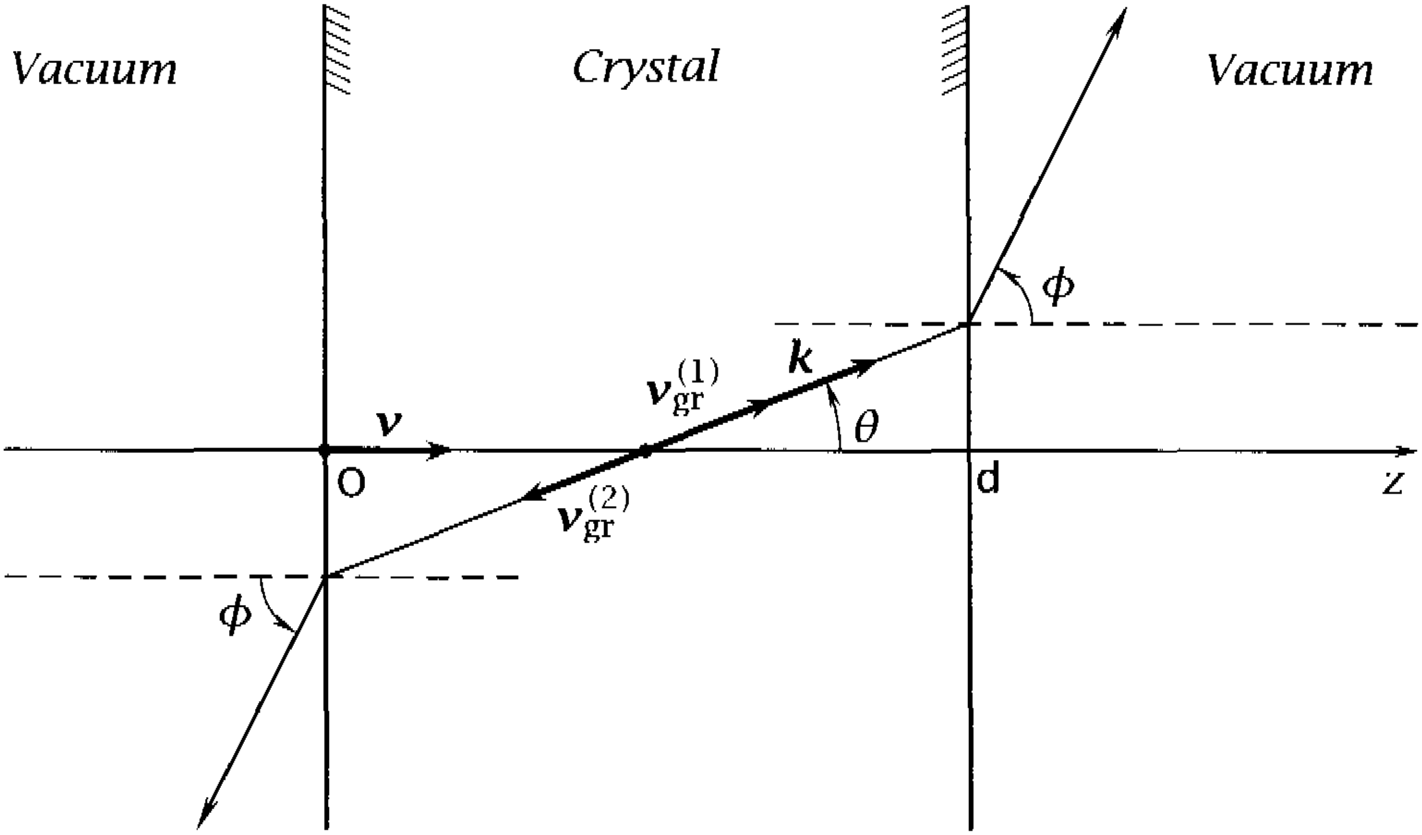

Figure 11: The direction of propagation of the waves of Cherenkov radiation, when spatial dispersion is taken into account, for the ordinary wave (subscript 1) and the anomalous wave (subscript 2) (Adapted from Ref. [49]).

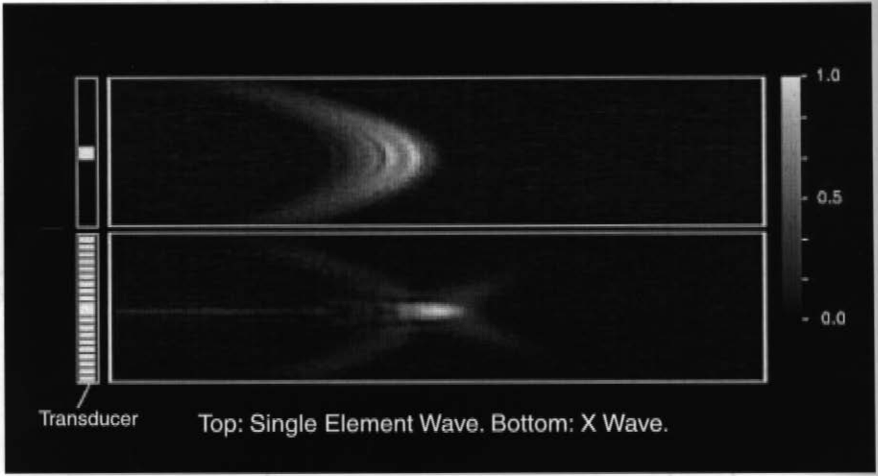

Figure 12: Normal sound propagation (upper figure), and the excitation interpreted as a supersonic soliton (lower figure); from reference [3] (We thank W. A. Rodrigues and J. E. Maiorino for providing us with a postscript file of this picture).

6.4 Comportamento complexo em biosistemas: uma abordagem teórico-informacional

A questão particular do transporte de energia vibracional em biosistemas é considerada dentro do escopo do modelo de Fröhlich-Davydov. É mostrado que as ondas solitárias de Davydov, fortemente amortecidas em condições de quase equilíbrio, podem apresentar uma propagação de longo alcance quando viajam sobre o condensado de Fröhlich. Este último consiste na emergência de uma estrutura dissipativa auto-organizada (no sentido de Prigogine), assemelhando-se a um condensação de não-equilíbrio tipo Bose-Einstein na parte inferior dos modos de freqüência de vibração, uma vez que um nível crítico de alimentação de energia metabólica é alcançado.

Submetido para publicação em *Chaos, Solitons and Fractals.*

Complex Behavior in Biosystems: An Information-Theoretic Approach

Áurea R. Vasconcellos, Marcus V. Mesquita, Roberto Luzzi

Instituto de Física 'Gleb Wataghin',
Universidade Estadual de Campinas, Unicamp
13083-970 Campinas, São Paulo, Brazil

The particular question of transport of vibrational energy in biosystems is considered within the scope of Fröhlich-Davydov's model. It is shown that Davydov's solitary waves, strongly damped in near equilibrium conditions, can display long-range propagation when travelling in Fröhlich's condensate. The latter consists in the emergence of a self-organized dissipative structure (in Prigogine's sense), resembling a nonequilibrium Bose-Einstein-like condensation in the low-lying in frequency modes of vibration, once a critical level of pumping of metabolic energy is achieved.

Key words: Complex Biosystems; Bioenergetic processes; Informational"-Statistical Thermodynamics; Nonequilibrium Kinetics.

Group Home Page: http://www.ifi.unicamp.br/~aurea

1. INTRODUCTION

Nonlinearity is known to be the source of new and unexpected phenomena that characterize complex behavior in physico-chemical systems. This is particularly the case in dissipative systems far from equilibrium [1]. Quite recently, the question concerning the theoretical description of the macroscopic behavior of dissipative open many-body systems in arbitrarily far-from-equilibrium conditions has been encompassed in a seemingly powerful, concise, and elegant formalism, established on sound basic principles. This is the Nonequilibrium Statistical Operator Method (NESOM) [8–13] which appears to be encompassed in Jaynes' Predictive Statistical Mechanics [14, 15]. The NESOM allows for the construction of a nonlinear quantum transport theory of a large scope [8, 11, 16] and a thermodynamics of irreversible processes, termed Informational Statistical Thermodynamics (IST; sometimes referred to as Information-theoretic Thermodynamics, which is briefly reviewed with accompanying historical notes in Ref. [17]), which provides the foundations for the treatment of dissipative open macrosystems away (either near or far) from equilibrium.

Particularly, biological matter consists of nonequilibrium thermodynamic open systems where energy is always available, through metabolic processes, that is, the open biosystem "feeds" on this energy and is driven away from equilibrium. A quite fundamental point is that the evolution of the system has associated a nonlinear kinetics (which can be described in NESOM-IST). This nonlinearity in the equations of evolution of the macroscopic properties of the system is of fundamental relevance for the emergence of synergetic phenomena. Complex behavior in matter is a subject that is attracting more and more interest in science [20, 21].

Quite interesting and illustrative examples of nonlinearity at work, producing what can be relevant biological effects, are Fröhlich's condensate [19, 23, 24] and Davydov's solitons [25–30]. Fröhlich's effect consists in that, under appropriate conditions a phenomenon quite similar to a Bose-Einstein condensation may occur in substances with vibrational polar modes. If energy is fed into these modes and thence transferred to other degrees of freedom of the substance (a thermal bath), then a stationary state will be reached in which the energy content of the vibrational modes is larger than in thermal equilibrium. This excess energy is found to be channelled into the modes lowest in frequency — similarly to the case of a Bose condensation — provided the energy supply exceeds a critical value. Under these circumstances a random supply of energy is thus not completely thermalized but partly used in maintaining a coherent behavior in the substance. On the other hand, A. S. Davydov showed that due to nonlinear interactions, of the same type as those responsible for Fröhlich's effect, it is expected to arise a novel mechanism for the localization and transport of vibrational energy in protein, namely the propagation of a solitary-like wave. The equivalence of the Hamiltonians used to describe Fröhlich and Davydov models, when both are placed in a representation in terms of normal coordinates, was shown by Tuszynski *et al.* [31]. Hence, while Fröhlich's approach is connected with the study of the steady state in the model pumped by external sources of metabolic energy, Davydov's approach refers to the dynamic aspect of propagation of the information-carrying oscillations. Davydov's theory has received plenty of attention, and a long list of results published up to the first half of 1992 are discussed in the excellent review by A. C. Scott [32]. We address here this question, through a study of the Fröhlich-Davydov model in nonequilibrium thermodynamic conditions.

We consider a system where modes of polar vibrations are excited by a continuous supply of metabolic energy. These polar modes are in interaction with a bath of acoustic-like vibrations through a nonlinear dynamics. The kinetic equations of evolution for the population of the vibrational modes are derived in NESOM. After a short transient time there follows a steady state, where, after a certain threshold of the pumping intensity is achieved, there follows Fröhlich's condensation, as described in section 2. In section 3, we consider the propagation of oscillations in the polar system. The equation of evolution for the NESOM-averaged amplitude is of the Davydov's soliton type, but with damping. The lifetime of the excitation in normal conditions is very short, but it is shown that it increases enormously for the modes in Fröhlich's condensate. In last section we summarize and discuss the results.

2. THE MODEL AND FRÖHLICH'S CONDENSATE

Let us consider a model biosystem which can sustain longitudinal polar vibrations in interaction with a thermal bath of acoustic-like vibrations. We write for the Hamiltonian of the system

$$H = H_{01} + H_{02} + H_{11} + H_{12} + H_{13} + H_{14} + H_{21} + H_{22} + H_{23} + H_{24} + H_f \,, \tag{1}$$

$$H_{01} = \sum_q \hbar\omega_q \left(a_q^\dagger a_q + \frac{1}{2} \right) \,, \tag{2a}$$

is the Hamiltonian of the free polar vibrations, with $\omega_{\boldsymbol{q}}$ being their frequency dispersion relation ($\boldsymbol{q}$ runs over the reciprocal space Brillouin zone); $a(a^\dagger)$ are creation (annihilation) operators in mode $\boldsymbol{q}$;

$$H_{02} = \sum_{\boldsymbol{q}} \hbar\Omega_{\boldsymbol{q}} \left(b_{\boldsymbol{q}} b_{\boldsymbol{q}}^\dagger + \frac{1}{2} \right) \tag{2b}$$

is the Hamiltonian of the bath of free acoustic-like vibrations; $b(b^\dagger)$ are creation (annihilation) operators in mode $\boldsymbol{q}$ with frequency $\Omega_{\boldsymbol{q}}$. The other terms in Eq. (1) are the anharmonic interactions given by

$$H_{11} = \sum_{\boldsymbol{q}\boldsymbol{q}'} V^{(1)}_{\boldsymbol{q}\boldsymbol{q}'} a_{\boldsymbol{q}} b_{\boldsymbol{q}'} b^\dagger_{\boldsymbol{q}+\boldsymbol{q}'} + \text{H.c.}\,; \qquad H_{12} = \sum_{\boldsymbol{q}\boldsymbol{q}'} V^{(1)}_{\boldsymbol{q}\boldsymbol{q}'} a_{\boldsymbol{q}} b^\dagger_{\boldsymbol{q}'} b_{-\boldsymbol{q}+\boldsymbol{q}'} + \text{H.c.}\,; \tag{2c,d}$$

$$H_{13} = \sum_{\boldsymbol{q}\boldsymbol{q}'} V^{(1)}_{\boldsymbol{q}\boldsymbol{q}'} a_{\boldsymbol{q}} b_{\boldsymbol{q}'} b_{-\boldsymbol{q}-\boldsymbol{q}'} + +\text{H.c.}\,; \qquad H_{14} = \sum_{\boldsymbol{q}\boldsymbol{q}'} V^{(1)}_{\boldsymbol{q}\boldsymbol{q}'} a_{\boldsymbol{q}} b^\dagger_{\boldsymbol{q}'} b^\dagger_{\boldsymbol{q}-\boldsymbol{q}'} + \text{H.c.} \tag{2e,f}$$

$$H_{21} = \sum_{\boldsymbol{q}\boldsymbol{q}'} V^{(2)}_{\boldsymbol{q}\boldsymbol{q}'} a_{\boldsymbol{q}} a_{\boldsymbol{q}'} b^\dagger_{\boldsymbol{q}+\boldsymbol{q}'} + \text{H.c.}\,; \qquad H_{22} = \sum_{\boldsymbol{q}\boldsymbol{q}'} V^{(2)}_{\boldsymbol{q}\boldsymbol{q}'} a_{\boldsymbol{q}} a_{\boldsymbol{q}'} b_{-\boldsymbol{q}-\boldsymbol{q}'} + \text{H.c.}\,; \tag{2g,h}$$

$$H_{23} = \sum_{\boldsymbol{q}\boldsymbol{q}'} V^{(2)}_{\boldsymbol{q}\boldsymbol{q}'} a^\dagger_{\boldsymbol{q}} a_{\boldsymbol{q}'} b_{\boldsymbol{q}-\boldsymbol{q}'} + \text{H.c.}\,; \qquad H_{24} = \sum_{\boldsymbol{q}\boldsymbol{q}'} V^{(2)}_{\boldsymbol{q}\boldsymbol{q}'} a_{\boldsymbol{q}} a^\dagger_{\boldsymbol{q}'} b^\dagger_{\boldsymbol{q}-\boldsymbol{q}'} + \text{H.c.}\,; \tag{2i,j}$$

$V^{(1)}$ and $V^{(2)}$ are the matrix elements of the interaction potential. Finally,

$$H_f = \sum_{\boldsymbol{q}} \varphi_{\boldsymbol{q}} a^\dagger_{\boldsymbol{q}} + \text{H.c.}\,, \tag{2k}$$

stands for the energy of interaction between the pumping source and the polar modes; $\varphi(\varphi^\dagger)$ are annihilation (creation) operators of excitations in the source, also containing the coupling strength. Further, we introduce — as required by the NESOM — the partial Hamiltonians

$$H_0 = H_{01} + H_{02}, \tag{3a}$$

$$H' = H_{11} + H_{12} + H_{13} + H_{14} + H_{21} + H_{22} + H_{23} + H_{24} + H_f, \tag{3b}$$

Once the system Hamiltonian is given, the next step in NESOM is the choice of the basic set of variables deemed appropriate for the description of the macroscopic state of the system: We introduce the populations of the polar vibrations

$$\nu_q(t) = \mathrm{Tr}\left\{a_q^\dagger a_q \bar{\varrho}(t,0)\right\}, \tag{4}$$

of relevance to evidence *a posteriori* Fröhlich effect, and, assuming the thermal bath to be constantly kept at a fixed physiological temperature by means of an efficient homeostatic mechanism, we introduce the energy of the acoustic-like vibrations, namely

$$E_b(t) = \mathrm{Tr}\left\{\sum_q \hbar\Omega_q \left(b_q^\dagger b_q + \frac{1}{2}\right) \bar{\varrho}(t,0)\right\}, \tag{5}$$

In Eqs. (4) and (5), $\bar{\varrho}(t,0)$ is the auxiliary (coarse grained) nonequilibrium operator in NESOM, in the present case given by

$$\bar{\varrho}(t,0) = \exp\left\{-\phi(t) - \beta H_{02} - \sum_q F_q(t) a_q^\dagger a_q\right\}, \tag{6}$$

where ϕ ensures its normalization, $\beta = (k_B T_0)^{-1}$ (with T_0 being the constant temperature of the bath; k_B is Boltzmann constant), and $F_q(t)$ is the intensive variable thermodynamically conjugated to the population number operator in the variational approach to the NESOM [12]. The complete (fine grained) nonequilibrium statistical operator is a superoperator depending on the coarse-grained distribution of Eq. (6), which in Zubarev's approach to the NESOM [8, 9], to be used in what follows, is given by

$$\varrho_\varepsilon(t) = \exp\left\{ -\hat{S}(t,0) + \int_{-\infty}^{t} dt' \, e^{\varepsilon(t'-t)} \frac{d}{dt'} \hat{S}(t', t'-t) \right\}, \tag{7}$$

$$\hat{S}(t,0) = -\ln \bar{\varrho}(t,0) \tag{8a}$$

is the so-called informational-entropy operator, and

$$\hat{S}(t', t'-t) = \exp\left\{ -\frac{1}{i\hbar}(t'-t)H \right\} \hat{S}(t,0) \exp\left\{ \frac{1}{i\hbar}(t'-t)H \right\} . \tag{8b}$$

In Eq. (7) ε is a positive infinitesimal which ensures irreversible evolution from the initial state of preparation of the system, and goes to zero after the trace operation in the calculation of averages has been performed. Moreover, we notice that in Eqs. (8) the two time variables in the argument of $\hat{S}$ correspond, the first one, to the evolution of the thermodynamic variables (here ϕ and F_q, since β is constant), and the second indicates the evolution of the dynamical operators in Heisenberg representation.

Since β is assumed to be constant in time, we are simply left to calculate the equations of evolution for the population of the polar modes of Eq. (4). As noted in the Introduction these equations are derived resorting to the nonlinear quantum generalized transport theory that the NESOM provides. We introduce an approximate treatment, however appropriate for the present case since the anharmonic terms in Eq. (3b) are expected to be weak interactions, consisting of the so-called second order approximation in relaxation theory [16], usually referred to as the quasi-linear theory of relaxation [8, 34], which is a Markovian approximation and exact up to second order in the interaction strengths in H'.

The calculation shows that, because of the symmetry properties of the system and the selected choice of basic variables, several contributions to the collision operators in the NESOM-SOART transport equations vanish in this case, surviving the one that corresponds to the Golden Rule of quantum mechanics averaged over the nonequilibrium ensemble characterized by the NESO of Eq. (7). The final expression is

$$\frac{d}{dt}\nu_{\mathbf{q}}(t) = I_{\mathbf{q}} + \sum_{j=1}^{5} J_{\mathbf{q}_{(j)}}(t) \, , \tag{9}$$

$$J_{\mathbf{q}_{(1)}}(t) + J_{\mathbf{q}_{(2)}}(t) = -\tau_{\mathbf{q}}^{-1}[\nu_{\mathbf{q}}(t) - \nu_{\mathbf{q}}^{(0)}] \, , \tag{10a}$$

with $\nu_{\mathbf{q}}^{(0)}$ being the $\mathbf{q}$-mode-population in equilibrium, i.e. Planck distribution at temperature T_0, and $\tau_{\mathbf{q}}$ is a relaxation time given by

$$\tau_{\mathbf{q}}^{-1} = \frac{4\pi}{\hbar^2}\frac{1}{\nu_{\mathbf{q}}^{(0)}}\sum_{\mathbf{q}'} |V_{\mathbf{q}\mathbf{q}'}^{(1)}|^2 \nu_{\mathbf{q}'}^{B} \nu_{\mathbf{q}\ \mathbf{q}'}^{B} \left[\delta(\Omega_{\mathbf{q}'} + \Omega_{\mathbf{q}-\mathbf{q}'} - \omega_{\mathbf{q}}) + 2e^{\beta\hbar\Omega_{\mathbf{q}'}}\delta(\Omega_{\mathbf{q}'} - \Omega_{\mathbf{q}-\mathbf{q}'} + \omega_{\mathbf{q}})\right] , \tag{10b}$$

where $\nu_{\mathbf{q}}^{B}$ is the population of the vibrational modes of the bath at temperature T_0, given by the Planck distribution

$$\nu_{\mathbf{q}}^{B} = [\exp(\beta\hbar\Omega_{\mathbf{q}}) - 1]^{-1} \, , \tag{11}$$

and the other remaining terms are

$$J_{q_{(3)}}(t) = \frac{8\pi}{\hbar^2} \sum_{q'} |V^{(2)}_{qq'}|^2 \left[\nu^B_{q-q'}(\nu_{q'} - \nu_q) - \nu_q(1 + \nu_{q'})\right] \delta(\Omega_{q-q'} + \omega_{q'} - \omega_q) \,, \tag{12a}$$

$$J_{q_{(4)}}(t) = \frac{8\pi}{\hbar^2} \sum_{q'} |V^{(2)}_{qq'}|^2 \left[\nu^B_{q-q'}(\nu_{q'} - \nu_q) + \nu_{q'}(1 + \nu_q)\right] \delta(\Omega_{q-q'} - \omega_{q'} + \omega_q) \,, \tag{12b}$$

$$J_{q_{(5)}}(t) = \frac{8\pi}{\hbar^2} \sum_{q'} |V^{(2)}_{qq'}|^2 \left[\nu^B_{q+q'}(1 + \nu_{q'}) - (\nu_{q'} - \nu^B_{q+q'})\nu_q\right] \delta(\Omega_{q+q'} - \omega_{q'} - \omega_q) \,, \tag{12c}$$

Furthermore, we have expressed the time-dependent correlations involving the operators associated to the external source in terms of a spectral density, namely

$$\frac{2\pi}{\hbar^2} \left\langle \left[\varphi_q(t), \varphi^\dagger_q\right]\right\rangle = \int_{-\infty}^{\infty} \frac{d\omega}{\pi} I_q(\omega)\, e^{i\omega t} \,, \tag{13}$$

where $I(\omega)$ represents the intensity of the source over the spectrum of frequencies.

Equation (9) is of the type of equation proposed by Fröhlich. The rate of change of $\nu_q(t)$ is composed of a pumping term (increasing the population); a relaxation term to the thermal bath, decreasing the population at a rate τ^{-1}; $J_{(5)}$ is also a relaxation term (containing contributions nonlinear in the mode populations); while $J_{(3)}$ and $J_{(4)}$ are those to be responsible for Fröhlich effect: they account for, through the nonlinear terms, the transfer of energy to the low-frequency polar modes.In fact, they contain nonlinear contributions proportional to

$$\sum_{q'} |V^{(2)}_{qq'}|^2 \nu_q(t)\nu_{q'}(t) \left[\delta(\Omega_{q-q'} - \omega_{q'} + \omega_q) - \delta(\Omega_{q-q'} + \omega_{q'} - \omega_q)\right] \,, \tag{14}$$

and we may notice that for modes $\boldsymbol{q}'$ such that $\omega_{\boldsymbol{q}} > \omega_{\boldsymbol{q}'}$ the energy conservation as required by the first delta function is satisfied, while this is not possible for the second: hence this nonlinear contribution tends to increase the population in mode $\boldsymbol{q}$ at the expenses of the other modes higher in frequency. It has been argued that contributions coming from $J_{\boldsymbol{q}(5)}$ wash away the effect [35]. Fröhlich [36] has countered that it has a small contribution as a result of the different form of energy conservation in both processes, what is clearly evidenced by our expressions in Eqs. (12); in particular for the usual case when the frequencies of the polar modes are higher than those of the acoustic modes, $J_{\boldsymbol{q}(5)}$ vanishes. The equation of evolution for the mode population, here derived in NESOM-SOART and normal coordinates, resemble the one obtained by Wu and Austin [37] and Mills [38].

Equation (9) is a complicated set of coupled integro-differential equation for the populations of the modes, the coupling involving all modes contained in the Brillouin zone. We contour this difficulty resorting to a simplified model. Taking into account the established fact that high frequency modes transfer energy to the low frequency ones, we introduce a crude model, in which we consider as identical the energy transferring modes, having frequency ω_0 and contained in a region $\mathcal{R}_0$ of the Brillouin zone, and a second representative set of modes receiving that energy, having frequency ω_1 and contained in a region $\mathcal{R}_1$ of the Brillouin zone (hence $\omega_0 > \omega_1$).

Further we assume, as it is generally the case, that the polar mode frequencies are always higher than the acoustic mode frequencies, what then excludes the contributions of $J_{\boldsymbol{q}(1)}$, $J_{\boldsymbol{q}(3)}$, and $J_{\boldsymbol{q}(3)}$ because energy conservation cannot be satisfied. We are then left with only two coupled equations for the representative modes in the model, which are

$$\frac{d}{dt}\nu_0(t) = I_0 - \tau_0^{-1}[\nu_0(t) - \nu_0^{(0)}] - g_1\eta[e^{\beta\hbar\Delta}\nu_0(t) - \nu_1(t)] - g_1\nu_0(t)\nu_1(t), \quad (15a)$$

$$\frac{d}{dt}\nu_1(t) = I_1 - \tau_1^{-1}[\nu_1(t) - \nu_1^{(0)}] + g_0\eta[e^{\beta\hbar\Delta}\nu_0(t) - \nu_1(t)] + g_0\nu_0(t)\nu_1(t), \quad (15b)$$

$$\Delta = \omega_0 - \omega_1 , \qquad \eta = \left[e^{\beta\hbar\Delta} - 1\right]^{-1} , \quad (16a,b)$$

$$g_0 = \frac{8\pi}{\hbar^2}\sum_{q'\in\mathcal{R}_0} |V^{(2)}_{q_0q'}|^2\delta(\Omega_{q_0\ q'} - \Delta) , \quad g_1 = \frac{8\pi}{\hbar^2}\sum_{q'\in\mathcal{R}_1} |V^{(2)}_{q_1q'}|^2\delta(\Omega_{q_1\ q'} - \Delta) , \quad (16c,d)$$

$\nu_0^{(0)}$ and $\nu_1^{(0)}$ are the distributions in equilibrium, $\boldsymbol{q}_0$ and $\boldsymbol{q}_1$ label each type of representative modes. Quantities g_0 and g_1 are a measure of the intensity of the coupling between the two sets of modes, involving the strength of the interaction, contained in the matrix element, and the region in energy-momentum space available for the scattering events, determined by the energy conserving delta function [momentum conservation is automatically accounted for in the expression for the Hamiltonian of Eqs. (1) and (2)].

Consider now the stationary state, i.e. $\dot{\nu}_0 = 0$ and $\dot{\nu}_1 = 0$ (where the upper dot stands for time derivative), in which case, from Eqs. (15), we find that

$$\bar{\nu}_0 = \frac{A_0 + C_0\bar{\nu}_1}{B_0 + g_1\bar{\nu}_1} , \qquad \bar{\nu}_1 = \frac{A_1 + C_1\bar{\nu}_0}{B_1 - g_0\bar{\nu}_0} , \quad (17a,b)$$

where the bar over the populations stands for stationary state values, and

$$A_0 = I_0 + \tau_0^{-1}\nu_0^{(0)} ; \qquad A_1 = I_1 + \tau_1^{-1}\nu_1^{(0)} ; \quad (18)$$

$$B_0 = \tau_0^{-1} + g_1\eta\exp(\beta\hbar\Delta); \qquad B_1 = \tau_1^{-1} + g_0\eta ; \quad (19)$$

$$C_0 = g_1\eta; \qquad\qquad C_1 = g_0\eta\exp(\beta\hbar\Delta)\,. \tag{20}$$

We look next for a numerical solution of the coupled pair of algebraic equations (17). First we multiply coefficients A, B, and C, as well as g_0 and g_1 by a scaling factor $\bar{\tau}$ with dimensions of time, to be determined later on [see arguments following Eqs. (42)]. For illustrative purposes we take $g_0\bar{\tau} = 0.9$, $g_1\bar{\tau} = 0.1$, $\tau_0^{-1}\bar{\tau} = 15$, $\tau_1^{-1}\bar{\tau} = 18$, $\omega_0 = 10^{13}$ s^{-1}, $\omega_1 = 8.7\times 10^{12}$ s^{-1}, and take $I_0\bar{\tau} = S$, and $I_1 = 0$. The numerical results are displayed in Fig. 1.

Inspection of Fig. 1 clearly shows the onset of Fröhlich effect at an intensity threshold $S_c = 500$, roughly given by the value of S where ν_1 steeply increases, and the pumping modes, represented by ν_0, acquire a nearly constant value. Hence, it is undoubtedly evidenced the condensation of excitations in the modes low in frequencies.

Furthermore, it is worth mentioning that using the NESO of Eq. (6) in Eq. (4), we find that

$$\nu_q(t) = \{\exp[F_q(t)] - 1\}^{-1}\ , \tag{21}$$

what defines the NESOM Lagrange multiplier $F_q(t)$. Making the choice

$$F_q(t) = \beta[\hbar\omega_q - \mu_q(t)]\,, \tag{22}$$

Equation (21) takes a form reminiscent of a Bose-Einstein distribution with temperature

T but a different chemical potential for each mode. Using this expression, we find that

$$\beta\mu_q(t) = \beta\hbar\omega_q - \ln\left[1 + \frac{1}{\nu_q(t)}\right] , \tag{23}$$

In our model with two sets of modes, with increasing population ν_1 of the low frequency modes after the critical threshold, μ_1 approaches $\hbar\omega_1$ (see Fig. 2) and there follows a kind of Bose-Einstein phase transformation, here not in equilibrium, but in nonequilibrium conditions. We noticed that μ_1 approaches asymptotically ω_1 for S going to infinity, but never coincide with it.

As a final question in this section, let us consider the energetic implications of the results. Considering an intensity $S \simeq 1000$ (beyond the critical point), using $\tau_0 \simeq \tau_1 \simeq 10$ picoseconds, and ω_0 being of the order of 10^{13} s^{-1}, this requires a pumping power of 6.4×10^{-9} Watts per mode. Assuming that this power is provided through hydrolysis of ATP, which produces 7.3 kcal/mol, in the event of an almost total absorption of this energy in the process, to sustain a stationary Fröhlich condensate would require hydrolysis of 2×10^{-13} moles of ATP per mode per second. Consider a near one-dimensional system (e. g. the α-helix protein):the Brillouin-zone length is roughly 10^7 cm^{-1}, and if we consider a sample, say, 10 cm long, the number of modes is $\sim 3 \times 10^7$. If the propagation of the signal (as discussed in next section) takes, say, 10^{-5} s for riding the length of 10 cm (implying in a group velocity of 10^6 cm/s), for the process to be completed in Fröhlich condensate it would require $\sim 10^{-10}$ moles of ATP, a seemingly easily accessible value.

Another important consideration is the one related to the transient time that must elapse between the switch on of the pumping source and the emergence of the stationary-state Fröhlich condensate. Solution, in the given model, of the equations of evolution allows us to estimate this time as being in the picosecond range, that is, Fröhlich effect follows very rapidly after the pumping of metabolic energy into the vibrational modes has begun.

Having dealt with the stationary state of the model, let us consider in next section the dynamic aspects associated to the propagation of signals.

3. PROPAGATION OF EXCITATIONS

To consider the dynamical description of the system we introduce in NESOM, besides the basic variables of Eqs. (4) and (5), the operators for the amplitudes of vibration, a_q and $a_q^\dagger$. Hence the auxiliary statistical operator of Eq. (6) is extended to take the form

$$\bar{\varrho}(t,0) = \exp\left\{-\phi(t) - \beta H_{02} - \sum_q \left[F_q(t)a_q^\dagger a_q - \left(f_q(t)a_q + f_q^*(t)a_q^\dagger\right)\right]\right\} , \tag{24}$$

where f and f^* are the NESOM-Lagrange multipliers associated to the added dynamical quantities [39].

Introducing the canonical transformation (reminiscent of Glauber [40] transformation to coherent states in laser theory)

$$\tilde{a}_q = a_q - \langle a_q|t\rangle \ , \tag{25}$$

where $\tilde{a}$ is a new annihilation operator and $\langle a_q|t\rangle = \mathrm{Tr}\{a_q\ \bar{\varrho}(t,0)\}$, we find that

$$\tilde{\varrho}(t,0) = \exp\left\{-\tilde{\phi}(t) - \sum_q F_q(t)\tilde{a}_q^\dagger \tilde{a}_q\right\} , \tag{26a}$$

$$\tilde{\phi}(t) = \phi(t) - \frac{|f_q(t)|^2}{F_q(t)} , \tag{26b}$$

$$\langle a_q|t\rangle = \frac{f_q^*(t)}{F_q(t)} , \qquad \nu_q(t) = \tilde{\nu}_q(t) + |\langle a_q|t\rangle|^2 , \tag{26c,d}$$

$$\tilde{\nu}_q(t) = \{\exp[(F_q(t)] - 1\}^{-1} \tag{26e}$$

has the form of the expression of Eq. (21), i.e. the mode population in the absence of variables $\langle a_q|t\rangle$.

Resorting to NESOM-SOART, together with the use of Eqs. (26), after some algebra we arrive to the equations of evolution for the variables a, namely

$$\begin{aligned}\frac{\partial}{\partial t}\langle a_q|t\rangle = &-\mathrm{i}\,\tilde{\omega}_q\,\langle a_q|t\rangle - \Gamma_q\,\langle a_q|t\rangle - \mathrm{i}\,W_q\,\langle a_q|t\rangle^* + \\ &+\Gamma_q\,\langle a_q|t\rangle^* + \sum_{q_1 q_2}\left[R_{q_1 q_2}\,\langle a_{q_1}|t\rangle\,\langle a_{q_2}|t\rangle\,\langle a_{q_1+q_2\ \ q}|t\rangle^* + \text{c.c.}\right] ,\end{aligned} \tag{27a}$$

$$\frac{\partial}{\partial t}\langle a_q^\dagger|t\rangle = \frac{\partial}{\partial t}\langle a_q|t\rangle^* = \text{the c.c. of the r.h.s of Eq. (27a)} , \tag{27b}$$

$$\tilde{\omega}_q = \omega_q + W_q , \tag{28}$$

$$\begin{aligned}\Gamma_q(t) = &\frac{1}{2}\tau_q^{-1}(t) + \frac{4\pi}{\hbar^2}\sum_{q'}|V_{qq'}^{(2)}|^2\left[1 + \nu_{q'} + \nu^B_{q\ \ q'}\right]\delta(\Omega_{q-q'} + \omega_{q'} - \omega_q) \\ &- \frac{4\pi}{\hbar^2}\sum_{q'}|V_{qq'}^{(2)}|^2\left[\nu_{q'} - \nu^B_{q\ \ q'}\right]\delta(\Omega_{q-q'} - \omega_{q'} + \omega_q) \\ &+ \frac{4\pi}{\hbar^2}\sum_{q'}|V_{qq'}^{(2)}|^2\left[\nu_{q'} - \nu^B_{q+q'}\right]\delta(\Omega_{q+q'} - \omega_{q'} - \omega_q) .\end{aligned} \tag{29}$$

with τ_q given by Eq. (10b), and we omit to write down the long expression for W_q, which is a term of renormalization of frequency which will not be of interest in the following analysis. Furthermore,

$$R_{q_1 q_2} = \mathrm{i}\,\frac{2\pi}{\hbar^2}\,|V^{(2)}_{qq'}|^2 \Big\{(\omega_{q_1} + \omega_{q_2} - \Omega_{q_1+q_2} + \mathrm{i}\,\varepsilon)^{-1} + (\omega_{q_1} + \omega_{q_2} + \Omega_{q_1+q_2} + \mathrm{i}\,\varepsilon)^{-1} + $$

$$+ \ (\omega_{q_1} + \omega_{q_2} + \Omega_{q_1+q_2} + \mathrm{i}\,\varepsilon)^{-1} + (\omega_{q_1} - \omega_{q_2} - \Omega_{q_1+q_2} + \mathrm{i}\,\varepsilon)^{-1}\Big\} \ , \quad (30)$$

where ε is taken in the limit $+0$, producing a principal value part and an energy conserving delta function.

The coupled equations (27) contain linear and tri-linear terms. Ignoring the latter, the resulting linearized equation has as solutions damped wave motion, with frequency $\tilde{\omega}_q$ and lifetime Γ_q^{-1}. The complete equations are of the Davydov's soliton type, but with damping. In fact, if we introduce a representation in direct space, defining the operators

$$a_j = \sum_q a_q\, \mathrm{e}^{\mathrm{i}\, \boldsymbol{q}\cdot \boldsymbol{R}_j} \ , \quad (31)$$

where $\boldsymbol{R}_j$ is the position of the j-th oscillating center, and assuming that these centers are periodically spaced, we find that

$$\frac{\partial}{\partial t}\langle a_j|t\rangle = -\mathrm{i}\sum_l \Big\{[\omega_{jl} + W_{jl} - \mathrm{i}\,\Gamma_{jl}]\,\langle a_l|t\rangle + [W_{jl} - \mathrm{i}\,\Gamma_{jl}]\,\langle a_l|t\rangle^*\Big\}$$

$$+ \sum_{lm}\left[R_{jlm}\langle a_l|t\rangle\langle a_m|t\rangle\langle a_j|t\rangle^* + \text{c.c.}\right] \ , \quad (32)$$

$$\omega_{jl} = \sum_{q} \omega_{q}\, \mathrm{e}^{\mathrm{i}\, \boldsymbol{q}\cdot(\boldsymbol{R}_j - \boldsymbol{R}_l)} \,, \qquad W_{jl} = \sum_{q} W_{q}\, \mathrm{e}^{\mathrm{i}\, \boldsymbol{q}\cdot(\boldsymbol{R}_j - \boldsymbol{R}_l)} \,, \tag{33a,b}$$

$$\Gamma_{jl} = \sum_{q} \Gamma_{q}\, \mathrm{e}^{\mathrm{i}\, \boldsymbol{q}\cdot(\boldsymbol{R}_j - \boldsymbol{R}_l)} \,, \qquad R_{jlm} = \sum_{q_1 q_2} R_{q_1 q_2}\, \mathrm{e}^{\mathrm{i}\, \boldsymbol{q}_1\cdot(\boldsymbol{R}_j - \boldsymbol{R}_k)}\, \mathrm{e}^{\mathrm{i}\, \boldsymbol{q}_2\cdot(\boldsymbol{R}_j - \boldsymbol{R}_m)} \,. \tag{33c,d}$$

Consider now a one-dimensional chain [29, 32] and let us introduce the average field operators in the continuum

$$\psi(x,t) = \sum_{q} \langle a_{q} | t \rangle\, \mathrm{e}^{\mathrm{i} q x} \,. \tag{34}$$

Moreover, the frequency dispersion relation is approximated by

$$\omega_q = \omega_0 - \alpha q^2 \,, \tag{35}$$

where ω_0 and α are constants. Then, after neglecting the coupling terms with the conjugated equation (what is equivalent to introducing a truncated Hamiltonian in the so-called rotating wave approximation [41]), we obtain that

$$\begin{aligned} \mathrm{i}\hbar \frac{\partial}{\partial t}\psi(x,t) = (\hbar\omega_0 + \hbar\alpha \frac{\partial^2}{\partial x^2})\psi(x,t) - \mathrm{i}\hbar \int dx'\, \Gamma(x - x')\psi(x',t) + \\ + \int dx' dx'' R(x,x',x'')\psi(x'',t)\psi(x'',t)\psi^*(x,t) \,, \end{aligned} \tag{36}$$

$$R(x,x,x'') = \sum_{q_1 q_2} R_{q_1 q_2}\; \mathrm{e}^{\mathrm{i} q_1 (x - x') + \mathrm{i} q_2 (x - x'')} \,, \tag{37}$$

$$\Gamma(x - x') = \sum_{q} \Gamma_q\; \mathrm{e}^{\mathrm{i} q (x - x')} \,. \tag{38}$$

Equation (36) is a nonlinear Schrödinger-type equations with damping [39]. Introducing a local approximation (that is, neglecting space correlations) what is accomplished using the expressions

$$R(x,x',x'') = K\delta(x-x')\delta(x-x'') \, , \tag{39}$$

$$\Gamma(x-x') = \gamma\delta(x-x'), \tag{40}$$

we obtain that Eq. (36) becomes

$$\mathrm{i}\hbar\frac{\partial}{\partial t}\psi(x,t) = \left(\hbar\omega_0 + \hbar\alpha\frac{\partial^2}{\partial x^2}\right)\psi(x,t) - \mathrm{i}\hbar\gamma\psi(x,t) + K|\psi(x,t)|^2\psi(x,t) \, . \tag{41}$$

Equations (32) and (41) are of the form of the equations derived by Davydov in an alternative way, but here clearly showing damping effects.

In the simplified model consisting of two representative set of modes, the damping constants of Eq. (29) are

$$\bar{\Gamma}_0 = \frac{1}{2}(\bar{\tau}_0{}^{1} + \exp(\beta\hbar\Delta)\bar{g}_1\eta + \bar{g}_1\nu_1) \, , \qquad \bar{\Gamma}_1 = \frac{1}{2}(\bar{\tau}_1^{-1} + \bar{g}_0\eta - \bar{g}_0\nu_0) \, , \tag{42a,b}$$

where $\bar{\Gamma} = \Gamma\bar{\tau}$ and $\bar{g} = g\bar{\tau}$, with $\bar{\tau}$ being a scaling time. In equilibrium conditions at temperature 300 K, for the numerical values used in section 2, $\bar{\Gamma}_0^{(0)} = 9.22$ and $\bar{\Gamma}_1^{(0)} = 20.71$. Γ_0 can be obtained from linewidths of scattering bands (see for example Ref. [42]), and then it can be estimated the value of $\bar{\tau}$. Since the lifetimes are of the order of a few tens of picoseconds, a pulse signal impinged on the system would be carried a few micrometers, since the group velocity is expected to be in the order of 10^5 to 10^6 cm/s.

However, the situation is substantially modified if the excitation propagates in a nonequilibrium background, namely the one provided by the stationary Fröhlich's condensate discussed in section 2. This is a result of the fact that the damping constants depend on the actual state of the system, being affected by the nonlinear anharmonic interactions that are responsible, on the one hand, for Fröhlich effect, and [last term in Eqs. (27)] for Davydov's mechanism of exciton propagation. In the case of the model of section 2 we can obtain the two characteristic damping constants in terms of the pumping intensity, as shown in Fig. 3.

As a result, while the lifetime of the high frequency modes largely decreases ($\bar{\Gamma}_0$ increases in the figure), after the critical point for the onset of Fröhlich effect the lifetime of the low frequency modes in the Fröhlich-Bose condensate increases enormously ($\bar{\Gamma}_1$ decreases to near zero in the figure). Consequently we may expect that in Eqs. (27) there occur a very rapid (pico- to subpicosecond scale) damping of the amplitudes $\langle a_{\boldsymbol{q}}|t\rangle$ for values of $\boldsymbol{q}$ contained in the region $\mathcal{R}_0$ of the Brillouin zone described in section 2 (high frequency modes), while those of the region $\mathcal{R}_1$ (low frequency modes) are practically undamped. If we introduce the expression

$$\langle a_{\boldsymbol{q}}|t\rangle = A_{\bar{q}}(t)\exp\left[-\mathrm{i}\tilde{\omega}_{\boldsymbol{q}}t - \Gamma_{\boldsymbol{q}}t\right] \ , \tag{43}$$

after replacing it in Eqs. (27) we obtain that

$$\exp\left[-\mathrm{i}\,\tilde{\omega}_{\boldsymbol{q}}t - \Gamma_{\boldsymbol{q}}t\right]\frac{\partial}{\partial t}A_{\bar{q}}(t) = (-\mathrm{i}\,W_{\boldsymbol{q}} + \Gamma_{\boldsymbol{q}})A^{*}_{\bar{q}}(t)\exp\left[-\mathrm{i}\,\tilde{\omega}_{\boldsymbol{q}}t - \Gamma_{\boldsymbol{q}}t\right] +$$

$$+\sum_{\boldsymbol{q}_1\boldsymbol{q}_2}\left[R^{*}_{\boldsymbol{q}_1\boldsymbol{q}_2}A_{\bar{q}_1}(t)A_{\bar{q}_2}(t)A^{*}_{\bar{q}_1+\boldsymbol{q}_2-\boldsymbol{q}}(t)\right]\times$$

$$\times \exp\left[-\mathrm{i}(\tilde{\omega}_{\boldsymbol{q}_1} + \tilde{\omega}_{\boldsymbol{q}_2} - \tilde{\omega}_{\boldsymbol{q}_1+\boldsymbol{q}_2-\boldsymbol{q}})t\right] \exp\left[-\mathrm{i}(\Gamma_{\boldsymbol{q}_1} + \Gamma_{\boldsymbol{q}_2} - \Gamma_{\boldsymbol{q}_1+\boldsymbol{q}_2-\boldsymbol{q}})t\right] . \quad (44)$$

Hence, those amplitudes with small lifetime decay rapidly, and survive those corresponding to modes in Fröhlich's condensate, where Γ is practically null. Consequently, in the expression for the average field operator in the continuum of Eq. (34), after a very short transient (expected to be in the subpicosecond range) only the contributions from the modes in the condensate survive, i.e. the summation in Eq. (34) can be restricted to modes $\boldsymbol{q} \in \mathcal{R}_1$ in reciprocal space. Then in Eq. (41) the damping term disappears ($\gamma = 0$), and we recover an equation for an undamped Davydov's soliton. Summarizing, according to the results thus far derived there should follow propagation of a coherent-Davydov's soliton-like excitation, composed by the low-lying excited vibrational states, which can travel very long distances, once metabolic energy has been provided to produce a Fröhlich-Bose-Einstein-like condensation in the open system in nonequilibrium thermodynamic conditions.

4. SUMMARY AND CONCLUDING REMARKS

We have considered a model of biological systems (e.g. the a-helix protein chain) of the type proposed by Fröhlich and Davydov. Polar vibrational modes that are pumped by a source of energy, are in nonlinear anharmonic interaction with a thermal bath that remains at constant temperature and which is modelled as a system of acoustic-type vibrations. The vibrational polar modes are then an open system in (arbitrary) nonequilibrium conditions.

Two main results arise out of the particular application we presented: on the one hand (Section 2), we have been able to demonstrate that such system displays complex behavior, namely, that at a certain distance from equilibrium, i.e. for a threshold value of the pumping intensity, there occurs a steeply increase in the population of the modes with low frequencies, in a way reminiscent of a Bose-Einstein condensation. This was predicted by H. Fröhlich, and then we have called it *Fröhlich's effect.* There is a kind of self-organization in the system, governed by nonlinear effects in the equations of evolution, and thus, this phenomenon may be considered as the emergence of a dissipative structure in Prigogine's sense [1,21]. On the other hand in section 3 we have addressed the question of long-range propagation of excitations in the system we considered in section 2. As noted, A. S. Davydov proposed that this is possibly accomplished through propagation of solitary waves, resulting from the nonlinearity in the equations of evolution. However, it was pointed out that in realistic physiological conditions it should occur strong damping of the wave. We derived the equivalent of Davydov's equations [Eqs. (27)] in general thermodynamic conditions, where the damping effect is clearly evidenced. But our calculation allowed to show that this damping is dependent on the macroscopic state of the system, and influenced by the same nonlinearities responsible for both, Fröhlich effect and Davydov's soliton. As a consequence, after Fröhlich condensation sets in, the lifetimes of the low frequency vibrations (i.e. those modes in the Fröhlich-Bose condensate) increase enormously. This implies that a coherent excitation composed by the low-lying in frequency excited states form *a Davydov's soliton-like wave which travels undamped in Fröhlich condensate.*

In summary, long-range propagation of excitations (informational energy) in biosystems can follow in the Fröhlich condensate, which are, otherwise, strongly dampened. That is, metabolic energy needs be provided to largely increase the population of the low-lying-in-frequency modes, for, on this so prepared background, to be possible dissipation-free signals to proceed. The results were derived on the basis of a simplified model, but we believe that the general outlook is correct. A detailed calculation, allowing for exact results in the case of the α-helix structure in protein is in development [49] and preliminary results agree with those presented here. Figure 4, taken from that reference shows, for the case of the α-helix structured chain, the composition in frequencies of the modes in Fröhlich's condensate, what gives better justification to the model of two sets of representative modes that we used. As a final word we remark on a curious point consisting on the fact that it can be noticed certain similitude of the phenomenon described here with laser action. Furthermore, we noticed that another novel phenomenon, also driven by the nonlinearities in the equations of evolution, consists in the possible emergence of a Cherenkov-like effect [50] in this media: It consists in that when the soliton is propagating with a velocity v larger than the average group velocity of the phonons in the bulk medium, corresponding to the modes in Fröhlich condensate, it is predicted a large emission of phonons in priviledged directions. In the case of acoustic vibrations, with sound velocity s, the emission occurs in a direction with angle θ such that $\cos\theta \approx s/v$ [?]. This may be the particular excitation noticed in experiments in ultrasonography [52] where it was dubbed as an X-wave. Additional considerations on Fröhlich effect and Davidov's Soliton are presented in the works listed in Ref. [?].

We gratefully acknowledge financial support to our Group provided in different opportunities by the São Paulo State Research Foundation (FAPESP); the National Research Council (CNPq); the Ministry of Planning (Finep); Unicamp Foundation (FAEP); and the John Simon Guggenheim Memorial Foundation (USA). One of the authors (MVM) is a Ministry of Education (CAPES) Pre-Doctoral Fellow, and the other two (ARV, RL) are CNPq Research Fellows.

REFERENCES

[1] G. Nicolis, in *The New Physics*, edited by P. Davies (Cambridge Univ. Press, Cambridge, 1989), pp. 316–347.

[2] I. Prigogine, in *From Theoretical Physics to Biology*, edited by M. Marois (North Holland, Amsterdam, 1969).

[3] G. Nicolis and I. Prigogine, *Self-organization in Nonequilibrium Systems* (Wiley-Interscience, New York, 1977).

[4] H. Haken, *Synergetics* (Springer, Berlin, 1978).

[5] H. Fröhlich, Rivista del Nuovo Cimento **3**, 490 (1973).

[6] S. Kauffman, *The Origins of Order: Self-organization and selection in evolution* (Oxford Univ. Press, New York, 1993); *At Home in the Universe: The Search for the Laws of Self-Organization and Complexity* (Oxford Univ. Press, New York, 1995).

[7] R. Rosen, *Life itself: A comprehensive inquiry into the nature, origin, and fabrication of life* (Columbia Univ. Press, New York, 1991).

[8] D. N. Zubarev, *Nonequilibrium Statistical Thermodynamics* (Consultants Bureau, New York, 1974), [*Neravnovesnaia Statisticheskaia Termodinamika* (Idz. Nauka, Moscow, 1971)].

[9] D. N. Zubarev, V. N. Morozov, and G. Röpke, *Statistical Mechanics of Nonequilibrium Processes, Vol. 1: Basic Concepts; Kinetic theory* (Akademie Verlag, Berlin, 1996).

[10] M. S. Green, J. Chem. Phys. **20**, 1281 (1952); J. Chem. Phys. **22**, 398 (1954).

[11] A. I. Akhiezer and S. V. Peletminskii, *Methods of Statistical Physics* (Pergamon, Oxford, 1981).

[12] R. Luzzi and A. R. Vasconcellos, Fortschr. Phys./Prog. Phys. **38**, 887 (1990).

[13] J. G. Ramos, A. R. Vasconcellos, and R. Luzzi, Fortschr. Phys./Prog. Phys. **43**, 265 (1995).

[14] E. T. Jaynes, in *Complex Systems: Operational Approaches,* edited by H. Haken (Springer, Berlin, 1985).

[15] E. T. Jaynes, in *Frontiers of Nonequilibrium Statistical Physics,* edited by G. T. Moore and M. O. Scully (Plenum, New York, 1986).

[16] L. Lauck, A. R. Vasconcellos, and R. Luzzi, Physica A **168**, 789 (1990).

[17] L. S. Garcia-Colin, A. R. Vasconcellos, and R. Luzzi, J. Non-Equilib. Thermodyn. **19**, 24 (1994); R. Luzzi and A. R. Vasconcellos, Physica A **241**, 677 (1977); R. Luzzi, A. R. Vasconcellos, J. Casas-Vázquez, and D. Jou, J. Chem. Phys. **107**, 7383 (1997); Physica A, **248**, 111 (1998)

[18] H. Fröhlich, in *From Theoretical Physics to Biology,* edited by M. Marois (North Holland, Amsterdam, 1969), pp. 13-22.

[19] H. Fröhlich, *Advances in Electronics and Electron Physics* (Academic Press, New York, 1980), Vol. 17, pp. 85-152.

[20] P. W. Anderson, Science **117**, 393 (1972).

[21] G. Nicolis and I. Prigogine, *Exploring Complexity* (Freeman, New York, 1989).

[22] P. Davies, in *The New Physics,* edited by P. Davies (Cambridge Univ. Press, Cambridge, 1989).

[23] H. Fröhlich, Int. J. Quantum Chem. **2**, 641 (1968).

[24] H. Fröhlich, Nature **228**, 1093 (1970).

[25] A. S. Davydov and N. I. Kislukha, Phys. Stat. Sol. B **59**, 465 (1973).

[26] A. S. Davydov, J. Theor. Biol. **38**, 559 (1973).

[27] A. S. Davydov, J. Theor. Biol. **66**, 379 (1977).

[28] A. S. Davydov, Phys. Scr. **20**, 387 (1979).

[29] A. S. Davydov, *Biology and Quantum Mechanics* (Pergamon, Oxford, 1982).

[30] A. S. Davydov, in *Nonlinear and Turbulent Processes in Physics*, edited by R. Z. Sagdeev (Harwood, London, 1984).

[31] J. A. Tuszynski, R. Paul, R. Chaterjee, and S. R. Sreenivasan, Phys. Rev. A **30**, 2666 (1984).

[32] A. C. Scott, Phys. Rep. **217**, 1 (1992).

[33] A. R. Vasconcellos, R. Luzzi, and L. S. Garcia-Colin, Phys. Rev. A **43**, 6622 (1984); *ibid.* **43**, 6633 (1984); also, R. Luzzi and A. R. Vasconcellos, Physica A **241**, 677 (1997).

[34] V. P. Kalashnikov, Teor. Mat. Fiz. **35**, 127 (1978).

[35] M. Y. Yushina, Phys. Lett. A **91**, 372 (1982), [The original argument is due to M. A. Lifshits in *Biofiz.* **17**, 694 (1972)].

[36] H. Fröhlich, Physics Lett. A **93**, 105 (1982).

[37] T. M. Wu and S. Austin, J. Theor. Biol. **71**, 209 (1978).

[38] R. E. Mills, Phys. Rev. A **28**, 379 (1983).

[39] K. Valyasek, D. N. Zubarev, and A. L. Kuzemskii, Theor. Math. Phys. **5**, 2 (1971).

[40] R. J. Glauber, Physics Rev. **131**, 276 (1963).

[41] H. Haken, Laser Theory, in *Handbuch der Physik XXV/2C*, edited by S. Flügge (Springer, Berlin, 1970).

[42] S. J. Webb, Phys. Rep. **60**, 201 (1980).

[43] J. N. Kapur and H. K. Kesavan, *Entropy Optimization Principles with Applications* (Academic, San Diego, CA, 1992).

[44] E. T. Jaynes, in *E. T. Jaynes Papers on Probability, Statistics, and Statistical Physics*, edited by R. D. Rosenkrantz (Dordrecht, Reidel, 1983).

[45] E. T. Jaynes, in *Maximum Entropy and Bayesian Methods*, edited by J. Skilling (Kluwer, Dordrecht, 1989), pp. 1–27.

[46] E. T. Jaynes, in *Maximum Entropy and Bayesian Methods*, edited by W. T. Grandy and L. H. Schick (Kluwer, Dordrecht, 1990), pp. 1–13.

[47] E. T. Jaynes, in *Physics and Probability: Essays in honor of E.T. Jaynes*, edited by W. T. Grandy and P. W. Milonni (Cambridge Univ. Press, Cambridge, 1993).

[48] M. V. Mesquita, A. R. Vasconcellos, and R. Luzzi, Selective Amplification of Coherent Polar Vibrations in Biopolymers, Phys. Rev E **48**, 4049–4059 (1993).

[49] M. V. Mesquita, Ph. D. Thesis (UNICAMP Campinas, SP, Brazil, 1998)

[50] V. M. Agranovich and V. L. Ginsburg, *Spatial Dispersion in Crystal Optics and the Theory of Excitons*, Wiley-Interscience, London, 1966.

[51] A. R. Vasconcellos, M. V. Mesquita, and R. Luzzi, Phys. Rev. E, submitted.

[52] J. Lu and J. F. Greenleaf, IEEE Trans. Ultrason. Ferroelect. Freq. Contr. **39**, 19 (1992); **39**, 441 (1992); J. Lu, Z. Hehong, and J. F. Greenleaf, Ultrasound Med. Biol. **20**, 403 (1994).

FIGURE CAPTIONS

Figure 1: Mode populations of the representative high frequency modes (index naught) and low frequency modes (index one) for increasing intensity of the power source.

Figure 2: The quasi-chemical potential (in units of $\hbar\omega_1$) of the representative low frequency modes vs. the intensity of the power source.

Figure 3: Reciprocal lifetime of the representative high frequency modes (index naught) and low frequency modes (index one) vs. the intensity of the power source.

Figure 4: Mode populations (in frequency space) in Fröhlich's condensate for the case of a near one-dimensional model for the α-helix protein. After Ref. [48].

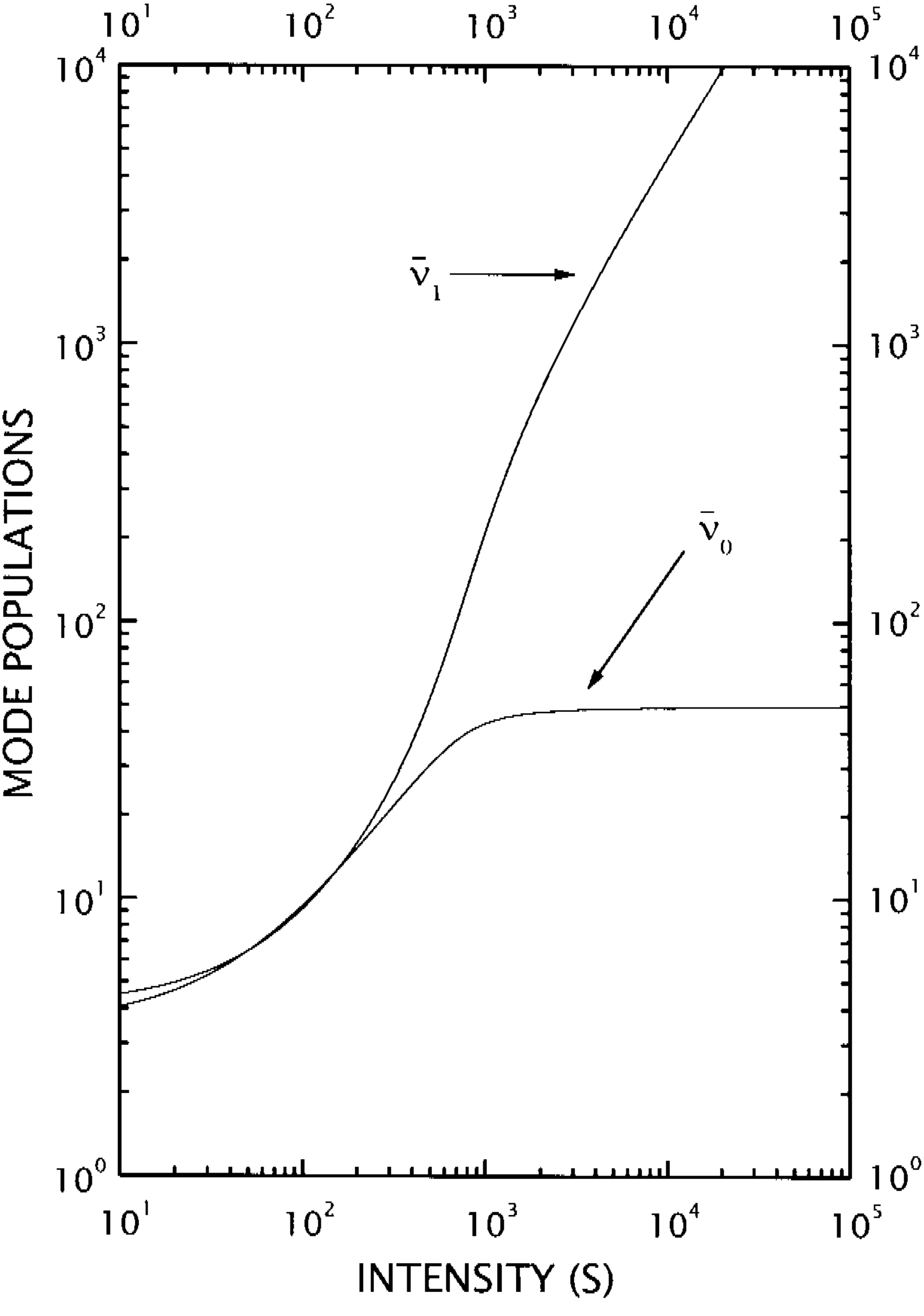

Figure 1: Mode populations of the representative high frequency modes (index naught) and low frequency modes (index one) for increasing intensity of the power source.

VASCONCELLOS *et al.* FIGURE 1

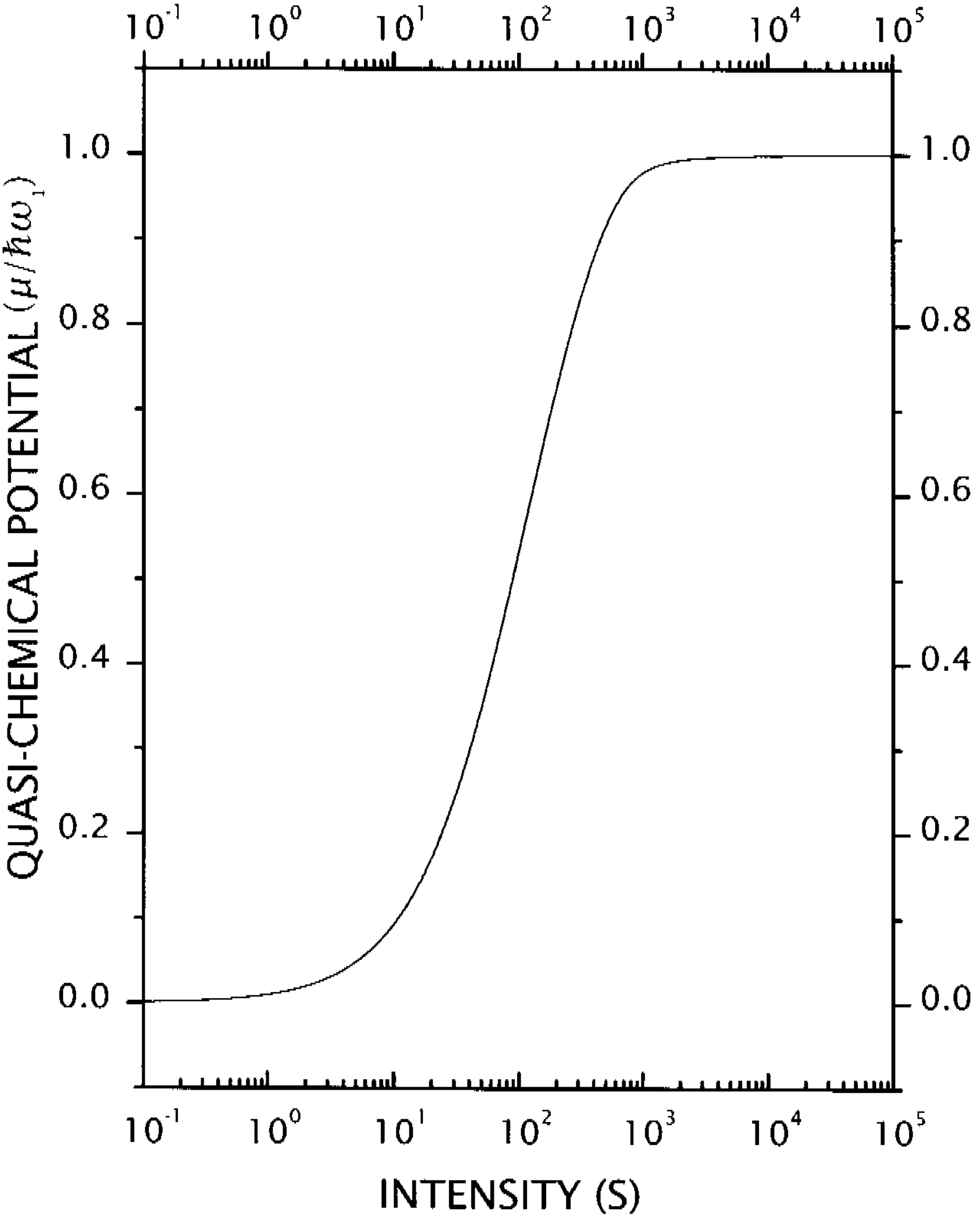

Figure 2: The quasi-chemical potential (in units of $\hbar\omega_1$) of the representative low frequency modes vs. the intensity of the power source.

VASCONCELLOS *et al.* FIGURE 2

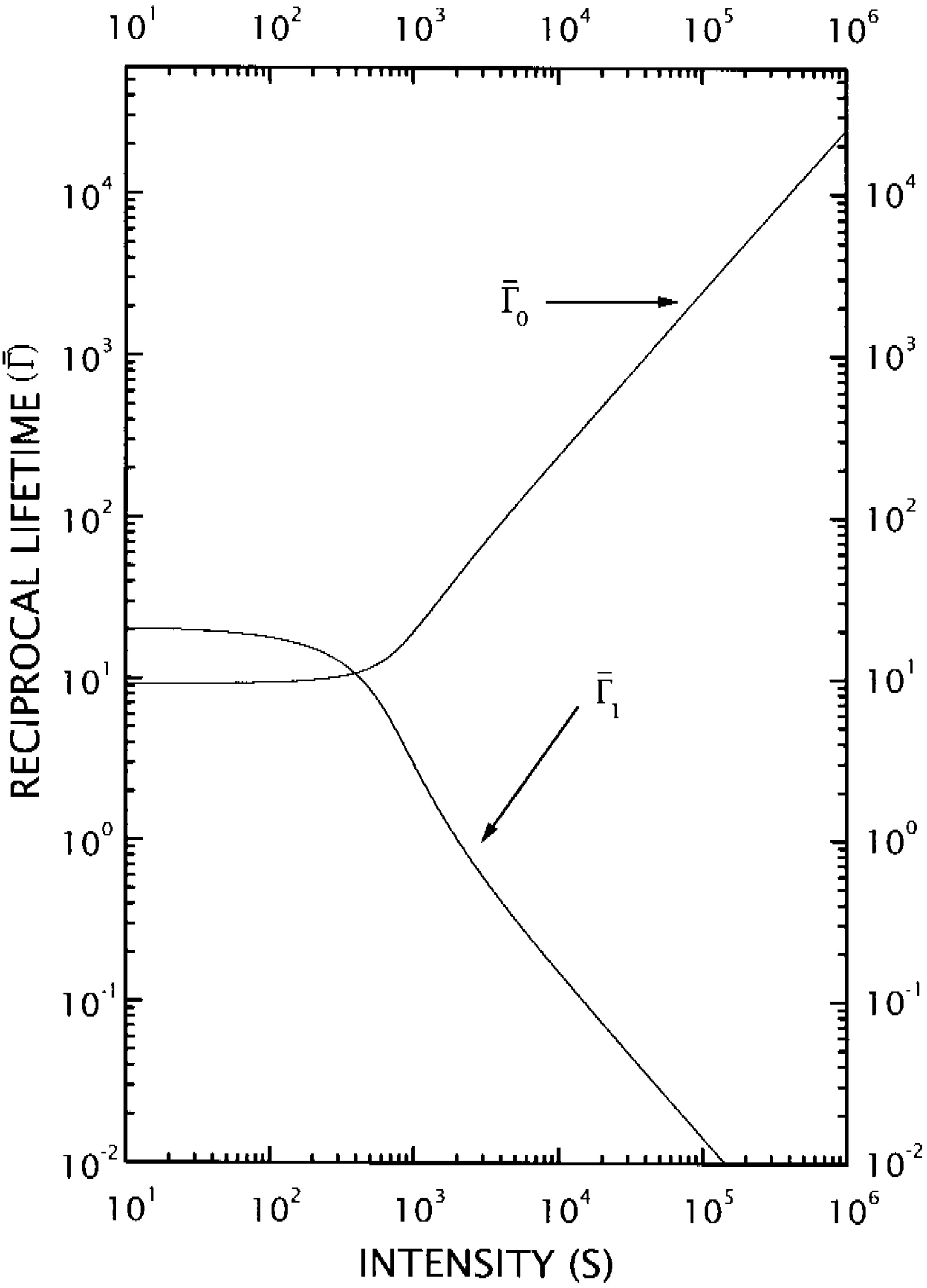

Figure 3: Reciprocal lifetime of the representative high frequency modes (index naught) and low frequency modes (index one) vs. the intensity of the power source.

VASCONCELLOS *et al.* FIGURE 3

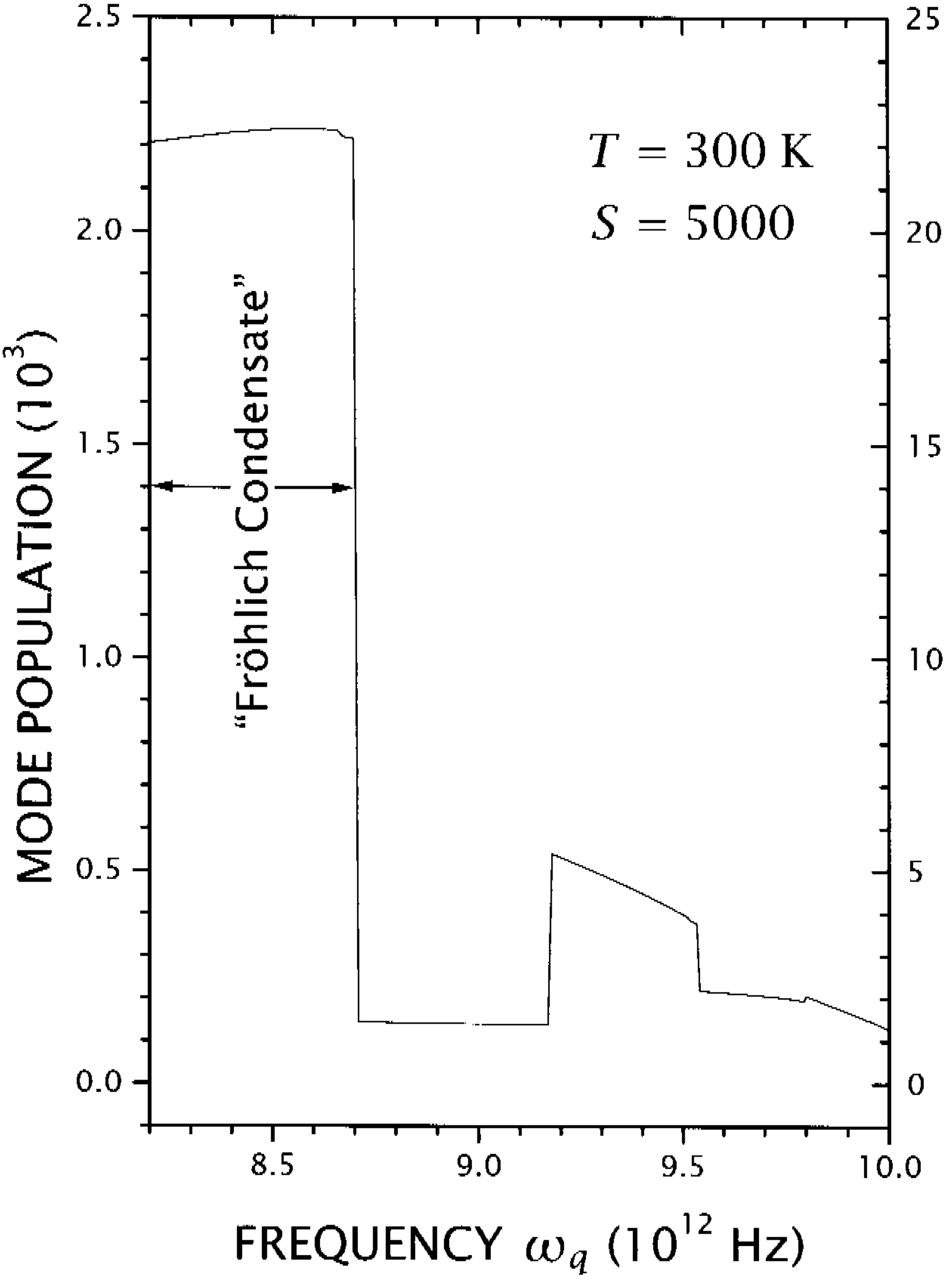

Figure 4: Modes (in frequency space) in Fröhlich's condensate for the case of a near one-dimensional model for the α-helix protein. After Ref. [48]

VASCONCELLOS *et al.* FIGURE 4

Capítulo 7

CONCLUSÕES

O objetivo desta tese, como já foi indicado na Introdução, foi o de apresentar uma Mecânica Estatística de Sistemas Não-lineares e uma Termodinâmica Irreversível apropriadas para tratar os assim chamados sistemas complexos. Mais precisamente, foi o de utilizar dois poderosos enfoques para o tratamento de sistemas dinâmicos não-lineares, a saber:

- a Mecânica Estatística Preditiva — baseada na Teoria da Informação — na parte correspondente ao Formalismo dos Ensembles de Não-Equilíbrio (NESOM), onde usamos o enfoque de Zubarev;
- a Termodinâmica Estatística Informacional (IST).

Estas teorias foram aplicadas ao estudo de sistemas de partículas tipo boson, como são os fonons e éxcitons em matéria condensada.

Deixamos o esclarecimento de que na tese não foi desenvolvida nenhuma extensão ou aperfeiçoamento destas teorias; com base no seu desenvolvimento já existente foram diretamente aplicadas ao estudo de sistemas com uma dinâmica não-linear e aparecimento de comportamento complexo.

Sumarizamos brevemente a contribuição resultante, visto que cada capítulo apresenta a discussão dos resultados.

Basicamente tratamos, via o uso do formalismo MaxEnt-NESOM, da Termodinâmica Irreversível (IST) e da Teoria da Função Resposta dele derivadas, de sistemas dinâmicos afastados (perto ou longe) do equilíbrio termodinâmico, realizando um estudo com certa profundidade do comportamento macroscópico de matéria condensada quando efeitos não-lineares estão presentes. No caso dos bosons considerados — fonons ópticos e acústicos e éxcitons em polímeros orgânicos, sistemas biológicos e semicondutores — pudemos, a partir de uma base mecânica microscópica, evidenciar comportamento complexo num nível macroscópico e analisar particularmente tal comportamento nesses sistemas dinâmicos não-lineares, evidenciando três notáveis fenômenos, que são:

- Condensação Fröhlich-Bose-Einstein (Efeito Fröhlich);
- Propagação de sólitons de Schrödinger-Davydov de vida média muito longa;
- O efeito Fröhlich-Cherenkov.

No caso de polímeros, como a acetanilida, consideramos as vibrações polares ("CO-streching" ou Amida I) em interação e em equilíbrio com o meio circundante. Mostramos de forma conclusiva — na literatura existente era conjectura — que a banda dita "anômala" no espectro de absorção infravermelha corresponde à excitação conhecida como sóliton de Schrödinger-Davydov. Este é resultado do comportamento não-linear das equações de evolução das amplitudes de vibração, proveniente da interação anarmônica dos modos polares com o meio circundante.

Outra análise que levou aos mesmos resultados consistiu em analisar os éxcitons criados num semicondutor pela ação de um pulso de radiação gerado por um laser.

Em ambos os casos a vida média da excitação é muita curta.

No caso das vibrações polares tipo Amida I — existentes e relevantes em sistemas biológicos como a hélice α em proteinas —, sob ação de excitação contínua, que leva o sistema para longe do equilíbrio, temos estudado com certo detalhe a emergência de uma condensação tipo Bose-Einstein numa estrutura no estado dissipativo de não-equilíbrio, mas não uma transição de fase no sentido usual. Temos denominado o fenômeno como *efeito Fröhlich* em razão de ter sido primeiramente sugerido por Herbert Fröhlich.

Como notado no texto principal, tal efeito pode ser de grande revelância no funcionamento de sistemas biológicos. Não se pode descartar o fato de que o efeito possa estar presente em outros casos em matéria condensada: um é o caso de éxcitons em simicondutores tratados no Cap. 5, e outro candidato seria as oscilações de plasma em materiais dopados, incluindo aqui os biológicos onde as proteínas são dopadas do tipo p. Neste ultimo caso dos plasmons o comportamento complexo a surgir poderia ser do tipo de formação de uma onda estacionário de carga. Esta pode ser considerada como um tipo particular de eletreto, com uma situação similar — i. e. formação de eletreto — podendo estar presente no caso das vibrações polares como um estado meta-estável.

Sendo mostrado que o efeito Fröhlich e a formação de sóliton são conseqüência das mesmas não-linearidades presentes no sistema (na literatura existente têm sido estudados separadamente a partir de modelagens diferentes), temos procedido ao estudo da propagação de ondas solitárias no substrato consistente no condensado de Fröhlich-Bose-Einstein. Como visto pode ser mostrado a existência de um novo fenômeno consistente em que a excitação correspondente a um sóliton de Schrödinger-

Davydov se propaga no condensado com uma vida média ordens de grandeza maiores que na ausência de fonte externa de alimentação.

O fenômeno tem sido evidenciado no caso do assim chamado "excitoner". Como temos demonstrado, esta amplificação espontânea de éxcitons coerentes a partir de éxcitons incoerentes — numa forma similar ao que acontece com os fotons no laser — consiste em um sóliton de Schrödinger-Davydov formado num condensado de Fröhlich-Bose-Einstein. O sinal detectado experimentalmente é explicado pela presença do sóliton "vestido" por um nuvem de éxcitons incoerentes.

Finalmente, no Cap. 6, procuramos tratar sistemas biológicos modelados. Por um lado reforçamos que a condensação Fröhlich-Bose-Einstein e as ondas solitárias não-amortecidas propagando-se nesse substrato podem ter relevância muito importante em Biofísica, particularmente em Bioenergética. Por outro lado consideramos, em conexão com certos resultados na área médica de imagem por ultrasonografia, o caso de vibrações acústicas. Mostramos que, em completa analogia com o caso das vibrações polares ópticas, apresentam-se os fenômenos da condensação Fröhlich-Bose-Einstein (mais fácil de surgir como resultado das freqüências acústicas serem muito menores que as ópticas) e da propagação a grandes distâncias do sóliton de Schrödinger-Davydov.

Além disso, mostramos também outro fenômeno novo e peculiar, também presente nos casos de vibrações ópticas, que lembra o efeito Cherenkov no caso de propagação de cargas em meios materiais, e que denominamos de efeito Fröhlich-Cherenkov. Consiste em larga emissão de fonons em determinadas direções, quando a velocidade do sóliton é maior que a velocidade do som no meio. A emissão acontece ao longo de cones com vértice no sóliton e um ângulo de abertura dado por $\cos\theta \approx s/v$. Isto explica os chamadas ondas X em processos de ultrasonografia.

Como palavras finais diremos que estes estudos, por um lado, convalidam as teorias propostas (MaxEnt-NESOM e IST) proporcionando formalismos promissores mecânico-estatísticos para tratar sistemas não-lineares e mostrar a eventual emergência de comportamento complexo dando idéia de sua origem ao nível molecular atômico ou de partículas. Por outro lado eles abrem uma excelente perspectiva para que se possa tratar um amplo conjunto de fenômenos associados a comportamento complexo em sistemas físicos, químicos e biológicos abertos e levados para longe do equilíbrio.

Bibliografia

ANDERSON, P. W. [1972]. More is different. *Science*, **177**, 393-6.

ANDERSON, P. W. [1991]. Is Complexity Physics? Is it Science? What is it? *Phys. Today*, **44**(7), 9.

ANDERSON, T. & ROTH, S. [1994]. Conducting Polymers: Electrical Transport and Current Applications. *Braz. J. Phys.*, **24**(3), 746–54.

BEARDSLEY, T. [1997]. Plastic Power. *Sci. Am.*, **276**(4), 39–40.

BECK, A. H. [1976]. *Statistical Mechanics, Fluctuations, and Noise* (Arnold, London). Cap. 10.

BERNARDES, N. [1996]. *Holotropic Theory of Thermodynamics* (CLE-Unicamp, Campinas – SP). Versão condensada e futuro livro.

BOGOLIUBOV, N. N. [1962]. Some Topics in Quantum Statistics. In: *Studies in Statistical Mechanics I* (edited by DE BOER, J. & UHLENBECK, G. E.) (North Holland, Amsterdam).

BOGOLIUBOV, N. N. [1967]. *Lectures in Quantum Statistics*, vol. 1 (Gordon and Breach, New York).

BOGOLIUBOV, N. N. [1970]. *Lectures in Quantum Statistics*, vol. 2 (Gordon and Breach, New York).

BUISHVILI, L. L. & ZVIADADZE, M. D. [1972]. On the quasi-thermodynamic theory of magnetic relaxation. *Physica*, **59**, 697.

CASIMIR, H. B. G. & DU PRÉ, F. K. [1938]. Thermodynamic interpretation of paramagnetic relaxation phenomena. *Physica*, **5**, 507–11.

CHANG, C. S. W., UHLENBECK, G. E., & DE BOER, J. [1964]. In: *Studies of Statistical Mechanics, vol. 2* (edited by DE BOER, J. & UHLENBECK, G. E.) (North Holland, Amsterdam).

COURANT, R. & HILBERT, D. [1953]. *Methods of Mathematical Physics: Vol. I* (Wiley-Interscience, New York).

DAVYDOV, A. S. [1982]. *Biology and Quantum Mechanics* (Pergamon, Oxford).

FESCHBACH, H. [1987]. *Phys. Today*, (November issue), 9.

FRÖHLICH, H. [1947]. On the theory of dielectric breakdown in solids. *Proc. Roy. Soc. London*, **188A**, 521–32.

FRÖHLICH, H. [1969]. Quantum Mechanical Concepts in Biology. In: *From Theoretical Physics to Biology* (edited by MAROIS, M.), pp. 13–22 (North Holland, Amsterdam).

FRÖHLICH, H. [1973]. The connection between macro- and micro-physics. *Rivista del Nuovo Cimento*, **3**, 490–534.

FRÖHLICH, H. [1975]. Evidence for Bose-condensation-like excitation of coherent modes in biological systems. *Phys. Lett. A*, **51**, 21–2.

FRÖHLICH, H. [1980]. The Biological Effects of Microwaves and Related Questions. In: *Advances in Electronics and Electron Physics*, vol. 17, pp. 85–152 (Academic Press, New York).

GELL-MANN, M. [1995]. What is Complexity? *Complexity*, **1**(1), 16–9.

GLANSDORFF, P. & PRIGOGINE, I. [1971]. *Thermodynamic Theory of Structure, Stability, and Fluctuations* (Wiley-Interscience, New York).

GRANT, N. & HYLAND, G. J. [1998]. Preprints of the main talks at the Microwave Application Workshop, to be held in the University of São Paulo (São Paulo, Brazil, tentatively in the Autumn (Southern Hemisphere) of 1998). We thank Dr. Norman Grant (Matra-Marconi Space-United Kingdom) and Prof. Oswaldo Massambani (São Paulo Univ.) for calling our attention to the Workshop, and providing us in advance the preprints of the invited talks.

GRMELA, M. & ÖHTTINGER, H. C. [1997]. Dynamics and thermodynamics of complex fluids. I. Development of a general formalism. *Phys. Rev. E*, **56**, 6620-32.

Grupo MESD [1990-1998]. LUZZI, R. & VASCONCELLOS, A. R. [1990]. On the Nonequilibrium Statistical Operator Method. *Fortschr. Phys./Prog. Phys.*, **38**, 887-922; RAMOS, J. G., VASCONCELLOS, A. R., & LUZZI, R. [1995]. A Classical Approach in Predictive Statistical Mechanics: A Generalized Boltzmann Formalism. *Fortschr. Phys./Prog. Phys.*, **43**, 265-300; TENAN, M. A., VASCONCELLOS, A. R., & LUZZI, R. [1997]. Statistical Mechanical Foundations for a Generalized Thermodynamics of Dissipative Processes. *Fortschr. Phys./Prog. Phys.*, **45**, 1-37; LUZZI, R., VASCONCELLOS, A. R., & RAMOS, J. G. [1998*a*]. On the Statistical Foundations of Irreversible Thermodynamics. *Fortschr. Phys./Prog. Phys.*, **00**, 000; LUZZI, R., VASCONCELLOS, A. R., & RAMOS, J. G. [1998*b*]. *Statistical Foundations of Irreversible Thermodynamics.* In: *Texte zur Physik Series* (edited by EBELING, W.) (Teubner, Berlin), no prelo; LUZZI, R., VASCONCELLOS, A. R., & RAMOS, J. G. [1998*c*]. *Foundations of a Nonequilibrium Statistical Ensemble Formalism.* In: Fundamental Theories of Physics Series (edited by VAN DER MERWE, A.) (Elsevier-Kluwer Academic, Amsterdam-Dordrecht), em preparação.

HAKEN, H. [1970]. *Handbuch der Physik XXV/2C* (Springer, Berlin).

HAKEN, H. [1978]. *Synergetics* (Springer, Berlin).

HAUS, H. A. [1993]. Molding light into solitons. *IEEE Spectrum*, (March Issue), 48-53.

HEGER, A. J., KIVELSON, S., SCHRIEFFER, J. R., & SU, W. P. [1988]. Solitons in Conducting Polymers. *Rev. Mod. Phys.*, **60**, 781-850.

HEISENBERG, W. [1930]. *The Physical Principles of the Quantum Theory* (Univ. of Chicago Press, Chicago).

HOBSON, A. [1966*a*]. Irreversibility and Information in Mechanical Systems. *J. Chem. Phys.*, **45**, 1352-57.

HOBSON, A. [1966*b*]. Irreversibility in Simple Systems. *Am. J. Phys.*, **34**, 411-6.

JAYNES, E. T. [1957*a*]. Information Theory and Statistical Mechanics I. *Phys. Rev.*, **106**, 620–30.

JAYNES, E. T. [1957*b*]. Information Theory and Statistical Mechanics II. *Phys. Rev.*, **108**, 171–90.

JAYNES, E. T. [1978]. "Where do we stand on maximum entropy?". In: *The Maximum Entropy Formalism* (edited by TRIBUS, M. & LEVINE, R. D.) (MIT Press, Cambridge, MA).

JAYNES, E. T. [1983]. Reprinted Articles and Notes. In: *E. T. Jaynes Papers on Probability, Statistics, and Statistical Physics* (edited by ROSENKRANTZ, R. D.) (Reidel, Dordrecht).

JAYNES, E. T. [1986]. Predictive Statistical Mechanics. In: *Frontiers of Nonequilibrium Statistical Physics* (edited by MOORE, G. T. & SCULLY, M. O.), pp. 33–55 (Plenum, New York).

KUBO, R. [1978]. Oppening address to Oji Seminar on Nonlinear Nonequilibrium Statistical Mechanics, Oji, Japan, 1977. *Sup. Prog. Theor. Phys. (Japan)*, **64**, 1–11.

LANDAU, L. D. [1936]. Kinetic equation for the Coulomb effect. *Fiz. Z. Sowjet*, **10** (2), 154–64 [also in *Collected Papers of L. D. Landau* (edited by TER HAAR, D.) (Pergamon, Oxford)].

LANDAUER, R. [1987]. Nonlinearity: Historical and Technological View. In: *Nonlinearity in Condensed Matter* (edited by BISHOP, A. R., CAMPBELL, D. K., KUMAR, P. & TRULLINGER, S. E.) (Springer, Berlin).

LOUISSEL, W. H. [1973]. *Quantum Statistical Properties of Radiation* (Wiley, New York).

LU, J. & GREENLEAF, J. F. [1992]. Nondiffracting X-waves. *IEEE Trans. Ultrason. Ferroelect. Freq. Contr.*, **39**, 19–31.

LUZZI, R. & VASCONCELLOS, A. R. [1990]. On the Nonequilibrium Statistical Operator Method. *Fortschr. Phys./Prog. Phys.*, **38**, 887–922.

LUZZI, R. & VASCONCELLOS, A. R. [1991]. Mechanical Statistical of Dissipation and Order. *Ciência e Cultura,* **43**, 423-31.

LUZZI, R., VASCONCELLOS, A. R., JOU, D., & CASAS-VAZQUEZ, J. [1997]. Thermodynamic variables in the context of a nonequilibrium statistical ensemble approach. *J. Chem. Phys.*, **107**(18), 7383-96.

LUZZI, R., VASCONCELLOS, A. R., & RAMOS, J. G. [1998]. *Foundations of a Nonequilibrium Statistical Ensemble Formalism.* In: Fundamental Theories of Physics Series (edited by VAN DER MERWE, A.) (Kluwer Academic, Amsterdam-Dordrecht). Em preparação.

MADUREIRA, J. R., VASCONCELLOS, A. R., LUZZI, R., CASAS-VAZQUEZ, J., & JOU, D. [1998*a*]. Evolution of dissipative processes in a statistical thermodynamic approach II. Thermodynamic properties of a fluid of bosons. *J. Chem. Phys.*, **108**, 7580-6.

MADUREIRA, J. R., VASCONCELLOS, A. R., LUZZI, R., & LAUCK, L. [1998*b*]. Markovian kinetic equations in a nonequilibrium statistical ensemble formalism. *Phys. Rev. E*, **57**, 3637-40.

MASCARENHAS, S. [1987]. Bioelectrets: Electrets in Biomaterials and Biopolymers. In: *Electrets* (edited by SESSLER, G. M.), pp. 321-46 (Springer, Berlin).

MILLER, P. F. & GEBBIE, H. A. [1996]. Laboratory millimeter wave measurements of atmospheric aerosols. *Int. J. Infrared Milli.*, **17**(10), 1573-91.

MORI, H. [1965]. Transport, collective motion and Brownian motion. *Progr. Theor. Phys. (Japan),* **33**, 423-45.

NICOLIS, G. [1986]. Dissipative Systems. *Rep. Prog. Phys.*, **49**, 873-949.

NICOLIS, G. [1989]. Physics of Far-From-Equilibrium Systems and Self-Organization. In: *The New Physics* (edited by DAVIES, P.), pp. 316-47 (Cambridge Univ. Press, Cambridge).

NICOLIS, G. [1995]. *Introduction to Nonlinear Science* (Cambridge University Press, Cambridge).

NICOLIS, G. & DAEMS, D. [1998]. Probabilistic and thermodynamic aspects of dynamical systems. *Chaos*, **8**(2), 311–20.

NICOLIS, G. & PRIGOGINE, I. [1977]. *Self-organization in Nonequilibrium Systems* (Wiley-Interscience, New York).

PELETMINSKII, S. V. & YATSENKO, A. A. [1968]. Contribution to the quantum theory of kinetic and relaxation processes. *Soviet Phys. JETP*, **26**, 773–8.

PRIGOGINE, I. [1947]. *Étude Thermodinamique des Phénomènes Irreversibles* (Desoer, Liège).

PRIGOGINE, I. [1955]. *Introduction to the Thermodynamics of Irreversible Processes* (Thomas, New York).

PRIGOGINE, I. [1969]. Structure, Dissipation, and Life. In: *From Theoretical Physics to Biology* (edited by MAROIS, M.) (North Holland, Amsterdam).

PRIGOGINE, I., NICOLIS, G., & BABLOYANTZ, A. [1972*a*]. Thermodynamics of Evolution I. *Phys. Today*, **25**(11), 23–8.

PRIGOGINE, I., NICOLIS, G., & BABLOYANTZ, A. [1972*b*]. Thermodynamics of Evolution II. *Phys. Today*, **25**(12), 38–44.

RAMOS, J. G., VASCONCELLOS, A. R., & LUZZI, R. [1995]. A Classical Approach in Predictive Statistical Mechanics: A Generalized Boltzmann Formalism. *Fortschr. Phys./Prog. Phys.*, **43**, 265–300.

REDLICH, O. [1976]. *Thermodynamics* (Elsevier, Amsterdam).

SCOTT-RUSSELL, J. [1844]. Report on Waves. *Proc. Roy. Soc. Edinburgh*, pp. 319–20.

SHAH, J. & LEITE, R. C. C. [1969]. Radiative recombination from photoexcited hot carriers in GaAs. *Phys. Rev. Lett.*, **22**, 2844.

SHAH, J., LEITE, R. C. C., & SCOTT, J. F. [1970]. Photoexcited hot LO phonons in GaAs. *Sol. St. Comm.*, **8**, 1089.

SHANNON, C. E. & WEAVER, W. [1964]. *The Mathematical Theory of Communication.* (Univ. Illinois Press, Urbana).

SHEN, Y. R. [1997]. Solitons made simple. *Science*, **276**, 1520.

SHKLOVSKII, V. A. [1975]. Overheat of electrons as a cause of critical current hysteresis in resistive state of superconductors. *Fiz. Tverd. Tela*, **17**(10), 3076–8. [Solid State **17**, 2040 (1976)].

SNOKE, D. [1996]. Coherent exciton waves. *Science*, **273**, 1351–52.

SNYDER, A. W. & MITCHELL, D. J. [1997]. Accessible solitons. *Science*, **276**, 1538–41.

TISZA, L. [1991]. Concluding Remarks. In: *Thermodynamics: History and Philosophy* (edited by MARTINAS, K., ROPOLYI, L., & SZEGEDI, P.), pp. 515–22 (World Scientific, Singapore).

UHLENBECK, G. E. [1963]. The Boltzmann equation. In: *Studies in Statistical Mechanics I* (edited by KAC, M.) (Ed. Am. Math. Soc, Providence, RI).

VALYASEK, K., ZUBAREV, D. N., & KUZEMSKII, A. L. [1971]. Schrödinger-Type Equation with Damping for a Dynamical System in a Thermal Bath. *Theor. Math. Phys.*, **5**, 2.

VASCONCELLOS, A. R., ALGARTE, A. C., & LUZZI, R. [1990]. On the relaxation-time hierarchy in dissipative systems — an example from semiconductor physics. *Physica A*, **166**, 517–39.

VASCONCELLOS, A. R., MESQUITA, M. V., & LUZZI, R. [1998]. Stimulated Amplification and Propagation of Excitons' Beams. *Phys. Rev. Lett.* Submitted.

WOLFRAM, S. [1996]. *The Mathematica Book* (Wolfram Media & Cambridge University Press, Redwood City, California), 3rd edn.

ZAKHAROV, V. E. & SHABAT, A. B. [1972]. Exact Theory of Two-dimensional Self-focusing and one-dimensional Self-modulation of Waves in Nonlinear Media. *Soviet Physics JETP*, **34**(1), 62–9.

ZUBAREV, D. N. [1974]. *Nonequilibrium Statistical Thermodynamics* (Consultants Bureau, New York). [*Neravnovesnaia Statisticheskaia Termodinamika* (Izd. Nauka, Moscow, 1971)].

ZUBAREV, D. N., MOROZOV, V. N., & RÖPKE, G. [1996, 1997]. *Statistical Mechanics of Nonequilibrium Processes. Vol. 1: Basic Concepts, Kinetic Theory; Vol. 2: Relaxation and Hydrodynamic Processes* (Akademie Verlag, Berlin).

Apêndice A

Metodologia

A.1 O Método do Operador Estatístico de Não-Equilíbrio

O Método do Operador Estatístico de Não-Equilíbrio (MOENE), em qualquer uma de suas formulações, baseia-se no princípio estabelecido por Bogoliubov [Bogoliubov 1962; Uhlenbeck 1963] de que a descrição do estado macroscópico de um sistema fora do equilíbrio termodinâmico pode ser feita com um número contraído de variáveis, se houver uma hierarquia de tempos de relaxação tal que o sistema continuamente perca memória da evolução prévia, o assim chamado princípio de enfraquecimento de correlações. Desse modo, pode-se definir um conjunto básico de variáveis dinâmicas $\{\hat{P}_j(\boldsymbol{r})\}$, $j = 1, \ldots, n$, com, em geral, um número n de elementos muito menor que o número de graus de liberdade do sistema considerado, para efetuar tal descrição em dado estágio de evolução do sistema.

O conjunto de macrovariáveis $\{Q_j(\boldsymbol{r}, t)\}$ associadas aos $\{\hat{P}_j(\boldsymbol{r})\}$ é constituído pelas médias estatísticas das variáveis dinâmicas, $\langle \hat{P}_j(\boldsymbol{r}) | t \rangle$, as quais devem corresponder às medidas obtidas experimentalmente. Essas macrovariáveis, em termos do Operador Estatístico de Não-Equilíbrio (OENE), $\varrho(t)$, são dadas por:

$$Q_j(\boldsymbol{r}, t) = \mathrm{Tr}\left\{\hat{P}_j(\boldsymbol{r}) \varrho(t)\right\} \equiv \langle \hat{P}_j(\boldsymbol{r}) | t \rangle \, , \tag{A.1}$$

onde $\varrho(t)$ é o operador estatístico de não-equilíbrio (OENE), que depende destas e apenas das variáveis dinâmicas $\{\hat{P}_j(\boldsymbol{r})\}$. A contração do número de variáveis está ligada com a separação do hamiltoniano total em duas contribuições

$$\hat{H} = \hat{H}_0 + \hat{H}' \, , \tag{A.2}$$

onde $\hat{H}_0$ é a parte do hamiltoniano que contém os efeitos dinâmicos associados com a parte da energia cinética e com interações que produzem efeitos de relaxação com tempos de decaimento menores que o tempo característico do experimento, que é tipicamente da ordem do tempo de resolução do instrumento; enquanto H' contém as interações responsáveis por mecanismos mais lentos de relaxação; exemplos ilustrativos são proporcionados no estudo de sistemas de spin [Buishvili & Zviadadze 1972] e de semicondutores fortemente fotoexcitados [Vasconcellos *et al.* 1990].

A determinação deste conjunto $\{\hat{P}_j(\boldsymbol{r})\}$ é um dos problemas capitais da Mecânica Estatística do Não-Equilíbrio, não havendo um método definitivo para chegar a uma decisão única. Para cada problema em particular pode-se chegar a mais de uma opção. Contudo, a escolha dessas variáveis deve obedecer necessariamente uma condição de fechamento, denominada *condição de simetria de Zubarev-Peletminskii*,

$$\frac{1}{i\hbar}[\hat{P}_j(\boldsymbol{r}), \hat{H}_0] = \sum_k \alpha_{jk} \hat{P}_k(\boldsymbol{r}) \, , \tag{A.3}$$

onde os α_{jk} são operadores diferenciais [Peletminskii & Yatsenko 1968] em uma representação quântica apropriada.

As macrovariáveis $\{Q_j(\boldsymbol{r},t)\}$ definem o estado macroscópico ou mesoscópico, dependendo do caso, ou seja, o estado termodinâmico de não-equilíbrio do sistema. Observemos que, embora as quantidades $\{\hat{P}_j(\boldsymbol{r})\}$ variem no tempo com a evolução do estado dinâmico do sistema, o experimento não acompanha a evolução microscópica, porém a evolução macroscópica do sistema através das macrovariáveis $\{Q_j(\boldsymbol{r},t)\}$. Os resultados de semelhante experimento devem ser descritos por equações de transporte generalizadas da forma:

$$\frac{\partial}{\partial t}Q_j(\boldsymbol{r},t) = \mathcal{R}_j\left\{Q_1\left(\boldsymbol{r},t\right),\ldots,Q_n\left(\boldsymbol{r},t\right);t\right\} \ , \tag{A.4}$$

onde os $\mathcal{R}_j$ são funcionais das macrovariáveis $Q_j(\boldsymbol{r},t)$, sendo em geral de caráter não-linear, não-local e acompanhados de efeito de memória. Assim, as Eqs. (A.4) são as equações fundamentais à descrição da evolução macroscópica do sistema.

O OENE $\varrho(t)$ satisfaz à equação de Liouville, que apresenta dois tipos de solução, as soluções retardadas (evolução rumo ao futuro) e as soluções avançadas (volta do futuro para o passado), e assim temos reversibilidade temporal. O comportamento irreversível na descrição do estado macroscópico do sistema pode ser conseguido mediante a introdução *ad hoc* de uma hipótese não-mecânica, que consiste na imposição de uma quebra da simetria de reversão temporal da equação de Liouville, o que é feito negligenciando o conjunto das soluções avançadas. Na prática, isto é conseguido introduzindo o conceito de quasi-médias de Bogoliubov [Bogoliubov 1967, 1970].

Na formulação do OENE de Zubarev, que será utilizado nesta tese, isto é feito adicionando uma fonte infinitesimal à equação de Liouville e, após o cálculo das quasi-médias, fazendo o limite tender a zero. A construção desse operador é feita utilizando-se um princípio variacional, o Formalismo da Maximização de Entropia Estatística (MaxEnt), proposto por Jaynes [1957*a*,*b*, 1978, 1983, 1986]. De acordo com este autor, a teoria de informação proporciona um critério construtivo para obter distribuições de probabilidade com base em um conhecimento parcial do estado do sistema, levando para um tipo de estatística por inferência. A base é a contribuição de Shannon à teoria de informação [Shannon & Weaver 1964; Beck 1976]. De acordo com Jaynes, o estado de conhecimento do observador é dado por inferência probabilística, que consiste em determinar a distribuição de probabilidade p_j dos eventos x_j, maximizando a quantidade $S_I = \quad k\sum_j p_j \ln p_j$, a assim chamada entropia informacional, onde k é uma constante positiva, e S_I está sujeita às condições do conhecimento existente sobre o sistema [Jaynes 1957*a*,*b*, 1978, 1983, 1986]. Detalhes da construção desse operador podem ser encontrados em Zubarev *et al.* [1996, 1997]; Luzzi & Vasconcellos [1990]; Ramos *et al.* [1995]; Luzzi *et al.* [1998].

O OENE na formulação de Zubarev, ϱ_ε, é dado por

$$\varrho_\varepsilon(t) = \exp\left\{\ln\bar{\varrho}(t,0) - \int_{-\infty}^{t} dt' e^{\varepsilon(t'-t)} \frac{d}{dt'} \ln\bar{\varrho}(t', t'-t)\right\} , \tag{A.5}$$

onde $\bar{\varrho}(t,0)$ é um operador auxiliar de relevância importante na teoria dado pela distribuição tipo Gibbs instantânea:

$$\bar{\varrho}(t,0) = \exp\left\{-\phi(t) - \sum_j F_j(t)\hat{P}_j(r)\right\} , \tag{A.6a}$$

e

$$\bar{\varrho}(t',t'-t) = \exp\left\{-\frac{1}{i\hbar}(t'-t)H\right\}\bar{\varrho}(t',0)\exp\left\{\frac{1}{i\hbar}(t'-t)H\right\}, \tag{A.6b}$$

onde $\phi(t)$ assegura a normalização de $\bar{\varrho}$, e as variáveis termodinâmicas intensivas de não-equilíbrio $F_j(t)$ são os multiplicadores de Lagrange que o método introduz.

Usando a Eq. (A.5) é possível mostrar que o OENE é composto de dois termos:

$$\varrho_\varepsilon(t) = \bar{\varrho}(t,0) + \varrho'_\varepsilon(t) . \tag{A.7}$$

O termo $\bar{\varrho}(t,0)$ é um operador auxiliar de grão grosso que dá valores médios instantâneos das observáveis do sistema, e que não leva em conta a dissipação do sistema, e o termo $\varrho'_\varepsilon(t)$ está associado com a informação dinâmica microscópica indispensável para descrever-se a evolução irreversível e os processos dissipativos que ocorrem no sistema. Além disso, tem-se que

$$Q_j(\boldsymbol{r},t) = \mathrm{Tr}\left\{\hat{P}_j\varrho_\varepsilon(t)\right\} = \mathrm{Tr}\left\{\hat{P}_j\bar{\varrho}(t,0)\right\} . \tag{A.8}$$

A.2 Teoria cinética

Consideremos um sistema quântico cujo hamiltoniano separamos em dois termos:

$$\hat{H} = \hat{H}_0 + \hat{H}' . \tag{A.9}$$

Nesse sistema, $\hat{H}_0$ é a parte do hamiltoniano que contém os efeitos dinâmicos associados na evolução dos $\{\hat{P}_j(\boldsymbol{r})\}$ com a parte da energia cinética e com interações que produzem efeitos de relaxação rápidos, enquanto H' contém as interações responsáveis por mecanismos mais lentos de relaxação [cf. Eq. (A.2)]

Diferenciando-se a Eq. (A.1) com relação ao tempo, obtemos:

$$\frac{\partial}{\partial t} Q_j(\boldsymbol{r},t) = \frac{d}{dt} \mathrm{Tr}\{\hat{P}_j(\boldsymbol{r})\varrho_\varepsilon(t)\} = \mathrm{Tr}\left\{(\mathrm{i}\hbar)^{-1}[\hat{P}_j(\boldsymbol{r}),\hat{H}]\varrho_\varepsilon(t)\right\} . \tag{A.10}$$

Levando em conta a Eq. (A.7), obtemos:

$$\frac{\partial}{\partial t} Q_j(\boldsymbol{r},t) = \mathrm{Tr}\left\{(\mathrm{i}\hbar)^{-1}[\hat{P}_j(\boldsymbol{r}),H]\bar{\varrho}(t,0)]\right\} + \mathrm{Tr}\left\{(\mathrm{i}\hbar)^{-1}[\hat{P}_j(\boldsymbol{r}),H]\varrho'_\varepsilon(t)]\right\} . \tag{A.11}$$

Com a separação de H dada pela Eq. (A.9), podemos escrever

$$\mathrm{Tr}\left\{(\mathrm{i}\hbar)^{-1}[\hat{P}_j(\boldsymbol{r}),H]\bar{\varrho}(t,0)]\right\} = J_j^{(0)}(\boldsymbol{r},t) + J_j^{(1)}(\boldsymbol{r},t) , \tag{A.12}$$

onde

$$J_j^{(0)} = \mathrm{Tr}\left\{(\mathrm{i}\hbar)^{-1}[\hat{P}_j(\boldsymbol{r}),\hat{H}_0]\bar{\varrho}(t,0)\right\} \equiv (\mathrm{i}\hbar)^{-1}\langle[\hat{P}_j(\boldsymbol{r},\hat{H}_0)]|t\rangle_0 , \tag{A.13a}$$

$$J_j^{(1)} = \mathrm{Tr}\left\{(\mathrm{i}\hbar)^{-1}[\hat{P}_j(\boldsymbol{r}),\hat{H}']\bar{\varrho}(t,0)\right\} \equiv (\mathrm{i}\hbar)^{-1}\langle[\hat{P}_j(\boldsymbol{r},\hat{H}')]|t\rangle_0 . \tag{A.13b}$$

Levando em conta as Eq. (A.3), (A.7) e (A.8), podemos mostrar que:

$$\mathrm{Tr}\left\{(\mathrm{i}\hbar)^{-1}[\hat{P}_j(\boldsymbol{r}),H_0]\varrho'_\varepsilon(t)\right\} = 0 , \tag{A.14}$$

de maneira que podemos escrever o segundo termo do lado direito da Eq. (A.11) como:

$$\mathrm{Tr}\left\{(\mathrm{i}\hbar)^{-1}[\hat{P}(\boldsymbol{r}),H]\varrho'_\epsilon(t)\right\} = \mathrm{Tr}\left\{(\mathrm{i}\hbar)^{-1}[\hat{P}_j(\boldsymbol{r}),H']\varrho'_\epsilon(t)\right\} \equiv \mathcal{J}_j(\boldsymbol{r},t)\ . \tag{A.15}$$

O operador de colisão $\mathcal{J}(\boldsymbol{r},t)$ é extremamente complicado, contendo efeitos altamente não-lineares, não-locais e de memória (a história prévia, mecânica e termodinâmica até o tempo t). Com as propriedades das Eqs. (A.3) e (A.9) podemos escrever este operador de colisão como uma série infinita de operadores de colisão organizados em potências sucessivas da interação:

$$\mathcal{J}_j(\boldsymbol{r},t) = \sum_{k=2}^{\infty} J_j^{(k)}(\boldsymbol{r},t)\ , \tag{A.16}$$

onde o índice k representa a ordem de interações. Dessa forma, podem ser introduzidas aproximações através do truncamento da série de operadores de colisão parciais, numa dada ordem de interação. A teoria de transporte baseada no MOENE constitui uma generalização abrangente das idéias e do formalismo de Mori [Mori 1965] (vide, por exemplo, Madureira *et al.* [1998*a*]), sendo altamente não-linear e, em princípio, aplicável a qualquer situação arbitrariamente longe do equilíbrio. Até segunda ordem na intensidade de interação resultante no limite Markoviano, tem-se a a expressão aproximada [Luzzi & Vasconcellos 1990; Madureira *et al.* 1998*b*]:

$$\begin{aligned} \mathcal{J}_j(t) \approx J_j^{(2)}(\boldsymbol{r},t) &= (\mathrm{i}\hbar)^{-2}\int_{-\infty}^{t} dt'\, \mathrm{e}^{\varepsilon(t'-t)}\langle[H'(t'-t)_0,[H',\hat{P}_j(\boldsymbol{r})]]\mid t\rangle_0 \\ &+ (\mathrm{i}\hbar)^{-1}\int_{-\infty}^{t} dt'\, \mathrm{e}^{\varepsilon(t'-t)}\sum_k \frac{\delta J_j^{(1)}(\boldsymbol{r},t)}{\delta Q_k(\boldsymbol{r},t)}\langle[H'(t'-t)_0,\hat{P}_k(\boldsymbol{r})]\mid t\rangle_0\ , \end{aligned} \tag{A.17}$$

onde $H(t'-t)_0$ é o operador na representação de Heisenberg na evolução com H_0, δ indica derivada funcional [Courant & Hilbert 1953], e lembramos que definimos

$$\langle \cdots \mid t\rangle_0 \equiv \mathrm{Tr}\left\{\ldots\bar{\varrho}(t,0)\right\} . \tag{A.18}$$

Na aproximação proposta, a Eq. (A.10) pode ser escrita com o auxílio das Eqs. (A.12) e (A.16) como:

$$\frac{d}{dt}Q_j(\boldsymbol{r},t) = \frac{d}{dt}\langle \hat{P}_j(\boldsymbol{r}) \mid t\rangle = J_j^{(0)}(\boldsymbol{r},t) + J_j^{(1)}(\boldsymbol{r},t) + J_j^{(2)}(\boldsymbol{r},t) , \tag{A.19}$$

obtendo-se assim no MOENE a especificação dos funcionais $\mathcal{R}_j$ da Eq. (A.4).

Essa expressão constitui o conjunto de equações generalizadas de transporte, construído, relembramos, usando-se o Operador Estatístico de Não-Equilíbrio na aproximação Markoviana de segunda ordem na intensidade de interação, que é o termo de ordem mais baixa a produzir efeitos dissipativos.

Para o **OENE** de Zubarev, o termo $J_j^{(2)}(\boldsymbol{r},t)$ tem a seguinte expressão:

$$J_j^{(2)}(\boldsymbol{r},t) = (\mathrm{i}\hbar)^{-2}\int_{-\infty}^{0} dt' e^{\epsilon t'} \langle [H'(t')_0, [H', \hat{P}_j(\boldsymbol{r})] + \mathrm{i}\hbar\sum_k \frac{\delta J_j^{(1)}(t)}{\delta\langle \hat{P}_k(\boldsymbol{r}) \mid t\rangle}\hat{P}_k(\boldsymbol{r})] \mid t\rangle_0 . \tag{A.20}$$

A.3 Teoria da Função Resposta

Outro item de grande importância, e ligado à teoria cinética descrita na seção A.2, é o da construção de uma teoria da Função Resposta. Isto é descrito na reprodução a seguir de um artigo que está sendo submetido para publicação no *Journal of Statistical Physics*. A seção 2 desse artigo — por consistência em sua apresentação — tem uma discussão do formalismo nos moldes do que já foi apresentado nas seções anteriores deste apêndice.

Integração da Equação de Schrödinger Não-linear pelo Método do Espalhamento Inverso

B.1 O método

Nosso problema consiste em achar as soluções do problema de valor inicial para a equação:

$$i\frac{\partial\psi(x,t)}{\partial t}+\frac{\partial\psi(x,t)}{\partial x^2}+g\left|\psi(x,t)\right|^2\psi(x,t)=0 \tag{B.1}$$

com a seguinte condição inicial:

$$\psi(x,0)=\psi_0(x), \tag{B.2}$$

com $\psi_0(x)$ correspondendo a uma função arbitrária decrescendo rapidamente no infinito ($x \to \infty$). Zakharov & Shabat [1972] criaram um método para resolver esse problema, o assim chamado Método do Espalhamento Inverso (MEI). Eles mostraram que a solução da esse problema pode ser colocado em correspondência com o problema do espalhamento para os autovetores

$$v = \begin{pmatrix} v_1 \\ v_2 \end{pmatrix}, \tag{B.3}$$

satisfazendo o sistema de equações:

$$\frac{dv_1}{dx} + \mathrm{i}\zeta v_1 = q(x)v_2 \tag{B.4a}$$

$$\frac{dv_2}{dx} - \mathrm{i}\zeta v_2 = -q^*(x)v_1 \tag{B.4b}$$

com autovalores $\zeta = \xi + \mathrm{i}\eta$, e

$$q(x) = i\sqrt{g}\psi_0(x). \tag{B.5}$$

O método proposto por esses autores consiste em achar soluções do sistema (B.4) tais que, em uma função fixada $q(x)$ e um autovalor ζ, possuam o seguinte comportamento assintótico:

$$v(\zeta, x) \to \begin{cases} \begin{pmatrix} 1 \\ 0 \end{pmatrix} \mathrm{e}^{-\mathrm{i}\zeta x} & , \text{ se } x \to -\infty \\ \begin{pmatrix} 1 \\ 0 \end{pmatrix} a(\zeta)\mathrm{e}^{-\mathrm{i}\zeta x} + \begin{pmatrix} 0 \\ 1 \end{pmatrix} b(\zeta)\mathrm{e}^{\mathrm{i}\zeta x} & , \text{ se } x \to \infty \end{cases} \tag{B.6}$$

onde $a(\zeta)$ é o coeficiente de transmissão e $b(\zeta)$ é o coeficiente de reflexão de uma onda plana incidente no potencial $q(x)$ da região $x \approx \infty$.

A relação entre $b(\zeta)$ e $a(\zeta)$ determina o coeficiente de reflexão:

$$R = \frac{b(\zeta)}{a(\zeta)} \; . \tag{B.7}$$

As funções em (B.6) admitem continuação analítica no semiplano superior $\eta > 0$ de uma variável complexa ζ. Zakharov & Shabat [1972] provam que, uma vez conhecidas $a(\zeta)$ e $b(\zeta)$ em um tempo $t = 0$, pode-se obter seus valores em $t > 0$ por meio das relações:

$$a(\zeta, t) = a(\zeta), \tag{B.8a}$$

$$b(\zeta, t) = b(\zeta)\exp(4\mathrm{i}\zeta^2 t). \tag{B.8b}$$

Nos valores ζ_j, $j = 1, \dots, N$, no semiplano superior em que os coeficientes $a(\zeta)$ se anulam, a forma assintótica da função $v(\zeta_j, x)$ é dada por

$$v(\zeta_j, x) \to \begin{cases} \begin{pmatrix} 1 \\ 0 \end{pmatrix} \mathrm{e}^{-\mathrm{i}(\xi_j + i\eta_j)x} \;, \text{ se } x \to -\infty \\ \begin{pmatrix} 0 \\ 1 \end{pmatrix} b(\xi)\mathrm{e}^{\mathrm{i}(\xi_j + i\eta_j)x} \;, \text{ se } x \to \infty . \end{cases} \tag{B.9}$$

A função $v(\zeta_j, x)$ decresce assintoticamente em $x \to \pm\infty$; ela descreve, portanto, os estados ligados correspondentes aos autovalores complexos ζ_j nas Eqs. (B.4).

Os assim chamados dados do espalhamento, por meio dos quais se pode determinar a função $q(x,t)$ em um momento arbitrário t, são dados por

$$\zeta_j, \quad c_j(t) = b(\zeta_j,t)\left[\frac{\partial a(\zeta)}{\partial \zeta}\right]^{-1}_{\zeta=\zeta_j}, \quad R(\zeta,t) = \frac{b(\zeta,t)}{a(\zeta)}. \tag{B.10}$$

A função $q(x,t)$ no MEI é dada por

$$q(x,t) = -2K(x,x), \tag{B.11}$$

onde a função $K(x,y)$ é a solução da equação integral de Gelfand-Levitan-Marchenko:

$$K(x,y) = F^*(x+y,t) - \int_x^\infty ds \int_x^\infty dz F^*(s+y,t)F(s+z,t)K(x,z), \tag{B.12}$$

onde a função $F(x,t)$ é dada em termos dos dados do espalhamento (Eq. B.10):

$$F(x,t) = \frac{1}{2\pi}\int_{-\infty}^{\infty} R(\zeta,t)e^{i\zeta x}d\zeta + \sum_{j-1}^{N} c_j(t)e^{i\zeta_j x}. \tag{B.13}$$

Uma vez determinada a função $q(x,t)$ por meio da Eq. (B.11), pode-se usar a Eq. (B.5) para obter $\psi(x,t)$

$$\psi(x,t) = \frac{-iq(x,t)}{\sqrt{g}}, \tag{B.14}$$

que é a solução da Eq. (B.1) com a condição inicial especificada pela Eq. (B.2).

B.2 Aplicação do método

Como aplicação do MEI, resolveremos a equação

$$\mathrm{i}\frac{\partial\psi(x,t)}{\partial t}+\frac{\partial\psi(x,t)}{\partial x^2}+2g\left|\psi(x,t)\right|^2\psi(x,t)=0 \tag{B.15}$$

com uma condição inicial na forma de uma secante hiperbólica:

$$\psi(x,0)=\psi_0(x)=\frac{A}{\sqrt{g}}\mathrm{e}^{\mathrm{i}2kx}\operatorname{sech}(Ax). \tag{B.16}$$

Para calcular os dados do espalhamento, temos de encontrar as soluções assintóticas do sistema (B.4).

Usando a Eq. (B.4b), podemos escrever que:

$$v_2=\frac{v_1'+i\zeta v_1}{q(x)}\;. \tag{B.17}$$

Substituindo a Eq. (B.17) na Eq. (B.4a), obtemos a equação:

$$v_1''-\frac{q'(x)}{q(x)}v_1'+(\zeta^2+\left|q(x)\right|^2-\mathrm{i}\frac{q'(x)}{q(x)})v_1=0. \tag{B.18}$$

Para a condição inicial da Eq. (B.16) o potencial $q(x)$ é dado por

$$q(x)=\mathrm{i}A\mathrm{e}^{2\mathrm{i}kx}\operatorname{sech}(Ax), \tag{B.19}$$

de maneira que a Eq. (B.18) se reduz a:

$$v_1'' - (2ik - A\tanh(Ax))v_1' + [\zeta^2 + A^2\mathrm{sech}^2(Ax) + (2k + iA\tanh(Ax))\zeta]v_1 = 0. \tag{B.20}$$

O comportamento assintótico da equação acima quando $x \to \pm\infty$ é:

$$v_1'' - (2ik \mp A)v_1' + [\zeta^2 + (2k \pm iA)\zeta]v_1 = 0. \tag{B.21}$$

A solução geral da Eq. (B.21) é:

$$v_1 = c_1 e^{\ i\zeta x} + c_2 e^{i[\zeta + (2k \mp iA)]x}, \tag{B.22}$$

com c_1 e c_2 constantes arbitrárias a serem determinadas tal que v_1 satisfaça a condição

$$v_1 \to e^{-i\zeta x}, \tag{B.23}$$

quando $x \to -\infty$. Com isso, obtemos que:

$$v_1 = \begin{cases} e^{(2ik + i\zeta + A)x}\ , \text{ se } x \to -\infty, \text{ com } \zeta = -k + \frac{1}{2}iA \\ e^{-i\zeta x}\ , \text{ se } x \to \infty. \end{cases}, \tag{B.24}$$

e, usando a Eq. (B.17),

$$v_2 = 0, \quad \text{para } x \to \pm\infty. \tag{B.25}$$

Uma vez que em $x \to \infty$, $v_2 = b(\xi)\mathrm{e}^{\mathrm{i}\zeta x}$, é imediato que

$$b(\xi) = 0, \tag{B.26}$$

de maneira que o valor de R na Eq. (B.10) é

$$R(\xi, t) = 0, \tag{B.27}$$

e o valor da função auxiliar $F(x,t)$ da Eq. (B.13) é:

$$F(x,t) = \sum_{j=1}^{N} c_j(t)\mathrm{e}^{\mathrm{i}(\xi_j)x} \tag{B.28}$$

Em nosso caso, $N = 1$, [cf. Eq. (B.24)], de modo que:

$$F(x,t) = c_1(t)\mathrm{e}^{\mathrm{i}\zeta x}, \tag{B.29}$$

com $\zeta = -k + \frac{1}{2}\mathrm{i}\Lambda$. Substituindo a Eq. (B.29) na Eq. B.12, e assumindo $K(x,y)$ na forma

$$K(x,y) = f(x)\mathrm{e}^{-\mathrm{i}\zeta^* y}, \tag{B.30}$$

obtemos:

$$f(x)\mathrm{e}^{-\mathrm{i}\zeta^* y} = c_1^*(t)\mathrm{e}^{-\mathrm{i}\zeta^*(x+y)} - \int_x^\infty ds \int_x^\infty dz\, |c_1(t)|^2\, \mathrm{e}^{-\mathrm{i}\zeta^*(s+y)}\mathrm{e}^{-\mathrm{i}\zeta(s+z)} f(x)\mathrm{e}^{-\mathrm{i}\zeta^* z}. \tag{B.31}$$

Resolvendo para $f(x)$, encontra-se que:

$$f(x) = \frac{c_1^*(t)\mathrm{e}^{-\mathrm{i}\zeta^* x}}{1 + \frac{|c_1(t)|^2}{A^2}\mathrm{e}^{-gx}}\,. \tag{B.32}$$

O valor de $c_1(t)$ é dado por [cf. Eq. (B.8b)]

$$c_1(t) = \mathrm{i}A\mathrm{e}^{\mathrm{i}(4k^2 - A^2)t}\mathrm{e}^{4kAt}. \tag{B.33}$$

Utilizando as Eqs. (B.32), (B.33), (B.11) e (B.14), obtém-se

$$\psi(x,t) = \frac{2A}{\sqrt{g}}\mathrm{e}^{\mathrm{i}[2kx-(4k^2-A^2)t]}\frac{\mathrm{e}^{A(4kt - x)}}{1 + \mathrm{e}^{2A(4kt - x)}}, \tag{B.34}$$

que pode ser colocada na forma:

$$\psi(x,t) = \frac{A}{\sqrt{g}}\,\mathrm{e}^{\mathrm{i}[2kx-(4k^2-A^2)t]}\,\mathrm{sech}^2[A(x-4kt)], \tag{B.35}$$

que é a solução procurada para a Eq. (B.15) com a condição inicial dada pela Eq. (B.16).

Apêndice C

Valores Médios de Operadores

Para calcularmos os valores médios de operadores com o operador auxiliar $\bar{\varrho}(t,0)$, podemos diagonalizá-lo com o auxílio de uma transformação canônica:

$$a_q = b_q + \lambda_q \,, \qquad\qquad a_q^\dagger = b_q^\dagger + \lambda_q^* \,, \tag{C.1}$$

onde λ_q é um número complexo. Com isso $\bar{\varrho}(t,0)$ toma a forma:

$$\begin{aligned}\bar{\varrho}(t,0) = \exp\Big\{-\phi - \sum_q [F_q(t) b_q^\dagger b_q + (F_q(t)\lambda_q^* + f_q(t)) b_q \\ + (F_q(t)\lambda_q + f_q^*(t)) b_q^\dagger + F_q(t)\lambda_q\lambda_q^* + f_q(t)\lambda_q + f_q^*(t)\lambda_q^*]\Big\} \,,\end{aligned} \tag{C.2}$$

onde

$$\begin{aligned}\phi = \ln \mathrm{Tr} \exp\Big\{-\sum_q [F_q(t) b_q^\dagger b_q + (F_q(t)\lambda_q^* + f_q(t)) b_q \\ + (F_q(t)\lambda_q + f_q^*(t)) b_q^\dagger + F_q(t)\lambda_q\lambda_q^* + f_q(t)\lambda_q + f_q^*(t)\lambda_q^*]\Big\} \,.\end{aligned} \tag{C.3}$$

Se tomarmos

$$\lambda_q = -\frac{f_q^*(t)}{F_q(t)}\,, \qquad \lambda_q^* = -\frac{f_q(t)}{F_q(t)}\,, \tag{C.4}$$

a expressão para $\bar{\varrho}(t,0)$ reduz-se a:

$$\bar{\varrho}(t,0) = \frac{\exp\left\{-\sum\limits_q F_q(t) b_q^\dagger b_q\right\}}{\operatorname{Tr}\exp\left\{-\sum\limits_q F_q(t) b_q^\dagger b_q\right\}}\,, \tag{C.5}$$

e nessa forma podemos calcular as médias que aparecem ao longo dos cálculos das equações de evolução.

C.1 Cálculo de $\langle a_q | t\rangle$ e $\langle a_q^\dagger \mid t\rangle$

$$\langle a_q \mid t\rangle = \operatorname{Tr}\{a_q \bar{\varrho}(t,0)\} = \operatorname{Tr}\{(b_q + \lambda_q)\,\bar{\varrho}(t,0)\}$$

$$= \operatorname{Tr}\{b_q \bar{\varrho}(t,0)\} + \lambda_q \operatorname{Tr}\{\bar{\varrho}(t,0)\} = \lambda_q \tag{C.6}$$

$$\langle a_q^\dagger \mid t\rangle = \operatorname{Tr}\left\{a_q^\dagger \bar{\varrho}(t,0)\right\} = \operatorname{Tr}\left\{\left(b_q^\dagger + \lambda_q^*\right)\bar{\varrho}(t,0)\right\}$$

$$= \operatorname{Tr}\left\{b_q^\dagger \bar{\varrho}(t,0)\right\} + \lambda_q^* \operatorname{Tr}\{\bar{\varrho}(t,0)\} = \lambda_q^*\,, \tag{C.7}$$

onde usamos o fato de que $\operatorname{Tr}\{\bar{\varrho}(t,0)\} = 1$.

C.2 Cálculo de $\langle a_{q_1}^{\dagger} a_{q_2} \mid t \rangle$

$$
\begin{aligned}
\langle a_{q_1}^{\dagger} a_{q_2} \mid t \rangle &= \mathrm{Tr}\{a_{q_1}^{\dagger} a_{q_2} \bar{\varrho}(t,0)\} = \mathrm{Tr}\{(b_{q_1}^{\dagger} + \lambda_{q_1}^{*})(b_{q_2} + \lambda_{q_2})\bar{\varrho}(t,0)\} \\
&= \mathrm{Tr}\{b_{q_1}^{\dagger} b_{q_2} \bar{\varrho}(t,0)\} + \lambda_{q_2}\, \mathrm{Tr}\{b_{q_1}^{\dagger} \bar{\varrho}(t,0)\} \\
&+ \lambda_{q_1}^{*}\, \mathrm{Tr}\{b_{q_2} \bar{\varrho}(t,0)\} + \lambda_{q_1}^{*}\lambda_{q_2}\, \mathrm{Tr}\{\bar{\varrho}(t,0)\} \\
&= \frac{1}{e^{F_{q_1}} - 1}\delta_{q_1,q_2} + \langle a_{q_1}^{\dagger} \mid t \rangle \langle a_{q_2} \mid t \rangle \; . \qquad \text{(C.8)}
\end{aligned}
$$

Quando $\boldsymbol{q}_1 = \boldsymbol{q}_2$, temos

$$
\langle a_{q_1}^{\dagger} a_{q_1} \mid t \rangle = \langle n_{q_1} \mid t \rangle = \frac{1}{e^{F_{q_1}} - 1} + \left| \langle a_{q_1} \mid t \rangle \right|^2 \; , \qquad \text{(C.9)}
$$

de maneira que podemos escrever a Eq. (C.8) como

$$
\langle a_{q_1}^{\dagger} a_{q_2} \mid t \rangle = \langle a_{q_1}^{\dagger} \mid t \rangle \langle a_{q_2} \mid t \rangle + \Big(\langle n_{q_1} \mid t \rangle - \left| \langle a_{q_1} \mid t \rangle \right|^2 \Big)\, \delta_{q_1,q_2} \; . \qquad \text{(C.10)}
$$

C.3 Cálculo de $\langle a_{q_1}^{\dagger} a_{q_2} a_{q_3} \mid t \rangle$

$$
\begin{aligned}
\langle a_{q_1}^{\dagger} a_{q_2} a_{q_3} \mid t \rangle &= \mathrm{Tr}\left\{a_{q_1}^{\dagger} a_{q_2} a_{q_3} \bar{\varrho}(t,0)\right\} = \mathrm{Tr}\left\{\left(b_{q_1}^{\dagger} + \lambda_{q_1}^{*}\right)(b_{q_2} + \lambda_{q_2})(b_{q_3} + \lambda_{q_3})\,\bar{\varrho}(t,0)\right\} \\
&= \mathrm{Tr}\left\{\left(b_{q_1}^{\dagger} b_{q_2} b_{q_3} + \lambda_{q_3} b_{q_1}^{\dagger} b_{q_2} + \lambda_{q_2} b_{q_1}^{\dagger} b_{q_3} + \lambda_{q_2}\lambda_{q_3} b_{q_1}^{\dagger}\right)\bar{\varrho}(t,0)\right\} \\
&+ \mathrm{Tr}\left\{\left(\lambda_{q_1}^{*} b_{q_2} b_{q_3} + \lambda_{q_1}^{*}\lambda_{q_3} b_{q_2} + \lambda_{q_1}^{*}\lambda_{q_2} b_{q_3} + \lambda_{q_1}^{*}\lambda_{q_2}\lambda_{q_3}\right)\bar{\varrho}(t,0)\right\}
\end{aligned}
$$

$$
\begin{aligned}
&= \lambda_{q_3}\,\mathrm{Tr}\left\{b^{\dagger}_{q_1} b_{q_2}\bar{\varrho}(t,0)\right\} + \lambda_{q_2}\,\mathrm{Tr}\left\{b^{\dagger}_{q_1} b_{q_3}\bar{\varrho}(t,0)\right\} + \lambda^{*}_{q_1}\lambda_{q_2}\lambda_{q_3}\,\mathrm{Tr}\left\{\bar{\varrho}(t,0)\right\} \\
&= \langle a^{\dagger}_{\mathbf{q}_1} \mid t\rangle\langle a_{\mathbf{q}_2} \mid t\rangle\langle a_{\mathbf{q}_3} \mid t\rangle + \\
&\quad + \left(\langle n_{\mathbf{q}_1} \mid t\rangle - \left|\langle a_{\mathbf{q}_1} \mid t\rangle\right|^2\right)\left(\langle a_{\mathbf{q}_2} \mid t\rangle\delta_{\mathbf{q}_1,\mathbf{q}_3} + \langle a_{\mathbf{q}_3} \mid t\rangle\delta_{\mathbf{q}_1,\mathbf{q}_2}\right) \ , \qquad \text{(C.11)}
\end{aligned}
$$

onde fizemos uso da Eq. (C.10).

Cálculo de $\langle a^{\dagger}_{\mathbf{q}_1} a^{\dagger}_{\mathbf{q}} a_{\mathbf{q}_2} a_{\mathbf{q}_3} \mid t\rangle$

$$
\begin{aligned}
\langle a^{\dagger}_{\mathbf{q}_1} a^{\dagger}_{\mathbf{q}} a_{\mathbf{q}_2} a_{\mathbf{q}_3} \mid t\rangle &= \mathrm{Tr}\left\{a^{\dagger}_{\mathbf{q}_1} a^{\dagger}_{\mathbf{q}} a_{\mathbf{q}_2} a_{\mathbf{q}_3}\bar{\varrho}(t,0)\right\} \\
&= \mathrm{Tr}\left\{\left(b^{\dagger}_{\mathbf{q}_1} + \lambda^{*}_{\mathbf{q}_1}\right)\left(b_{\mathbf{q}} + \lambda_{\mathbf{q}}\right)\left(b_{\mathbf{q}_2} + \lambda_{\mathbf{q}_2}\right)\left(b_{\mathbf{q}_3} + \lambda_{\mathbf{q}_3}\right)\bar{\varrho}(t,0)\right\} \\
&= \mathrm{Tr}\left\{\left(b^{\dagger}_{q_1} b^{\dagger}_{q} b_{q_2} b_{q_3} + \lambda_{q_3} b^{\dagger}_{q_1} b^{\dagger}_{q} b_{q_2} + \lambda_{q_2} b^{\dagger}_{q_1} b^{\dagger}_{q} b_{q_3} + \lambda_{q_2}\lambda_{q_3} b^{\dagger}_{q_1} b^{\dagger}_{q}\right)\bar{\varrho}(t,0)\right\} \\
&\quad + \mathrm{Tr}\left\{\left(\lambda^{*}_{q} b^{\dagger}_{q_1} b_{q_2} b_{q_3} + \lambda^{*}_{q}\lambda_{q_3} b^{\dagger}_{q_1} b_{q_2} + \lambda^{*}_{q}\lambda_{q_2} b^{\dagger}_{q_1} b_{q_3} + \lambda^{*}_{q}\lambda_{q_2}\lambda_{q_3} b^{\dagger}_{q_1}\right)\bar{\varrho}(t,0)\right\} \\
&\quad + \mathrm{Tr}\left\{\left(\lambda_{q_1} b^{\dagger}_{q} b_{q_2} b_{q_3} + \lambda^{*}_{q_1}\lambda_{q_3} b^{\dagger}_{q} b_{q_2} + \lambda^{*}_{q_1}\lambda_{q_2} b^{\dagger}_{q} b_{q_3} + \lambda^{*}_{q_1}\lambda_{q_2}\lambda_{q_3} b^{\dagger}_{q}\right)\bar{\varrho}(t,0)\right\} \\
&\quad + \mathrm{Tr}\left\{\left(\lambda^{*}_{q}\lambda^{*}_{q_1} b_{q_2} b_{q_3} + \lambda^{*}_{q}\lambda^{*}_{q_1}\lambda_{q_3} b_{q_2} + \lambda^{*}_{q}\lambda^{*}_{q_1}\lambda_{q_2} b_{q_3} + \lambda^{*}_{q}\lambda^{*}_{q_1}\lambda_{q_2}\lambda_{q_3}\right)\bar{\varrho}(t,0)\right\} \\
&= \mathrm{Tr}\left\{b^{\dagger}_{q_1} b^{\dagger}_{q} b_{q_2} b_{q_3}\bar{\varrho}(t,0)\right\} + \lambda^{*}_{q}\lambda_{q_3}\,\mathrm{Tr}\left\{b^{\dagger}_{q_1} b_{q_2}\bar{\varrho}(t,0)\right\} \\
&\quad + \lambda^{*}_{q}\lambda_{q_2}\,\mathrm{Tr}\left\{b^{\dagger}_{q_1} b_{q_3}\bar{\varrho}(t,0)\right\} + \lambda^{*}_{q_1}\lambda_{q_3}\mathrm{Tr}\left\{b^{\dagger}_{q} b_{q_2}\bar{\varrho}(t,0)\right\} \\
&\quad + \lambda^{*}_{q_1}\lambda_{q_2}\mathrm{Tr}\left\{b^{\dagger}_{q} b_{q_3}\bar{\varrho}(t,0)\right\} + \lambda^{*}_{q}\lambda^{*}_{q_1}\lambda_{q_2}\lambda_{q_3}\mathrm{Tr}\left\{\bar{\varrho}(t,0)\right\} \ . \qquad \text{(C.12}
\end{aligned}
$$

Usando o teorema de Wick [Louissel 1973], podemos escrever que

$$\mathrm{Tr}\left\{b^\dagger_{q_1}b^\dagger_q b_{q_2}b_{q_3}\bar{\varrho}(t,0)\right\} = \mathrm{Tr}\left\{b^\dagger_{q_1}b_{q_2}\bar{\varrho}(t,0)\right\}\mathrm{Tr}\left\{b^\dagger_q b_{q_3}\bar{\varrho}(t,0)\right\}$$
$$+ \mathrm{Tr}\left\{b^\dagger_{q_1}b_{q_3}\bar{\varrho}(t,0)\right\}\mathrm{Tr}\left\{b^\dagger_q b_{q_2}\bar{\varrho}(t,0)\right\}, \qquad (C.13)$$

de modo que

$$\langle a^\dagger_{q_1}a^\dagger_q a_{q_2}a_{q_3} \mid t\rangle = \mathrm{Tr}\left\{b^\dagger_{q_1}b_{q_2}\bar{\varrho}(t,0)\right\}\mathrm{Tr}\left\{b^\dagger_q b_{q_3}\bar{\varrho}(t,0)\right\}$$
$$+ \mathrm{Tr}\left\{b^\dagger_{q_1}b_{q_3}\bar{\varrho}(t,0)\right\}\mathrm{Tr}\left\{b^\dagger_q b_{q_2}\bar{\varrho}(t,0)\right\} + \lambda^*_q\lambda_{q_3}\mathrm{Tr}\left\{b^\dagger_{q_1}b_{q_2}\bar{\varrho}(t,0)\right\}$$
$$+ \lambda^*_q\lambda_{q_2}\mathrm{Tr}\left\{b^\dagger_{q_1}b_{q_3}\bar{\varrho}(t,0)\right\} + \lambda^*_{q_1}\lambda_{q_3}\mathrm{Tr}\left\{b^\dagger_q b_{q_2}\bar{\varrho}(t,0)\right\}$$
$$+ \lambda^*_{q_1}\lambda_{q_2}\mathrm{Tr}\left\{b^\dagger_q b_{q_3}\bar{\varrho}(t,0)\right\} + \lambda^*_q\lambda^*_{q_1}\lambda_{q_2}\lambda_{q_3}\mathrm{Tr}\left\{\bar{\varrho}(t,0)\right\}$$
$$= \langle a^\dagger_{q_1} \mid t\rangle\langle a_{q_2} \mid t\rangle\langle a_{q_3} \mid t\rangle\langle a^\dagger_q \mid t\rangle$$
$$+ \left(\langle n_{q_1} \mid t\rangle - |\langle a_{q_1} \mid t\rangle|^2\right)\langle a^\dagger_q \mid t\rangle\left(\langle a_{q_2} \mid t\rangle\delta_{q_1,q_3} + \langle a_{q_3} \mid t\rangle\delta_{q_1,q_2}\right)$$
$$+ \left(\langle n_q \mid t\rangle - |\langle a_q \mid t\rangle|^2\right)\langle a^\dagger_{q_1} \mid t\rangle\left(\langle a_{q_2} \mid t\rangle\delta_{q,q_3} + \langle a_{q_3} \mid t\rangle\delta_{q,q_2}\right)$$
$$+ \left(\langle n_q \mid t\rangle - |\langle a_q \mid t\rangle|^2\right)\left(\langle n_{q_1} \mid t\rangle - |\langle a_{q_1} \mid t\rangle|^2\right)\left(\delta_{q_1,q_2}\delta_{q,q_3} + \delta_{q_1,q_3}\delta_{q,q_2}\right). \qquad (C.14)$$

Apêndice D

Deltas de Conservação

D.1 Introdução

Para calcularmos as várias integrais que aparecem nas equações de transporte para $\nu_{\boldsymbol{q}}$, $a_{\boldsymbol{q}}$ e $a^{\dagger}_{\boldsymbol{q}}$, utilizamos a relação

$$\delta(f(x)) = \sum_i \frac{\delta(x - x_i)}{|f'(x_i)|} , \tag{D.1}$$

onde os x_i são as raízes de f, e $f'(x_i)$ é a derivada de $f(x)$ em $x = x_i$. Uma vez fixadas as relações de dispersão, podemos calcular as raízes das funções que aparecem nas deltas para expandi-las. As deltas de conservação que aparecem nas equações são:

$$\delta(f_1(q_1)) = \delta(\Omega_{q_1} + \Omega_{q-q_1} - \omega_q) , \tag{D.2a}$$

$$\delta(f_2(q_1)) = \delta(\Omega_{q_1} - \Omega_{q+q_1} + \omega_q) , \tag{D.2b}$$

$$\delta(f_3(q_1)) = \delta(\Omega_{q-q_1} + \omega_{q_1} - \omega_q) , \tag{D.2c}$$

$$\delta(f_4(q_1)) = \delta(\Omega_{q-q_1} - \omega_{q_1} + \omega_q) , \tag{D.2d}$$

$$\delta(f_5(q_1)) = \delta(\Omega_{q+q_1} - \omega_{q_1} - \omega_q) . \tag{D.2e}$$

Analisaremos cada uma das funções f_i para o caso dos modos ópticos e para o caso dos modos acústicos.

D.2 Modos ópticos

Neste caso, a relação de dispersão para o sistema é $\omega_q = \omega_0 - \alpha q^2$, e para o reservatório é $\Omega_q = s_B q$. Levando em conta essas relações, podemos escrever as Eqs. (D.2) como:

$$\delta(f_1(q_1)) = \delta(s_B|q_1| + s_B|q - q_1| - \omega_0 + \alpha q^2) \; , \tag{D.3a}$$

$$\delta(f_2(q_1)) = \delta(s_B|q_1| - s_B|q + q_1| + \omega_0 - \alpha q^2) \; , \tag{D.3b}$$

$$\delta(f_3(q_1)) = \delta(s_B|q - q_1| - \alpha(q_1^2 - q^2)) \; , \tag{D.3c}$$

$$\delta(f_4(q_1)) = \delta(s_B|q - q_1| + \alpha(q_1^2 - q^2)) \; , \tag{D.3d}$$

$$\delta(f_5(q_1)) = \delta(s_B|q + q_1| - 2\omega_0 + \alpha(q_1^2 + q^2)) \; . \tag{D.3e}$$

Analisaremos a seguir cada uma das funções f_i, calculando suas raízes e as condições em que elas existem.

D.2.1 Análise de f_1.

i) Para $q < 0$, a expressão para f_1 é:

$$f_1 = \begin{cases} -2s_B q_1 s_B + s_B q - \omega_0 + \alpha q^2, & \text{se } q_1 < q\,, \\ -s_B q - \omega_0 + \alpha q^2\,, & \text{se } q \leq q_1 \leq 0\,, \\ 2s_B q_1 s_B - s_B q - \omega_0 + \alpha q^2\,, & \text{se } q_1 > 0\,. \end{cases} \tag{D.4}$$

Neste caso, a função f_1 possui duas raízes:

$$q_1 = \begin{cases} r_1 = \dfrac{s_B q - \omega_0 + \alpha q^2}{2s_B}, & \text{se } q_1 < q\,, \\ r_2 = \dfrac{s_B q + \omega_0 - \alpha q^2}{2s_B}, & \text{se } q_1 > 0\,. \end{cases} \tag{D.5}$$

Para que a condição $q_1 < q$ seja satisfeita, q deve satisfazer à relação $\zeta^{(\ )} < q < 0$. Igualmente, para que a condição $q_1 > 0$ seja satisfeita, devemos ter que $\zeta^{(-)} < q < 0$, com:

$$\zeta^{(-)} = \frac{s}{2\alpha} - \sqrt{\left(\frac{s}{2\alpha}\right)^2 + \frac{\omega_0}{\alpha}}\,. \tag{D.6}$$

Podemos então escrever, usando a Eq. (D.1), que:

$$\delta(f_1(q_1)) = \frac{1}{2s_B}[\delta(q_1 - r_1) + \delta(q_1 - r_2)][\Theta(q - \zeta^{(-)}) - \Theta(q)]\,, \tag{D.7}$$

onde Θ é a função degrau de Heaviside.

ii) Para $q \geq 0$, a expressão para f_1 é:

$$f_1 = \begin{cases} -2s_B q_1 s_B + s_B q - \omega_0 + \alpha q^2, & \text{se } \ q_1 < 0 \,, \\ s_B q - \omega_0 + \alpha q^2 \,, & \text{se } \ 0 \leq q_1 \leq q \,, \\ 2s_B q_1 s_B - s_B q - \omega_0 + \alpha q^2 \,, & \text{se } \ q_1 > q \,. \end{cases} \tag{D.8}$$

Neste caso, a função f_1 possui duas raízes:

$$q_1 = \begin{cases} r_1, & \text{se } \ q_1 < 0 \,, \\ r_2, & \text{se } \ q_1 > q \,. \end{cases} \tag{D.9}$$

Para que a condição $q_1 < 0$ seja satisfeita, q deve satisfazer a relação $0 < q < -\zeta^{(-)}$. Igualmente, para que $q_1 > q$ seja satisfeita, devemos ter que $0 < q < -\zeta^{(-)}$.

Podemos então escrever, usando a Eq. (D.1), que:

$$\delta(f_1(q_1)) = \frac{1}{2s_B}[\delta(q_1 - r_1) + \delta(q_1 - r_2)][\Theta(q) - \Theta(q + \zeta^{(-)})] \,. \tag{D.10}$$

Assim, para um q geral, podemos escrever:

$$\delta(f_1(q_1)) = \frac{1}{2s_B}[\delta(q_1 - r_1) + \delta(q_1 - r_2)][\Theta(q - \zeta^{(-)}) - \Theta(q + \zeta^{(-)})] \,. \tag{D.11}$$

D.2.2 Análise de f_2.

i) Para $q < 0$, a expressão para f_2 é:

$$f_2 = \begin{cases} s_B q + \omega_0 - \alpha q^2, & \text{se } q_1 \leq 0 , \\ 2 s_B q_1 + s_B q + \omega_0 - \alpha q^2, & \text{se } 0 < q_1 < -q , \\ -s_B q + \omega_0 - \alpha q^2, & \text{se } q_1 \geq -q . \end{cases} \tag{D.12}$$

Neste caso, a função f_2 possui uma raiz:

$$q_1 = -r_1 = -\frac{s_B q + \omega_0 - \alpha q^2}{2 s_B} , \tag{D.13}$$

se e apenas se for satisfeita a relação $0 < q_1 < -q$. Para tanto, q deve satisfazer à condição $-\zeta^{(+)} < q < \zeta^{(-)}$, com

$$\zeta^{(+)} = \frac{s}{2\alpha} + \sqrt{\left(\frac{s}{2\alpha}\right)^2 + \frac{\omega_0}{\alpha}} . \tag{D.14}$$

Podemos então escrever, usando a Eq. (D.1), que:

$$\delta(f_2) = \frac{1}{2 s_B} [\delta(q_1 + r_1)] [\Theta(q + \zeta^{(+)}) - \Theta(q - \zeta^{(-)})] . \tag{D.15}$$

ii) Para $q \geq 0$, a expressão para f_2 é:

$$f_2 = \begin{cases} s_B q + \omega_0 - \alpha q^2, & \text{se } \; q_1 \leq -q \, , \\ -2 s_B q_1 - s_B q + \omega_0 - \alpha q^2 \, , & \text{se } \; -q < q_1 \leq 0 \, , \\ -s_B q + \omega_0 - \alpha q^2, & \text{se } \; q_1 > 0 \, . \end{cases} \tag{D.16}$$

Neste caso, a função f_2 possui uma raiz:

$$q_1 = -r_2 \, , \tag{D.17}$$

se e apenas se for satisfeita à condição $-q < q_1 \leq 0$. Para tanto, q deve satisfazer a relação $-\zeta^{(-)} \leq q < \zeta^{(+)}$.

Podemos então escrever, usando a Eq. (D.1), que:

$$\delta(f_2(q_1)) = \frac{1}{2 s_B} [\delta(q_1 + r_2)] [\Theta(q + \zeta^{(-)}) - \Theta(q - \zeta^{(+)})] \, . \tag{D.18}$$

Assim, para um q geral, podemos escrever:

$$\delta(f_2(q_1)) = \frac{1}{2 s_B} \Big\{ [\delta(q_1 + r_1)] [\Theta(q + \zeta^{(+)}) - \Theta(q - \zeta^{(-)})] + \\ [\delta(q_1 + r_2)] [\Theta(q + \zeta^{(-)}) - \Theta(q - \zeta^{(+)})] \Big\} \, . \tag{D.19}$$

D.2.3 Análise de f_3.

A expressão para f_3 é:

$$f_3 = \begin{cases} +s_B(q_1 - q) - \alpha(q_1^2 - q^2) \,, & \text{se } q_1 \geq q \,, \\ -s_B(q_1 - q) - \alpha(q_1^2 - q^2) \,, & \text{se } q_1 < q \,. \end{cases} \tag{D.20}$$

Neste caso, a função f_3 possui três raízes:

$$q_1 = \begin{cases} q, \, -q + \dfrac{s_B}{\alpha} & \text{se } q_1 \geq q \,, \\ -q - \dfrac{s_B}{\alpha} & \text{se } q_1 < q \,. \end{cases} \tag{D.21}$$

Levando em conta que a derivada de f_3 não existe em $q_1 = q$, podemos então escrever, usando a Eq. (D.1), que:

$$\delta(f_3) = -\frac{1}{2\alpha q - s_B}[\delta(q_1 + q - \frac{s_B}{\alpha})][1 - \Theta(q - \frac{s_B}{2\alpha})] + \frac{1}{2\alpha q + s_B}[\delta(q_1 + q + \frac{s_B}{\alpha})]\Theta(q + \frac{s_B}{2\alpha}) \,. \tag{D.22}$$

D.2.4 Análise de f_4.

A expressão para f_4 é:

$$f_4 = \begin{cases} s_B(q_1 - q) + \alpha(q_1^2 - q^2) \,, & \text{se } q_1 \geq q \,, \\ -s_B(q_1 - q) + \alpha(q_1^2 - q^2) \,, & \text{se } q_1 < q \,. \end{cases} \tag{D.23}$$

Neste caso, a função f_4 possui três raízes:

$$q_1 = \begin{cases} q, -q - \dfrac{s_B}{\alpha}, & \text{se} \;\; q_1 \geq q \, , \\[2ex] -q + \dfrac{s_B}{\alpha}, & \text{se} \;\; q_1 < q \, . \end{cases} \tag{D.24}$$

Levando em conta que a derivada de f_4 não existe em $q_1 = q$, podemos então escrever, usando a Eq. (D.1), que:

$$\delta(f_4) = -\frac{1}{2\alpha q + s_B}[\delta(q_1 + q + \frac{s_B}{\alpha})][1 - \Theta(q + \frac{s_B}{2\alpha})] + \\ \frac{1}{2\alpha q - s_B}[\delta(q_1 + q - \frac{s_B}{\alpha})]\Theta(q - \frac{s_B}{2\alpha}) \, . \tag{D.25}$$

D.2.5 Análise de f_5.

A expressão para f_5 é:

$$f_5 = \begin{cases} s_B(q_1 + q) - 2\omega_0 + \alpha(q_1^2 + q^2) \, , & \text{se} \;\; q_1 \geq -q \, , \\[2ex] -s_B(q_1 + q) - 2\omega_0 + \alpha(q_1^2 + q^2) \, , & \text{se} \;\; q_1 < -q \, . \end{cases} \tag{D.26}$$

Neste caso, a função f_5 possui quatro raízes:

$$q_1 = \begin{cases} \kappa_1^{(+)} \, , & \text{se} \;\; q_1 \geq -q \, , \\[2ex] \kappa_2^{(+)} \, , & \text{se} \;\; q_1 < -q \, , \end{cases} \tag{D.27}$$

onde:

$$\kappa_1^{(\pm)} = -\frac{s_B}{2\alpha} \pm \sqrt{\left(\frac{s_B}{2\alpha}\right)^2 - q\left(\frac{s_B}{\alpha}\right) - q^2 + \frac{2\omega_0}{\alpha}}\,, \tag{D.28a}$$

$$\kappa_2^{(\pm)} = \frac{s_B}{2\alpha} \pm \sqrt{\left(\frac{s_B}{2\alpha}\right)^2 + q\left(\frac{s_B}{\alpha}\right) - q^2 + \frac{2\omega_0}{\alpha}}\,. \tag{D.28b}$$

Para que $\kappa_1^{(+)} \geq -q$, devemos ter:

$$-\iota^{(+)} \leq q \leq -\sqrt{\frac{\omega_0}{\alpha}} \qquad \vee \qquad \sqrt{\frac{\omega_0}{\alpha}} < q \leq \iota^{(-)}\,, \tag{D.29}$$

com $\iota^{(\pm)}$ dados por:

$$\iota^{(\pm)} = \pm\frac{s_B}{2\alpha} + \sqrt{\frac{s_B^2}{2\alpha^2} + \frac{2\omega_0}{\alpha}}\,. \tag{D.30}$$

Para que $\kappa_1^{(-)} \geq -q$, devemos ter:

$$-\sqrt{\frac{\omega_0}{\alpha}} \leq q \leq \sqrt{\frac{\omega_0}{\alpha}}\,. \tag{D.31}$$

Para que $\kappa_2^{(+)} < -q$, devemos ter:

$$-\iota^{(-)} \leq q < -\sqrt{\frac{\omega_0}{\alpha}} \qquad \vee \qquad \sqrt{\frac{\omega_0}{\alpha}} < q \leq \iota^{(+)}\,. \tag{D.32}$$

Para que $\kappa_2^{(-)} < -q$, devemos ter:

$$-\sqrt{\frac{\omega_0}{\alpha}} < q < \sqrt{\frac{\omega_0}{\alpha}}\,. \tag{D.33}$$

Podemos então escrever, usando a Eq. (D.1), que:

$$\begin{aligned}
\delta(f_5) = {} & \frac{1}{2\alpha\kappa_1^{(+)} + s_B}\delta(q_1 - \kappa_1^{(+)})[\Theta(q + \iota^{(+)}) - \Theta(q - \iota^{(-)}) - 1 + \Theta(|q| - (\omega_0/\alpha)^{1/2})] - \\
& \frac{1}{2\alpha\kappa_1^{(-)} + s_B}\delta(q_1 - \kappa_1^{(-)})[1 - \Theta(|q| - (\omega_0/\alpha)^{1/2})] + \\
& \frac{1}{2\alpha\kappa_2^{(+)} - s_B}\delta(q_1 - \kappa_2^{(+)})[\Theta(q + \iota^{(-)}) - \Theta(q - \iota^{(+)}) - 1 + \Theta(|q| - (\omega_0/\alpha)^{1/2})] - \\
& \frac{1}{2\alpha\kappa_2^{(-)} - s_B}\delta(q_1 - \kappa_2^{(-)})[1 - \Theta(|q| - (\omega_0/\alpha)^{1/2})] \, .
\end{aligned} \tag{D.34}$$

D.3 Modos acústicos

Neste caso, a relação de dispersão para o sistema é $\omega_q = s_A q$, e para o reservatório é $\Omega_q = s_B q$. Levando em conta essas relações, podemos escrever as Eqs. (D.2) como:

$$\delta(f_1(q_1)) = \delta(s_B|q_1| + s_B|q - q_1| - s_A|q|);, \tag{D.35a}$$

$$\delta(f_2(q_1)) = \delta(s_B|q_1| - s_B|q + q_1| + s_A|q|) \, , \tag{D.35b}$$

$$\delta(f_3(q_1)) = \delta(s_B|q - q_1| + s_A|q_1| - s_A|q|) \, , \tag{D.35c}$$

$$\delta(f_4(q_1)) = \delta(s_B|q - q_1| - s_A|q_1| + s_A|q|) \, , \tag{D.35d}$$

$$\delta(f_5(q_1)) = \delta(s_B|q + q_1| - s_A|q_1| - s_A|q|) \, . \tag{D.35e}$$

D.3.1 Análise de f_1.

i) Para $q < 0$, a expressão para f_1 é:

$$f_1 = \begin{cases} 2s_B q_1 + (s_A - s_B)q\,, & \text{se } q_1 \geq 0\,, \\ -2s_B q_1 + (s_A + s_B)q\,, & \text{se } q_1 \leq q\,, \\ (s_A - s_B)q\,, & \text{se } q < q_1 < 0\,. \end{cases} \tag{D.36}$$

Neste caso, a função f_1 possui duas raízes:

$$q_1 = \begin{cases} \varsigma^{(+)}q, & \text{se } q_1 \geq 0\,, \\ \varsigma^{(-)}q, & \text{se } q_1 \leq q\,, \end{cases} \tag{D.37}$$

com $\varsigma^{(+)}$ dado por:

$$\varsigma^{(\pm)} = \frac{1}{2}\left(1 \pm \frac{s_A}{s_B}\right)\,. \tag{D.38}$$

Podemos então escrever, usando a Eq. (D.1), que:

$$\delta(f_1(q_1)) = \frac{1}{2s_B}\left[\delta(q_1 - \varsigma^{(+)}q) + \delta(q_1 - \varsigma^{(-)}q)\right]\Theta(s_A - s_B)\,. \tag{D.39}$$

ii) Para $q \geq 0$, a expressão para f_1 é:

$$f_1 = \begin{cases} 2s_B q_1 - (s_A + s_B)q \,, & \text{se } \; q_1 > q \,, \\ -2s_B q_1 - (s_A - s_B)q \,, & \text{se } \; q_1 < 0 \,, \\ -(s_A - s_B)q, & \text{se } \; 0 \leq q_1 \leq q \,. \end{cases} \tag{D.40}$$

Neste caso, a função f_1 possui duas raízes:

$$q_1 = \begin{cases} \varsigma^{(+)} q, & \text{se } \; q_1 > q \,, \\ \varsigma^{(-)} q, & \text{se } \; q_1 < 0 \,. \end{cases} \tag{D.41}$$

Podemos então escrever, usando a Eq. (D.1), que:

$$\delta(\, f_1(q_1)) = \frac{1}{2s_B}[\delta(q_1 - \varsigma^{(+)} q) + \delta(q_1 - \varsigma^{(-)} q)]\Theta(s_A - s_B) \,, \tag{D.42}$$

expressão idêntica à Eq. (D.39), o que indica que ela é válida para qualquer valor de q.

D.3.2 Análise de f_2.

i) Para $q < 0$, a expressão para f_2 é:

$$f_2 = \begin{cases} (s_A + s_B)q \,, & \text{se } \; q_1 \geq -q, \\ -2s_B q_1 + (s_A - s_B)q \,, & \text{se } \; 0 \leq q_1 < -q \,, \\ (s_A - s_B)q \,, & \text{se } \; q_1 < 0 \,. \end{cases} \tag{D.43}$$

Neste caso, a função f_2 possui uma raiz:

$$q_1 = -\varsigma^{(-)}q, \qquad \text{se } 0 \leq q_1 < -q \, . \tag{D.44}$$

Podemos então escrever, usando a Eq. (D.1), que:

$$\delta(f_2(q_1)) = \frac{1}{2s_B}[\delta(q_1 + \varsigma^{(-)}q)]\Theta(s_A - s_B) \, . \tag{D.45}$$

ii) Para $q \geq 0$, a expressão para f_2 é:

$$f_1 = \begin{cases} 2s_B q_1 - (s_A - s_B)q \, , & \text{se } -q \leq q_1 < 0 \, , \\ -(s_A - s_B)q \, , & \text{se } q_1 \geq 0 \, , \\ -(s_A + s_B)q \, , & \text{se } q_1 < -q \, . \end{cases} \tag{D.46}$$

Neste caso, a função f_2 possui uma raiz:

$$q_1 = -\varsigma^{(-)}q \, , \qquad \text{se } -q \leq q_1 < 0 \, . \tag{D.47}$$

Podemos então escrever, usando a Eq. (D.1), que:

$$\delta(f_2(q_1)) = \frac{1}{2s_B}[\delta(q_1 + \varsigma^{(-)}q)]\Theta(s_A - s_B) \, , \tag{D.48}$$

expressão idêntica à Eq. (D.45), o que indica que ela é válida para qualquer valor de q.

D.3.3 Análise de f_3.

i) Para $q < 0$, a expressão para f_3 é:

$$f_3 = \begin{cases} (s_A + s_B)q_1 + (s_A - s_B)q\,, & \text{se } \; q_1 \geq 0\,, \\ -(s_A + s_B)(q_1 - q)\,, & \text{se } \; q_1 < q\,, \\ -(s_A - s_B)(q_1 - q)\,, & \text{se } \; q \leq q_1 < 0\,. \end{cases} \tag{D.49}$$

Neste caso, a função f_3 possui duas raízes:

$$q_1 = \begin{cases} -\varkappa\, q, & \text{se } \; q_1 \geq 0\,. \\ q, & \text{se } \; q_1 < 0\,, \end{cases} \tag{D.50}$$

onde

$$\varkappa = \frac{s_A - s_B}{s_A + s_B}\,. \tag{D.51}$$

Levando em conta que a derivada de f_3 não existe em $q_1 = q$, podemos então escrever, usando a Eq. (D.1), que:

$$\delta(\,f_3(q_1)) = \frac{1}{s_A + s_B}\left[\delta(q_1 + \varkappa\, q)\right]\Theta(s_A - s_B)\,. \tag{D.52}$$

ii) Para $q \geq 0$, a expressão para f_3 é:

$$f_3 = \begin{cases} (s_A - s_B)(q_1 - q)\ , & \text{se}\ \ 0 \leq q_1 < q\ , \\[2ex] (s_A + s_B)(q_1 - q)\ , & \text{se}\ \ q_1 \geq q\ , \\[2ex] -(s_A + s_B)q_1 - (s_A - s_B)q\ , & \text{se}\ \ q_1 < 0\ . \end{cases} \tag{D.53}$$

Neste caso, a função f_3 possui duas raízes:

$$q_1 = \begin{cases} q\ , & \text{se}\ \ 0 \leq q_1 \leq q\ , \\[2ex] -\varkappa\, q\ , & \text{se}\ \ q_1 < 0\ . \end{cases} \tag{D.54}$$

Levando em conta que a derivada de f_3 não existe em $q_1 = q$, podemos então escrever, usando a Eq. (D.1), que:

$$\delta(\,f_3(q_1)) = \frac{1}{s_A + s_B}\left[\delta(q_1 + \varkappa\, q)\right]\Theta(s_A - s_B)\ , \tag{D.55}$$

expressão idêntica à Eq. (D.51), o que indica que ela é válida para qualquer valor de q.

D.3.4 Análise de f_4.

i) Para $q < 0$, a expressão para f_4 é:

$$f_4 = \begin{cases} -(s_A - s_B)q_1 - (s_A + s_B)q\,, & \text{se } q_1 \geq 0\,, \\ (s_A - s_B)(q_1 - q)\,, & \text{se } q_1 \leq q\,, \\ (s_A + s_B)(q_1 - q)\,, & \text{se } q < q_1 < 0\,. \end{cases} \tag{D.56}$$

Neste caso, a função f_4 possui duas raízes:

$$q_1 = \begin{cases} -\sigma q\,, & \text{se } q_1 \geq 0\,, \\ q\,, & \text{se } q_1 < 0\,, \end{cases} \tag{D.57}$$

com $\sigma = \varkappa^{-1}$.

Levando em conta que a derivada de f_4 não existe em $q_1 = q$, podemos então escrever, usando a Eq. (D.1), que:

$$\delta(f_4(q_1) = \frac{1}{s_A - s_B}[\delta(q_1 + \sigma q)]\Theta(s_A - s_B). \tag{D.58}$$

ii) Para $q \geq 0$, a expressão para f_4 é:

$$f_4 = \begin{cases} -(s_A + s_B)(q_1 - q)\,, & \text{se } 0 \leq q_1 \leq q\,, \\ -(s_A - s_B)(q_1 - q)\,, & \text{se } q_1 > q\,, \\ (s_A - s_B)q_1 + (s_A + s_B)q\,, & \text{se } q_1 < 0\,. \end{cases} \tag{D.59}$$

Neste caso, a função f_4 possui duas raízes:

$$q_1 = \begin{cases} -\sigma q\,, & \text{se } q_1 < 0\,, \\ \\ q\,, & \text{se } q_1 \geq 0\,. \end{cases} \tag{D.60}$$

Levando em conta que a derivada de f_4 não existe em $q_1 = q$, podemos então escrever, usando a Eq. (D.1), que:

$$\delta(\,f_4(q_1)) = \frac{1}{s_A - s_B}[\delta(q_1 + \sigma q)]\Theta(s_A - s_B)\,, \tag{D.61}$$

expressão idêntica à Eq. (D.58), o que indica que ela expressão acima é válida para qualquer valor de q.

D.3.5 Análise de f_5.

i) Para $q < 0$, a expressão para f_5 é:

$$f_5 = \begin{cases} -(s_A - s_B)q_1 + (s_A + s_B)q\,, & \text{se } q_1 \geq -q\,, \\ \\ -(s_A + s_B)q_1 + (s_A - s_B)q\,, & \text{se } 0 \leq q_1 < -q\,, \\ \\ (s_A - s_B)(q_1 + q)\,, & \text{se } q_1 < 0\,. \end{cases} \tag{D.62}$$

Neste caso, a função f_5 possui duas raízes:

$$q_1 = \begin{cases} \sigma q\,, & \text{se } q_1 \geq -q\,, \\ \\ \varkappa q\,, & \text{se } 0 \leq q_1 < -q\,. \end{cases} \tag{D.63}$$

Podemos então escrever, usando a Eq. (D.1), que:

$$\delta(f_5(q_1)) = \left\{\frac{1}{s_A + s_B}[\delta(q_1 - \varkappa q)] + \frac{1}{s_A - s_B}[\delta(q_1 - \sigma q)]\right\}\Theta(s_B - s_A) \ . \tag{D.64}$$

ii) Para $q \geq 0$, a expressão para f_5 é:

$$f_5 = \begin{cases} -(s_A - s_B)(q_1 + q) \ , & \text{se} \ \ q_1 \geq 0 \ , \\ (s_A + s_B)q_1 - (s_A - s_B)q \ , & \text{se} \ \ -q \leq q_1 < 0 \ , \\ (s_A - s_B)q_1 - (s_A + s_B)q \ , & \text{se} \ \ q_1 < -q \ . \end{cases} \tag{D.65}$$

Neste caso, a função f_5 possui duas raízes:

$$q_1 = \begin{cases} \varkappa q \ , & \text{se} \ \ -q \leq q_1 < 0 \ , \\ \sigma q \ , & \text{se} \ \ q_1 < -q \ . \end{cases} \tag{D.66}$$

Podemos então escrever, usando a Eq. (D.1), que:

$$\delta(f_5(q_1)) = \left\{\frac{1}{s_A + s_B}[\delta(q_1 - \varkappa q)] + \frac{1}{s_A - s_B}[\delta(q_1 - \sigma q)]\right\}\Theta(s_B - s_A) \ . \tag{D.67}$$

expressão idêntica à Eq. (D.64), o que indica que ela é válida para qualquer valor de q.

Apêndice E

Pacote para o cálculo de comutadores, valores médios de operadores e integrais

E.1 Introdução

O sistema de computação simbólico *Mathematica* [Wolfram 1996] oferece uma linguagem de programação avançada que possibilita implementar elegantemente cálculos algébricos, apresentando ainda a vantagem de encontrar-se facilmente disponível para ambientes UNIX, Windows e DOS, entre outros. Por essa razão, escolhemos essa linguagem para construir um pacote (*package*) para o cálculo de várias quantidades ao longo desta tese, cujo código reproduzimos abaixo, com comentários pertinentes sempre que possível.

E.2 O código

Declarações iniciais do pacote:

```
BeginPackage["Comutadores‘Operadores‘"]

(*: Início do pacote *)
(*: Arquivo: Operadores.M *)
(*: Nome: Comutadores‘Operadores‘ *)
(*: Contexto: Comutadores‘Operadores‘ *)
```

Inicialmente, definimos propriedades gerais de comutadores, usando como operador de multiplicação não-comutativa a função Dot:

```
Unprotect[Power,Dot,Times,NumberQ]
SetAttributes[delta,Orderless]
Dot[x_?NumberQ,y_]:=x y
Dot[x_?NumberQ y_?NumberQ, z]=x y z
Dot[z_, x_?NumberQ y_?NumberQ]=x y z
Dot[x_,y_?NumberQ]:= y x
Dot[x_, n_?NumberQ y_]:=n x.y
Dot[x_ n_?NumberQ, y_]:=n x.y
Dot[x_,-y_]:= -x . y
Dot[-x_, y_]:= -x . y
Dot[x_,y_+z_]:=x.y+x.z
Dot[(x_+y_).z_]:=x.z+y.z
Dot[x_+y_,z_,w_]:=x.z.w+y.z.w
Dot[x1_ . x2_ + y1_ . y2_,z_]:=x1.x2.z+y1.y2.z
Dot[n_?NumberQ x1_ . x2_ + y1_ y2_,z_]:=n x1.x2.z+y1.y2.z
Dot[ x1_ . x2_ + n_?NumberQ y1_ . y2_,z_]:= x1.x2.z+n y1.y2.z
Dot[ n_?NumberQ * (x1_ . x2_ + y1_ . y2_),z_]:= x1.x2.z+n y1.y2.z
Dot[Exp[x_],Exp[y_]]:=Exp[x+y];
Dot[x_,y_ Exp[z_]]:=Dot[x,y] Exp[z];
Dot[x_ Exp[y_],z_]:=Dot[x,z] Exp[y];
Dot[x_,y_ / Exp[z_]]:=Dot[x,y]/Exp[z];
Dot[x_ / Exp[y_],z_]:=Dot[x,z]/Exp[y];
Dot[x_ Exp[x1_],y_ Exp[z_]]:=Dot[x,y] Exp[x1+z];
Dot[x_ / Exp[x1_],y_ / Exp[z_]]:=Dot[x,y]/Exp[x1+z];
Dot[x_ / Exp[x1_],y_ Exp[z_]]:=Dot[x,y] Exp[-x1+z];
Dot[x_ Exp[x1_],y_ / Exp[z_]]:=Dot[x,y] Exp[x1-z];
```

A seguir, implementamos a álgebra dos comutadores:

```
com[x_,y_]:=x.y-y.x
com[(x_em|x_emc) y_,(w_em|w_emc) z_]:=x w com[y,z]
com[(x_em[t_]|x_emc[t_]) y_, (w_em[t]|w_emc[t_]) z_]:=x w com[y,z]
com[(x_em[t_]|x_emc[t_]) y_, (w_em|w_emc) z_]:=x[t] w com[y,z]
com[(x_em|x_emc) y_, (w_em[t]|w_emc[t_]) z_]:= w[t] x com[y,z]
com[x__?NumberQ . y_,z_]:=x com[y,z]
com[x_, y_ + z_]:=com[x,y]+com[x,z]
com[a_,f_[a_]]:=0
com[x_?NumberQ,y_]:=0
com[a_ . b_,c_]:= a . com[b,c]+ com[a,c] . b
com[a_ ,b_ . c_]:=com[a,b] . c + b . com[a,c]
com[n_?NumberQ a_ . b_,c_]:= n a . com[b,c]+ n com[a,c] . b
com[a_ ,n_?NumberQ b_ . c_]:=n com[a,b] . c + n b . com[a,c]
```

Propriedades dos operadores bosons e fermions:

```
Dot[z_?NumberQ*(x_ba|x_fa), y_ba|y_fa]:=z Dot[x,y]
Dot[z_?NumberQ*(x_bc|x_fc), y_bc|y_fc]:=z Dot[x,y]
Dot[z_?NumberQ, x_ba|x_fa, y_ba|y_fa]:=z Dot[x,y]
Dot[z_?NumberQ, x_bc|x_fc, y_bc|y_fc]:=z Dot[x,y]
Dot[x_ba|x_fa, z_?NumberQ, y_ba|y_fa]:=z Dot[x,y]
Dot[x_bc|x_fc, z_?NumberQ, y_bc|y_fc]:=z Dot[x,y]
Dot[x_ba|x_fa, y_ba|y_fa, z_?NumberQ]:=z Dot[x,y]
Dot[x_bc|x_fc, y_bc|y_fc, z_?NumberQ]:=z Dot[x,y]
```

Álgebra de bosons com propriedades várias:

```
com[ba[a_[q1_]],bc[a_[q2_]]]:=delta[q1,q2]
com[bc[a_[q1_]],ba[a_[q2_]]]:=-delta[q1,q2]
com[a_ba,b_ba]:=0
com[a_bc,b_bc]:=0
com[a_ba,b_bc]:=0
com[(x_ba|x_bc),(y_fa|y_fc)]:=0
```

Funções para ordenamento canônico de produtos de operadores tipo boson:

```
OrdBos[x_+y_]:=OrdBos[x]+OrdBos[y]
OrdBos[n_?NumberQ x_]:=n OrdBos[x]
OrdBos[Boson_]:=FixedPoint[ (Expand[#] /. (ba[a_[x_]] . bc[a_[y_]]->delta[x,y]
                + bc[a[x]] . ba[a[y]]))& ,Boson]
```

A seguir, definimos funções delta de Kronecker, e algumas propriedades necessárias de objetos a serem usadas:

```
delta[q_,q_]:=1
delta[q1_+q2_,q1_]:=delta[q2,0]
delta[q1_+q2_,0]:=delta[q1,-q2]
delta[-x_,-y_]:=delta[x,y]
delta[x_+y_,z_+y_]:=delta[x,z]
DiracDelta[-xx_]:=DiracDelta[xx]
DiracDelta[-(xx_+yy_)]:=DiracDelta[xx+yy]
DiracDelta[-(xx_+yy_-zz_)]:=DiracDelta[xx+yy-zz]
PV[1/(-xx_+yy_-zz_)]:=-PV[1/(xx-yy+zz)]
NumberQ[delta[q1_,q2_]]^:=True
delta[i_,j_]^n_?IntegerQ:=delta[i,j]
NumberQ[x_ y_]:=NumberQ[x]&&NumberQ[y]
NumberQ[x_ . y_]:=NumberQ[x]&&NumberQ[y]
NumberQ[em[x_]]^:=True;
```

```
NumberQ[emc[x_]]^:=True;
NumberQ[em[x_][t]]^:=True;
NumberQ[emc[x_][t]]^:=True;
```

A seguir, definimos algumas funções e suas propriedades, que serão utilizadas no cálculo dos comutadores:

```
soma[ind_,x_+y_]:=soma[ind,x]+soma[ind,y]
soma[ind_,(x_+y_) z_]:=soma[ind,x z]+soma[ind,y z]
soma[ind,x_ y_]:=  soma[ind,x soma[ind,y]]
soma[ind_,x_ . (y_ + z_)]:=soma[ind,x . y ]+soma[ind, x . z]
soma[ind_, (x_ + y_) . z_]:=soma[ind,x . z ]+soma[ind, y . z]
soma[ind_,x_ . y_]:=  soma[ind,x . soma[ind,y]]
soma[ind_, expr_]:=Module[{Delta, i1, indices, n, regra, exptem},
  n=Count[expr,x_delta,Infinity];
  exptem=Expand[expr];
  Which[n==0, exptem,
        n==1, (Delta=exptem[[Sequence @@ Flatten[Position[expr,x_delta]]]];
               i1=Table[Delta[[i]],{i,2}];
               regra=Flatten[Solve[i1[[1]]==i1[[2]],ind]];
               exptem /. regra),
        n==2, indices=Flatten[Position[exptem,x_delta,Infinity]];
              Deltas=Table[exptem[[indices[[i]]]],{i,Length[indices]}];
              eqs=Table[Deltas[[i,1]]==Deltas[[i,2]],{i,Length[Deltas]}];
              regras=Flatten[Solve[eqs,{q2,ind}]];
              exptem /. regras]]
coms[x_,y_]:=Module[{result},
          result=Expand[com[x,y]];
          result=soma[q2,soma[q1,result]];
          Ordena[IndMudo[result]]]
Ordena[(x_) + (y_)] := Ordena[x] + Ordena[y]
Ordena[expr_] := Module[{CoefNum, Operadores, Banho, Sistema},
   CoefNum := Apply[Times, Cases[expr, (y_)?NumberQ]];
    Operadores := DeleteCases[expr, (y_)?NumberQ];
    Banho := DeleteCases[Operadores, ba[a[x_]]|bc[a[x_]]|ba[f[x_]]
            |bc[f[x_]], Infinity];
    Sistema := DeleteCases[Operadores, ba[b[x_]]|bc[b[x_]], Infinity];
    CoefNum*(Sistema . Banho)]
Ordbf[x_+y_]:=Ordbf[x]+Ordbf[y]
Ordbf[expr_] := Module[{CoefNum, Operadores, Bosons, Fermions},
    CoefNum := Apply[Times, Cases[expr, (y_)?NumberQ]];
    Operadores := DeleteCases[expr, (y_)?NumberQ];
    Bosons := DeleteCases[Operadores, fa[c_[x_]]|fc[c_[x_]], Infinity];
    Fermions := DeleteCases[Operadores, ba[a_[x_]]|bc[a_[x_]], Infinity];
    Expand[CoefNum*(OrdFer[Fermions] . OrdBos[Bosons])] ]
Com[x_,y_]:=Ordbf[Expand[com[x,y]]]
ComSim[x_,y_]:=Ordena[Plus@@ ((Table[soma[q2,soma[q1,
                Expand[com[x[[i]],y]]]],{i,Length[x]}]) /. {q2->q1})]
Comutador[x_,y_]:=  Module[{aux},
```

```
    aux=Table[soma[q1,soma[q2,soma[q3,Expand[com[x[[i]],y[[j]]]]]]],
                  {i,Length[x]},{j,Length[y]}];
    aux=Plus @@ Flatten[aux];
    Ordena[aux]]
```

Implementamos agora as regras para o cálculo dos valores médios do banho:

```
NumberQ[vr[x_]]^:=True
vm[x_+y_]:=vm[x]+vm[y]
vm[ba[b[x_]]|bc[b[x_]]]:=0
vm[ba[b[x_]] . ba[b[y_]]]:=0
vm[bc[b[x_]] . bc[b[y_]]]:=0
vm[ba[a[x_]] . ba[a[y_]]]:=0
vm[bc[a[x_]] . bc[a[y_]]]:=0
vm[bc[b[x_]] . ba[b[y_]]]:=vr[x] delta[x,y]
vm[ba[b[x_]] . bc[b[y_]]]:=(1+vr[x]) delta[x,y]
vm[(x_bc|x_ba) . (y_bc|y_ba) . (z_bc|z_ba)]
                 :=vm[x.y]*vm[z]+vm[x.z]*vm[y]+vm[y.z]*vm[x]
vm[(x_bc|x_ba) . (y_bc|y_ba) . (z_bc|z_ba) . (w_bc|w_ba)]
                 :=vm[x.y]*vm[z.w]+vm[x.z]*vm[y.w]+vm[x.w]*vm[y.z]
vm[ba[a[x_]]]:=0
vm[bc[a[x_]]]:=0
vm[bc[a[x_]] . ba[a[y_]]]:=v[x] delta[x,y]
vm[ba[a[x_]] . bc[a[y_]]]:= Expand[(1+v[x]) delta[x,y]]
vm[E^(y_)*(x_)] := Exp[y]*vm[x]
vm[emc[v_]*em[x_]*(y_)] := em[x]*emc[v]*vm[y]
vm[em[x_] y_]:=em[x] vm[y]
vm[emc[x_] y_]:=emc[x] vm[y]
```

Implementamos agora as regras para o cálculo dos valores médios do sistema:

```
NumberQ[AA[q_]]^:=True;
NumberQ[AAc[q_]]^:=True;
bc[aa[q_]]:=bc[ã[q]]-AAc[q]
ba[aa[q_]]:=ba[ã[q]]-AA[q]
ba[aa[q1_]].bc[aa[q2_]]:=bc[aa[q2]].ba[aa[q1]]+delta[q1,q2]
ba[ã[q1_]].bc[ã[q2_]]:=bc[ã[q2]].ba[ã[q1]]+delta[q1,q2]
Tr[r] = 1
Tr[r x_ . y_ . z_ . w_]:=
              Tr[r x.y]*Tr[r z.w]+Tr[r x.z]*Tr[r y.w]+Tr[r x.w]*Tr[r y.z]
Tr[r x_ . y_ . z_]:=Tr[r x.y]*Tr[r z]+Tr[r x.z]*Tr[r y]+Tr[r y.z]*Tr[r x]
Tr[r*ba[aa[q_]]] = -AA[q]
Tr[r*((x_) + (y_))] := Tr[x*r] + Tr[y*r]
Tr[r*ba[ã[q_]]] = 0
Tr[x_ y_?NumberQ]:=y Tr[x]
Tr[(x_) + (y_)] := Tr[x] + Tr[y]
Tr[r bc[aa[q1_]].ba[aa[q2_]]] :=
   Expand[v[q1]*delta[q1, q2] + AAc[q1] AA[q2] (1-delta[q1, q2])]
Tr[bc[ã[q_]] r]:=0
```

```
Tr[bc[ă[q1_]].ba[ā[q2_]] r]:=(v[q1]-AAc[q1] AA[q2]) delta[q1,q2]
Tr[bc[ă[q1_]].bc[ā[q2_]] r]:=0
Tr[r ba[ă[q1_]].ba[ā[q2_]]]:=0
vms[xx_]:=Module[{aux1,aux2,aux3},
                 aux1=Expand[xx/.{a[q_]->aa[q]}];
                 aux2=Expand[Tr[Expand[r aux1]]];
         aux3=aux2/.Tr[x_]->0;
         Expand[aux3/.{AA[q_]->-A[q],AAc[q_]->-At[q]}]]
spur[0]=0
spur[bc[a[q]]]=At[q]
spur[ba[a[q]]]=A[q]
spur[x_+y_]:=spur[x]+spur[y]
spur[expr_] := Module[{CoefNum, Operadores, Banho, Sistema, nb, ns},
   CoefNum := Apply[Times, Cases[expr, (y_)?NumberQ]];
    Operadores := DeleteCases[expr, (y_)?NumberQ];
    nb = Count[Operadores, ba[b[x_]]|bc[b[x_]], Infinity];
    If[nb==0,
      Banho = 1,
      Banho = vm[DeleteCases[Operadores, ba[a[x_]]|bc[a[x_]], Infinity]]];
    ns = Count[Operadores, ba[a[x_]]|bc[a[x_]], Infinity];
    If[ns==0,
       Sistema=1,
       Sistema := vms[DeleteCases[Operadores, ba[b[x_]] |
                      bc[b[x_]], Infinity]]];
    Expand[CoefNum*Sistema*Banho]]
IndMudo[x_+y_]:=IndMudo[x]+IndMudo[y]
IndMudo[n_?IntegerQ x_]:=n IndMudo[x]
IndMudo[x_]:=Module[{n1,n2,n3},
n1=Length[Position[x,q1,Infinity]];
n2=Length[Position[x,q2,Infinity]];
n3=Length[Position[x,q3,Infinity]];
If[n1>=1,
        If[n2>=1,x, If[n3>=1,x/.{q3->q2},x]],
        If[n2>=1,If[n3>=1,x/.{q2->q1,q3->q2},x/.{q2->q1}],x/.{q3->q1}]]]
```

Agora, definimos funções para realizar o cálculo de integrais com partes reais e valores principais e também funcões que simplifiquem ao máximo os resultados obtidos do cálculo das integrais:

```
Integral[termo_]:=Module[{Integre, coef},
     coef=DeleteCases[termo,x_Power,1];
     Integre[Exp[i t x_]]:= Pi DiracDelta[x]-i PV[1/x];
     Integre[Exp[-i t x_]]:= Pi DiracDelta[x] + i PV[1/x];
     Expand[coef Integre[Cases[termo,x_Power,1][[1]]]]];
Integral1[termo_]:=Module[{Integre, coef},
     coef=DeleteCases[termo,x_Power,1];
     Integre[Exp[i t x_]]:= Pi DiracDelta[x];
     Integre[Exp[-i t x_]]:= Pi DiracDelta[x];
```

```
     Expand[coef Integre[Cases[termo,x_Power,1][[1]]]];
Integral2[termo_]:=Module[{Integre, coef},
     coef=DeleteCases[termo,x_Power,1];
     Integre[Exp[i t x_]]:= -i PV[1/x];
     Integre[Exp[-i t x_]]:=  i PV[1/x];
     Expand[coef Integre[Cases[termo,x_Power,1][[1]]]];
Simplifique[expr_]:=Module[{i,j,ind,t,k,fin},
   ind=Union[Cases[expr,DiracDelta[x_],Infinity]];
   t=Table[Position[expr,ind[[i]],Infinity],{i,Length[ind]}];
   k=Table[t[[j]][[i,1]],{j,Length[t]},{i,Length[t[[j]]]}];
   fin=Table[expr[[k[[i]]]],{i,Length[k]}];
   Plus @@ Table[Simplify[ fin[[i]] ],{i,Length[fin]}] ]
SimpPV[expr_]:=Module[{i,j,ind,t,k,fin},
   ind=Union[Cases[expr,PV[x_],Infinity]];
   t=Table[Position[expr,ind[[i]],Infinity],{i,Length[ind]}];
   k=Table[t[[j]][[i,1]],{j,Length[t]},{i,Length[t[[j]]]}];
   fin=Table[expr[[k[[i]]]],{i,Length[k]}];
   Plus @@ Table[Simplify[ fin[[i]] ],{i,Length[fin]}] ]
```

Definimos agora os dezesseis termos da hamiltoniano que utilizamos:

```
H[1] = em[V[1][q1,q2]] ba[a[q1]] . ba[b[q2]] . bc[b[q1 + q2]]
H[2] = em[V[2][q1,q2]] ba[a[q1]] . ba[b[q2]] . ba[b[-q1-q2]]
H[3] = em[V[3][q1,q2]] bc[a[q1+q2]] . ba[b[q1]] . ba[b[q2]]
H[4] = em[V[4][q1,q2]] ba[a[q1]] . bc[b[q2]] . ba[b[q2-q1]]
H[5] = emc[V[1][q1,q2]] ba[b[q1 + q2]] . bc[b[q2]] . bc[a[q1]]
H[6] = emc[V[2][q1,q2]] bc[b[-q1-q2]] . bc[b[q2]] . bc[a[q1]]
H[7] = emc[V[3][q1,q2]] bc[b[q2]] . bc[b[q1]] . ba[a[q1+q2]]
H[8] = emc[V[4][q1,q2]] bc[a[q1]] . bc[b[q2-q1]] . ba[b[q2]]
H[9] = em[W[1][q1,q2]] ba[a[q1]] . ba[a[q2]] . bc[b[q1 + q2]]
H[10] = em[W[2][q1,q2]] bc[a[q1]] . ba[a[q2]] . ba[b[q1-q2]]
H[11] = em[W[3][q1,q2]] ba[a[q1]] . ba[a[q2]] . ba[b[-q1-q2]]
H[12] = em[W[4][q1,q2]] ba[a[q1]] . bc[a[q2]] . bc[b[q1-q2]]
H[13] = emc[W[1][q1,q2]] ba[b[q1+q2]] . bc[a[q2]]. bc[a[q1]]
H[14] = emc[W[2][q1,q2]] bc[b[q1-q2]] . bc[a[q2]] . ba[a[q1]]
H[15] = emc[W[3][q1,q2]] bc[b[-q1-q2]] . bc[a[q2]] . bc[a[q1]]
H[16] = emc[W[4][q1,q2]] ba[a[q2]] . bc[a[q1]] . ba[b[q1-q2]]
```

A dependência temporal dos vários coeficentes que aparecem nos comutadores:

```
tempo = {em[x_]->em[x][t], emc[y_]->emc[y][t]}
tempos = { em[V[1][q,q]][t]->em[V[1][q,q]] Exp[-i(w[q]+Omega[q])t],
emc[V[1][q,q]][t]->emc[V[1][q,q]] Exp[i(w[q]+Omega[q])t],
em[V[1][q1_,q2_]][t]->em[V[1][q1,q2]] *
             Exp[-i(w[q1]+Omega[q2]-Omega[q1+q2])t],
em[V[2][q1_,q2_]][t]->em[V[2][q1,q2]] *
             Exp[-i(w[q1]+Omega[q2]+Omega[-q1-q2])t],
em[V[3][q1_,q2_]][t]->em[V[3][q1,q2]] *
             Exp[i(w[q1+q2]-Omega[q1]-Omega[q2])t],
```

```
em[V[4][q1_,q2_]][t]->em[V[4][q1,q2]] *
            Exp[-i(w[q1]-Omega[q2]+Omega[q2-q1])t],
emc[V[1][q1_,q2_]][t]->emc[V[1][q1,q2]] *
            Exp[i(w[q1]+Omega[q2]-Omega[q1+q2])t],
emc[V[2][q1_,q2_]][t]->emc[V[2][q1,q2]] *
            Exp[i(w[q1]+Omega[q2]+Omega[-q1-q2])t],
emc[V[3][q1_,q2_]][t]->emc[V[3][q1,q2]] *
            Exp[-i(w[q1+q2]-Omega[q1]-Omega[q2])t],
emc[V[4][q1_,q2_]][t]->emc[V[4][q1,q2]] *
            Exp[i(w[q1]-Omega[q2]+Omega[q2-q1])t],
em[W[1][q1_,q2_]][t]->em[W[1][q1,q2]] Exp[-i(w[q1]+w[q2]-Omega[q1+q2])t],
em[W[2][q1_,q2_]][t]->em[W[2][q1,q2]] Exp[-i(-w[q1]+w[q2]+Omega[q1-q2])t],
em[W[3][q1_,q2_]][t]->em[W[3][q1,q2]] Exp[-i(w[q1]+w[q2]+Omega[-q1-q2])t],
em[W[4][q1_,q2_]][t]->em[W[4][q1,q2]] Exp[-i(w[q1]-w[q2]-Omega[q1-q2])t],
emc[W[1][q1_,q2_]][t]->emc[W[1][q1,q2]] Exp[i(w[q1]+w[q2]-Omega[q1+q2])t],
emc[W[2][q1_,q2_]][t]->emc[W[2][q1,q2]] Exp[i(-w[q1]+w[q2]+Omega[q1-q2])t],
emc[W[3][q1_,q2_]][t]->emc[W[3][q1,q2]] Exp[i(w[q1]+w[q2]+Omega[-q1-q2])t],
emc[W[4][q1_,q2_]][t]->emc[W[4][q1,q2]] Exp[i(w[q1]-w[q2]-Omega[q1-q2])t]}
```

Agora, definimos mais algumas funções e realizamos alguns cálculos considerando os elementos de matrizes constantes e levando em conta algumas propriedades das deltas de Dirac:

```
hc[x_+y_]:=hc[x]+hc[y]
hc[x_ Dot[y_, z_]]:=(hc[x]Reverse[Dot[y.z]])/.
                                {bc[x1_]->ba[x1],ba[y1_]->bc[y1]}
hc[em[x_]]:=emc[x]
hc[emc[x_]]:=em[x]
hc[x_ y_]:=hc[x] hc[y]
cc=DeleteCases[#,(x_em|x_emc),Infinity]&;
HSR = Plus @@ Array[H,16]
HSRT = Plus @@ Array[HT,16]
equa[x_,y_]:=IndMudo[soma[q1,soma[q2,spur[Comutador[x,y]]]]]
mal={bc[a[q1_]]->bc[a[q1]]Exp[i w[q1] t],
     ba[a[q2_]]->ba[a[q2]]Exp[-i w[q2] t],
     bc[b[q3_]]->bc[b[q3]]Exp[i Omega[q3] t],
     ba[b[q4_]]->ba[b[q4]]Exp[-i Omega[q4] t],
     emc[X_[i_][q1_,q2_]][t_]->emc[X[i][q1,q2]],
     em[Z_[j_][q3_,q4_]][t_]->em[Z[j][q3,q4]] }
zeit[x_]:=Module[{aux},
            aux=x/.mal;
            Simplify[aux]];
freq={w[q_]->w0-Ó q^2, Omega[q_]->s Abs[q]};
coef = { emc[W[4][q1_, q2_]]->W4c, em[W[4][q1_, q2_]]->W4,
   emc[W[3][q1_, q2_]]->W3c, em[W[3][q1_, q2_]]->W3,
   emc[W[2][q1_, q2_]]->W2c, em[W[2][q1_, q2_]]->W2,
```

```
    em[W[1][q1_, q2_]]->W1, emc[W[1][q1_, q2_]]->W1c,
    emc[V[1][q1_, q2_]]->V1c, em[V[1][q1_, q2_]]->V1,
    emc[V[2][q1_, q2_]]->V2c, em[V[2][q1_, q2_]]->V2,
    emc[V[3][q1_, q2_]]->V3c, em[V[3][q1_, q2_]]->V3,
    emc[V[4][q1_, q2_]]->V4c, em[V[4][q1_, q2_]]->V4 }
hf1=em[V[1][q1,q1]] ba[b[q1]].bc[a[q1]];
hf1=hf1+hc[hf1];
hf2=em[V[2][q1,q2]] bc[a[q1]].bc[a[q2]].ba[b[q1+q2]];
hf2=hf2+hc[hf2];
hp = (h*w[q1])/2 + h*bc[a[q1]] . ba[a[q1]]*w[q1]
ha= (h*Omega[q1])/2 + h*Omega[q1]*bc[b[q1]] . ba[b[q1]]
NumberQ[w[x_]]^:=True
NumberQ[Omega[x_]]^:=True
NumberQ[h]^:=True;
x1=ba[a[q1]]+bc[a[-q1]]
x2=ba[a[q2]]+bc[a[-q2]]
X1=ba[b[q1]]+bc[b[-q1]]
X2=ba[b[q2]]+bc[b[-q2]]
X3=ba[b[q3]]+bc[b[-q3]]
cf1={V1c->V1,V2c->V1,V3c->V1,V2->V1,V3->V1,V4->V1,V4c->V1,
W1c->W1,W2c->W1,W3c->W1,W3->W1,W2->W1,W4->W1,W4c->W1};
delta[q,0]=0
delta[0,q]=0
PV[1/Omega[0]]=0;
dp1={DiracDelta[Omega[0]]->0,
  DiracDelta[Omega[q-q1]+Omega[q1]+w[-q]]->0,
  DiracDelta[Omega[-q-q1]+Omega[q1]+w[q]]-> 0,
  DiracDelta[Omega[q-q1]+w[-q]+w[q1]]->0,
  DiracDelta[Omega[-q-q1]+w[q]+w[q1]]->0,
  DiracDelta[Omega[-q1-q2]+w[q1]+w[q2]]->0}
dp2={DiracDelta[Omega[0]]->0,
  DiracDelta[Omega[q-q1]+Omega[q1]+w[-q]]->0,
  DiracDelta[Omega[-q-q1]+Omega[q1]+w[q]]->0,
  DiracDelta[Omega[q-q1]+w[-q]+w[q1]]->0,
  DiracDelta[Omega[-q-q1]+w[q]+w[q1]]->0,
  DiracDelta[Omega[-q1-q2]+w[q1]+w[q2]]->0};
dp3={DiracDelta[Omega[q-q1]+Omega[q1]+w[-q]]->0,
    DiracDelta[-Omega[0]+Omega[-q]+w[q]]->0,
    DiracDelta[Omega[0]+Omega[-q]+w[q]]->0,
    DiracDelta[Omega[-q-q1]+Omega[q1]+w[q]]->0,
    DiracDelta[Omega[(-q-q1)/2]+Omega[(q-q1)/2]+w[q1]]->0,
    DiracDelta[Omega[(q-q1)/2]+Omega[-q/2-q1/2]+w[q1]]->0}
```

Cuidamos agora da formatação dos resultados obtidos, para que tenham uma apresentação usual. Primeiro, a hamiltoniano, e então, outras funções:

```
Format[(x1_ba|x1_bc).(x2_ba|x2_bc)(y_em|y_emc)]:=SequenceForm[y,x1.x2]
Format[(x1_ba|x1_bc).(x2_ba|x2_bc).(x3_ba|x3_bc)(y_em[t_]|y_emc[t_])]:=
        SequenceForm[y[t],x1.x2.x3]
```

```
Format[(x1_ba|x1_bc).(x2_ba|x2_bc)*(y1_em|y1_emc)(y2_em[t_]|y2_emc[t_])]:=
         SequenceForm[y2[t],y1,x1.x2]
Format[(x1_ba|x1_bc).(x2_ba|x2_bc)*n_?IntegerQ*
               (y1_em|y1_emc)(y2_em[t_]|y2_emc[t_])]:=
         SequenceForm[n y2[t],y1,x1.x2]
Format[(x1_ba|x1_bc).(x2_ba|x2_bc) (y_em|y_emc) (z_delta)]:=
         SequenceForm[y,x1.x2,z]
Format[(x1_ba|x1_bc).(x2_ba|x2_bc) (y_em|y_emc) n_?IntegerQ]:=
         SequenceForm[n y,x1.x2]
Format[(x1_ba|x1_bc).(x2_ba|x2_bc) (y_em|y_emc) n_?IntegerQ z_delta]:=
         SequenceForm[n y x1.x2,z]
Format[((x1_ba|x1_bc).(x2_ba|x2_bc).(x3_ba|x3_bc)) (y_em|y_emc)]:=
         SequenceForm[y,(x1.x2.x3)]
Format[((x1_ba|x1_bc).(x2_ba|x2_bc).(x3_ba|x3_bc))
         (y_em|y_emc)z_?IntegerQ]:=SequenceForm[z y,x1.x2.x3]
Format[((x1_ba|x1_bc).(x2_ba|x2_bc).(x3_ba|x3_bc)) *
        ((y1_em|y1_emc)(y2_em|y2_emc))]:=SequenceForm[y1 y2,x1.x2.x3]
Format[((x1_ba|x1_bc).(x2_ba|x2_bc).(x3_ba|x3_bc)) *
((y1_em[t_]|y1_emc[t_])(y2_em|y2_emc))]:=SequenceForm[y1[t],y2,x1.x2.x3]
Format[((x1_ba|x1_bc).(x2_ba|x2_bc).(x3_ba|x3_bc)) *
        ((y1_em[t_]|y1_emc[t_])(y2_em|y2_emc)) z_?IntegerQ]:=
         SequenceForm[z y1[t],y2,x1.x2.x3]
Format[((x1_ba|x1_bc).(x2_ba|x2_bc).(x3_ba|x3_bc).(x4_ba|x4_bc)) *
        (y1_em|y1_emc)(y2_em|y2_emc)]:=SequenceForm[y1 y2,x1.x2.x3.x4]
Format[((x1_ba|x1_bc).(x2_ba|x2_bc).(x3_ba|x3_bc).(x4_ba|x4_bc))*
       ((y1_em|y1_emc)(y2_em|y2_emc)) z_?IntegerQ]:=
         SequenceForm[z y1 y2,x1.x2.x3.x4]
Format[((x1_ba|x1_bc).(x2_ba|x2_bc).(x3_ba|x3_bc).(x4_ba|x4_bc)) *
        (y1_em[t_]|y1_emc[t_])(y2_em|y2_emc)]:=
         SequenceForm[y1[t],y2,x1.x2.x3.x4]
Format[((x1_ba|x1_bc).(x2_ba|x2_bc).(x3_ba|x3_bc).(x4_ba|x4_bc))*
       ((y1_em[t_]|y1_emc[t_])(y2_em|y2_emc)) z_?IntegerQ]:=
         SequenceForm[z y1[t],y2,x1.x2.x3.x4]

Format[Power[E,x_]]:=SequenceForm["e", Superscript[x]]
Format[AA[q_]]:=SequenceForm["<a",Subscript[q],">"];
Format[AAc[q_]]:=SequenceForm["<a",Superscript["+"],Subscript[q],">"];
Format[ba[ã[q_]]]:=SequenceForm[ã,Subscript[q]]
Format[bc[ã[q_]]]:=SequenceForm[ã,Superscript["+"],Subscript[q]]
Format[vr[x_]]:=SequenceForm["v",Superscript["R"],Subscript[x]]
Format[v[x_]]:=SequenceForm["v",Subscript[x]]
Format[ba[a_[q_]]]:=SequenceForm[a,Subscript[q]];
Format[bc[a_[q_]]]:= SequenceForm[Sequence[a,Superscript["+"],
                     Subscript[q]]];
Format[fa[c_[q_]]]:=SequenceForm[c,Subscript[q]];
Format[fc[c_[q_]]]:= SequenceForm[Sequence[c,Superscript["+"],
                     Subscript[q]]];
Format[delta[q1_,q2_]]:=SequenceForm[Sequence["\[Delta]",
                        Subscript[q1,",",q2]]];
Format[(x_em|x_emc) (y_em[t_]|y_emc[t_])]:=SequenceForm[y[t],x]
Format[delta[x_]]:=SequenceForm["\[Delta]",Subscript[x]]
Format[x_ . (y_ z_delta)]:=SequenceForm[x.y,z]
Format[A[x_]]:=SequenceForm["<a",Subscript[x],">"]
Format[At[x_]]:=SequenceForm["<a",Superscript["+"],Subscript[x],">"]
```

```
Format[(x_+y_) DiracDelta[z_+w_]]:=SequenceForm["(",x+y,")",DiracDelta[z+w]]
Format[Exp[x_] y_]:=SequenceForm[y, Exp[x]]
Format[em[V_[ui_][li1_,li2_]]]:=Module[{inf,sup,result},
                 sup={Superscript["("],Superscript[ui],Superscript[")"]};
                 inf={Subscript[li1],Subscript[","],Subscript[li2]};
                 result=Join[sup,inf];
                 SequenceForm[V,Sequence @@ result]]
Format[emc[V_[ui_][li1_,li2_]]]:=Module[{inf,sup,result},
                 sup={Superscript["("],Superscript[ui],Superscript[")"],
                      Superscript["*"]};
                 inf={Subscript[li1],Subscript[","],Subscript[li2]};
                 result=Join[sup,inf];
                 SequenceForm[V,Sequence @@ result]]
Format[w[q_]]:=SequenceForm[w,Subscript[q]]
Format[Omega[q_]]:=SequenceForm["Omega",Subscript[q]]
Format[DiracDelta[x_]]:=SequenceForm["\[Delta](",x,")"]
Format[n_?IntegerQ * x_ DiracDelta[y_]]:=SequenceForm[n x,DiracDelta[y]]
Format[x_ DiracDelta[y_]]:=SequenceForm[x,DiracDelta[y]]
Format[x_ . y_]:=SequenceForm[x,y]
Format[n_?IntegerQ * Dot[x1_,x2_] (y1_emc|y1_em)*(y2_em|y2_emc)]:=
        SequenceForm[n y1 y2,x1.x2]
Format[n_?IntegerQ * Dot[x1_,x2_,x3_] (y1_emc|y1_em)*(y2_em|y2_emc)]:=
        SequenceForm[n y1 y2,x1.x2.x3]
Unprotect[Pi, Abs, Complex]
Format[Pi]:= Pi
Format[Abs[x_]]:=SequenceForm["|",x,"|"]
Complex[0,1]=i
Protect[Pi, Abs, Complex]
Protect[Power,Dot,Times,NumberQ];
sss[xx_]:=Collect[xx,{v[q],A[q],At[q],At[-q],A[q1],A[q2],At[q1],At[q2]}];
vvv[xx_]:=Cases[xx,PV[yy_],Infinity][[1]];
ddd[xx_]:=Cases[xx,DiracDelta[yy_],Infinity][[1]];
fun={Omega[-q-q1]+Omega[q1]-w[-q], Omega[q1]-Omega[-q+q1]+w[-q],
   -Omega[q1]+Omega[q+q1]+w[-q], Omega[q-q1]+Omega[q1]-w[q],
   -Omega[q1]+Omega[-q+q1]+w[q], Omega[q1]-Omega[q+q1]+w[q],
   Omega[-q-q1]+w[q]-w[-q1], Omega[q+q1]-w[q]+w[-q1],
   -Omega[q-q1]+w[q]+w[-q1], Omega[-q+q1]+w[q]+w[-q1],
   Omega[q+q1]+w[-q]-w[q1], Omega[-q+q1]+w[q]-w[q1],
   Omega[-q-q1]-w[-q]+w[q1], -Omega[-q+q1]+w[-q]+w[q1],
   Omega[q-q1]-w[q]+w[q1], -Omega[q+q1]+w[q]+w[q1],
   Omega[q1-q2]-w[q1]+w[q2], -Omega[q1+q2]+w[q1]+w[q2]};
```

Em seguida, o código de finalização do pacote:

```
End[]
EndPackage[]
```

E.3 *Notebook* para os cálculos

Com o pacote pronto, podemos agora realizar os diversos cálculos necessários mediante um *notebook* do *Mathematica*. Como tivemos problemas de memória com o *Mathematica* devido a complexidade e o tamanho dos cálculos com a hamiltoniano que usamos, subdividimos o cálculo em várias etapas. Assim, criamos *notebooks* para os cálculos pertinentes a cada uma das variáveis de base. Uma vez que cada *notebook* é idêntico, com exceção da segunda linha, em que a variável nq assume para cada *notebook* o correspondente valor da variável de base, damos apenas o código do *notebook* para a variável de base a_q:

```
«\m\Operadores.m
nq=ba[a[q]]
hsa=coms[HSR,nq]/.q1->q3

h1=HSR[[1]]+HSR[[9]]
ht=h1/.tempo
r1=Comutador[ht,hsa]
r2=IndMudo[soma[q1,soma[q2,spur[r1]]]];
r3=r2/.tempos
eqtem=-Integral /@ r3;
preal1=eqtem/.PV[1/x_]->0
pima1=eqtem/.DiracDelta[x_]->0
pr1=preal1/.coef
pi1=pima1/.coef
h2=HSR[[2]]+HSR[[10]]
ht=h2/.tempo
r1=Comutador[ht,hsa]
r2=IndMudo[soma[q1,soma[q2,spur[r1]]]];
r3=r2/.tempos
eqtem=-Integral /@ r3;
preal2=eqtem/.PV[1/x_]->0
pima2=eqtem/.DiracDelta[x_]->0
pr2=preal2/.coef
pi2=pima2/.coef

h3=HSR[[3]]+HSR[[11]]
ht=h3/.tempo
r1=Comutador[ht,hsa]
r2=IndMudo[soma[q1,soma[q2,spur[r1]]]];
r3=r2/.tempos
```

```
eqtem=-Integral /@ r3;
preal3=eqtem/.PV[1/x_]->0
pima3=eqtem-preal3
pr3=preal3/.coef
pi3=pima3/.coef

h4=HSR[[4]]+HSR[[12]]
ht=h4/.tempo
r1=Comutador[ht,hsa]
r2=IndMudo[soma[q1,soma[q2,spur[r1]]]];
r3=r2/.tempos
eqtem=-Integral /@ r3;
preal4=eqtem/.PV[1/x_]->0
pima4=eqtem/.DiracDelta[x_]->0
pr4=preal4/.coef
pi4=pima4/.coef

h5=HSR[[5]]+HSR[[13]]
ht=h5/.tempo
r1=Comutador[ht,hsa]
r2=IndMudo[soma[q1,soma[q2,spur[r1]]]];
r3=r2/.tempos
eqtem=-Integral /@ r3;
preal5=eqtem/.PV[1/x_]->0
pima5=eqtem/.DiracDelta[x_]->0
pr5=preal5/.coef
pi5=pima5/.coef

h6=HSR[[6]]+HSR[[14]]
ht=h6/.tempo
r1=Comutador[ht,hsa]
r2=IndMudo[soma[q1,soma[q2,spur[r1]]]];
r3=r2/.tempos
eqtem=-Integral /@ r3;
preal6=eqtem/.PV[1/x_]->0
pima6=eqtem/.DiracDelta[x_]->0
pr6=preal6/.coef
pi6=pima6/.coef
h7=HSR[[7]]+HSR[[15]]
ht=h7/.tempo
r1=Comutador[ht,hsa]
r2=IndMudo[soma[q1,soma[q2,spur[r1]]]];
r3=r2/.tempos
eqtem=-Integral /@ r3;
preal7=eqtem/.PV[1/x_]->0
pima7=eqtem/.DiracDelta[x_]->0
pr7=preal7/.coef
pi7=pima7/.coef

h8=HSR[[8]]+HSR[[16]]
ht=h8/.tempo
r2=IndMudo[soma[q1,soma[q2,spur[r1]]]];
r3=r2/.tempos
eqtem=-Integral /@ r3;
```

```
preal8=eqtem/.PV[1/x_]->0
pima8=eqtem/.DiracDelta[x_]->0
pr8=preal8/.coef
pi8=pima8/.coef

prt=Simplifique[(pr1+pr2+pr3+pr4+pr5+pr6+pr7+pr8)/.dp1]
pit=SimpPV[pi1+pi2+pi3+pi4+pi5+pi6+pi7+pi8]
pra=Collect[prt/.cf1,{A[q],At[-q],A[q1],A[q2],At[q1],At[q2]}]
vpa=Collect[prt/.cf1,{A[q],At[-q],A[q1],A[q2],At[q1],At[q2]}]
```

Cólofon

Esta tese foi composta em TEX, utilizando-se o conjunto de macros LATEX 2_ε. Os diversos pacotes auxiliares utilizados foram: `doublesp`, `t1enc`, `inputenc`, `mathematica`, `graphics`, `babel`, `natbib`, `feynmp`, `fancyhdr`, `pstricks`, `afterpage`, `calc`, `path`.

Os capítulos foram digitados no editor de textos Tse Pro 32, da SEMWARE, em um computador Pentium utilizando o sistema operacional Windows NT e compilados com o TEX de 32 bits da Y&Y. A versão final em *postscript* foi criada usando-se o programa dvipsone, também da Y&Y. Os gráficos foram feitos nos programas Origin 5 e Maple V, gerados em *postscript* encapsulado (EPS), e incluídos diretamente no corpo do texto. Detalhes adicionais necessários nos gráficos foram feitos com o programa Corel Draw.

A fonte do corpo principal do texto está em `Lucida Bright`; a das equações, em `Lucida New Math`; e a listagem dos programas no apêndice E, em `Lucida Typewriter`. O texto de Schiller está em `Goudy Text Lombardi`.